CONF-780301--

GASEOUS DIELECTRICS

(Proceedings of the International Symposium on Gaseous Dielectrics, Knoxville, Tennessee, USA, March 6-8, 1978)

•

Hosted by

Oak Ridge National Laboratory

Sponsored by

Oak Ridge National Laboratory
United States Department of Energy
Electric Power Research Institute

and

in cooperation with
Institute of Electrical and Electronics Engineers, Inc.
Power Engineering Society

CONF-780301

GASEOUS DIELECTRICS

(Proceedings of the International Symposium on Gaseous Dielectrics, Knoxville, Tennessee, USA, March 6-8, 1978)

Loucas G. Christophorou
Editor

Date Published: May 1978

Hosted by

Oak Ridge National Laboratory

Sponsored by

Oak Ridge National Laboratory
United States Department of Energy
Electric Power Research Institute

&

in cooperation with
Institute of Electrical and Electronics Engineers, Inc.
Power Engineering Society

1978

CONF-780301

GASEOUS DIELECTRICS

(Proceedings of the International Symposium on Gaseous Dielectrics, Knoxville, Tennessee, USA, March 6-8, 1978)

Loucas G. Christophorou
Editor

Sponsors

Oak Ridge National Laboratory
U.S. Department of Energy
Electric Power Research Institute

TABLE OF CONTENTS

AC, IMPULSE AND TIME VOLTAGE CHARACTERISTICS

Session III - Monday, March 6, 1978
CHAIRMAN: T. Nitta
Mitsubishi Electric
Corporation, Japan

EFFECTS OF PARTICLE CONTAMINANTS AND SURFACE ROUGHNESS ON BREAKDOWN

Session IV - Monday, March 6, 1978
CHAIRMAN: M. S. Mashikian
Detroit Edison Company, USA

NEW GASES AND GAS MIXTURES
Session V - Tuesday, March 7, 1978
CHAIRMAN - T. F. Garrity
U.S. Department of Energy, USA

APPLICATIONS
Session VI - Tuesday, March 7, 1978
CHAIRMAN: R. Samm
Electric Power Research Institute, USA

CONTRIBUTED PAPERS (EXTENDED ABSTRACTS)
Session VII - Wednesday, March 8, 1978
CHAIRMAN: A. V. Phelps
University of Colorado, USA

CONTRIBUTED PAPERS (EXTENDED ABSTRACTS)
Session VIII - Wednesday, March 8, 1978
CHAIRMAN: J. M. Googe
The University of Tennessee, USA

WELCOME

L. G. Christophorou
Oak Ridge National Laboratory
Oak Ridge, Tennessee 37830, USA

Ladies and Gentlemen: Good morning and welcome to Knoxville.

It is a distinct honor and an immeasurable pleasure to have you at this symposium.

In the energy era in which we are living, the need for energy conservation and energy cost reduction is overwhelmingly pressing. The demand for electric power in highly industrialized countries increases at alarming rates and so do the multiple needs for high voltage insulation.

It is the primary goal of this symposium to provide a forum for a report on, a comprehensive discussion of, and an exchange of ideas about current progress and problems relating to gaseous dielectrics.

It is also the hope of the organizing committee that this symposium, and perhaps future similar symposia, will provide an opportunity for a coordination of present and future efforts in both the basic and the applied and engineering aspects of gaseous insulation.

Prior to turning over the floor to the Chairman of the first session, I wish to express my gratitude to the sponsors of the symposium, the members of the program committee, and the members of the local arrangements committee. Special thanks are also due to many of you for your advice and to the personnel of the Oak Ridge National Laboratory's Laboratory Services Department for their assistance.

Thank you.

THE BASIC PHYSICS OF GASEOUS DIELECTRICS

J. Dutton
Department of Physics, University College of Swansea, University of Wales, U. K.

ABSTRACT

The mechanism of high voltage breakdown in molecular gases is discussed in terms of basic physical processes and the properties of charged particle swarms.

The three main areas surveyed are related to (i) static breakdown in uniform fields at voltages up to about 0.5 MV in relatively low electric fields ($<10^7$ V m^{-1}) where, as a result of experimental studies and theoretical simulations in recent years, the breakdown mechanism is now well understood for a range of gases including N_2, air, SF_6 and N_2O: (ii) the role of space charges in both uniform and non-uniform fields, with particular reference to experimental studies of the transition from uniform to non-uniform fields in the impulse breakdown of positive-sphere/earthed-plane systems and attempts to obtain a physically based breakdown criterion for such systems: and (iii) uniform-field breakdown in the same voltage range as in (i) above but at higher fields, which presents a difficult problem in surface physics which is discussed in the light of recent results.

INTRODUCTION

The ultimate limit of the voltage attainable in systems for the generation and distribution of high voltages is often set by the electrical breakdown of the gaseous dielectric which forms part of the insulation of such a system. Since there is strong interest, and considerable advantage, in operating systems at ever higher voltages, there is powerful motivation for understanding the basic physical processes which result in the transition, on a very short time scale, from good insulator to good conductor which characterises this breakdown.

This transition results from the chain of atomic and molecular processes initiated by one or more charged particles released in, and gaining energy from, the electric field which must exist between the high voltage electrode and earth. Thus, in principle, it should be possible to understand and make theoretical predictions about breakdown phenomena given the electric field distribution, a complete knowledge of the cross sections as a function of energy for all the collision processes involved in a given gas, and information concerning the processes of charged particle emission which results from the interaction of particles and radiation with boundary surfaces including, in particular, the electrodes. If this information is available an energy balance can be struck and an energy distribution function for the charged particles obtained, and the consequences in terms of the development of a current in the dielectric determined. In practice, however, except under special conditions there are a large number of individual processes occurring and there is often a lack of detailed knowledge of many of the cross sections involved. In addition, the procedure is a difficult one involving numerical integration of the equations and has only recently become possible with the advent of high speed computers.

SWARM COEFFICIENTS AND STATIC BREAKDOWN

In these circumstances, it has proved extremely valuable to obtain experimental values of the various averages for charged particle swarms corresponding to the cross sections of the various collision processes. These averages include the drift velocity W and diffusion coefficient D related to the cross section for momentum transfer and the coefficients of excitation ε, primary ionization α, electron attachment a, detachment d and ion-molecule reaction c, related to the corresponding atomic collision cross sections. Just as the total effective cross sections are dependent on energy and the gas number density n, so the swarm coefficients are dependent on the mean energy, which is determined by the parameter E/n (where E is the electric field) and on n. Investigation of the dependence of the coefficients on

these parameters can be used (a) to obtain information about cross sections,[1] (b) to identify the nature of the significant processes occurring in given cases,[2] and (c) to enable predictions to be made of the growth of ionization and breakdown, which are of particular importance in the present context. The power of this approach was, in fact, first shown in this connection through the early work of Townsend[3], who demonstrated experimentally that for relatively low voltages and under conditions when the only significant processes were electron ionization in the gas and secondary ionization by one of a variety of processes in the gas or at the cathode) the spatial growth of a current I_0, liberated from the cathode by external means was given at a constant value of E/n, by

$$I = I_0 e^{\alpha d} / [1 - (\gamma/\alpha)(e^{\alpha d} - 1)]. \qquad (1)$$

In this equation (γ/α) is a secondary ionization coefficient representing the number of secondary electrons produced per primary ionization. Furthermore, at a certain value of $d = d_s$,

$$(\gamma/\alpha)(e^{\alpha d_s} - 1) = 1 . \qquad (2)$$

Equation (2) is essentially a replacement condition and sets the lower limit to the region in which the current becomes self-sustaining. The voltage $V_s = (E/n)(\alpha d_s)$ is the static breakdown voltage which can thus be predicted from a knowledge of the swarm coefficients. These early experiments were conducted at relatively low voltages ($< 1{,}000$V) corresponding to relatively low values of the parameter αd_s and the interpretation is valid when the only significant processes are primary and secondary ionization.

II. V. BREAKDOWN IN UNIFORM STATIC FIELDS OF LESS THAN 10^7 V m^{-1}

Considerable effort has been devoted in recent years (a) to determining how the model can be generalized to take into account other processes such as attachment, detachment and ion conversion and a wide range of secondary ionization processes and (b) to establishing the range of validity of this generalised model.

Generalised Townsend Theory

The effect of including extra terms for the additional processes in the continuity equations leads to more involved expressions for the steady state solution. For example, when attachment, detachment and ion conversion from a negative ion species X^- which has a high detachment coefficient to a more stable species Y^- are included, in addition to primary and secondary ionization, the equation becomes[4, 5]

$$\frac{I}{I_o} = \frac{[A e^{\lambda_1 d} - B e^{\lambda_2 d} + D]}{1 - \frac{\omega}{\lambda_1 - \lambda_2}\left[\frac{\lambda_1 + c + \Delta}{\lambda_1}(e^{\lambda_1 d} - 1) - \frac{\lambda_2 + c + \Delta}{\lambda_2}(e^{\lambda_2 d} - 1)\right]} \qquad (3)$$

where λ_1 and λ_2 are the roots of the following equation

$$\frac{1}{2}\{\alpha - a_1 - a_2 - c - \Delta \pm [(\alpha - a_1 - a_2 - c - \Delta) + 4\{(a_1 + a_2)c + a_1\Delta\} + a_2]^{\frac{1}{2}}\} \qquad (4)$$

which involves the coefficients of attachment to the two ion species a_1 and a_2, the detachment coefficient Δ from X^- and the ion conversion coefficient c. The nature of this equation is such that very little detailed information about the individual coefficients or the processes underlying them can be obtained from swarm measurements under these conditions. Fortunately, however, the magnitude of the coefficients is such that an I, d curve at a constant value of E/n has, over much of its range, an analytical form the same as that of Equation (1) with α and ω/α replaced by effective ionization coefficients α' and $(\omega/\alpha)'$. These effective coefficients involve the coefficients of the individual processes in a way which depends on a knowledge of the particular processes occurring, but are useful even in the absence of such knowledge, because they can be used to predict the static breakdown voltage using a criterion of the same form as Equation (2).

Range of Validity

In order to test the range of validity of this generalized theory for breakdown in uniform fields, it is necessary to carry out swarm experiments over the widest possible range of parameters. Such measurements require a stable (fluctuations $\lesssim$ 1 part in 10^4) high voltage supply, the potential difference from which can be applied across an electrode system profiled to give a uniform field and contained within an enclosure which can be evacuated and filled with the required gas at high pressures. Using such a system, we have measured the spatial growth of ionization currents (range 10^{-13} to 10^{-7} A) at voltages up to a maximum of about 0.5 MV corresponding to values of nd_s up to about $59.93 \times 10^{23} m^{-2}$. For all the cases we have investigated which include N_2, air, SF_6, N_2O (see Refs. 6, 7, 8, 9, respectively) and mixtures, the spatial growth of ionization over a large range of d is analytically of the form given by Equation (1) provided the individual value of n is chosen at each value of E/n to ensure that $E \lesssim 10^7 V\ m^{-1}$. The values of the coefficients obtained under these conditions and the values of V_s determined from them are shown in Table 1. In all cases the values of V_s predicted from the swarm coefficients agree within the experimental error of about 1% with the measured values in our own laboratory[10, 11, 12, 13] and elsewhere[14, 15, 16, 17, 18, 19]. Other similar experiments on the growth of pre-breakdown ionization within this range in other laboratories (see Bibliography of Ref. 5) give results in agreement with the general conclusion that the spatial growth of prebreakdown ionization and the static breakdown voltage are in accord with the theory. This being so, it is of interest to determine whether the swarm coefficients can also be used to determine the temporal development of the spark when an impulse voltage $V \geq V_s$ is applied under these conditions.

IMPULSE H. V. BREAKDOWN IN UNIFORM FIELDS OF LESS THAN $10^7 V\ m^{-1}$

A priori, this would be expected to be the case because there is no reason to expect a change in the continuity equations (which together with the boundary conditions give the steady-state solution given in Equation (1) as the

Table 1. Values of the effective primary and secondary ionization coefficient in nitrogen, air and SF_6, together with the corresponding values of nd_s and V_s.

GAS	E/n (10^{-20} V m^2)	E (10^5 V m^{-1})	α'/n (10^{-24} m^2)	$10^4(\omega/\alpha)'$	V_s (kV)	nd_s (10^{23} m^{-2})
N_2	85	69.7	1.73	0.32	509	59.93
	88	72.4	2.5	0.57	343	39.04
	91	75.7	3.36	1.12	247	27.23
	94	79.6	4.39	1.48	184	19.53
	97	80.3	5.82	1.56	146	15.07
	100	82.3	9.7	1.19	123	12.23
Air	100	54.0	2.12	0.91	439	43.89
	101.5	54.8	3.54	0.48	285	28.07
	103	55.6	5.48	0.28	197	19.11
	106	56.4	9.81	0.064	129	12.17
	109	58.0	15.9	0.066	82	7.50
SF_6	358	11.8	42.0	2.89	68.7	1.921
	358.7	11.84	62.0	2.71	47.4	1.322
	359.4	11.86	76.0	3.83	38.0	1.056
	360.6	11.9	107.0	1.77	29.0	0.805

applied voltage increases above V_s.

Thus the current as a function of x and t in the simplest case, of primary ionization, together with secondary ionization at the cathode only, in a plane parallel electrode system can be obtained by solution of the continuity equations

$$\frac{\partial I_e}{\partial t} = W_e \left\{ \alpha I_e - \frac{\partial I_e}{\partial x} \right\}$$
$$\frac{\partial I_p}{\partial t} = W_p \left\{ \alpha I_p + \frac{\partial I_p}{\partial x} \right\} \qquad (5)$$

(in which I_e, I_p, W_e and W_p are the electron and ion currents and drift velocities, respectively, at plane x and time t) subject to the boundary conditions which are determined by the processes at the electrodes, in particular the secondary ionization processes at the cathode. For the early stages of the development of a small initial current when there is insufficient charge to distort the applied field, these equations are amenable to exact analytical solution [20 - 25]. These analytical solutions are useful when considering the early growth at relatively low pressures and over-voltages. In these conditions the space charge distortion is negligible, and the temporal growth of ionization exponential with a growth constant λ for many electron transit times, which represents a large fraction of the time taken for the glow discharge to develop[26]. At the relatively high pressures being considered here, however, the space charges build up much more rapidly often becoming significant during the transit time of an electron across the gap. During the phases of the growth where space charge becomes significant analytical solutions are no longer possible and to determine the temporal development of the current it is necessary (a) to be able to calculate the field due to the space charge and (b) to solve the continuity equations in conditions when the coefficients are not constant but vary continuously as the applied field is modified by the space-charge field.

The one dimensional form of the Poisson equation is found[27] to give values for the space charge field which are significantly in error. Thus, the first approach to the problem[28] was to develop a method for solving the equations numerically on the assumption that the discharge was of cylindrical cross section with charge density constant across a radius. This enabled the space charge field along the axis to be calculated, by the application of the inverse square law to the charges and their images in the electrodes, and the numerical integration of the one dimensional continuity equations using the so-called method of characteristics. In this method, the integration is carried out along the characteristic curves which follow the motion of the electrons and the ions. In the low pressure case at relatively low over-voltages, the development is such that the positive ion space charge has by far the bigger influence on the growth, but in the much more rapid development at high pressures it is essential to take into account the effects of both positive ion and electron space charges.

This method leads to a solution of the equations which gives electron density, ion density and electric field as functions of position and time. From these the light output as a function of time may also be obtained and streak photographs of the developing discharge simulated. A simulated streak photograph obtained in this way for nitrogen is shown in Fig. 1. This bears a striking visual resemblance to the experimentally observed streak photographs[29,30] showing the progression of luminous fronts usually referred to as the anode and cathode-directed streamers. Moreover, more detailed comparison between simulation and experimental photographs shows that there is good quantitative agreement between the times of identifiable features such as the arrival times of the streamers at the electrodes.

Additional processes can readily be incorporated into the equations and later computations by other groups, using similar methods have shown (i) that in air the inclusion of electron attachment and detachment greatly influences the growth[31] in agreement with experimental observations[32] and (ii) that the

Fig. 1. Computer simulated[28] streak photograph for breakdown in nitrogen for $n = 2.97 \times 10^{24}$ m^{-3} and $E/n = 1.76 \times 10^{-20}$ V m^2. The anode and cathode-directed streamers can be clearly seen. [The anode is at the top of the picture and is separated by a distance of 3 cm from the cathode at the bottom; time progresses from left to right on a scale from about 70 to 145 ns after the application of the voltage].

assumption of photo-ionization rather than photo-electric effect at the cathode as the dominant secondary ionization process changes the growth to a very small extent, except in the case of wide discharges at high over-voltages[33].

Subsequent development of the original analysis[34] has enabled the prediction of currents in good agreement with experiment[35] from a few initial electrons well into the region of the glow discharge, provided the experimental variations of the radius are taken into account. This change of radius of the developing discharge has also been shown[36] to have an important bearing on the discontinuity in the experimentally observed curves of formative time lag vs. over-voltage which is also in agreement with the theoretical predictions of the simulation.

In more recent work[37], the necessity to make assumptions about the change in radius is removed by extending the method to two dimensions. This work, together with some of the details of the earlier methods and results, is described in another paper[38] to be given at this Conference and thus will not be discussed further here except to note that it does not significantly alter the conclusions of the earlier work using the one-dimensional solution.

The concepts of [illegible] development of discharges [illegible] observed development [illegible] for on the basis of the same basic collision processes as those responsible for the spatial growth of ionization at $V = V_s$.

In this region a knowledge of the swarm coefficients and the coefficients of the electron emission processes at the cathode, enables not only the static breakdown potential of a gas and its electrical behaviour under pulse or d.c. voltages to be predicted. It should be noted, however, that where the effective ionization coefficients (which can be adequately measured by a variety of methods and are available for a large number of cases[5]) are sufficient for the calculation of V_s, the actual coefficients of the individual processes are needed for the predictions of temporal growth, and these cannot be accurately measured by existing methods in cases where electron attachment and detachment occur. The alternative approach of using swarm coefficients calculated from data on cross sections is limited to those relatively few cases for which all the required cross sections are sufficiently well known as a function of energy. That this procedure is now technically feasible even in gas mixtures, however, was recently shown by the calculation[39] of [illegible] at relatively high E/n for the gas laser mixture $CO_2 : N_2 : He$, the values obtained being subsequently confirmed by independent measurement[40].

II. V. BREAKDOWN IN NON-UNIFORM FIELDS AND IN UNIFORM FIELDS GREATER THAN 10^7 V m^{-1}

A large amount of experimental and theoretical research has been carried out on breakdown phenomena under these conditions, and a good deal of insight gained into the various phases of the discharge such as, for example, the corona, leader and leader-corona phases of positive rod-earthed plane systems, which have been observed in laboratory gaps of lengths from 1m in the early work of Allibone and Meek[41] to 13.5m in the recent extensive

measurements on long gaps by the Les Renardières Group[42]. It is nevertheless true to say that the understanding in terms of basic processes is not nearly as well established in either of these regions as in the region previously discussed. This is partly because in both these cases the phenomena themselves are more variable, and in the non-uniform case this is compounded by the difficulties of carrying out experiments in completely controlled atmospheres because of the large volumes required and by the fact that the theoretical capability of dealing with the two dimensional development of space charge, which is required even for axially symmetric breakdown, is only now being developed. The vast amount of work done in these areas has been the subject of a number of excellent reviews including those of Cookson[43] covering high uniform fields and those of Allibone[44] and Waters[45] which are the most recent in non-uniform field breakdown.

In these circumstances, rather than attempting a much abbreviated review it seemed to me better in this paper to concentrate attention on some current experiments in our laboratory designed to define and to attempt to solve some of the basic physics problems which remain in these regions.

Non-Uniform Fields

From the point of view of developing a criterion for breakdown in non-uniform fields in terms of basic collision processes, the *major* difference between low uniform fields considered previously and non-uniform fields is the relative importance of space charge. As has been shown above, in low uniform fields a criterion for V_s not involving space charge but only the ionization coefficients is adequate over a wide range of parameters. Space charges only become significant when conditions are established in which the current can increase with time, and then usually act in the later stages of the growth so as to enhance the growth of current to the spark. In non-uniform fields, on the other hand, space charges play a crucial role in determining the breakdown voltage, because the current in the gap in the pre-breakdown phase produces significant space charge which has an inhibiting effect.

In order to develop a criterion for breakdown in non-uniform fields on the basis of fundamental collision processes and their interaction, it is thus necessary to establish the distribution of this space charge. Thus we have recently started a series of measurements in collaboration with Dr. R. T. Waters' group at the University of Wales Institute of Science & Technology, to investigate the distribution of space charges in positive sphere-earthed plane systems. The system was designed to enable us to study the transition from uniform-field to non-uniform field breakdown of air for a range of electrode separations from 0.1 to 0.7m and of sphere diameters from 75 to 250mm, using lightning impulses with a rise time of 1.1 μs and a decay time of 58 μs. The electrode system was enclosed in an earthed wire mesh cylinder of 3m diameter, so that the applied field was well defined and the whole system was shrouded in a polythene tent through which filtered air was flowed to give some degree of control of the gaseous environment. (Further experiments are planned in a large metal ionization chamber to investigate the effects of humidity.) The first experiments with this system established clearly the expected transition in the 50% probability breakdown voltage (V_{50}) vs. distance for a given sphere diameter from a slope of about 3×10^6 V m^{-1} for uniform fields to about 0.55×10^6 V m^{-1} in non-uniform fields. Subsequent experiments were concentrated on corona events in the non-uniform field region which did not lead to breakdown, with a view to determining the way in which the space charge resulting from the corona was distributed. These measurements involved the use of a rotating vane fluxmeter[46] mounted in the centre of the plane electrode, and simultaneous photomultiplier observations at various positions in the gap. In the fluxmeter, a sectored disc of 15 cm diameter rotated above a similarly sectored stator, and the integrated signals from both discs were recorded by a digital recorder (sampling rate 20MHz) to enable the induced and conduction currents at the cathode to be measured. Hence the field at the cathode and the net charge arriving there can be determined: from these measurements it was established[47] that for the cathode to play an active role in the corona phase (i.e. for charge to be transferred to it) requires a field E of about 4.7×10^5 V m^{-1} to be established there. Thus at any given

value of pd, a voltage V_t is required before there is a transfer of charge at the cathode and this gives a characteristic curve V_t, d lying below the V_{50}, d characteristic. A typical signal from the stator in the case in which the cathode does not play an active part in the corona phase is shown in Fig. 2; the amplitude of the oscillation is a measure of the induced field at the cathode, and the displacement of the minimum of the oscillations from the axis at a time T_i after the initial pulse is a measure of the charge conducted. Thus, in this case the induced field remains practically constant as the ion space-charge approaches the cathode and then decreases as the ions begin to reach it at the time T_i. Such measurements give the total charge injected by the corona and the arrival time of this injected charge at the cathode, while simultaneous photo-multiplier observations give the extent of the corona. These results are found to be consistent with an earlier suggestion[48] from fluxmeter measurements that to a first approximation the charge injected by the corona can be regarded as located in a plane at some distance from the cathode. With this assumption and

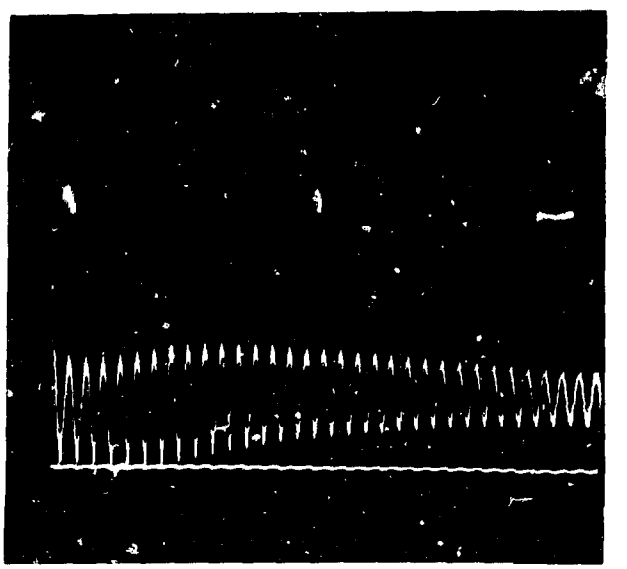

Fig. 2. Signal from the lower static electrode (see text) of a fluxmeter situated in the middle of the plane electrode of a positive sphere-earthed plane system subjected to a lightning impulse of 210kV peak voltage. Sphere diameter: 7.5 cm; Gap length: 45 cm; Gas: air at relative humidity about 10 g m^{-3}.
[The time scale is 2ms per cm].

using calculated values of the corona inception field[42] and the applied field at the cathode[49], together with experimentally established values of E_t, it is possible to predict the V_{50}, d characteristic. This characteristic has the same form as that experimentally observed and currently the two-dimensional computer simulation is being developed to calculate a more accurate distribution of space charge to see whether, in this way, a criterion for non-uniform field breakdown based entirely on basic processes and their interaction in the applied field as modified by space charge can be obtained.

Uniform Fields > 10^7 V m^{-1}

It has been known for a considerable time that as the pressure, and hence the field at a given value of pd_s, increases a region is reached in which the character of uniform-field breakdown becomes quite different from that described earlier. The characteristics of this region are that (a) the breakdown potential, even under well controlled conditions, ceases to be a well-defined value predictable on the basis of Equation (1), (b) there are marked departures from Paschen's law and (c) the sparking potential shows a strong dependence on the cathode material and state, the dependence being large enough to be observed despite the large range of values obtained with a given electrode. In order to investigate this region in as controlled an environment as possible, we have recently carried out a series of experiments[50, 51] on nitrogen, using an ionization chamber which could be initially evacuated to about 10^{-5} torr and into which nitrogen (filtered to remove particles above 1 μm in size, and dried over P_2O_5) could be subsequently admitted at pressures up to about 15 atmospheres. The electrodes were profiled to give a uniform field over the central region; the materials and surface finishes used were (a) aluminium polished with γ-alumina (b) titanium, as-machined giving a surface of $\sim 0.6\,\mu$m centre line average (CLA) as measured using a Talysurf, or medium polished with 600 carborundum ($\sim 0.1\,\mu$m CLA) or polished with diamond paste ($\sim 0.1\,\mu$m CLA), and (c) stainless steel medium polished ($\sim 0.1\,\mu$m CLA). A series of measurements of the breakdown voltage at a constant value of $nd_s = 1.69 \times 10^{24}$ m^{-2} enabled the transition from low to

high fields to be studied. For all the surfaces, V_s in the low field region was 162 ± 1kV as shown in Table 2, but at approximately the values of the pressure p_t given in the table for each surface, the static breakdown potential began to decrease and to show a scatter, the majority of the values at any given pressure lying within a band about 30kV wide but with single values occasionally lying even lower than the bottom of this band. Some of these very low values were followed by a decrease in the mean position of the band which then gradually recovered. The breakdown voltage for $p > p_t$ was characterised by V_m^p the mean of highest 25% at the pressure p. The values of V_m^{12} (i.e. V_m at p = 12 atmospheres) given in the table indicate that some of the curves of V_m, p cross each other so that the relative insulation strength with a given electrode at high pressure is not necessarily dependent on the pressure at which the transition to high field behaviour occurs.

The surface state of the electrodes was investigated before and after sparking using a talysurf and photo-graphic observation, and measurements of field emission were made for each electrode. The results are summarised in Table 2 and it can be seen that there is little correlation between surface topography, steady state field-emission and breakdown strength with a given electrode at a given pressure, except for the stainless steel electrodes. These surprisingly gave particularly low values of V_m and much higher field emission than any other surface. Further polishing showed that this probably resulted from the use of stainless steel which had not been vacuum cast and contained small porosities within the material itself. The lack of correlation between surface topography and breakdown was further indicated by the fact that the number of craters observed were about the same as the number of sparks and that when a deliberate surface scratch was introduced, breakdown did not occur there.

Measurements were also made of the spatial growth of pre-breakdown ionization and these showed that α in the high pressure region was identical with that at low pressures and that there was no marked enhancement of ω/α.

Table 2. Results of a study of the transition from breakdown at low uniform fields to that at high uniform fields in N_2 at $n\,d_s = 1.69 \times 10^{24}\ m^{-2}$.

Electrode surface	P_t (atm)	V_m^{12} (kV)	Surface after sparking	I_F (A)	V_s (kV)
Polished Al	4	120	Craters 25 μm deep and splash marks	$\sim 10^{-12}$	163
Medium polished Stainless Steel	4	81	Craters 2 - 5 μm deep and metal dust	$\sim 10^{-10}$	162
As-machined titanium	4.5	108			162
Medium polished titanium	6.5	103	Craters 2 - 5 μm deep	$\lesssim 10^{-12}$	162
Diamond polished titanium	6.5	117			162

Breakdown occurred at random along an I, d curve sometimes when a point in the middle of a given curve (which had shown that the steady-state ω/α at that distance was negligible) was being re-measured. It follows that the breakdown in the high pressure region is random, transient and localised. This is in agreement with the temporal studies of Müller[52] which showed that breakdown was initiated in these conditions by short bursts of about 10^3 electrons over a period of less than 3ns, although the nature of the sites from which the emission occurred was not established.

The above results show that it has not been possible to identify any readily measurable parameters of a surface or its pre-breakdown behaviour in the steady state which can be used to select electrodes likely to give the best insulation strength in a high-field insulating gap.

INTERACTION OF BASIC PHYSICS WITH TECHNOLOGY

Because there are fundamental connections with the use of gaseous dielectrics and semiconductors for high voltage transmission systems, it seems appropriate to conclude with some consideration of the way in which the study of the basic phenomena and interactions exist for use in technological developments.

There are in general three ways in which basic physics can interact with technology ranging from the use of known physical data to the solution of technological problems, whereas at the physicist could learn the controlled experiments of the uncontrolled case, on itself, based on those measurements which occur in the engineering context. In other words, technological improvements can be sought through essentially a theoretical materials approach, while on the latter, technological useful results are cannot likely to emerge (all the field is already well developed) from the solution of fundamental basic problems. Both situations exist in the field of h. v. breakdown.

The Materials Science of Gaseous Dielectrics

It is clear from the discussion in the earlier sections that the region in which the materials science approach is most likely to be successful is that of uniform field breakdown at fields $\leq 10^7$ V m^{-1}. Since in this region there is a well-defined accurately reproducible V_x which can be predicted either from a knowledge of cross sections or swarm coefficients, the physical properties for a dielectric of high insulator strength can be specified in general terms. These are that the ionization detachment coefficients should be small and the attachment coefficient large. Not only does knowledge of the cross sections of the processes involved as a function of energy enable prediction of the insulation performance of a given gas but also gives guidance as to the potentialities of gas mixtures. A great deal of interesting work of this sort is, of course, being undertaken in the Atomic, Molecular and High Voltage Physics Group at Oak Ridge National Laboratory, some of which is reported

in another paper[5,6] at this Conference. Another example is some recent work undertaken on N_2O in our laboratory. This arose from the initial question as to whether there were any common gases having the same fundamental property which makes SF_6 a good insulator, viz: a high attachment cross section at low energy. A search of the literature suggested that N_2O, which has an attachment cross section $\sim 10^{-17}$ cm^2 at about 2eV should be a good insulating medium, although no previous studies of ionization growth or breakdown had been made in N_2O itself. Our subsequent measurements[13] of V_s for N_2O which are given in Table 3, showed it to have a dielectric strength intermediate between N_2 and SF_6. The measurements of V_s, together with associated pre-breakdown measurements, gave results which required[9] account to be taken of the following six reactions for their interpretation:-

primary ionization:	$e + N_2O \rightarrow N_2O^+ + e + e$	(coefficient α),
dissociative attachment:	$e + N_2O \rightarrow N_2 + O^-$	(a),
negative-ion-molecule reactions:	$O^- + N_2O \rightarrow NO + NO^-$	(m_1),
	$O^- + 2N_2O \rightarrow N_2O + N_2O_2^-$	(m_2),
	$NO^- + 2N_2O \rightarrow N_2O + N_3O_2^-$	(μ)
collisional detachment:	$NO^- + N_2O \rightarrow N_2O + e + NO$	(δ)

Considerable pressure dependencies of the measured coefficients were observed resulting from the competition between the three-body ion-molecule reaction (converting the loosely bound NO^- to the lightly bound $N_3O_2^-$) and the detachment reaction. It was clear that if the detachment reaction rate could be reduced by, for example, the addition of small amounts of O_2 in which the charge transfer reaction

$$NO^- + O_2 \rightarrow NO + O_2^-$$

is known to occur with a fast reaction rate, the breakdown strength should be increased, even though O_2 itself has a much lower dielectric strength than N_2O.

Table 3. Sparking potentials for N_2O and for O_2/N_2O and SF_6/N_2O mixtures at $n \approx 13 \times 10^{24}\ m^{-3}$.

V_s (kV)									
	N_2O	$[O_2/(N_2+O_2)]$ %				$[SF_6/(N_2O+SF_6)]$ %			
		0.95	2.8	5.2	10.9	1.1	2.6	6.2	10.1
nd_s ($10^{22} m^{-2}$)									
10.0	17.30	18.14	18.45	18.62	18.5	19.18	20.48	22.57	24.06
15.0	25.02	26.28	26.73	27.1	26.86	28.02	30.02	33.29	35.60
30.0	48.29	50.4	51.7	52.2	51.8	54.5	58.7	65.3	70.3
45.0	71.6	74.6	76.4	77.1	76.2	80.7	87.3	97.3	104.9
60.0	94.7	98.6	100.7	101.4	100.4	107.4	115.9	129.3	139.6
75.0	117.9	122.4	124.9	125.8	124.1	134.2	144.3	161.4	174.4
90.0	141.0	146.0	148.6	149.3	147.6	160.4	172.4	192.5	207.7
100.0	156.3		164.7	165.4	163.1	176.9	186.1	203.6	222.1
105.0	162.1					179.2	187.8		224.1
110.0	164.0		173.2	177.1	173.5	180.9			

Breakdown measurements in O_2/N_2O mixtures[54], some of which are given in Table 3, confirmed this prediction and also showed, as expected, that the pressure dependence was reduced. These results led to an investigation of SF_6/N_2O mixtures[55] where on general grounds a reaction of the type

$$NO^- + SF_6 \rightarrow SF_6^- + NO$$

might be expected to occur. In this case the dielectric strength increases very rapidly with the addition of SF_6 as shown in Table 3, giving for a 20% mixture, for example, a dielectric strength over 70% of that of SF_6 alone at about 40% of the cost. Recent measurements on N_2/SF_6 in a similar system show an almost identical pattern, although the fundamental reasons must be quite different. This would make an investigation of pre-breakdown currents in this mixture and in the triple mixture $N_2/N_2O/SF_6$ of interest.

Technologically Interesting Basic Problems

In the other regions which have been discussed, the basic physics has not reached the level of understanding which is required for the materials science approach, but there are some clearly identifiable basic problems the solution to which could well be useful technologically. For example, in non-uniform field breakdown, there is the prospect that further experimental research on the distribution of space charge, together with two-dimensional computer simulations, will lead to completely physically based breakdown criteria, at least for axially symmetric geometries in which the applied field is well specified. Even if these methods are too complex for every-day practical use, they will be helpful as absolute theories against which to test existing empirical and semi-empirical expressions (as well as any further ones which may arise from the investigations themselves) in novel and extrapolated situations. The overall aim of predictive criteria of this kind being, of course, to reduce the amount of experimental testing required.

In uniform-field breakdown at high pressures it is clear that the basic problem for solution is not mainly concerned with the gaseous dielectric itself, but with the electrode-surface/dielectric interface. Ideally, what is required to determine the initiation mechanism in this regime, is a method of studying microscopical developments on an electrode surface in the presence of a high pressure gas on a time-scale of at least microseconds, and possibly nano-seconds. This does not seem technically feasible at present, so more indirect methods are required, possibly along the lines of previous work[56] in which the effect on the breakdown strength of introducing known types of imperfections on single crystal surfaces was investigated. The identification of the nature and evolution of the sites at which breakdown is initiated is clearly a difficult problem. Identification is, however, the first step in assessing whether such sites can be controlled or eliminated. If this proved possible it would have considerable consequences for the design of h. v. insulation because it would lead to less erratic spark breakdown voltages and a much improved level of insulation for a given gas pressure.

REFERENCES

1. L. G. Christophorou, Atomic and Molecular Radiation Physics, Chapters 4 and 5: Wiley - Interscience (1971).

2. J. Dutton, F. M. Harris and F. Llewellyn-Jones, Proc. Phys. Soc., 82, Part 4, 528, 581 (1963).

3. J. S. Townsend, Electricity in Gases: Oxford, Clarendon Press (1915).

4. R. W. L. Thomas, Ph. D. Thesis, University of Wales (1968).

5. J. Dutton, J. Phys. Chem. Ref. Data 4, 577 (1975).

6. T. N. Daniel, Ph. D Thesis, University of Wales (1968).

7. J. Dutton and W. T. Morris, Brit. J. Appl. Phys. 18, 1115 (1967).

8. G. J. Jones, Ph. D. Thesis, University of Wales (1973).

9. J. Dutton, F. M. Harris and D. B. Hughes, J. Phys. B : Atom. Molec. Phys. 8, 313 (1975).

10. T. N. Daniel and F. M. Harris, J. Phys. B : Atom. Molec. Phys. 3, 363 (1970).

11. W. T. Morris, Ph.D. Thesis, University of Wales (1967).

12. J. Dutton, F. M. Harris and G. J. Jones, Proc. IEE, 118, 733 (1971).

13. J. Dutton, F. M. Harris and D. B. Hughes, Proc. IEE, 120, 941 (1973).

14. E. A. Schröder, Z. angew Phys. 13, 567 (1961).

15. H. A. Boyd, F. M. Bruce and D. J. Tedford, Nature, Lond. 210, 719, (1966).

16. O. Farish and D. J. Tedford, Brit. J. Appl. Phys. (J. Phys. D) 2, 1555, (1969).

17. T. N. Daniel, J. Dutton and F. M. Harris, Brit. J. Appl. Phys. (J. Phys. D) 2, 1559 (1969).

18. M. S. Bhalla and J. D. Craggs, Proc. Phys. Soc. 80, 151 (1962).

19. D. W. George and P. H. Richards, Brit. J. Appl. Phys. 2, 1470 (1969).

20. P. M. Davidson, Brit. J. Appl. Phys. 4, 170 (1953).

21. P. M. Davidson, Phys. Rev. 103, 1897 (1956).

22. P. M. Davidson, Phys. Rev. 106, 1 (1957).

23. P. M. Davidson, Proc. Roy. Soc. A249, 237 (1958).

24. P. M. Davidson, Proc. Roy. Soc. 80, 143 (1962).

25. A. J. Davies and C. J. Evans, CERN(Geneva) Report 73- (1973).

26. C. G. Morgan and W. T. Williams, Proc. Phys. Soc. 85, 443 (1965).

27. A. J. Davies and C. J. Evans, Proc. IEE. 114, 1547 (1967).

28. A. J. Davies, C. S. Davies and C. J. Evans, Proc. IEE, 118, 816 (1971).

29. K. H. Wagner, Zeits für Phys. 189, 465 (1966).

30. I. D. Chalmers, H. Duffy and D. J. Tedford, Proc. Roy. Soc. A329, 171 (1972).

31. P. Bayle and M. Bayle, Z. Phys. 266, 275 (1974).

32. I. D. Chalmers, H. Duffy and D. J. Tedford, Proc. Roy. Soc. A329, 171 (1972).

33. L. E. Kline, J. Appl. Phys. 45, 2046 (1974).

34. A. J. Davies, C. J. Evans and P. M. Woodison, Proc. IEE 122, 765, (1975).

35. A. A. Doran, Zeits für Phys. 208, 427 (1968).

36. A. J. Davies, C. J. Evans and P. M. Woodison, Proc. 3rd Int. Conf. on Gas Discharges, (London), 1, 119 (1974).

37. A. J. Davies, C. J. Evans, P. Townsend and P. M. Woodison, Proc. IEE 124, 179 (1977).

38. A. J. Davies, C. J. Evans and P. M. Woodison, Proc. Int. Symp. on Gaseous Dielectrics (Knoxville) (1978).

39. J. J. Lowke, A. V. Phelps and B. W. Irwin, J. Appl. Phys. 44, 4664 (1973).

40. S. C. Haydon and A. I. McIntosh, Proc. 4th Int. Conf. on Gas Discharges, (Swansea), 1, 184 (1976).

41. T. E. Allibone and J. M. Meek, Proc. Roy. Soc. A166, 97 (1938).

42. "Les Renardières Group", Electra No. 53, 31 (1977).

43. A. H. Cookson, Proc. IEE 117, 269 (1970).

44. T. E. Allibone, Lightning (Editor: R. H. Golde) : Academic Press, Chapter 7 (1978).

45. R. T. Waters, The Electrical Breakdown of Gases (Editors: J. M. Meek and J. D. Craggs) : 2nd Edn : Wiley: Chapter 5 (In the press) (1978).

46. R. T. Waters, T. E. S. Rickard and W. B. Stark, Proc. Roy. Soc. A304, 187 (1968).

47. P. Bye, A. J. Davies, J. Dutton and R. T. Waters, Proc. 4th Int. Conf. on Gas Discharges (Swansea), 137 (1976).

48. R. T. Waters, T. E. S. Rickard and W. B. Stark, Proc. Roy. Soc. A315, 1 (1970).

49. J. M. Mattingley and H. M. Ryan, Proc. IEE 118, 720 (1971).

50. R. Coates, J. Dutton and F. M. Harris, Proc. 3rd Int. Conf. on Gas Discharges (London), 1, 403 (1974)

51. R. Coates, J. Dutton and F. M. Harris, Proc. 4th Int. Conf. on Gas Discharges (Swansea), 1, 133 (1976).

52. E. K. Müller, Zeits angew Phys. 21, 219, 475 and 554 (1966).

53. D. R. James, L. G. Christophorou, R. Y. Pai, M. O. Pace, R. A. Mathis, I. Sauers and C. C. Chan, Proc. Int. Symp. on Gaseous Dielectrics (Knoxville), (1978).

54. J. Dutton, F. M. Harris and D. B. Hughes, J. Phys. D : Appl. Phys. 8, 1640 (1975).

55. J. Dutton, F. M. Harris and D. B. Hughes, Proc. IEE 121, 223 (1974).

56. Y. L. Stankevich and V. G. Kelinen, Sov. Phys. Tech. Phys. 11, 1120, (1967).

DISCUSSION

SIOMOS: 1. What is the physical meaning of the constant C in your equation $I_c = \frac{I_o}{C}$? 2. How do you explain the measured departure of the Paschen law and do you see any consequences because of this?

BUTTON: 1. I should have mentioned that I_c is the constant measured at some given low value of E/N, so that since $I = f(E/N)$, $I_o = CI_c$. The advantage of measuring I_c rather than attempting to determine I_o is that it leads to more accurate evaluation of the ionization coefficients. The reason for this is that although the I, E/N curve is often assumed to saturate at a value of I_o it does not in practice do so and thus I_o can only be obtained by extrapolation. This, in turn, means that the accuracy with which I_o can be determined is less than that attainable in the measurement of I_c and I. 2. The explanation clearly lies in the high value of the fields at which the departure occurs and the influence this has on the electrode/gas interface. The details of the processes occurring at the interface are, however, an unsolved and very interesting problem. Our experiments in N_2 show that the magnitude of the departures are not readily related to surface topography, electrode material, steady-state field emission or prebreakdown current, but indicate an agreement with the earlier time-resolved field emission measurement of Müller, that the phenomena are transient and localized.

The consequences for insulation are considerable because if the sites at which breakdown is initiated could be identified and eliminated, this would reduce the scatter in the breakdown voltage and increase its value to that corresponding to the Paschen value. Ideally, what is

needed is a method of studying the electrode surfaces in the presence of a field of $>10^7$ V cm^{-1} and of a gas at high pressure on a time scale of μsec or even nsec. This does not seem feasible at the moment, and we are currently using a more indirect approach involving the use of single crystal electrodes and the effect of introducing imperfections at the surface.

BLAIR: You report measurements of breakdown voltage as a function of pressure with different electrode materials and different cathode-surface roughnesses. To what extent could the differences between materials be caused by different rates of change of surface roughness with repeated sparking? Were the quoted roughnesses measured before or after sparking?

DUTTON: The roughness was measured both before and after sparking, the figures quoted on the slide being those before breakdown which ranged from 0.1 to 0.6 μm CLA. After breakdown, there were craters ~25 μm deep on Al and ~2-5 μm deep on the stainless steel and tungsten electrodes. These craters did not seem to play a significant role in initiating breakdown however, because there was no suggestion of discharges being anchored to craters, the number of craters being of the same order as the number of sparks. There was little correlation of the breakdown behavior with any of the steady-state parameters which we measured.

ELECTRON SWARM PARAMETERS IN GASES AND VAPOURS

J. Lucas
Department of Electrical Engineering and Electronics, University of Liverpool, P.O. Box 147, Liverpool L69 3BX, England.

ABSTRACT

Electron swarm parameters have been measured for a number of years over a wide range of E/N (electric field to gas number density) by using both a time of flight and a steady state technique. The parameters investigated have been the ionisation coefficient, attachment coefficient, drift velocity, excitation coefficient, and both radial and longitudinal diffusion coefficients. Measurements have been made for $1 \lesssim E/N \lesssim 2000$ Td ($1\ \text{Td} = 10^{-17}\ \text{V cm}^2$) in a wide range of molecular gases (H_2, N_2, CO, CO_2, O_2, CH_4, CF_4) and atomic gases (He, Ar, Ne) and a recent development is measurements in CO_2 laser gas mixtures (CO_2-N_2- He) and metal vapours (Hg, Na, Tl).

Theoretical values have been computed for the electron swarm parameters by using the Boltzmann equation and the Monte Carlo simulation technique. For each gas/vapour a set of cross-sections have been selected which give theoretical values of the parameters in agreement with their experimental values. The cross-sections used include total collision, elastic collision, differential scattering and inelastic collisions. The majority of the computations have been done using the Monte Carlo technique because it directly simulated the time of flight and steady state experimental methods.

INTRODUCTION

Electron swarms drifting across a uniform electric field in gas are represented by at least six swarm parameters namely:- ionisation coefficient (α), drift velocity (v), attachment coefficient (η), radial (D_r) and longitudinal (D_L) diffusion coefficient and a radiation coefficient (α_r) for a single or a group of wavelengths. These parameters describe all of the physical properties of the swarm as shown in Fig. 1. If n_o electrons are emitted as a point source from the cathode at z = 0 then after a time t the mean distance travelled is $\bar{z}_t = vt$, the radial spreading is $\overline{r_t^2} = 4 D_r t$ and the axial spreading is $\overline{(z - \bar{z})_t^2} = 2 D_L t$. The electron swarm has increased in number from n_o to $n_t = n_o e^{(\alpha-\eta)vt}$ and has produced $\frac{\alpha}{\alpha-\eta}(n_t - n_o)$ positive ions, $\frac{\eta}{\alpha-\eta}(n_t - n_o)$ negative ions and $\frac{\alpha_r}{\alpha-\eta}(n_t - n_o)$ photons. The swarm parameters give us a lot of preliminary information concerning the electron energy distribution. The ratio of radial diffusion coefficient to mobility (D_r/μ) is a measure of the mean electron energy ($\bar{\varepsilon}$) since $\bar{\varepsilon} \simeq 3/2\ (D_r/\mu)$. The presence of ionisation indicates that some of the electrons have attained the ionising energy ($\lesssim$15 eV for molecular gases) whilst presence of attachment indicates that some electrons have reached the

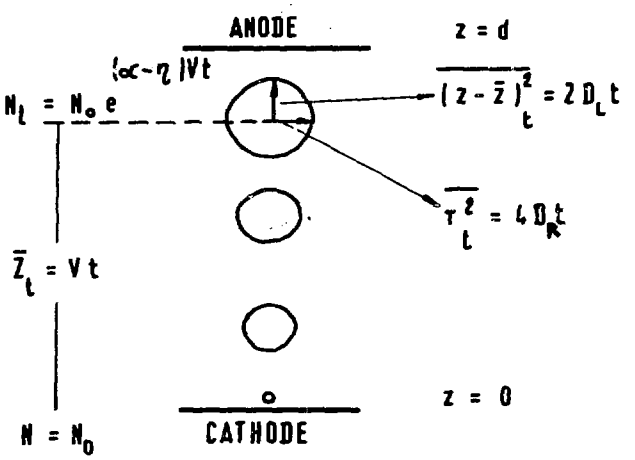

Fig. 1 A Schematic Diagram of Swarm Motion

attachment energy (~3 eV for O^- in oxygen) and the attachment reaches its peak value when the swarm mean energy corresponds to the electron energy which produces the maximum attachment cross-section.

A detailed theoretical study will produce accurate values for the mean electron energy and the energy distribution. It requires knowledge of all the collision cross-sections and is achieved by solving Boltzmann's equation or by using the Monte Carlo simulation. The accuracy of the computations is assured by obtaining a satisfactory agreement between the experimental and theoretical values for the four main parameters the drift velocity, the ionisation coefficient, the radial diffusion coefficient and the longitudinal diffusion coefficient (see Fig. 2) although it may be necessary to scale some of the doubtful

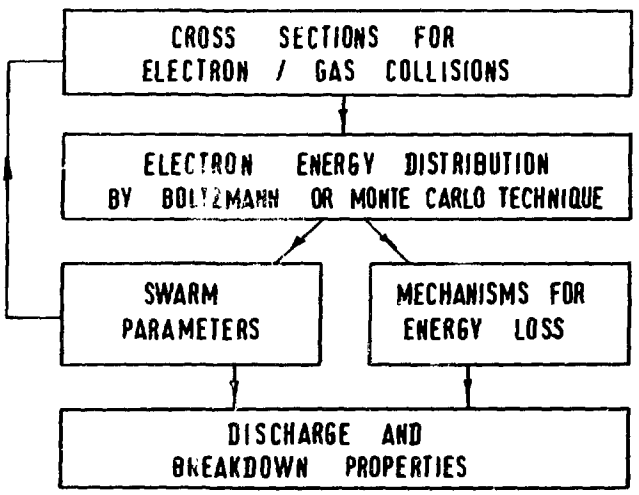

Fig. 2 The Interrelationship between Swarm Parameters

cross-sections (Frost and Phelps [1]). It is convenient to calculate for each E/N all the sources of energy loss by the electron/gas collisions because these have many uses in assessing the discharge and breakdown properties. For gas laser mixtures it is useful to compute the fractional energy producing radiation of a certain wavelength (e.g. 9.6 μm to 10.6 μm radiation in CO_2-N_2-He gas mixtures by Nighan [2]). In the temporal growth of prebreakdown current the dominant mechanisms for the production of secondary electrons needs to be known (e.g. the relative numbers of ions, metastable atoms and

radiation in the breakdown of helium gas by Davies et al [3]. The swarm parameters themselves will provide valuable information concerning the growth of prebreakdown current (e.g. the $\alpha = \eta$ condition in N_2-SF_6 gas mixtures).

The majority of swarm parameters for low E/N and the corresponding set of collision cross-sections have been well documented (see Laborie et al [4]) for all gases. In recent years we have concentrated on measuring swarm parameters at high E/N. A summary of our techniques and results are given in this paper.

APPARATUS

Two apparatus have been constructed to u.h.v. standards. The first is by Lakshminarasimha et al [5] and is for steady state measurement and the second is by Saelee et al [6] and is for time of flight measurements. The apparatus are shown schematically in Figs. 3 and 4.

The steady state apparatus consisted of a fixed cathode and a movable anode made of concentric rings. The anode could be moved along the central axis with a special bellows arrangement and the gap distance could be varied between 0-10 cm and measured accurately (to 0.1 mm) using a dial gauge. The anode had a central disc of radius 0.24 cm surrounded by nine concentric annuli having radii of 0.64, 1.04, 1.44, 1.84, 2.44, 3.04, 3.64, 4.24 and 5.00 cm respectively. Nine guard rings, made of stainless steel, provided equipotentials at 1 cm intervals. The guard ring assembly together with anode and cathode was enclosed in a glass lined stainless steel vacuum chamber. The initial electrons were produced by back illumination of a palladium coated quartz disc with an ultra-violet lamp. The coated quartz disc was fitted into a groove in the cathode and a central hole of 1 mm diameter allowed the electrons to enter the discharge chamber. The anode was kept at earth potential and a negative voltage was applied to the cathode. The anode currents could be measured to an accuracy of 1% using two special electrometers having ranges of 10^{-8} - 10^{-12}A. Under all conditions the leakage currents were of the order of 10^{-15}A.

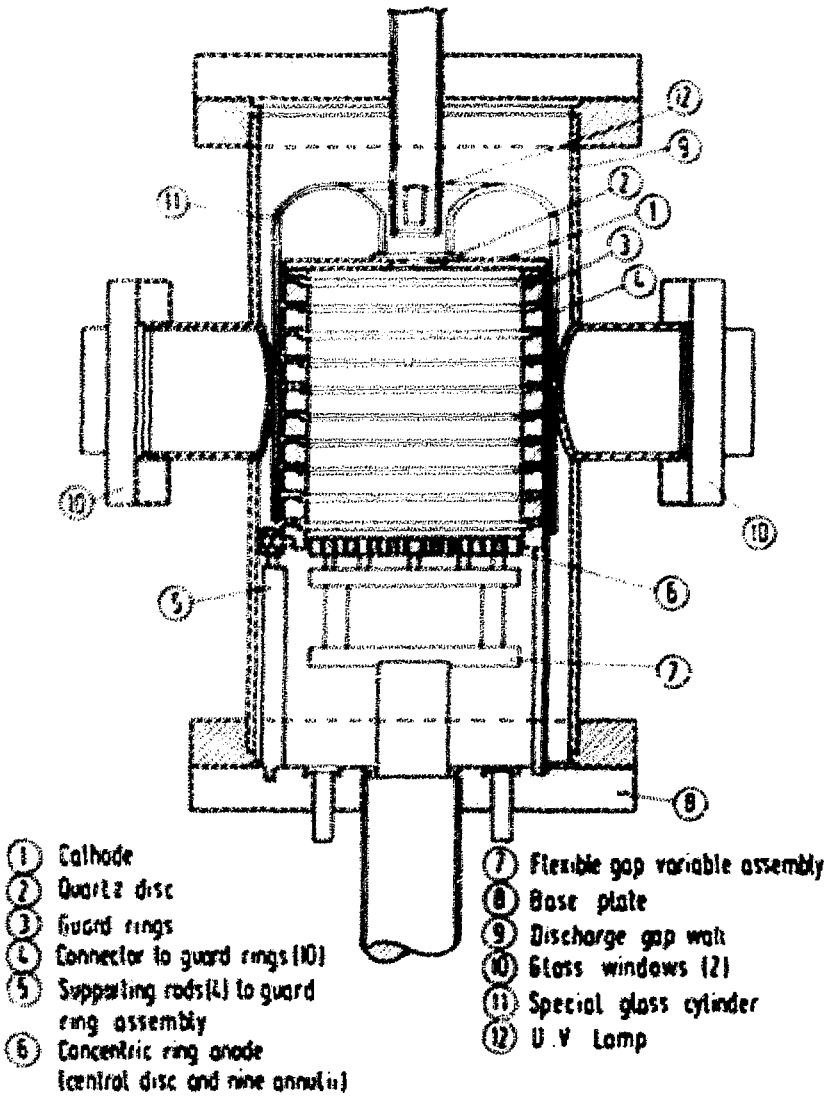

Fig. 3 The Steady State Apparatus

The time of flight apparatus was also constructed from a thick guard ring assembly to give equipotential planes at 2 cm intervals. The guard rings were made of stainless steel with an o.d. of 22 cm and an i.d. of 19.7 cm. The anode position was variable and the maxium gap separation was 20 cm. and the system had a choice of two anodes. The first anode was 16.3 cm. in diameter and was enclosed in a fine meshed screen to prevent induced charges from being recorded. The second anode had a central disc of 8cm diameter and two annuli of 18.5 cm o.d. and 19.5 cm o.d. and was unscreened and this anode was only used for radial diffusion measurements.

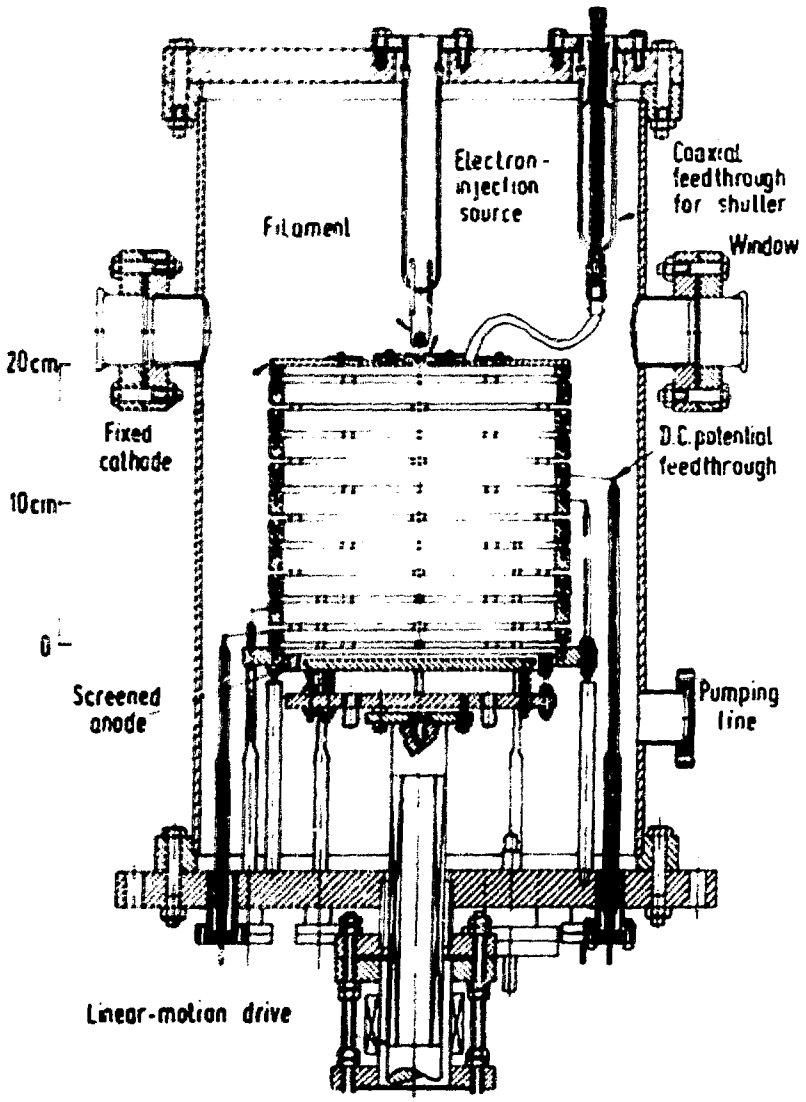

Fig. 4 The Time of Flight Apparatus

The cathode was fixed to the guard ring system and had a central hole of diameter 0.5 cm into which an electron injector source was fixed. The electron source was a heated filament and electrons were injected into the gap by applying an impulse voltage to a cone shaped grid placed between the filament and the cathode. The grid was normally biased negative with respect to the filament so that no electrons were injected into the gap unless a pulse was applied. The electrons were injected into the discharge gap for a time duration variable between 20 and 150 ns. For low E/N

(~ 50 Td) the anode current was fed into a 500 Ω resistor, and an impedance converter (100 MHz bandwidth) enabled the circuit to be matched to two 50 Ω cascaded amplifiers having a total gain of 60 dB. For high E/N (~ 300 Td) because gas amplification was present the current was directly fed into a 50 Ω amplifier with 40 db gain. The output voltage from the amplifier was then fed into a "box car" detector system to improve the signal/noise ratio. The voltage profiles were displayed on an X-Y recorder. The use of high gain amplifier (150 MHz bandwidth) required careful shielding to reduce ringing and distortion on the output profile. The anode capacitance was nominally 200 pF so that the time constant of the centre circuit was approximately 11 ns.

The vacuum chambers could be evacuated to less than 10^{-8} torr using both a trapped oil diffusion pump, backed by a rotary pump, and an ion pump. The pressure of the gas in the chamber could be measured to an accuracy of ± 3% using two MKS Baratron gauges with overlapping ranges varying from 0.01 to 1000 torr.

ANALYSIS

Experimental-Steady State

Measurements on the steady state apparatus have given values for the ionisation coefficient (α) and the ratio of radial diffusion to mobility (D_r/μ). These parameters are related to the total anode current I(d) and its radial distribution (Virr et al. [7]) such that

$$\alpha_d = \frac{\partial}{\partial d} \left\{ \ln I(d) \right\}$$

and

$$\frac{D}{\mu_d} = \frac{E}{4} \frac{\partial}{\partial d} \left\{ \overline{r^2}\,(d) \right\},$$

where d is the gap separation and E is the electric field. (α_d is the same as α_T Townsend's ionisation coefficient).

When strong ionisation and secondary electrons are present then a more detailed analysis is required (Kontoleon et al. [8]).

Experimental - Time of Flight

The drift velocity (v_d) and the ratio of longitudinal diffusion coefficient to mobility are primarily measured with the TOF apparatus (Saelee et al [6]). The mean value $\bar{T}(d)$ and the standard deviation ϵ (d) of the transit time are measured for each gap separation d. The swarm parameters are determined by

$$v_d = \left[\frac{\partial}{\partial d}\left\{\bar{T}(d)\right\}\right]^{-1}$$

and

$$\left(\frac{D_L}{\mu_d}\right) = \frac{v_d^3}{2}\frac{\partial}{\partial d}\left\{\epsilon^2(d)\right\}$$

When secondary electrons or the Penning effect are present it is advantageous to use the time of flight measurement in order to separate the fast primary electrons from the slow secondary electrons (Lakshminrasima et al. [9]). For this condition

$$\alpha_T = \frac{\partial}{\partial d}\left\{\ln N(d)\right\}$$

where

$$N(d) = \int_0^{\bar{T}+3\epsilon} I(d, t)\, dt$$

In the presence of attachment some electrons are converted into negative ions. Again the use of the TOF technique allows the fast electron current to be separated from the slow negative ion current. (Lakshminarasimha et al [9]).

Finally in the presence of secondary electrons it is advantageous to do TOF measurements of D_r/μ. This is achieved by using the unscreened anode having a central disc and annulus. The fraction F(d) of the integrated current collected by the disc allows $(D_r/\mu)_d$ to be obtained by using the Huxley [10] equation.

Theoretical Analysis

The electron motion has been simulated by using the Monte Carlo technique (Saelee and Lucas [11]). The advantage of this method is that it directly simulates the experimental procedures, measurements and analysis. It allows the electron current to be emitted as a point source and computes the amplification, the arrival times and radial spreading of the anode current for each gap separation. For each gas it is necessary to specify all the electron/gas collision cross-sections as a function of energy including the differential scattering cross-sections. The total cross-section gives the distance between collisions whilst the type of collision either elastic or inelastic collision gives the energy loss. The frequency of occurrence of all the different types of collisions are monitored during the simulation and hence we can investigate in detail any collisions of special importance.

EXPERIMENTAL RESULTS AND THEORETICAL RESULTS

The experimental and theoretical results for hydrogen are shown in Figs. 5 to 8 covering an E/N range from 1 to 2800 Td (1Td = 10^{17} V cm^2). The electron-hydrogen molecule collisions were grouped into five types namely elastic, vibration, dissociation, excitation and ionisation. The magnitude of the cross-sections and their variation with electron energy are shown in Fig. 9. The total cross-section (Q_T) is about 10% higher than that given by Golden et al.[12] for energies less than 20 eV but runs into the values given by Normand [13] at the higher energies. The vibration cross-section (Q_V) is given by Ehrhardt et al.[14], dissociation cross-section (Q_D) by Corrigan [15] and total ionisation cross-section (Q_I) by Rapp and Englander-Golden [16]. The excitation cross-section (Q_{ex}) with an onset energy of 11.4 eV is found by fitting to the swarm parameters. The elastic differential scattering cross-sections are given by Ramsauer and Kollath [17] for energies less than 5 eV and by Bullard and Massey [18] and by Webb [19] for higher energies. Fig.10 shows the percentage of energy loss due to the various collisional processes as a function of E/N.

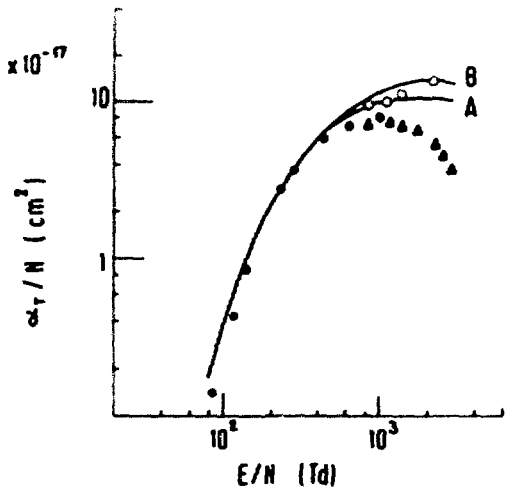

Fig. 5 The Ionisation Coefficient in Hydrogen (• Kontoleon et al.[21], ○ Golden et al.[20], △ Haydon and Stock [22])

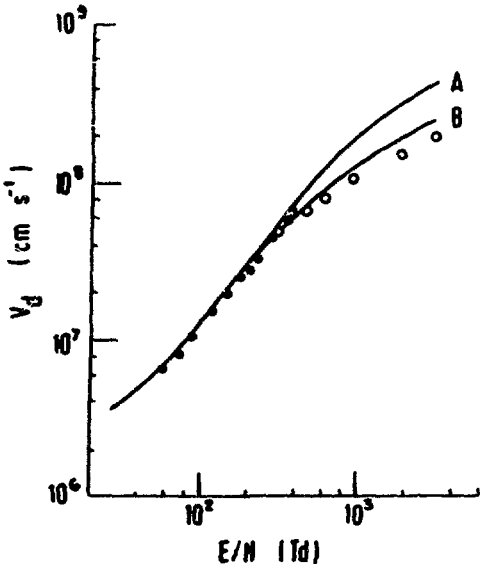

Fig. 6 The Drift Velocity in Hydrogen (• Saelee et al.[6], ○ Schlumbohm [23])

Figure 5 compares the computed to the recent experimental values of α_T/N. At present the values given by Golden et al.[20] give a better fit to the theoretical values than the results of both Kontoleon et al. [21] and Haydon and Stock [22]. The theoretical curves A and B refer to the nature of the

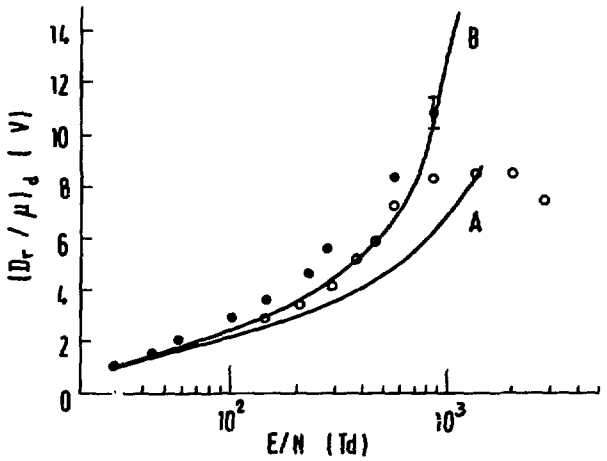

Fig. 7 The Ratio of Radial Diffusion Coefficient to Mobility in Hydrogen (• Virr et al.[7] and Kontoleon et al.[8], ○ Kucukarpaci [24])

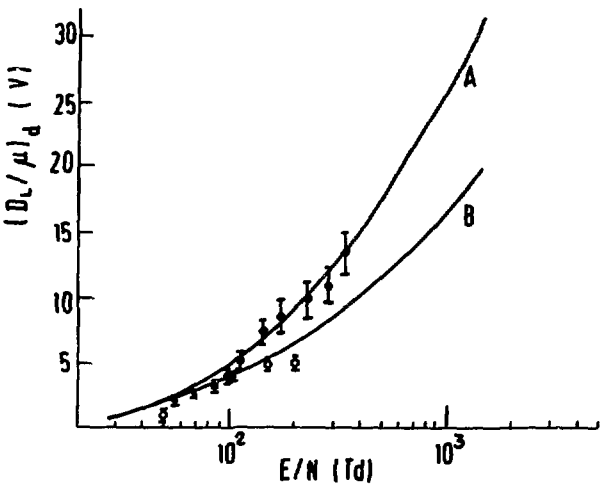

Fig. 8 The Ratio of Longitudinal Diffusion Coefficient to Mobility in Hydrogen (• Saelee et al.[6], ○ Blevin et al.[25])

inelastic differential scattering cross-sections. For curve A it is assumed to be the same as the elastic differential scattering cross-section whilst for curve B it is assumed to be isotropic.

Fig. 6 compares the computed and the experimental values of the drift velocity v_d. The results of Saelee et al.[6] give a good fit whilst the values of Schlumbohm[23] are too low.

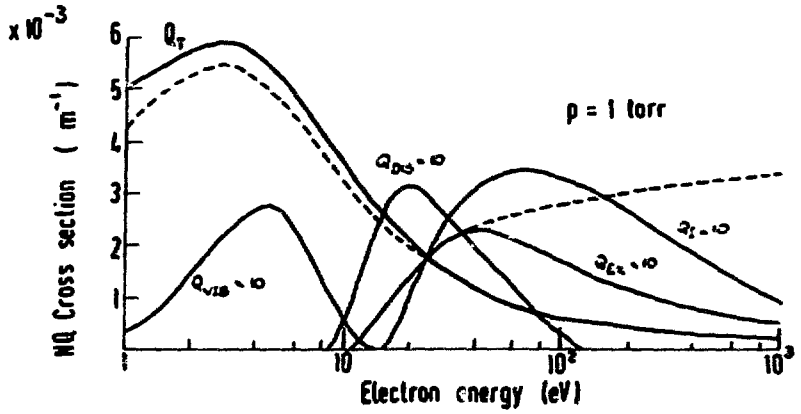

Fig. 9 The Cross-section in Hydrogen

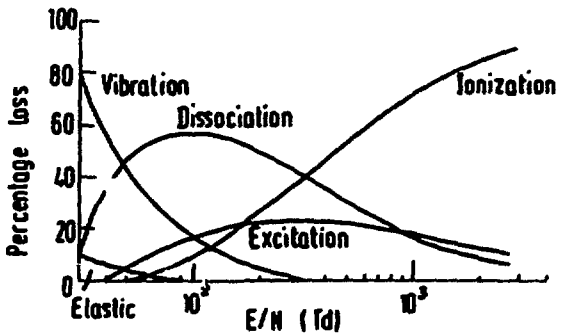

Fig. 10 Percentage Energy Losses in Hydrogen

Fig. 7 compares the computed values of $(D_r/\mu)_d$ with the steady state values of Virr et al.[7] and Kontoleon et al.[8]. A better agreement is obtained with our latest time of flight values (Kucukarpaci[24]).

Fig. 8 shows a comparison of the computed and experimental values of $(D_L/\mu)_d$. The experimental values of Saelee et al.[6] seem to agree best with the case A results whilst the values of Blevin et al.[25] lie below the case B results.

Summary of Measurements in Gases and Gas Mixtures

A summary is given in Table 1 of the experimental and theoretical measurement of swarm parameters.

Table 1 - Swarm Parameters by the Author and his Co-workers at high $\frac{E}{N}$

Gas	Experimental: α_T and $(D_r/\mu)_d$	Experimental: v_d and $(D_L/\mu)_d$	Theoretical
H_2	Virr et al [7] Kontoleon et al [8]	Snelson and Lucas [29]	Saelee and Lucas [11]
N_2	Kontoleon et al [21]	Saelee et al [6]	Limbeek [30]
CO	Lakshminarisimha et al [28]		Saelee and Lucas [11]
CO_2	Lakshminarisimha et al [28]		Limbeek [30]
He	Lakshminarisimha et al [9]	Saelee [26] and Kucukarpaci [24]	Saelee [26] and Kucukarpaci [24]
Ar	Lakshminarisimha and Lucas [27]		
Ne	Kucukarpaci [24]		
Kr			- -
O_2	Price et al [31]	- -	Lucas et al [32]
CH_4	Lakshminarasimha and Lucas [27]	Kucukarpaci [24]	- -
CF_4	Lakshminarasimha et al [9]	- -	- -
SF_6-N_2	Kucukarpaci [24]	Kucukarpaci [24]	Kucukarpaci [24]
SF_6-Ar			
SF_6-He			
CO_2-N_2-He	Lakshminarasimha et al [5]	Limbeek [30]	Limbeek [30]
Ar-Kr-NF_3	Limbeek [30]		
Hg	- -	Nakamura and Lucas [33]	Nakamura and Lucas [33]
Na			
Tl			

Metal Vapours

We have recently set up a heat pipe drift tube for the measurement of electron drift velocities. Measurements and calculations have so far been done in mercury, sodium and thallium vapours (Nakamura and Lucas [33]).

REFERENCES

1. L.S. Frost and A.V. Phelps, Phys. Rev., 127, 1621 (1962)
2. W.L. Nighan, Phys. Rev., 2, 1989 (1970).
3. D.K. Davies, F. Llewellyn Jones and C.G. Morgan, Proc. Phys. Soc., 83, 137 (1964).
4. P. Laborie, J.M. Rocard and J.A. Rees, Electronic Cross-sections and Macroscopic Coefficients, Vol. 1 and 2, Dunod, Paris, 1968, 1971.
5. C.S. Lakshminarasimha, J. Lucas, J.L. Moruzzi and I.J. Spalding, J. Phys. D, 9, 1727 (1976).
6. H.T. Saelee, J. Lucas and J.W. Limbeek, SSED-IEE, 1, 111 (1977).
7. L.E. Virr, J. Lucas and N. Kontoleon, J. Phys. D, 5, 542 (1972).
8. N. Kontoleon, J. Lucas and L.E. Virr, J. Phys. D, 5, 956 (1972).
9. C.S. Lakshminarasimha, J. Lucas and R.A. Snelson, Proc IEE, 122, 1162 (1975).
10. L.G.H. Huxley, Aust. J. Phys. 12, 171 (1959).
11. H.T. Saelee and J. Lucas, J. Phys. D, 10, 343 (1977).
12. D.E. Golden, H.W. Bandel and J.A. Salerno, Phys. Rev., 146, 40 (1966).
13. C.E. Normand, Phys. Rev., 35, 1217 (1930).
14. H. Ehrhardt, L. Langhans, F. Linder and H.S. Taylor, Phys. Rev., 173, 222 (1968).

15. S.J.B. Corrigan, J. Chem. Phys., 43, 4381 (1965).

16. D. Rapp and P. Englander-Golden, J. Chem. Phys., 43, 1464 (1965).

17. C. Ramsauer and R. Kollath, Ann. Physik, 12, 529 (1932).

18. E.C. Bullard and H.S.W. Massey, Proc. Roy. Soc., A133, 637 (1932).

19. G.M. Webb, Phys. Rev., 47, 384 (1935).

20. D.E. Golden, H. Nakano and L.H. Fisher, Phys. Rev., A138, 1613 (1965).

21. N. Kontoleon, J. Lucas and L.E. Virr, J. Phys. D, 6, 1237 (1973)

22. S.C. Haydon and H.M.P. Stock, Aust. J. Phys., 19, 795 (1966).

23. H. Schlumbohm, Z. Physik, 182, 317 (1965).

24. N. Kucukarpaci, M.Eng. Thesis, Liverpool University (1987).

25. H.A. Blevin, J. Fletcher and S.R. Hunter, J. Phys. D, 9, 1671 (1976).

26. H.T. Saelee, Ph.D. Thesis, Liverpool University (1976).

27. C.S. Lakshminarasimha and J. Lucas, J. Phys. D, 10, 313 (1977).

28. C.S. Lakshminarasimha, J. Lucas and N. Kontoleon, J. Phys. D., 7, 2545 (1974).

29. R.A. Snelson and J. Lucas, Proc IEE, 122, 333 (1975)

30. J.W. Limbeek, Ph.D. Thesis, Liverpool University (1978).

31. D.A. Price, J. Lucas and J.L. Moruzzi, J. Phys. D., 5, 1249 (1972)

32. J. Lucas, D.A. Price and J.L. Moruzzi, J. Phys. D., 6, 1503, (1973).

33. Y. Nakamura and J. Lucas, J. Phys. D., (accepted for publication).

DISCUSSION

PHELPS: In your high E/N experiments, has the electron energy distribution reached steady state in a distance that is short compared to the electrode separation?

LUCAS: The electron swarm has to travel an effective distance d_o across the gap before the electron energy distribution stabilizes. All our experimental techniques use a difference technique to eliminate this nonequilibrium region. This means that we effectively measure the equilibrium values for the swarm coefficients. Our Monte Carlo simulation indicates to us the probable value of d_o to be expected in our experiments and, therefore, guides us to the minimum voltage which we may use in our experimental measurements. The limit of our investigation is about E/N $\sim$3000 Td for which $Ed_o \sim V_B/3$ where V_B is the breakdown voltage.

CHRISTOPHOROU: 1. Are the cross sections designated "dissociation" on your slide on H_2 referring to dissociative ionization or to dissociation into neutrals or both? 2. Can your treatment be successfully extended to polyatomic gases and polyatomic gas mixtures with some hope of success? Presently there seems to be no basic electron transport data on polyatomic gas mixtures.

LUCAS: 1. The dissociation cross section is by S. J. B. Conigan, J. Chem. Phys. 43, 4381-6 (1965). The cross section for dissociative ionization is by D. Rapp, P. Englander-Golden, and D. D. Briglia, J.

Chem. Phys. 42, 4081-5 (1965) and this has been lumped into the ionization cross section for the cross-section plot. In the Monte Carlo simulation, it is treated separately because of the extra energy loss incurred.

2. Polyatomic gases do not have their cross sections well tabulated or known. A simple method of obtaining the electron energy distribution by computation has been used by Lucas, et al., for hydrogen and for oxygen, Int. J. Elec., 27, 201-20 (1969) and J. Phys. D, 6, 1503-13 (1973). This method uses three swarm parameters and up to three cross sections, e.g., α, v, D_r/μ with Q_m, Q_i for hydrogen, α or η, v, D_r/μ with Q_m, Q_η, Q_i for oxygen. You may find this method useful in mixtures whose cross sections are not well tabulated since momentum, ionization and attachment cross sections are usually the first to be measured in gases.

DAKIN: Does your curve indicating that the mean energy of the electrons is reached only after a voltage drop of 300 V indicate a limitation on the use of mean electron energies in calculating multiplication and breakdown in nonuniform electric fields?

LUCAS: As E/N increases, the electron swarm has to travel across larger voltages before it attains its equilibrium energy distribution. For E/N $\sim$3000 Td the Monte Carlo simulation indicates that the swarm only attains equilibrium after passing across 150V but maintains this equilibrium state until the breakdown voltage is obtained at $\sim$360V. In nonuniform fields this result means that the electron energy distribution may not correspond to the local value of E/N for these high values. It is better to investigate these nonuniform electric field

cases individually using the Monte Carlo simulation and the set of cross sections given in the paper. The main advantage of a Monte Carlo simulation is that it is able to exactly simulate the experimental geometry and conditions.

DUTTON: 1. On the question of whether a steady state is attained at high E/N, how do your conclusions agree with those of Haydon using the Gosseries method of analyzing spatial growth? 2. What is the accuracy of the measurements at high E/N and is it sufficient to distinguish between the theoretical curves you showed?

LUCAS: 1. The question of equilibrium is discussed in the paper by H. T. Saelee and J. Lucas, J. Phys. D 10, 343-54 (1977). For E/N = 1412 Td it seems possible to define an α coefficient although the swarm mean energy varies across the discharge gap for all voltages up to and including breakdown. However, the secondary electron coefficient varies with the gap voltage when produced by swarm radiation reaching the cathode. For these reasons I think it is important to measure α by using a time of flight technique in order to avoid the generation of secondary electrons rather than use a steady state measurement of pre-breakdown current. The method of Haydon uses a steady state technique but has made the assumption of constant secondary electron coefficient and this seems in doubt. The Gosseries plot is useful for eliminating "d_o" effects but careful use of Townsend's three-point method will give the same analytical result.

To understand why the mean energy varies across the gap while α remains constant requires us to solve Boltzmann's equation. Such a solution was presented in Int. J. Elec. 29, 465-77 (1970) and explains

the result.

2. The accuracy of computation and measurement is ·5% which is much less than the difference between the two computed curves marked A and B at the highest E/N. Therefore it should be possible to state which theoretical conditions appear to be the better.

THE ROLE OF NEUTRAL DENSITY VARIATIONS IN THE FORMATION OF STREAMER INDUCED SPARK

E.Marode F.Bastien

G.Berger M.Goldman

Laboratoire de physique des décharges
E.S.E. - C.N.R.S. équipe n° 114
Plateau du Moulon,91190 GIF SUR YVETTE, FRANCE

ABSTRACT

The breakdown of a small positive point-to-plane gap in electronegative mixtures near atmospheric pressure begins with the formation of a low conductivity filament by the space charge controlled streamer process. Within this filament, the rate of electron attachment exceeds the ionization rate and the external current decreases. However in spite of this attachment process, a sudden unexplained rise of current is observed leading to the transient spark which cannot be explained by negative ion detachment.

A new process is proposed. The current flowing through the filament leads to an enhancement of temperature and pressure, and the tendency of this excess pressure to relax quickly to the normal external pressure produces a decrease of density in the core of the filament which then leads to an increase of density at the discharge boundary. Within the core, E/N increases until the ionization rate becomes greater than that of attachment, leading to the final current growth. This model is supported by theoretical calculations, solving hydrodynamic and electrical equations together. For this model to be correct, then a sound wave should be launched from the filament boundary by the increase of neutral density. By means of a fast schlieren photography technique, the existence of a cylindrical wave around the filament has been shown.

The ionization growth processes leading to spark breakdown have been thoroughly investigated for many years. Two main processes have been proposed in order to explain the initial phase of the developing discharge: namely a generalized Townsend process involving electrode secondary effects or a local space charge controlled growth called streamer process [1] [2]. After this initial phase the space charge in general leads to a further discharge development in a filamentary form [3] [4] [5] . The complexity of this glow-like phase, however, is such that it is difficult to obtain clear information on the ionization processes. However in the subsequent stage whenever the electron density reaches approximately $10^{17} cm^{-3}$ the discharge state is close to L.T.E. and the situation can then be more clearly analysed [6] [7] . The problem remains to understand the ionizing process which allows this critical value of electron density to be reached during the glow-like phase, especially for the case of electronegative gases where electrons are removed by negative ion formation. Recently an explanation for small air gaps has been suggested which uses electron heating waves [8] . In this paper we propose an alternative explanation based on the dynamics of neutral species [9] and experimental confirmation of this point of view will be presented [10]. This investigation has been developed in order to study the streamer induced spark breakdown of $\simeq$ 1 cm positive point-to-plane gap in air at atmospheric pressure. However the proposed process may also hold for a wide range of geometries and gas compositions. It may further be of help in the understanding of laser instabilities since overvolted gaps often lead to a streamer controlled development of the discharge.

PROPOSED PROCESS

The present interpretation of the streamer induced spark formation in air at atmospheric pressure may be followed by means of the schematic drawing of figure 1 . Launched from the positive point towards the plane at high speed ($\simeq 10^8$ cm/s), the streamer creates an ionized track which finally bridges the entire gap with the formation of a cathode fall region at the cathode. At all stages of its development the discharge is similar to a glow discharge with a small high-field

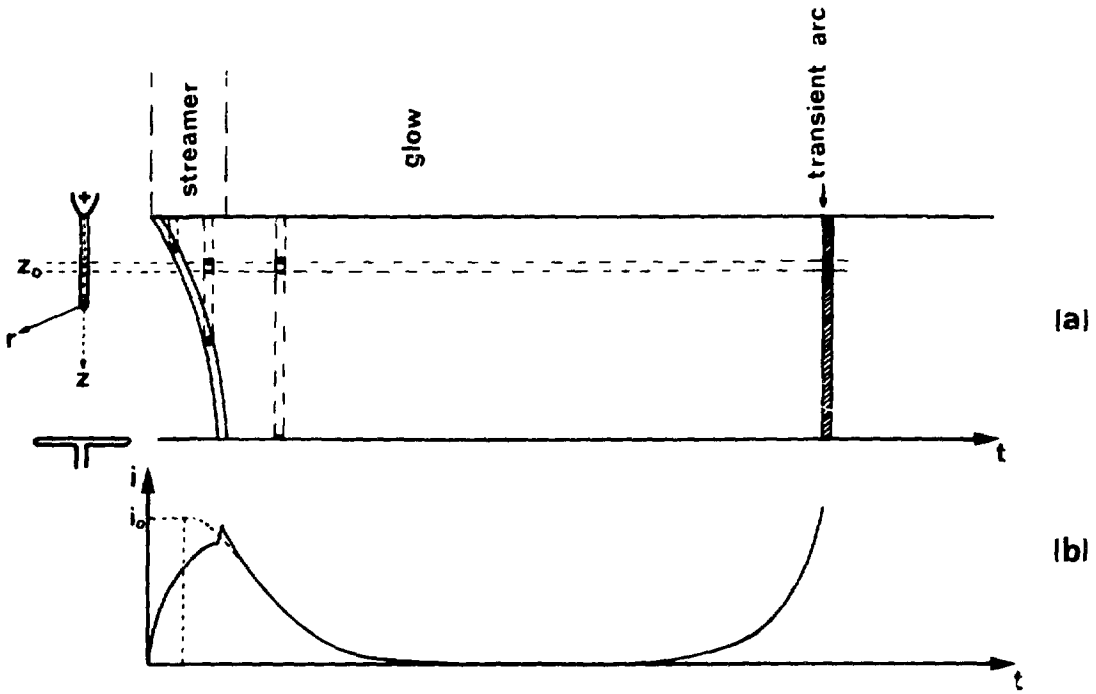

Fig. 1. a)Main sequences of the discharge
b)Discharge current measured at the point (——);
current flowing in the discharge at z_o (----)

region followed by a filamentary positive column. Within this positive column the small value of the field leads to an attachment rate higher than the ionization rate so that the discharge current decreases [5] . However, in spite of the presumed high attachment rate, this decrease may be followed by a rise in current leading to spark, if the current pulse associated to the streamer phase is large enough. Detachment of negative ions could be invoked as an explanation for this last current rise; but even if all the negative ions detach , the free electrons could not give a current higher than before attachment.

Actually, from a study based on Stark broadening of hydrogen lines, it has been possible to measure the current densities and discharge radius within the filament [11] :this led to the present proposal of another more effective process explaining the final ionization growth. In spite of the small heating of heavy species by electrons,a weak but substantial increase of the temperature of neutral species can occur which raises the pressure. The dynamics of neutral species will lead to a decrease in

this pressure so that the neutral density within the discharge region will also decrease. In turn the ratio of field strength to neutral density E/N will increase and if it reaches the critical value where the ionization coefficient α begins to surpass the apparent attachment coefficient η a new and final growth of ionization will occur leading to spark formation.

HYDRODYNAMIC EQUATIONS

In order to test the above hypothesis, hydrodynamic equations for neutral species together with those which apply to charged species have been written and solved. Only a small section located at a given distance z_o from the point (figure 1) need be analysed assuming, for the moment, that axial variations are negligible. It can be seen that a current will only flow through the section of interest after the streamer has reached z_o. The initial value i_o of the current through z_o can be estimated and is an initial condition for the solving of the problem. The hydrodynamic equations which describe the dynamics of neutral species, i.e., the continuity, momentum transfer and energy transfer equations respectively eq(1), (2) and (3) are given below:

$$\frac{\partial N}{\partial t} + \frac{1}{r}\frac{\partial}{\partial r}(rNV) = 0 \tag{1}$$

$$\frac{\partial (NV)}{\partial t} + \frac{1}{r}\frac{\partial}{\partial r}(rNV^2) + \frac{1}{m}\frac{\partial}{\partial r}(NkT) = \frac{1}{m}(A_{c+} + A_{cn}) \tag{2}$$

$$\frac{3}{2}\frac{\partial}{\partial t}(NkT) + \frac{3}{2}\frac{1}{r}\frac{\partial}{\partial r}(rNkT) + \frac{NkT}{r}\frac{\partial}{\partial r}(rV) + \frac{\lambda}{r}\frac{\partial}{\partial r}\left(r\frac{\partial T}{\partial r}\right) = M_c - (A_{c+} + A_{cn})V \tag{3}$$

where N, V, T are respectively the neutral density, the neutral radial velocity and the neutral temperature, m is the mass of neutral species, λ is the thermal conductivity, k is the Boltzmann constant, M_c , A_{c+}, A_{cn} are respectively the energy and momentum release from charged species to neutral species (A_{c+} and A_{cn} referring to positive and negative ions). The continuity equations for charged species are:

$$\frac{\partial n_e}{\partial t} + \frac{1}{r}\frac{\partial}{\partial r}(n_e V_e) = (\alpha - \eta) n_e \mu_e E_z - a_e n_e n_+ \tag{4}$$

$$\frac{\partial n_n}{\partial t} + \frac{1}{r}\frac{\partial}{\partial r}(n_n V_n) = n_e \mu_e E_z - a_i \left(\frac{T_o}{T}\right)^{2.5} n_n n_+ \tag{5}$$

where n_e , n_n are electron and negative ion densities, V_e ,V_n electron and negative ions radial velocities; α , η are the coefficients of ionization and apparent attachment (taking detachment into account); μ_e ,μ_n are the electron and negative ion mobilities; E_z is the axial field at z_o; a_e ,a_i are the two body electron-ion and ion-ion recombination coefficients with T_o=300 K. Assuming neutrality the positive ion density n_+ is given by:

$$n_+ = n_e + n_n \tag{6}$$

Using the momentum transfer equation for electron, to express the radial electrical field, the momentum transfer equations for positive and negative ions are found to be:

$$\frac{\partial}{\partial t}(n_+V_+) + \frac{1}{r}\frac{\partial}{\partial r}(rn_+V_+^2) + \frac{kT}{m}\left\{1 + \frac{T_e n_+}{T\, n_e}\frac{\partial n_e}{\partial r}\left(\frac{\partial n_+}{\partial r}\right)^{-1}\right\}\frac{\partial n_+}{\partial r} + \frac{k}{m}n_+\frac{\partial T_e}{\partial r} = -\frac{1}{m}A_{c+} \tag{7}$$

$$\frac{\partial}{\partial t}(n_nV_n) + \frac{1}{r}\frac{\partial}{\partial r}(rn_nV_n^2) + \frac{kT}{m}\left\{1 - \frac{T_e n_n}{T\, n_e}\frac{\partial n_e}{\partial r}\left(\frac{\partial n_n}{\partial r}\right)^{-1}\right\}\frac{\partial n_n}{\partial r} - \frac{k}{m}n_n\frac{\partial T_e}{\partial r} = -\frac{1}{m}A_{cn} \tag{8}$$

where T_e is the electron temperature.

From the continuity equation of charged species togetner with the equation of neutrality one obtains:

$$n_+V_+ = n_eV_e + n_nV_n \tag{9}$$

which means that no radial current flows out of the discharge.

Energy transfer equations for charged species are avoided by assuming thatthe temperature of the positive and negative ions is equal to that of neutral species and by assuming that the radial electron temperature is independent of time and given by eq (10) with $kT_{eo} \simeq 1.4$ eV [5]:

$$T_e(r) = T_{eo}\, e^{-\left(\frac{r}{r_o}\right)^2} + T_o \tag{10}$$

Eq. (10) expresses approximately the temperature equilibium appearing when the boundaries are defined as cold walls, r_o being a typical discharge radius. The collision terms are:

$$A_{c+} = \frac{kT}{D_+}n_+\,(V_+ - V) \tag{11}$$

$$A_{cn} = \frac{kT}{D_+}n_n\,(V_n - V) \tag{12}$$

$$M_c = (f_e j_e + f_n j_n + f_+ j_+) E_z \qquad (13)$$

where D_+ is the positive ion diffusion coefficient (assumed to be the same for negative ion); f_e , f_n , f_+ are the fractional energy loss of electron, positive and negative ion released as heat. Obviously $f_n = f_+ = 1$, while f_e is estimated to be of the order of 5.10^{-3} if electron elastic collisions and rotational deexcitation of nitrogen molecules excited by electron collisions are taken into account. The current densities are given by:

$$j_e = e\, n_e\, \mu_e\, E_z \quad j_n = e\, n_n\, \mu_n\, E_z \quad j_+ = e\, n_+\, \mu_+\, E_z \qquad (14)$$

It is interesting to note that initially $n_e = n_+$ and $n_n = 0$. Multiplying eq. (7) by $D_+ m/kT$ the third term of this equation becomes $D_+(1 + T_e/T)\, \partial n_+/\partial r = D_a\, \partial n_+/\partial r$ showing that ambipolar diffusion (D_a) controls partially the radial charged velocities.

The main assumption allowing closure of this set of equations is that the axial field E_z is constant in space and time. This is acceptable for small gaps [5] but may be an oversimplification for long gaps, where space charge redistribution can affect significantly the local field.

RESULTS

Normal neutral gas density and temperature, no radial neutral gas velocity and a Gaussian electron density distribution (consistent with a streamer formation of the filamentary discharge[12]) are taken as initial conditions. A value of E_z = 22kV/cm is chosen for the electric field, as it corresponds to the maximum axial field within the filament prior to breakdown [5] and from previous results [11] the radius of the filament is taken to be $r_o = 9.10^{-6}$m . The computed current (fig.2) shows a behaviour similar to that observed experimentally (fig.1): if the initial value of current i_o is too low, only a decrease of current is computed, whereas if i_o is above a critical value a current increase appears after the decrease of current while a further increase of i_o gives an earlier rise in current. Figs.3, 4 and 5 show the

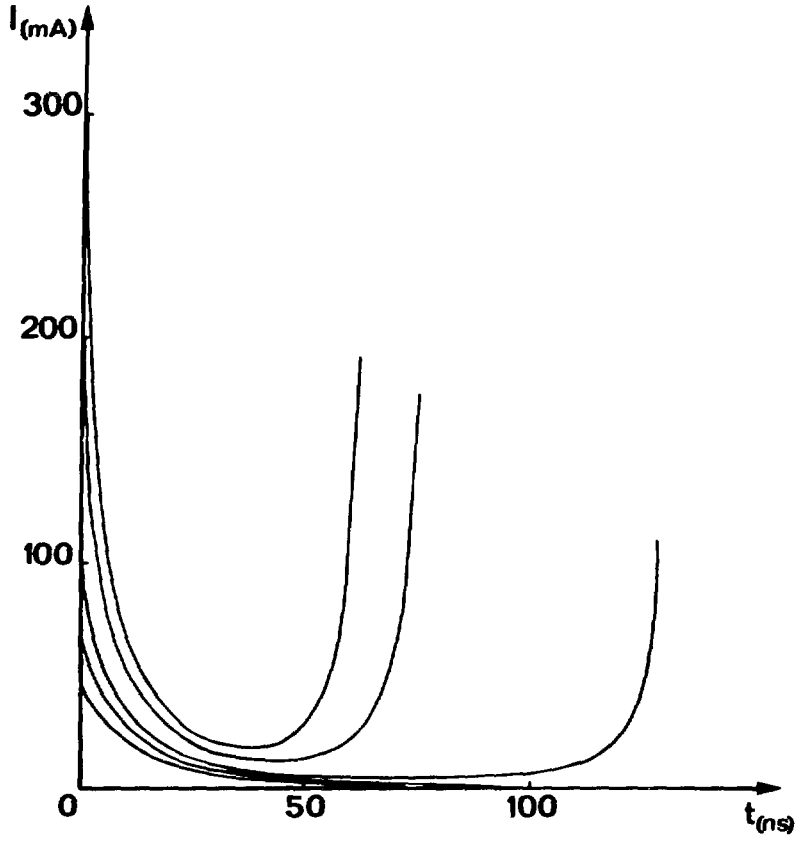

Fig. 2. Calculated current for different values of initial current

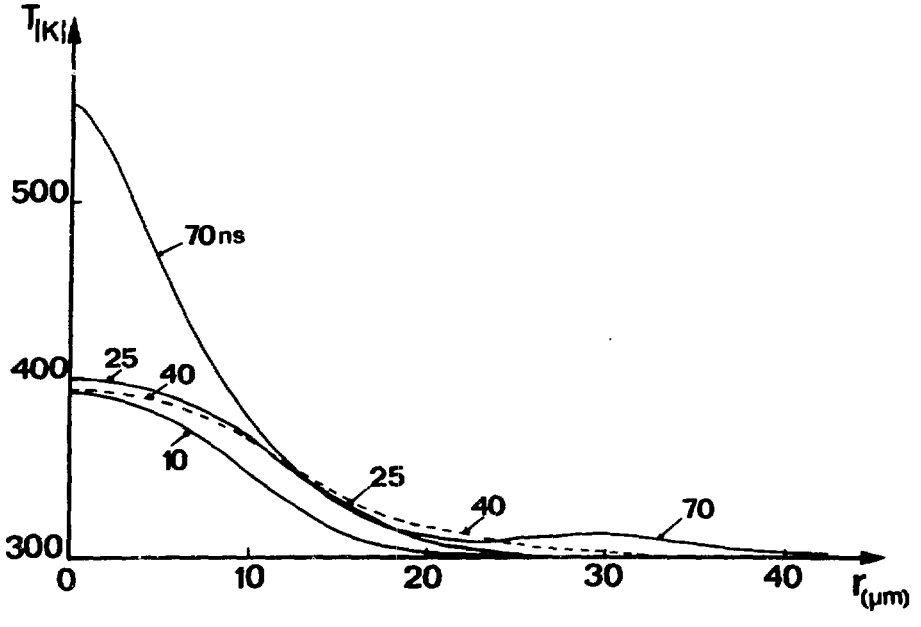

Fig. 3. Theoretical radial distribution of the temperature at different times (ns)

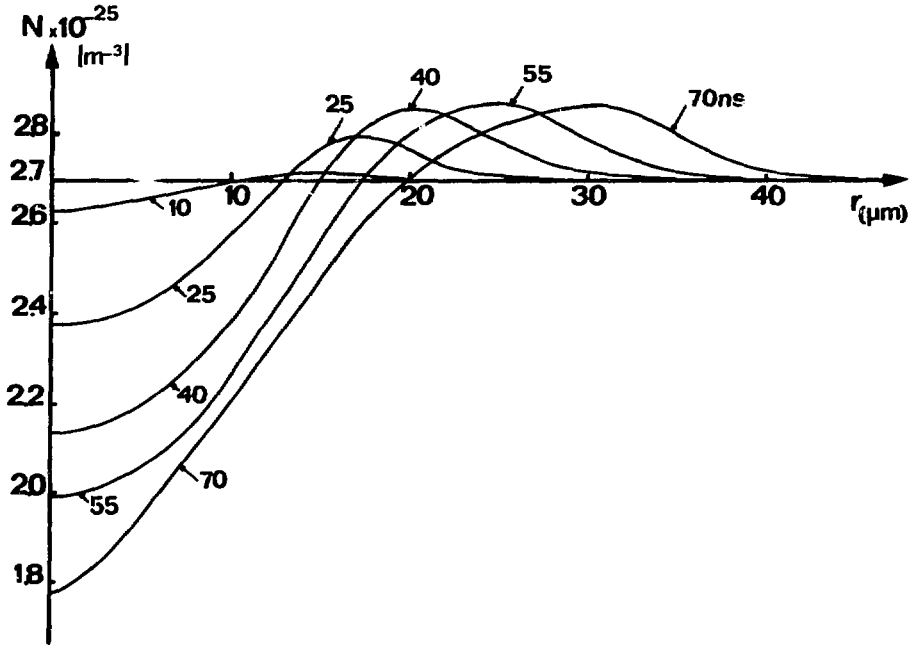

Fig. 4. Theoretical radial distribution of the neutral species density at different times (ns)

radial distribution of the heavy particle temperature, the neutral density and ($\alpha - r_i$), at various times, for the case of i_o = 200 mA. Three stages can be distinguished, the first one lasting from time zero to about 30 ns during which mainly attachment is occuring in the filamentary channel, but the energy transfer from ions to neutral particles induces a rise of temperature within the discharge . This increases the radial neutral velocity which in turn leads to a decrease in the neutral density near the axis of the filament . This decrease of density is of course balanced by an increase of density near the discharge boundary. These results show that the discharge evolves under conditions of neither constant volume or constant pressure. In the second stage, ionization becomes greater than attachment near the discharge axis . However for $t < 40$ ns attachment near the boundary remains high and the total current continues to decrease. The third stage corresponds to the final increase of current; the fall in density is now more pronounced and the ionization in the centre much more important. This leads to the rapid increase in temperature and to an electron density distribution which is no longer

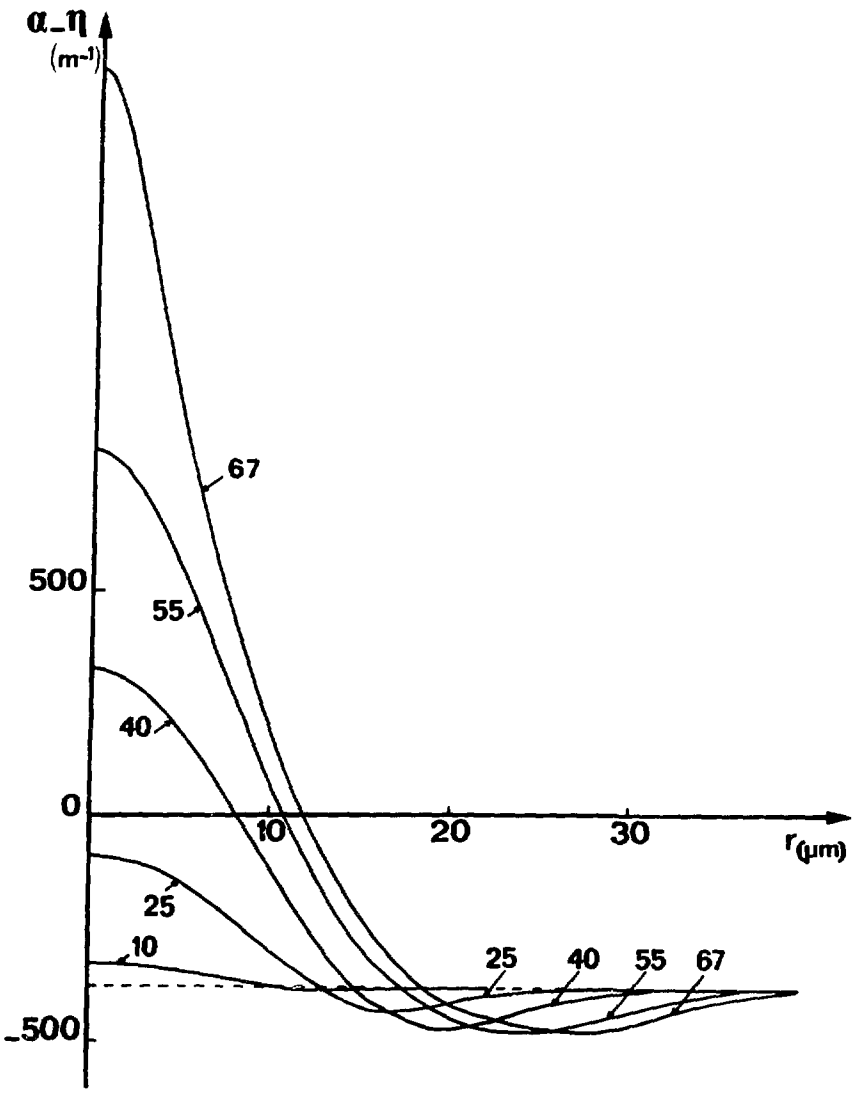

Fig. 5. Theoretical radial distribution of (α - η) at different times(ns). α :electron multiplication coefficient.
η : apparent electron attachment coefficient

Gaussian.At this stage the equation used ceases to be valid because L.T.E. appears and the Saha equation for ionization must be employed.

EXPERIMENTAL CONFIRMATION

The above model predicts a variation of the neutral gas density. To test this prediction a high speed schlieren technique has been employed whereby density variation is detected by a change in the light intensity of a given region in and around the discharge [10]. Using a single pass schlieren system having a light source of 350 watts,

and a high-gain photomultiplier, the discharge of a 1.5 cm point to plane gap has been observed, with $i_o \simeq 150$ mA. Fig. 6a reproduces schematically the photomultiplier pulse associated with the observation of a point on the discharge axis (spatial resolution is about 0.1 mm) . The first peak however corresponds to the light emitted by the discharge itself namely the streamer pulse. It can be seen that the shape of the photomultiplier pulse clearly resembles that predicted theoretically (Fig. 7). As well as a decrease of neutral gas density on the axis the model also predicts that a density perturbation is launched from the discharge boundary with a velocity of 350 m/s (Fig.4) . According to this, through a wide slit sighting an observed region of $2.5\ 10^{-4}$ m situated off axis a pulse of about 10^{-6}s should be obtained. Fig. 8 shows that the observation is in fair agreement with the prediction. Moreover changing the delay of the detected pulse by moving the slit permits to measure a velocity close to 350 m/s.

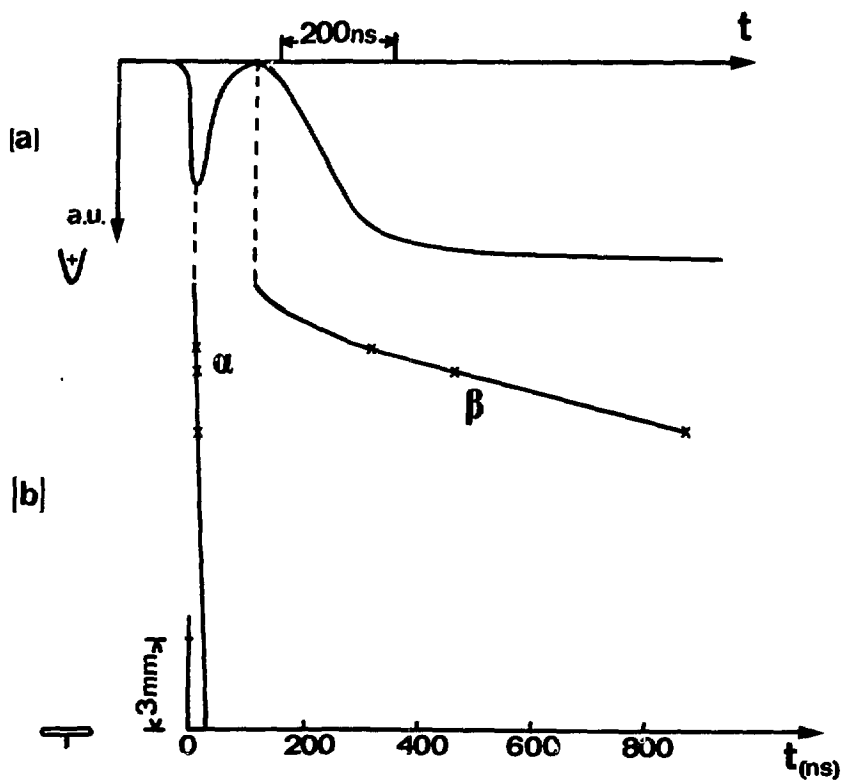

Fig. 6. a)Smoothed photomultiplier signal of the schlieren image for a point on the discharge axis
b)Time resolved sketch of the streamer progression (α) compared to the schlieren disturbance (β) off the discharge axis.

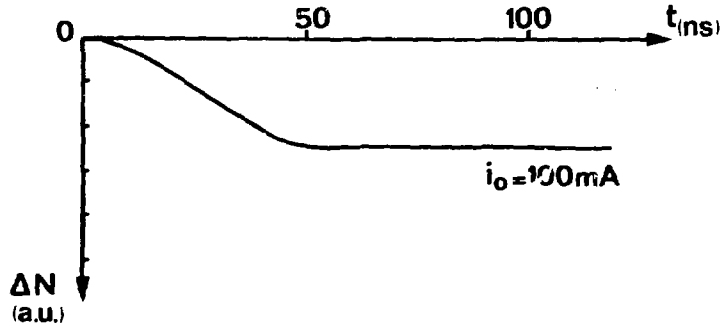

Fig. 7. Theoretical time variations in the neutral density for a point on the discharge axis.

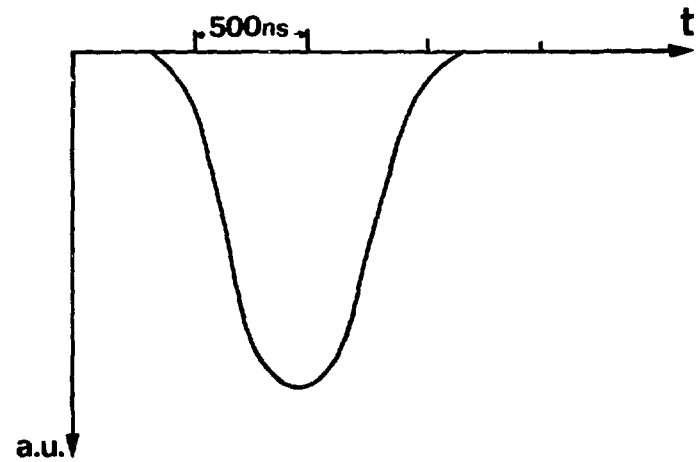

Fig. 8. Smoothed photomultiplier pulse for a point of the schlieren image off the discharge axis.

Some indication for a variation of the neutral gas density distribution in the z axis has been obtained using the schlieren technique. Fig. 8 shows that the neutral density variations on the discharge axis appear with a delay which increases with the distance from the positive point.

CONCLUSION

This paper is not the first to propose neutral density variations within a discharge. Obviously variations exist during the final breakdown phase [7], or during the spark breakdown itself where a shock wave is formed [6]. In long air gaps streamer discharges can form the so-called "leader" stage which has a longer life time than the discharge analysed in this paper. This leader stage evaluates rather under constant pressure and also exhibits neutral density variations as was recently shown [13].

However in this paper it is suggested that neutral variations play a fundamental role at a much earlier stage than indicated in the above papers. More precisely it is proposed that, as far as the spark

formation is concerned, the role of streamer and glow phase is not so much to increase the charged paricle concentration as to create something like a hole in the gas medium in which conditions for the final current rise are fulfilled.

REFERENCES

1. H.Raether,Electron avalanches and breakdown in gases,Butterworths, London(1964)
2. L.B.Loeb, Electrical Coronas, University of California press(1965)
3. A.Doran,Z.Phys.,208,427 (1968)
4. K.H.Wagner,Z.Phys.,189,465 (1966)
   Z.Phys.,204,177 (1967)
5. E.Marode,J.Appl.Phys.,5,2005 and 2016 (1975)
6. A.Tholl,Z.Naturforsch.,25a,420 (1970)
7. G.Rogoff,Phys.Fluids,15,1931 (1972)
8. E.Barreto,H.Jurenka and S.I.Reynolds,J.Appl.Phys.,48,4510 (1977)
9. E.Marode,F.Bastien and M.Bakker,30th Gaseous Electronics Conf.,Palo-Alto (U.S.A.),Abstracs,p109 (1977);paper to be published
10. G.Berger,G.Dastarac and A.Gibert,13th C.I.P.I.G.,East Berlin,547 (1977)
11. F.Bastien and E.Marode,J.Q.S.R.T.,17,453 (1977)
    J.Phys.Appliquée,12,1121 (1977)
    paper to be published
    F.Bastien,Thesis no 1871,Université Paris-sud (1977)
12. I.Gallimberti,J.Phys.D,5,2179 (1972)
13. I.Gallimberti,The characteristics of the leader channel in long spark,World Electrotechnical Cong.,Moscow (1977)

DISCUSSION

PHELPS: In your experiment, how were you able to distinguish between an increase in electron density and a decrease in neutral atom density? We have concluded theoretically that on axis we saw an increase in electron density.

BASTIEN: From schielren technique it is not possible to distinguish between an increase in electron density and a decrease in neutral density. I think that the neutral density variation is the most important factor especially off the axis, but a precise evaluation is necessary.

BREAKDOWN IN SF_6 AND ITS MIXTURES IN UNIFORM AND NONUNIFORM FIELDS

O. Farish
Department of Electrical Engineering, University of Strathclyde, United Kingdom

ABSTRACT

There is increasing interest in the dielectric properties of electron-attaching gases and particularly in those of SF_6 and mixtures containing SF_6. While breakdown of compressed attaching gases in reasonably uniform fields is fairly well understood, there is less information about the processes active in nonuniform-field configurations for which flashover may be preceded by a corona discharge. The paper reviews briefly recent work on breakdown in SF_6 and its mixtures in both uniform and nonuniform fields. The effects of such parameters as gas pressure, field non-uniformity, gas composition, electrode-surface roughness, gas flow, polarity and voltage waveform are discussed and illustrated mainly by experimental results obtained in our laboratory. For uniform fields, breakdown below the similarity-law value can be explained if ionisation near electrode microprotrusions is considered: there are indications that certain mixtures might have advantages over SF_6, but accurate prediction of their properties requires more information on swarm coefficients. With nonuniform fields, breakdown is corona-free only above a critical pressure p_c which seems to be related to the length of the ionisation zone relative to the free path for photoionising radiation. At lower pressures breakdown is corona-controlled and is strongly affected by gas composition, voltage waveform and gas flow. There is a need for further work on the relationship between quasiuniform-field and nonuniform-field breakdown.

INTRODUCTION

Sulphur hexafluoride is extensively used in high-voltage apparatus because of its excellent dielectric and heat-transfer properties. Under 'ideal' conditions of nearly uniform fields and smooth electrodes, its breakdown strength is about 2.5 times that of air, a property which is due to the strong electron affinity of the SF_6 molecule. Thus, the pressure-reduced ionisation coefficient (α/p) exceeds that for electron

attachment (η/p) only for values of the reduced field (E/p) greater than ~89 kV/cm: * the net ionisation coefficient $\bar{\alpha}$ in SF_6 is well represented, at least over the range $67 \leq E/p \leq 150$ kV/cm bar,[1] by the linear relationship

$$\bar{\alpha}/p = A(E/p) - B \qquad (1)$$

where $A = 27.8\ kV^{-1}$ and $B = 2460(\text{bar cm})^{-1}$. For perfectly uniform fields, the criterion for gas breakdown may be expressed as[2]

$$\bar{\alpha}d = k \qquad (2)$$

where d is the electrode spacing and k a constant, irrespective of whether the breakdown mechanism considered is a Townsend multiavalanche process or a streamer process involving breakdown initiated by a single electron avalanche. In the former case, $k = \bar{\alpha}/\gamma\alpha$, where γ is the secondary ionisation coefficient, and in the latter $k = \ln(N_{crit})$ where $N_{crit} = \exp(\bar{\alpha}d)$ is the electron multiplication required for streamer formation. For nonuniform fields, the Townsend equation becomes

$$\gamma \int_0^d \exp\left[\int_0^x \bar{\alpha}\,(x)\,dx\right] \alpha\,dx = 1 \qquad (3)$$

Pedersen[2] has shown that, for SF_6, the corresponding streamer criterion is

$$\int_0^x \bar{\alpha}\,dx = k \qquad (4)$$

and that this may be more applicable to many practical conditions than Eq. (3). Experimental studies have shown that the breakdown-voltage characteristics are strongly dependent on the degree of nonuniformity of the field, the polarity of the highly-stressed electrode, and the voltage waveform. For highly nonuniform fields Eq.(3) and Eq.(4) may give only the corona-onset voltage and breakdown will then be determined by corona space-charge effects. Breakdown under impulse conditions is further complicated by statistical time-lag effects and, in nonuniform fields, by factors governing the propagation of the streamer and leader discharges.

This paper is concerned with recent studies of breakdown characteristics in SF_6 and its mixtures. The section below on uniform-field breakdown is intended to include the case of quasiuniform fields in which corona does not occur before breakdown, while the nonuniform-field section deals only with breakdown in highly-divergent fields.

---

*In this paper, pressures are referred to 20°C.

BREAKDOWN IN UNIFORM FIELDS

Low-Pressure Studies

In SF_6, where $\bar{\alpha}/p$ is given by the linear relationship of Eq. (1), there is a limiting value of E/p for which $\bar{\alpha}/p = 0$ and below which breakdown should not occur. Several investigators have reported measurements of the static breakdown voltage V_s for SF_6 in uniform fields[3-6]. Figure 1 shows the results of Chalmers and Tedford[4] for pressures up to 2 bar. For pressures less than 1 bar, there is a range of spacings over which Paschen's Law is obeyed and V_s is a function of the product pd (pressure x spacing), with the breakdown value of E/p tending to a limiting value $(E/p)_{lim}$ of 88.4 kV/bar cm. At the larger spacings the apparent value of E/p at breakdown falls below $(E/p)_{lim}$; this has been shown[4,7] to be due to the phenomenon of edge breakdown, which results from enhancement of the field near the curved part of the uniform-field electrode. The increase with pressure in E/p indicated in figure 1 for pressures above 1 bar has been shown by Crichton and

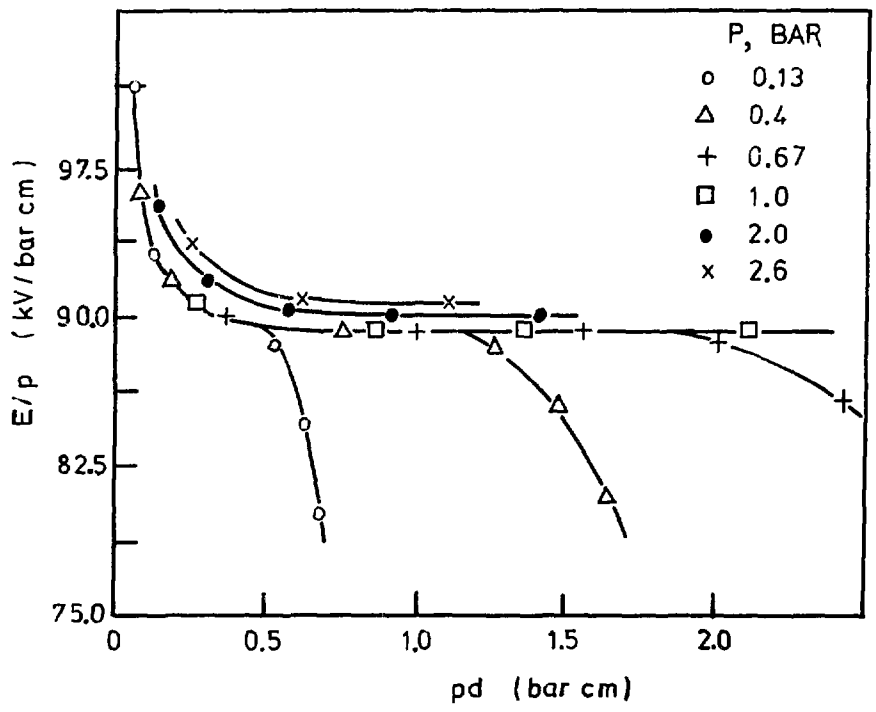

Fig. 1. E/p at breakdown against pd in SF_6.

Tedford[8] to be caused by non-ideal behaviour of the gas: with the introduction of a compressibility factor Z(p) such that p/Z(p) is proportional to number density N, the ionisation coefficient becomes $\bar{\alpha}/p = AE - Bp/Z(p)$ and Paschen's similarity law [$V_s = f(Nd)$] is obeyed.

High-Pressure Studies

Paschen Deviation and Spark Conditioning

It is well known that in technical applications the similarity-law strength of SF_6 is not easily achieved for pressures greater than ~2 bar and values of pd greater than ~20 bar mm[3,9]. In addition, increased pressure leads to spark-conditioning effects,[10-12] in which V_s increases with repeated sparking from an initial low level. If dust[10] or other particles are excluded, the conditioning process is an electrode phenomenon, and previously conditioned electrodes require further conditioning if the pressure is increased, even at constant pd.[12] Nitta et al[11] have shown that electrode area is important in determining the degree of conditioning observed. With relatively smooth electrodes, for example, there is little conditioning either for small electrode areas, where the Paschen level is quickly attained, or for very large areas, where there are enough 'weak points' on the surface to keep V_s low. For intermediate areas marked conditioning may occur, although even after spark conditioning the breakdown strength of the gas may still be lower than the similarity-law value.

The reduced insulation strength in compressed SF_6 represents breakdown for which the macroscopic field strength is less than the limiting value so that $\bar{\alpha}$ is apparently everywhere < 0. However, breakdown requires that a criterion of the form $\int_0^{x'} \bar{\alpha}(x)\,dx = k$ is satisfied somewhere in the gap, and several explanations have been proposed for this anomaly. In general, these do not assume any change in gas properties, but deal with such effects as enhanced cathode emission,[11,13] and enhanced ionisation in regions where the limiting field is exceeded locally due to electrode microprotrusions or to free conducting particles in the gas. An exception is the suggestion[14] that avalanche statistics in SF_6 are such that critical-avalanche conditions may be achieved when E/p is appreciably less than $(E/p)_{lim}$. Recent

calculations by Tedford et al[15] have shown that this is not the case, and that the probability of breakdown is negligible for E/p even a fraction of one percent below $(E/p)_{lim}$. The lack of any gas-dependent mechanism apart from the compressibility effect is also borne out by the fact that the similarity-law breakdown voltage can be attained under laboratory conditions at pressures up to 12 bar using carefully filtered gas with highly polished electrodes of very small stressed area.[16] For practical conditions, the important factors therefore appear to be particulate contamination and electrode-surface conditions.

Particle-Induced Breakdown

The breakdown voltage of SF_6-insulated systems can be reduced by the presence of particles of size greater than a few μm, and recent studies have established how V_s depends on particle material, size and shape.[17-21] The particle material may be important in coaxial systems[18,20] where its density determines whether the particle can cross to the high-field inner conductor at a given voltage. In general, the breakdown voltage is reduced as particle size increases, and elongated particles have a much greater effect than spherical ones.[18-21] Figure 2 shows data for ac breakdown in a coaxial 150 mm/250 mm system:[20] the results are typical in that with spherical particles V_s increases with pressure while with wires more than ~1 mm long V_s has a maximum at ~4 bar and falls at higher pressures to values which can be as low as 10% of the particle-free level. For both ac and dc stress, breakdown in coaxial systems occurs when the particles are at or near the centre conductor[21] and the breakdown voltage is usually lower when that conductor is positive, especially at the higher pressures,[17,21] while for particle-free gas the opposite is the case. Under impulse conditions large particles do not move significantly during the surge, but there is evidence that small particles can reduce the breakdown level.[22]

Several mechanisms have been proposed to explain particle-induced breakdown: these have included the effects of increased ionisation in the enhanced field at the particle tip,[18,19] processes associated with rapid charge reversal at contact with an electrode[20,21] and mechanisms based on microdischarges between particle and electrode.[18,20]

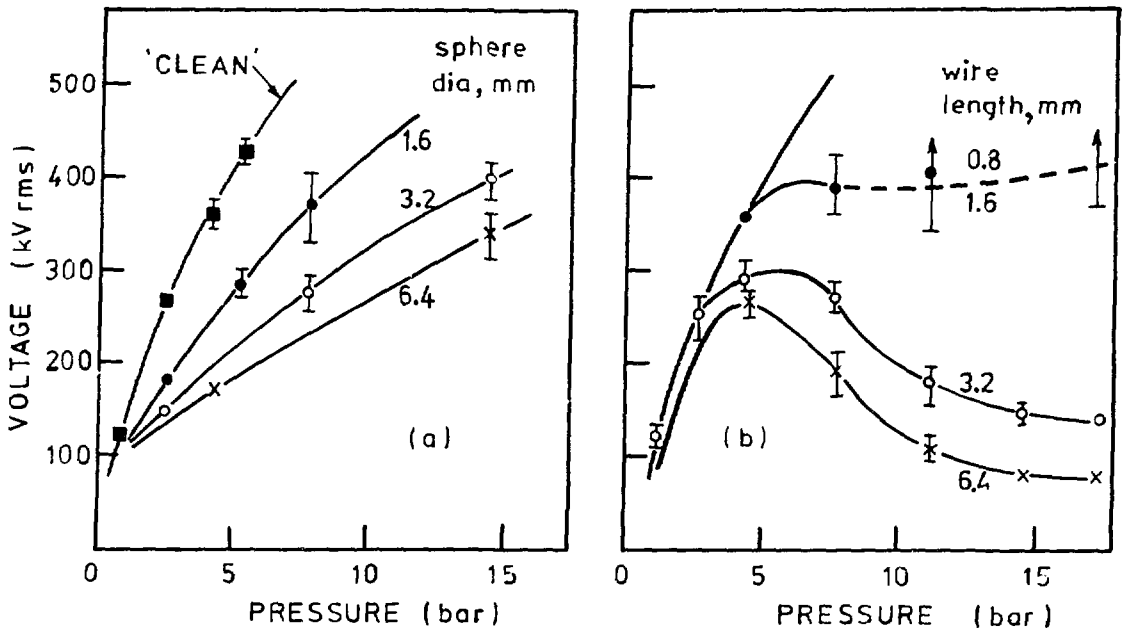

Fig. 2. Particle-initiated breakdown in SF_6: ac voltage-pressure characteristics for a 150 mm/250 mm coaxial-electrode system for breakdown initiated (a) by aluminium spheres (b) by 0.1-mm dia. copper wires.

Effect of Electrode-Surface Roughness

For practical electrodes, microscopic surface irregularities will cause local field intensification and this can lead both to electron emission and to locally-enhanced ionisation in the gas.[23] While the former process, coupled with space-charge effects, might be important in breakdown in compressed N_2 or H_2, the latter effect is especially important in SF_6, where $\bar{\alpha}/p$ increases very rapidly for $E/p > (E/p)_{lim}$.[1,24] Pedersen[25] has suggested that ionisation in the small region of enhanced field can reach the levels required for streamer formation, even when the macroscopic field is less than the limiting value. Experimental studies with artificial protrusions[26,27] and with electrodes of different surface roughness[11,28] have demonstrated this behaviour, and calculations for a single protrusion have shown[25,26] that the macroscopic value of E/p at breakdown is reduced from $(E/p)_{lim}$ to $\xi\,(E/p)_{lim}$ where ξ is a surface-roughness factor $(0<\xi\leq 1)$. These calculations consider ionisation within the distance x_c from the protrusion tip for which the protrusion-perturbed field exceeds $(E/p)_{lim}$ and use the linear relationship of

Eq. (1) for $\bar{\alpha}$ in SF_6 in the simple streamer criterion of Eq. (4). For the case of a hemispherical protrusion of radius ρ, for example, Pedersen has shown[25] that ξ is a function of $p\rho$ and is less than unity only for values of $p\rho$ greater than ~ 40 bar μm. Assuming that the maximum roughness R_{max} may be represented by the protrusion model, this suggests that roughness should reduce V_s only if pR_{max} exceeds this figure. Comparison with experimental results suggests that the protrusion model proposed by Pedersen is adequate to explain Paschen deviations in SF_6 up to ~ 6 bar.[25,29]

In an extension of Pedersen's analysis Somerville et al[15,30] have found that the condition for the occurrence of breakdown below the limiting field depends only on the height h of the protrusion and is independent of its shape. It can easily be shown that the condition is $ph = k/B$ where k and B are the constants in Eq. (1) and Eq. (4) above; for $k = 10.5$ and $B = 2460$ (bar cm)$^{-1}$ the maximum tolerable value of ph is 43 bar μm for any shape of particle.

For conditions where ph exceeds the critical value for the onset of roughness effects, the actual value of ξ depends on the protrusion shape. Figure 3 shows calculated values[30] of E/p at breakdown for prolate-spheroid protrusions for various ratios of height h to half width b. For large values of h/b, the field enhancement may be so great that the assumption of the linear relation Eq. (1) for $\bar{\alpha}$ is no longer valid: however a lower limit to the breakdown voltage may be obtained by assuming that the voltage drop over the ionisation zone where $\bar{\alpha} > 0$ can never be less than the Paschen-minimum voltage, which for SF_6 is 507 V. The dashed curve in figure 3 was calculated using this criterion for a protrusion with $h/b = 10$.

Breakdown in SF_6 Mixtures

Measurements of breakdown voltages in SF_6 mixtures in uniform[31,32] and slightly nonuniform fields[32-34] have shown that the addition of SF_6 to a nonattaching gas such as nitrogen results in a saturation effect such that increasing the SF_6 content above a given level does not appreciably improve the insulation strength. Baumgartner[31] has calculated smooth-electrode breakdown voltages for such mixtures using ionisation

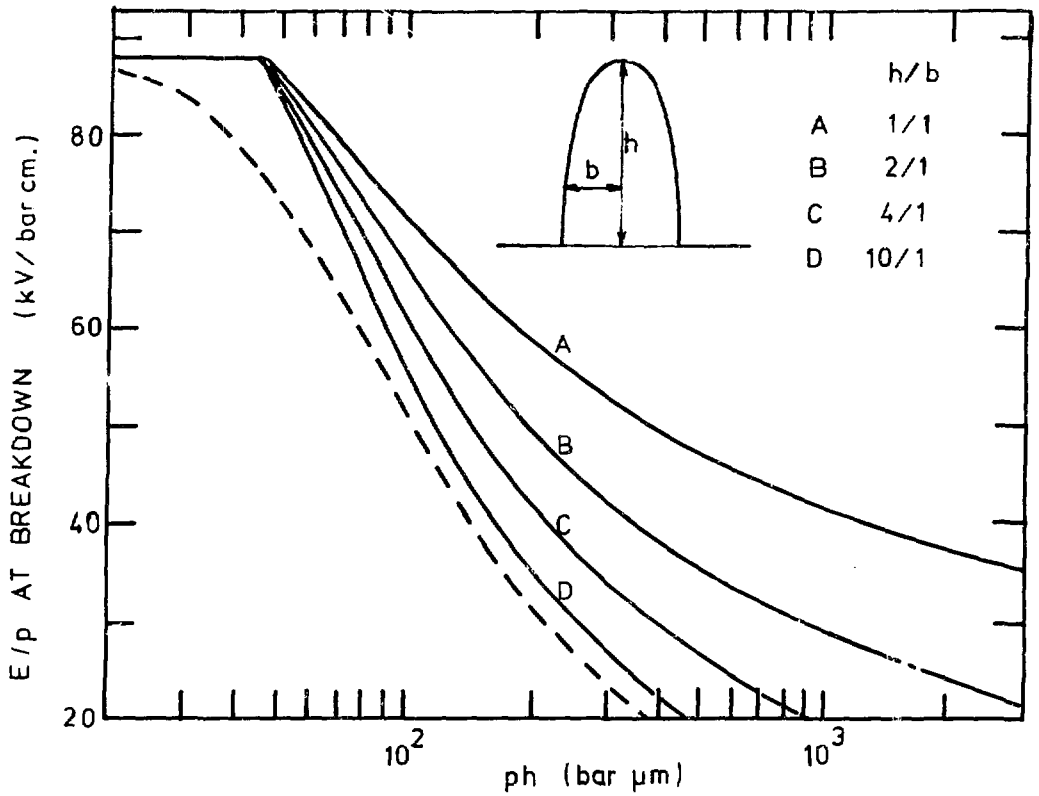

Fig. 3. Calculated values of the macroscopic breakdown value of E/p in SF_6 as a function of parameter ph for various prolate-spheroid protrusions. The dashed curve is calculated for h/b = 10 using a Paschen-minimum criterion.

coefficients obtained by interpolation on a partial-pressure basis between the data for the component gases and has found good agreement with experimental results.

Apart from the saturation effect, mixtures with nonattaching gases are attractive for practical applications because of recent indications that their insulation strength is less sensitive to electrode roughness[27] and to particle contamination.[35] Calculations of the influence of electrode roughness on breakdown in SF_6 mixtures have been made by Farish, Ibrahim and Crichton[27,36] using the hemispherical-protrusion model proposed by Pedersen. As shown in figure 4 for SF_6/N_2 mixtures, reduction of the SF_6 content leads to a progressive increase in the value of $p\rho$ which can be tolerated before ξ falls below unity. These calculations are subject to some uncertainty because of the technique for estimating $\bar{\alpha}$. Also, all roughness calculations depend on the value

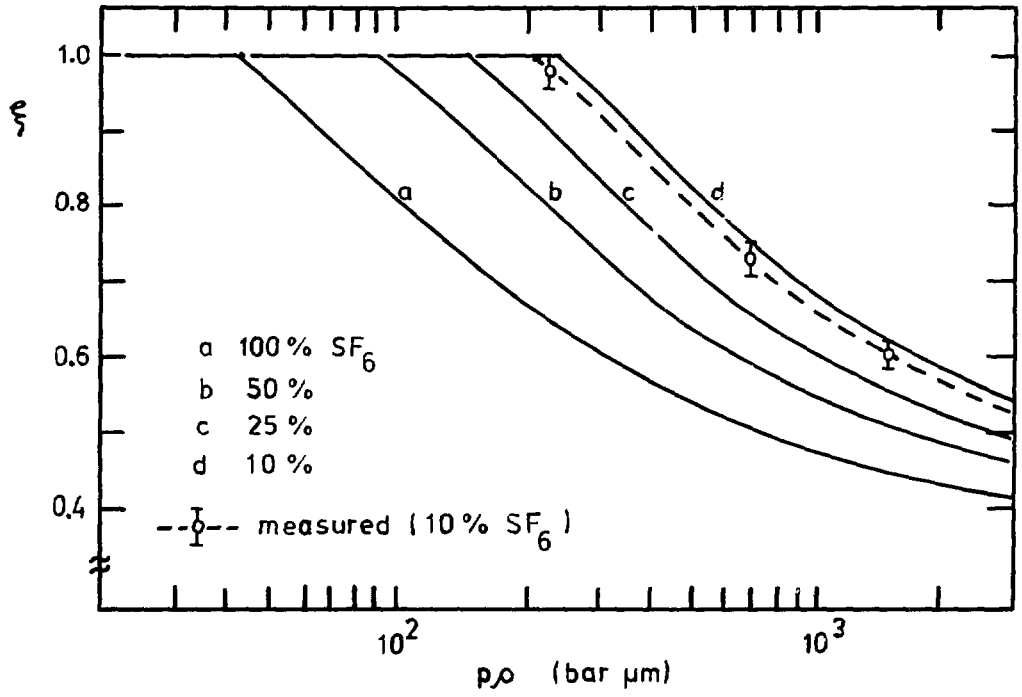

Fig. 4 Roughness factor ξ as a function of the product $p\rho$ (pressure x protrusion radius) for breakdown in SF_6/N_2 mixtures.

chosen for the streamer constant k, although the results are not very sensitive to k except near the deviation point. In the above calculations, the SF_6 content was $\geqslant 10\%$ and k was interpolated between the value of 18 generally used for air or nitrogen and that of 10.5 proposed for SF_6 by Pedersen.[25] Reasonable agreement is obtained between the calculations and values of ξ obtained from measurements with smooth electrodes and with a fixed cathode protrusion (dashed curve in figure 4): this suggests that no serious error results from the assumptions made, but there is obviously a need for experimental determination of $\bar{\alpha}$ and k for mixtures.

For the values of $p\rho$ of 50-500 bar μm that might be expected for large practical systems, the dependence of ξ in mixtures on $p\rho$ tends to compensate for the reduction in the Paschen-law strength with decreased SF_6 content: figure 5 shows the results of calculations of the maximum value at breakdown of the macroscopic field strength in SF_6/nitrogen mixtures for various conditions of roughness and gas pressure. For each pressure the upper curve corresponds to the smooth-electrode value (i.e. $pR \leqslant 40$ bar μm) while for roughness greater than the threshold level

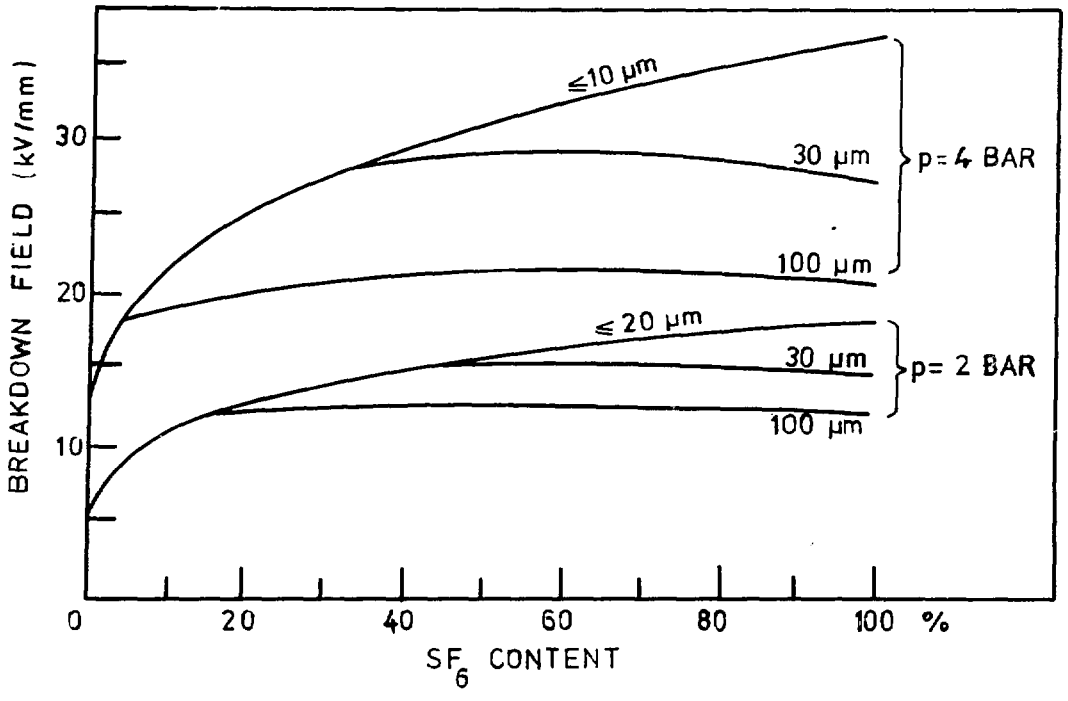

Fig. 5. Effect of electrode-surface roughness on calculated breakdown field/gas mixture characteristics in SF_6/N_2 mixtures.

there is an optimum mixture for each surface condition. At 4 bar, for example, a 30% SF_6 mixture is the best choice for a 30 µm finish while ~10% SF_6 would be adequate with 100 µm protrusions. It is interesting to note that experimental studies for practical electrode systems[37,38] do give the result that V_s in mixtures can be comparable to that for pure SF_6.

Voltage-Time Characteristics

For practical applications, there is considerable interest in the voltage time characteristics of SF_6 insulation, and these have been the subject of several recent experimental studies.[39-41] The prediction of these characteristics, however, presents considerable difficulties. The Pedersen criterion assumes the availability of an initiatory electron and will therefore find its application most readily for the case of a cathode protrusion where electron emission may be assumed. For the highly-stressed anode, an initiatory electron must be found in the region for which $\bar{\alpha} > 0$, and more specifically in that part of the region from which, for a given voltage, an avalanche is capable of developing to the critical size before reaching the anode. As this critical volume is vanishingly small at the

breakdown threshold, large values of the statistical time lag t_s can be expected in SF_6. Information on the factors controlling t_s will therefore be required before voltage-time characteristics can be predicted theoretically, although empirical methods have already been proposed.[39]

BREAKDOWN IN NONUNIFORM FIELDS

DC and Power-Frequency Studies

Voltage-Pressure Characteristics

Sulphur Hexafluoride.--Breakdown in highly divergent fields in SF_6, as in other electronegative gases, is characterised by the existence of a range of pressures over which breakdown for a given electrode arrangement takes place at a voltage considerably in excess of the corona-onset voltage V_c, while at higher pressures the breakdown voltage and corona-onset voltage coincide. In the lower pressure range the high breakdown voltage is due to stabilisation of the field near the high-stress electrode by space charge of the same polarity generated by the corona discharge; the voltage-pressure characteristics exhibit a peak in this range which is especially marked for dc and power-frequency voltages. There have been several recent investigations in which the influence of field divergence, gas pressure and polarity have been systematically studied for point-plane gaps[42-44] and coaxial-electrode systems.[45] These measurements have confirmed and extended previous observations (see ref. 43) and several general features of the characteristics can be identified. These are (1) over a range of pressure on the rising part of the characteristics V_s is almost independent of the radius of curvature r_o of the highly stressed electrodes;[43] (2) the critical pressure p_c at which V_s and V_c coincide is such that $p_c r_o$ is approximately constant; (3) the breakdown voltage V_{sc} at the critical pressure is almost independent of r_o and, for a given spacing, V_{sc} represents the minimum breakdown voltage for SF_6 irrespective of pressure (above 1 bar) and radius of curvature.[42,43]

The above features are illustrated by the curves for 100% SF_6 in figure 6, which shows data obtained in a study of corona and breakdown in point-plane gaps in SF_6 and its mixtures in static and flowing gas.[46,47]

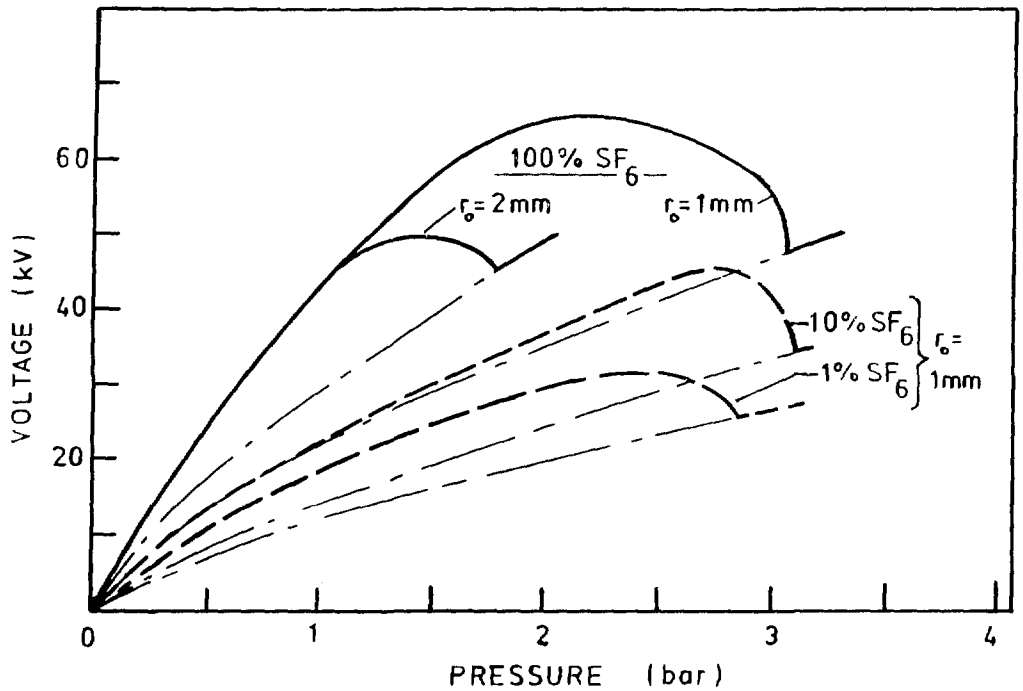

Fig. 6 Effect of point radius (r_o) and gas mixture on dc corona onset and breakdown in SF_6 and SF_6/N_2 mixtures in a 10-mm point-plane gap.

The results indicate that V_{sc} for the 10-mm gap is 45-48 kV and, as found for longer gaps,[43] the peak voltage in SF_6 corresponds to an average E/p at breakdown of about 35 kV/cm bar.

SF_6 Mixtures.-- Corona current/voltage characteristics and dc voltage-pressure characteristics have been measured in SF_6/nitrogen mixtures for various point-plane arrangements.[46,47] As shown in figure 6, p_c is almost unaffected by SF_6 content in the range 100% - 1%: this behaviour, which has also been reported by Ermel,[48] is in contrast to the results of impulse studies in SF_6 mixtures, in which p_c increased greatly with decreasing SF_6 content.[49] For a given pressure and gas mixture, the average corona current in the stabilisation region follows the relationship $I = cV(V-V_c)$ typical of coronas in which the field at the high-stress electrode is limited by space charge to its onset value.[46]

Effect of Gas Flow

The influence of gas flow on corona and breakdown in SF_6 is of interest both because flow is a factor in practical applications such as

gas-blast circuit breakers and because it affords an insight into the corona-stabilisation process.[47] Figure 7 shows voltage-pressure characteristics for a 10-mm positive point-plane gap in SF_6 for still gas and for flow at 30 m/s along the gap axis and transverse to it. The effect of axial flow towards the point is to increase V_s in the stabilisation region, while with transverse flow there is a considerable reduction in V_s over the pressure range p_1 - p_c. Figure 7 also shows the form of the spark channel for various conditions of pressure and gas flow: this will be discussed below.

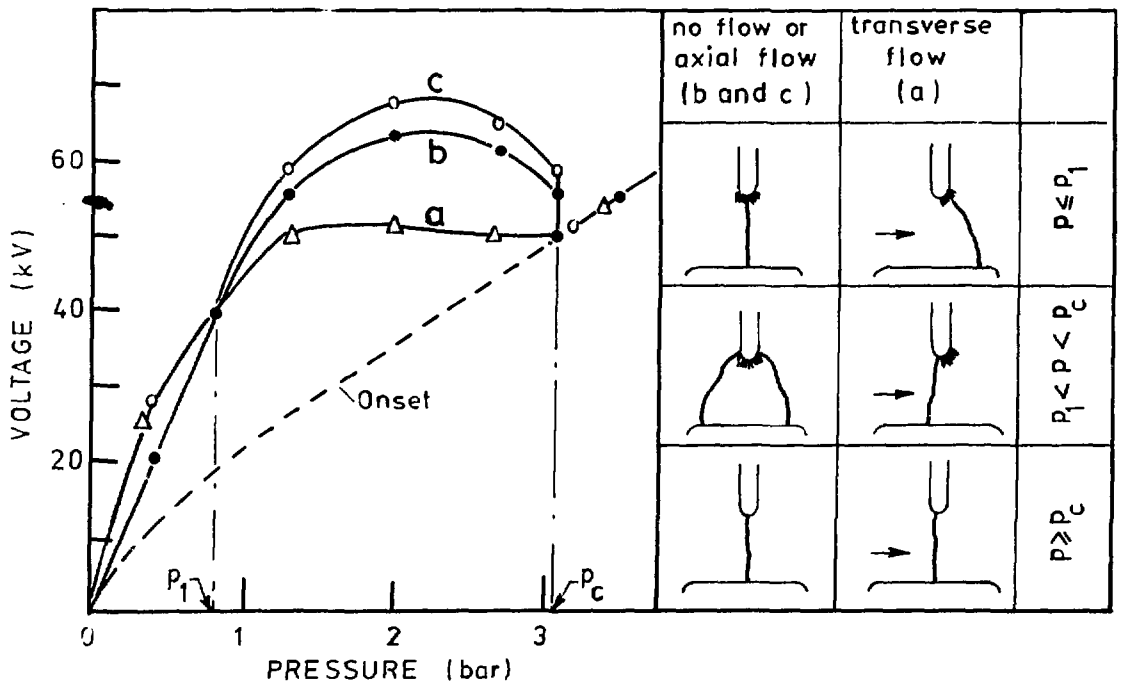

Fig. 7. The influence of gas flow at 30 m/s on dc corona onset and breakdown in SF_6 in a 10-mm point-plane gap with r_o = 1 mm.
(a) transverse flow (b) no flow (c) axial flow towards point.

Prebreakdown Corona

Apart from the work of Hazel and Kuffel[50] and Davidson et al[46,47] there is little information on corona in SF_6. The main features appear to be that, over most of the stabilisation region, individual pulses at onset give way at higher voltages to a continuous discharge, while near the critical pressure only streamer corona is observed.[50] At constant pressure within the stabilisation region, increasing voltage causes the corona to spread round the electrode tip.[50] The increase in the

breakdown voltage reported by Farish et al for axial gas flow towards the point is associated with a further increase in area covered by the discharge due to a redistribution of ions around the point[46] so that the stabilisation effect is enhanced.

The forms of the spark channel for still gas shown in figure 7 have been reported by several investigators.[43,44,47,50] At low pressures ($p \leqslant p_1$) where V_s is independent of r_o, the channel is axial and develops out of the corona: For $p_1 < p < p_c$ the channel is curved away from the axial region and originates at the edge of the corona; Hazel and Kuffel[50] suggest that the curvature of the channel is caused by a potential barrier in the axial region of the gap due to positive and negative-ion space charges. For $p \geqslant p_c$ the channel is again axial and no corona occurs. With transverse flow, the corona is displaced to the downstream side of the electrode and, for $p \leqslant p_1$, this supports the suggestion that breakdown in this range is controlled by the field near the plane cathode; thus, when the positive space charge, and hence the region of enhanced cathode field, is blown downstream the spark channel is curved in that direction.[47] In the range p_1 to p_c the spark is almost axial with flow. This is consistent with the idea that the stabilisation process fails when breakdown streamers form at the edge of the corona. With transverse flow, the upstream edge of the corona is very near the electrode tip and breakdown can occur at a lower voltage than for still gas.

The Critical Pressure

The corona-onset voltage V_c may be calculated using the streamer criterion of Eq. (4) and, if the mechanism controlling p_c is known, the minimum breakdown voltage V_{sc} may be determined. For a point-plane system, if the field near the point is taken as $E(r) = E(r_o)\, r_o^2/r^2$ then the onset voltage is given by[24]

$$V_c = (E/p)_{lim} \cdot \psi\, pd\, [1 + (k/Bpr_o)^{\frac{1}{2}}]^2 \qquad (5)$$

where $\psi = V/d\, E(r_o)$ is the field utilisation factor. Since ψ depends on d/r_o, V_c for a given pd should be a function of pr_o and this similarity-law behaviour has been well established in recent experimental studies.[43,44] The critical pressure p_c is that at which the onset

streamer leads directly to breakdown and may differ from the pressure p_c' at which continuous corona no longer occurs. For relatively large values of r_o, the two nearly coincide but with sharper points there can be a considerable pressure range where corona stabilisation is absent but onset streamers are unable to lead to breakdown. Hazel and Kuffel[50] have proposed a semiempirical criterion for p_c based on the effect on streamer propagation of the rate of change of field near the tip and the mean free path for ionising radiation. The condition for which continuous corona no longer occurs (pressure p_c') can be derived if it is assumed that the continuous component comprises avalanche pulses which occur within the ionisation zone for which $\bar{\alpha} > 0$, and which are initiated by detachment from negative ions produced by this Townsend discharge by photoionisation.[47] It can be shown that x_c varies as $1/p^{\frac{1}{2}}$ and, since the free path x_μ for ionising radiation varies as $1/p$, the critical pressure will be that at which $ax_\mu = x_c$, where a is a constant; at this pressure negative ions will no longer be produced in enough quantities to maintain the Townsend discharge, and the increased production of electrons within x_c will favour the development of streamer discharges. Thus for the point-plane case, $x_c = (kr_o/Bp)^{\frac{1}{2}}$ giving $p_c' = BC^2/kr_o$, where C is a constant containing μ. Comparison with experimental results[47] gives a value for C of ~ 0.05 bar cm.

IMPULSE STUDIES

Sulphur Hexafluoride

Recent measurements with 5-50 cm gaps using lightning-impulse[51] and switching-impulse voltages[51-54] have shown that for long gaps the 50% breakdown voltage V_{50} in SF_6 can be surprisingly low.[52,53] Further, the breakdown voltage at pressures above 1 bar is strongly dependent on the shape of the high-stress electrode. For a square-ended rod, V_{50} does not change significantly with pressure in the range 1-6 bar, and V_{50} for a 50 cm rod-plane gap in SF_6 at 6 bar can be lower than for the same gap in atmospheric air.[52]

Takuma and Watanabe suggested that these results might be due to reduced corona stabilisation effects in SF_6 and this has been

demonstrated by recent work by Kurimoto et al[49,53,54] who studied impulse corona and breakdown in SF_6 and SF_6 mixtures. For a 30-cm rod-plane gap with a 19-mm dia. hemispherically capped rod in SF_6 they found the stabilisation peak at $p_m \approx 0.4$ bar and the critical pressure p_c at ~ 1 bar. A study of the impulse-corona development using photomultiplier and high-speed camera techniques showed that, for $p < p_m$, a diffuse corona occurred which inhibited further corona for ~ 10 μs. In the range $p_m < p < p_c$, however, one or more of the diffuse coronas was followed by a series of filamentary discharges while for $p > p_c$ only filamentary discharges were observed. The filamentary discharge in SF_6 propagates in the stepped manner found in air at high pressures or in very long gaps, but the interval between successive discharges is much less (0.1 - 0.2 μs). Figure 8 shows typical records for pressures near p_c. There is a marked difference between positive and negative polarity in that in the former case the channel extends with each discharge while in the latter a series of reilluminations occurs before the channel is extended by a particularly vigorous discharge.

SF_6 Mixtures

In SF_6 mixtures, considerably more charge is injected during the impulse corona and the corona shielding is more pronounced and persists over a greater pressure range.[49] The result is that the breakdown strength of mixtures, even those containing very small ($\sim$1%) amounts of SF_6, can be much greater than that of pure SF_6. Figure 9 shows results obtained by Kurimoto for SF_6-air mixtures with positive switching impulses: It can be seen that the highest strength relative to SF_6 occurs with 1% SF_6 by volume, where p_m corresponds to p_c for SF_6. Similar results have been reported by Watanabe and Takuma,[55] and for SF_6/H_2 mixtures by Farish et al.[56,57] Figure 10 shows data for V_{50} in SF_6/H_2 mixtures for 1.5/40 μs impulses; even for a 10-cm gap, V_{50} with $\sim 0.4\%$ SF_6 at 2 bar exceeds the positive-impulse level for SF_6.[52] Cookson and Wootton[58] have found even higher breakdown voltages for ac conditions in such 'weak' mixtures, as shown by the ac curve in figure 10.

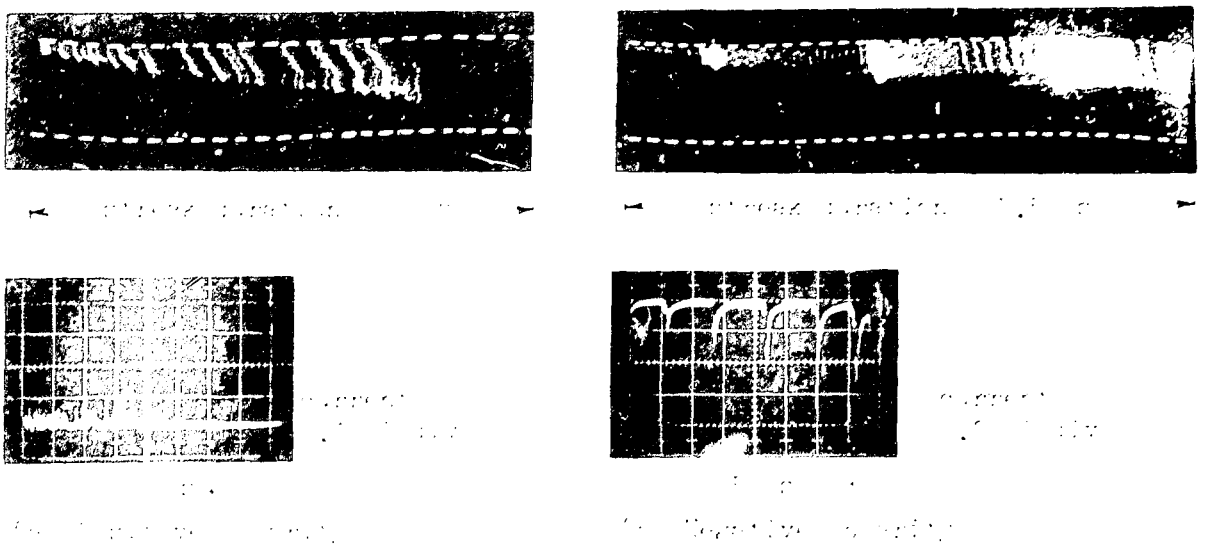

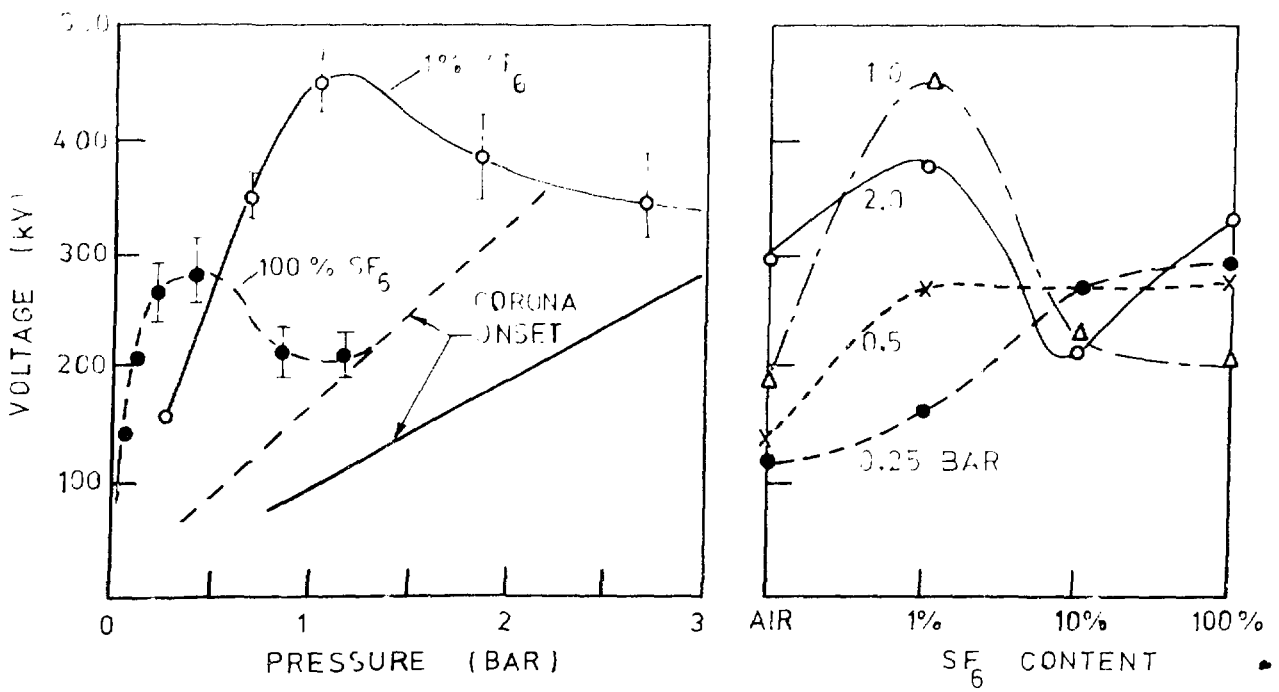

Fig. 9 50% corona-inception and impulse-breakdown voltage measurements in SF_6-air mixtures for a 30-cm rod-plane gap. (19-mm diameter rod, 130/2000 μs impulse).

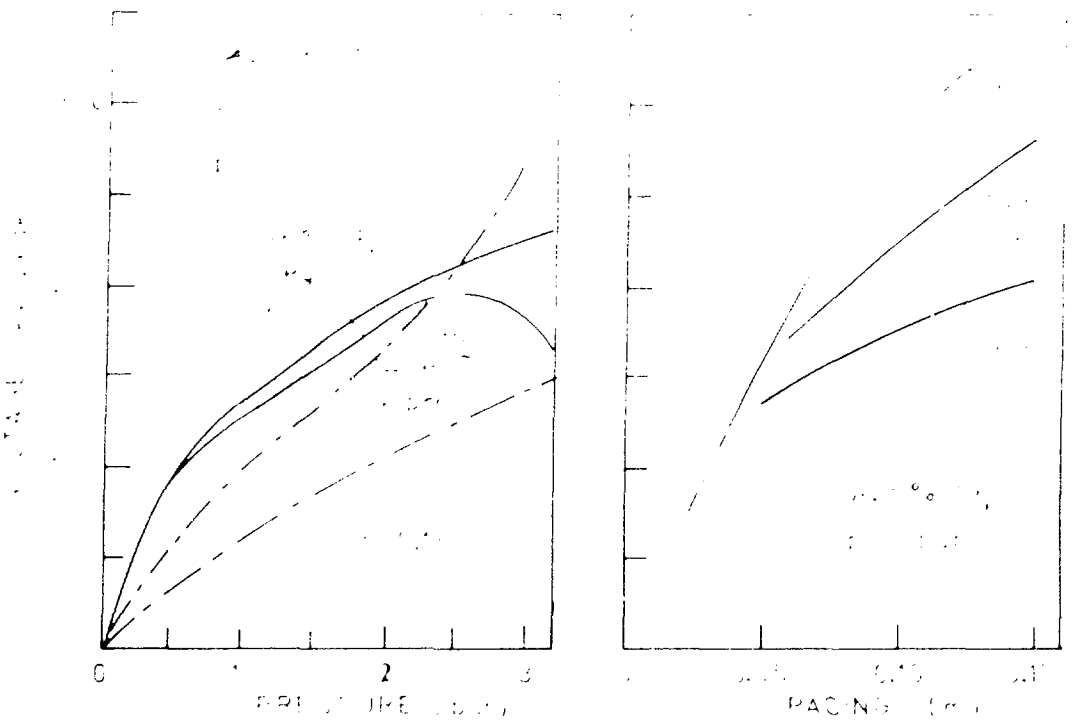

Fig. [illegible]. [illegible] mixtures. [illegible]

The high level of research activity since [illegible] and its mixtures reflects the increasing interest in the use of compressed-gas insulation in compact substation and power-transmission applications. In the search for superior insulants, the performance of a new gas or gas mixture should be evaluated for practical conditions of electrode roughness and particle contamination as well as for ideal conditions, since gases with high intrinsic strength might be subject to the same problems as SF_6. There is a need for reliable data on ionisation parameters in such gases to allow improved breakdown-voltage estimation and also for more information on time lags to breakdown and the statistics of breakdown under impulse-voltage conditions. The case of highly nonuniform fields is important in particle-contaminated systems and further work is required on corona characteristics and on factors determining the critical pressure: a study of the transition from quasiuniform-field to nonuniform-field breakdown would be of particular interest.

ACKNOWLEDGEMENTS

The author wishes to thank Prof. D.J. Tedford for his advice and encouragement, and D.T.A. Blair, A. Aked, I.D. Chalmers, B.H. Crichton, A. Kurimoto, I. Somerville, O.E. Ibrahim and C. Korasli for many useful discussions during the preparation of this paper.

REFERENCES

1. H.A. Boyd and G.C. Crichton, Proc.IEE, 118, 1872 (1971).
2. A. Pedersen, IEEE Trans, PAS-89, 2043 (1970).
3. T.W. Dakin, G. Luxa, G. Opperman, J. Vigreux, G. Wind and H. Winkelnkemper, Electra, 32, 61 (1974).
4. I.D. Chalmers and D.J. Tedford, Proc.IEE, 118, 1893 (1971).
5. J. Dutton, F.M. Harris and G.J. Jones, Proc.IEE, 118, 732 (1971).
6. H.A. Boyd and G.C. Crichton, Proc.IEE, 119, 275 (1972).
7. A. Pedersen, P.W. Karlsson, E. Bregnsbo and T. Munk Nielsen, IEEE Trans, PAS-93, 1820 (1974).
8. B.H. Crichton and D.J. Tedford, J.Phys.D., 9, 1079 (1976).
9. Y. Kawaguchi, K. Sakata and S. Menju, IEEE Trans, PAS-90, 1072 (1971).
10. C. Ikeda and B. Yoda, EE in Japan, 91, 67 (1971).
11. T. Nitta, N. Yamada and Y. Fujiwara, IEEE Trans, PAS-93, 623 (1974).
12. I.D. Chalmers and J. Thom, Int.Conf.Gas Discharges, IEE Publ. 143, 166 (1976).
13. M. Ermel, Int.Conf. Gas Discharges, IEE Publ 143, 191 (1976).
14. A. Rein, A. Arnesen and I. Johansen, IEEE Trans, PAS-96, 945 (1977).
15. D.J. Tedford, B.H. Crichton and I.C. Somerville, to be published in 1977 Annu.Rep.Conf.Elect.Insul. (1978).
16. R. Baumgartner, ETZ-A, 98, 369 (1977).
17. A. Diessner and J.G. Trump, IEEE Trans, PAS-89, 1970 (1970).
18. A.H. Cookson, O. Farish and G.M.L. Sommerman, IEEE Trans, PAS-91, 1329 (1972).
19. I.M. Bortnik and C.M. Cooke, IEEE Trans, PAS-91, 2196 (1972).
20. A.H. Cookson and O. Farish, IEEE Trans, PAS-92, 871 (1973).
21. C.M. Cooke, A.H. Cookson, R.E.Wootton, IEEE Trans, PAS-96, 768 (1977).
22. J.M.K. MacAlpine and A.H. Cookson, Proc.IEE, 117, 646 (1970).
23. V.A. Avrutskii, G.M. Goncharenko and E.N. Prokhorov, Sov.Phys. Tech. Phys., 18, 386 (1973).
24. T. Nitta and Y. Shibuya, IEEE Trans, PAS-90, 1065 (1971).

25. A. Pedersen, IEEE Trans, PAS-94, 1749 (1975).

26. C.M. Cooke, IEEE Trans, PAS-94, 1518 (1975).

27. O. Farish, O.E. Ibrahim and B.H. Crichton, Proc.IEE, 123, 1047 (1976).

28. B.A. Goryunov, Sov.Phys.Tech.Phys., 20, 60 (1975).

29. W. Zaengl and R. Baumgartner, ETZ-A, 96, 510 (1975).

30. I.C. Somerville, D.J. Tedford and B.H. Crichton, Proc. 13th Conf.Ion Phen.in Gases, Berlin, 429 (1977).

31. R.G. Baumgartner, Int.Conf.Gas Discharges, IEE Publ 118, 366 (1974).

32. D.R. James, L.G. Christophorou, R.Y. Pai, M.O. Pace, R.A. Mathis and D.W. Bouldin, to be published in 1977 Annu.Rep.Conf.Elect.Insul(1978).

33. J. Dutton, F.M. Harris and D.B. Hughes, Proc.IEE, 121, 223 (1974).

34. T. Takuma, T. Watanabe and K. Kita, Proc.IEE, 119, 927 (1972).

35. A.H. Cookson and R.E.Wootton, Int.Conf.Gas Discharges, IEE Publ 118, 385 (1974).

36. B.H. Crichton, O.E. Ibrahim and O. Farish, Int.Conf.Gas Discharges, IEE Publ 143, 117 (1976).

37. R.G. Baumgartner, Int.Symp.HV Tech., Zurich, 326 (1975).

38. W. Schmidt and D. Nguyen, Int.Symp. HV Tech., Zurich, 385 (1975).

39. T. Nitta, Y. Shibuya and Y. Fujiwara, IEEE Trans, PAS-93, 108 (1974).

40. W.L. Watson, H.M. Ryan, Int.Conf.Gas Disch., IEE Publ 143, 153 (1976).

41. W. Taschner, ETZ-A, 98, 153 (1977).

42. A.A. Azer and R.P. Comsa, IEEE Trans, EI-8, 136 (1973).

43. S. Sangkasaad, Int.Symp. HV Tech., Zurich, 379 (1975).

44. A.G. Lianin, V.I. Popkov and W.N. Shertsov, Int.Conf. Gas Discharges, IEE Publ. 143, 169 (1976).

45. M. Ermel, ETZ-A, 96, 505 (1975).

46. R.C. Davidson, B.R. Lynch and O. Farish, Int.Conf.Gas Discharges, IEE Publ 143, 242 (1976).

47. O. Farish, R.C. Davidson and D.J. Tedford, to be published in 1977 Annu.Rep.Conf.Elect.Insul. (1978).

48. M. Ermel, ETZ-A, 96, 231 (1975).

49. H.M. Ryan et al, CIGRE, paper 15-02 (1976).

50. R. Hazel and E. Kuffel, IEE Trans, PAS-95, 178 (1976).

51. R.C. Klewe, B.A. Tozer, Int.Conf.Gas Discharges, IEE Publ 70,36(1970).

52. T. Takuma and T. Watanabe, EE in Japan, 90, 166 (1970).

53. A. Kurimoto, S.J. Dale, A.Aked and D.J. Tedford, Int.Symp. HV Tech., Zurich, 349 (1975).

54. A. Kurimoto, A. Aked and D.J. Tedford, Int.Conf. Gas Discharges, IEE Publ 143, 162 (1976).

55. T. Watanabe and T. Takuma, J.Appl.Phys., 48, 3281 (1977).

56. O. Farish, S.J. Dale and A.M. Sletten, IEEE Trans, PAS-95,1639(1976).

57. O. Farish, S.J. Dale and A.M. Sletten, Paper F-77 070-6 IEEE Pwr. Eng. Soc. Winter Power Meeting, New York (1977).

58. A.H. Cookson and R.E.Wootton, Paper F-77 657-0 IEEE Pwr. Eng. Soc. Summer Power Meeting, Mexico (1977).

DISCUSSION

DUTTON: 1. On the question of the sensitivity of breakdown to surface roughness in N_2/SF_6 mixtures, our results at the extreme of N_2 suggest that it is not possible to interpret the data there in terms of the Pedersen equation or the equivalent criterion in terms of the equivalent Townsend criterion. Do you have any comments?

2. The interesting recent photographs of the critical pressure region you showed give an indication of the regions where the electron density and the field are high enough to give light output. Do you have any information about the negative ions? This is a region which we hope to investigate using the rotating vane fluxmeter.

3. In relation to the criterion $\int \alpha' ds = k$ used for determining the critical volume and relating it to the statistics of breakdown was the applied field used? I ask because simulation shows that the original field is very rapidly modified by the development of space charge.

FARISH: 1. I agree that for pure nitrogen an analysis based on enhanced ionization near microprotrusions is inadequate to explain the Paschen deviations which occur at high values of Pd. This would seem to suggest that an electrode process is involved in such breakdowns; there are several possible processes, including space-charge-enhanced field emission combined with low level ionization in the gas, and charging and subsequent breakdown of oxide or other tarnish layers on the electrodes. In our earlier experiments with compressed nitrogen, there seemed to be some evidence for the latter process in the way in which the system conditioned or deconditioned with different rates of sparking;

it would be very difficult experimentally to study the field emission process as this would involve monitoring the early stages of the discharge which would require very high spatial resolution, probably with subnanosecond time resolution.

2. Concerning the question on negative ions, we have as yet no information concerning the distribution of negative ions in the gap. From positive-point studies with transverse gas flow, however, we have indications that the continuous corona in the stabilization region is maintained by detachment from negative ions near the point.

3. The applied field is used in the Pedersen analysis, as in any streamer model, to calculate the avalanche carrier number.

SIOMOS: Under the assumption that particles exist in the space between the electrodes can you give any indication about the real nature and the sizes of these particles? Do you have any idea about the number density of these particles?

FARISH: The particle-initiated breakdown studies which I described were designed to provide information on the effects of size and shape, and used artificially introduced particles. In practical equipment, metallic particles may be introduced during assembly or produced by abrasion between moving parts; those which cause degradation of insulation strength are probably ≥ 5 μm in size.

CHANTRY: The equation you derive for the critical pressure $P'_c = BC^2/Kr_o$ above which corona stabilization does not occur, contains three "constants" B, C^2, and K, all of which change or are likely to change if the proportions in a gas mixture are changed. Experimentally, you find that in N_2/SF_6 mixtures P_c remains essentially constant, implying

cancellation of the effects of changing B, C, and K. Have you speculated as to how this occurs?

FARISH: I don't think the lack of sensitivity of P'_c to SF_6 content is well enough established yet to warrant trying to explain it on the basis of the above model, which itself requires further investigation. However, it is true that with increasing nitrogen concentration the constant B in the equation for $\bar{\alpha}$ should decrease, while C, which is proportional to $1/\mu$, should increase; it is therefore possible that this tends to keep P'_c constant.

THE NUMERICAL SIMULATION OF THE BREAKDOWN OF A GASEOUS DIELECTRIC

A. J. Davies, C. J. Evans and P. M. Woodison,

Department of Physics, University College of Swansea, University of Wales, U. K.

ABSTRACT

One and two-dimensional simulation methods are described, for investigating the breakdown of a gaseous dielectric, which can trace the growth of a discharge from its initiation to the space-charge controlled glow. The present paper is mainly concerned with the application of the two-dimensional simulation to discharges in nitrogen and air between parallel plane electrodes. Preliminary results are also presented for a sphere-plane configuration.

ONE-DIMENSIONAL SIMULATIONS

During the last few years, following the advent of high-speed computers, much interest has been shown in using numerical simulation techniques for studying the electrical breakdown of a gaseous dielectric. With the new techniques that have been developed it is now possible to follow the growth of a discharge from its initiation as far as the space-charge controlled glow with instantaneous currents up to 100A.

In essence the basis of all simulation methods for studying current growth is to solve the conservation equations, for each species of particle present, subject to the boundary conditions that apply in a given experimental or engineering situation. For example, neglecting photo-ionization, diffusion and recombination, the general equation of charge conservation for electrons is

$$\frac{\partial \rho_e}{\partial t} = \alpha \rho_e W_e - a \rho_e W_e + \delta \rho_n W_n - \nabla \cdot (\rho_e \underset{\sim}{W}_e), \tag{1}$$

and the boundary conditions will include specification of the initial charge distribution in the gap, the characteristics of the external electrical circuit, and the electric potentials on the boundaries of the discharge region*.

The simplest case one can consider is that of a discharge between infinite plane paralliel electrodes separated by a distance d and subject to an applied voltage V(t). If we restrict our attention to discharges in which only one species of positive and negative ion are present and further assume that the discharge is of constant radius with uniform particle densities across the cross-section, then only one space dimension need be considered and the relevant conservation equations are

$$\frac{\partial \rho_e}{\partial t} = \alpha \rho_e W_e - a \rho_e W_e + \delta \rho_n W_n - \frac{\partial}{\partial x} (\rho_e W_e), \tag{2a}$$

$$\frac{\partial \rho_p}{\partial t} = \alpha \rho_e W_e + \frac{\partial}{\partial x} (\rho_p W_p), \tag{2b}$$

$$\frac{\partial \rho_n}{\partial t} = a \rho_e W_e - \delta \rho_n W_n - \frac{\partial}{\partial x} (\rho_n W_n). \tag{2c}$$

If the cathode is at x = 0 and the anode at x = d, then the boundary conditions are

---

* A list of symbols and their meaning is given in the Appendix.

$$\rho_e(0,t)W_e(0,t) = J_o(t) + \gamma_i \rho_p(0,t)W_p(0,t)$$
$$+ \frac{\gamma_{ph}}{\tau_{ph}} \left\{\frac{\alpha}{\alpha_{ex}}\right\} V_s \int_0^t e^{-(t-t')/\tau_{ph}} \int_0^d \alpha_{ex}(x,t')\rho_e(x,t')W_e(x,t')dxdt' \quad (3a)$$

$$\rho_p(d,t) = 0, \quad (3b)$$

$$\rho_n(0,t) = 0, \quad (3c)$$

$$\int_0^d E(x,t)dx = V_g(t), \quad (3d)$$

where the gap voltage $V_g(t)$ will be determined by the characteristics of the external circuit and the total current flowing in the gap.

The electric field $E(x,t)$ is a function of the net charge density and one must be particularly careful in selecting a method for computing it since the various ionization coefficients are strongly varying functions of E. For wide discharges, whose radius is much greater than the gap separation, Poisson's equation in one dimension may be used to find the axial fields but for narrow discharges this procedure can introduce large errors[1]. In these cases the two-dimensional form of Poisson's Equation or the "disc method" due to Davies et al[1] may be used. In the latter method the discharge is divided into discs by planes perpendicular to the axis and the field on the axis computed by summing the contribution of each disc of charge, making the appropriate allowance for the image charges in the electrodes.

As pointed out by Davies et al[2], the stability of the simulations can be greatly improved by computing the net charge density, ρ, directly from the relation

$$\frac{\partial \rho}{\partial t} = \frac{\partial}{\partial x} (\rho_e W_e + \rho_p W_p + \rho_n W_n), \qquad (4)$$

which does not include any ionization terms. Numerical errors introduced in computing ρ_e, ρ_n and ρ_p separately from Equations (2a - 2c) can give large inaccuracies in ρ if it is evaluated from $\rho = \rho_p - \rho_n - \rho_e$, especially, for example, in the positive column of a discharge where ρ is small compared with the corresponding electron and ion densities.

In the numerical simulations, the charge conservation equations are put in their finite difference form and integrated using the Method of Characteristics[3]. In most of the work a constant mesh spacing in the axial direction was employed but recently the procedure has been modified to enable the mesh to be graded in the region of the cathode so as to be able to investigate in greater detail the cathode-fall region of the discharge in the later stages of growth. This work is to be published elsewhere.

The one-dimensional simulations using the above equations and boundary conditions have been successfully applied to discharges in air, N_2, and SF_6[2, 4, 5]. For example, Fig. 1 shows the computed contours of light output from a discharge in N_2 at 90 torr initiated by a pulse of 400 electrons, for a step function applied voltage 25.5% above the breakdown potential V_s, (a) when the effects of space charge distortion are neglected and (b) when distortion of the field is taken into consideration.

Fig. 1(a) essentially gives the same result as Davidson's exact solution[6] for ionization growth in uniform fields between plane electrodes and we clearly see the electron avalanche travelling to the anode with constant velocity W_e and the apparently infinite phase velocity towards the cathode of the isophot lines behind the primary avalanche. Fig. 1(b) on the other hand shows the apparent acceleration of the avalanche as it approaches the anode (the anode-directed streamer phase) and also the appearance of a sharp light maximum propagating

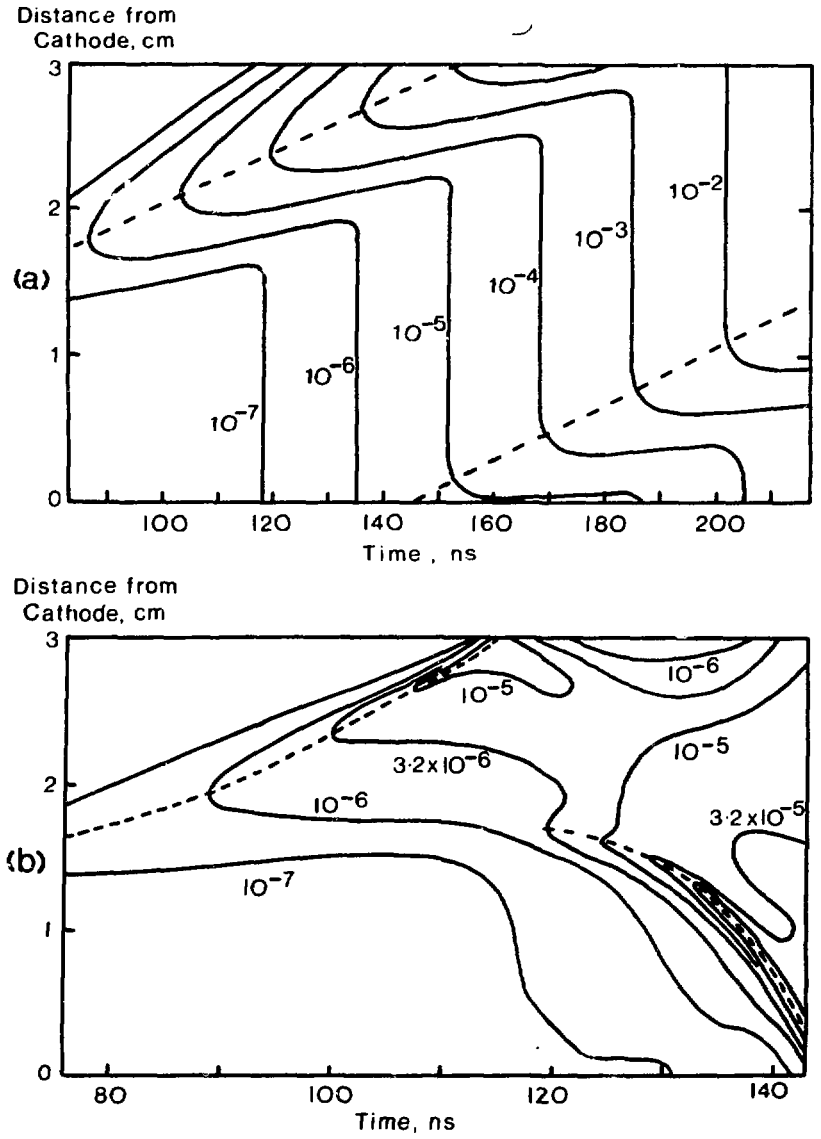

Fig. 1. Contour lines of equal light output (arbitrary units) plotted as a function of x and t (a) neglecting space-charge and (b) allowing for space-charge. Data: Nitrogen, p = 91 Torr, E/p = 62 V $cm^{-1}Torr^{-1}$. Discharge initiated by 400 electrons released from 0.5 mm diameter disc on cathode.

back towards the cathode (the cathode-directed streamer). Calculations with the appropriate experimental data have given velocities of propagation of the cathode and anode directed streamers which are in very good agreement with the measurements of Chalmers et al[7] and Wagner[8].

For narrow discharges it has been found that very good agreement is obtained between experiment and theory when only primary ionization and secondary electron production at the cathode are considered. It is interesting to note, however, that using similar methods Kline[9] found that at large over-voltages it was necessary to incorporate the effects of photoionization for large radius discharges such as those produced by Koppitz[10].

TWO-DIMENSIONAL SIMULATIONS.

The one-dimensional simulations described above have the obvious drawbacks of assuming that the discharge radius is constant and that the charge densities are uniform over the cross-section. The next natural step is, therefore, to extend the method to two space dimensions x and r so that both the radial and axial development of the discharge can be followed, but retaining the plane parallel electrode geometry and making the assumption that the discharge is axially symmetric.

Here the conservation equations and boundary conditions corresponding to Equations (2a-c) and (3a-c) are

$$\frac{\partial \rho_e}{\partial t} = \alpha \rho_e W_e - a \rho_e W_e + \delta \rho_n W_n - \nabla \cdot (\rho_e \underset{\sim}{W}_e) \tag{5a}$$

$$\frac{\partial \rho_p}{\partial t} = \alpha \rho_e W_e - \nabla \cdot (\rho_p \underset{\sim}{W}_p) \tag{5b}$$

$$\frac{\partial \rho_n}{\partial t} = a \rho_e W_e - \delta \rho_n W_n - \nabla \cdot (\rho_n \underset{\sim}{W}_n) \tag{5c}$$

with $\rho_p(d, r, t) = 0, \quad \rho_n(o, r, t) = 0$ (6a, b)

and $$J_e(o, r, t) = J_o(r, t) + \gamma_i(r, t)J_p(o, r, t) + \Gamma_{ph}\int_0^d \int_0^{r_d} \alpha_{ex}(x, r', t)g(x, r', r)J_e(x, r', t)2\pi r'dr'dx \quad (6c)$$

where Γ_{ph} is the mean number of secondary electrons produced per photon incident on the cathode and g(x, r', r) is a geometric factor[11] representing the fraction of the photons produced at (x, r') which fall on unit area of the cathode at a distance r from the axis. In Equation (6c) for simplicity the lifetime Γ_{ph} of the excited states is taken to be zero. The electric field is found from the axially symmetric form of Poisson's equation

$$\frac{\partial^2\phi}{\partial x^2} + \frac{1}{r}\frac{\partial}{\partial r}\left(r\frac{\partial\phi}{\partial r}\right) = -\frac{\rho}{\varepsilon_o}, \quad (7)$$

where $\underset{\sim}{E} = -\nabla\phi$, with ϕ specified on the boundaries.

Typical results of this two-dimensional simulation are shown in Fig. 2 for the experimental conditions of Doran[12] who worked with N_2 at 300 torr with an electrode separation of 2 cm, a breakdown voltage of 25772V and a step function applied voltage waveform corresponding to an overvoltage of 7.56%. Once again the discharge was initiated by a pulse of about 400 electrons at the cathode. The simulated shutter and streak photographs of the cathode streamer phase of discharge development shown in Fig. 2 are in very good agreement with the experimental measurements and the contraction in radius as the cathode streamer approaches the cathode is clearly seen.

Analysis of Time-Lag Measurements

The one and two-dimensional simulation programmes have also been used to compute time-lags in air in order to see whether any discontinuity is

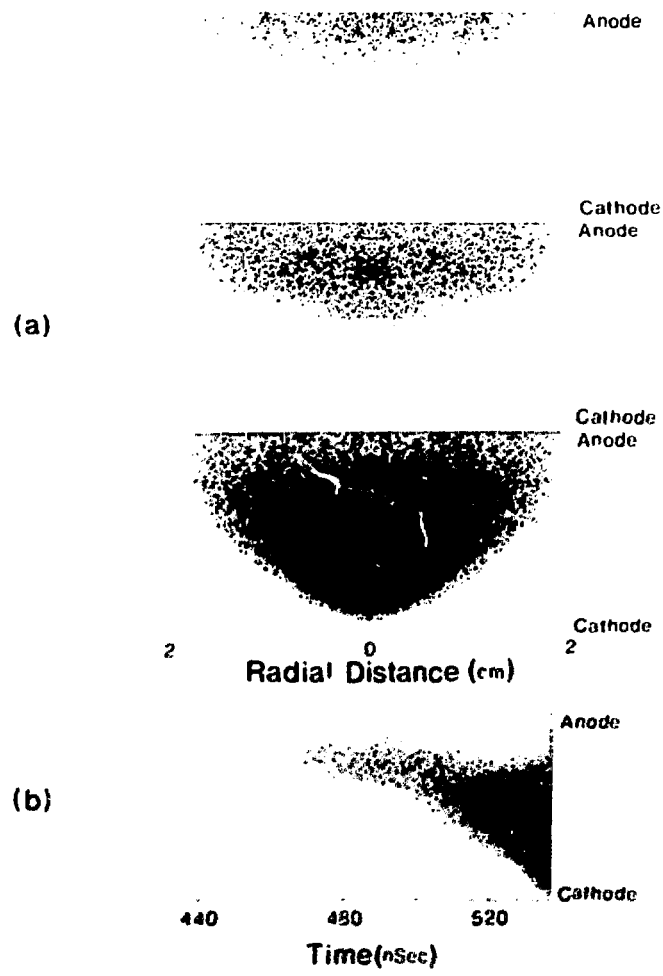

Fig. 2. Simulated photographs from a two-dimensional calculation for nitrogen, using the data of Doran[12]. The simulated shutter photographs (a) correspond to exposures from time zero up to 472, 513 and 536 ns respectively, while the streak photograph (b) displays the light passing through a narrow slit looking towards the axis of the discharge.

observable in the predicted time lag, t_f versus overvoltage curve as has been found by several workers including Crichton et al[13]. The latter measurements were made in dry air at a pressure of 500 torr using Bruce profile electrodes at a separation of 10 cm. Initiatory electrons were produced in the region of the cathode by ionizing radiation from a radioactive source 2mm below the centre of the cathode surface, the steady-state ionization current being of the order 10^{-11}A. Since the radioactive source was likely to give rise to bursts of electrons in the region of the cathode rather than a continuous stream, the computations were carried out for pulses of about 10 electrons although, as mentioned later, the effect of varying this number was investigated.

In the one-dimensional computations, the values of the ionization coefficients were taken from Dutton et al[14] and the time-lags were computed over the whole range of overvoltage (a) with the radius of the discharge equal to that of the initial electron pulse (~1 cm) and (b) with it equal to the effective radius of the electrodes (~ 10 cm). It was found that (a) gave good agreement with experiment at high over-voltages whereas (b) gave agreement at low over-voltages (i. e. long t_f), the transition being at time-lags of order of the electron transit time. The experimental result could thus be explained by an increase in the effective discharge radius for $t_f \gtrsim \tau_e$, corresponding to the spreading of the secondary electrons over the cathode surface. This change in radius could not be automatically followed by the one-dimensional computations, however, and it was therefore decided to check our conclusions by re-calculating the t_f overvoltage curve using the two-dimensional simulation programme.

The results obtained are shown by the solid curve in Fig. 3 which corresponds to t_f's calculated for pulses of 10 electrons leaving an area of about 3 cm^2 at the centre of the cathode. We see that good agreement is obtained at high and low overvoltages with a smooth transition between 3% and 4% overvoltage. As may be seen from Fig. 3, Crichton et al[13] found that any voltage in the transition region, the time lags fell into two distinct groups; one

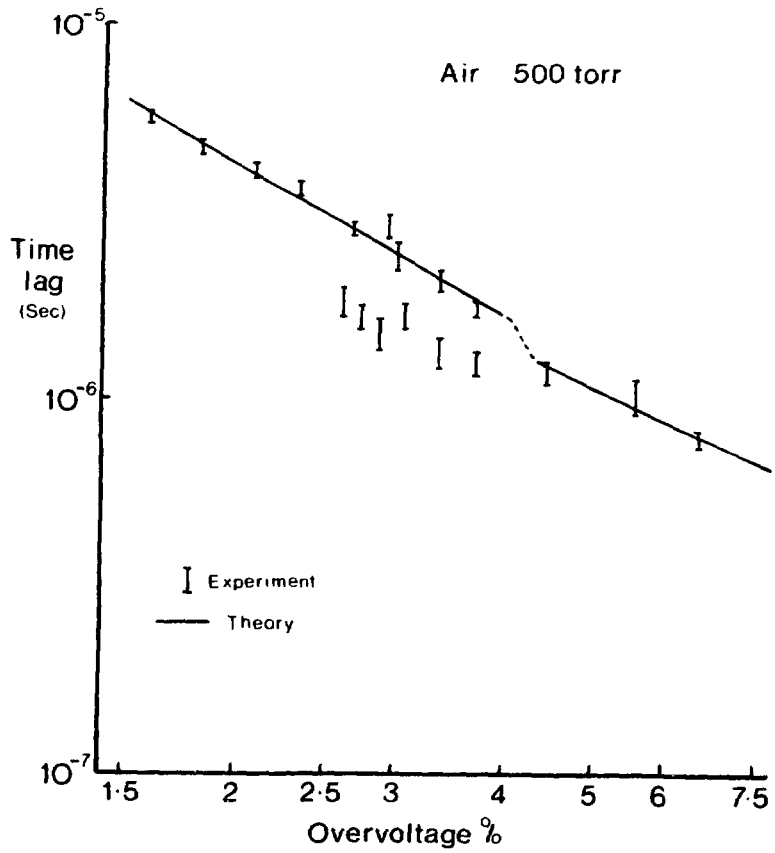

Fig. 3. Formative time-lags in air at 500 Torr, d = 10 cm. The experimental points are from Chalmers et al[7], while the curve is obtained from the two-dimensional simulation.

possible explanation is that these groups correspond to different numbers of initiating electrons. For example, in the simulations at 3% overvoltage, it was found that if the size of the initiating pulse was increased to about 100 electrons the lower values of t_f were obtained, the increase producing appreciable space charge effects within the first electron transit time, whereas space charge effects did not become effective until well into the second transit time for 10 initiatory electrons.

Time-lags were also computed in nitrogen for various experimental conditions but in no cases were any appreciable discontinuities in the t_f overvoltage curves predicted.

Non-uniform Electrode Geometries.

One of the main aims of our simulations was to investigate discharge growth in non-uniform field geometries (e.g. sphere-plane and rod-plane systems) which still, however, have axial symmetry. Considerable effort has been devoted to adapting the two-dimensional simulations to consider such cases. The biggest problem that is encountered is the highly localised high field region in the neighbourhood of the sphere or rod electrode. This field can be several orders of magnitude greater than the average applied field. It is highly desirable, therefore, to grade the finite difference mesh in both the radial and axial directions so that it is very fine in the high field region and more coarse in regions where the ionization processes are negligible. This procedure is fairly straightforward when integrating the charge conservation equations (5a - c) and, in this case, we have taken the axial mesh spacing to be inversely proportional to the primary ionization coefficient corresponding to the local value of the applied electric field. The radial mesh spacing increased in a simple geometric progression.

Since, however, in order to keep the computation times within reasonable limits, it is still necessary to use a direct method such as the Fast Fourier Transform algorithm due to Le Bail[15], to compute the field, the axial mesh must be of constant spacing when the field computations are carried out. This severely limits the accuracy of the computed fields in the high field region and eventually the calculations become unstable due to numerical errors. These problems could be overcome by returning to Successive Over-Relaxation (SOR) methods for computing the field when there is much more flexibility in varying the mesh spacing, but the increased computing times (by a factor of 10 approximately) make this prohibitive on a serial processing computer such as the CDC 7600 now used.

The advent of parallel processing computers, however, may change the situation completely during the next few years. International Computers Ltd., for example, are developing a Distributed Array Processor[16] which has 64 x 64

parallel processing elements and, although each individual processor is slow, the overall power of the machine is twenty times a CDC 7600 for SOR-type calculations, thus giving an effective increase in power of two for our problem, with greatly improved flexibility.

In our present simulations the Fast Fourier Transform technique has to be modified to consider irregular regions rather than the rectangular boundaries previously considered. In essence we follow the method due to Hockney[17], where an overall rectangular boundary is retained but the presence of the electrodes within the region is taken into account by placing a matrix of charges at the appropriate mesh points so as to produce the correct potential distribution on the interior boundaries. This so-called "capacity matrix" only has to be computed once at the start of the simulation and stored. In order to obtain a reasonable number of mesh points in the active region of the discharge, the field computations had to be performed in two stages, (i) over a coarse 128 x 40 mesh covering the whole region and (ii) over a smaller sub-region near the sphere or rod using the same number of meshes.

A problem that arises for negative polarity systems is the computation of the photon flux over the non-uniform field electrode. We have therefore initially restricted our attention to positive polarities where we compute the photon flux over the plane cathode using an identical method to that described[11] for the two-dimensional simulations in plane parallel systems.

Figs. 4 - 6 show preliminary results obtained for ionization growth in a sphere-plane system (sphere diameter 7.5 cm, gap separation 10 cm, plane cathode 60 cm radius, cylindrical walls at 60 cm radius) similar to that used in a parallel experimental investigation[18]. The initial conditions were taken to be a constant density of approximately 10^3 electrons cm^{-3} everywhere in space, with a step function impulse voltage equal to V_{50} being applied at time zero (the computations are easily modified to take into account any desired voltage waveform).

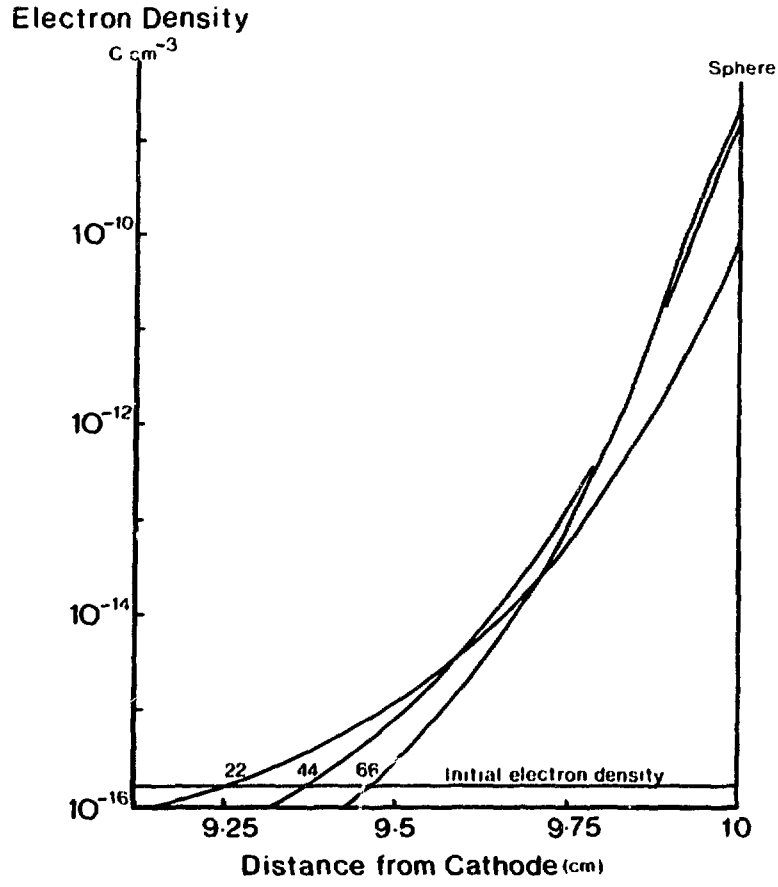

Fig. 4. Computed electron density along the axis of a sphere-plane electrode system at various times, indicated in ns on the curves.

We see in Fig. 4 the rapid growth of electron density near the anode surface which is quickly limited, by space charge effects and drift to the sphere, after about 50 nsec. The corresponding current growth curve is shown in Fig. 5, while Fig. 6 shows the contours of electron density in the neighbourhood of the anode, and we see how localised the active region of the discharge has become. Even though the field was calculated in a secondary region near the sphere and the maximum 128x40 mesh possible with the available computer was used to compute the fields, there were still only about 20 axial points in the region of ionization growth and the calculation failed after about 70 nsec due to the instabilities introduced by numerical errors. Work is in progress to improve the stability but, in the opinion of the authors, the use of parallel processing computers will provide the ultimate answer to the problem.

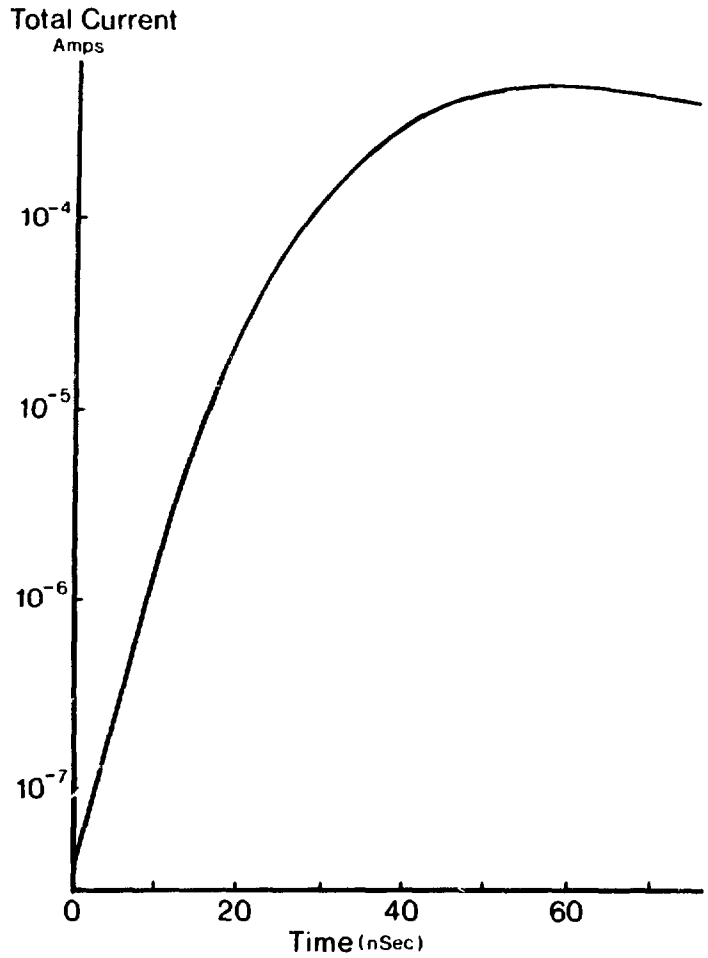

Fig. 5. Computed current for the sphere-plane system.

APPENDIX

List of Symbols

Independent of time for given set of experimental conditions:-

d	=	gas pressure
p	=	electrode separation
r_d	=	radius of discharge volume
g(x, r', r)	=	geometric factor for calculating photon flux
Γ_{ph}	=	photoelectric efficiency of cathode
V_s	=	breakdown potential
V_{50}	=	peak voltage of lightning-type impulse for which breakdown probability is 50%

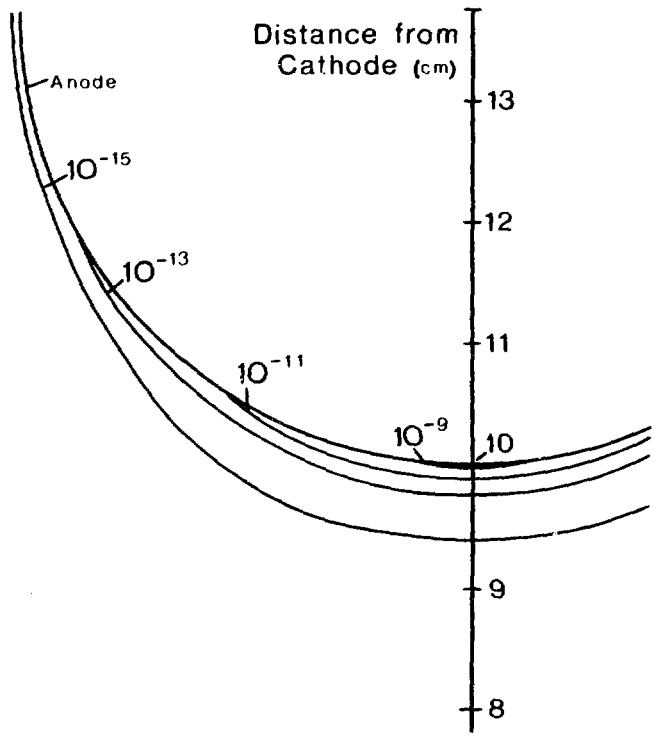

Fig. 6. Contour lines of equal electron density (indicated in C cm^{-3} on the curves) at time 66 ns, in the neighbourhood of the spherical electrode.

t_f = formative time lag

τ_e = electron transit time

γ_{ph} = photon secondary ionization coefficient

Dependent on t only

V_g = voltage across the discharge gap

Dependent on r and t only

γ_i = positive-ion secondary ionization coefficient

J_o = externally generated electron current density at cathode

Dependent on x, r and t

ρ_e, ρ_p, ρ_n = electron, positive-ion and negative-ion charge densities

J_e, J_p, J_n = electron, positive-ion and negative-ion current densities

$\underset{\sim}{W}_e$, $\underset{\sim}{W}_p$, $\underset{\sim}{W}_n$ = electron, positive-ion and negative-ion drift velocities

$\underset{\sim}{E}$	=	electric field
ϕ	=	electric potential
α	=	primary ionization coefficient
a	=	attachment coefficient
δ	=	detachment coefficient
α_{ex}	=	excitation coefficient

REFERENCES

1. A. J. Davies and C. J. Evans, Proc. IEE 114, 1547 (1967).

2. A. J. Davies, C. J. Evans and P. M. Woodison, Proc. IEE 122, 765 (1975).

3. A. Ralston and H. S. Wilf, Mathematical Methods for Digital Computers, Wiley, New York, (1960).

4. A. J. Davies, C. S. Davies and C. J. Evans, Proc. IEE 118, 816 (1971).

5. A. J. Davies, C. J. Evans and P. M. Woodison, Proc. IIIrd Int. Conf. on Gas Discharges, IEE, London, 119 (1974).

6. P. M. Davidson, Brit. J. Appl. Phys., 4, 170 (1953).

7. I. D. Chalmers, H. Duffy and D. J. Tedford, Proc. Roy. Soc. A 329, 171 (1972).

8. K. H. Wagner, Z. Phys. 189, 465 (1966).

9. L. E. Kline, J. Appl. Phys. 45, 2046 (1974).

10. J. Koppitz, J. Phys. D. 6, 1494 (1973).

11. A. J. Davies, C. J. Evans, P. Townsend and P. M. Woodison, Proc. IEE 124, 179, (1977).

12. A. A. Doran, Z. Phys. 208, 427 (1968).

13. B. H. Crichton, D. J. Tedford and P. Chalmers, Proc. IIIrd Int. Conf. on Gas Discharges, IEE, London, 100 (1974).

14. J. Dutton, F. M. Harris and F. Llewellyn-Jones, Proc. Phys. Soc. 81, 52 (1963).

15. [illegible], Use of fast Fourier transforms for solving partial differential equations in physics, [illegible] (1971).

16. [illegible], Numerische Mathematik 9, No. 2, 21 (1977).

17. [illegible], FOUT4 - a fast three dimensional Poisson solver for the rectangle with non-mixed boundary conditions and internal electrodes, [illegible] (1974), 1978.

18. [illegible], A. J. Davies, J. Duran and R. T. Waters, Proc. IVth Int. Conf. on Gas Discharges, IEE, Swansea, 141 (1976).

DISCUSSION

CHRISTOPHOROU: Your time lag versus overvoltage data show some distinct discontinuity. Is it genuine?

DUTTON (For DAVIES, et al.): The discontinuity has been observed in a number of experiments and is also given by the simulation with a constant number of initiating electrons, so I think there is no doubt that it is genuine.

THE BREAKDOWN OF GASES AT LOW PRESSURE

A.B. Parker

Department of Electrical Engineering and Electrons, University of Liverpool, P.O. Box 147, Brownlow Hill, Liverpool L69 3BX, England.

ABSTRACT

Although the Townsend theory of breakdown is generally accepted to apply at high pressure, difficulties arise at low pressure, because the long electron mean free path negates the definition of Townsend's primary coefficient α. The paper shows how the problem is overcome by considering the total electron multiplication M, between cathode and anode. A method of calculating M is given, as well as a theoretical estimate of . experimental values are also published for several gases.

INTRODUCTION

Gases may be changed from insulators to conductors by applying a sufficiently high voltage and this property has been of interest in engineering for many decades, both in its prevention and application [1]. The mechanism of this dielectric breakdown has been studied by many investigators [2], with the objective of relating it to basic atomic data such as, for example, ionisation cross-section values. It is generally agreed that a pre-breakdown current growth equation of the Townsend type can be used to explain breakdown at and to the high pressure side of the Paschen minimum [2].

This equation contains two basic coefficients, a primary coefficient (α) and a secondary coefficient (γ). The first is defined as the average number of electrons produced by a single electron undergoing ionising collisions in

unit distance of drift in the direction of the electric field. The secondary coefficient may represent all or some of several processes, e.g. the average number of secondary electrons produced by positive ion impact on the cathode; photo-emission from the cathode etc. The primary coefficient is related to the ionisation cross-section. Until recently, little effort [3,4,5] had been expended on considering the applicability of Townsend's theory to the low pressure side of the Paschen minimum, i.e. towards vacuum breakdown. No pre-breakdown current measurements had been reported, and only qualitative or semi-empirical models existed. In this pressure region, where the number density of atoms is low, there will be few electron-atom collisions. Hence, electrons cannot achieve a mean drift velocity, which is essential in the concept of Townsend's primary coefficients. Hence a new pre-breakdown current equation was needed. A desirable object is the derivation of values of the primary ionising coefficient from the ionisation cross-section of the gas atoms. Much effort has been devoted to such derivations at higher pressures [2]. Thus it is seen that there are three parts to the investigation of breakdown, the obtaining of the Paschen curve; the measurement of pre-breakdown current and an adequate theoretical model connecting basic atomic data with breakdown voltages via ionisation coefficients. In the following sections, apparatus for carrying out the experimental work is first described briefly and then the appropriate theory formulated.

EXPERIMENTAL TECHNIQUE

Two discharge chambers have been used in the investigation, the second being identical in design and form, but with all important linear dimensions twice those of the first. The first chamber has been fully described previously, and the second only will be considered. The earlier version had an upper voltage limitation of 10 kV, whilst results have been obtained up to 30 kV with the larger chamber.

The main practical problem which besets experiments on low gas pressure breakdown is the existence of the so-called 'long-path' breakdown, i.e. the breakdown voltage decreases as the path increases. A direct consequence is that a small clearance must exist between the electrodes and the enclosing chamber walls. After several electrodes had been tried, the most successful model proved to be a modified version of that first suggested by Schonhuber [6]. The electrodes are plane ended cylinders, which fit closely in a precision bore boro-silicate tube 15 cm long with a clearance of 0.25 mm. A direct consequence of such a close fit was the flow of wall currents between cathode and anode, which was larger than the pre-breakdown currents. The method of eliminating these wall currents is illustrated in Fig. 1.

It is seen that the anode is split into two sections viz an outer cylinder connected to earth and an inner cylinder which is isolated from the inner by small ruby spheres. Thus leakage currents are conducted away, and do not add to pre-breakdown current. A linear motion drive allows the electrode separation to be varied.

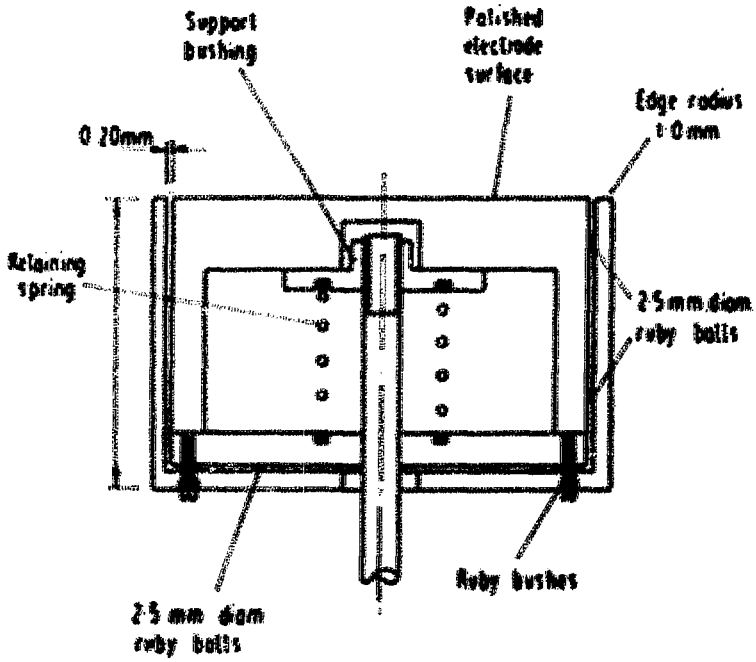

Fig. 1 Split Anode to Eliminate Wall Currents

Conventional ultra high vacuum techniques are used to attain a base pressure of less than 10^{-7} Pa, with a leak rate of less than 10^{-5} Pa S^{-1}; operating pressures were measured with a Baraton pressure gauge.

Conventional high voltage sources and measurement techniques were used. The divider system and 'kicking-off' circuit allowed voltage differences of 0.1 volts to be detected over the range of operating voltages used.

Both vibrating reed electrometers and x - t recorders were used in the low current measurements.

As usual with such experiments, reproducible results were obtained only when the vacuum chamber, its contents and system were properly processed, i.e. the electrodes were ultrasonically cleaned before assembly and were conditioned by a glow discharge before measurements were started.

EXPERIMENTS AND RESULTS

In all the experiments involving breakdown measurements, the validity of Paschen's law was tested by determining values of breakdown voltages over a range of electrode separation for several pressures. The pre-breakdown currents were measured for a set of electrode separations, for various values of E/N, again for several pressure values.

Fig. 2 shows breakdown curves for the smaller chamber for several gases, whilst Fig. 3 shows results for the same gases with larger chamber. It is to be noted that the results shown are only a selection of those obtained, as both the cathode and anode material affects the breakdown voltage.

Typical sets of pre-breakdown currents are shown in Figs. 4 and 5. Again, both the anode and cathode affect these values for any gas.

Analysis of such current-distant curves is straightforward at higher pressures, where an initial linear portion enables the calculation of Townsend's α, and

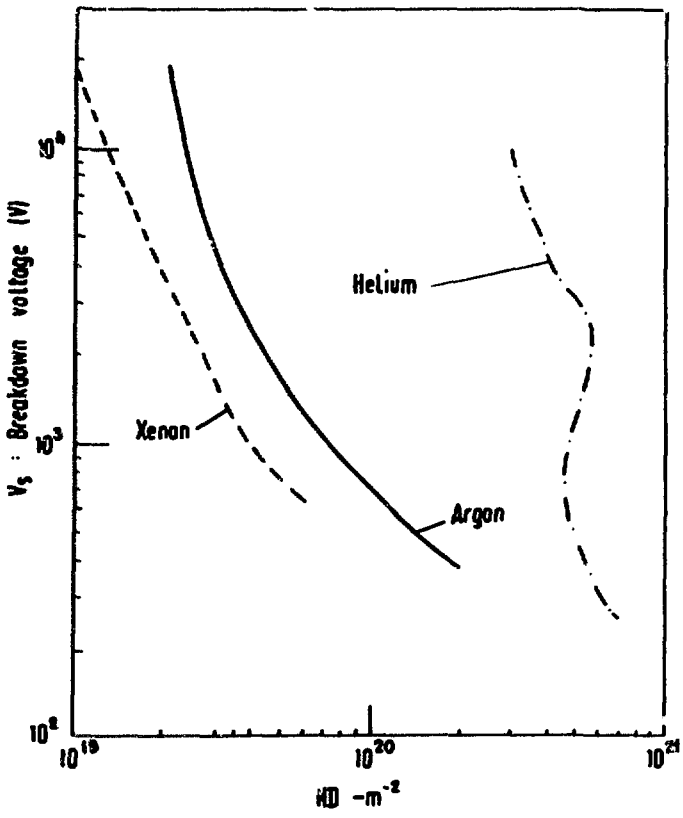

Fig. 2 Paschen Curves with Small Chamber

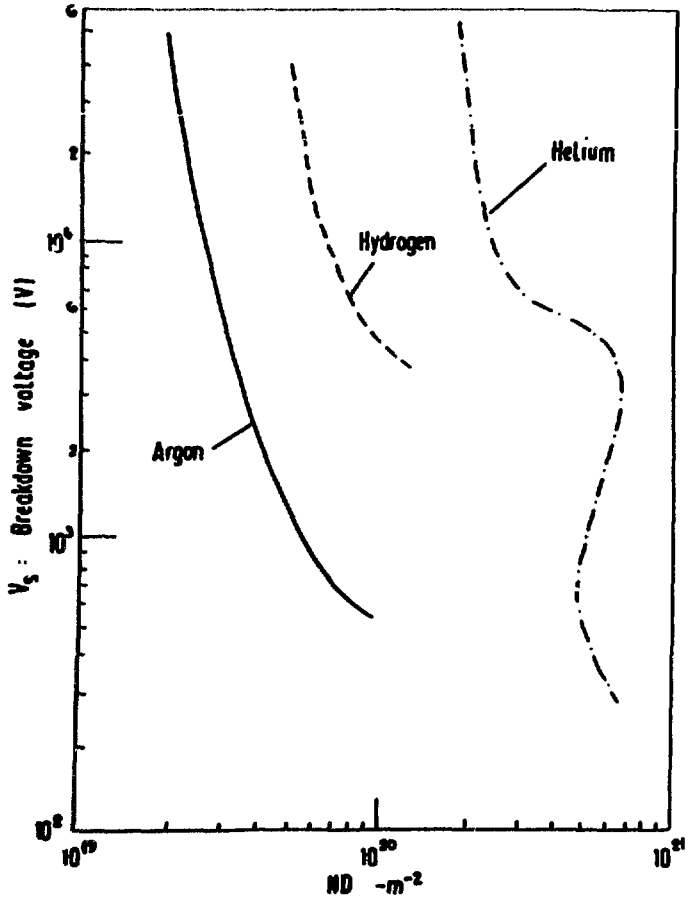

Fig. 3 Paschen Curves with Large Chamber

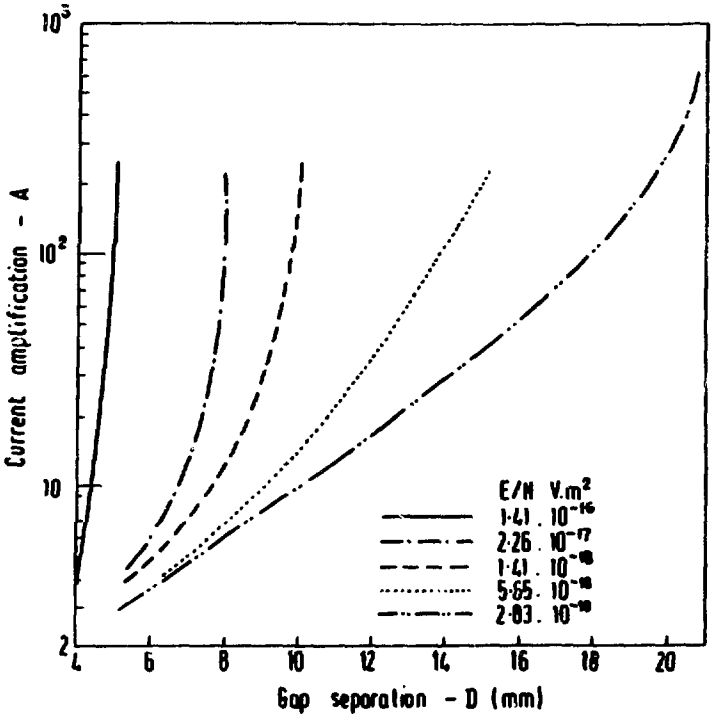

Fig. 4 Pre-breakdown Current - Small Chamber

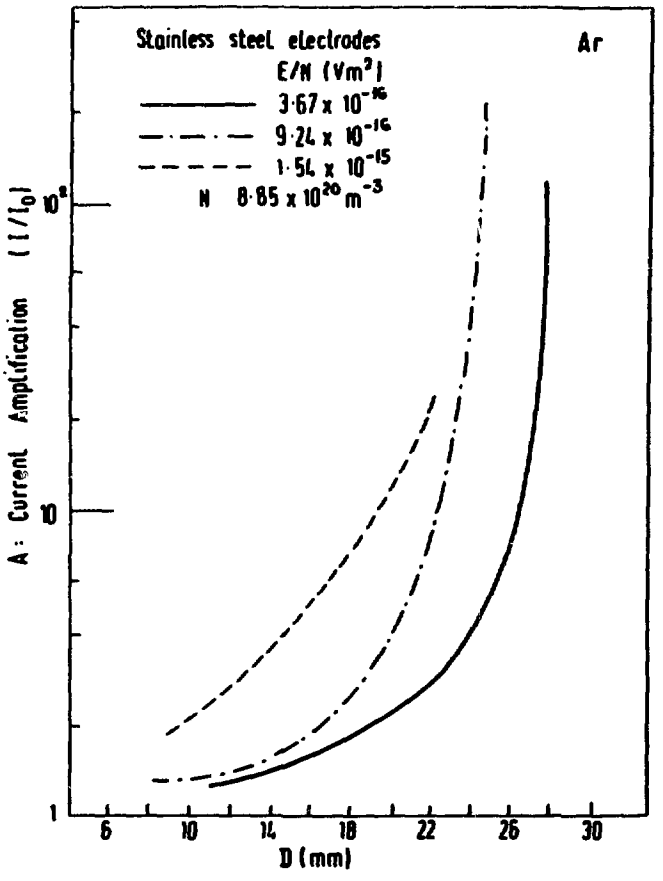

Fig. 5 Pre-breakdown Current - Large Chamber

the later non-linear portion gives a value of γ. It is seen that no linear region exists in Figs. 4 and 5. However, it has been shown [5] that by using both the Paschen and pre-breakdown curves, it is possible to calculate values of both M and γ at low pressures. Typical theoretical values of the multiplication factor M are shown in Fig. 6. The main features to note are that the coefficient varies with the product (ND) as well as with E/N. It is also interesting to note the low values compared with the electron multiplication attained at lower values of (E/N). The corresponding curve for the secondary coefficient γ is shown in Fig. 7. These coefficients for several gases have been reported in earlier publications for the smaller chamber [4].

In a more recent publication, the results have been presented for argon at even higher values of (E/N) [5]. A new difficulty arose under these conditions; the values of M become even smaller and γ larger. Then the method [5]

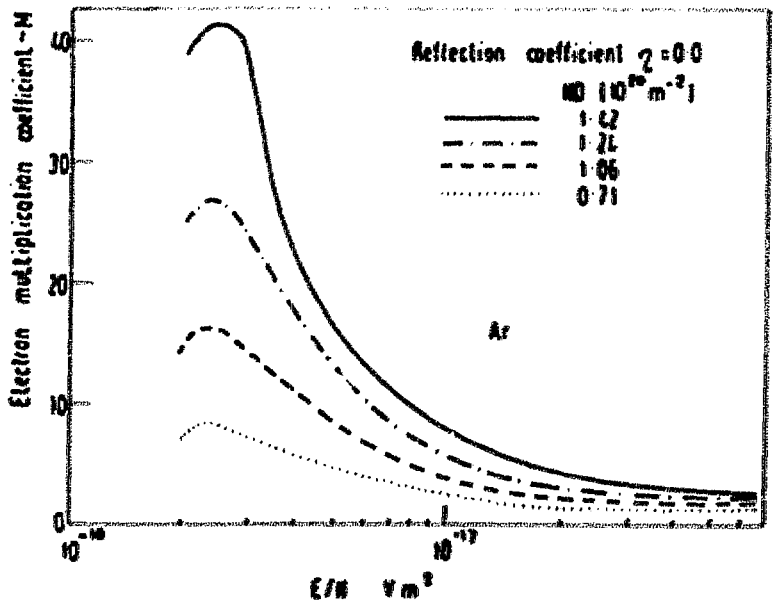

Fig. 6 Values of Measured Electron Multiplication M

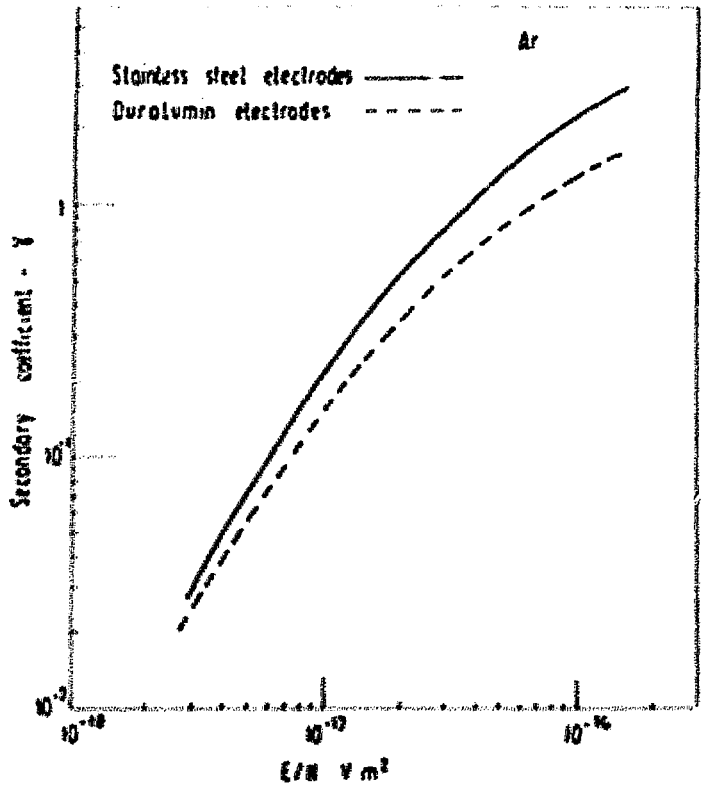

Fig. 7 Values of Secondary Coefficient - Small Chamber

of analysis of the current electrode separation curve makes accurate estimation of the ionisation coefficients impossible. The only solution to this difficulty appears to be that the coefficient M must be calculated theoretically, and the values of the coefficient $\bar{\gamma}$ then derived from the current-separation curves. This is justifiable, because measured and theoretical values of M agreed in the experiments with the smaller chamber, as will be shown later. When this operation is carried out, it is found that the coefficient $\bar{\gamma}$ is not only dependent on (E/N) but also on D. Values of $\bar{\gamma}$ calculated in this way are shown in Fig. 8. It is seen that in all cases, the secondary coefficient increased with electrode separation. As calculated values of the coefficients M were essential to analyse the pre-breakdown current wave forms, it is convenient to outline the method of their calculation at this stage.

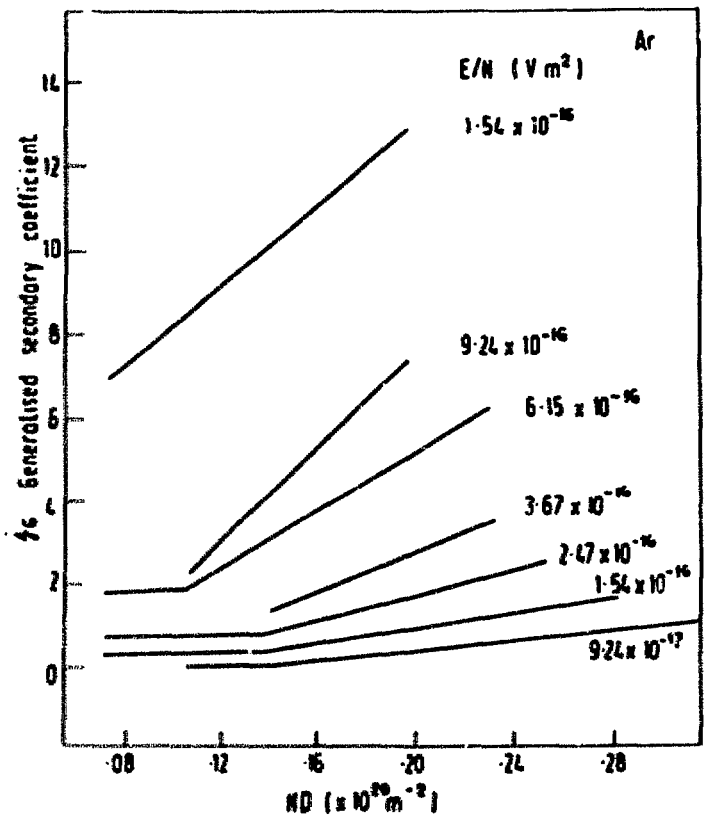

Fig. 8 Values of Secondary Coefficient - Large Chamber

THEORY

A full account [3] has been given of the method used to calculate the coefficient M for any gas from its ionisation cross-section using a Monte Carlo (random walk) computer program. The basis of the program is the simulation of the movement of test electrons along the electric field. It is assumed that the only collisions which occur are ionising, and also that electron movement is forward only, i.e. a one dimensional model. The gap D is divided into 1000 equal cells, and the ionising collision probability is calculated for each. A store of test electrons is set up at the cathode, and each is moved towards the anode, in turn. The probability of ionisation for the electron is summed and compared with a pseudo-random number at a predetermined value of the accumulated probability. If the random number is less than the accumulated probability, then it is assumed that an ionising

collision has occurred. Otherwise no collision occurs and the probability is taken to zero. The initial electron is then taken along its path to the anode, tests on collision being taken as it travels. All the initial electrons and their progeny are processed in this way. Electrons backscattered from the anode are also taken into account, as a substantial fraction can be reflected with a range of energies. Thus the overall multiplication M of the electron by ionisation can be calculated. It is interesting to note that for the larger values of M reported, the number of test electrons was 100. In the later work when $M \lesssim 2$ it was necessary to use a considerably larger number of test electrons to get meaningful results. For the smallest values of M, the quantity had to be increased to 10,000 electrons. The electron energy distribution at the anode is shown in Fig. 9. The values of M calculated always agreed with those obtained from the experimental pre-breakdown currents within experimental accuracy.

A similar computer program has enabled the calculation of the secondary coefficient γ by the simulated motion of the positive ions. Then charge exchange and ionisation by positive ions have been assumed as two important processes as well as release of secondary electrons from the cathode bombardment. Reasonable order-of-magnitude agreement has been achieved with the experimental values of the secondary coefficient.

DISCUSSION

It has been demonstrated that a new pre-breakdown current equation can be used to determine two ionisation coefficients, the total electron multiplication M, and the secondary coefficient γ, for pressures approaching 10^{-2} torr, and voltages as high as 30 kV on the low pressure side of the Paschen minimum. A computer program to calculate M from ionisation cross-sections has been developed. Thus a satisfactory theory of pre-breakdown has been formulated for this low pressure region between gas breakdown and vacuum breakdown. Some extra points of interest will now be indicated.

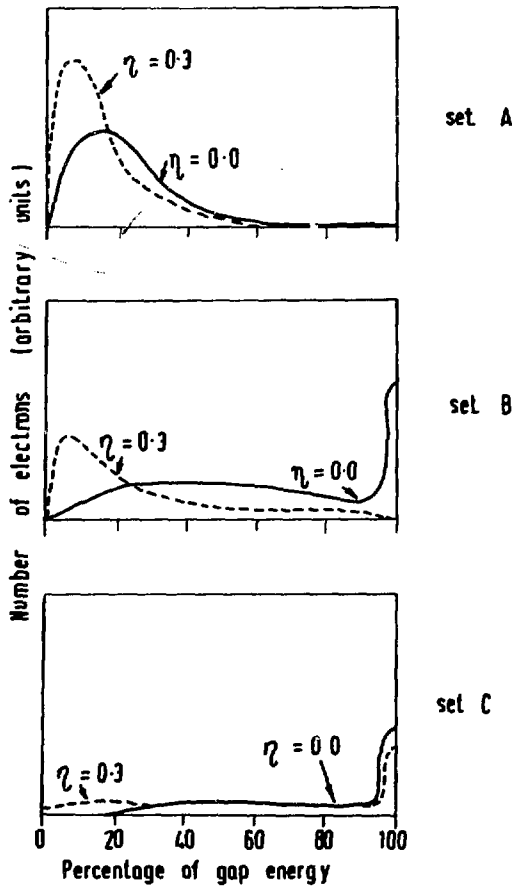

set	E/N (V m^2)	Full gap energy (eV)
A	$8{\cdot}49 \times 10^{-18}$	780
B	$2{\cdot}83 \times 10^{-17}$	1133
C	$5{\cdot}66 \times 10^{-17}$	1703

Fig. 9 Electron Energy Distribution at Anode - Theoretical

For each chamber a limitation of usage was reached. This happened when spurious bursts of current made the measurement of pre-breakdown current impossible. The value of electric field at which the effect was observed was only 10^4 volts/cm. However, this effect must have been due to some form of field emission, probably enhanced by ionisation of gas atoms. It is just possible that this may also contribute to the secondary mechanism. The latter needs further investigation.

It is interesting to speculate on possible future work. For example, it is obviously possible to calculate the coefficient M for several other gases. However, a search of the literature shows that very few values of ionisation cross-sections have been reported for electron energy above 20 keV. It might be possible to calculate such cross-sections from atomic theory. It is desirable to operate at lower pressures in order to approach even closer the region called vacuum breakdown.

Finally, work has already started on time lag studies. It is hoped that this will give more information on the nature of the secondary effect.

ACKNOWLEDGEMENTS

It is necessary to thank the Science Research Council for their financial support of this work.

The essential contributions of Dr. P.C. Johnson, Dr. J.D. Pace and Dr. D. Bhasavanich, is also acknowledged.

REFERENCES

1. J.D. Cobine, Gaseous Conduction.

2. F. Llewellyn Jones, Ionisation and Breakdown in Gases.

3. A.B. Parker and P.C. Johnson, Proc. Roy. Soc. A, 511, 325 (1971).

4. J.D. Pace and A.B. Parker, J. Phys. D.6, 1525 (1973).

5. D. Bhasavanich and A.B. Parker, Proc. Roy. Soc. A, 385, 358 (1978).

6. M.J. Schönhuber, Inst. Elect. Eng. Electra Trans. PAS 88, 100 (1969).

DISCUSSION

CRANBERG: In the energy region of 50, how much uncertainty is contributed by the assumption of only forward scattering, and whatever assumptions were made regarding the division of energy between the two electrons?

PARKER: The assumption of forward scattering is not unreasonable under the conditions considered, i.e., where the electron energy at a maximum is high -- usually of the order of 100 eV. I believe there is certainly some evidence supporting this for helium.

It is assumed that the energy of the colliding electron is shared equally between both the original and resultant electron, after allowance is made for the energy needed to ionize the atom.

CHAIRPERSON: I might be make a comment and then ask a question.

Comment: At low energy and beyond, the ionization cross sections should be given sufficiently accurate by the Born approximation calculations.

Question: Have you tried this analysis for something like Cs? In this case one may observe structure in the Q vs. E/M functions.

PARKER: I agree that the Born approximation could be used above 20 keV, but it would still be a good thing if experimental values were available.

We have not attempted to determine Q for Cs as yet. However, I see no reason why it could not be done, and would certainly be willing to carry out such a calculation.

SHARBAUGH: I would like to encourage Dr. Parker to continue his attention to the long-neglected low pressure regime to the left of the Paschen minimum. As he bridges the gap between very high vacuum regime and the present case, there will be a point where the metal vapor produced by the vacuum arc will come into prominence. I think it is generally forgotten that a so-called "vacuum" breakdown involves transient pressures of metal vapor atoms which may approach that of atmospheric values. So such a breakdown is not so different from "gaseous" breakdown as we might expect.

EXPERIENCE IN DESIGN AND TESTING OF GAS-INSULATED SYSTEMS

By J. C. Cronin

Gould Inc.
Power Systems Division
Greensburg, PA

ABSTRACT

The dielectric capability of SF_6 insulated systems is reviewed and compared with today's design practices. It is found that there is some potential for increasing impulse stress limits but that one minute power frequency factory test stress levels are already close to the limit. There is increasing interest in long term 50/60 Hz performance and results to date indicate very high stress levels can be maintained indefinitely. Contamination is a serious problem, particularly with insulators, but field conditioning techniques can help deactivate particles. Results to date on the voltage-time characteristics of SF_6 are contradictory and more work must be undertaken. D-c performance is important because of field testing requirements and the possibility that trapped charges will sometimes impose a d-c voltage on the system.

INTRODUCTION

In recent years there has been increasing use of compressed gas insulation for both power switching stations and power transmission lines. The technology has rapidly moved from the status of being considered novel and experimental, to one where feasibility and reliability have been demonstrated. Increasingly, the decision to use a compressed gas insulated system is made on the basis of economic considerations and consequently much of the industrial R&D effort is devoted to expanding the application range and reducing cost. In the switching station area there are installations at all levels in the voltage range 145 kV through 550 kV and the basic R&D effort has been concluded at 800 kV[1]; work is now starting on 1200 kV systems.

The upsurge in application of commercial gas insulated systems has been accompanied by a parallel and equally intense effort in the basic R&D area. Numerous papers have appeared during the past ten years and considerable progress has been made towards identifying, in a quantitative manner, the factors controlling and limiting performance. Ultimate dielectric capability is being explored so that more economical designs can be developed, particularly at the higher voltage levels. The influence of conducting particles (contaminants) has been studied extensively and attention is now focussing on control techniques. Voltage-time characteristics are being explored so that insulation coordination can be improved. Insulator design has also received considerable attention with most of the efforts being directed towards making the designs more tolerant of contamination. Overall, a considerable volume of information has been generated and there is now a need for efficient correlation so that trends and interdependencies can be discerned and the most productive directions for future work identified.

SYSTEM VOLTAGES

Prior to reviewing the status of work in the various areas it is desirable to consider the types of voltage to which equipment will be subjected in normal service.

Steady State Voltages

Power Frequency

Power frequency voltage imposes the normal steady state dielectric stress and must be a prime influence in establishing the long term reliability of the system. One minute withstand tests are applied in the field. The long term exposure occurs during field conditioning (to move particles into low stress areas) and involves holding the voltage for perhaps hours at a number of levels up to, and perhaps including, the field test level (75% of factory test level[2]). There is no generally accepted conditioning procedure and manufacturers usually recommend a procedure for their equipment.

At 145 kV the short term (factory) test voltage is 1.7 times the service voltage but this ratio decreases fairly continuously at higher system voltages, reaching 1.9 at 800 kV. This situation arises because test voltages are determined by impulse levels rather than operating voltage levels. The practical significance is that more attention must be directed to continuous dielectric stresses at higher system voltages and, in fact, the latter may become dominant in determining system dimensions.

D-C Voltage

In addition to continuous power frequency dielectric stresses there is also a probability that d-c voltage stresses may be imposed on the system due to trapped charges following line dropping. The duration of the d-c voltage is difficult to predict as it depends on a number of system parameters which differ from utility to utility. However, in systems where cables are used, the d-c voltage can exist for several hours with an initial amplitude that can equal, or exceed, peak line to ground voltage.

D-c voltage is occasionally used to field test gas-insulated systems but the technique is considered severe and interpretation can be difficult.[3] However, there may be no other choice when a suitable power frequency test source is not available and/or the utility has a trapped charge situation. In particular d-c is the only practical way to test long gas insulated cables due to charging current limitations on portable 60 Hz test sets. Therefore, despite the somewhat controversial nature of d-c testing, it cannot be ignored when defining the dielectric capability of gas insulated systems.

Transient Overvoltages

In defining the capability of gas insulated systems the impact of transient overvoltages must also be considered. While power frequency dielectric studies are increasingly concerned with predicting the mean time to failure at some continuous dielectric stress the transient overvoltage studies focus on establishing the probability of failure when short term overvoltages are applied (infrequently) during the life

of the system.

Impulse

Impulse overvoltages occur because of lightning strikes on connected overhead lines. The amplitude and waveshape of the overvoltages appearing in the gas insulated equipment depend on a number of parameters and the subject is too complex to treat here.[4,5] However, because of lightning arrester characteristics and reflections at discontinuities (open switches, etc.) the most severe overvoltages are caused by steep front waves. This gives rise to interest in the voltage-time characteristic as an increase in dielectric strength at short times to crest may have a favorable impact on insulation coordination.

At the present time the impulse withstand levels used at the various system voltages are as follows.

Table I. Impulse Insulation Levels in Range 145 kV through 800 kV

System Voltage, kV (rms)	145	242	362	550	800
Impulse Insulation Level, kV	650	900	1050	1550	1800

It is easily seen that the impulse to 60 Hz ratio decreases as system voltage increases, emphasizing that long term 60 Hz stresses may become dominant at the higher voltage levels.

Switching Surge

Switching surges can be expected to occur fairly frequently but are generally not considered as serious a threat to the insulation system as steep front lightning surges. This is because the slow wavefronts eliminate reflected wave problems and the surge arresters are able to limit the overvoltages to well defined and predictable levels.

DIELECTRIC STRENGTH OF SF_6

In the preceeding section the various types of voltage that can impinge on gas insulated systems have been identified. When relating these voltages to the dielectric strength of gas insulated systems it is appropriate, and less confusing, to initially consider the voltage

types separately and to explore the factors which can influence performance. However, once dielectric strength data has been developed an integrated approach must be followed to allow practical design limits to be proposed. When reviewing dielectric strength data it is also essential to remember that equipment designers are generally interested in consistent withstand levels whereas researchers tend to be more interested in flashover levels. This does not normally present a problem as long as flashover studies generate statistical information which allows withstand levels to be predicted.

Area Effect

During early dielectric studies on SF_6 very high strengths were frequently measured due to the use of relatively small area electrode systems. The subsequent development of transmission lines and station components showed these high strengths could not always be achieved and led, for a period of time, to a significant interest in the influence of electrode area on performance. In the early 1970's Gould conducted an extensive correlation of both published and in house test data and concluded the influence of area could be ignored once the area of the most highly stressed electrode exceeded approximately 6000 square cm. A much more comprehensive, statistically oriented, study by Nitta et al[6] resulted in essentially the same conclusion. Therefore, there is no problem applying test results generated with reasonably sized laboratory samples to practical systems.

Intrinsic Strength of SF_6

While the ultimate dielectric strength of SF_6 is never approached in commercial systems it is of interest because obviously it gives a measure of how much the technology could (theoretically) be exploited. There is fairly general agreement that the limiting dielectric strength is described by the equation:[7,8]

$$(E/P)_{out} = 89 \text{ (kV/cm. atm)}$$

where

E = Maximum stress in kV/cm

P = SF_6 pressure in atmospheres (absolute)

Most systems are designed to operate in the range of 3 through 4.5 atm so the theoretical maximum strength should lie in the range 270 through 400 kV/cm. However, these stress levels can only be achieved with small, highly polished electrodes and test results with larger area systems show a 0.5% flashover probability in the range 150 through 200 kV/cm.[6] If the intrinsic strength could be achieved in practical apparatus a 550 kV, 1550 kV BIL system could be contained in a 21 cm (8 inch) diameter enclosure, compared to the approximately 50 cm (20 inch) diameters now used.

50/60 Hz Strength of SF_6

Short Term Performance

In clean coaxial systems with normal (extruded) electrode surfaces flashover stress levels of from 90 kV (rms)/cm at 2.5 atm to 110 kV (rms)/cm at 4 atm can easily be achieved. Generally, consistent one minute withstands can be observed by reducing stress a few percent below the flashover level. These levels were established in a 27 cm/11.5 cm coaxial system approximately 250 cm long and agree well with the results of Hogg et al[9]. Increased dielectric strength can be obtained at higher pressures but this tends to be somewhat academic as pure SF_6 liquefies at temperatures below $-30^{o}C$, when pressure exceeds 5 atm. In addition there is also a tendency for the dielectric stress-pressure relationship to level off and it becomes increasingly more difficult to take advantage of higher pressures by operating at higher dielectric stress.

In most of the gas insulated systems built to date 60 Hz factory test stresses lie in the range 65 kV (rms)/cm. through 90 kV (rms)/cm. The specific level depends on gas pressure and the design criteria (including degree of cleanliness) imposed by the various manufacturers. The margin between factory test stress and demonstrated maximum capability is only 20% and there is therefore no significant potential for reducing size by designing to higher factory test stresses.

Long Term Performance

While good one minute performance is very important, the predicted time to failure under much lower operating stress is of prime importance when determining system reliability. Work in this area has been very limited because of the difficulty involved in making meaningful tests. Invariably, the tests involve measuring times to failure at relatively high dielectric stresses and using statistical techniques to extrapolate the results to the 30 year lifetime associated with practical systems. Bortnick[10] concludes that at 3 atm stresses as high as 100 kV/cm can be tolerated indefinitely but it is not clear if this is on an rms or peak basis. The work of Cooke[11] also indicates that very high stress levels can be sustained but the conclusion is based on d-c testing. Brown et al[12] conclude that system length is also a factor in determining long term reliability and their approach can be used to calculate a 0.1 probability of failure (in 20 years) if stress is limited to 81 kV (rms)/cm.[13] The maximum steady state stress in the installations built to date is approximately 35 kV (rms)/cm. So there is obviously potential for increasing working stress levels. However, it must also be emphasized that more consistent experimental data, with better theoretical interpretation, is needed and the influence of contamination must be considered more carefully.

Contamination

It is well known that conducting particles can reduce the dielectric strength of SF_6 and this subject has been studied exhaustively during the past ten years. Numerous publications have appeared detailing what appears to be an endless list of experiments involving particle shapes ranging from fine dust to spheres to relatively long wires. (It is not intended to review the literature in detail and a good summary of current thinking may be found in references 14 to 16.) Work has involved calculating liftoff stresses, measuring flashover levels, evaluating the influence of gas pressure and investigating particle deactivation techniques. All studies agree that particles reduce dielectric strength with the long needle type particles being most severe;

dielectric strength can easily be reduced to 10% of the uncontaminated value, causing flashovers well below operating voltage. It is difficult to see why there has been so much emphasis on needle type particles as these can be detected by even the most elementary quality control techniques and removed from the system. Small particles are more difficult to detect and are much more likely to be encountered in practical systems. Sensitive partial discharge measurements are always made on each section shipped and this helps detect even small particles.

Experiments with a variety of shop floor type contaminants have confirmed that 0.5 inch long slivers of aluminum can easily reduce dielectric strength by 50% while small particles reduce strength by 25%.[17] These are significant reductions and it is obvious that sections must be relatively clean to tolerate the factory test voltage, which of course emphasizes its value as a quality control technique.

In recent years attention has also been directed to particle motion and contamination control techniques.[13] It has been shown that even large particles can move along the enclosure at voltages well below operating voltage and that particles can be directed to, and sometimes contained in, low stress areas. This is the basis for the conditioning sequence frequently used during field testing. There is no general agreement on the best combination of voltage and time for effective field conditioning and this is an area worthy of future study.

Insulated Coatings

Early d-c work with coaxial systems suggested an increase in dielectric strength could be obtained by applying an insulating coating to the electrodes.[18] During the course of various research programs the influence of coatings was explored and no significant benefit was found when applying 60 Hz voltage to a clean system. The results of tests at 2 atm are summarized in Table 2.

Table 2. Evaluation of Dielectric Coatings on Conductor of Gas Insulated System

COATING	BARE	EPOXY (.006")	EPOXY (.01")	EPOXY-VINYL (.125")	TEFLON TAPE (.003")	ANODIZE (.001")
Flashover Stress kV (rms)/cm	93	93	93	85	95	101

The best performance was obtained with the hard anodize but the improvement is somewhat marginal and it is doubtful if the added cost could be justified. At a pressure of 4 atm the six mil epoxy coating gave a 13% improvement in performance but no benefit was observed with the ten mil epoxy coating. More refined experiments would help clarify the situation but it is obvious that no spectacular improvements in performance can be anticipated.

When a fifteen mil epoxy coating was applied to the enclosure the flashover stress increased by 8% but, again, this improvement is hardly enough to justify the added cost and complexity of a coating. During studies of particle motion it was observed that a dielectric coating on the enclosure tended to reduce particle mobility but that particles could still be deposited on the insulators. Therefore, while coatings can be beneficial they are not a universal solution to the contamination problem.

Impulse Strength of SF_6

In systems without insulators there is fairly good agreement between various investigators on the impulse performance levels that can be achieved. Generally the negative polarity flashover level is lower than positive polarity and negative is therefore the dominant influence in system design. In the range 3 to 5 atm the 50% flashover stress varies from 200 kV/cm. to 280 kV/cm. and the standard deviation is less than 5%.[9] Therefore, consistent withstands can be obtained in the range 180 kV/cm. to 250 kV cm. and this conclusion is also supported by the work of Ryan et al.[19]

The systems built to date appear to have maximum impulse stresses of less than 190 kV/cm. (at 4 atm). Extensive test experience has been

accumulated at 175 kV/cm. on a great number of components and generally no flashovers are observed during a forty shot test series. This implies the mean flashover stress is at least two standard deviations above the withstand stress and the results are consistent with those reported above. There is a good chance that design stress levels could be increased and 220 kV/cm. would not seem unreasonable for systems operating at 4 atm.

When specifying impulse (or switching surge) levels it is well to consider that the test technique has a significant influence on determining what is meant by withstand level. The IEC standards call for fifteen applications of voltage and allow two failures. Some users specify forty applications of voltage and allow only one failure. Obviously, the forty application test is more severe and both techniques are more severe than the three by three or five by five test procedures sometimes used.

Previously, it was reported that the intrinsic strength of SF_6 was 89 kV/cm-atm and this gives a theoretical capability of 356 kV/cm. at 4 atm. Obviously, this level is not even being approached and there may be potential for improvement in this area.

Volt-Time Characteristic

More efficient insulation coordination can be achieved if complete information on the voltage-time characteristic of the insulation system is available. To date is has generally been assumed that the characteristic is essentially flat for impulse voltages and that no upturn in strength occurs for front times less than one microsecond. This conclusion was supported by the work of Ryan and Watson[20] but more recent work by Taschner [21] shows an appreciable upturn below two microseconds. According to Taschner the 50% flashover strength can increase by 15% at one microsecond and 30% at half a microsecond. Nitta et al[22] previously came to a similar conclusion but as they investigated relatively non-uniform fields the findings were not too surprising. However, Taschner used a coaxial geometry and further experimental work is obviously needed.

Contamination

In systems without insulators the impulse strength is not affected by contamination unless the particles are large enough to disrupt the dielectric field at the enclosure. However, when insulators are involved the situation is very different and this will be discussed later.

Switching Surge

Switching surge behavior is very similar to impulse and most designers assume the switching surge withstand level will be some constant fraction of the impulse level. Experience indicates consistent switching surge withstands can easily be achieved at 85% of the impulse level and this is in agreement with the findings of Taschner[21] and Hogg et al[9]. However, Ryan and Watson[20] have established a 70% of impulse relationship for both the flashover and withstand levels and the reason for the disagreement is not obvious.

Switching surge tests in clean gas insulated systems show none of the scatter normally observed during tests in air. This is because the fields (in gas insulated systems) are quasi uniform and the highly non-uniform fields associated with high voltage air insulated equipment are not encountered. Standard deviation is generally below 5% while Ryan and Watson[20] have measured 3%.

D-C Voltage

A substantial volume of work has been published on d-c performance but it is not proposed to review it in detail; references 23 to 25 summarize the current status. In very clean systems the d-c flashover stress is almost equal to the power frequency flashover stress (on a voltage peak basis) but more typically the d-c level equals the power frequency rms level.[3]

The great problem with d-c is that particles lift off the enclosure at very low stresses and proceed with high velocity to impact on the conductor and insulators. Positive polarity seems to concentrate particles on the insulators while negative polarity favors the conductor.[13] The great difference between 60 Hz and d-c can be appreciated by con-

sidering that with 60 Hz particles begin to move at an enclosure stress of 1 to 2 kV (rms)/cm. and have still not lifted very far above the enclosure at 6 kV (rms)/cm; with d-c, particles can impact on the conductor and insulators at stresses as low as 2 kV/cm.[13]

The character of particle motion under d-c makes it impossible to condition a system by moving the particles into low field areas; in fact one d-c system was conditioned with 60 Hz.[25] Even when 60 Hz conditioning is undertaken particles can still be forced out of the low field areas if a subsequent d-c stress exceeds certain levels.[13] Overall the peculiarities of d-c make it difficult to accurately correlate d-c and 60 Hz field test results and the d-c can identify "problems" which would never cause trouble in actual service. However, it must be admitted that d-c detects contamination and many systems are operating successfully after d-c testing.

INSULATORS

The data presented so far has ignored what is perhaps the most important component in the system -- the insulator, which locates and supports the conductor in the center of the enclosure. A variety of designs have been used successfully (discs, cones and posts) and there is general agreement that a good design should not reduce the performance achieved with gas alone. This performance is achieved by controlling stress on the surface of the insulator and ensuring it does not exceed the stress on the conductor surface.[26] Practical experience indicates that excellent performance can be achieved with conical insulators even when insulator surface stress equals, or slightly exceeds, conductor stress.

The greatest problem with insulators is that conducting particles can lie on the surface and reduce dielectric strength with all types of voltage.[27] It is impractical to predict the magnitude of the reduction as it depends on design stress level, stress distribution on insulator surface, particle shape and size, particle location, etc. However, performance can be severely impaired especially if the particle is large or if the insulator somehow accumulates a number of small particles.

frequently, but the stress with metallic particles off the insulator surface can also be very detrimental.[13] The best safeguard against contamination is to impose high quality control standards in both factory and field and to follow through with stringent test programs. This approach has been used on most installations to date and operating experience has been excellent.

Bruggeman and Fleming[28] have made one of the most detailed studies to date on the performance of both clean and contaminated insulators, at pressures up to 15 atm. The work shows that even very small particles make it difficult to take advantage of high pressures and suggests operating pressures in excess of 5 atm may be impractical.

While most of the insulator work to date has been concerned with negative stationary there is increasing emphasis on the long term 60 Hz performance of the solid material. This trend has resulted from the development of higher voltage systems where impulse and switching surge overvoltages tend to be reduced relative to the steady state 60 Hz voltage. Under these conditions impulse is no longer the dominant design influence and 60 Hz stress in both gas and solid material can be more important. Work to date has focused on establishing the maximum permissible operating stress levels in epoxy and indications are that levels in excess of 50 kV (rms)/mm. will be acceptable.[29]

Summary

At the present time, in the range of pressures normally used, it is possible under laboratory conditions to work SF_6 at 45% and 75% of its intrinsic strength for 60 Hz and impulse voltages respectively. In practical systems the 60 Hz and impulse stresses have been restricted to 15% and 30% of the intrinsic strength and it appears higher impulse levels could be used without any significant change in technology. This may be beneficial at the lower system voltages where impulse is normally the dominant constraint. However, at 550 kV and above, steady state 60 Hz stresses dominate and higher levels must be tolerated before advantage can be taken of increased impulse capability. Work to date indicates higher continuous 60 Hz stresses are feasible.

Under ideal conditions higher gas pressures allow significant increases in dielectric strength but extreme cleanliness is essential and this may make the high pressure/high stress approach impossible to use in practical systems.

CURRENT RESEARCH

Most of the research and development work to date has been concerned with SF_6 at relatively moderate pressures (3 to 6 atm) and at room temperature. Projects underway are designed to explore other design options so that the full capability of compressed gas-insulated systems can be realized. These projects involve studies of higher operating temperatures, gas mixtures for higher operating pressures, alternate gases to SF_6 etc.

High Temperatures

It has long been accepted that SF_6 has very high thermal capability and work during a recent EPRI/ERDA project confirmed the impulse and 60 Hz insulation strength is retained up to at least 150°C.[13]

Table 3. Effect of Temperature on Impulse and 60 Hz Tests in a 27 cm/11.5 cm Coaxial System at 3.5 atm.

Temperature °C	25	150
60 Hz Flashover Stress kV (rms)/cm	108	113
60 Hz Withstand Stress kV (rms/cm	104	108
Impulse Flashover Stress kV/cm	216	228
Impulse Withstand Stress kV/cm	208	214

The dielectric strength is slightly higher at 150°C but this may be due to experimental error. In any event it is clear that dielectric strength is not degraded and the challenge now is to develop an insulator which can operate reliably at 150°C. This involves both material development and basic design and work is proceeding under EPRI sponsorship.

Gas Mixtures

As mentioned previously it is virtually impossible to operate at SF_6 pressures above 6 atm and attention has been focussed on using SF_6/N_2 mixtures to increase the total pressure without introducing liquification problems at low temperatures. A number of studies have demonstrated that mixtures are very effective[13,19] and the problem now is to control contamination so that advantage can be taken of higher stress levels.

Alternate Gases

SF_6 has been used exclusively to date but efforts are underway to find better gases. Experiments with various fluorocarbons indicate the dielectric strength of SF_6 can at least be equaled but flashovers tend to generate free carbon.[13] There is also some hope that other gases (or mixtures of gases) may be more tolerant of contamination and this, if true, could allow a major advance in the technology.

FUTURE DEVELOPMENT

It is obvious that the dielectric strength of compressed gas insulated systems can be predicted with a high degree of confidence and that the factors which influence reliability are well understood. The most promising areas for future work would appear to be as follows:

1. Higher Dielectric Stresses - the work to date suggests impulse stress levels could be increased without too much difficulty. However, this change leads to an increase in 60 Hz working stress levels, in both gas and solid insulation and work is needed to define limits more accurately. The benefits of higher stresses need to be evaluated economically and one study indicates increased losses may negate the benefits of higher dielectric stresses in gas insulated cable systems.[30] However, the situation is much more favorable in substations.

2. Conducting particles are obviously the performance limiting factor in many situations and more effective scavenging techniques would be very beneficial. Existing conditioning techniques could be refined but there is need for an approach that would also remove or deactivate particles on solid insulation.

3. A better definition of the voltage-time characteristic may allow insulation levels to be reduced. However, this depends on how frequently very steep front overvoltages are encountered and systems work to date indicates wavefront rise times less than one microsecond may be almost impossible in gas insulated systems.[4]

4. It is probably feasible to work closer to the intrinsic strength of SF_6 by improving electrode surface quality but the economics of this approach may be difficult to justify, unless breakthroughs are made.

REFERENCES

1. J. C. Cronin et al, Design and Testing of 800 kV Gas Insulated Substation Components, to be published.

2. IEEE Working Group 70.1 - Proposed Standards for Gas Insulated Substations.

3. H. W. Graybill, J. C. Cronin and E. J. Field, IEEE T-PAS 93, 404 (1974).

4. J. C. Cronin, R. G. Colclaser and R. F. Lehman, IEEE Paper F 77 197-7.

5. J. D. Tranen, IEEE Paper A 77 729-7.

6. T. Nitta, N. Yamada and Y. Fujiwara, IEEE T-PAS 93, 623 (1974).

7. Y. Kawaguchi, K. Sakata and S. Menju, IEEE T-PAS 90, 1072 (1971).

8. T. Nitta and Y. Shibuya, IEEE T-PAS 90,1065 (1971).

9. P. Hogg, W. Schmidt and H. Strasser, CIGRE Paper 23-10 (1972).

10. I. M. Bortnick, IEEE Underground Transmission Conference - Supplement, 317 (1972).

11. Final MIT Report on ERC Project RP 78-2.

12. G. W. Brown, R. Samm and J. C. Cronin, IEEE Paper F 77 018-5.

13. Final Report on EPRI Project 7825; ERDA Project E(49-18)-1615.

14. A. H. Cookson et al, CIGRE Paper 15-09 (1976).

15. A. H. Cookson and O. Farish, IEEE T-PAS 92,871 (1973).

16. E. B. Ganger and A. A. Leibold, IEEE Paper A 76 152-9.

17. J. C. Cronin, IEEE Underground Transmission Conference - Supplement, 323 (1972).

18. H. C. Doepken, IEEE Trans. on PAS 88,364 (1969).

19. H. M. Ryan et al, CIGRE Paper 15-02 (1976).

20. H. M. Ryan and W. L. Watson, IEEE Paper F 76 390-5.

21. W. Taschner, ETZ A 2, 153 (1977).

22. T. Nitta, Y. Shibuya and Y. Fujiwara, IEEE T-PAS 94, 108 (1975).

23. C. M. Cooke and R. Velazquez, IEEE Paper F 77 094-6.

24. C. M. Cooke, R. E. Wootton and A. H. Cookson, IEEE T-PAS 96, 768 (1977).

25. R. Nakata and E. J. Tuohy, IEEE Paper A 77 198-5.

26. T. Takuma and T. Watanabe, Proc. IEE 122, 183 (1975).

27. J. C. Cronin and E. R. Perry, IEEE T-PAS 92, 558 (1973).

28. B. F. Hampton and S. P. Fleming, Proc. IEE 120, 514 (1973).

29. V. H. Tahiliani and D. H. Reighter, IEEE Paper A 78 191-9.

30. J. C. Cronin et al, IEEE Paper A 78 189-3.

DISCUSSION

GARRITY: 1. On the slide depicting impulse levels, was the level the statistical (50%) withstand or the design withstand? 2. To what rate of rise lightning impulse have you investigated the fast front transient performance?

CRONIN: The impulse level is the two sigma withstand level; generally this is defined by allowing not more than one flashover in a forty shot-test series. Rates of rise up to 2000 kV/μs have been investigated.

KUWAHARA: We have a very useful computer program by which we can evaluate the voltage-time characteristic of practical systems based on the test results obtained under controlled conditions. I would like to show an example by a slide (Fig. 1). This slide shows voltage-time

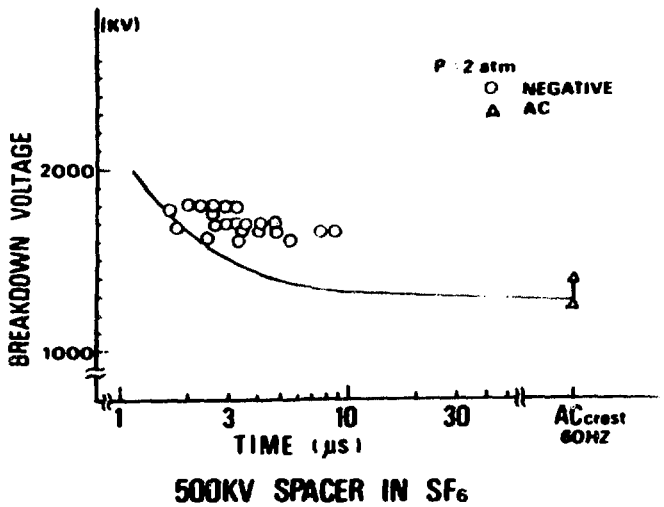

Figure 1

characteristic for 500 kV bus section with an insulator. Dr. Cronin said that the estimation of steep front region was difficult. One reason

is the measuring problem in fast rising region. The solid curve is the estimated minimum level and plots are experimental values for impulse and AC. The estimated curve is in good agreement with the test data. So we think that we can evaluate the design of a gas system based on the test results under controlled conditions.

CRONIN: Computer programs are fine but the output is only as good as the input. Our experience is that accurate voltage-time data on complex, practical systems are presently not available and accordingly we have designed on the (pessimistic) assumption that the characteristic is flat.

CHRISTODOULIDES: 1. In the "Areas of Interest," you have mentioned gas mixtures. In your analysis, you talked about the intrinsic breakdown strength of SF_6, the laboratory test limit, and the actual operating limit. Have you tried such analysis for a mixture of SF_6 with some other gas or gases, not necessarily N_2? 2. In one of your slides, an increase of breakdown strength with "conditioning time" is shown. How do you actually define "conditioning time?"

CRONIN: 1. We have undertaken work with SF_6/N_2 mixtures and have also explored mixtures of various fluorocarbons with nitrogen. This work is reported in EPRI Report 7825. We have not evaluated mixtures of SF_6 with other gases. 2. Conditioning time is the time taken to move all, or some significant fraction of, conducting particles to low field areas. A precise definition has not been formulated but, in the referenced work, the degree of conditioning was evaluated by measuring the one minute 60 Hz withstand capability.

ERIKSSON: Which assumption has been made as regards voltage-time characteristics for the arresters in the given example?

CRONIN: The voltage-time characteristics have been taken from manufacturers data (mainly Ohio Brass) and were represented by a function with six linear sections. A problem with manufacturers data is the lack of information at rise-times in excess of 2000 kV/μs and flashover statistics are also not readily available.

VLASTOS: I would like to make a comment on Dr. Cronin's data on the influence of the voltage steepness on the breakdown voltage of SF_6 in a quasihomogeneous field. Our experiments performed with impulse voltages with different fronts and pulse lengths show that for bare electrodes the influence of front steepness is of minor importance; however, the pulse length is decisive. The reason may be that for bare electrodes the breakdown happens at the tail of the impulse voltage. Figs. 2 and 3 show the results obtained with a negative standard full or chopped impulse voltage (chopping times 2 and 6 μs respectively) and Figs. 4 and 5 the results with a full negative 0.5/50 μs and for impulses chopped after 1.5 and 6μs respectively. The results refer to coaxial cylinders 30/70 mm 250 mm long at 5 bar pure SF_6 gas.

CRONIN: This is a very interesting explanation and we have sometimes observed flashovers 2 to 10 μs after voltage crest; usually this observation is made when the flashover is across an insulator. However, most of the flashovers we observe (including insulator flashovers) are before or at the crest of the wave.

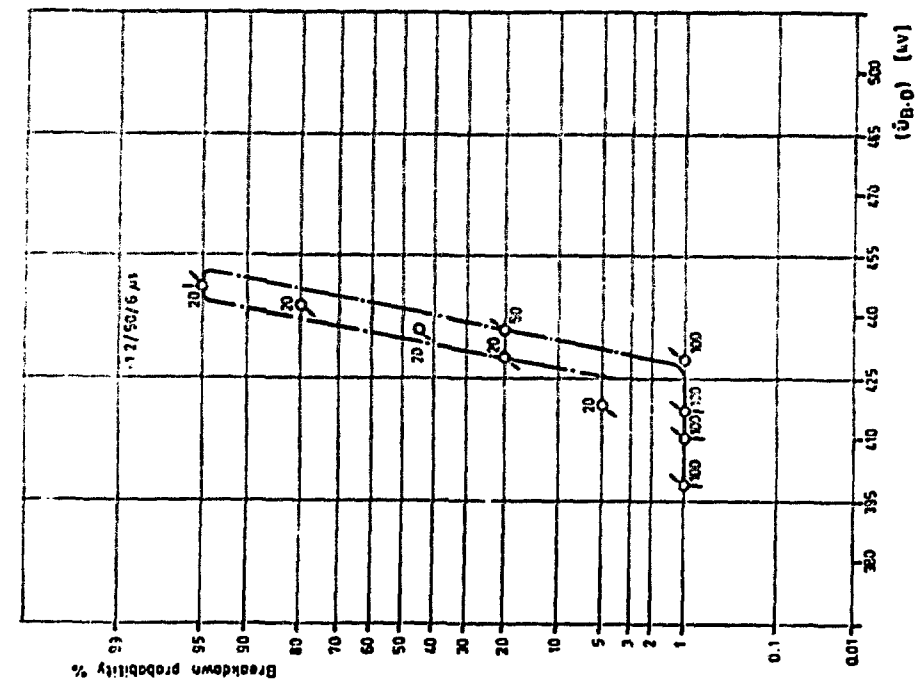

Figure 3

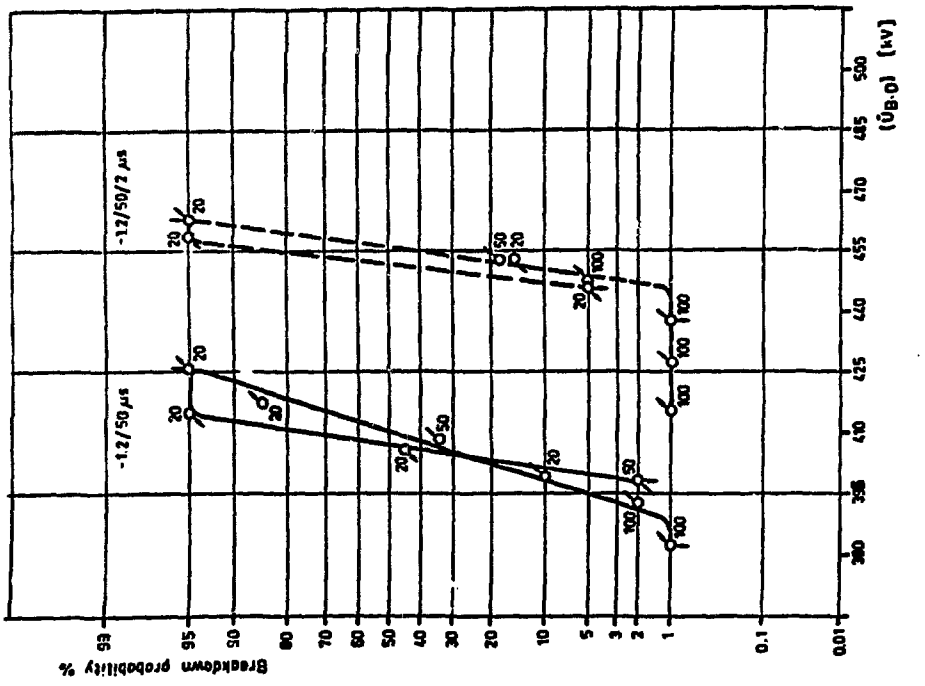

Figure 2

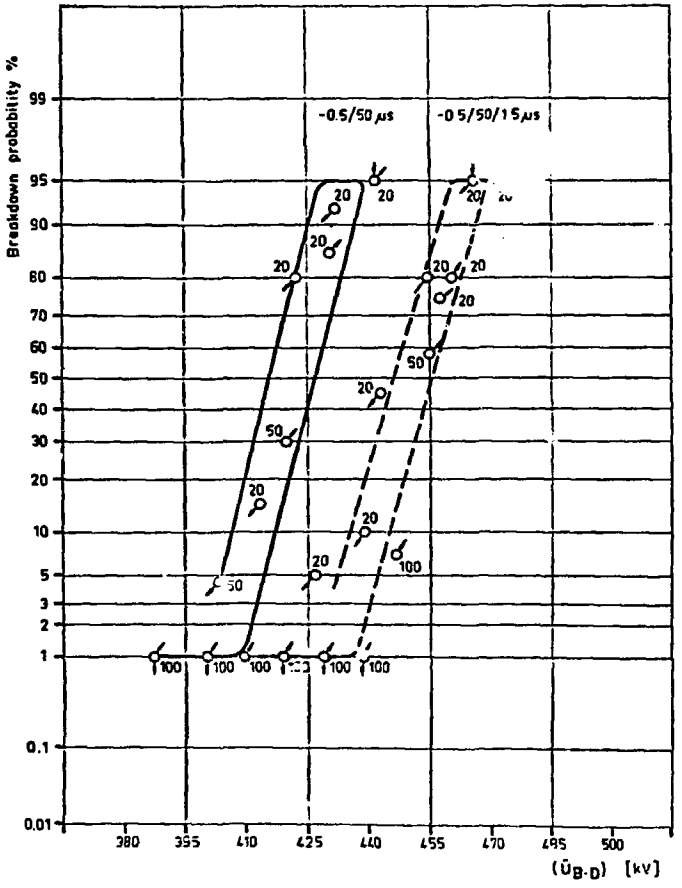

Figure 4

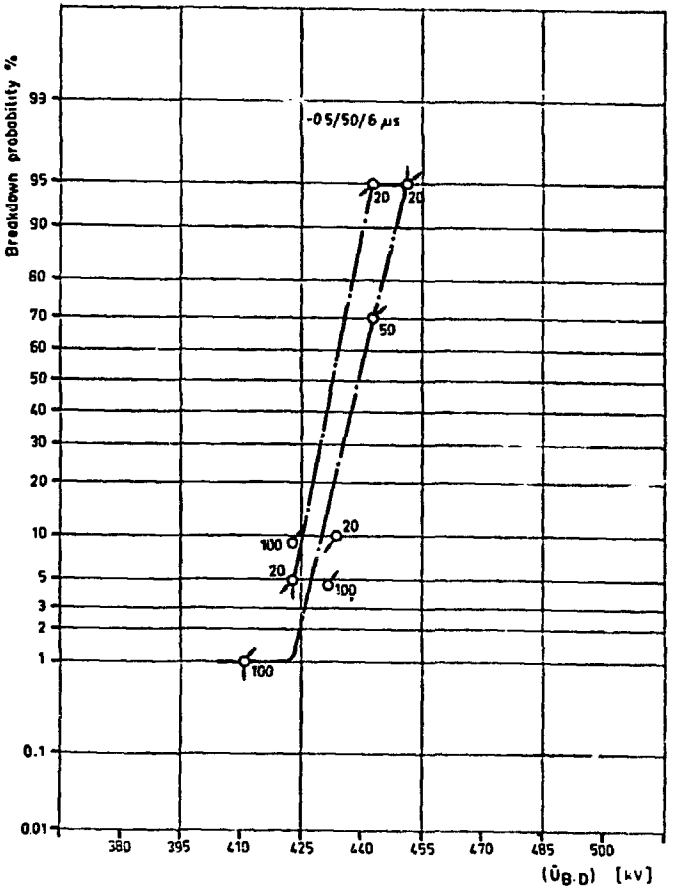

Figure 5

INFLUENCE OF PREEXISTING DC VOLTAGE ON THE BREAKDOWN PERFORMANCE OF SF_6 UNDER IMPULSE VOLTAGE

E. Gockenbach
Technical University Darmstadt, West Germ

ABSTRACT

The dielectric strength of SF_6 is determined at a voltage stress, which is typical for HVDC-converter stations, in uniform and nonuniform electrical field configurations. This voltage is verified by superposition of dc and impulse voltage. The addition of the two voltages results in the breakdown voltage, which is independent of the preexisting dc voltage in uniform and quasiuniform electrode configurations. In nonuniform electrical field configurations the breakdown voltage decreases evidently with increasing dc voltage.

INTRODUCTION

The power transmission in densely populated areas needs new technologies regarding the high consumption of electrical energy, the restriction of the transmission lines, and the increasing importance of the environmental factors[1]. Therefore compact, metalclad stations may be used for high voltage alternating as well as for direct current transmission. In both cases the application of a gaseous insulant with highly insulating stress is necessary. The following paper investigates, whether the application of the electro-negative gas SF_6, well known from the HVAC technique, is practicable as an insulant in a HVDC-converter station with its special voltage stress.

TEST FIXTURE

The voltage stress in HVDC terminals is very variable. Some parts are applied with pure sine-shaped ac voltage, others with pure dc voltage, but there is also mixed voltage, which can be reproduced by superimposing dc and lightning impulse voltage[2]. Figure 1 shows the block diagram of the test arrangement. The impulse voltage generator produces an impulse wave of 1,2 /50 µs by an amplitude of 140 kV. A damped-capacitive voltage divider is used to measure the impulse voltage U_I.

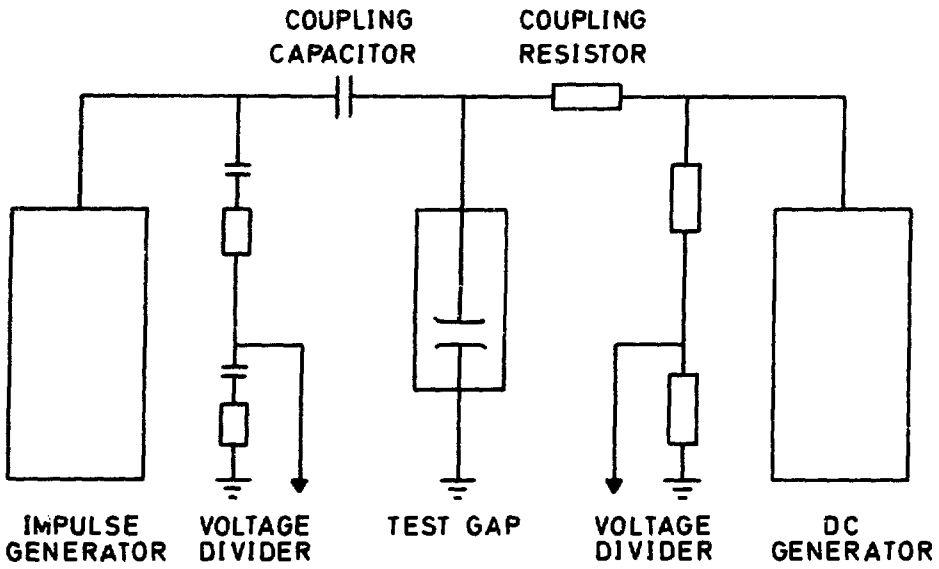

Fig. 1. Experimental circuit arrangement

The test gap is situated within a Plexiglas tube of 120 mm diameter and 300 mm height. Breakdown voltages of plane-plane, sphere-plane with various diameter of the spheres, and rod-plane electrode configurations are investigated. The gap is irradiated under an ultra-violet light with a line spectrum between 200 and 600 nm, reducing the breakdown voltage scatter. The dc voltage is applied by charging a capacitor via rectifier. The amplitude is also 140 kV. The coupling elements (shown in figure 1) are necessary to protect the two generators and they have no influence on the measurements and the test parameters. The error in measurements is less than 3 %.

TEST PROCEDURE

After cleaning and installing of the electrodes the test tube is evacuated until 0,4 mbar and then filled with SF_6 until the desired pressure is obtained. Then the gap length is set by a micrometer screw. After a time of about 1/2 h the percentage breakdown probability of the impulse voltage is determined as a function of the constant preexisting dc voltage. The time function of the voltage stress is shown in figure 2, where you can find two unipolar applications, one with posi-

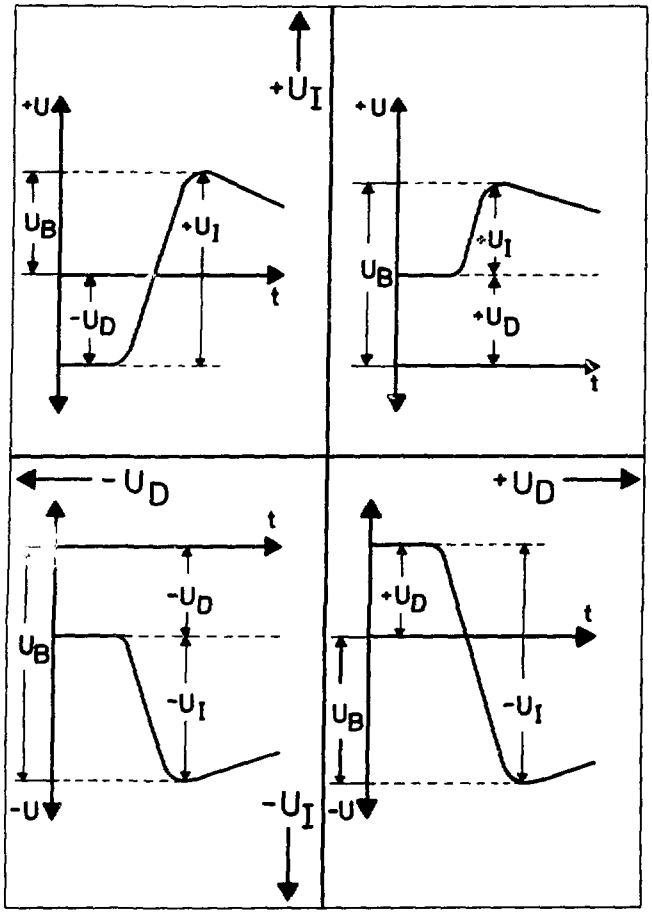

Fig. 2. Time-function of voltage stress

tive dc and impulse voltage at the first quadrant, and one with negative dc and impulse voltage at the third quadrant, moreover two bipolar applications, one with negative dc and positive impulse voltage at the second quadrant, and one with positive dc and negative impulse voltage at the fourth quadrant. The designation U_D gives the dc voltage, U_I the impulse voltage and U_B the breakdown voltage, which can be calculated by the addition of the two voltages U_I and U_D. The breakdown probability is determined at 100 impulses of constant amplitude of the impulse voltage as well as the dc voltage. Then the test points are noted in a diagram whose axis of ordinate is divided according to the Gaussian distribution and whose abscissa is linearly divided. For nonuniform field configurations with stable corona many test points (about 50) are

necessary to describe the shape of the breakdown probability as a function of the impulse voltage. For uniform field configurations only few test points (3 or 4) are necessary.

The impulse voltage with a breakdown probability of 0,2 % is determined graphically and this value is called breakdown voltage U_B in the following diagrams and evaluations.

RESULTS

UNIFORM FIELD

Figure 3 shows the shape of the breakdown probability as a function of the impulse voltage for various preexisting dc voltages in a uniform field (plane-plane, gap length 5 mm).

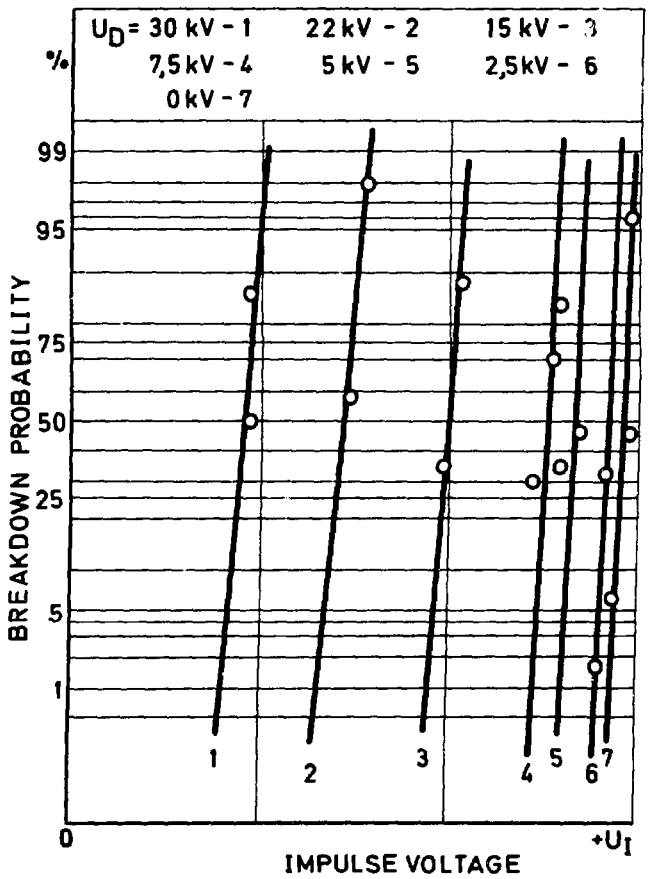

Fig. 3. Breakdown probability of positive impulse voltage as a function of the preexisting positive dc voltage for uniform field configuration

The polarity is positive for both voltages. The linear shape of the breakdown probability points out that this probability obeys a normal distribution because the axis of ordinate is divided according to the Gaussian distribution. Moreover the linear shape shows that only one parameter is significant due to the breakdown[3]. With decreasing dc voltage the straight lines shift parallel to higher values of impulse voltage. The shape of breakdown probability of the other three quadrants corresponds with figure 3.

Figure 4 shows the impulse voltage U_I as a function of the dc voltage U_D(full line) and also the breakdown voltage U_B (broken line).The breakdown voltage is independent of the dc voltage.

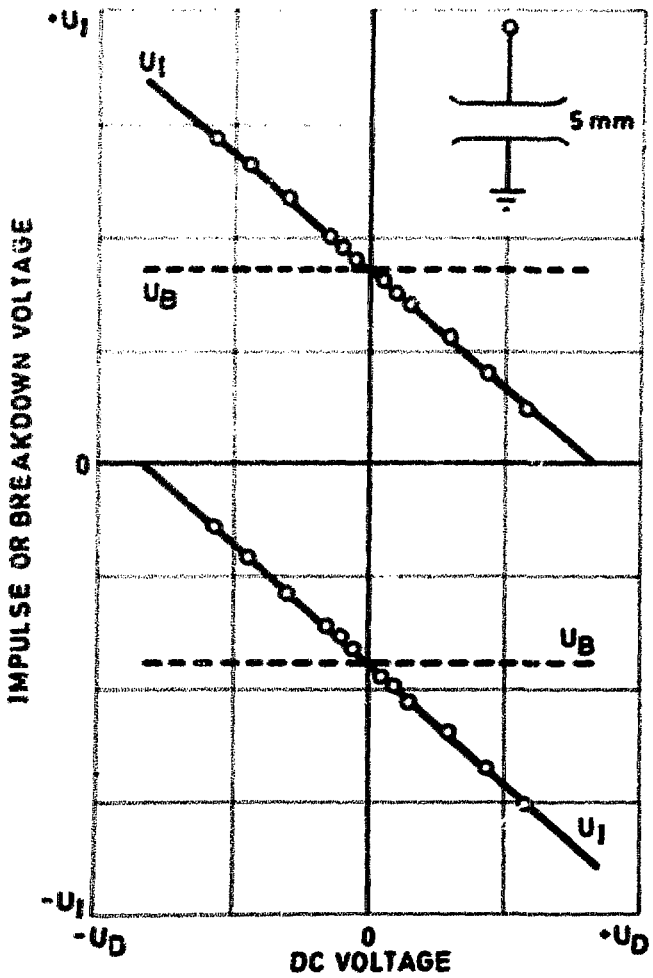

Fig. 4. Impulse or breakdown voltage as a function of the preexisting dc voltage

That means, that a value of the voltage exists, which is critical at the breakdown. This value can be reached with a high dc and low impulse voltage or with a low dc and high impulse voltage. In consequence of the symmetrical electrode configuration and the production of the initial electrons due to irradiation no difference between dc and impulse breakdown voltage exists. The same results are obtained by the investigation at all other gap lengths (up to 10 mm) and at all other gas pressures (up to 3 bar). In the case of high gas pressure the breakdown probability runs parallel to the axis of ordinate, because the term of the electron multiplication obeys the following Eq. (1)[1]:

$$\alpha - \eta = p\,k\,(E/p - (E/p)_{crit}) \qquad (1)$$

where α, η = ionization or attachment coefficient, 1/cm
p = gas pressure, bar
E/p = referred field strength, kV/cmbar
E/p_{crit} = referred field strength at $\alpha=\eta$, 88 kV/cmbar

The electrode configurations sphere-plane have the same behaviour, shown in figure 4, if the utilization factor u

$$u = E_{max}/E_{mean} \qquad (2)$$

where E_{max} = maximum value of the field strength, kV/cm
E_{mean} = mean value of field strength, kV/cm

is greater than o.5 .Therefore the representation of the measuring results of this electrode configuration is given. All the breakdowns occur within the front of the impulse, so that the breakdown time is between 1 and 1.5 µs.

NONUNIFORM FIELD

Figure 5 shows the principal shape of the breakdown probability due to various electrode configurations and various preexisting dc voltages. With increasing inhomogeneity of the configuration the declination of the line decreases if no corona exists. This is caused by longer breakdown times and

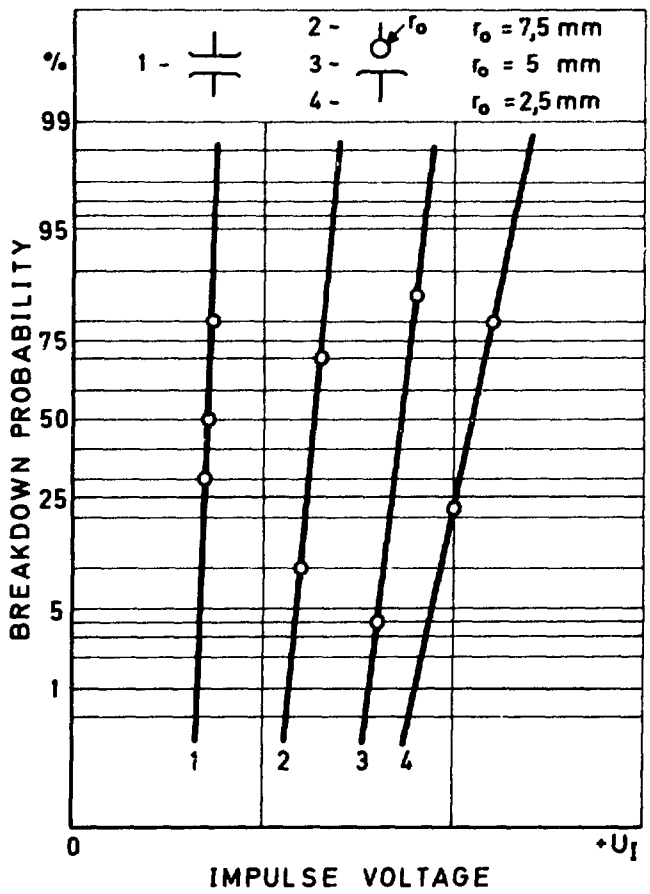

Fig. 5. Breakdown probability of positive impulse voltage for various electrode configurations

smaller voltage stressed volumes. If stable corona exists due to the preexisting dc voltage, the breakdown probability does not obey a normal distribution.The reason for the deviation of the normal distribution is the fact that now more than one parameter is significant due to the breakdown. It is difficult to determine the breakdown voltage in such a case. Nevertheless the impulse voltage and "breakdown" voltage of a sphere-plane configuration is shown, as an example, in figure 6 as a function of the dc voltage.The breakdown voltage increases slightly for positive dc and negative impulse voltage, but is essentially independent of the dc voltage.With positive dc and impulse voltage the breakdown voltage is independent of the preexisting dc voltage. At negative dc voltage the breakdown voltage is constant and also independent of the dc voltage, until predischarges

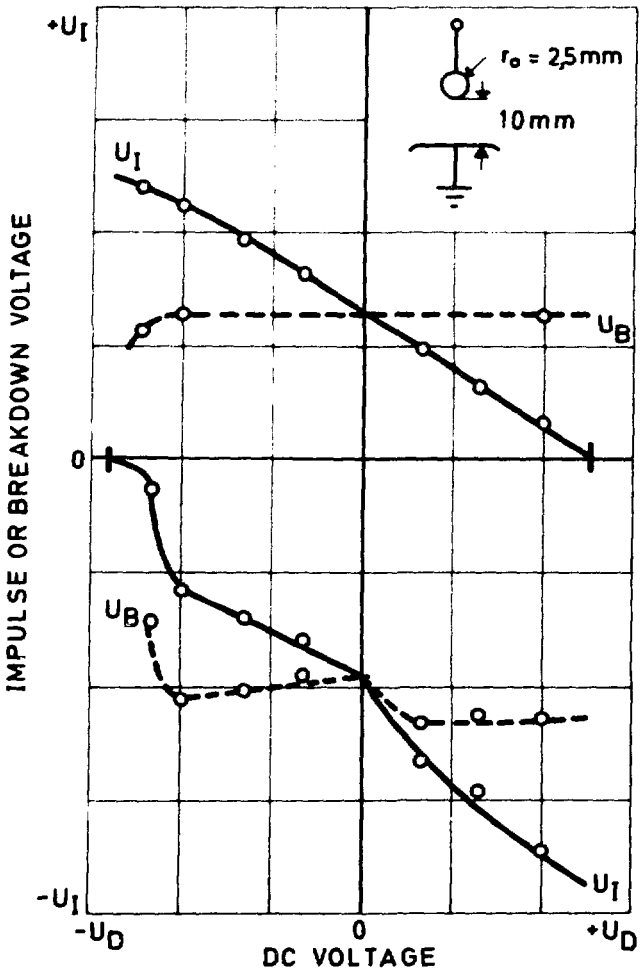

Fig. 6. Impulse or breakdown voltage as a function of the preexisting dc voltage

occur. Then the breakdown voltage decreases strongly and the breakdown time is very long and reaches values up to 100 µs. At high gas pressure no corona exists and the breakdown voltage is independent of the dc voltage[6].

CONCLUSIONS

The breakdown voltage, composed of the addition of dc and impulse voltage, is constant and independent of the kind of voltage combination in uniform and quasiuniform electrical field configurations. The predischarges change the normal distribution to a mixed distribution and the breakdown voltage decreases strongly. In a uniform field it is possible to estimate the dielectric strength under mixed voltage stress

knowing the breakdown voltage of the components. On the contrary the knowledge of the breakdown voltage of the components leads to incorrect estimates of the dielectric strength in nonuniform field configurations.

REFERENCES

1. Elektrische Hochleistungsübertragung, ETZ-A 98, 11 (1977)
2. W. Mosch, E. Lemke, I. Fahd, Elektrie 26, 10 (1972)
3. N. W. Smirnow, Mathematische Statistik in der Technik, VEB Verlag der Wissenschaften, 1970
4. T. Nitta, Y. Shibuya, IEEE Power App. Syst. 90, 4 (1971)
5. K. Feser, Bull. ASE 62, 6 (1971)
6. D. Berg, C. N. Works, IEEE Power App. Syst. 78, 5 (1958)

DISCUSSION

NAKATA: Dr. Gockenbach's findings on the independence of SF_6 breakdown with DC bias for a clean system is gratifying since for a practical HVDC converter system, the gas bus and thyristor valve must be capable of instantaneous (actually by smooth commutation) polarity reversal in order to change the direction of power flow. Then, too, Dr. Cronin's paper wherein he mentioned that an AC gas bus system could suddenly find itself to be a DC gas bus system if it performed capacitive switching duty is to be kept in mind. Under such a DC state any transient surge on the capacitively switched AC bus system constitutes the type of stress which Dr. Gockenbach investigated. In our own work, we have designed a DC gas bus which was biased to 500 kV DC of one polarity. This bus was subjected to a truly instantaneous (microseconds) polarity reversal to 500 kV DC of the opposite polarity for 4 hours (soak) only to be reversed again. This test was demonstrated for 72 hours of such reversals continuously without failure. While this design was shown to be adequate for the present EPRI project, I would like to propose (as Dr. Christophorou suggested at the start of the session for development suggestion items) that the study of fundamental materials behavior under high electrical stresses be included in a subsequent conference. Otherwise all the excellent work on SF_6 gas will be naught if practical insulators to support the conductor in the gas could not be thoroughly understood and built. Whereas Dr. Gockenbach showed that the SF_6 is sensitive only to the net peak voltage (and not to any pre-bias) the physical insulator with trapped charges (caused by DC bias prior to the impulse stresses)

constitutes a threat unless it is understood and designed for accordingly.

VLASTOS: What influence has the coupling condenser on the wave form of the impulse voltage applied to the gap?

GOCKENBACH: The coupling capacitor has no influence on the wave form and the error in measurement of the impulse voltage is very small, because the coupling capacitor has a capacitance of about 10 nF and the test gap of about 10 pF. For practical configurations with a voltage range of some hundred kV it may be better to measure directly the impulse voltage on the test gap with a capacitive voltage divider.

DAKIN: In experiments done at the Westinghouse Research Laboratory by Dr. Daniel Berg about 15-20 years ago (and published) he found the reduced positive point impulse breakdown voltage was increased when the gap was pre-stressed with a positive DC voltage to produce a positive space charge at the point. This was done to indicate that the lower impulse breakdown was due to the time delay for corona space charge development with the impulse voltage.

DALE: I would like to present some results from breakdown voltage studies with 60 Hz AC and superimposed 1.5/50 μs impulses in a coaxial electrode system of 76/250 mm diameter electrodes with a 6.4 mm long, 0.45 mm diameter wire particle fixed on the central conductor. The results are consistent with those presented by Dr. Gockenbach in that the super-position breakdown voltage is unaffected by the AC voltage amplitude below the AC corona onset voltage. However, the presence of AC corona from the fixed particle can significantly increase the super-position

breakdown voltage in the part of the voltage-pressure characteristic corresponding to the space charge stabilized breakdown region for impulses applied to the peak of the AC voltage (See Fig. 7). Impulses applied at the instant of zero voltage on the AC waveform resulted in an insignificant deviation from the impulse breakdown voltage even when corona occurred on the positive and negative peaks of the AC voltage.

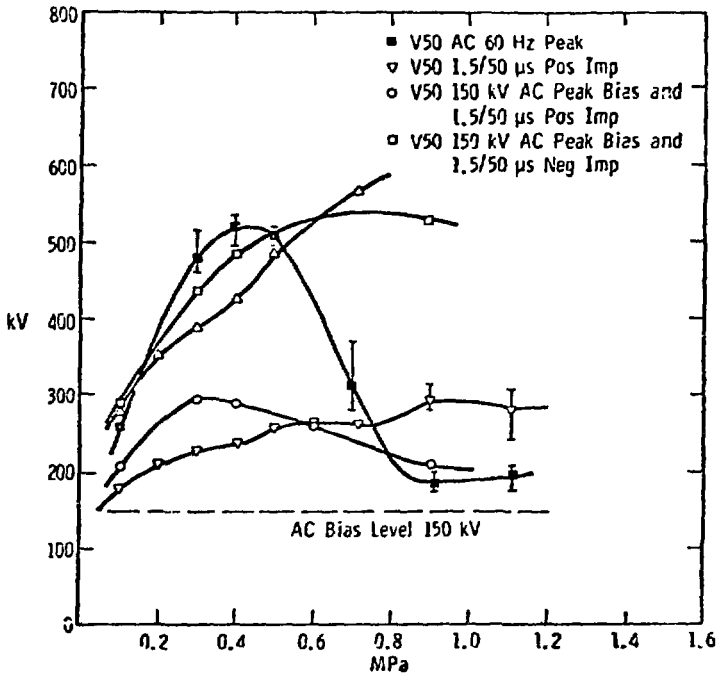

Fig. 7 — Breakdown voltage-pressure characteristics for 76/250 mm coaxial electrodes in SF_6 with one 6.4 mm long, 0.45 mm diam. particle fixed on the inner conductor.

VOLTAGE-TIME CHARACTERISTICS AND AREA EFFECT OF BREAKDOWN IN SF_6

Inge Johansen
Asgaut Rein
The Norwegian Institute of Technology.
N-7034 Trondheim-NTH, Norway
Asle Schei
The Norwegian Research Institute of
Electricity Supply, EFI
N-7034 Trondheim-NTH, Norway
Arne Arnesen
National Industri, N-1701 Sarpsborg, Norway

ABSTRACT

The influence of the statistical time lag on the voltage-time characteristics of SF_6 has been calculated. This gives a rise in the breakdown voltage for decreasing times in the microsecond region for certain combinations of stressed electrode area and gas pressure.

In the calculations the effect of the formative time lag is not taken into account. This would be the dominating time lag for combinations of stressed electrode area and pressure that are found in most SF_6 insulated high voltage equipment.

The calculations are based on a streamer criterion where the statistical nature of the availability of starting electrons and the statistical distribution of the size of electron avalanches are taken into account.

INTRODUCTION

The growing recognition of SF_6 as a high voltage insulation, notably for space-saving switchgear, substations and power cables, has created the need of studying the behavior of SF_6 insulation from an insulation point of view. In this respect the voltage-time curve for SF_6 gas is important.

In recent papers [1 - 9] the voltage-time curves for SF_6 insulation have been studied experimentally and theoretically.

In Fig. 1 the general form of the voltage-time characteristic is given.[11] This curve shows that there is an increase in the breakdown voltage when the voltage is applied for less that a few micro seconds. Why this increase is of practical importance is demonstrated in Fig. 2[11] which shows the voltage waveforms calculated for an actual SF_6 station.

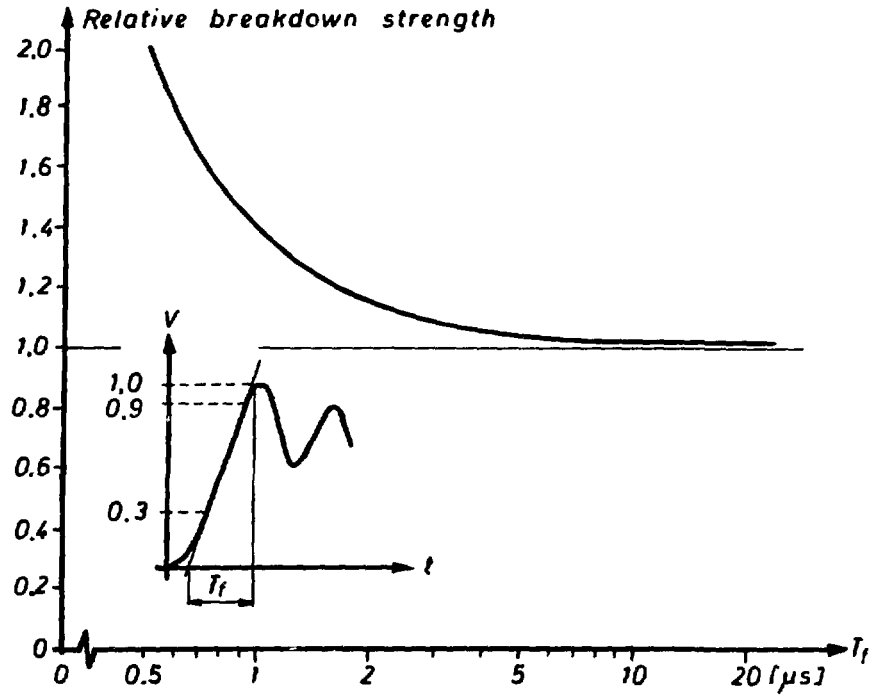

Fig. 1. General form of voltage-time characteristic for SF_6 insulation.

Several studies have been reported.[1,2,5 - 9] To simulate practical designs coaxial cylinders and sphere-sphere configuration have been studied with voltages of positive and negative polarity. In all cases the electric field has been rather uniform in agreement with the practical design situation.

The influence of the electrode area on the voltage-time curve has not been systematically determined.

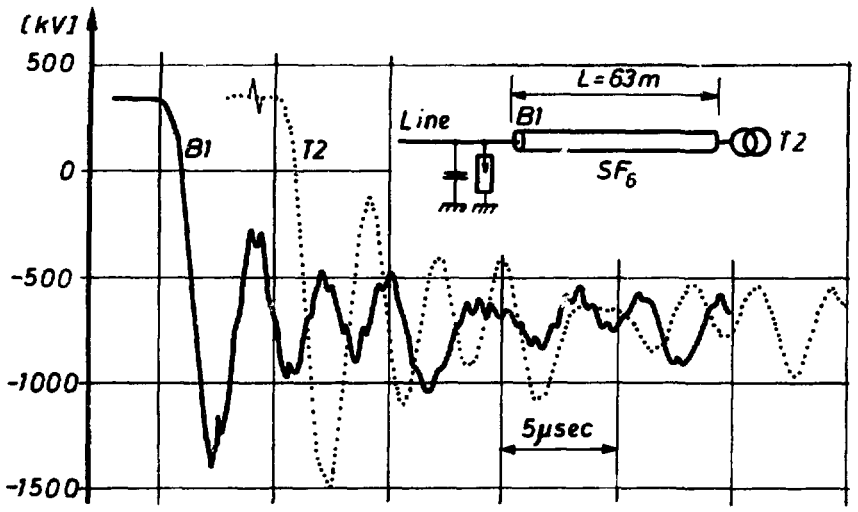

Fig. 2. Example of overvoltage in a SF_6 insulated station for one particular lightning stroke to the overhead line.[11]

The increase in the breakdown voltage with decreasing time, is due to the time lag in the physical processes governing the breakdown phenomena. This time lag can be divided into a statistical and a formative time lag.

This paper deals with the statistical time lag when the highly stressed electrode has negative polarity. It utilizes a theoretical concept given in a paper [14] where the statistical nature of the electronic avalanches which develop into breakdown is taken into account. This concept has successfully explained the variation in the impulse breakdown voltage with pressure and stressed electrode area, as shown in Fig. 3.[14]

For simplification the formative time lag is not taken into account in this analysis. This can be done by using the concept[9] that a certain voltage-time area above a critical voltage is necessary to complete the breakdown. In most practical cases it is in fact this time lag which will determine the voltage-time curve of the configuration.

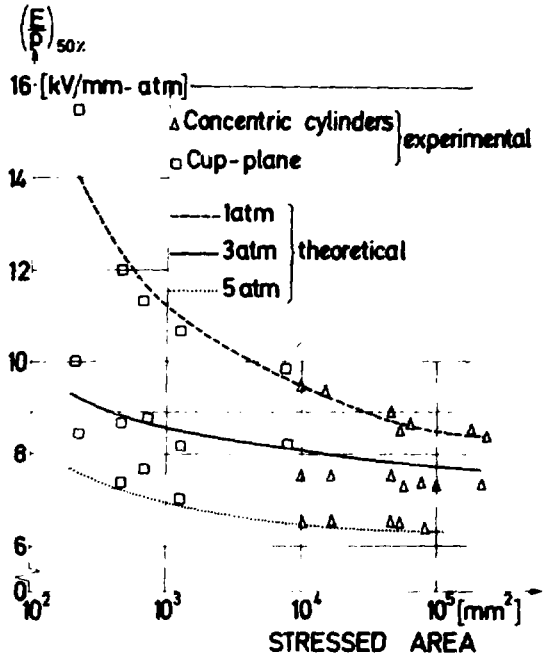

Fig. 3. Negative lightning impulse breakdown field strength. Experimental and theoretical values.[14]

EXPERIMENTAL RESULTS

Fig. 4 shows some experimental breakdown values as a function of time in a coaxial configuration [9,12]. Studies of voltage-time curves appearing in the literature [9,12] show the variation to be steeper for negative polarity at the inner cylinder and that the breakdown values are lower in this case than for positive polarity. Experimental voltage-time curves on configurations where the electrode area has systematically been varied has to the knowledge of the authors not been performed. As will be seen from the analysis given below, this is also a parameter which should be taken into account.

THEORETICAL ANALYSIS

In determining the influence of the statistical time lag on the breakdown strength, the theoretical concept given in reference 14 will be the basis. This concept is essentially a streamer criterion, but takes the stochastic nature of the electronic avalanche processes that start the streamer into account.

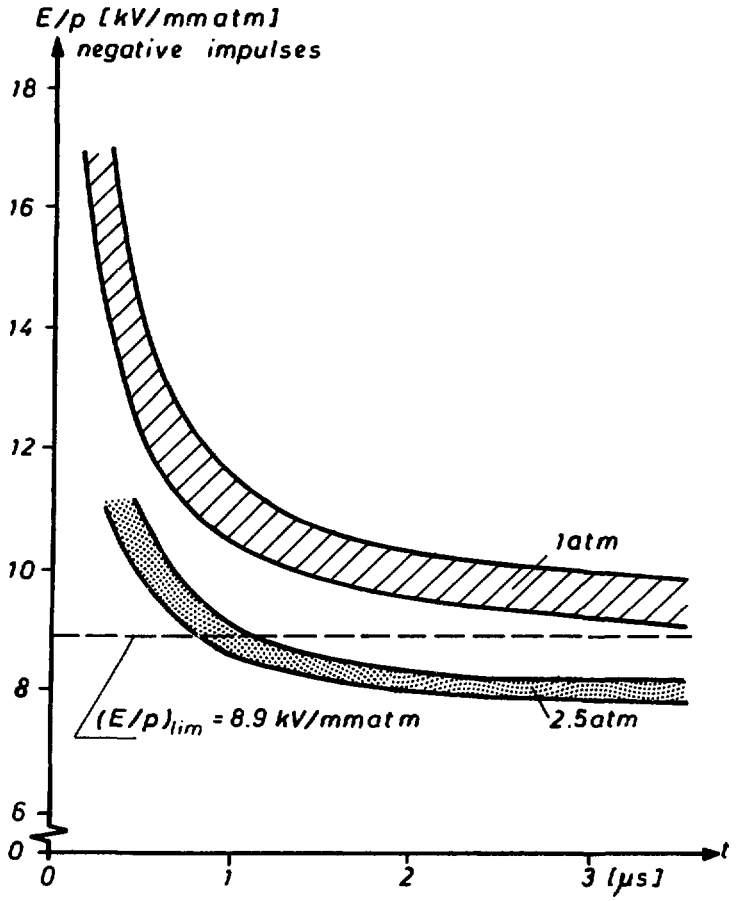

Fig. 4. Experimental voltage-time curves for SF_6.[9, 12]

The streamer criterion predicts breakdown to take place when the number of electrons in an avalanche exceeds a critical value of 10^5 - 10^8 electrons. This criterion is generally based on an average avalanche where the number of electrons can be calculated as

$$\exp\left[\int_0^{z_0}(\alpha-\eta)\,dz\right]$$

where

α = ionization coefficient

η = attachment coefficient

z_0 = critical length of avalanche

Due to the high steepness in the function

$$\frac{\alpha-\eta}{p} = f\left(\frac{E}{p}\right)$$

in SF_6 around $\alpha-\eta = 0$, the criterion predicts breakdown to take place when the maximum field strength E is such that $\frac{E}{p}$ is slightly above 8.9 kV mm^{-1} atm^{-1} where $\alpha-\eta=0$. As demonstrated in Fig. 4 this criterion is not able to explain the pressure variation in the breakdown values. This is also pointed out by others. [8,9]

The criterion is not able to explain the variation of the breakdown strength with the size of the electrode area. When the statistical nature of the electron avalanches is taken into consideration, both the influence of the pressure and the electrode area on the breakdown strength can be accounted for. It can also predict the standard deviation of the breakdown values.

In this paper the new concept will be used to calculate the statistical time lag before breakdown occurs.

The basic streamer criterion as developed by Raether, shows that a single avalanche with a size of about 10^8 electrons develops into a streamer leading to breakdown. The probability of this development increases with the avalanche size with very low probability below a critical limit.

When the electric field is such that the average avalanche contains 10^8 electrons, there are chances that both smaller and larger avalanches can be found. The statistical distribution of the avalanche sizes can be calculated, [14, 15] when no distortion of the field is assumed. It will be the first single avalanche exceeding the critical size that will trigger the breakdown. The chance for finding a single avalanche of such a magnitude will be determined by the electric field and by the probability of finding a starting electron. When there is a great number of starting (primary) electrons present, there is a chance of finding avalanches exceeding the critical value (10^5 - 10^8) even at electric field strengths below the value which gives $\alpha = \eta$.

This is the case when the high field is at the negative electrode at high pressure, and when the stressed electrode area is large.

An applied voltage of short duration and low breakdown field strength, i.e. low pressure, will give few starting electrons and the field has to be increased in order to ensure that one of the few occuring avalanches will reach critical size. In such cases the field strength may be above the value corresponding to $\alpha = \eta$ before breakdown occurs.

The statistical distribution of the avalanche sizes is calculated theoretically by Legler.[15] These distributions are applied to obtain the results presented below.

The next information needed is the availability of starting electrons. There is very little information available on this subject, and in most theoretical models it is simply assumed that free electrons serving as starting electrons are at the right position at the right time, with the exception that it may introduce a certain statistical time delay.

In these calculations where the highest electric field strength is at the cathode, field emission is assumed to be the source of electrons. This approach was also used to determine the influence of electrode area and pressure [14] with results as shown in Fig. 3. It should also be a reasonable assumption when calculating the statistical time lag.

Before demonstrating the theoretical results some further considerations about the availability of free electrons should be made. In references 5 and 9 it is assumed a certain number of electrons are generated per unit volume and time in the gas volume. The number is fitted so that theoretical and experimental values coincide, and is thought to apply when the electrode with the highest electric stress is positive. It is concluded, however, that when the stressed electrode is at negative field emitted electrons will be the major source of starting electrons. The authors agree with this conclusion.

Although it is outside the scope of this paper, comments will be made on the source of starting electrons when the stressed electrode is positive. In this case the electrons have to be found in the gas volume. These are thought to be electrons drifted from the cathode, and on their way starting avalanches below the critical size which will increase the electron population. Even though most electrons will be attached to neutral SF_6 molecules to make negative ions, some electrons will reach the region of the anode where the field is high. The transit time is determined by the drift velocity of electrons which is expected to be about 10^5 m/sec. The electrode configurations which are experimentally investigated, have distances in the order of 0.1 m, which gives a transit time of about 1 μs. In this time region it is also seen from experimental studies that the breakdown strength increases fast.

Foreign sources give a very low electron generation and cannot be considered as an important electron source. It may be that it enhances the influence of the electric field at the cathode. The short statistical time lag that is observed is not consistent with foreign sources as the only source for the generation of starting electrons.

Figs. 5 and 6 show the results of theoretical calculations of the breakdown strength as a function of time. Two coaxial cylinder models were used in the calculations:

Model 1:

Diameter ratio D/d = 225/45 mm, length L = 10 mm
Area of high voltage electrode: $A = 1.4 \cdot 10^3$ mm^2
Utilization factor $\mu = \frac{E_{average}}{E_{max}} = 0.4$

Model 2:

D/d = 280/100 mm, L = 600 mm
$A = 1.9 \cdot 10^5$ mm^2
$\mu = 0.57$

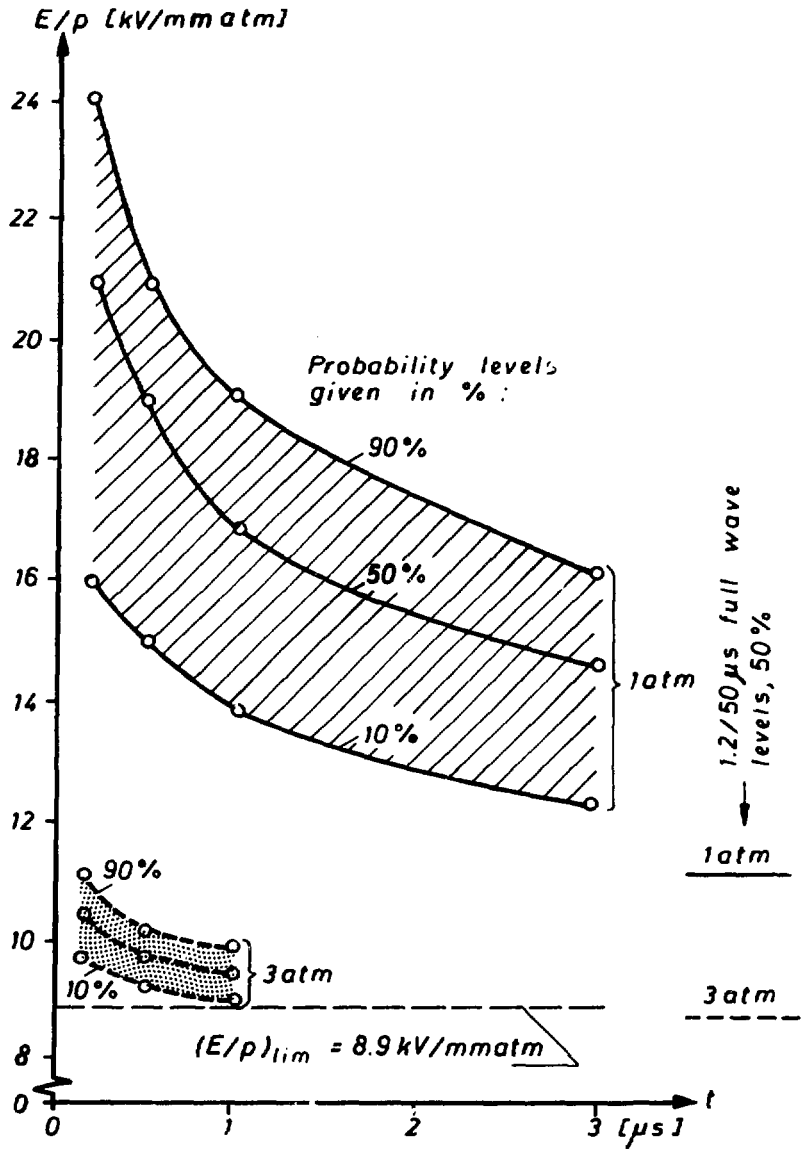

Fig. 5. Calculated breakdown field strength for Model 1 assuming zero formative time lag.

Linearly rising negative voltages are used in the calculations. Field emitted electrons are thought to be the source of starting electrons for avalanches. The statistical distribution of the avalanches, given by the electric field, will determine the probability that one of the starting electrons gives an avalanche with critical size resulting in breakdown.

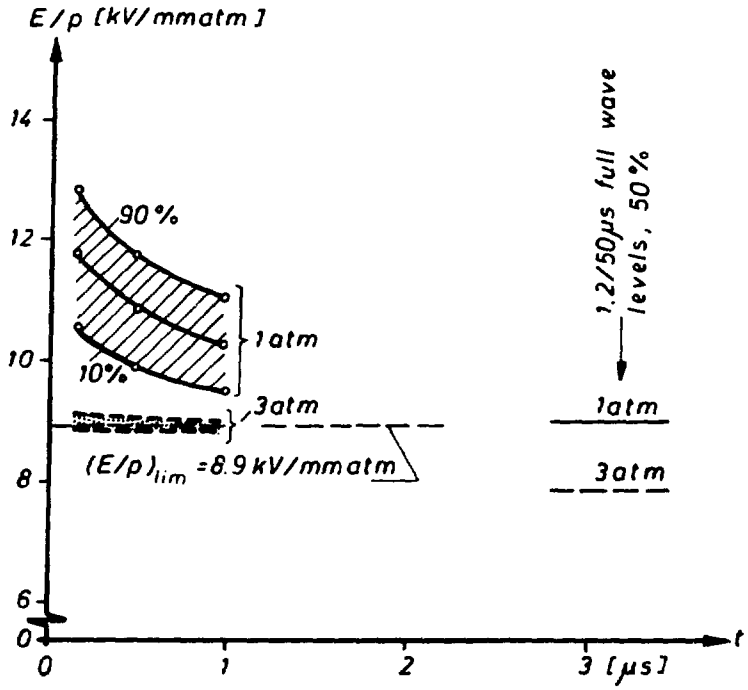

Fig. 6. Calculated breakdown field strength for Model 2 assuming zero formative time lag.

The model gives probability levels for the breakdown field strength, a concept which is used in insulation coordination.

It is seen from Fig. 5 and 6 that it is in the low pressure case (1 atm) and when the stressed electrode area is low that the statistical time lag is of importance for the breakdown strength. It is seen from Fig. 6 that for stressed areas as occuring in high voltage substations and with pressure 3 atm and above the statistical time lag will be of no importance for the breakdown strength. However, in applications where low pressure is utilized and the geometric dimension of the negative electrode area is small it will bend the voltage-time curve upwards in the μs-region.

It must be emphasized that the voltage-time curves calculated are not what would be measured experimentally. In these calculations the influence of the formative time lag is not taken into account.

The effect of this would certainly be the main factor in determining the voltage-time curve when the pressure is high and the stressed electrode area is large, as is the case in the experimental values given in Fig. 4.

CONCLUSION

It is shown theoretically that the statistical time lag in the breakdown process in SF_6 insulation is of influence only in determining the voltage-time curve of SF_6 equipment when the pressure is low and the negative electrode has a small area. This is based on a theoretical approach that successfully has predicted the variation of the breakdown strength for negative impulse voltages with pressure and stressed electrode area.

REFERENCES

1. T. Nitta, Y. Shibuya, Y. Fujiwara, IEEE Trans. PAS No. 1, 108-115 (1975).
2. V. N. Borin, Gas Discharge IEE Conference, September 11-15, 1972.
3. S. Menju, H. Aoyagi, K. Takahashi, and H. Ohno, IEEE Trans. PAS 93, No. 5 (1974).
4. H. M. Ryan and W. L. Watson, ISH/Zurich, 1975. supplement p. 12-16.
5. W. Boeck, ETZ-A Bd. 96, H.7. (1975).
6. W. L. Watson and H. M. Ryan, IEE Conference Publication No. 143.
7. W. Taschner, ETZ-A Bd. 97, H.2. (1976).
8. W. Taschner, ETZ-A Bd. 98, H.2. (1977).
9. W. Knorr, ETZ-A Bd. 98, H.8. (1977).
10. R. W. Crowe, J. Appl. Phys. 37, 1515 (1966).
11. Olsen, Ulriksen, Huse, Schei, CIGRE Paper No. 33-01 (1978).
12. CIGRE, Working Group 15.03, insulating gases, private communication.
13. T. Nitta, N. Yamada, and Y. Fugiwara, IEEE PAS 93, No. 2 (1974).
14. A. Rein, A. Arnesen, and I. Johansen, IEEE PAS 96, No. 3 (1977).
15. W. Legler, Z. Phys 140 (1955).

DISCUSSION

NITTA: Have you ever tried to apply your theory to explain the V-t characteristics published in the literature on various gaps?

JOHANSEN: It is observed that the theory gives results in qualitative agreement with the reported measurements. However, in the theoretical results the formative time lag is not taken into account. Even though this time lag is small, it makes the comparison uncertain. Next, in reported measurements, not all parameters are given. There is also a considerable spread in the measured results. I think the most important part of this contribution is that it may be a guide to further measurements.

BLAIR: 1. The analysis we give in another paper (page 360) in this Symposium makes it difficult for me to accept your explanation of breakdown below the limiting E/P in terms of the statistics of avalanche growth; we should discuss this when the other paper has been presented. 2. It seems to me that, in your model, formative time lags will be very small, so that the voltage-time characteristics will be determined largely by statistical time lags. Do you agree?

JOHANSEN: The model presented does not say anything about the formative time lag. I regard the formative time lag as the sum of the times it takes for an electron to form a critical streamer, the time it takes for a streamer to develop into a channel across the gap, and the time it takes to make that channel into a good conductive arc. Although I consider that to be a short time I think it will have an influence on the voltage/time characteristic, which is not accounted for in the present paper.

PARTICLE CONTAMINATION IN COMPRESSED GAS INSULATION, LIMITATIONS AND CONTROL

Chathan M. Cooke

Massachusetts Institute of Technology

ABSTRACT

The sensitivity of compressed gas electrical insulation to contaminant particles constitutes a basic limitation for practical apparatus which becomes even more severe in compact higher gradient systems. Though only a physically small perturbation, contaminants strongly reduce breakdown voltages in the gas gap as well as across solid insulating supports and are a major cause for substantial variations in performance. Recent studies on compressed gas insulation which emphasize methods of controlling contaminants and their effects are described. Remedies include changes which increase the tolerance of systems to the inevitable particles and also techniques for rendering them harmless. Although particle motion is complex and often determines whether or not a particle triggers failure, it can be utilized by appropriately designed electrodes which provide one way entrances into inactivating low-field trap regions. The results indicate the possibilities of substantial increases in the reliable gradients insulated by gases and improved testing strategies for installed apparatus.

INTRODUCTION

The electrical insulation strength of compressed gases is subject to various adverse factors. Among the more important are inhomogeneities such as conducting particles located in the active insulation region. An emphasis on such contaminants deserves attention since even single, physically small particles or multiple particles of still smaller size can trigger breakdown in the gas at voltages as low as 1/5 that obtained without the added contaminants.[1,2] Experimental evidence increasingly shows that particle movement can be responsible for substantial variations in performance so that a given contaminated system might at one

time withstand a certain test voltage, and at another time withstand only 1/3 as much.[3] Testing such a "dynamic" insulation system for defects is therefore difficult and any breakdowns subject to various interpretations.[4] Particles which are notably more destructive to performance are typically of extended length and of electrically conducting metal or other materials such as insulating fibers in combination with fine conducting powder.[5]

Practical SF_6 gas-insulated power apparatus for 138 to 500 kV systems commonly employ operating stresses of 30 to 40 kV/cm peak in the bus duct regions.[6 - 9] For the gas pressures used in these systems, this amounts to electric stresses of only about 10% the ideal ionization limit. Yet even at such low operating levels particle contamination can be of real concern. Besides the use of clean-room assembly techniques to reduce the amount of contamination, methods to capture and inactivate particles in low-field regions[1] or on adhesive surfaces[10,11] have been described. The successful application of particle trapping methods has been demonstrated for both AC and DC systems.[12,13]

This report classifies particle contaminant effects in quantitative terms and then identifies several factors found to be significant in achieving improved particle control. Most of the experimental results were obtained in coaxial electrode systems of outer electrode size from 250mm to 760mm and inner electrode size from 25mm to 250mm. Test voltages reached 3000 kV DC and peak low-frequency AC of about 1 Hz. SF_6 gas pressures ranged from 1 to 14.6 atm abs. For reproducibility of the test results, controlled quantities of particles were injected and were often of wire or sphere shape.

PARTICULATE ACTIVITIES

Gas Gap

Particles are of concern in insulation systems because they may act to trigger spark breakdown at abnormally low voltages. For SF_6 gas insulation, the amount of loss in withstand voltage caused by particles depends on the particles and on the gas pressure. To quantify this reduction in insulation strength the DC performance of three coaxial gaps ranging in size from 9 to 34cm was studied with and without added particulates. The results shown in Figure 1 were obtained using aluminum wire particles 6.4mm long, 0.45mm dia. which would move prior to breakdown development. The maximum reduction or loss in insulation strength as measured by the breakdown voltage ratio is about 50% at 1 atm SF_6 and does not change greatly even to about 3 atm. However, by 6 atm the loss is in excess of 80% and remains near that point even at higher pressures. In other words, much to the frustration of those who desire compact apparatus, high pressure and hence high gradient systems are more sensitive to contamination.

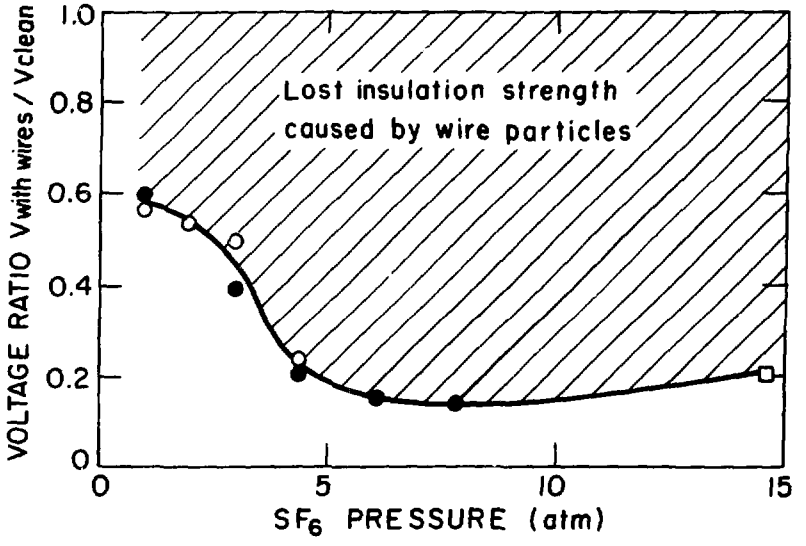

Figure 1 Loss in SF_6 insulation strength due to wire shape particles.

Numerous experimental studies reported in the literature confirm that particles can cause a large reduction in breakdown voltage. However, particle movement prior to the actual initiation of breakdown has been noted to strongly influence performance. An understanding of general particle activity in gas gaps is therefore useful before considering possible remedies to the particle initiated breakdown problem.

Modes of Motion

Particles respond to an applied DC voltage in a variety of ways. At very low voltages there is no noticeable activity, while at higher stresses movement within the gap and electrical effects are detected. Three distinct modes of movement have been observed: bouncing in back and forth traversals between two electrodes: rapid oscillation near only one electrode (sometimes referred to as a "firefly" due to the optical effects it produces): and hovering (where the particle remains in mid-gap for an extended period of time without contacting any electrode).

An overview of particle response is provided by Figure 2 which indicates the applied electric stresses in each of five coaxial systems hav-

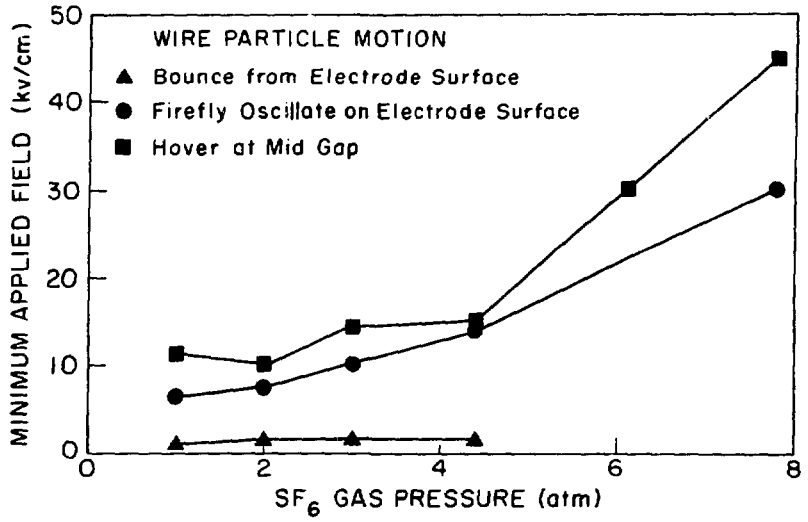

Figure 2 Minimum electric fields for different modes of wire particle motion in SF_6.

ing these different modes of motion. Although each mode was observed to occur for a broad range of applied voltages, the minimum electric field needed to sustain movements was found to be relative consistent from system to system. Figure 2 shows these minimum electric fields for the case of the 6.4mm long, 0.45mm dia aluminum wire particles.

Bouncing motion occurs at the lowest stresses and is independent of gas pressure. Rapid oscillations (i.e. fireflies) and hovering occur at higher fields which increase with gas pressure in a manner to be anticipated from gas ionization inception levels. The fields shown are the applied ambient values at the location of particle movement, those for hovering being the mid-gap applied values. Minimum fields for rapid oscillations were the same for both inner and outer electrodes. Thus because of the coaxial geometry and the preference for this mode on the negative electrode, several times higher positive voltages were needed to achieve the rapid oscillation mode in comparison to negative polarity voltages on the center conductor. The following more detailed descriptions help characterize the three modes of movement, and provide a basis for evaluating methods of particle control.

Bouncing.--Particle motion begins when electrostatic forces exceed gravity and adhesion. Hence, lift-off depends on the applied electric field, particle shape, particle material, and the surfaces involved. Typical lifting fields where there is no grease or other adhesive material range from 4.6 to 14.5 kV/cm and from 2.7 to 8.5 kV/cm for aluminum particles of elongated and spherical shape of 0.1 to 1mm diameter. Once lifted, the particle may traverse the gap, exchange charge at the opposite electrode, and return in a repetitive manner so as to move back and forth in the bouncing mode between electrodes. The bounce frequency increases with increased applied voltage. For coaxial gaps observed frequencies have ranged from 2 Hz to more than 50 Hz. Small electrical

currents result from the charge transported by such bouncing motion and are on the order of 10^{-8} amperes for millimeter size particles. The impact forces from bouncing motion have been observed to deform particles as well as electrodes.

Due to asymmetries in particles and/or electrodes a component of movement tangential to the electrode surface can be introduced on each bounce. In horizontal coaxial electrodes irregularly shaped particles can attain substantial lateral components to their movement whereas smooth shapes will not be strongly affected and therefore will move in relatively straight radial paths. For example, spheres would move laterally on the order of only 1% of the gap spacing during one round trip bounce. Wire particles, on the other hand, were more dynamic and often travelled laterally a distance equal to 30 to 40% of the gap spacing during a single hop. Gravitational forces are significant and bouncing particles demonstrated a tendency to stay on the bottom side of the coax under the center conductor. However, while this preference for the lower side was consistently exhibited by the sphere, the wires deviated substantially from this pattern because of their greater random motion. At high stresses they even bounced entirely around the center conductor to all parts of the coax.

Because particle orientation and electrode surface features will be different with each impact, every hop may be considered essentially independent of the last and a randomization occurs. A statistical model which uses average characteristics may therefore be employed to simulate the bounce pattern. Each succeeding position is determined on the basis of a probability distribution for moving a given distance in one bounce. An accumulation of position probabilities after each discrete bounce then provides a method of tracing movement and predicting particle location after a specified number of bounces.

Such a discrete bounce analysis was used to evaluate observed motion along a coax. In one case studied experimentally, a 760/152mm coaxial system of 1.6 meters length was used. Aluminum wire particles 6.4mm long initially located at the center, required an average time of 30 seconds to bounce out one end or the other when 400 kV DC was suddenly applied to the center conductor. Films of the bounce action indicated a bounce frequency of 3 Hz, an average tangential bounce distance in either direction of 9.1 cm, and a standard deviation of 3.0 cm. The statistical model of this system predicts that 50% of the particles will leave in 27 seconds. Particle position probabilities calculated from a start location at the center after 3 and 7 seconds are shown in Figure 3. Those that have moved out the ends are shown as X's.

Besides the factors of gravity and impact randomization, bouncing motion is influenced by electrode configuration. A fringing field arrangement can actively move bouncing particles to regions of lower average field. This results from the tangential component of the electric lines of force and is easily seen in tests with parallel flat disk electrodes where particles are literally flung out the side when near the edge. Planar, non-parallel electrodes have also been used to illustrate the importance of configuration. Even for relative electrode angles as small as a few degrees smooth bouncing particles show a tendency to move in the direction of wider gap separation. These forces were demonstrated sufficiently to provide a pumping action which can move particles up hill against gravity when the electrode assembly is tilted.

In general the bouncing mode of particle motion under DC voltages provides a means for extensive particle movement. This movement can be expected to permit particle entry into most regions of typical bus duct structures.

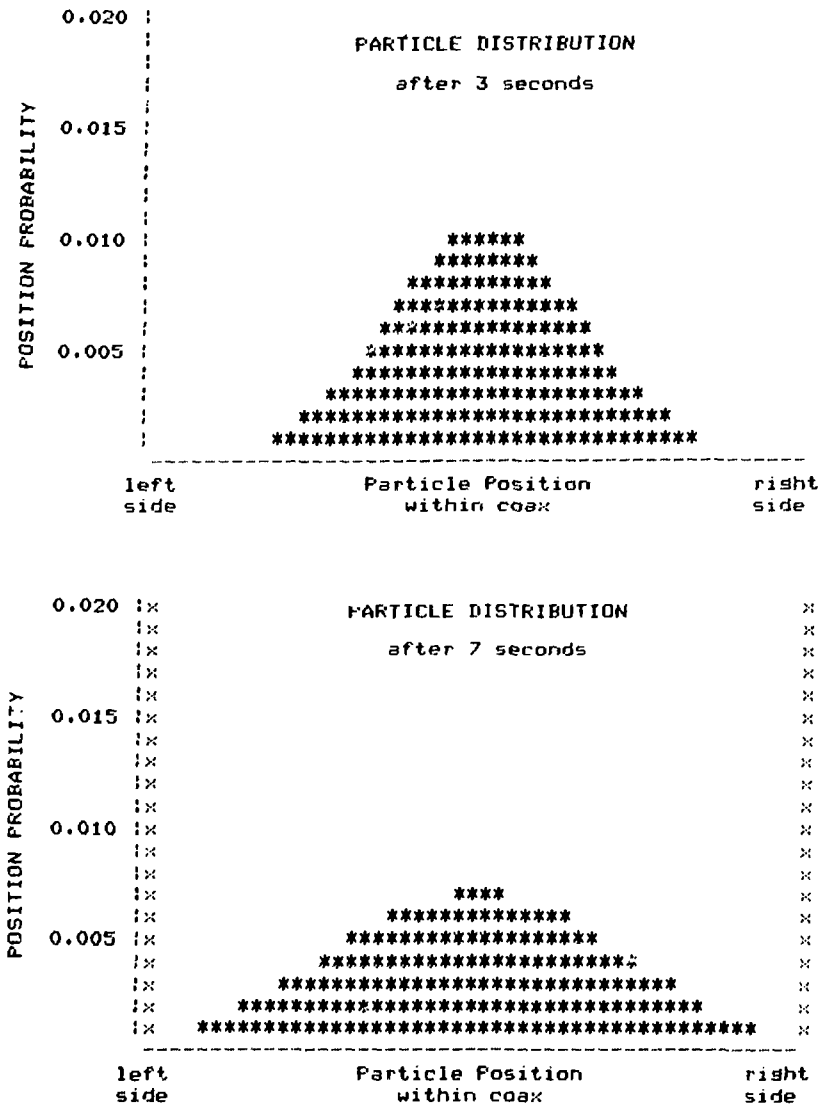

Figure 3 Calculated bouncing wire particle position probabilities.

Rapid Oscillation (the Firefly).--Particle motion in a gas gap does not necessarily involve a bouncing movement back and forth between the electrodes. Because particle forces result from the product of field and charge, a variation in charge during transit will also alter particle motion. This effect is easily distinguished in experiments with DC voltages where elongated particles are observed to slow down and reverse direction in mid-gap. An extreme case of such charge alteration is the so-called "firefly" or rapid oscillation effect. This rapid oscill-

ation of a particle near one electrode is always accompanied by ionization and emitted light and seems to be related to the particle exchanging charge in its own ionization generated space-charge cloud.[1]

In SF_6 there is a strong preference for this type of motion to occur on the negative polarity electrode surface at either the inner or outer conductor of a coaxial system. Particles with large length to width ratios were more frequently seen in this mode, presumably because they more easily produce the needed ionization. Interelectrode currents ranged from less than a microamp to more than 100 microamps, light emission increasing with current.

The movement of particles under the rapid oscillation mode appears random with frequent changes in direction. At low electric stresses the motion is relatively slow and is seen to be affected by gravity since the particle remains at the lower side of the electrode on which it is moving. At high stresses the movement is more rapid and appears less dependent upon gravity, the particle easily traveling around the center conductor. This motion can typically result in the particle staying near one location for an extended period or traveling along the surface quickly, a distance of 10cm in less than a second.

Hovering.--An additional form of movement, the hovering mode, occurred when an elongated particle was aligned radially in the coaxial gap. A hovering particle would remain in the mid-gap region for an extended period of time without moving close to either electrode even though a DC voltage was applied. This was observed especially on the lower side of coaxial systems with outer to inner electrode diameter ratios of 5 to 10, and at positive voltages above gas ionization levels. It appears that an equilibrium is achieved in which gas ionization and slight radial movement allow the particle to charge and discharge so as to just balance the force of gravity. This was the least stable form of

motion, though on occasion lateral movement also occurred. In one such case the particle was seen to "float" down the mid-gap region and on out one end.

Dielectric Support Surfaces

A solid insulating surface which spans across a gas gap can introduce new features to the breakdown process. For example, it may promote discharge development due to vapors, or it may hold static charges and solid particulates for substantial periods of time. However, for a number of clean epoxy materials used as mechanical supports in SF_6 gas, there is no evidence that breakdown necessarily occurs at much lower stresses on insulating surfaces than in the gas gap remote from such insulators. To the contrary, surface flashover gradients have been found to be comparable to those for gas gap breakdown.[14]

The influence of contaminants on dielectric surfaces is clearly significant. Particles can initiate surface flashover whether loosely held by electrostatic forces or firmly fixed by adhesive. For single conductive particles, surface flashover occurs at voltages comparable to those when the same particle is in the adjacent gas gap, although somewhat lower results have been found with rapid polarity reversals for the firmly affixed situation. Currents which decay, currents which are steady, and ultimately surface flashover can all be induced by elongated fixed particles. The rapid decay of initial currents observed for constant unipolar DC voltage indicate surface charging of the dielectric may act to suppress steady gas ionization.

Experimental studies were conducted with 6.4mm long aluminum wires attached to the equator of a cast epoxy post-type spacer to demonstrate the characteristics with contaminates held in isolation midway along an insulating surface. Though initial currents would decay, steady currents could be maintained at elevated voltages. As depicted in

Figure 4 the pressure dependence of the current-voltage relation for such an attached, floating-potential wire is similar to the familiar positive point-to-plane characteristics.[15]

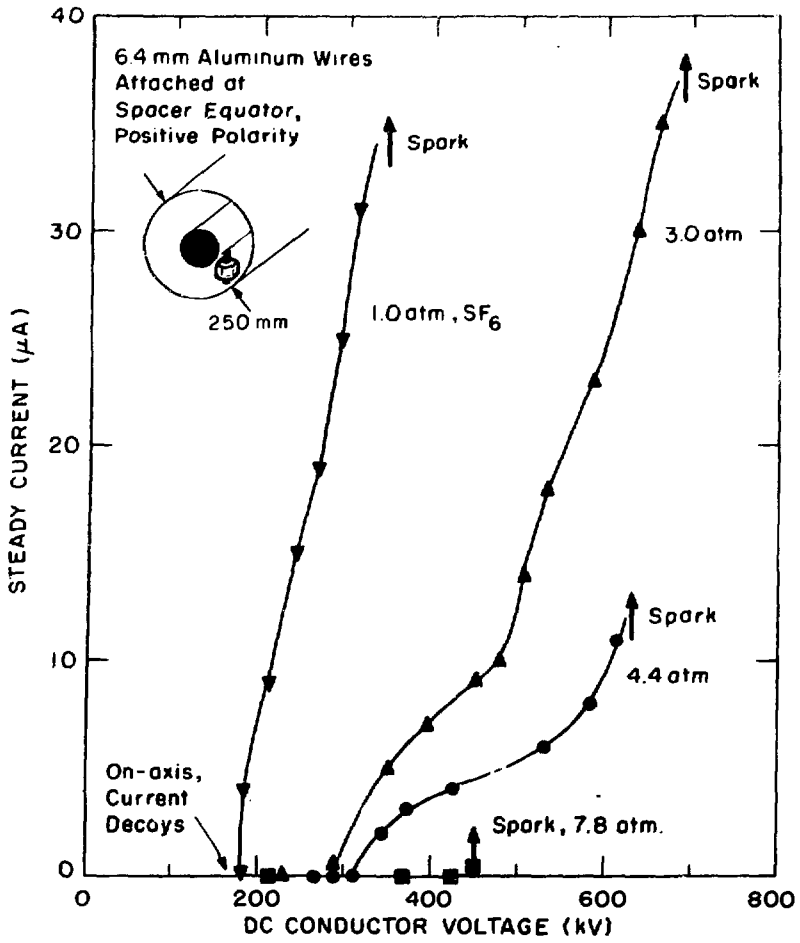

Figure 4 Gap currents for wire particle fixed to spacer surface.

The presence of particles can greatly alter charge accumulation on dielectric supports. Under relatively low voltage conditions, our recent studies have shown surface charges on clean epoxy posts in coaxial lines accumulate at a moderate rate, form a relatively smooth distribution and are of polarity equal to the center conductor. However, as seen in Figure 5 the charge accumulation pattern is very different with

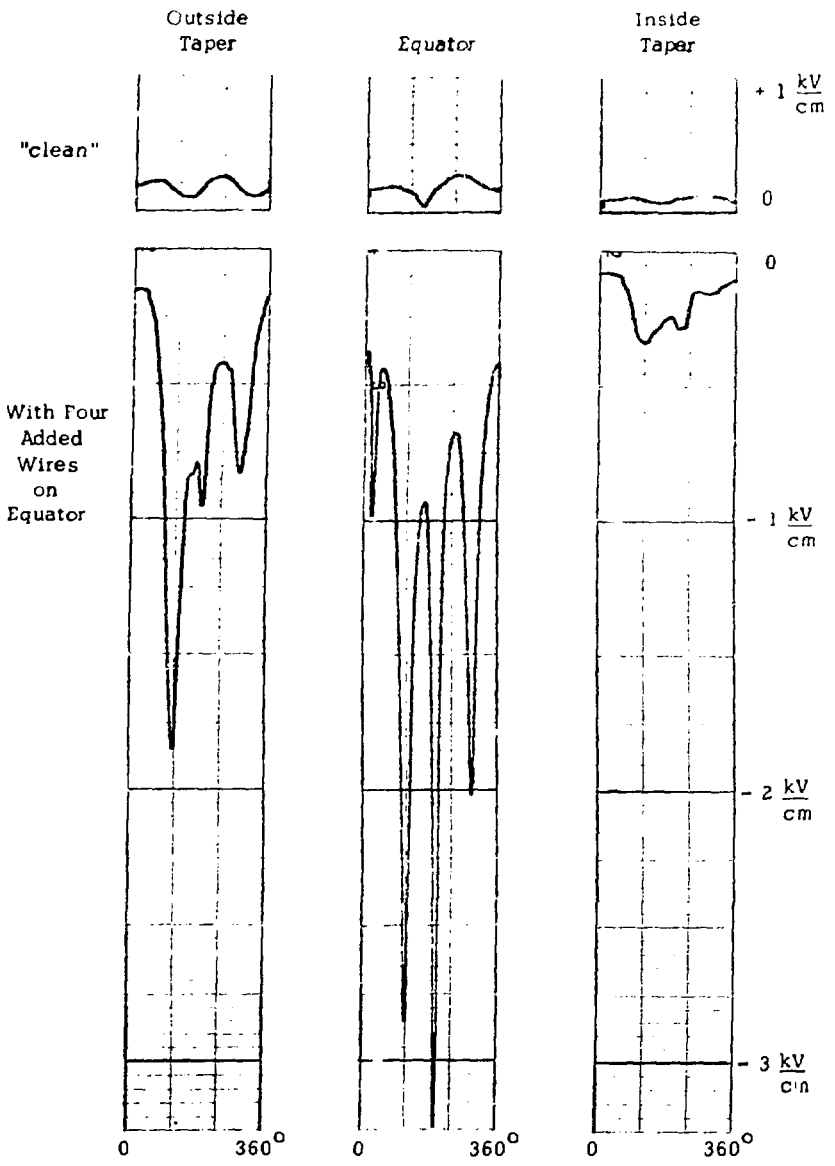

Figure 5 Fields from static charge accumulated on a spacer during 1 minute at positive 200kV DC voltage in 4.4 atm SF_6.

metallic particles on the surface. Not only are there sharp peaks in intensity, corresponding to the wire positions, but the polarity is also reversed. Thus even though the center conductor is positive the insulator surface becomes charged strongly negative, and vice versa. Substantial alterations in the stress distribution can therefore be anticipated when contaminates are present.

The triggering of surface flashover by single wire particles can occur for a wide range of particle positions. However, low voltage breakdowns were often observed when loose particles move by chance to regions where the surface stress was highest in the absence of particles. In the two configurations depicted in Figure 6, the particle was located in a high field region and flashover voltages were low even though the discharge path was relatively tortuous.

The motion of loose particles in a coaxial system is also influenced by insulating support spacers. Bouncing particles could readily move to and stay on such supports. This behavior seemed more notable when residual charges and gradients in electric fields are likely to have been on the surface. Rapid oscillations, i.e. fireflies, were frequently seen to approach the vicinity of spacers, and then to move away without touching or hopping on to the insulating surface.

Besides introducing variations in initial test results particle effects can cause changes over the long term. Particles which eventually move to more sensitive areas such as high field regions on the electrodes or dielectric surfaces may ultimately reduce the insulation strength of a system. On the other hand, movement of a particle to a less sensitive region can result in improved insulating strength. Control of particulate movement thus affords the opportunity for increasing both the reliability of testing and of long term performance. Though it is tempting to solve the particle problem by simply eliminating all contamination, this is usually impractical and allows no margin for error that would introduce a particle. In addition, due to the dynamics of some equipment, particles will be generated on the interior necessitating particle control. The next section is devoted to the consideration of various control techniques.

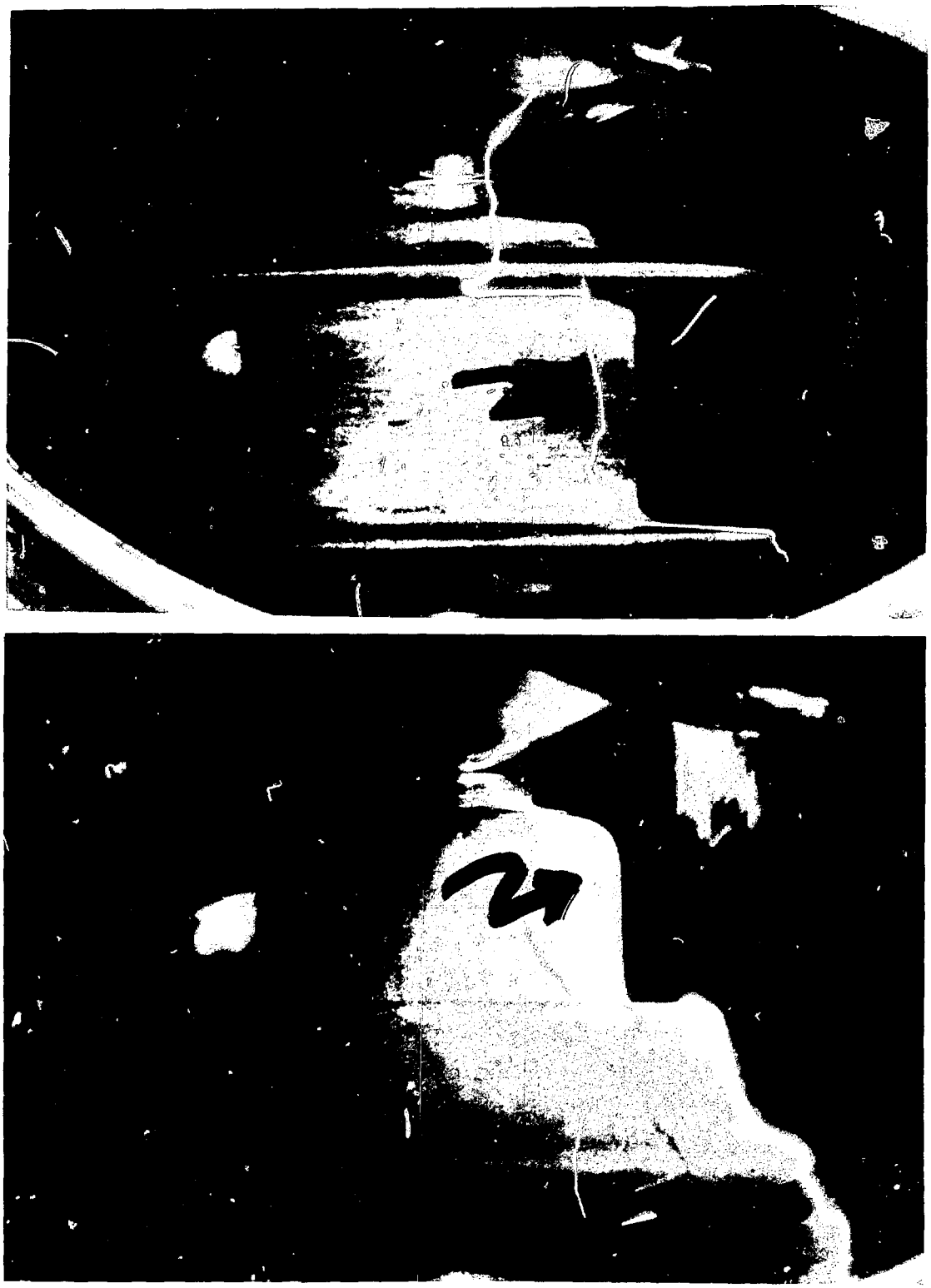

Figure 6 Spacer surface flashover initiated by loose wire particles (indicated at arrow), in 6-8 atm SF_6, negative conductor.

CONTROL OF PARTICLE EFFECTS

Particle effects can be controlled by either of two substantially different methods. One approach seeks to make gas-insulation systems more tolerant of particles, while the other involves methods which remove or prevent particles from entering sensitive, active insulation regions. To increase the tolerance of a system, one or more of the following techniques can be employed.

1. dielectric coatings
2. different gas compositions
3. improved support spacers

Particle removal and elimination on the other hand may make use of:

1. adhesive surfaces
2. ionizing radiation
3. barriers
4. particle traps

Results of our studies indicate that improvements can be achieved by both the tolerance and removal methods.

Particle Tolerant Support Spacers

Because particulates can be attracted to make contact with and even be held by solid insulating supports, the surfaces of these insulators take on special importance. One feature commonly considered in the design of insulators for open-air service is surface contour. However, in the hermetic, high-gradient environment of compressed gas insulated equipment conditions are substantially different than open-air so that fundamental principals need to be reexamined to determine what surface characteristics are important.

Perhaps it is because gases are so sensitive to excessive electric fields that commensurate gains in withstand voltage do not follow directly with increased end-to-end path length provided by corrugations or

other contour forms. As seen in the previous breakdown pictures, the surface flashover path can readily dip into a corrugation and move uphill against a reverse ambient gradient, passing a potential well to continue to the finish. Thus it can be expected that once a discharge is started, it will follow complicated paths where necessary to complete breakdown. In some instances this can include the puncture of intervening solid dielectric.

The minimum insulation strength obtained with four different post-type insulator configurations under rapidly applied DC voltages is depicted in Figure 7. Gas gap and worst case surface flashover voltages without added particles are shown as the dashed lines. When 6.4mm long aluminum wire particles were added, surface flashover occurred over a broad range of voltages. The minimum flashover values for each of the 4 configurations are within the hatched regions. A distinction is made between two types of initiation; in one case the particle was seen on the surface as the voltage was increased and in the other the particle was seen to be moving in rapid oscillation on the inner or outer conductor near the spacer prior to ultimately triggering surface flashover. None of the designs were very superior over the entire pressure range. However, the two shapes in the Figure on the left, WO and SU, generally failed at lower voltages than the two on the right, SD and F2.

The results indicate certain gains in performance can be made and provide design guidelines:

1. There is a trade-off with corrugations. Due to intensified regions of electric stress, the uncontaminated insulation strength of the spacer is lowered in order to increase the contaminated strength.
2. A longer surface path length does not necessarily increase the contaminated insulation strength.

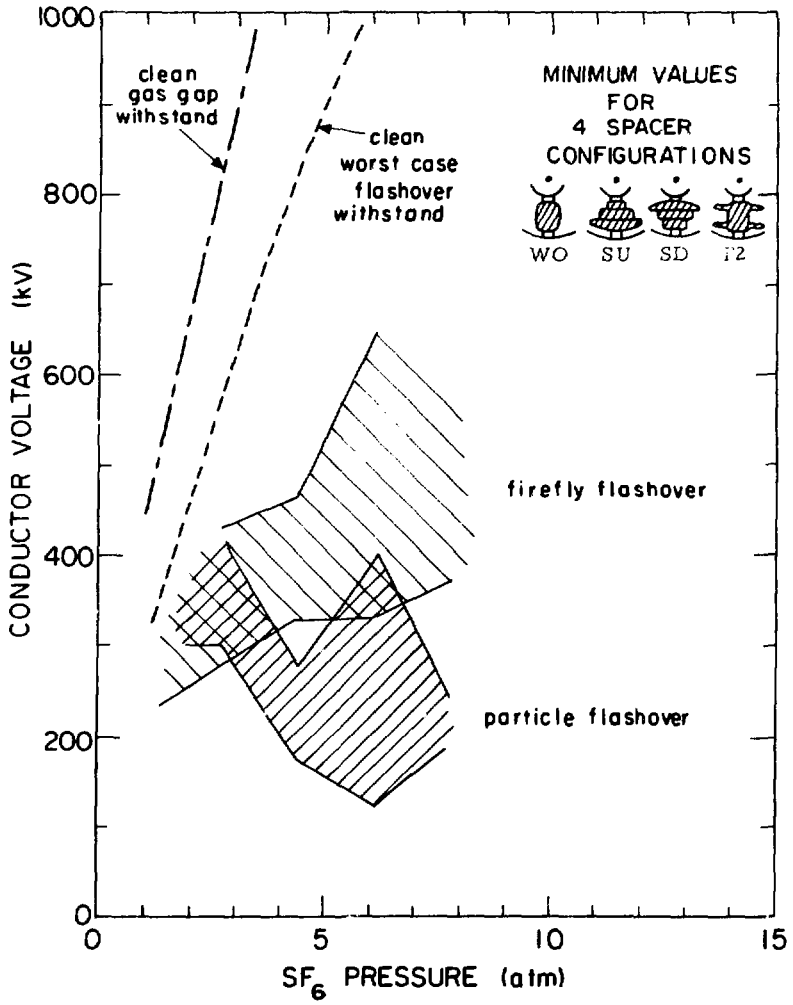

Figure 7 Minimum spacer surface flashover for 4 configurations.

3. Insulating surfaces should avoid high stress regions where an elongated particle can reside. For example by sitting across a distance amounting to ambient equipotentials of only 10% the total voltage, such particles can cause a 5-fold reduction in surface flashover voltage.

Because supports may be exposed to a variety of voltage transients and waveforms after particles have collected on the surface, it is important to include investigations of time dependent effects to confirm the performance of tolerant designs.

Particle Barriers and Traps

In practical gas insulated equipment such changes in geometry as corners, connections, and supports can produce localized regions of higher electric stress. Systems with some particle tolerance may result from methods which prevent movement of contaminant particles into the sensitive regions thereby improving overall performance and reliability. Barriers are therefore of interest to generally limit movement or to move particles away from certain regions.

Particle motion may also be turned into an advantage. Where traps are employed, movement can cause the particles to enter regions where they cannot escape or act to trigger failure. Low-field particle traps achieve this result by use of cavities or other electrode configurations which sufficiently reduce the field in a local region where particles can migrate.

Particle Barriers

The influence of barrier structures on particle motion can be complicated. Typical barriers in our investigations have included metal rings slid into a coaxial line arrangement. For DC voltages vertical face rings with a half-round radius on their tops have not been found effective in restricting particle motion. Aluminum wire particles placed on one side of the barrier were not excluded from crossing to the other section of the line in either the bouncing or rapid oscillation modes of motion. Although there was a tendency for the particles to stay in the vicinity of these rings during rapid oscillation, wire particles at negative polarity on the center conductor in SF_6 could move near, hop up onto the top and move on over to the other side of such structures.

However, a simple structure for preferentially moving particles in one direction has now been conceived and reduced to practice at MIT. In this barrier structure the ring form is still used, but rather than being

symmetrical as in previous devices, this ring is tapered so that there is a relatively long ramp on one side and a sharp drop on the other. Particles in the rapid oscillation mode of motion demonstrate a strong preference for walking up this ramp to the higher field region at the top, movement off the ring being easier from its sharp face. By creating a preferential direction for particle movement, the tapered ring acts as a particle pump. When such assymetric rings are located at intervals along a coaxial line, a distributed pumping action can be achieved.

The causes for this pumping action seem to be associated with the mechanisms for the rapid oscillating motion itself. The assymetry in the applied fields results in assymmetric, ionization induced space charges. The particle being repeatedly charged and uncharged then experiences a net lateral force. The angle of the ring's taper was not found to be especially critical, one minimum length would require that on random excursions the particle does not walk all the way back down the ramp before returning to the top.

Though it is reasonable to combine particle pumping with particle trapping configurations to more effectively move particles to trap regions, this combination was generally not needed in the experimental studies. The usual technique was to instead inject particles near the areas being investigated.

Particle Traps

Our recent studies have also emphasized contamination control by means of low-field particle traps. The size, shape, and interior of a trap can influence the electric field distribution and were found to be important in determining particle trapping characteristics. Since a particle must travel to a trap before it can drop inside it, these studies distinguished between trapping behavior observed with the two types of particle motion, bouncing and rapid oscillation.

As noted earlier, the trapping action of a low-field particle trap relies on sufficient reduction of the field in a localized region to prevent further activity. Calculations for various cavity configurations indicate that it is not difficult to achieve such low fields. Even values well below the experimental level of a few kV/cm needed to elevate elongated aluminum particles are easily produced. For example, the field strength at the bottom of a slot shaped trap of depth D and width W is reduced by about 10 raised to the -1.36 D/W power. A ten thousand-fold reduction therefore occurs for a slot just 3 times deeper than its width. The efficient trapping of particles in practice thus centers around promoting their movement to the trap and into its interior.

Elongated aluminum wire particles can easily be activated into either bouncing or rapid oscillation motions and thus have been used to obtain data on relative trapping efficiencies. Testing of a variety of different trap designs in coaxial electrode systems with DC voltages showed that particles did not always have a tendency to fall into traps. Especially under conditions where rapid oscillation motion exists, the particles can "walk around or hop over hole shaped traps with a diameter larger than the particle length. In contrast, a bouncing particle once headed for a trap would always drop into it.

Measurements indicate that the area of a trap's opening is most significant with bouncing particles. Substantially all bouncing particles would be trapped within seconds when the trap opening area in the general vicinity of the bouncing reached about 1% the total area of the outer conductor. Though particles in rapid oscillation in effect "walk up" to a trap and then fall in, the length of the trap edge was not the only consideration. Edge contour was also influential, relatively sharp radius edges of less than 1/2cm on a trap lip being about twice as effective in trapping fireflies as larger radius edges of 2 to 5cm. Still further gains

could be made by using even sharper edges. Figure 8 shows measured trapping efficiencies for hole and slot shaped traps under both modes of motion.

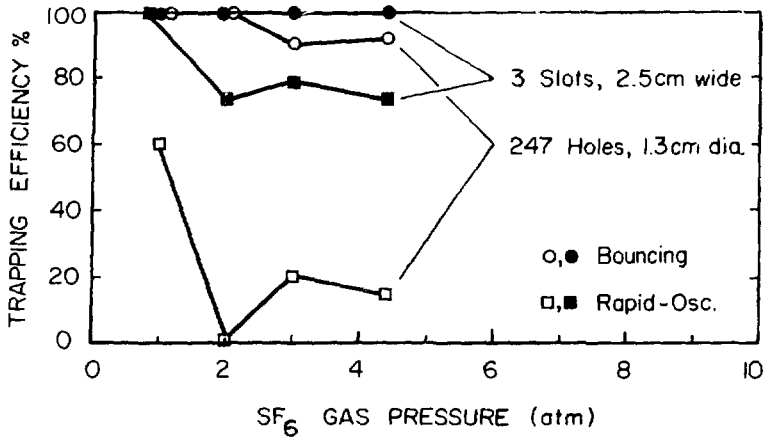

Figure 8 Particle trapping in coaxial electrodes.

Trapping of particles in the bouncing mode can be effectively modelled. The procedure follows that outlined previously in the Section on bouncing motion where no traps were employed. The particle position is traced on a bounce by bounce basis. The portion of particles that land in trap regions are accumulated and removed from further activity in the gap. By looking at the total fraction trapped after each bounce, a distribution of times to trapping for a given configuration can be determined and compared to measured results. Figure 9 provides a comparison of trapping times in a 760/254 coaxial electrode test system having 19 equally spaced, slot shaped traps that were each 6.4mm wide by 25cm long. Within 5 seconds 90% of the particles were trapped. Studies with several arrangements did not show a strong influence on trap effectiveness for SF_6 gas pressures from 1 to 4.4 atm.

Motion pictures of particle movement and trapping within the experimental test system indicate that the model is a reasonable representation of the physical process. Once established, such a model is a useful

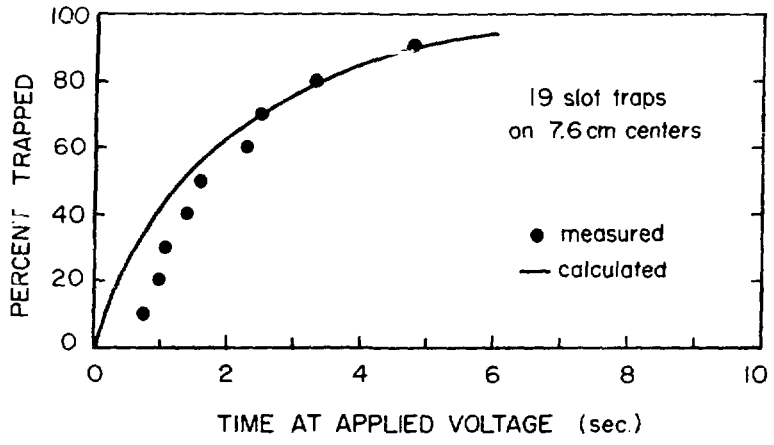

Figure 9 Time for trapping bouncing wire particles.

simulation tool. Not only can estimates of time to trapping be made, but also many other parameters can be studied. These include influences on trapping efficiency of trap size and distribution within a bus duct and of particle starting positions.

In a trap configuration designed to be effective for both modes of particle movement, relatively sharp trap edges and sufficient trap area were included in one design. This system used a series of 3 long slots, 2.5cm wide and 2.5cm deep, separated by 46 cm. Within 30 seconds, 97% of the bouncing particles and 78% of the rapidly oscillating particles were trapped. This demonstrates that good efficiencies can be achieved in a single design. Nevertheless it may still be advantageous for more complete particle removal, to energize the system at different voltages and waveforms so that a greater confidence in the trapping procedure is obtained. It may even be useful to periodically repeat such a procedure.

In conclusion, the control of particle contamination can lead to very substantial gains in the electrical performance of compressed gas insulated equipment. There are several modes of particle motion which result in substantially different particle movement patterns. Such modes of movement are influential to particle control and need to be considered when evaluating control techniques. Improvements to performance can be

achieved by raising the tolerance to particle contaminants or by actively controlling and trapping them. Better designs for support spacers, barriers which control particle location, and more effective low-field particle traps can each be useful for limiting the effects of particle contamination in compressed gas insulation. Ultimately, the goals of more efficient and reliable insulation can be expected to depend upon the better control of contamination.

ACKNOWLEDGEMENT

The program of research on compressed gas insulation at M.I.T. has been a team effort at the High Voltage Research Laboratory and is supported by the U. S. Department of Energy and the Electric Power Research Institute. The author wishes to acknowledge his indebtedness to contributing students at the Laboratory including Charles Rollman, Roberto Velazquez, Nombumitsu Kobayashi, Thomas Jones, Christopher Manglesdorf, and William Heil and especially to Professor John G. Trump.

REFERENCES

1. A.Diessner and J.G.Trump, "Free conduction particles in a coaxial compressed gas insulated system", IEEE Trans.PAS 89, 1970 (1970).

2. E.B.Ganger, A.A.Leibold, "The influence of foreign particles on dielectric strength in SF_6 installations", IEEE N.Y. PES Mtg.Paper A 76 152-9 (1976).

3. C.Cooke, R.Wootton, and A.Cookson, "Influence of particles on AC and DC electrical performance of gas insulated systems at extra-high-voltage", IEEE PAS 96, 768 (1977).

4. S.A.Boggs and F.L.Ford, "Acceptance testing of SF_6-insulated installations", NAS Conf.on elec.Insul.and Diel.Phen. N.Y.Oct.(1977).

5. H.Kuwahara et al, "Effect of solid impurities on breakdown in compressed SF_6 gas", IEEE PAS, 1546 (1974).

6. T.Takagi, T.Higashiro, E.Kusakabe et al, "Development of 500 kV gas spacer cable", IEEE PES Mexico City Mtg., paper F77635-6 (1977).

7. J.C.Cronin et al, "Basic design characteristics of a three conductor gas-insulated power transmission system", IEEE PES Vancouver Mtg. paper C73 499-1 (1973).

8. G.P.Baer, A.Diessner, G.F.Luxa, "420 kV SF_6-insulated tubular bus for the Wehr pumped-storage plant electric tests", IEEE PAS 95, 1552 (1976).

9. B.O.Pedersen, H.C.Doepken, Jr. and P.C.Bolin, "Development of a compressed-gas-insulated transmission line", IEEE PAS 90, 2631 (1971).

10. I.M.Bortnik and C.M.Cooke, "Electrical breakdown and the similarity law in SF_6 at extra-high-voltages", PAS 91, 2156 (1972).

11. T.Morva, U.S. Patent No. 3,553,410 (1971).

12. B.L.Johnson and H.C.Doepken, Discussion to paper of J.C.Cronin and E.R.Perry, IEEE PAS-92, 563 (1973).

13. R.Nakata, "Particle scavenging studies leading to the development of a HVDC gas bus system", NAS Conf.on Elec.Insul.and Dielect. Phen.,Colonie,N.Y. Oct. (1977).

14. C.M.Cooke and J.G.Trump, "Post-type support spacers for compressed gas-insulated cables", IEEE Trans. PAS 92, 1441 (1973).

15. C.N.Works and T.W.Dakin, "Dielectric breakdown of sulfurhexafluoride in nonuniform fields", Trans.AIEE 78, 682 (1953).

DISCUSSION

NAKATA: Our experience during the development of the HVDC gas bus was that particles go into the rapidly dancing state at the conductor surface (at voltages higher than the full gap traverse voltage) predominantly at the negative electrode. Thus for the motion picture you showed, the rapid dancing particle did indeed occur at the outer enclosure(which was negative relative to the positive central conductor). Further, we find that when the central conductor is negative, an untrapped particle could cause stress inversion such that particles already trapped in long traps 1/4" wide by 3/4" deep would be re-levitated. We will show this behavior of polarity and particle motion with a film at this symposium. When the central conductor was positive,we could not cause a similar re-levitation. Have you experienced such polarity effect or re-levitation?

COOKE: The induced removal of particles from your traps may be the result of an insulating layer, perhaps from oxides on the metal surfaces,which allow the particles to acquire substantial amounts of charge. Our studies indicate particles are always elevated when the charge and field produce forces sufficient for lift-off, whether in a trap or not.

DUTTON: 1. All the particles you mentioned were 6.4 mm wires and you showed the effect of voltage on the type of motion. Do you have information about the effect of size of the particle on the motion?
2. Was the simulation of particle ation that you talked about for a particle with bouncing mode?

COOKE: Particle size and shape can change the relative stresses at which the different modes of motion occur. Both rapid oscillation and

hovering take place more readily for longer particles than for shorter particles. This is expected in view of the fact that these motion modes always occurred at voltages where ionization is found. Initiation of bouncing motion, on the other hand, was essentially independent of length for particles of the same material, as has been reported previously.

Yes, these movement simulation studies were for the motion patterns in the bouncing mode.

FARISH: 1. I was interested in the technique of using a particle guide in the high-stress conductor to move particles in a desired direction. Does this work equally well for smaller particles assuming that they can be persuaded to adopt the oscillatory motion? 2. I noticed that the slot-type particle traps were tested with particles similar in width to the particle length. Could you indicate how trap performance depends on the length and shape of the particle present and how you would select an "optimum" trap aperture for a practical system? 3. In earlier work, we observed that particles would interact so that several small particles could possibly give the same effect as a single large one. Could you give some guidance on the conditions under which multiple particles are liable to interact and what this implies for contamination control based on maximum particle size?

COOKE: Smaller particles also demonstrated the preference for following our particle guide. As to particle trap dimensions, the data reported includes designs of width substantially greater than particle size (see Fig. 8). Such designs proved to be very effective. The

optimum appears to be a compromise in achieving sufficient interior field reduction versus width; a width several times the maximum particle length seems to be appropriate. Edge contour can be important, too. Sharper edges, rather than rounded corners, encourage trapping under rapid oscillation. For multiple particles at one time, collisions can take place. Such collisions increase tangential motion and can produce even higher electric stresses in the gas. Unless the number density of particles is large, particle-particle collisions seem to be relatively rare.

SLETTEN: I take it that your experiments were made in SF_6. What was the gas pressure? Have you experimented with other gases and pressures?

COOKE: Our particle studies have included some measurements to pressures above 10 atm SF_6. The general effects described for the lower pressures were also seen at the higher pressures. The studies shown in the motion picture film employed 2 atm SF_6. Tests in other gases have also shown the different modes of motion, but of course the stresses to induce these may be substantially different. For example, in N_2 rapid oscillation can occur at lower stresses.

PACE: As you increase pressure, do you see the three modes tend to appear in the same order they appear as you increase voltage?

COOKE: For the tested pressures of 1 to 4.4 atm SF_6, the three modes of movement may occur even at a single fixed value of voltage. However, the minimum stresses where each mode was observed did follow the sequential order indicated in the Fig. 1. This order remained the same for changes in pressure.

LAWRENCE: Have you tried other metals than aluminum such as copper, silicone, and other metals and organic materials with possible metals imbedded?

COOKE: A variety of other particle materials have been studied and the single most significant feature appears to be that they have sufficient conductivity to readily acquire and release charges.

SECOND LIMITING FIELD STRENGTH IN SF_6 GAS DISCHARGE - QUANTITATIVE ESTIMATION OF EFFECT OF ELECTRODE SURFACE ROUGHNESS ON BREAKDOWN

T. Takuma T. Watanabe
T. Kawamoto
Electric Engineering Laboratory, Central Research Institute
of Electric Power Industry, Japan

ABSTRACT

This paper describes the effect of surface roughness on discharge characteristics of compressed SF_6 gas. Prebreakdown dark current characteristics were found to vary greatly with surface roughness. Three different patterns of prebreakdown current appear for highly polished surfaces, surfaces with regular rounded unevenness and surfaces with irregular fine protrusions, respectively.

Then, the macroscopic field strength giving the discharge inception was calculated for sharp protrusions as extreme cases. A sharp blade-like protrusion (two-dimensional) gives as the discharge field strength approximately const. $\times\sqrt{p/h}$, where p is gas pressure and h protrusion height. A sharp needle-like protrusion, on the other hand ,ives const. /h, which becomes 3800/h (kV/cm, h in μm) if 10.5 is adopted for K ($K = \int(\alpha - \eta)\,dx$). This value, which the authors call "the second limiting field strength in SF_6 gas discharge", means the lowest limit of discharge field strength when an electrode has a protrusion of height h. It presents a strong contrast to the first limiting value 89p (p in atm), which gives the discharge condition for ideal gaps without protrusions. Experiments have shown that some uniform gaps with large electrode surface area give a totally saturated breakdown voltage against pressure as predicted by the value const./h.

INTRODUCTION

A number of papers have been published which discuss the relationship between electrode surface roughness and breakdown characteristics of SF_6 gas. They are divided into two main treatments: macroscopic and microscopic. In the macroscopic treatment first Cookson[1] and then Nitta et al[2] applied the extreme statistics to the distribution of weak points leading to breakdown in SF_6 gas. In the latter's analysis, the effect of the surface conditions is included in a constant λ of a Weibull-distribu-

tion. $\lambda = \lambda_0 \exp(1.15\ p)$ where p is gas pressure and λ_0 is a constant which depends only on the electrode material and roughness. Although Nitta et al give values of λ_0 experimentally for two kinds of roughness, it is not clear what λ_0 means and how λ_0 is related to various practical electrode surface conditions.

In the microscopic treatment, on the other hand, a single protrusion of suitable shape is assumed as a high field source leading to breakdown. As a protrusion form, for example, Pedersen[3] adopted a hemisphere, Avrutskii[4] a spheroid and Berger[5] a hemispherically capped rod, respectively. They calculated the breakdown voltage caused by a protrusion and compared it with the experimental value.

We first studied prebreakdown current characteristics in compressed SF_6 gas and then developed the microscopic treatment of the roughness effect to find a limiting relation between a protrusion height and the discharge inception field strength.

PREBREAKDOWN CURRENT

In this experiment, we used three different surfaces for an upper electrode of various materials in a 5cm diameter sphere-to-plane arrangement:

--- highly polished smooth surface
--- surface having regular rounded unevenness of 50 μm height
--- surface rubbed with an emery paper No. 80, which was found by an electron-microscopic photography to have fine irregular protrusions of maximum height 25 μm.

Prebreakdown current was measured in a short gap length of 3mm with negative dc voltage under atmospheric pressure and 5 atm of SF_6. No clear difference of current characteristics between electrode materials of aluminum, stainless-steel and brass was observed. Other main results are summarized briefly because of space limitations.

Under atmospheric pressure, no prebreakdown current was detected above the measurable limit of 10^{-10} A regardless of the cathode material and roughness until breakdown suddenly occurred. At 5 atm, the current

characteristics were found to vary greatly with surface conditions and to be divided into the following three types:
Type A (smooth surface) : Prebreakdown current flows only as a few short pulses of several nA and, in most cases, only during the voltage application to the first breakdown.
Type B (rounded unevenness) : Current also flows briefly but for a longer time (sometimes several minutes) than Type A. If the voltage is raised in steps, the current generally flows during the voltage rise or directly after the step.
Type C (sharp protrusions) : Prebreakdown current has a steady component as well as pulsive ones. The steady component amounted to the order of 100 nA immediately before breakdown.

Examples of prebreakdown currents for these three types are shown in Fig. 1. We may explain these characteristics with breakdown voltage for three electrode surfaces as follows:
In Type A, pulsive prebreakdown current is probably attributed to remaining very fine protrusions or perhaps also to attached free particles. They melt during the first voltage application by high field (stress conditioning) or by later sparks, which causes breakdown voltage to rise with the breakdown number. In Type B, transient current is also considered due to melting of remaining protrusions, which, owing to the surface unevenness, may be larger than in Type A. For Type B, little or no rise of the breakdown voltage with the application number was observed. On the other hand, the electrode surface for Type C has many breakdown current sources, which cause a steady component. The spark conditioning needed much more breakdowns than for Type A.

Two possible mechanisms are suggested for prebreakdown current in SF_6: field emission and ionization multiplication (microdischarge) at protrusion tips. We recorded the faint light in a Type C gap by exposing film several minutes at a voltage slightly lower than the breakdown. This means that prebreakdown current is caused not by field emission but by microdischarge, at least in a coarse electrode surface. We consider that microdischarge is a more probable cause than field emission in Types A and B as well, because transient pulsive current suggests the sudden current

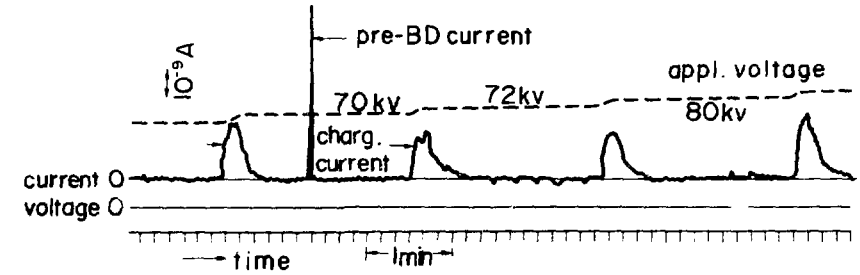

(a) Type A (smooth electrode, brass)

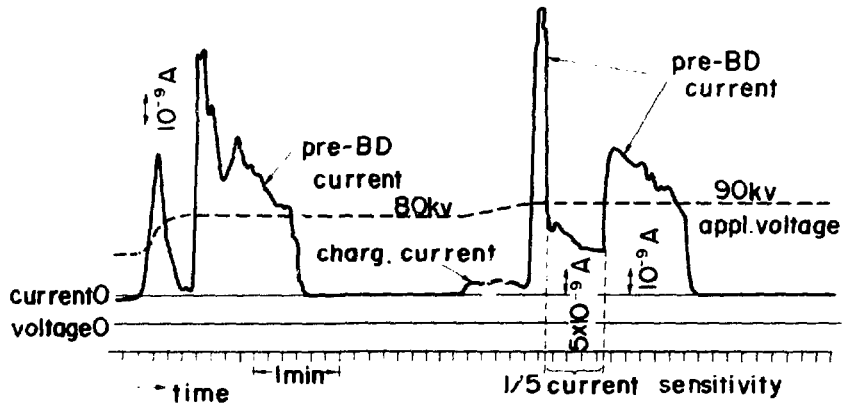

(b) Type B (rounded unevenness, stainless-steel)

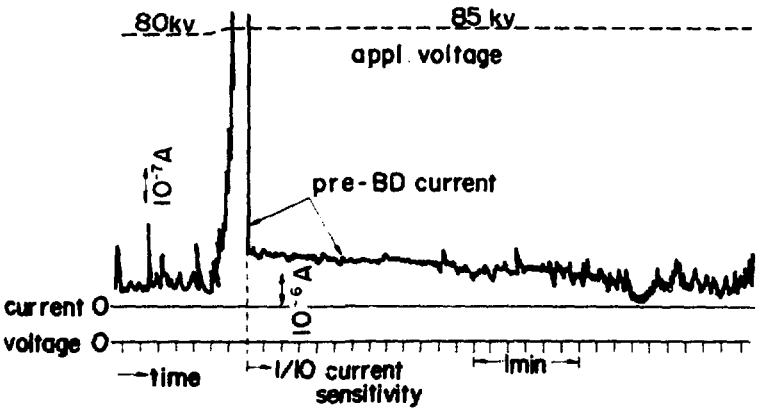

(c) Type C (sharp protrusion, Aluminum)

Fig. 1 Examples of Prebreakdown Current with Applied Voltage

increase at the instant when the discharge condition is satisfied.

SECOND LIMITING FIELD IN SF_6 GAS DISCHARGE

1. Discharge Inception Caused by a Sharp Protrusion

In the microscopic treatment of the surface roughness effect, the discharge inception caused by a single protrusion is calculated from

$$\int_{x_m}^{x_\ell} (\alpha - \eta)dx = K \qquad (1)$$

where

α and η = ionization and attachment coefficients,

x_m and x_ℓ = points where the field strength is maximum and $E_\ell(\alpha - \eta)$, respectively, in a gap.

If we use

$$\alpha - \eta = 27.7\ (E - 89p) \qquad (2)^6$$

where

E = field strength in kV/cm,

p = gas pressure in atm,

we can derive a simple discharge condition,

$$V(x_\ell) - 89\, x_\ell = K/27.7 \qquad (3)$$

Both x_m and the potential at x_m can be taken as zero without losing generality. The term K is problematic, as it is not insignificant in nonuniform fields. As the value of K, we[7] have suggested 18.6 + ℓn d (d = gap length) in uniform fields and Nitta et al[8] used 18. But for safety and a reason described in the Appendix, we here adopt 10.5 which Pedersen[3] and others recently used.

Figure 2 shows E_d/p (E_d = macroscopic discharge inception field strength) for some protrusions calculated from Eqs. (1) ~ (3) similarly as made by Pedersen[3] or Berger[5]. The dotted line is E_d/p for the electrode arrangement consisting of a 5cm diameter sphere with 50 μm regular un-

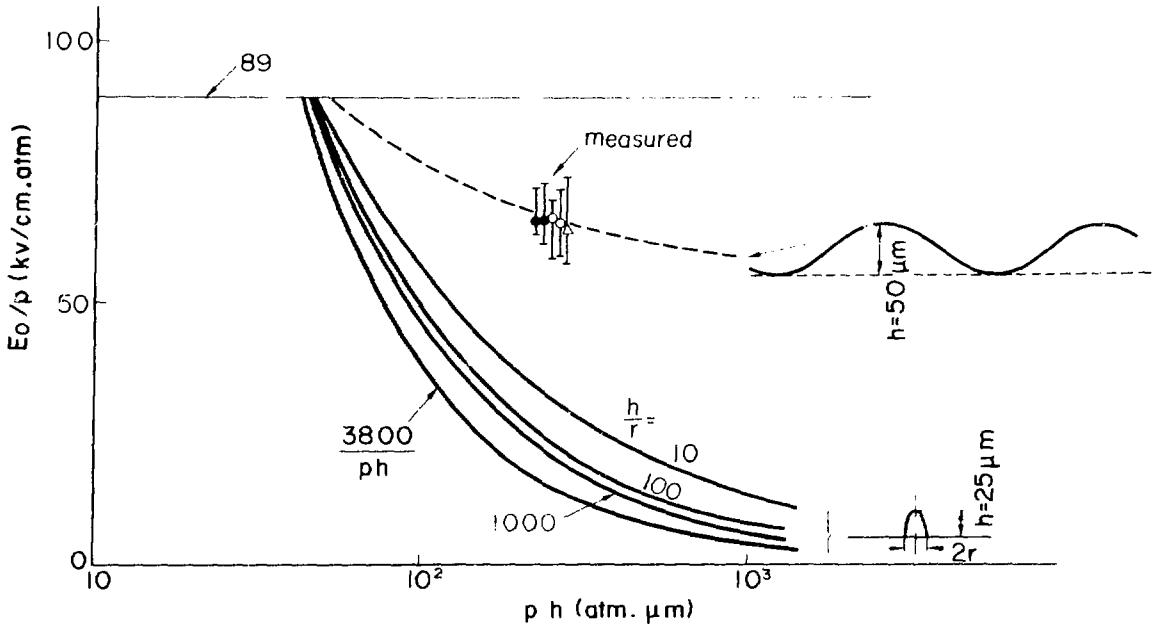

Fig. 2 E_0/p versus ph (E_0 = Macroscopic Discharge Inception Field Strength, p = Gas Pressure, h = Protrusion Height)

evenness and a plane that was used for measuring prebreakdown current. It agrees very well with the measured values for three electrode materials. Solid curves show E_d/p calculated for sharper spheroidal protrusions of 25 μm height. It is important that E_d/p is much lower for a sharper protrusion in spite of the smaller height especially when p is higher. Therefore, we derived the discharge field strength for sharpest protrusions.

(i) Needle-like Protrusion

The field distribution at a needle-like protrusion with height h can be analytically obtained by making thin a prolate spheroid which protrudes towards a uniform field E_0. If we take x from the protrusion end towards the field direction, we find as a limit a singular field distribution

$V = 0$ and E is infinitely high at $x = 0$

$V = E_0 (x + h)$ and $E = E_0$ at $x > 0$

On applying this distribution to Eq.(3),

$$E_n(kV) = 3800/h \quad (h \text{ in } \mu m) \tag{4}$$

(ii) Blade-like Protrusion

A very thin blade-like protrusion can be given as a limit of an ellyptic cylinder in a uniform field E_0. The field strength at x from the protrusion end is

$$V = E_0 \sqrt{x^2 + 2hx},$$

$$E = E_0 (x + h)/\sqrt{x^2 + 2hx}$$

This field distribution gives as the discharge field strength

$$E_b(kV) = 100\sqrt{67.5ph - 1440}/h \quad (h \text{ in } \mu m) \tag{5}$$

2. The Second Limiting Field Strength in SF_6 Gas Discharge

The field strength E_ℓ(= 89p) was first derived by Geballe et al[9]. They called this value "the limiting field strength" for SF_6 gas discharge by suggesting that E_ℓ is the discharge field strength in a uniform gap of SF_6 for larger $p \times d$. If we compare two field strengths, E_n and E_b, with E_ℓ, E_ℓ = const. $\times$ p, E_n for a needle-like protrusion = const. /h and E_b for a blade-like one = const. $\times\sqrt{p/h}$ when $p \times h$ is large.

E_ℓ (= 89p) is considered the field strength causing discharge in ideal conditions of SF_6 gas, while E_n (= 3800/h) is the lowest limit of the discharge field strength that a protrusion of height h may cause. Therefore, we would like to call this value "the second limiting field strength in SF_6 gas discharge". E_n is a very simple expression and has a marked feature that it is independent of the gas pressure p. Figure 3 shows the discharge field strength E_n and E_b for needle-like and blade-like protrusions of h = 25 and 50 μm with E_ℓ. These curves show that, at higher pressures, a sharp needle-like protrusion will determine the discharge inception in SF_6, even if it has a smaller height than a rounded or a blade-lke one.

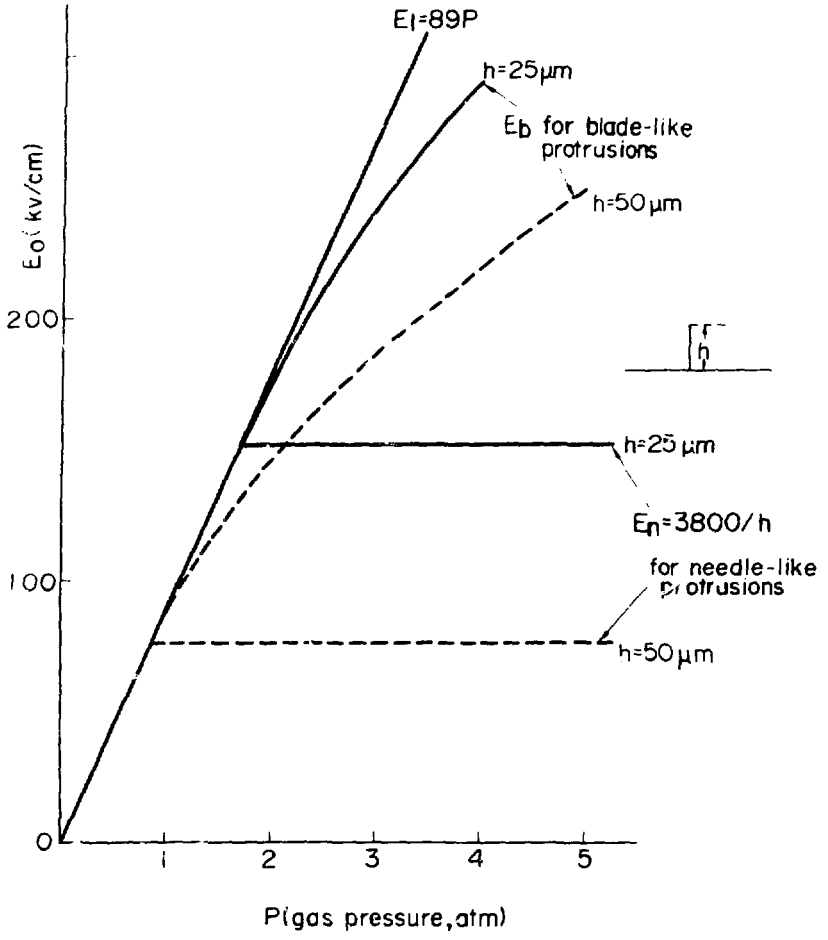

Fig. 3 Relation between Discharge Inception Field Strength E_0 and Kind of Protrusion

EXPERIMENT WITH UNIFORM GAPS

We studied the relation between electrode surface roughness and discharge voltage experimentally with two Rogowski electrodes having comparatively large surface area. One of them is Aluminum-Aluminum, 15cm in plane diameter, and the other Graphite-Graphite, 16cm in plane diameter. Protrusion heights on the surface were measured with a contact-needle method (10 μm end diameter) on eight lines at 45-degrees intervals that stretch radially from the center of the electrode surface. Although, in practice, surface roughness is generally expressed by the difference between protrusion height and depression depth within a fixed length, we adopted the protrusion height above a properly chosen surface level as the

height which affects discharge inception. Figure 4 shows a cumulative number distribution F(t) of these protrusion heights t on a logarithmic normal probability chart for Aluminum and Graphite.

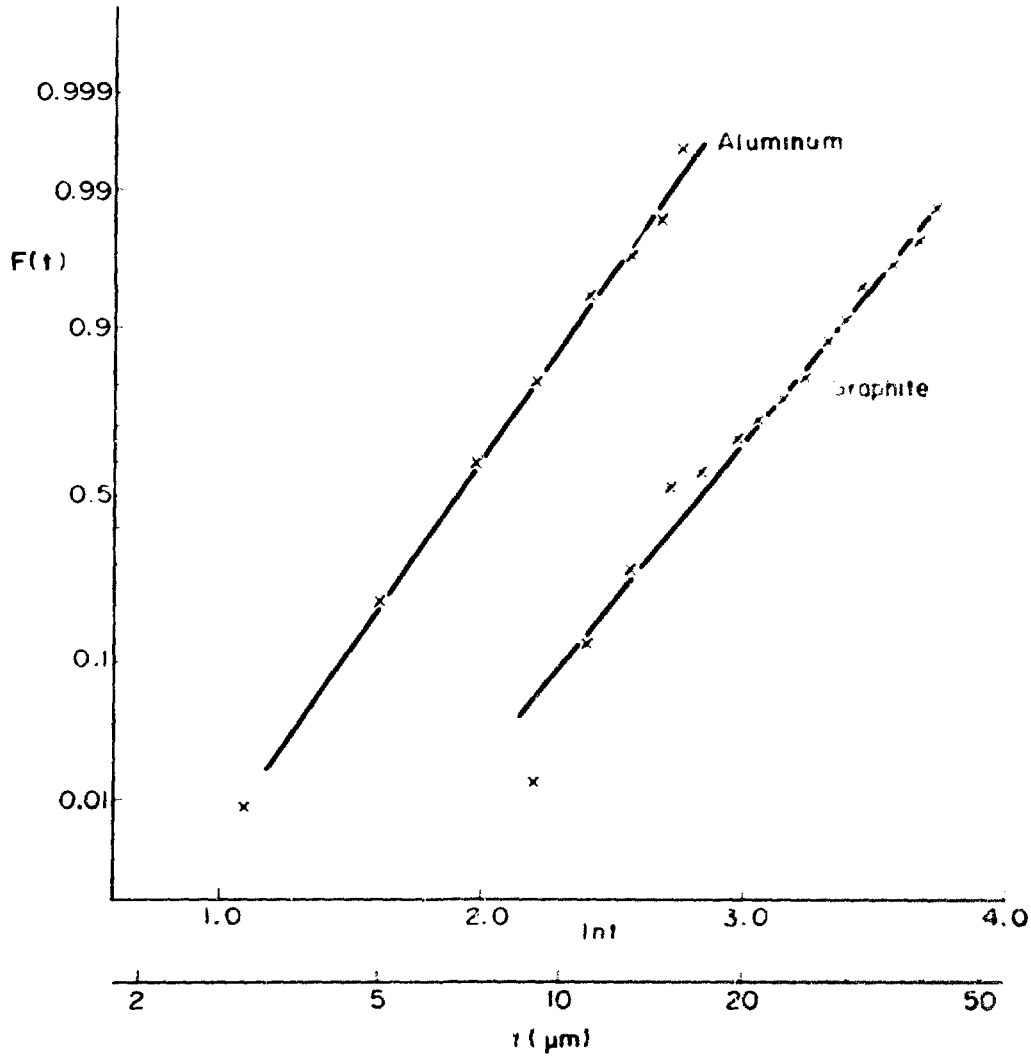

Fig. 4 Cumulative Number Distribution F(t) of Protrusion Heights t on a Logarithmic Normal Probability Chart

It is not easy, however, to obtain from these measurements the protrusion height h which gives the second limiting field strength. Two methods may be possible:

(a) Maximal measured heights : The five largest values of t were 14.7 ~ 17.5 μm for Aluminum and 32 ~ 43 μm for Graphite. The problem is that

firstly these values depend on the measured surface area and secondly the protrusion shape is not considered.

(b) Heights corresponding to a certain number of protrusions on the surface : For this, F(t) was extrapolated to higher values of t by assuming this as a linear function of ℓn t on a normal probability chart as shown in Fig. 4. Then, the number of heights on the surface which surpass t is roughly given by

$$N(t) = (1 - F(t)) S/\Delta S \qquad (6)$$

where ΔS and S - area measured by a contact-needle and total area of the plane surface.

For example, the protrusion height corresponding to N(t) $10^3 \sim 10^4$ is 14.5 ~ 18.5 μm for Aluminum and 34 ~ 48 μm for Graphite. These values do not differ greatly from those given in (a). In this estimation, however, the problem is an assumed function of F(t), because sufficient data are not easily obtained in larger values of t.

Figure 5 shows dc breakdown voltages in SF_6 gas for these two electrodes. Hatched areas show the range given by the second limiting field strength for protrusion heights t which correspond to $10^3 \sim 10^4$ of N(t). The agreement between this range and the measured values is not so good in the case of the Graphite electrode which has larger surface roughness. However, as expected by the expression of E_n, the breakdown voltage shows saturation against the gas pressure at higher pressures and is proportional to the electrode separation.

DISCUSSION

We here list and discuss briefly main problems concerning "the second limiting field strength", E_n. They are :

(a) on deriving E_n,

--- assumption of an extremely fine needle-like protrusion,

--- validity of the discharge condition Eq.(1) in a very small non-uniform region.

As can be seen in Fig. 2, however, the discharge inception field strength

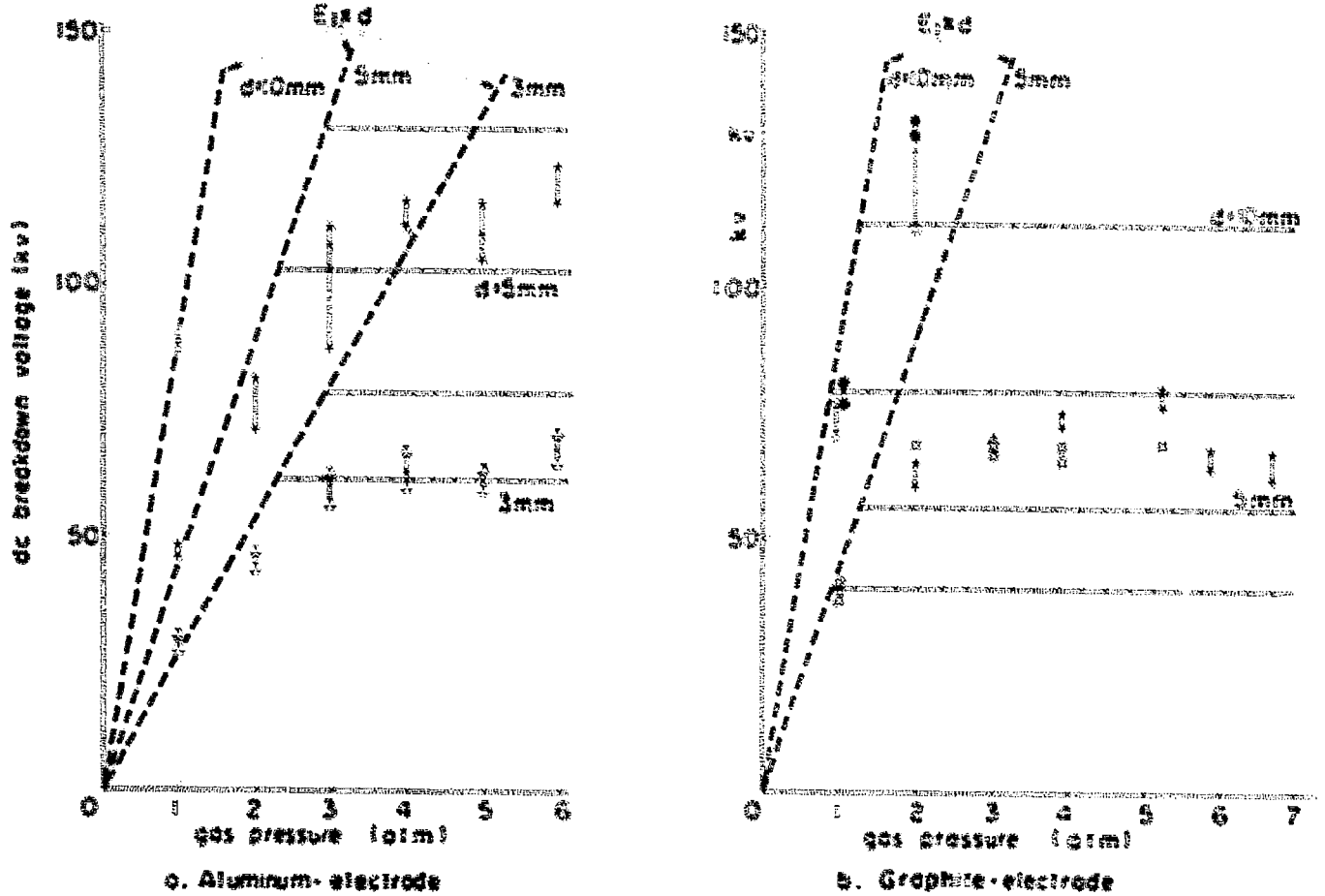

Fig. 6 DC Breakdown Voltage for Rogowski Electrodes (d = Gap Length. Hatched Areas are Explained in the Text.)

does not differ too much for sharper spherical protrusions if the ratio of two radii is not exceeds 100. So the second limiting field strength is considered as upper value as far as a fine protrusion leads to breakdown.
--- value of k in Eq.(1).
This point is briefly discussed in the Appendix.
(b) an uncertainty surface roughness.
--- deformation of sharp protrusions by a measuring needle,
--- definition of a plane surface level for obtaining effective protrusion heights,
--- determination of a protrusion height for E_0 which corresponds to a certain number of protrusions on the electrode surface.
All of them are factors which bring an uncertainty in giving E_0 from measured practical protrusion heights. Our work which may more reliably relate a practical surface condition to breakdown voltage is now in progress.
(c) an evaluating E_0 with experiment,
--- that the measured value is not generally discharge inception voltage but breakdown voltage,
--- surface change due to the conditioning effect during experiment.
It was observed in the experiment with the discharge photomultiplier tube that pre-breakdown current pulse in flow at about 70 to 90% of the breakdown voltage for type C and this inception voltage tends to increase with the breakdown number.
--- effect of applied voltage shape and electrode arrangement.
Probably the large electrode surface with dc voltage application, as we here used, will give the lowest discharge voltage as expected by E_0. For rather it has many sharp protrusions which are not easily destroyed by conditioning.

APPENDIX

Value of k in Eq.(1)[7]

We assume that discharge occurs in Δr_c when the space charge field strength of an electron avalanche exceeds the limiting field strength E_r. If we assume that the space charge forms a sphere of radius r,

$$\frac{1}{4\pi\varepsilon_0} \cdot \frac{eN}{r^2} = E_f \qquad (7)$$

where

$N = \exp \int (\alpha - \eta)\, dx$ total number of electrons in an avalanche,

e electron charge,

ε_0 dielectric constant in vacuum.

At time t measured from the avalanche start, r is expressed as three-dimensional diffusion radius with a diffusion coefficient D as

$$r^2 = 6Dt \qquad (8)$$

In such molecular gases as the drift velocity of an electron is proportional to E/p, Eq.(7) gives

$$E = [illegible] \frac{24\pi\varepsilon_0 D}{e\mu} E_f \int_{x_{cr}}^{x_f} [illegible]\, dx$$

Under steady state of these gases, also

$$D/\mu = kT_e/e$$

where

k Boltzmann constant,

μ and T_e electron mobility and temperature.

If we take $kT_e \approx 1$ eV in electronegative gases,[11]

$$E \approx [illegible] E_f \int_{x_{cr}}^{x_f} [illegible]\, dx$$

For uniform gaps, $E \approx E_f$. Therefore

$$E \approx [illegible] \quad (V \text{ in cm})$$

In extremely nonuniform gaps, E is much smaller because E becomes larger and ionization distance $(x_f - x_{cr})$ becomes much shorter. For example, E

may be of the order of 8 to 11 for a sharp spheroidal protrusion with 100 ~ 1000 of h/r.

REFERENCES

1. A. H. Cookson, Proc. Instn. Elect. Engrs. 117, 1, 269 (1970).
2. T. Nitta et al., IEEE Paper T74-465-1, (1974-7).
3. A. Pedersen et al., ibid. PAS-94, 5, 1749 (1975).
4. V. A. Avrutskii et al., Soviet Phys. Techn. Phys. 18, 3, 386 (1973).
5. S. Berger, IEEE, PAS-95, 4, 1073 (1976).
6. H. A. Boyd et al., Proc. Instn. Elect. Engrs. 118, 12, 1872 (1971).
7. T. Takuma et al., CRIEPI-Report No. 68065, (1968).
8. T. Nitta et al., IEEE, PAS-90, 3, 1065 (1971).
9. R. Geballe et al., Phys. Rev. 92, 4, 867 (1953).
10. von Engel, Ionized Gases, p249, Oxford at the Clarendon Press, 1965.

DISCUSSION

FARISH: In our calculations at Strathclyde for various ratios h/b of protrusion height/width, we were concerned that, for values of h/b $\lesssim$ 10, the measured values of $\bar{\alpha}/P$ and the linear relation $\alpha/P = A(E/P) - B$ might no longer be applicable. How have you resolved this problem in calculations for protrusions with h/b = 1000? Also, have you any comments on the conditions of h and h/b for which the calculation predicts corona onset rather than direct breakdown?

TAKUMA: The purpose of our paper is to show the existence of the lowest discharge inception field strength. Even if $\bar{\alpha}/P$ breaks away from and becomes lower than the linear relation at higher E/P as you say, E_n is the lower limit in the safety side. On the second point of your question, E_n always predicts corona onset when corona precedes breakdown. I have no idea of the boundary value of h and h/b for the transition. It certainly depends on the pressure.

COOKSON: On the calculation of the effect of surface roughness in SF_6 would one expect corona stabilization at the tips to effectively shield the high field site?

TAKUMA: You are strictly right in that the calculation is applicable only to the field without space charge. I only claim that, for short protrusion (where E_n is relatively high), the breakdown voltage is near the discharge inception voltage and that in such cases, E_n may be a practical estimate of the breakdown field strength.

DUTTON: I agree with the last two speakers that the influence of space charge at the points has to be considered carefully. Relevant to this is the magnitude of the emission current which you discussed at the beginning of your paper. Could you please tell us the order of magnitude of the emission currents you measured in the different surface states?

TAKUMA: I also agree that the calculation is applicable only to the field without space charge. The magnitude of the current was several 10^{-9}A for Type A and Type B, and 10^{-7} - 10^{-6}A for Type C. Examples are shown in the paper. Furthermore, I consider, as described in the paper, that the pre-breakdown current was caused not by emission but by ionization multiplication (local discharge), because firstly we observed a faint light for Type C and secondly the pre-breakdown current for Type A and B rises suddenly.

EFFECT OF DURATION OF VOLTAGE APPLICATION AND NUMBER OF CONDUCTING PARTICLES ON THE AC BREAKDOWN STRENGTH OF COMPRESSED SF_6 IN A COAXIAL SYSTEM

R. E. Wootton, F. T. Emery
Westinghouse Research & Development Center, 1310 Beulah Rd., Pgh.,PA 15235
and
A. H. Cookson
Westinghouse CGIT Laboratory, Westborough, MA 01581

ABSTRACT

Breakdown results are presented showing the effect of duration of application of ac voltage on the strength of a 7.5/25 cm coaxial electrode system containing free conducting particles and filled with compressed SF_6. Significant differences in strength are shown to be obtained with a step procedure in which the voltage is maintained at a constant level for three minutes compared with a ramp increase in voltage at 2.3 kV/s.

Further results are given which show the effect of having various number of free particles present in the electrode system. Significant differences in strength are obtained with variation in the number of particles from one to sixteen with both the above methods of test. Breakdown paths involving more than one particle are reported to occur in some cases.

The above results are discussed in terms of statistical effects which arise from interactions between the alternating-voltage, the particle motion and a critical particle-to-electrode spacing required for breakdown in SF_6.

Some possible consequences in the area of field conditioning and in procedures for field testing practical systems are discussed.

The work was performed at the Westinghouse Research and Development Center under a research contract on "Particle-initiated breakdown" sponsored jointly by the Electric Power Research Institute and the U.S. Department of Energy.

INTRODUCTION

The concept of transmitting large amounts of low frequency power through coaxial conductors insulated by compressed gas is now a well established practical procedure, and installations exist in many parts of the world. Their reliability is achieved through careful quality control and testing both in the factory and after assembly in the field. Existing methods are, however, not able to eliminate all free conducting particles

from the system during assembly in the field, and these particles are often potentially able to lead to a failure of the system by initiating a flashover in the compressed gas. By suitable conditioning procedures it is possible to transfer these particles from regions in which they can cause failure into particle-traps where they are harmless. The system is finally proved to be fully conditioned and free of active particles by an ac proof field test at a voltage well above the working level.

This paper reports results obtained using fixed or free particles or both, in a coaxial electrode system with SF_6 over a range of gas pressures. The effect of using a stepped increase in voltage is compared with using a linearly increasing ramp voltage having a faster average rate of rise of voltage. The effect on the breakdown voltage of varying the number of free particles simultaneously present is reported, as are the effects on particle motion of interactions between a fixed particle and free particles. These results are discussed in relation to field testing procedures. Breakdown with more than one particle in the flashover path, and the effect on breakdown strength of multi-particle breakdown is reported and discussed.

The strong statistical effects found in these experiments are closely related to results previously reported[1] by the authors on the critical dependence of breakdown voltage on the particle-to-electrode spacing at the instant of breakdown for particle-initiated ac breakdown in compressed SF_6. For instance, for 6.4 mm long aluminum particles in SF_6 at 0.44 MPa (the working pressure of many practical SF_6 systems) the dependence of breakdown voltage on the particle-to-electrode spacing is such that a displacement of the particle from the critical by less than half a millimeter (either towards or away from the electrode) increases the breakdown voltage by about forty percent. Movement of the particle into contact with the electrode doubles the breakdown voltage. This critical spacing of a free particle normally exists for only a small fraction of the time because of its rapid motion to and fro between the electrodes.

In addition, the peak ac voltage exists for only a small fraction of each cycle and only positive polarity is favorable for breakdown.

This paper reports the strong statistical effects which are observed as a result of these phenomena mainly as a strong dependence of breakdown voltage on time of application of voltage in the range of minutes to hours and a dependence of the breakdown strength on the number of free particles present.

APPARATUS

Coaxial aluminum electrodes with an inner conductor of 76 mm OD and an outer conductor of 250 mm inside diameter were used inside a cylindrical steel pressure vessel, 0.73 m in diameter by 1.7 m high inside. A 450kV 60Hz 0.5A 3-cascade transformer was used for breakdown tests with a 180 kohm series resistor. Visual observations of particle movement and corona were made via four windows in the wall of the steel pressure vessel. Corona measurements were made using the signal developed across a small inductor in the ground connection to the electrode system. Sixty Hertz and dc corona current measurements employed the same bridge circuit as in previous experiments[2].

RESULTS

Fig. 1(a) shows the variation of 60Hz breakdown voltage (or maximum withstand voltage) with SF_6 gas pressure for a coaxial electrode system containing an aluminum particle 6.4 mm long by 0.45 mm diameter One of the three curves on the figure applies to the case where the particle is fixed perpendicular to, and is in electrical contact with, the inner coaxial conductor.No free particles are present. The second curve applies to the case where the particle is free to move to and fro between the electrodes under the influence of the 60Hz voltage. In both the above cases the test voltage is raised from zero at a constant rate of 2.3kV/s until breakdown occurs. The third curve is also for a free particle, but the voltage is raised in 5kV steps at three-minute intervals, the voltage remaining at a constant rms value between steps.

Breakdown with Ramped or Stepped Voltage Test Procedures

Considering first the two curves of Fig. 1(a) each relating to a single free particle it can be seen that there is a significant difference in the breakdown strength depending on whether the voltage is raised at a constant rate of 2.3kV/s, or is raised in 5kV steps with the voltage maintained at a constant level for three minutes between steps. The curve plotted in Fig. 1(a) for the latter case is the highest withstand voltage. The lowest breakdown voltage is 5kV higher since 5kV voltage steps are used. The bars on the ramped curve represent the range of breakdown voltages recorded. It may be seen that the lowest breakdown voltage for the stepped voltage test is less than the lowest breakdown voltage using ramped voltages over the whole range of gas pressures used. Similar experiments with two, four, eight and sixteen free particles present show that the breakdown voltage with the stepped-voltage procedure is significantly lower in each case than where the voltage is ramped upwards (Figs. 1 and 2).

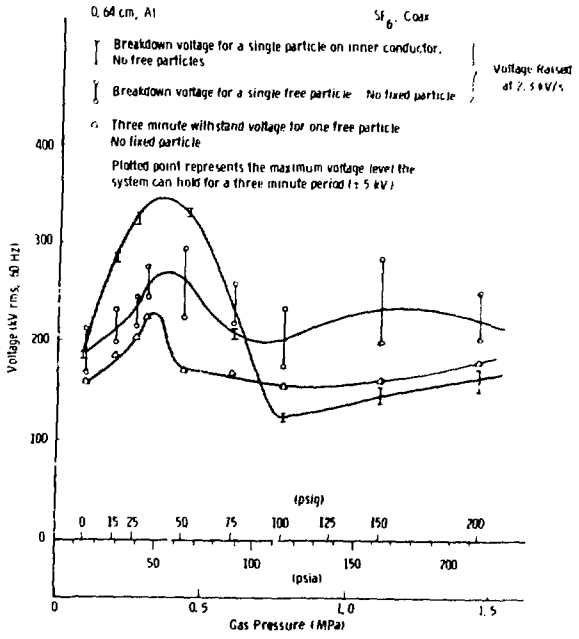

Fig.1(a)-Breakdown voltage for a single fixed 6.4 mm long x 0.45 mm diameter aluminum particle attached to the Inner conductor compared to the breakdown voltage for a single free 6.4 mm particle.

(b)

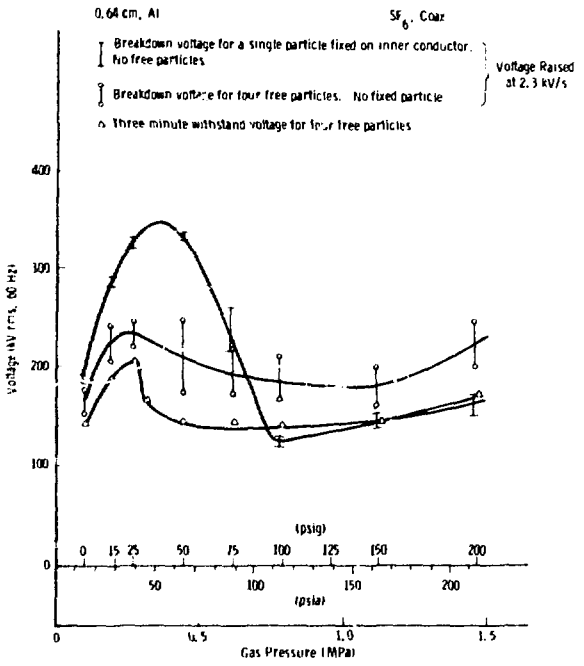

(c)

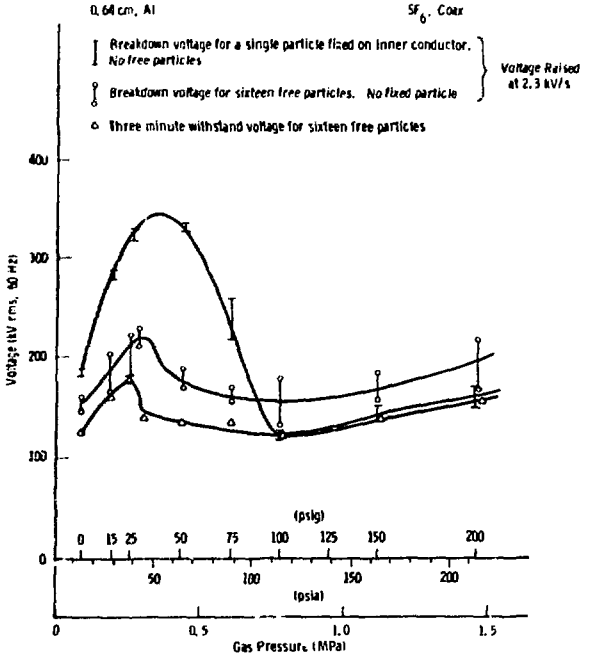

Fig. 1(b) and (c)-Breakdown voltage for a single fixed 6.4 mm long x 0.45 mm diameter aluminum particle attached to the Inner conductor compared with the breakdown voltage for ((b)top) four free particles and ((c) bottom) sixteen free particles.

Breakdown with Fixed or Free Particles

We have reported previously[1] the considerable difference between the 16-free-particle breakdown voltage at gas pressure less than about 0.8 MPa (100 psig) and the corresponding breakdown level for a single particle fixed perpendicularly on the inner conductor and in electrical contact with it (Fig. 1(c)). The 16-free-particle breakdown level is frequently only half of the fixed-particle level over this gas pressure range despite the fact that the free particle is very near the inner electrode at the instant of breakdown and therefore in a position similar to that occupied by the fixed particle. The breakdown strength with 16-free particles differs little with gas pressure over this range. These points will be discussed later.

Breakdown with Various Numbers of Free Particles

Over the whole range of SF_6 gas pressures the breakdown voltages generally decrease with increasing number of particles with both testing procedures. This can be seen for the ramped-voltage test in Fig. 2(a) and for the stepped tests in Fig. 2(b). The numbers on the curves indicate the number of free particles in the test. Fig. 2 also demonstrates a point made above viz. that the breakdown voltages obtained with the lower average rate of voltage rise (the stepped-voltage procedure) are lower than for ramped-voltage tests for each number of free particles (compare 2(a) with 2(b)).

Breakdown with More Than one Free Particle in the Breakdown Path

Many photographs were obtained with more than one free breakdown in the breakdown path. The lowest multi-particle breakdown (Table 1) is generally at a higher voltage than the lowest single-particle breakdown voltage. However, in considering this result it should be noted that the great majority of breakdowns involve only one particle. Thus, although multi-particle breakdown occurs it does not generally decrease the mean breakdown voltage to a significant extent. It is possible that breakdown is initiated by the particle near the inner coaxial conductor, and the presence or absence of another (or more) particles in the breakdown path has little or no effect on the magnitude of the breakdown voltage.

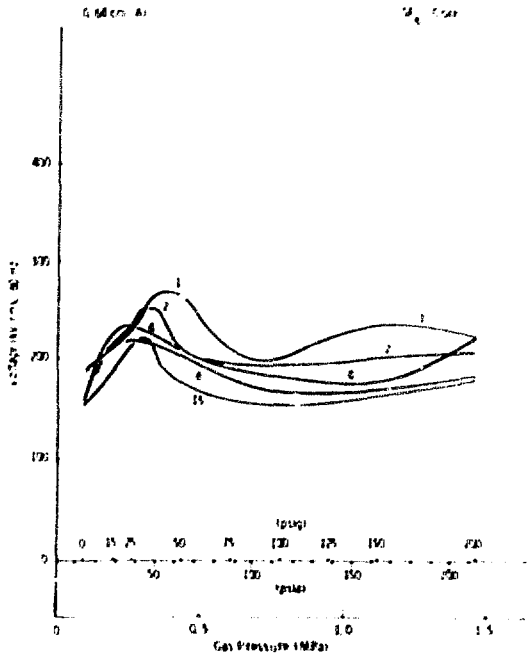

Fig. 2(a)-Breakdown voltage in a 7.6/25 cm diameter Coaxial system in SF_6 with various numbers of free 6.4 mm long x 0.45 mm diameter aluminum particles. Voltage raised at 2.3kV/s. The number of particles is shown on each curve.

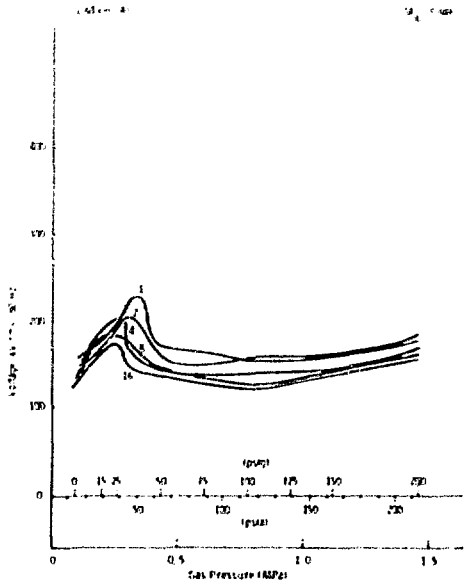

Fig. 2(b)-Maximum voltage which can be maintained for three minutes without breakdown in a 7.6/25cm diameter Coaxial system in SF_6 with various numbers of free 6.4 mm long x0.45 mm diameter aluminum particles. The number of particles is shown against each curve.

Interactions Between a Fixed Particle and Free Particles

SF_6 Gas Pressures Higher Than About 0.8 MPa (100 psig).--In this pressure range a particle fixed on the inner conductor, and in electrical contact with it, exerts a strong attractive force on free particles. It is not unusual for breakdown to be initiated with a free particle standing on the tip of the fixed particle (Fig. 3), and hence effectively forming a single particle of twice the length. However the breakdown voltages observed are not appreciably different from those obtained for a single fixed particle in the absence of free particles (Fig. 4).

SF_6 Gas Pressures Between 0.1 MPa and 0.8 MPa (100 psig).--In this pressure range a fixed particle on the conductor strongly repels free particles. This effect is so powerful that in our tests all free particles are ejected from the electrode system (Fig. 4(a)) while the voltage is being raised and before breakdown in tests at pressures less than about 0.8 MPa (100 psig). Thus,although several particles are present initially, the breakdown voltage is that for a single fixed particle, all the free particles having left the system during the 100s or so that is required to raise the voltage. At SF_6 pressures of near to 0.6 MPa (75 psig) the repulsion is not so marked and, with rapidly ramped voltages, breakdown occurs at a lower voltage than with a fixed particle alone, and usually occurs with one or more free particles still present within the electrode system (Fig. 4(b)).

Table 1. Comparison of Breakdown Voltages with Single Particle and Multi-particle Involvment

SF_6 Pressure (psig)	SF_6 Pressure (MPa)	Number of Free Particles in 7.6/25cm Coaxial System	Lowest[a] B/D[b] Strength with One Free Particle Involved in B/D Path	Lowest[a] B/D[b] Strength with n Free Particle Involved in B/D Path	
			B/D(kV rms)	B/D(kV rms)	n
200	1.46	16	180	195	2
150	1.12	16	164	160	≥4
100	0.78	16	135	169	≥4
75	0.71	8	162	167	2
50	0.44	16	176	176	3

[a]Lowest out of five breakdown measurements.

[b]B/D means breakdown.

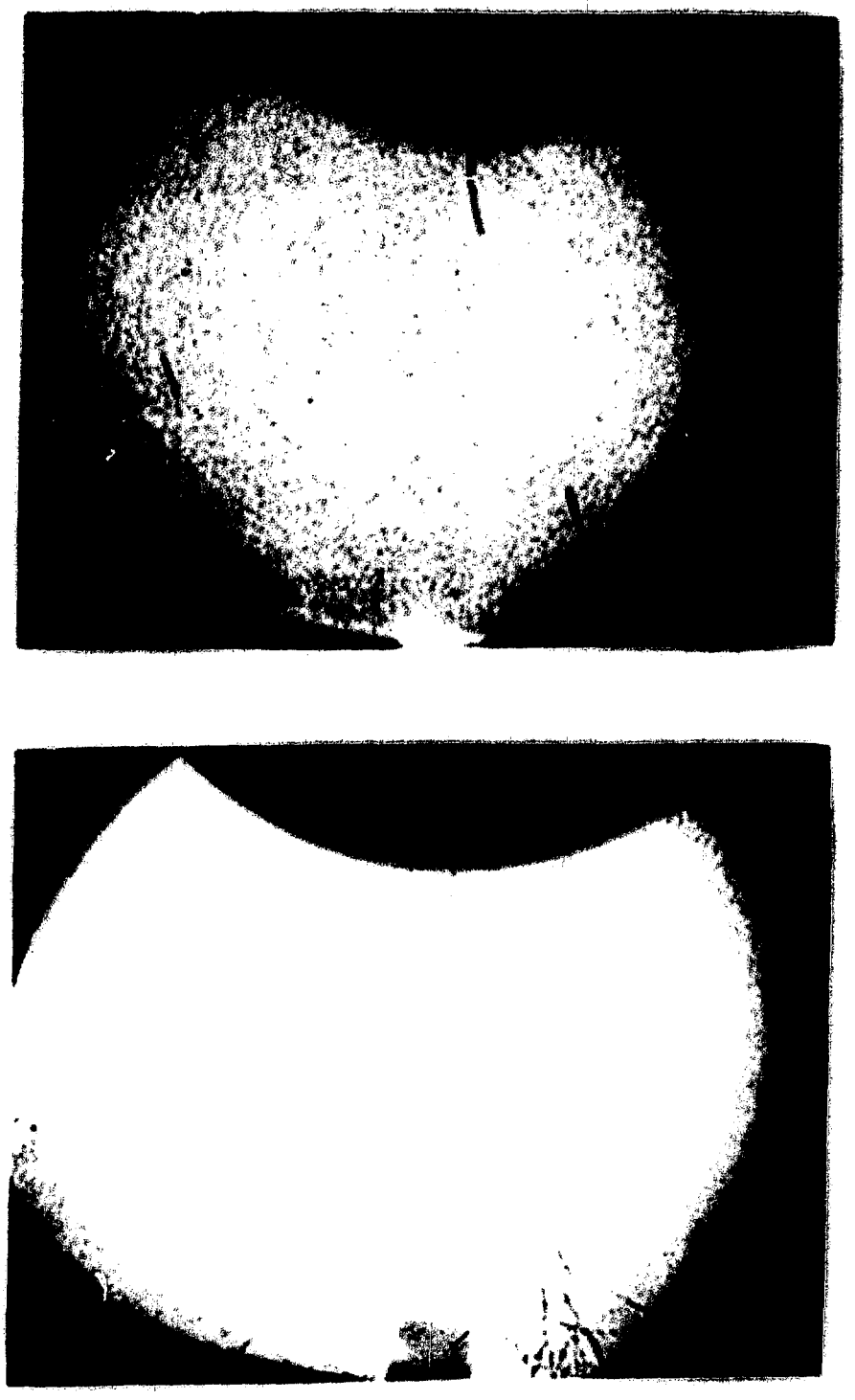

Fig. 3(a) and (b)-Consecutive frames from a movie taken at 5000 frames per second showing ((a) top) one of four free particles approaching a single particle fixed on the inner conductor of a coaxial electrode system in SF_6 at 1.46 MPa and 250kV rms, and ((b) bottom) breakdown occurring through both particles.

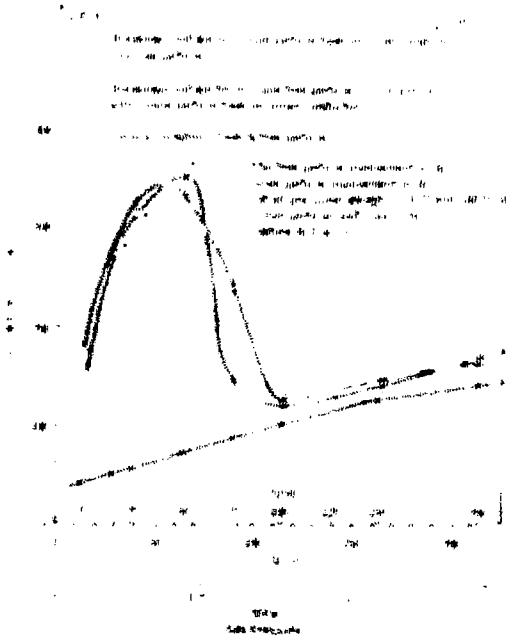

Fig. 4(b)-60Hz breakdown, corona inception in SF_6 in a 7.5/3.5 cm diameter system with a single fixed 6.4 mm long x 0.25 mm diameter aluminum particle on the inner conductor. Also shown are the breakdown results for a single fixed particle in conjunction with multiple free particles.

DISCUSSION

A Particle and Wire-to-Wire Breakdown Mechanism Explaining the Experimental Data for Minimum Breakdown Voltage

An experimentally reproducible, point-to-point breakdown occurs with three point-to-point spacings at the experimental pressure which is three point-to-point spacings at lower pressure, just what is consistent with the theory presented above. The experimental data for minimum breakdown voltage show maximums with increasing point separation from zero to 1 mm at 0.5 psia for zero point at 0.4 psia (1000 points). At 0.47 psia (94% points) it is about 0.4 mm (Fig. 7 and Ref. 18).

The Probability of Breakdown is Low at the Minimum Possible Breakdown Voltage

At this pressure (0.47 psia) and spacing (0.4 mm) the breakdown voltage is critically dependent on the spacing. For instance, an increase in the spacing to 0.9 mm, or a decrease to 0.22 mm, results in an increase in breakdown voltage by some 40%. A decrease in the spacing to zero increases the breakdown voltage by 100%. High-speed movie films show that particles normally transport the conductor under breakdown conditions at speeds of up to 20 m/s, although there are sometimes occasions in which the particle remains near the conductor recommended by a person for comparatively long periods. Particles which transport at high speed normally bounce away again with only a small loss of speed, and hence the dwell time at a particle-to-electrode spacing near to the critical value is very short. For instance, for a speed of 20 m/s the travel time from a spacing of 0.9 mm to one of 0.22 mm (at which spacings the breakdown voltage is 30% above that at 0.4 mm) is 9 microseconds. The particle then generally bounces back to the lower electrode, or otherwise makes an excursion away from the inner electrode, which usually occupies many cycles of 60Hz voltage. Thus the particle will typically occupy a critical position for breakdown for about 20 microseconds out of perhaps 0.1s or one five thousandth of the available time. The voltage on the electrodes is alternating so that the instantaneous voltage will be near to the peak value for only a small fraction of a cycle. Thus, breakdown is generally possible for only a small fraction of the approaches of particles to the inner electrode. Since breakdown only occurs when the inner electrode is positive

the polarity of the voltage will be favourable on only half the occasions where the above factors are all favourable. Since breakdown delays of the order of tens of microseconds are observed in impulse tests in compressed SF_6 systems[3] it seems possible that even when all the above factors are favourable, breakdown may still not always develop into a complete flashover between the electrodes. The electrode area between the particle and the electrode is also very small (~ 0.003 mm^2)and the gap has a very small volume of stressed gas ($\sim 3 \times 10^{-5}$ mm^3). For negative lightning impulse waves the electric strength, and the standard deviation of strength, both increase with decreasing electrode area[4]. Thus it appears that breakdown will occur on only a small fraction of the occasions when particles bounce on the inner conductor and this is observed in practice. It has also constituted one of the major experimental difficulties in studying particle initiated breakdown. This difficulty may be overcome by using a particle fixed at the critical spacing[1].

The "Number-of-Particles" and "Rate-of-Voltage-Rise" Effects Both Result from the Low Probability of Breakdown at the Minimum Breakdown Voltage

The dependence of the particle-initiated breakdown voltage on the number of particles and on the procedure for raising the voltage are thus both consequences of the statistical nature of breakdown initiated by particles. The average rate of rise of voltage in the tests using ramped voltages is some eighty times greater than that using stepped voltage increments, and thus results in eighty times fewer particle bounces on which breakdown might be initiated. The corresponding increase in mean breakdown voltage is about twenty percent (Fig. 2).

The decrease in breakdown strength with increase in number of free particles from one to sixteen varies somewhat with gas pressure but is about fifteen percent over most of the gas pressure range for both procedures of raising the voltage. Thus, if the effect of a larger number of particles is only to increase the number or frequency of impacts on the electrode at which breakdown conditions are favourable, then an increase in the number of impacts by a factor of sixteen results in a decrease in the breakdown strength by some fifteen percent. This is compatible with the previous result that an increase in the number of impacts by a factor of eighty reduces the breakdown voltage by a factor of about twenty percent. These results are similar to the reductions

in electric strength reported by Hauschild[5] of four, nine and fourteen percent for five, ten and thirty spherical particles in SF_6 at 1 bar.

Application to Tests on Practical Equipment

In applying these results to the field testing of practical systems it may be noted that there is a detectable difference between the results for 8 and for 16 particles using the 3-minute stepped-voltage procedure. On the basis of the number of bounces being the significant factor one might therefore expect there to be a similar difference between results for a single particle tested with a voltage stepped up at 8x3=24 minute intervals compared with one stepped at 48 minute intervals.

Breakdown at the lowest possible voltage for a particular particle in a particular system appears to occur with a very low probability. Thus, field test voltages to demonstrate the absence of particles may have to be applied for long periods of the order of hours or days. The effect of the ac voltage in moving particles into effective traps would eliminate the need for a long duration test.

Multi-Particle Breakdown

Although breakdowns are observed in these tests in which more than one particle is present in the breakdown arc, the associated breakdown voltage is not lower than the minimum for single-particle breakdown and there is thus little effect on the breakdown results in these experiments (Table 1). In a practical system the probability of a multi-particle breakdown occurring at a significantly lower voltage than for a single particle over a long period of time is very low. Since most particles will be moved into traps at an early stage in conditioning, multi-particle breakdown is not likely.

Interactions Between Fixed and Free Particles

Attraction of Free Particles by a Fixed Particle at High Gas Pressures

At high pressures in SF_6 ($\sim$0.8 MPa) the locally high field near the tip of a particle fixed on the inner conductor strongly attracts free particles which acquire a dipole charge and also possibly a net charge. The dipole charge leads to an attractive force towards the fixed particle and at breakdown the free particle is sometimes observed sitting on the

tip of the fixed particle (Fig. 3). The breakdown voltage is, however, rarely decreased by its presence. Any high-field regions will attract free particles in this manner to some extent.

Repulsion of Free Particles by a Fixed Particle at Lower Gas Pressures

At SF_6 gas pressures of less than about 0.8 MPa (100 psig) the tip of the fixed particle is surrounded by a corona glow discharge and strong electric wind effects are observed, as well as appreciable electric currents e.g. peak currents of 0.12mA at 250kV making an instantaneous power of 30W available to drive an electric wind.

In this pressure range the breakdown voltage for a fixed particle is considerably above (e.g. 100% above) the corona inception and electric wind starting voltage. At voltages above the corona starting voltage the free particles are promptly ejected from the space between the electrodes. The mechanism is not certain, but it is probably a combination of the force of the electric wind and of electrical charging of the free particles by the charge in the wind i.e. if the fixed point is of positive polarity, so is the space charge in the electric wind and this will tend to charge the free particles positive also. There will then be a repulsion between the fixed and free particles carrying like charges. The dipole attraction which dominates at high pressures will still be present, but it is evidently overwhelmed by the two forces described above and the free particles are ejected rapidly from the electrode region. It appears likely that in this pressure range free particles also repulsively interact with each other. Such behaviour is noticeable where wire-like particles tend to space themselves out evenly while executing low-amplitude hopping motion inside a coaxial electrode system.

CONCLUSION

The dependence of the free-particle initiated breakdown voltage on both the number of free particles present in the system and on the rate of rise of voltage has been reported, and both have been shown to be associated with the low probability of breakdown at the minimum breakdown voltage. This low probability of breakdown is in turn associated with a critical particle-to-electrode spacing which is necessary for breakdown at the minimum voltage, and the rapid increase in breakdown voltage with change in spacing away from the critical spacing.

Thus, the statistics of particle-initiated breakdown are such that extended duration tests are required to determine minimum breakdown levels.

Multi-particle breakdown is reported but does not result in significantly lower breakdown voltages.

Strong interactions between free particles and a particle fixed on the inner conductor of a coaxial system are reported for the first time. At high pressures above about 0.8 MPa (100 psig) the force is generally attractive while at lower pressures it is repulsive leading to expulsion of the free particles from the electrode system or into particle traps.

ACKNOWLEDGMENT

The still frames shown in Figure 3 are from a 16 mm film taken by Dr. O. Farish.

REFERENCES

1. R. E. Wootton, F. T. Emery and A. H. Cookson, Paper E-12, 1977 Ann. Report on the NSF Conf. on El. Ins. and Diel. Phen., Oct. 17-20, 1977.

2. A. H. Cookson and R. E. Wootton, IEEE Paper F77 657-0, Summer Power Meeting, 1977.

3. T. Nitta, Y. Shibuya and Y. Fujiwara, IEEE PAS-94, No. 1, p. 108-115, Jan. 1975.

4. A. Rein, A. Arnesen and I. Johansen, IEEE PAS-96, No. 3, p. 945-954, May 1977.

5. W. Hauschild, S. Schierig and J. Speck, Elektrie, 30, No. 7, p. 354-356, 1976.

DISCUSSION

DAKIN: The breakdown behavior with particles fixed at a short distance from the electrode and with moving particles which occasionally reach this position can be understood by recalling that the impulse strength with point electrodes is lower than the AC or positive DC strength in the pressure range where corona space charge reduces the local stress. When a particle near an electrode sparks to the electrode high on the AC cycle this would produce a sudden higher impulse potential at the particle tip, resulting in a reduced breakdown voltage since there is a time delay for space charge development.

WOOTTON: A single answer is given to both this comment and that by Roy Nakata. (See below).

NAKATA: I concur with Dr. Dakin's explanation of Mr. Wootton's test which showed that particles situated a short distance from the center electrode cause breakdown to occur (at moderate to low Pd) at voltages lower than for a fixed particle cemented to the central conductor. Motion picture films taken with an all quartz optical system (which will be shown in the panel discussion) show the impulse type of sparking which takes place at the center electrode and hovering particle, so that corona stabilization does not occur. By contrast, the cemented fixed particle can establish a steady state corona stabilized space charge thereby resulting in a higher breakdown voltage.

WOOTTON: The results of the work with particles fixed a short distance from the inner conductor (and electrically isolated from it) have been

published previously, (see Ref. 1 of the paper) and Dr. Dakin's explanation is identical to that given in Ref. 1, i.e., that the corona stabilization space-charge is able to adjust its magnitude and distribution to the comparatively slowly changing 60Hz voltage, but is unable to cope with the rapid potential changes resulting from breakdown of the small particle-to-electrode gap. The temporarily inadequate stabilization then leads to breakdown of the large gap. The AC free-particle initiated breakdown behavior is thus partially dependent on the impulse response of the gas. With regard to the comment on sparking at the center conductor, breakdown occurs above the corona inception voltage at low gas pressures for both isolated particles and for particles connected to the electrode so that stabilization is occurring in all these cases (Fig. 4 of the paper). Current is continuously injected into the corona space charge at the tip of the particle high on the 60Hz cycle and is being carried away partly by ion drift and partly by the corona wind. This current has to be supplied via the small particle-to-electrode gap. Photomultiplier, current and discharge detector measurements show (Ref. 1 of the paper) that this conduction current is carried sometimes as pulses and sometimes as an arc. The final breakdown occurs near the peak AC voltage after (conduction) current has been crossing the small gap for some hundreds or thousands of microseconds. The film which I will show tomorrow during the Applied Panel Session will illustrate that corona stabilization and electric winds also occur around free particles remote from the electrodes. Jets of gas can be seen streaming away from the tips of the particles. It seems probable that some degree of corona stabilization (maybe small in some cases) preceded breakdown in all the low pressure experiments using 6.4 mm long particles.

The explanation of "fire fly" behavior also depends on the existence of corona currents under both AC and DC conditions.

COOKE: The long duration time delay to breakdown associated with particle movement you have reported is good news to those of us trying to describe area effects and long-term reductions in insulation strength in gas insulated apparatus. Would you comment as to whether such area and time effects may be the result of this type of delay with naturally occurring particles?

WOOTTON: It appears entirely possible that this type of mechanism may apply to microparticles as well as to the larger particles used in our experiments. With microparticles the electric stress at breakdown would be higher but the delays may also be greater because of the smaller gas volumes involved in the particle-to-electrode gap. On the other hand, the volume of the corona stabilized charge is also smaller and readjustment of the space charge magnitude and volume after breakdown of the particle-to-electrode gap may occur very rapidly.

DIELECTRIC STRENGTHS OF NEW GASES AND GAS MIXTURES*

D. R. James, L. G. Christophorou,† R. Y. Pai, M. O. Pace,†
R. A. Mathis, I. Sauers, and C. C. Chan
Health and Safety Research Division, Oak Ridge National Laboratory,
Oak Ridge, Tennessee 37830

ABSTRACT

We have argued earlier and we emphasize further in this paper that the most effective gaseous dielectrics are gas mixtures with components chosen on the basis of fundamental physicochemical knowledge, especially on low-energy electron-molecule interactions. On the basis of such knowledge, especially on electron attachment and electron slowing down, a number of new gases and gas mixtures have been found with breakdown strengths superior to pure SF_6. These include the unitary gases c-C_4F_8 (perfluorocyclobutane), C_4F_8 (perfluorobutene-2), C_4F_6 (perfluoro-2-butyne), C_6F_{10} (perfluorocyclohexene), C_5F_8 (perfluorocyclopentene), and C_6F_{12} (perfluorodimethylcyclobutane), and the multicomponent gas mixtures 20% C_4F_6 + 80% SF_6, 40% C_4F_6 + 60% N_2, 50% C_4F_6 + 50% SF_6, and 30% C_4F_6 + 20% SF_6 + 50% N_2 with DC breakdown strengths relative to SF_6 of 1 equal to 1.4, 1.8, 2.2, 2.1, 2.2, 2.4, 1.3, 1.4, 1.75, and 1.33, respectively. Our findings on these and other systems will be presented and discussed. Results will be presented and discussed, also, on the dielectric strengths of some of the above new gases measured with cylindrical electrode geometries using different center conductor diameters. Finally, our findings on the initial decomposition products of some of the new insulators caused by electron impact will be presented and their implications assessed.

INTRODUCTION

As electric transmission line voltage levels continue to increase, there is a corresponding need to upgrade the performance of gaseous dielectrics. Existing gaseous insulators clearly do not meet all of

*Research sponsored by the Department of Energy under contract with Union Carbide Corporation.

†Also, The University of Tennessee, Knoxville, Tennessee 37916.

the requirements of the power industry, and it is unlikely that any single gas will be satisfactory for all conditions. Solutions, therefore, to the many and varied problems and needs relating to high voltage insulation (and improvements over present procedures) must be sought in the development and use of multicomponent gas mixtures.

We anticipate that the best multicomponent gaseous insulators will be comprised of components selected according to basic knowledge on their physical and chemical properties. Especially significant among these are the basic processes involved in the interaction of low-energy electrons with the dielectric gas molecules, such as electron attachment, electron energy loss, and electron impact ionization, as a function of electron energy and the relation of these to molecular structure.

We have undertaken a systematic investigation of the basic and applied aspects of the dielectric strengths of unitary and multicomponent gaseous systems, and in this paper we present and briefly discuss some of the pertinent findings of this work.

APPARATUS

Two pieces of apparatus have been employed in the present investigations of breakdown voltages of gases and gas mixtures. The first apparatus consisted of a small stainless steel chamber approximately 6 liters in volume which could be evacuated to less than 10^{-6} torr. The high voltage electrode was a 3/4-in. stainless steel sphere and the ground electrode was a 3-1/2-in. stainless steel plane mounted onto a micrometer drive. Negative high voltage was applied to the sphere by a 60-kV power supply. The electrode separation was kept small to approximate uniform field conditions (e.g., a 1-mm electrode gap resulted in a field nonuniformity of $\sim$3.5%).

The second apparatus comprised a larger chamber of $\sim$40 liters volume which was routinely evacuated to less than 10^{-6} torr before gas was admitted to the chamber. The electrode assembly consisted of two stainless steel planes, the profiles of which were designed according to the work of Pearson and Harrison.[1] A 300-kV DC power supply (Deltatron L300-2C) from Delta Ray Corporation provided a negative high voltage relative to the grounded electrode.

Both apparatuses had similar controllers which automatically ramped the voltage, detected the spark, and held the breakdown voltage reading on a digital voltmeter. Ultraviolet light from a deuterium lamp was used to irradiate the electrodes. To obtain a data point, usually a minimum of ten breakdowns were recorded at each value of P and d (P is the gas pressure and d is the electrode separation), and the average value and standard deviation were calculated. The ratio of the standard deviation to the mean was used as a measure of the scatter in the data. In general this scatter was ≲2% for the sphere-plane geometry, although at the highest values of Pd employed, this scatter was at times larger (still, however, <5%). With the plane-plane electrode geometry the scatter was ≲1% below 200 kV and typically between 2 to 3% above ∿200 kV.

BREAKDOWN STRENGTHS - UNITARY GASES

Dielectric Gases with Vapor Pressures in Excess of One Atmosphere

In our investigations we have found a number of high vapor pressure (>1 atm at ambient temperature) gases which have high dielectric strengths. Some of these gases, their dielectric strengths relative to that of SF_6, and their vapor pressures at ambient temperatures are listed in Table I. In Fig. 1 are shown the breakdown voltages, V_s, for a number of unitary gases as functions of Pd. The fluorocarbons were found to have the highest dielectric strength; C_4F_6 (perfluoro-2-butyne) in particular has more than twice the dielectric strength of SF_6. The double-bonded C_4F_8 (perfluorocyclobutene-2) and the cyclic-C_4F_8 (perfluorocyclobutane) compounds are two other fluorocarbons with high dielectric strengths. Perfluoropropane (C_3F_8), although with eight fluorine atoms, has a dielectric strength slightly lower than SF_6. This molecule, however, has no double bonds and attaches low-energy electrons very weakly.[3]

The breakdown voltage, V_s, in uniform electric fields was found to be a function of Pd and not an explicit function of P alone. A possible exception, however, seems to be SF_6 which for pressures >2000 torr shows[4] deviation from Paschen's law.

Table I. Relative DC Breakdown Strengths of Some Unitary Gases (Vapor Pressures ≥1 Atm)[a]

Gas	Relative Strength	Vapor Pressure Atm (°C)
C_4F_6 (perfluoro-2-butyne)	2.2	~4.8[b] (23)
C_4F_8 (perfluorobutene-2)	1.7-1.8	2.02[c] (21.1)
c-C_4F_6 (perfluorocyclobutene)	1.7	~1[d]
C_4F_6 (perfluoro-1,3-butadiene)	1.4	~1[e]
c-C_4F_8 (perfluorocyclobutane)	1.3-1.4	2.9[f] (24.3)
SF_6 (sulfur hexafluoride)	1.0	22.77[c] (21.1)
C_3F_8 (perfluoropropane)	0.93	7.81[c] (21.1)
N_2 (nitrogen)	0.40	g
CO_2 (carbon dioxide)	0.37	57.5[c] (21.1)

[a]All breakdown strength data are from Ref. 4 except those on c-C_4F_6 which are unpublished recent results by the Oak Ridge group.

[b]Present estimated value.

[c]William Braker and Allen L. Mossman, Matheson Gas Data Book, 5th Ed., Matheson Gas Products, East Rutherford, New Jersey, 1971.

[d]Boiling point = 7.4-7.6°C.

[e]Boiling point = 5-6°C.

[f]E. C. Coyner and D. Hanesian, Freon Technical Bulletin EL-5, E. I. du Pont de Nemours and Company, Inc., 1964.

[g]Critical temperature -147.1°C; N_2 cannot be liquefied at temperatures higher than this.

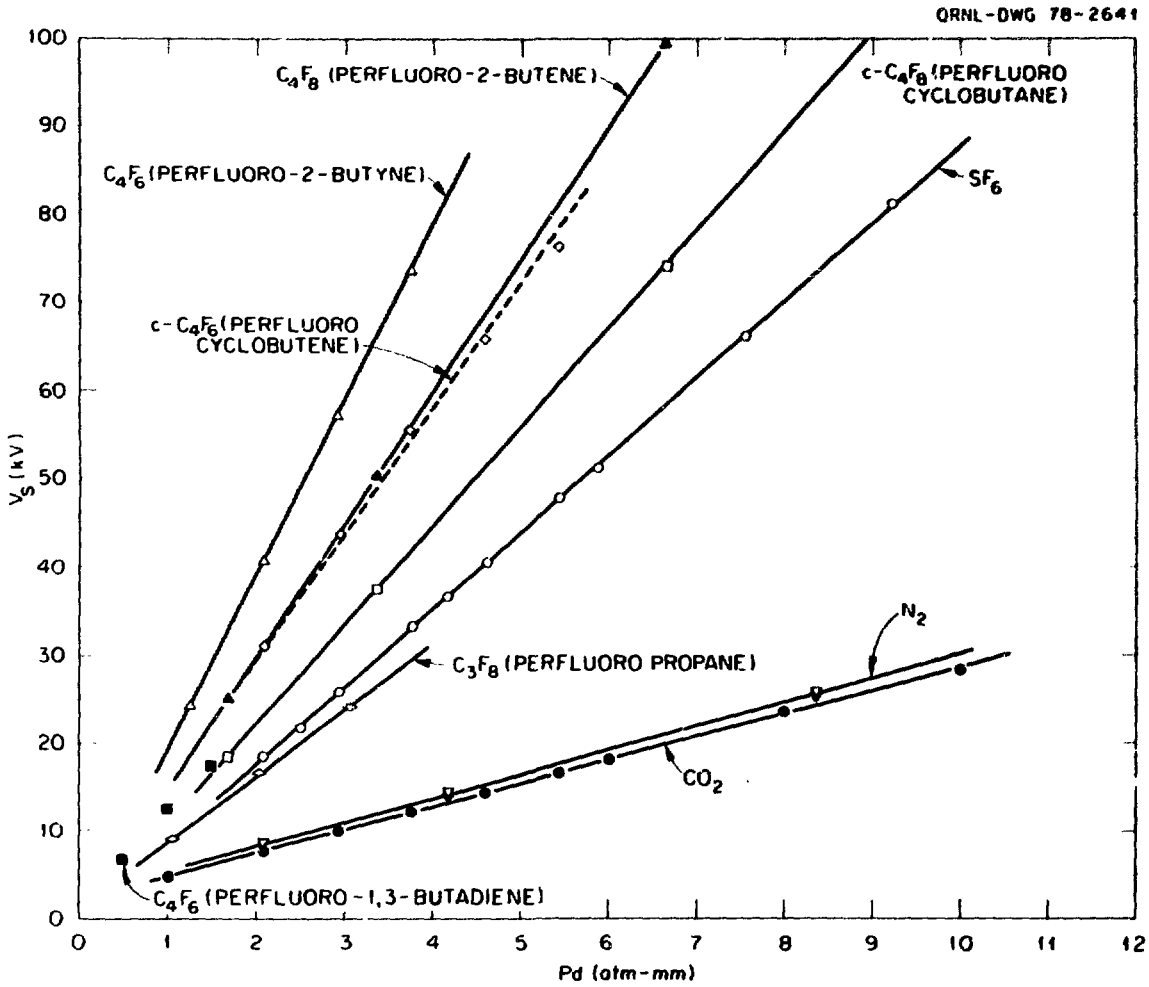

Fig. 1. Breakdown voltage, V_S, as a function of Pd for high pressure ($\gtrsim$1 atm) unitary gases. The CO_2 data are from Ref. 2.

Dielectric Gases with Vapor Pressures Less Than One Atmosphere

Many compounds with vapor pressures less than one atmosphere at room temperature were found to have higher dielectric strengths than SF_6 at comparable pressures. The relative breakdown strengths of some of these are given in Table 2, and the V_S vs Pd curves are shown in Fig. 2. The pressures employed ranged from 20 torr for C_7F_8 (octafluorotoluene) to 281 torr for C_4F_6 (hexafluoro-1,3-butadiene). Comparisons with SF_6 were made only when SF_6 could be measured at the same or nearly the same pressure. The curvature of the breakdown voltage vs Pd seen in Fig. 2 is due to the low pressures employed which required the electrode

Table 2. Relative DC Breakdown Strengths of Some Low Vapor Pressure Compounds[a]

Compound	Relative Strength
C_6F_{12} (mixture of 1,2- and 1,3-perfluorodimethylcyclobutane)[b]	2.3-2.4
C_5F_8 (perfluorocyclopentene)[c]	2.1-2.2
C_6F_{10} (perfluorocyclohexene)	1.9-2.2
C_7F_{14} (perfluoromethylcyclohexane)[d]	2.1
C_8F_{16} (perfluoro-1,3-dimethylcyclohexane)	~2.3[e]
C_7F_8 (octafluorotoluene)	~2[f]
C_7F_{14} (perfluoroheptene-1)	1.2
SF_6 (sulfur hexafluoride)	1.0

[a]Data from Ref. 4 except as noted.

[b]At 26.7°C the vapor pressure is 394.3 torr.

[c]Boiling point = 25°C.

[d]At 21.7°C the vapor pressure is ~95 torr.

[e]At low pressures the V_s for this compound was found to be 1.3 times that of C_4F_6 under identical experimental conditions.

[f]Unpublished result of the Oak Ridge group, measured with respect to C_8F_{16} under identical experimental conditions.

separation to be relatively large (up to 10 mm in some cases) in order to obtain Pd values in the range $0.5 \lesssim Pd \lesssim 2.5$ atm-mm. Hence, the electric field was highly nonuniform in these cases, and in general the breakdown voltage was not a linear function of Pd.

These low vapor pressure compounds, although unsuitable by themselves as dielectrics due to their low vapor pressures at room temperature, may

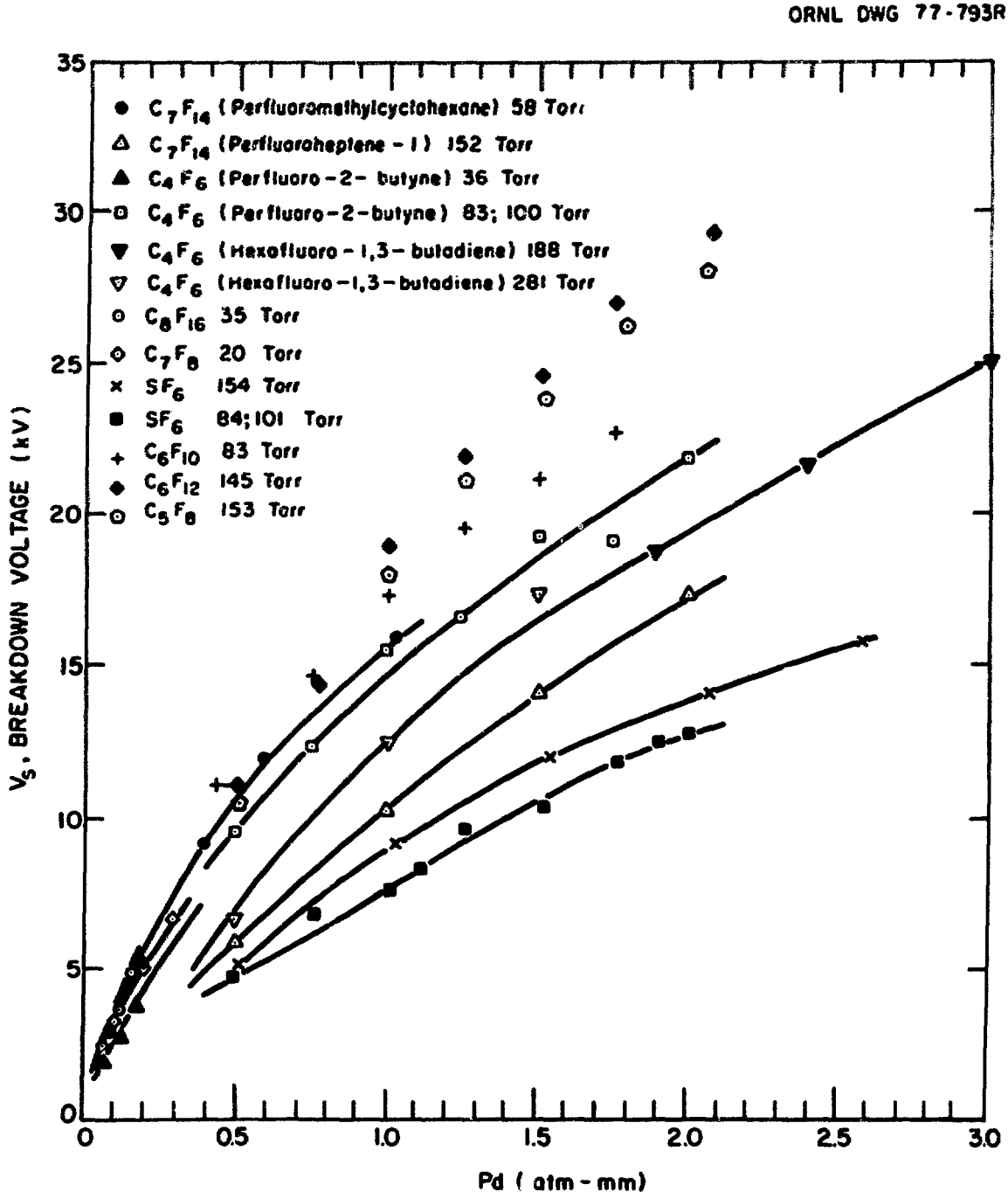

Fig. 2. Breakdown voltage, V_S, as a function of Pd for low pressure (<1 atm) unitary gases at the indicated pressures for sphere-plane electrode geometry.

have potential use as additives to higher pressure buffer gases such as N_2. For example, a 10% C_6F_{10}/90% N_2 mixture at 500 torr total pressure has a 20% higher breakdown voltage than a 10% SF_6/90% N_2 mixture at the same pressure. But, even more importantly, the study of these gases provides basic information necessary for the understanding of the role of fundamental physical processes in the electrical breakdown.

The Role of Electron Attachment as a Function of Electron Energy

In order to develop new improved gas dielectrics, the basic physical properties of the dielectric itself must be identified and understood, especially in relation to their effect on the breakdown voltage. We have been investigating the role of one such basic property of the dielectric; namely, electron attachment as a function of electron energy. Although our systematic study of the electron attachment properties of the compounds in Tables 1 and 2 is still not complete, the data presented in Fig. 3 are quite revealing.

Let us, then, draw our attention to Fig. 3 where the electron attachment cross section as a function of electron energy, $\sigma_a(\varepsilon)$, is plotted for several gases of high dielectric strength.[4-6] The line designated as $\pi\lambda\!\!\!^{-2}$ represents the maximum s-wave capture cross section ($\lambda\!\!\!^{-} = \lambda/2\pi$ and λ is the electron deBroglie wavelength). The $\sigma_a(\varepsilon)$ for SF_6 approaches the theoretical maximum at near-thermal energies and is quite large at $\sim$0.3 eV. (The peak at $\sim$0.3 eV is due to SF_5^- while at thermal energies SF_6^- is the dominant ion formed.) At energies $\gtrsim$0.4 eV, the SF_6 capture cross section rapidly decreases so that SF_6 cannot effectively capture electrons with kinetic energies in excess of this energy. It is seen from Fig. 3 that the attachment cross sections for c-C_4F_8, C_4F_8, and C_4F_6 remain substantial to electron energies $\gtrsim$1 eV. These latter gases, therefore, are capable of capturing effectively electrons to much higher energies than SF_6. Our breakdown measurements (Table 1) clearly show that for the latter group of compounds the breakdown strengths are significantly higher than that of SF_6. On the basis of these findings and additional measurements currently in progress,[6]

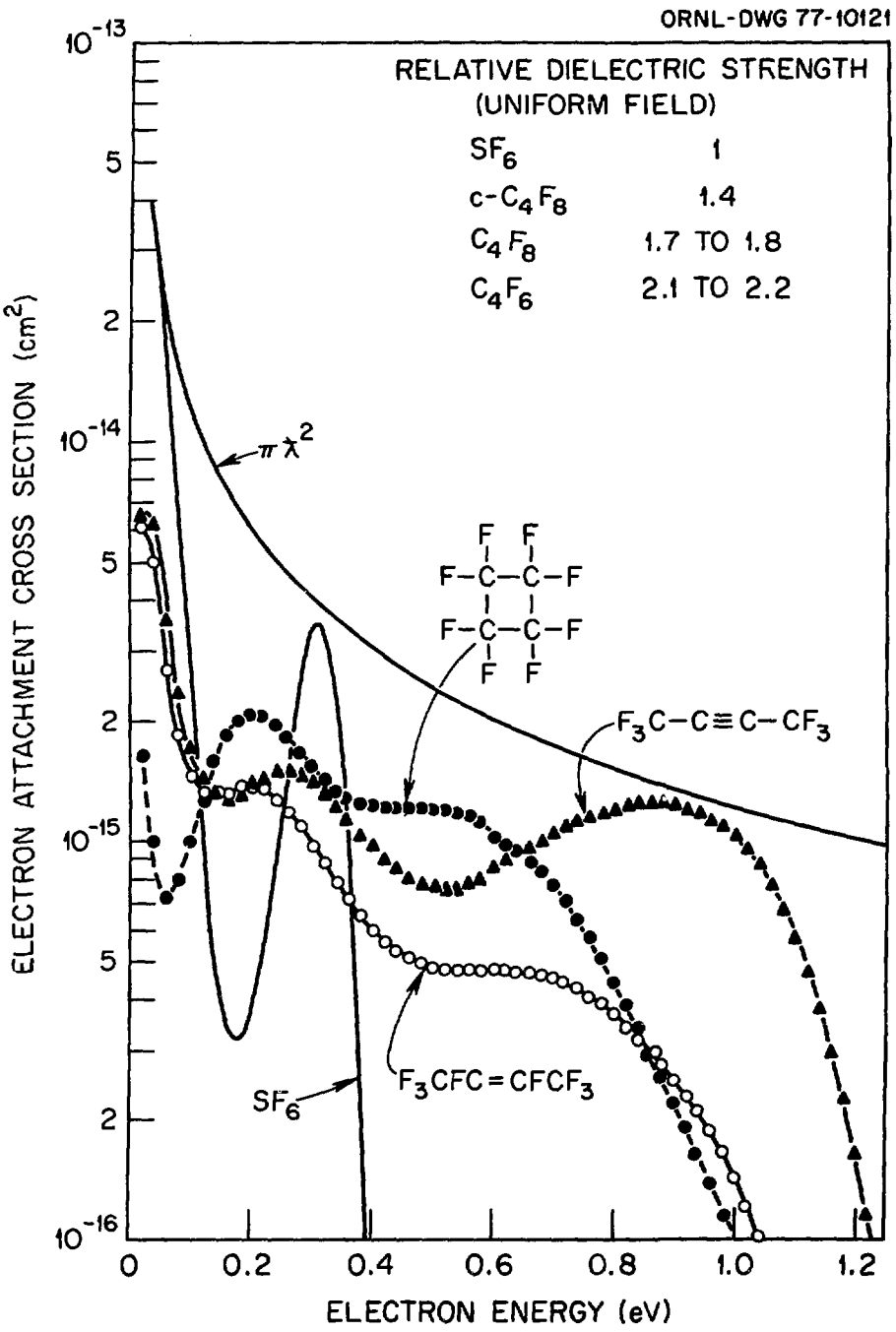

Fig. 3. Electron attachment cross sections as a function of electron energy for SF_6, c-C_4F_8, C_4F_8 (perfluorobutene-2), and C_4F_6 (perfluoro-2-butyne). $\pi\lambda^2$ is the maximum s-wave electron capture cross section (Refs. 5 and 6).

the efficient capture of electrons in the range of energies $0.4 \leq \varepsilon \leq 1.2$ eV evidently reduces significantly the number of free electrons available for initiating breakdown, with a resultant increase in the breakdown strength of the dielectric. More generally, the overlap of the electron energy (or velocity) distribution with the electron attachment cross section must be sufficiently large to cause a substantial increase in the breakdown voltage.

Optimizing the Gaseous Dielectric

We have suggested earlier[5] the criteria for an optimum gas dielectric; namely, that a good dielectric should maximize the quantity

$$\int_0^\infty \sigma_a(\varepsilon) f(\varepsilon, E/P) d\varepsilon \qquad \text{[maximize]} \tag{1}$$

and minimize the quantity

$$\int_I^\infty \sigma_i(\varepsilon) f(\varepsilon, E/P) d\varepsilon \qquad \text{[minimize]}, \tag{2}$$

where $\sigma_a(\varepsilon)$ and $\sigma_i(\varepsilon)$ are the electron-attachment and electron-impact ionization cross sections, respectively, and $f(\varepsilon, E/P)$ is the electron energy distribution function as a function of electron energy ε and pressure reduced electric field E/P, and I is the ionization threshold energy.

Condition (1) is satisfied when $\sigma_a(\varepsilon)$ is as large as possible over as wide an energy range as possible. Since electron attachment processes are resonant processes with cross sections decreasing with increasing energy position of the resonance (see Fig. 3 and Ref. 5), $f(\varepsilon, E/P)$ should be shifted to as low an energy as possible. To fulfill condition (2), the ionization threshold would need to be high and the energy distribution shifted to low energies. Thus in each case the electron energies should be reduced as much as possible. Such a reduction in the electron energy is accomplished by elastic and especially

inelastic electron scattering processes, some of which are discussed in the next section on dielectric mixtures.

Important as the electron energy distribution function is in assessing the role of the various basic processes on breakdown [see relations (1) and (2)], to our knowledge presently there are no direct measurements of this quantity for gaseous media under prebreakdown conditions. There exists only a limited indirect knowledge of $f(\varepsilon,E/P)$ for some simple gases. The main difficulty in computing $f(\varepsilon,E/P)$ from electron transport data lies in the fact that a large amount of basic detailed information on the microscopic cross sections is required, which for a complex molecular gas or a gas mixture makes the indirect deduction of $f(\varepsilon,E/P)$ very uncertain. Plans to measure directly $f(\varepsilon,E/P)$ for pure polyatomic gases and gas mixtures under prebreakdown conditions are under consideration at our laboratory.

Prior to closing this section, it is emphasized that important as the process of electron attachment is in affecting the dielectric strength of a gaseous medium, it is not the only gas property which determines the behavior of the gaseous dielectric. Elastic and inelastic (especially indirect via negative ion resonances[5]) electron scattering as well as electron impact ionization at low energies can also be crucial [see relations (1) and (2)]. It can be seen, for example, from Fig. 3 that the electron attachment cross section above thermal energies for $c\text{-}C_4F_8$ is generally higher than that for C_4F_8 (perfluorobutene-2), although the breakdown voltage of $c\text{-}C_4F_8$ is substantially less than that of its isomer. This may be due to the presence of the double bond in perfluorobutene-2, since, as we have shown earlier for a number of hydrocarbons,[3] the presence of double and triple bonds lowers the average electron energy at a given E/P.

Basic studies at our laboratory have been and are being aimed at the identification of the mechanisms of electron energy loss and on the dependence of the cross sections of these on the details of the molecular structure. It is on the basis of such knowledge that we would hope to optimize our choice of dielectric gases.

BREAKDOWN STRENGTHS - GAS MIXTURES

Gas mixtures as dielectrics have the advantage that they can be tailored to a specific need, whereas a unitary gas must be universally good under all conditions. For example, SF_6 performs well in uniform fields, but in the presence of nonuniform fields (as in the case of particle contamination) its strength deteriorates considerably. It is quite possible that gas mixtures can have a greatly improved nonuniform field performance.

There are several ways to approach systematically the development of dielectric gas mixtures, all of which require detailed knowledge of basic cross sections in order to assess the compatibility of the component gases and to maximize synergistic effects. One approach involves the use of several electron attaching gases in combination to map as wide an energy range as possible with large electron attachment cross sections. In this manner, one attempts to approach the theoretical maximum electron attachment cross section (see Fig. 3) and hence maximize expression (1). As far as electron attachment is concerned, this would be the optimal dielectric. Another approach involves the use of efficient electron attaching and electron slowing down gases, the latter being used for the purpose of shifting $f(\varepsilon,E/P)$ to lower energy and in such a way as to optimize (1) and (2).

Binary Mixtures of Efficient Electron Attaching Gases

In Table 3 data are presented on the relative breakdown strengths of binary mixtures of C_4F_6 and SF_6. The relative breakdown strength of the binary mixture increases with the amount of C_4F_6. The measured relative strengths were in each case larger than the weighted average (fraction of C_4F_6 x relative strength of C_4F_6 + fraction of SF_6 x relative strength of SF_6) calculated by using a relative breakdown strength of 2.2 for C_4F_6. These results indicate a synergistic effect between the two gases.

Table 3. Relative Breakdown Strengths of Binary Mixtures of SF_6 and C_4F_6 (perfluoro-2-butyne) ($T = 298°K$, $P_{total} = 500$ torr)

Percentage of Mixture		Measured Relative Breakdown Strength	Weighted Average[a]
C_4F_6	SF_6		
5	95	1.10	1.06
10	90	1.17	1.12
20	80	1.30	1.24
50	50	1.75	1.60
0	100	1.00	1.00

[a]See text.

From the discussion given earlier in this section, synergism in the dielectric behavior of a gas mixture must be traced to the details of the interaction of free electrons with the gas molecules comprising the mixture and the magnitudes and energy dependences of the associated cross sections. If the component gases interact with electrons in different energy ranges and with large cross sections, then—depending on the magnitude and energy dependence of their cross sections—they may cooperate in ameliorating the effects of free electrons, especially if the cross sections of each are small outside of a narrow energy range. Sulfur hexafluoride (SF_6) with an attachment cross section $\sigma_a(\varepsilon)$ confined mostly to thermal energies would be expected to show a great degree of synergism as an additive with other gases. This is borne out by the data in Tables 3 and 4.

Figure 4 shows the breakdown voltage of a 20% C_4F_6/80% SF_6 mixture at a high ($\sim$4.7 atm) total pressure. The relative improvement over pure SF_6 is the same as for the low pressure mixture in Table 3.

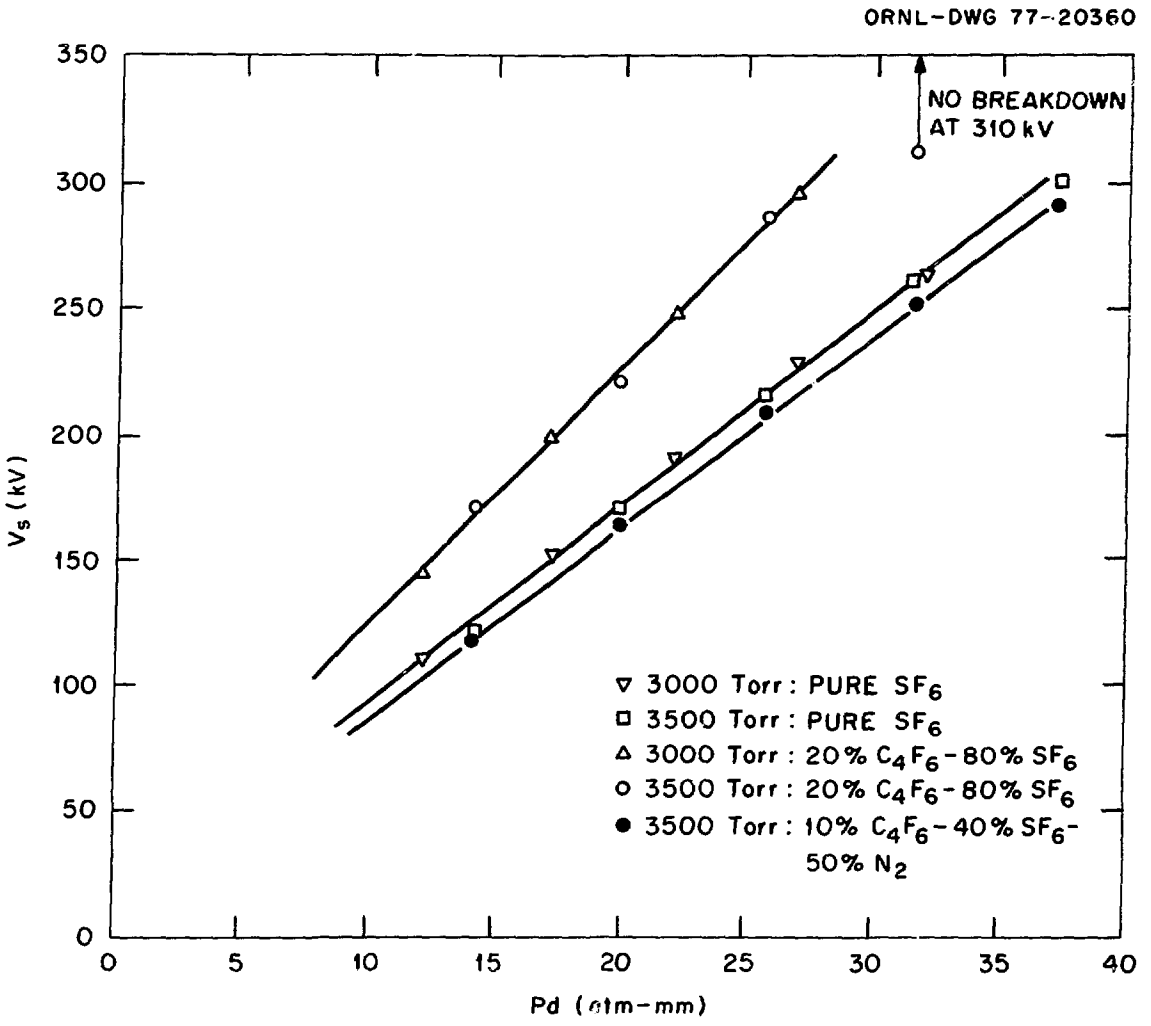

Fig. 4. Breakdown voltage, V_s, for pure SF_6 and for SF_6/C_4F_6 (perfluoro-2-butyne) and $SF_6/C_4F_6/N_2$ mixtures as a function of Pd for pressures 3000 to 3500 torr (sphere-sphere electrode geometry).

Binary Mixtures of Efficient Electron Attaching and Electron Slowing Down Gases

Although basic physicochemical knowledge does not yet permit a quantitative prediction of the breakdown strength and other dielectric properties of a gas, the available basic knowledge can be used as a guide for a systematic study of mixtures. An investigation of the breakdown voltages for several electron attaching gas mixtures using N_2 as the electron slowing down agent or buffer gas was made, and the results appear in Fig. 5. The Pd value was held constant at 4.6 atm-mm. By

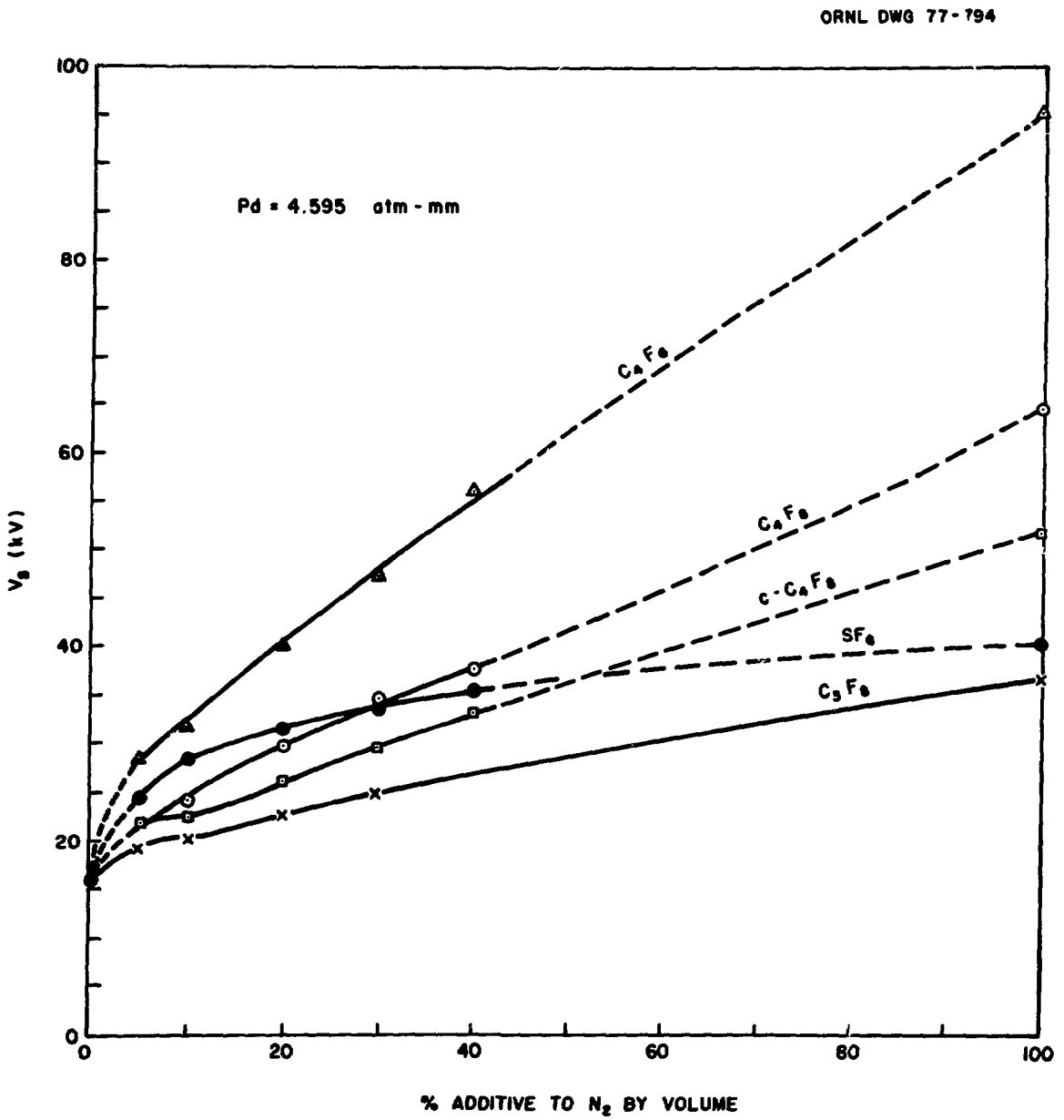

Fig. 5. Breakdown voltages, V_s, vs percent of electron attaching additive to N_2 by volume (plane-plane electrode geometry).

measuring the breakdown voltage as a function of the percentage of the electron attaching gas, we can compare the synergistic effect of each in combination with N_2.

For all five gases (SF_6, C_4F_6, C_3F_8, C_4F_8, and c-C_4F_8) the corresponding binary mixtures with N_2 show synergism. As expected from the electron attachment cross sections (Fig. 3), the mixtures with SF_6

show the largest synergism. A mixture of 40% SF_6/60% N_2 realizes 80% of the dielectric strength of pure SF_6. The rest of the electron attaching gases show a sharp increase in V_s at low percentage mixtures, but subsequently V_s increases essentially linearly with concentration showing no evidence of the saturation effect evident in the SF_6/N_2 mixtures.

Carbon dioxide (CO_2) also exhibits synergism when combined with electron attaching gases. In Table 4, the breakdown voltage is shown for mixtures of 20% of an efficient electron attaching gas and 80% CO_2, or 40% CO_2 + 40% N_2, or 80% N_2. It is clearly seen that CO_2 is slightly better than N_2 as a buffer gas for c-C_4F_8. A slight synergism between CO_2 and N_2 is also discernable for the C_4F_8 containing mixtures. These synergistic effects must relate to the electron slowing down properties of CO_2.[5,7]

Synergism in Multicomponent Gas Mixtures

Cooperative effects arising from proper combinations of electron attaching and electron slowing down gases can be seen from the data in Table 5, where the dielectric strengths of mixtures (see Ref. 4 for a complete list of these) comprising the gases N_2, SF_6, C_4F_6, and C_3F_8 are listed. Two of the salient features of these data are: (1) C_4F_6, as is expected from its dielectric strength in the pure form, is very effective as an additive. Thus entries 11 and 12 with the highest percentage of C_4F_6 have the highest breakdown voltage. (2) C_3F_8 by itself or in mixtures with only N_2 (entries 2 and 6) is not particularly effective. When, however, C_3F_8 is used in combination with N_2, C_4F_6, and SF_6—as in entries 9 and 10, 11 and 12, and 13 and 14—it is more effective than an equal amount of SF_6.

Effect of Indirect Electron Scattering Via Negative Ion Resonances on the Dielectric Strength of Binary Mixtures

The significance of negative ion resonances (NIRs) in slowing down subionization and especially subexcitation electrons has been discussed earlier.[5] A number of studies have shown that for many substances (see,

Table 4. Mixtures of Effective Electron Attaching Gases with CO_2
(T = 298°K, P ≈ 0.66 atm, Pd = 4.6 atm-mm)

Mixture	Breakdown Voltage[a,b] (kV)	Weighted Average (kV)
20% c-C_4F_8/80% N_2	25.0	23.1
20% c-C_4F_8/40% CO_2/40% N_2	25.7	22.2
20% c-C_4F_8/80% CO_2	26.0	21.3
20% C_4F_8/80% N_2	28.7	26.3
20% C_4F_8/40% CO_2/40% N_2	28.9	25.4
20% C_4F_8/80% CO_2	28.5	24.5
20% C_4F_6/80% N_2	40.1	31.3
20% C_4F_6/40% CO_2/40% N_2	39.1	30.4
20% C_4F_6/80% CO_2	38.1	29.5
20% C_3F_8/80% N_2	22.8	20.1
20% C_3F_8/40% CO_2/40% N_2	22.4	19.2
20% C_3F_8/80% CO_2	20.8	18.3
20% SF_6/80% N_2	30.1	20.7
20% SF_6/40% CO_2/40% N_2	28.7	19.8

[a]The uncertainty is less than 0.1 kV.

[b]These breakdown voltages are averages of ten breakdown measurements taken with plane-plane electrode geometry and 0.275-in. electrode gap.

for example, Refs. 8 and 9) electron scattering (elastic and inelastic) at low energies proceeds predominantly through such states. These electron-molecule (negative ion) states are formed[7,8,10] when slow electrons interact with molecules and are nonstationary (i.e., they decay, often

Table 5. Dielectric Strengths of Unitary, Binary, and Multicomponent Mixtures of N_2, SF_6, C_4F_6, and C_3F_8 ($T = 298°K$, $P \approx 0.66$ atm)[a]

	Percent Component				V_s (kV)
No.	N_2	SF_6	C_4F_6	C_3F_8	
1	—	100	—	—	40.1
2	—	—	100	—	93.5
3	—	—	—	100	36.4
4	80	20			30.1
5	80	—	20	—	40.1
6	80	—	—	20	22.8
7	80	10	10		36.0
8	80	10		10	29.8
9	60	20	20	—	45.2
10	60	10	20	10	47.7
11	50	20	30		53.7
12	50	10	30	10	55.4
13	50	20	20	10	47.0
14	50	10	20	20	48.3

[a]Average of ten independent measurements at a Pd value of 4.6 atm-mm (plane-plane electrode geometry).

in as short a time as $\sim 10^{-10}$ sec). Upon decay, the neutral molecule can retain part or all of the impacting electron's energy, the electron being slowed down in the process.

We have investigated the use of systems possessing such NIRs as "electron slowing down" gases in mixtures with one or more highly

electron attaching gases. The electron slowing down gases we used do not normally attach electrons themselves but act to lower the energy of the free electrons so that the electron attaching additive(s) can efficiently remove them in the form of negative ions.

Figure 6 shows the cross sections for vibrational excitation via NIR for CO, N_2, and H_2 as a function of electron energy. These gases were used since basic data for them already exist. Additional basic data are needed. For CO and N_2 the cross sections are the sums of the first eight vibrational levels[11]; for H_2 the cross section for only the first vibrational level is given since the higher ones are very much lower in magnitude. The H_2 cross section has been multiplied by 1.4 to correct for anisotropic scattering.[7] The magnitude of the cross sections decrease in the order CO > N_2 > H_2. One would expect on the basis of the NIR cross section data alone that the breakdown voltage should decrease in the order CO > N_2 > H_2. This is clearly seen from the uniform-field measurements on V_s presented in Table 6. V_s decreases in the order CO > N_2 > H_2. Since the electron attachment cross sections for these systems are exceedingly small or zero,[7] the differences in their dielectric strength is attributed to their relative effectiveness in slowing down electrons via their respective NIRs. Similar conclusions can be drawn from the results on binary mixtures of C_4F_6 and SF_6 each with H_2, N_2, and CO presented in Table 6.

BREAKDOWN STRENGTHS OF GASES/MIXTURES WITH CYLINDRICAL ELECTRODES

In Fig. 7 a and b, preliminary data[4] are presented on the breakdown voltages of mixtures of SF_6 and c-C_4F_8 each with N_2 obtained using cylindrical electrodes comprising an inner stainless steel electrode of 0.4 cm radius inside an outer cylinder of inner radius of 2 cm. The total pressure was 760 torr (1 atm), and the SF_6/N_2 and c-C_4F_8/N_2 concentration fraction was varied from 0 to 100% by pressure. The outer cylinder was at ground potential, and the inner cylinder was at either polarity of high voltage. Each data point is the average of at least ten breakdowns and for each the random scatter (standard deviation ÷ mean) was less than 3%. The uniform field breakdown strength data shown in

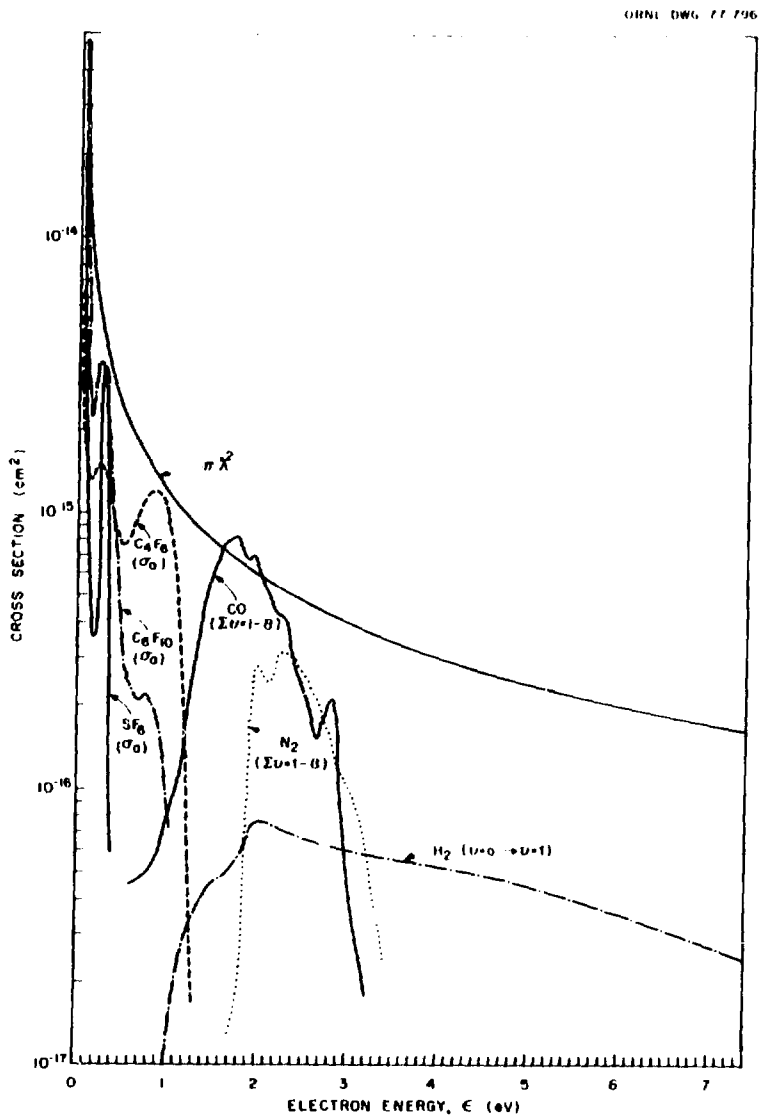

Fig. 6. Electron attachment cross sections, σ_a, as a function of electron energy, ε, for the three electron attaching gases, SF_6, C_4F_8, and C_6F_{10}, and vibrational excitation cross sections via negative ion resonances for CO, N_2, and H_2 (see text and Ref. 7).

Fig. 5 for SF_6/N_2 and c-C_4F_8/N_2 mixtures have been normalized to the nonuniform field value of the V_s for pure N_2. Although the normalized uniform and nonuniform field data are not dramatically different, it is interesting to see that the dependence of V_s on the amount of SF_6 in N_2 shows a stronger "saturation" effect in uniform than in nonuniform fields. In the uniform field case, the SF_6/N_2 mixtures which contain more than 40 to 50% of SF_6 showed little additional improvement in V_s. In the

Table 6. Effect of Negative Ion Resonances on Breakdown[a,b]

Percentage of Component Gas					Slope (kV/atm-mm)	Intercept (kV)	$(V_s)_R$[c]
C_4F_6	SF_6	H_2	N_2	CO			
10		90			4.39	0.82	0.55
10			90		6.18	0.66	0.73
10				90	6.71	1.02	0.82
33		67			8.76	0.68	1.01
33			67		8.93	1.41	1.10
33				67	10.74	0.61	1.22
66		34			15.05	0.55	1.66
66			34		14.16	0.22	1.52
66				34	16.12	0.49	1.76
	10	90			3.27	0.69	0.40
	10		90		4.83	1.18	0.60
	10			90	5.75	1.13	0.71
	33	67			4.79	1.13	0.59
	33		67		6.55	0.83	0.78
	33			67	7.18	1.04	0.86
	66	34			6.70	0.83	0.80
	66		34		7.56	1.03	0.91
	66			34	8.28	0.66	0.96
100					17.55	2.00	2.09
	100				8.49	0.87	1.00
		100			1.55	1.30	0.25
			100		2.74	1.56	0.40
				100	3.52	1.80	0.50

[a] From Ref. 4.

[b] Total pressure 2 atm; sphere-plane electrode geometry.

[c] Breakdown strength relative to SF_6 of 1.

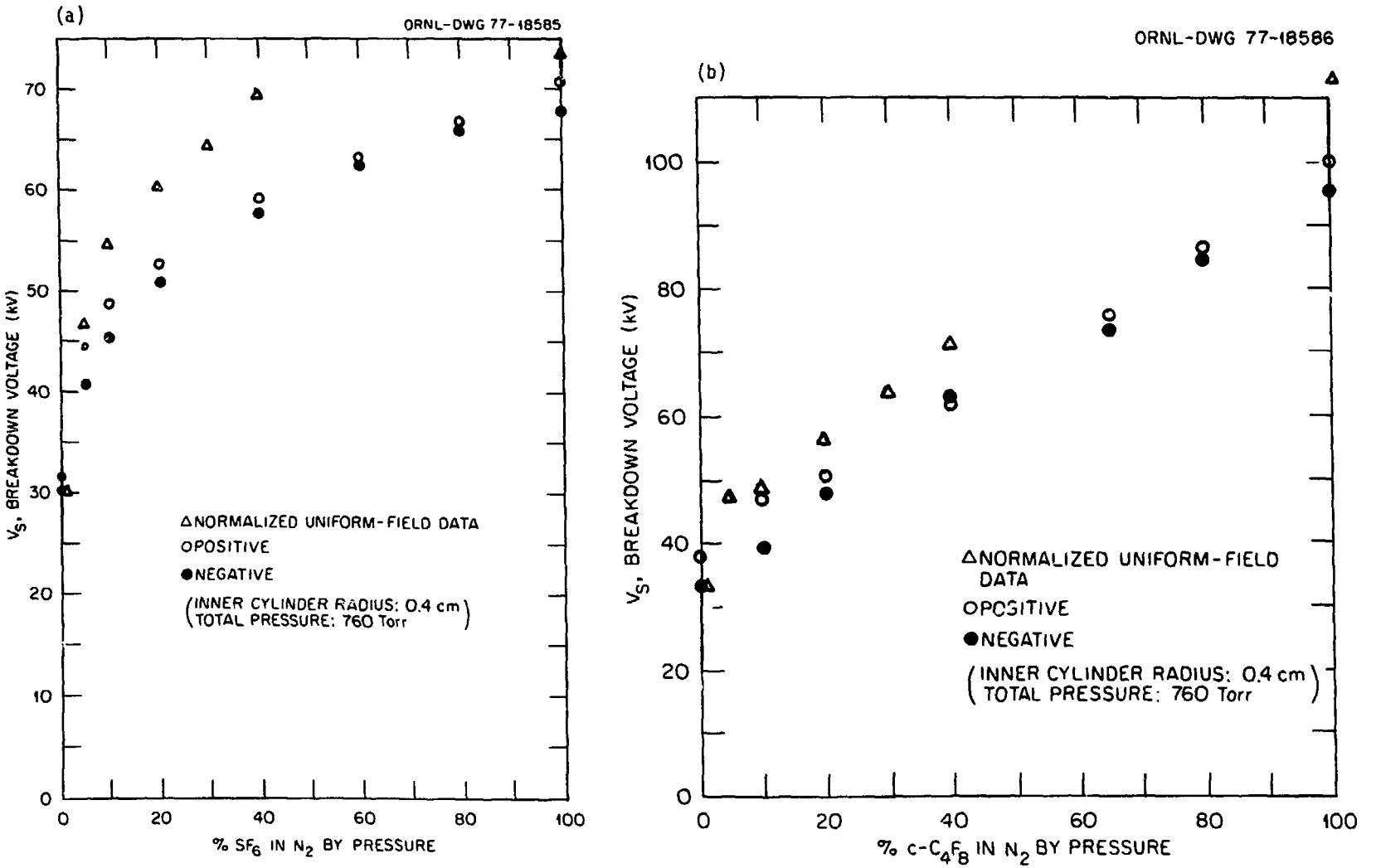

Fig. 7. a. Breakdown voltages for SF_6/N_2 mixtures with cylindrical electrode radii 0.4 and 2 cm. (o) inner electrode at positive potential, (●) inner electrode at negative potential, (Δ) normalized uniform field data. b. Breakdown voltages for c-C_4F_8/N_2 mixtures with cylindrical electrode radii 0.4 and 2 cm. (o) inner electrode at positive potential, (●) inner electrode at negative potential, (Δ) normalized uniform field data.

nonuniform fields of concentric cylinder geometries, the V_s vs % SF_6 curves exhibit less of this saturation. From similar data[4] using inner electrode radii of 1.4, 0.75, and 0.4 cm, each inside the outer cylinder of inner radius of 2 cm, it seems that the difference between the uniform and nonuniform field values of V_s increases with increasing field inhomogeneity. This could be attributed to the fact that the electron energy distribution function is shifted to higher energies in the case of nonuniform fields and to remove the same number of electrons more SF_6 is needed because the electron attachment cross section for SF_6 is small for electrons with energies $\gtrsim$0.4 eV (see Fig. 3). Consistent with this interpretation are the data in Fig. 7b on c-C_4F_8/N_2 where it is seen that when the uniform field data on V_s vs % c-C_4F_8 in N_2 are normalized to the nonuniform field data on the same system, minor differences are observed and practically no saturation effect is evident in either. The superior behavior of c-C_4F_8 compared with SF_6 is attributed to the fact that the electron attachment cross section for this molecule extends to higher energies than that for SF_6 (Fig. 3). This explanation is, however, tentative and requires further scrutiny. Our experiments so far indicate that in the nonuniform fields of concentric cylinders, c-C_4F_8, C_4F_8, and C_4F_6 continue to be far superior insulating gases to SF_6. Further work in this area and on the effect of surface roughness and electrode material on V_s is in progress at our laboratory.

ENVIRONMENTAL ASPECTS OF DIELECTRIC GASES; ANALYSIS OF BREAKDOWN PRODUCTS OF NEW GAS INSULATORS

An important consideration in the study of gaseous dielectrics is that of decomposition of the original gas/gas mixture. Decomposition results in possible loss of dielectric strength and in the possible formation of products which may be harmful to the system, to the environment or to both. Knowledge of the extent and nature of the decomposition products is necessary for any possible chemical intervention to neutralize the toxic or otherwise harmful products formed.

Presently at our laboratory a program is underway to systematically study the processes which lead from the initial electron impact induced fragmentation to the final long-lived products formed after breakdown.

There are essentially three aspects to this program: (1) determination of the initial products (parent ions, fragment ions, and radicals) resulting from single electron-molecule collisions as a function of electron energy by application of time-of-flight mass spectrometry; (2) analysis of decomposition products by a combination of gas chromatography and mass spectrometry; and (3) a study of the intermediate ion-molecule reactions which lead from the initial to the final products by high pressure mass spectrometry.

As an example to this approach, we have studied[12] C_4F_6 (perfluoro-2-butyne). The time-of-flight mass spectrum of C_4F_6 shows that low-energy ($\lesssim$10 eV) electron impact results predominantly in the formation of $C_4F_6^-$ ions, contributing >98% of all negative ions produced in this energy range. The remaining (<2%) ions consist of $C_3F_3^-$, F^-, and CF_3^- (see Table 7 and Fig. 8 for the relative intensity and energy dependence of these ions). It is thus indicated by these findings that C_4F_6 is not easily decomposed under electron bombardment. The resistance to fragmentation, seen in the C_4F_6 molecule, can be more fully appreciated when it is compared with the electron impact induced fragmentation of another good dielectric, namely, C_4F_8 (perfluorobutene-2). Perfluorobutene-2 (C_4F_8) exhibits far more extensive fragmentation (see Table 7) including the formation of $C_4F_7^-$, $C_4F_6^-$, $C_3F_5^-$, $C_3F_3^-$, $C_2F_3^-$, CF_3^-, and F^- ions with F^- being the most abundant ion in the vicinity of 5 eV. Quite unlike the results for C_4F_6, the negative ion fragments $C_4F_7^-$ and $C_4F_6^-$ were produced at near-zero energies in the case of C_4F_8. From the standpoint of initial electron impact induced fragmentation, C_4F_6 appears to be quite stable.

The problem of tracing the reaction pathways leading from the initial ion fragments to the final stable products is very complex, requiring a study of the ion-molecule reaction processes using high pressure mass spectrometry. This phase of our work in which the intermediates will be identified will be undertaken in the near future.

The last step of the decomposition problem lies in the identification and quantification of the products formed in gases which have been subjected to electrical breakdown. To accomplish this, gases which have

Table 7. Parent and Fragment Negative Ions Produced in C_4F_6 (Perfluoro-2-butyne) and C_4F_8 (Perfluorobutene-2) by Electron Impact

Negative Ion	Position of Maximum Ion Intensity	Relative Peak Ion Intensity
	C_4F_6 (perfluoro-2-butyne)	
$C_4F_6^{-*}$[a]	∿0.0	1000
$C_3F_3^-$	1.5	2.4
	5.0	4.0
CF_3^-	5.9	0.2
F^-	5.3	3.1
	C_4F_8 (perfluorobutene-2)	
$C_4F_8^{-*}$[a]	∿0.0	1000
	4.1	∿0.5
	7.4	∿0.3
$C_4F_7^{-*}$[a]	∿0.0	9.5
$C_4F_6^{-*}$[a]	∿0.0 (shoulder)	
	∿0.7	1.5
$C_3F_5^{-*}$[a]	2.3	0.8
	4.2	2.3
$C_3F_3^-$	5.1	0.9
$C_2F_3^-$	5.4	0.4
CF_3^-	5.3	1.3
F^-	5.2	26.7

[a]These ions were found to be metastable with autodetachment lifetimes $>10^{-5}$ sec.

been sparked under controlled conditions have been analyzed in a gas chromatograph followed by an ionization mass spectroscopy detection system. Preliminary work on a pure sample of C_4F_6 shows that the nontoxic[13] gases CF_4 (perfluoromethane), C_2F_4 (perfluoroethylene), and

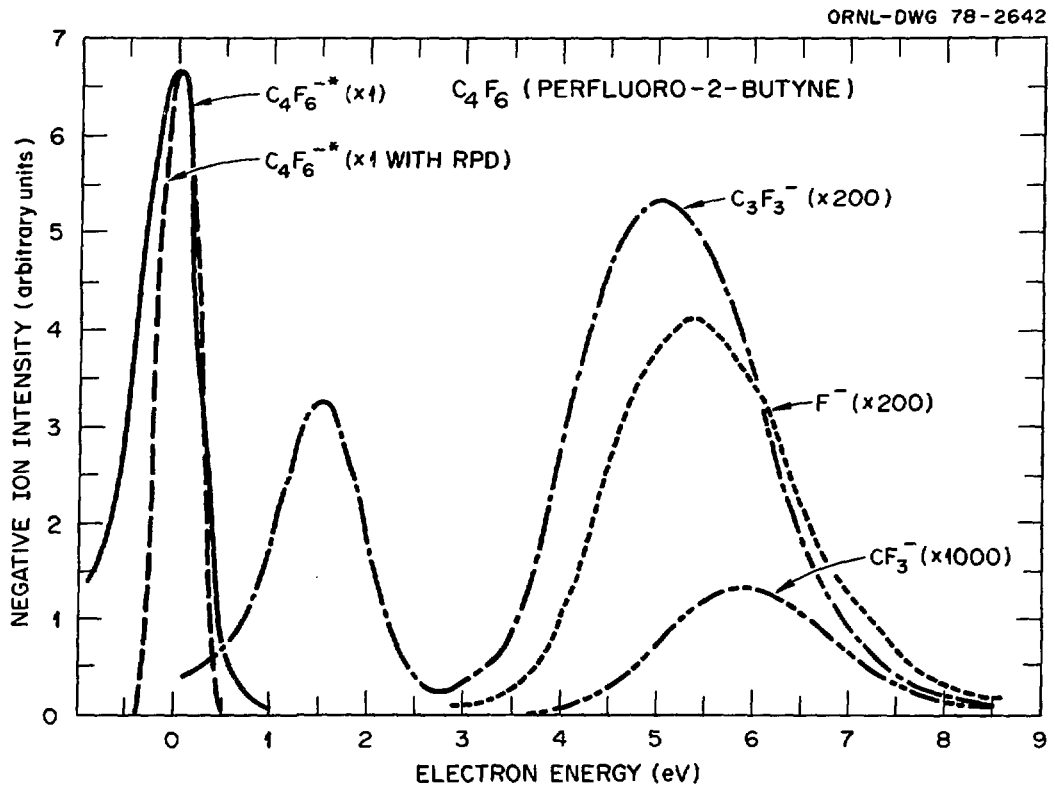

Fig. 8. Negative ion intensity as a function of electron energy for C_4F_6 (perfluoro-2-butyne). Except where noted the spectra were taken without the retarding potential difference (RPD) method.

C_2F_6 (perfluoroethane) are produced. The extent of decomposition of the dielectric as a function of the energy delivered to the system for both unitary and multicomponent gas mixtures is under investigation.

TOXICITY AND CARBON DEPOSITS

A comment on the toxicity and carbon deposits of sparked gases is in order. The toxicity of fluorocarbon compounds varies enormously with relatively small changes in their structure. Thus c-C_4F_8 is nontoxic (an 80% mixture with 20% oxygen substituted for air and breathed for four hours did not affect rats[14]), while iso-C_4F_8 (perfluoroisobutene) at 0.5 parts per million in air was found to be lethal to animals if breathed for four hours.[15]

Each new compound recommended for large-scale commercial use must be individually subjected to prior testing for toxicity. In such toxicity tests care must be taken to ensure that various compounds used as precursors in the manufacturing of fluorocarbons are eliminated, since such compounds often tend to be very toxic and trace amounts—which could be eliminated with careful manufacturing procedures—may be overlooked in small-scale laboratory preparations and can thus lead to erroneous conclusions as to the toxicity of a compound. For example, C_4F_6 samples can be contaminated with $C_4F_6Cl_2$—a known toxic compound used in the preparation of C_4F_6—which can be eliminated by a careful manufacturing procedure.

Another major problem connected with the use of perfluorocarbon compounds in electrical apparatus is the formation and deposition of carbon from the gas under an arc. This carbon can settle on insulators and short them out. Two possible ways to overcome this problem are: (1) appropriate designs of insulators which can relieve the effect of the carbon deposits on the insulators and (2) the use of SF_6 and N_2 (and perhaps other gases) in mixtures with perfluorocarbons. Such mixtures (e.g., $C_4F_6/SF_6/N_2$) can greatly reduce carbon deposits while increasing the dielectric strength above that of SF_6 (see Ref. 4).

REFERENCES

1. J. S. Pearson and J. A. Harrison, J. Phys. D (Appl. Phys.) 2, 77 (1969).

2. H. Winkelnkemper, Z. Krasucki, J. Gerhold, and T. W. Dakin, Electra 52, 67 (1977).

3. L. G. Christophorou, D. R. James, R. Y. Pai, M. O. Pace, R. A. Mathis, D. W. Bouldin, and D. E. Tittle, High Voltage Research, Third Quarterly Report, Oak Ridge National Laboratory Report ORNL/TM-5806, February 1977.

4. L. G. Christophorou, D. R. James, R. Y. Pai, R. A. Mathis, M. O. Pace, D. W. Bouldin, A. A. Christodoulides, and C. C. Chan, High Voltage Research, Semiannual Report, Oak Ridge National Laboratory Report ORNL/TM-6113, November 1977.

5. L. G. Christophorou, "Elementary Electron-Molecule Interactions and Negative Ion Resonances at Subexcitation Energies and Their Significance in Gaseous Dielectrics," paper presented at the International Conference on Phenomena of Ionized Gases, Berlin, September, 1977; Conference Proceedings, Vol. II (in press).

6. A. A. Christodoulides, R. Y. Pai, and L. G. Christophorou, Electron Attachment to Dielectric Gases (to be published).

7. L. G. Christophorou, Atomic and Molecular Radiation Physics, Wiley-Interscience, New York, 1971.

8. G. J. Schulz, Rev. Mod. Phys. 45, 423 (1973).

9. L. G. Christophorou, "Interactions of O_2 with Slow Electrons," paper presented at the International Conference on Singlet Oxygen and Related Species in Chemistry and Biology, Pinawa, Canada, August 1977; Photochem. Photobiol. (in press).

10. L. G. Christophorou, M. W. Grant, and D. L. McCorkle, Advances in Chemical Physics 36, 413 (1977).

11. G. J. Schulz, Phys. Rev. A 135, 988 (1964).

12. I. Sauers, L. G. Christophorou, and J. G. Carter (to be published).

13. W. Braker and A. L. Mossman, Matheson Gas Data Book, Fifth Edition, Matheson Gas Products, New Jersey, 1971.

14. J. W. Clayton, Jr., M. A. Delaplane, and D. B. Hood, Ind. Hyg. J. 21, 382 (1960).

15. J. W. Clayton, Jr., J. Occup. Med. 4, 262 (1962).

DISCUSSION

SHARBAUGH: Dr. J. C. Devins [J. Chem. Phys. 25, 1053 (1956); Nature 179, 976 (1957); Nature 187, 409 (1960); Dielectrics 1, 61 (1962)] of the General Electric Research and Development Center has been approaching the search for SF_6 replacement gases in quite a different manner than that reported by Dr. James. Devins has made an empirical determination of the "cross section" of various atomic groups and bonds by measuring the electric strength (at Pd = 100 torr cm) of certain homologous series of gases--alkanes, perfluoroalkanes, alkanes with one double bond, alkanes with one triple bond, and perfluoroalkylnitriles. In this fashion he has ascribed a semi-quantitative value of the contribution of a particular bond to the expected composite electric strength of the molecule; e.g., C-H, C-C, C=C, C≡C, -C≡N, C-F, C-Cl, C-Br. These are used to guide us to compounds with a desirable boiling point as well as high electric strength. The bond electric strengths are consistent with the spatial electronic configuration of the bonds. It is gratifying to see that Dr. James' approach has lead to some candidates which are among those yielded by the Devins' approach.

JAMES: The authors appreciate the comments of Dr. Sharbaugh on the work of Dr. Devins concerning the relationship between molecular structure and breakdown strength. It is particularly interesting to see that the presence of the double bond in the olefins increased the breakdown voltage over the corresponding single bonded alkanes. These findings are consistent with our results on compounds with multiple bonds and show the importance of understanding the fundamental properties of gaseous dielectrics.

CHRISTOPHOROU: Important as the observations of Dr. Devins are, they can only serve as a vague guide in the choice of unitary gases. A quantitative assessment, and especially a quantitative and realistic development of multicomponent gas mixtures, can only be achieved on the basis of the physicochemical data presented and emphasized by Dr. James, especially on the basis of quantitative knowledge on the various cross sections as a function of electron energy.

SLETTEN: Having had a near disaster in our laboratory, I was disturbed about the fact that one of your slides showed measurements on 33% SF_6 in hydrogen. This mixture can react explosively. It is worth checking the gas mixtures used for possible exothermic reactions before testing.

JAMES: Dr. Sletten's comment is quite relevant to all researchers involved with new gases or gas mixtures. We make a thorough literature search on new systems before we subject them to sparking in our laboratory. It is also important to ensure that impurities which may undergo exothermic reactions with the gas are not present in the sample. The particular mixture you mentioned was tried with extreme care. It was an important one in establishing the role of negative ion resonances on the breakdown strength of a gaseous dielectric and it was tried just for this reason.

DUTTON: A comment rather than a question, but I should like to show some results on a much simpler molecular gas which was motivated by a similar philosophy to that which you had in your investigations. These concern sparking potential and pre-breakdown measurement in N_2O and mixtures of N_2O with O_2 and SF_6, which are mentioned in the written version

of my paper yesterday but which I did not have time to mention.

JAMES: Dr. Dutton's comments are welcomed and are very interesting, especially the synergism observed in the N_2O and O_2 mixtures. These synergisms can probably be understood on the basis of detailed knowledge of the electron attachment and inelastic scattering cross sections and the stabilities of the negative ions involved.

VLASTOS: 1. Do you know something about the toxicity of the gas and the decomposition products?

2. Are these gases as stable as SF_6 is?

3. How these gases behave in the non-homogeneous field?

JAMES: 1. Regarding toxicity of the gases studied, we have found that many of the fluorocarbons such as $c\text{-}C_4F_8$ are considered nontoxic. However, the toxicity of some is either not known or is uncertain at the present time. In toxicity studies steps must be taken to ensure that no toxic impurities are present in the gas. For example, as mentioned in the paper, the toxic compound $C_4F_6Cl_2$ was found in a quantity of C_4F_6 (perfluoro-2-butyne) which was not removed in the manufacturing process. Also details of the toxicity test must be scrutinized to make sure that it is a realistic test.

2. The fluorocarbon gases we have investigated do exhibit varying degrees of solid deposits which appear after arcing. The pure gases at high pressure are generally the worst case. However, we have some preliminary information that in certain mixtures (e.g. $C_4F_6/SF_6/N_2$) the deposits can be significantly reduced.

3. There is little data available on most of the fluorocarbon gases we have studied. We believe that the fluorocarbons are in general relatively inert. As indicated in the paper we found the stability of C_4F_6 to be quite good under electron impact. Further work on the other gases studied is underway.

We have made measurements of the breakdown strength of c-C_4F_8, C_4F_8, and C_4F_6 using cylindrical electrode geometry and found them to have much higher breakdown voltages than SF_6. We continue work in this area of non-uniform fields.

COOKE: An assumption when considering composition of different gases is that the total amount of attachment, ionization, or other fundamental interaction can be determined according to the cross-section partial-pressure-weighted sum of the individual components. In your measurements of attachment in gases have you established that this assumption is valid by comparing attachment rates in individual components against values obtained in mixtures of these components?

JAMES: Since the electron attachment cross section describes a collision between a single electron and a single molecule, the electron attachment cross section of a mixture of gases is the partial pressure weighted sum of the attachment cross sections for the individual components. However, the electron energy distribution function for a mixture of gases will not in general be the partial pressure weighted sum of the distribution functions for the separate components. The distribution functions for mixtures, as well as for most single gases, are not known at the present time. The attachment rate as a function of electron energy

can be determined only if the distribution function for the particular mixture is known.

PACE: A comment as to breakdown products. Brock and Eiseman of DuPont (National Research Council Publication 1356, 1965 Conference on Electrical Insulation) studied solid breakdown products of SF_6 and three other gases. They found that SF_6 was the worst producing solid products of lowest resistivity. Brock and Eiseman found, for example, that $c\text{-}C_4F_8$ products had resistivity 100 times larger than that for SF_6 products (and the quantity was slightly less for $c\text{-}C_4F_8$ products). With 10% N_2O added to $c\text{-}C_4F_8$, that number changed from 100 to $3x10^4$. I would suggest that an intense study of the feared low resistance of fluorocarbon gas solid breakdown products in applications is in order.

JAMES: I agree with Dr. Pace that more information is needed about decomposition products of gaseous dielectrics. It is important in practical systems to eliminate or at least limit the amount of conducting deposits. At Oak Ridge National Laboratory we have already done some work on this and are in the process of expanding our investigations of breakdown products by looking at the initial products of electron impact and also the final long-lived species and products following sparking.

KLINE: It appears that the V_s data shown in Fig. 7a for the 0.4 cm/2 cm coaxial system would agree much more closely with the uniform field data if the data were normalized at 100% SF_6 rather than 0% SF_6. In addition, normalization at 100% SF_6 seems physically more reasonable since V_s is likely to be related to the limiting E/N in both systems. Do you have any

comments?

PACE: The uniform field curve could indeed be normalized at 100% SF_6. Our purpose in plotting it as is shown in Fig. 7a was primarily to see how field nonuniformity changes the curve <u>shape</u> between end points. This plot clearly shows that N_2 tolerates field nonuniformity better than does SF_6.

DIELECTRIC PROPERTIES FOR SF_6 AND SF_6 MIXTURES PREDICTED FROM BASIC DATA

L. E. Kline, D. K. Davies, C. L. Chen, and P. J. Chantry
Westinghouse R&D Center, Pittsburgh, PA 15235

ABSTRACT

We have calculated α and η, the ionization and attachment coefficients, and $(E/N)^*$ the limiting breakdown electric field-to-gas density ratio, in SF_6 and SF_6 mixtures by numerically solving the Boltzmann equation for the electron energy distribution. The calculations require a knowledge of several electron collision cross sections. Published momentum transfer and ionization cross sections for SF_6 were used. We measured various attachment cross sections for SF_6 using electron beam techniques with mass spectrometric ion detection. We determined a total cross section for electronic excitation of SF_6 by comparing the predicted values of α, η and $(E/N)^*$ with our measured values obtained from spatial current growth experiments in SF_6 in uniform fields over an extended range of E/N. With this self-consistent set of SF_6 cross sections, together with published He cross sections, it was then possible to predict the dielectric properties of SF_6-He mixtures. Published experimental values of α for these mixtures lie between the values of α calculated with and without ionization of SF_6 by excited He atoms. Published experimental values of $(E/N)^*$ agree with our calculations to within 5%.

INTRODUCTION

Gas mixtures are being studied as a means for improving the performance and reducing the cost of gas insulation. Extensive measurements are required to determine the dielectric properties of mixtures of two or more gases because a very large parameter space must be studied. Consequently a method for theoretically predicting the dielectric properties of mixtures is very desirable. Although some simple approaches have been proposed, these approaches have limited applicability. For example, when the method described by Baumgartner[1] is applied to SF_6-He mixtures $(E/N)^*$ is underestimated by 50% for a mixture with 10% SF_6 and by an order of magnitude for a mixture

containing 1% SF_6. The theory of the behavior of electrons in gases provides a much more general approach for predicting the dielectric properties of gas mixtures. The theory used here was formulated by Frost and Phelps[2] and has been described in detail by Huxley and Crompton[3]. This theory has been used by Lowke, Phelps and Irwin[4] to accurately predict the discharge properties of gas laser mixtures. This theory can be applied if the required electron collision cross sections are known.

In this paper we describe the results of a combined experimental-theoretical study designed to understand and predict the dielectric properties of SF_6 and SF_6 mixtures. Both attachment cross sections, which describe single electron behavior, and ionization and attachment coefficients, which describe the average behavior of the electrons in a swarm, were measured in SF_6. The theory uses a complete set of cross sections as input data and predicts swarm properties such as ionization and attachment coefficients. In this study, the theory was used to determine a cross section for electronic excitation in SF_6 and to adjust other measured cross sections so that the measured and calculated ionization and attachment coefficients for SF_6 are in good agreement. The set of SF_6 cross sections determined in this way provides the necessary data base from which we can predict the dielectric properties of any mixture containing SF_6, provided the relevant cross sections are known for the other gas(es). In the present study SF_6-He mixtures were chosen because experimental data were available and because the very different dielectric properties of SF_6 and He provide a stringent test of the theory.

CROSS SECTION MEASUREMENTS

The apparatus used for the measurements of the electron attachment cross-sections in SF_6 has been described previously.[5] Most of the measurements were made using the "High Temperature Apparatus" described in Ref. 5, but we restrict ourselves here to data taken with the collision chamber unheated, and the reported cross-sections are those appropriate to room temperature gas. Use of the retarding potential difference (RPD) technique[6,7] gave an effective energy resolution of typically 80-100 meV. The electron energy scale was calibrated by

the known onsets of He^+/He, Xe^+/Xe and the peak position of O^-/N_2O. The data is plotted on a scale corresponding to the most probable electron energy of the effective distribution, the estimated accuracy of the latter being $\pm$ 0.1 eV. The magnitudes of the cross-sections were determined by also measuring the various positive ion cross-sections and calibrating their sum with the total ionization cross-section measurements of Rapp and Englander-Golden[8]. The resulting absolute cross-sections are shown in Fig. 1.

The cross-sections of the negative ions produced above 2 eV have also been measured by Lehmann[9]. The predominant ion in that region is F^-, and comparison of Lehmann's data with the present data is shown for this ion in Fig. 2. For the purpose of this comparison Lehmann's data has been shifted to lower energies by 0.6 eV. No adjustment was made to the magnitudes of the cross-sections, which agree rather well. Similar agreement in magnitude and shape exists for the other ions, provided that Lehmann's data is consistently shifted to lower energies.

The two ions formed at low electron energies, SF_6^- and SF_5^-, are plotted separately on a log-log plot in Fig. 3. The broad peak in the SF_5^- cross-section centered at 0.38 eV is formed by a direct dissociative attachment process, as are the smaller ion fragments observed at higher energies. Of the negative ion cross-section measurements reported here this particular peak is measured with the highest degree of confidence, since it relies on a direct comparison of the ion counts for SF_5^- and SF_5^+, which should be transmitted with equal efficiencies through the ion collection lens system.

At very low energies (<0.2 eV) electron capture leads to SF_6^- or SF_5^-. The cross-sections for these ions have additional uncertainties attached to them. Firstly, both the SF_6^- peak and the SF_5^- peak, which occur at essentially zero electron energy, are in fact very narrow, their true width being unknown. In all measurements to date the observed width of the SF_6^- peak is acknowledged to be instrumental, and the present work is no exception. In Fig. 3 no attempt has been made to define the cross-section below 0.01 eV. The shape between 0.01 and 0.1 eV is instrumental, and only the energy integrated cross-section is known with any confidence to that point. Beyond 0.1 eV the cross-section has

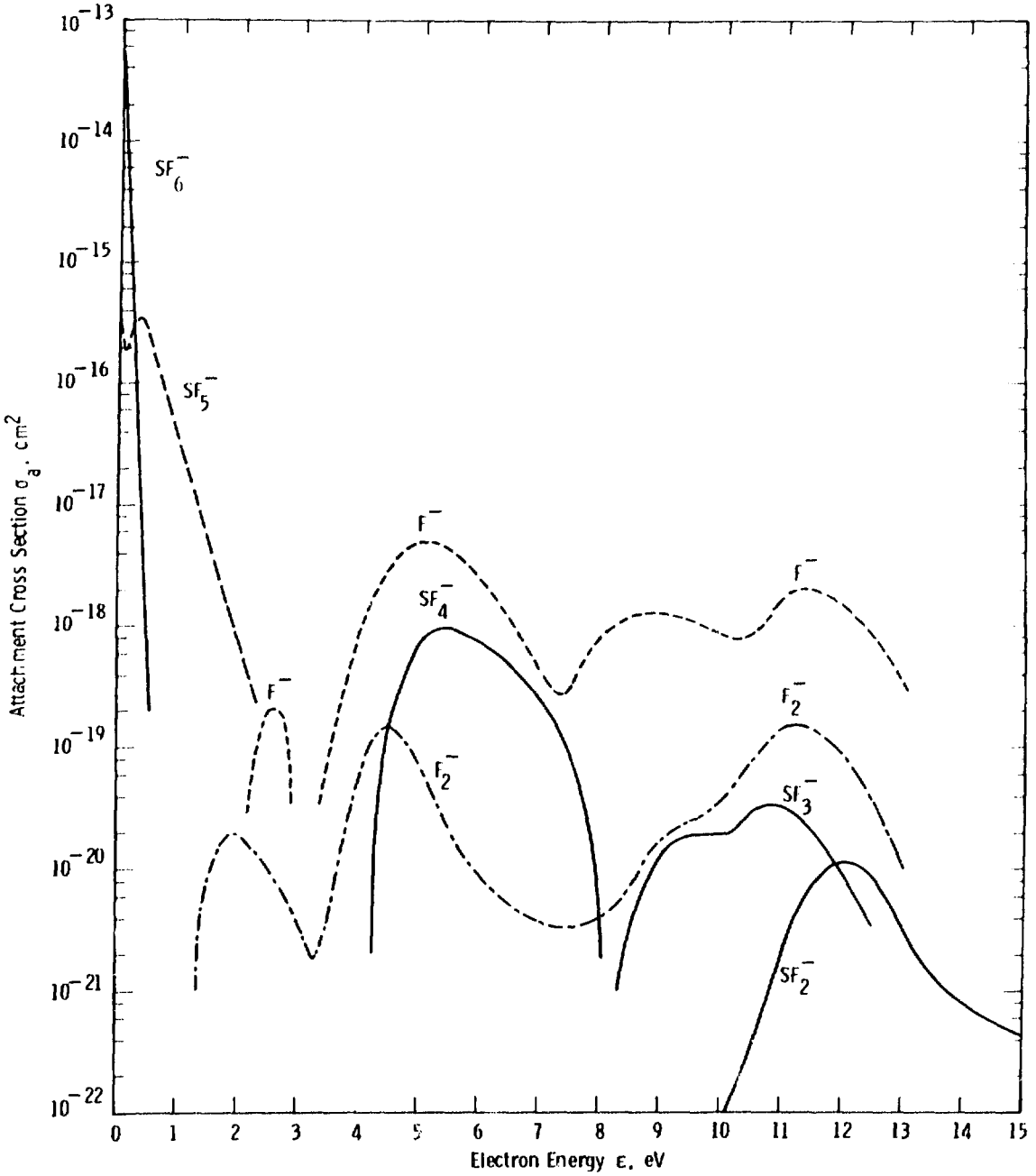

Figure 1 Cross sections for the various attachment processes in SF_6 leading to the indicated ions as measured in the present work.

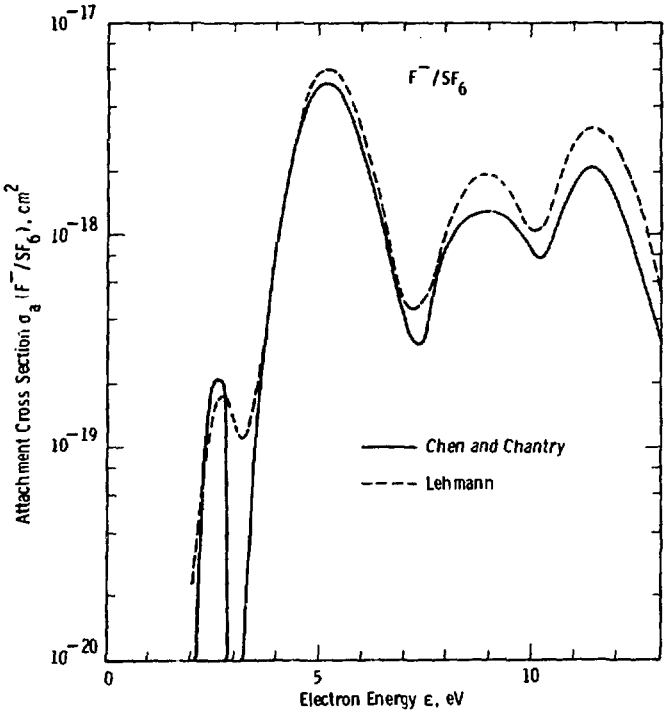

Figure 2 Comparison of the F^- production cross section measured in the present work with that of Lehmann (Ref. 9). Note that the latter has been shifted to lower energies by 0.6 eV.

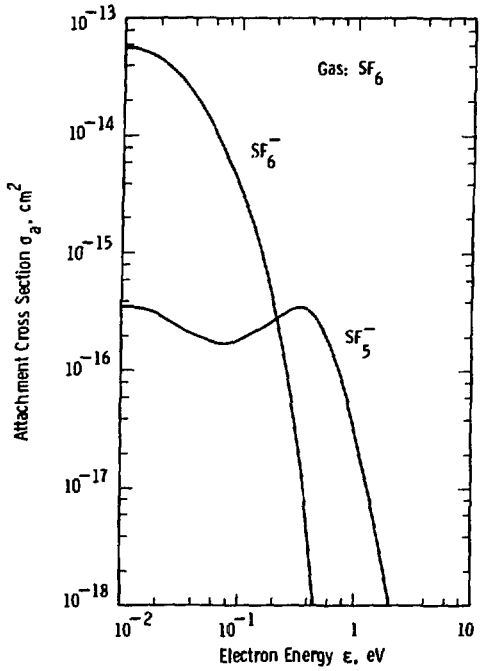

Figure 3 Low energy attachment cross sections measured in SF_6 at room temperature.

been shown[10] to decrease exponentially with increasing energy, the e-folding energy, ε', being typically 0.043 eV.

An additional uncertainty exists in the overall magnitude of the SF_6^- cross-section, due to the finite auto-detachment lifetime of the ion being detected. A correction has been made for the attenuation of the detected SF_6^- signal arising from in-flight autodetachment. This was done by measuring the ratio of the peak SF_6^- signal to the 0.38 eV peak SF_5^- signal for a range of ion transit times and extrapolating to zero ion transit time. This gave a value of 7.0×10^{-14} cm^2 for the peak SF_6^- cross-section. In addition, total ion collection measurements were performed on a second apparatus, the "Low Temperature Apparatus" described in Ref. 5, which gave a peak value of 4.5×10^{-14} cm^2. Based on these two independent measurements we have chosen a "best value" of $(5.5 \pm 2.0) \times 10^{-14}$ cm^2 for the peak of our measured shape.

It should perhaps be emphasized that the autodetachment lifetime of the $(SF_6^-)^*$ formed by direct electron capture of very low energy electrons is sufficiently great ($10^{-2} > \tau > 10^{-5}$ secs) that under the pressure conditions usually prevailing in an insulation application this ion is efficiently stabilized by subsequent collisions with other neutrals. Hence the cross-section relevant to such situations is the initial capture cross-section.

MEASUREMENTS OF SWARM PARAMETERS

The coefficients for net ionization (λ_1/N), ionization (α/N), and effective attachment (η'/N) in SF_6 have been determined from spatial current growth measurements in uniform fields E for values of gas density N in the range $3.54 \times 10^{16} \leq N \leq 88.4 \times 10^{16}$ cm^{-3}. The apparatus and procedure for the analysis of the measurements have been described in detail previously.[11,12] The values of λ_1/N as a function of E/N are compared with previous measurements[13-19] in Figs. 4 and 5. As may be seen from Fig. 4, the present data confirm the linear dependence of λ_1/N on E/N for values of E/N in the vicinity of the

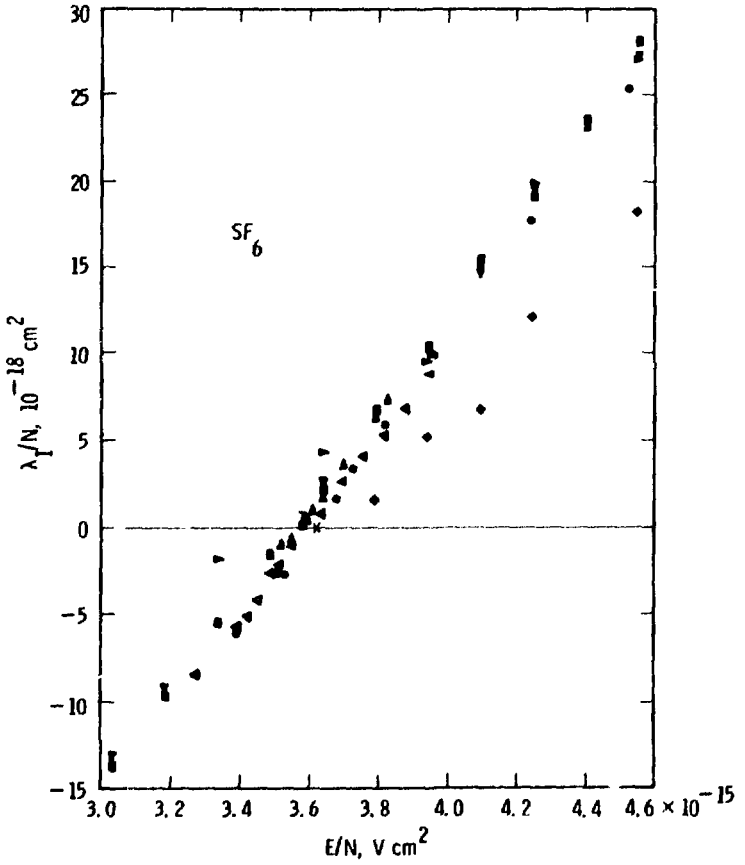

Symbol	Author	Ref.
× ●	Present	
■	CH	13
▼	BLC	14
I	DHJ	15
▲	BOC	16
◆	TS	17
◀	TB	18
▶	MN	19

Key to Figs. 4, 5, and 6

Figure 4 Comparison of present values of λ_1/N as a function of E/N with previous data in the vicinity of $(E/N)^*$.

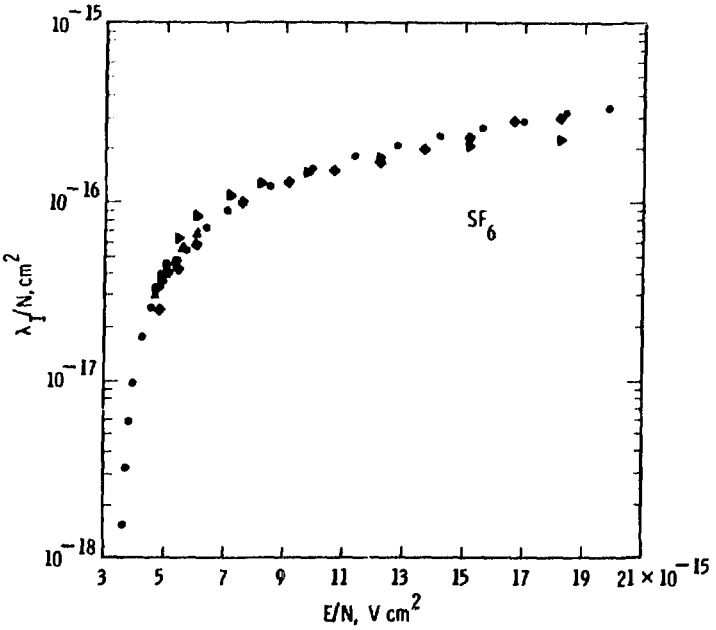

Figure 5 Log-linear plot of present values of λ_1/N as a function of E/N compared with previous data extending to large values of E/N.

limiting value $(E/N)^*$ where $\alpha = \eta'$. In this range there is good agreement among all the measurements with the exception of those of Teich and Sangi and those of Maller and Naidu at the lower values of E/N. The limiting value of $(E/N)^* = 3.62 \times 10^{-15}$ Vcm^2, determined in the present work from a careful search for the value of E/N for which a linear spatial growth of current obtains, is in excellent agreement with the value determined by Teich and Branston[18] from an analysis of avalanche waveshapes. For high values of E/N (Fig. 5), the present data are in good agreement with the results of Teich and Sangi[17] but diverge with increasing E/N from the values of Maller and Naidu,[19] the difference amounting to ~30% at $E/N \sim 2 \times 10^{-14}$ Vcm^2.

In general, the determination of the individual coefficients from current-growth measurements is limited to the range of E/N for which $\alpha/\eta' \lesssim 10$. The values of α/N and η'/N determined over this range of E/N in the present work are compared with previous values in Fig. 6. The present values of α/N are given to within $\pm$ 6% by the relationship $\alpha/N = 4.19 \times 10^{-16} \exp(-9.79 \times 10^{-15}\ N/E)$, where α/N and E/N are in cm^2 and Vcm^2, respectively. The spread among the different values of α/N and η'/N is much larger than that of λ_1/N particularly for values of $E/N < 4.5 \times 10^{-15}$ Vcm^2 (corresponding to values of $\alpha/\eta' < 2$). At present it is not clear whether the large variation in the coefficients α/N and η'/N is due to experimental uncertainties in the measurements or to inaccuracies in the analysis of the data in the event that electron detachment is significant. In the following comparison of the experimentally determined coefficients with those calculated from cross section measurements it is assumed that the measured effective attachment coefficient may be identified with the true attachment coefficient. Even in the presence of detachment, this is a reasonably good approximation provided the detaching ion can alternatively form a stable ion and that the detachment coefficient is small compared with the charge transfer coefficient.

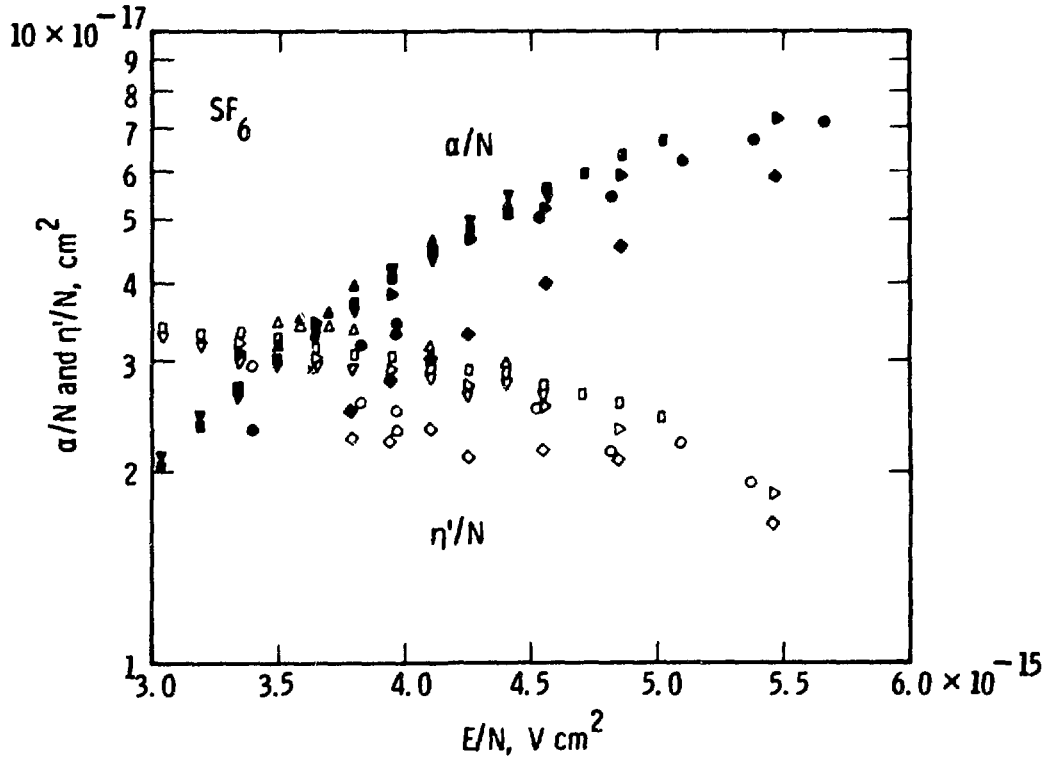

Figure 6 Present values of α/N (solid points) and η'/N (open points) as a function of E/N compared with previous data.

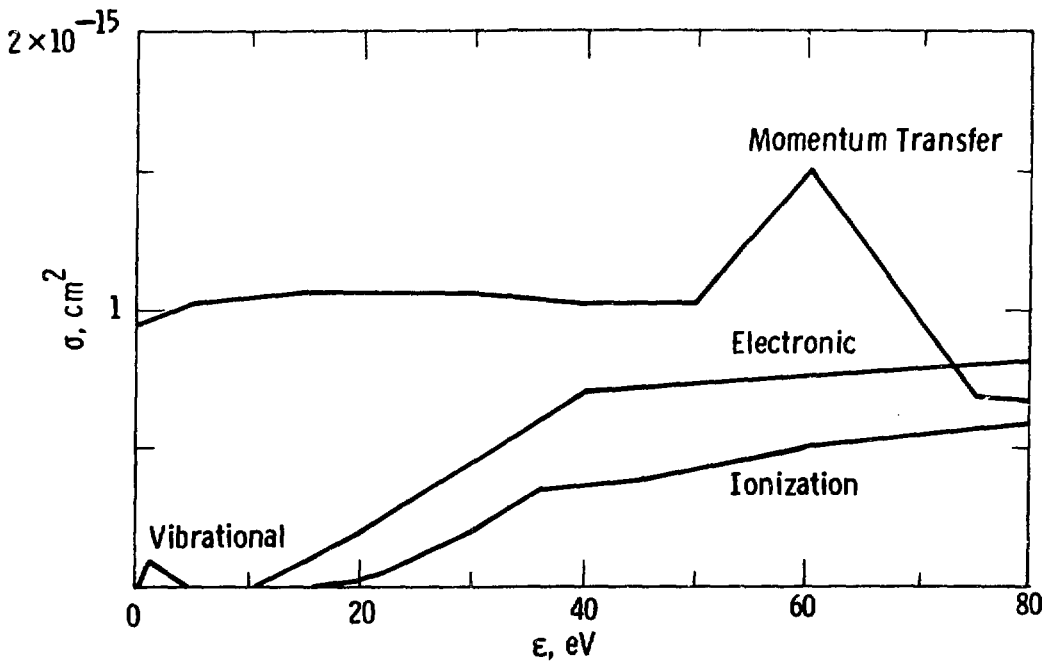

Figure 7 Cross sections used in the calculations. See text for description.

THEORY

Pure SF_6

The primary objective of the theoretical analysis was prediction of the dielectric and discharge properties of gas mixtures containing SF_6. Hence, we have emphasized the determination of a set of SF_6 cross sections which accurately predicts α and η in the the range 0.8 (E/N)* to 1.6 (E/N)* where separate values of α and η can be determined.

The theoretical analysis[2-4] proceeds as follows. First, a complete set of electron collision cross sections is used as input data to calculate the electron energy distribution (EED) by numerically solving the Boltzmann equation. The EED is then used to calculate swarm experiment parameters such as the electron drift velocity, w, and characteristic energy, D/μ, and the ionization and attachment coefficients α and η. Thus the theory can be used to check for consistency between measured cross sections and measured swarm parameters or to estimate a cross section based on measured swarm parameters.

As shown in Fig. 1, the four largest measured peak attachment cross sections are, in order, those for the product ions SF_6^-, SF_5^-, F^-, and SF_4^-. These cross sections were used in the analysis along with the momentum transfer cross section measured by Srivastava et al.[20] and the measured ionization cross section of Ref. 8. The latter two cross sections are shown in Fig. 7 along with the vibrational cross section used in the calculations. Recently Rohr[21] has measured the vibrational cross section at 1 eV to be 10^{-15} cm^2 which is an order of magnitude larger than we assumed. However, the predicted values of α and η in the E/N range of interest are insensitive to an order of magnitude increase in the vibrational cross section.

The total cross section for electronic excitation, σ_x, shown in Fig. 7 was determined by comparing measured and calculated values of α. The 10 eV threshold for σ_x was based on the measurements of Simpson et al.[22] The measured and calculated values of α/N are shown in Fig. 8. The shape and magnitude of σ_x has been adjusted to give good agreement in the range 0.8(E/N)* to 1.6(E/N)*. The calculated values of α/N in

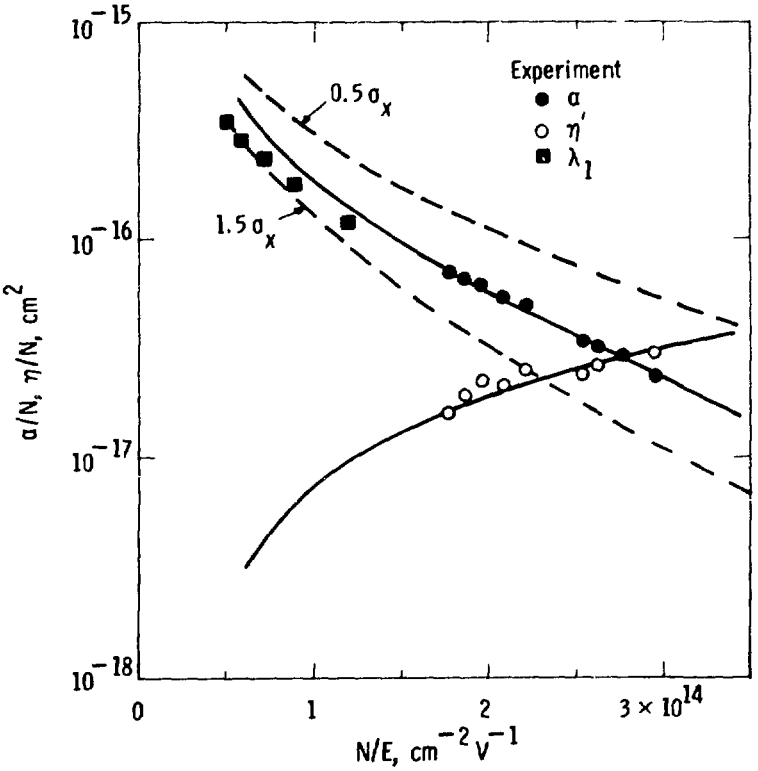

Figure 8 Comparison of measured and calculated values of the ionization and attachment coefficients in SF_6.

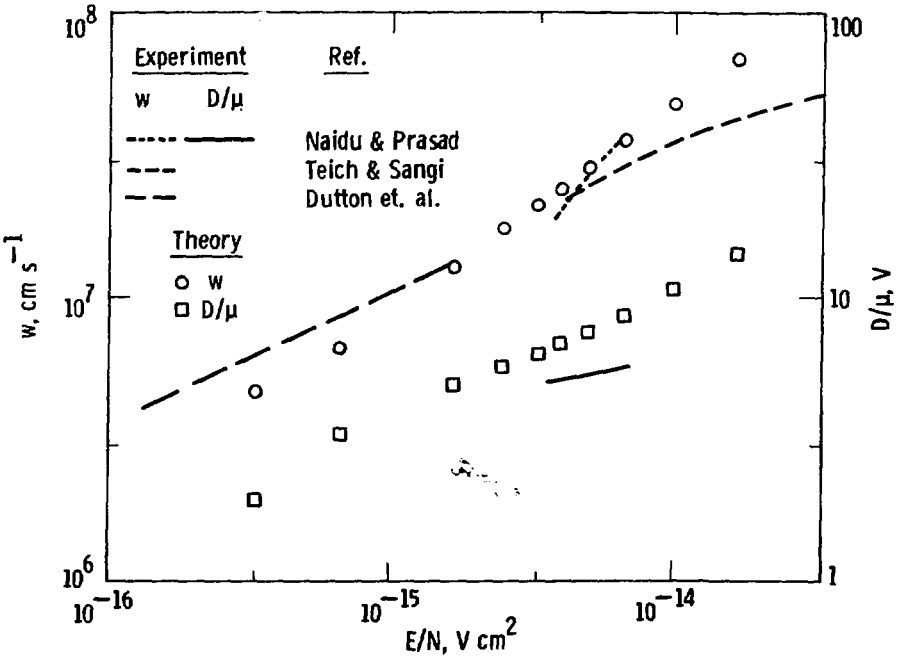

Figure 9 Calculated values of the electron drift velocity and characteristic energy in SF_6 compared with the measured values of Refs. 18, 25, and 26.

this range are quite sensitive to the magnitude of σ_x as indicated by the dashed curves in Fig. 8 which give the values of α/N which are calculated when σ_x in Fig. 7 is changed by $\pm$ 50%. Our value of σ_x at 20 eV is about three times as large as the 'order of magnitude' cross section recently determined by Trajmar and Chutjian.[23] The disagreement between the measured and calculated values of α/N at larger values of E/N is due, in part, to the neglect of the added electron in ionizing collisions.[24]

When the measured attachment cross sections of Fig. 1 were used, the predicted values of η/N were about 25% below the measured values. Good agreement between the measured values of η' and the calculated values of η was obtained by increasing the magnitude of the cross sections shown in Fig. 1 uniformly by 35%. The resulting calculated values are compared with the measured values in Fig. 8. When $E/N = (E/N)^*$, the mean electron energy is $\bar{\varepsilon} = 8.7$ eV and the attachment processes contribute to the total calculated value of η in the proportions: $SF_6^-:SF_5^-:F^-:SF_4^- = 0.19:0.40:0.31:0.08$. The remaining attachment cross sections shown in Fig. 1 are too small to change the predicted values of η by more than a few percent.

Although the emphasis here has been on determining a cross section set which accurately predicts α and η, the predicted values of the electron drift velocity, w, and characteristic energy, D/μ, are in fair to good agreement with the experimental results of Dutton et al.,[25] Teich and Sangi,[18] and Naidu and Prasad[26] as shown in Fig. 9.

SF_6 - He Mixtures

We next used our SF_6 cross sections, together with the helium cross sections of Ref. 4, to predict α, η and $(E/N)^*$ for several SF_6-He mixtures which have been studied experimentally.

Calculated values of α/N and η/N for four different mixtures are shown in Fig. 10. Note that two curves of α/N are shown in each case. The larger value of α/N is calculated by assuming that all excited helium atoms contribute to ionization by ionizing an SF_6 molecule

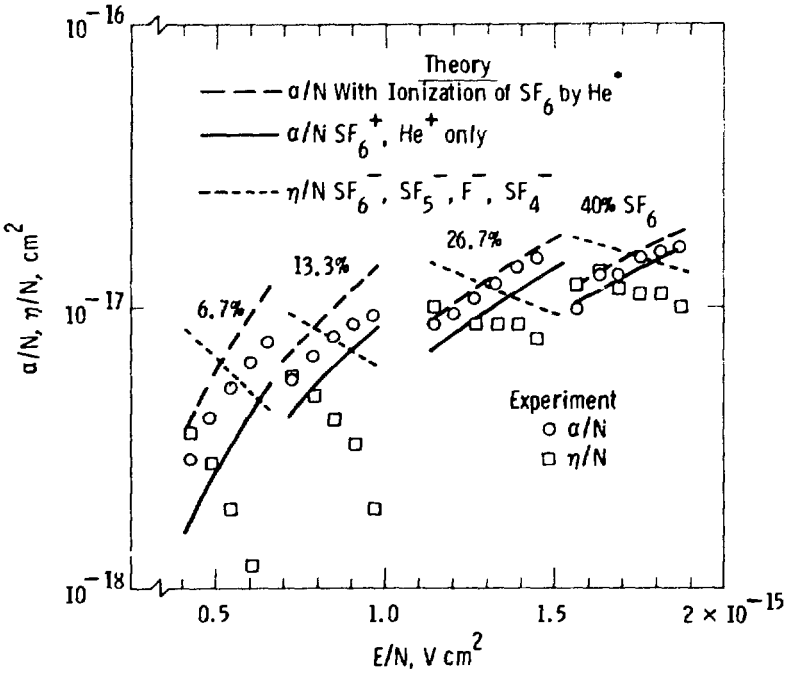

Figure 10 Calculated values of the ionization and attachment coefficient for four SF_6-He mixtures compared with the measured values of Moruzzi and Craggs (Ref. 27).

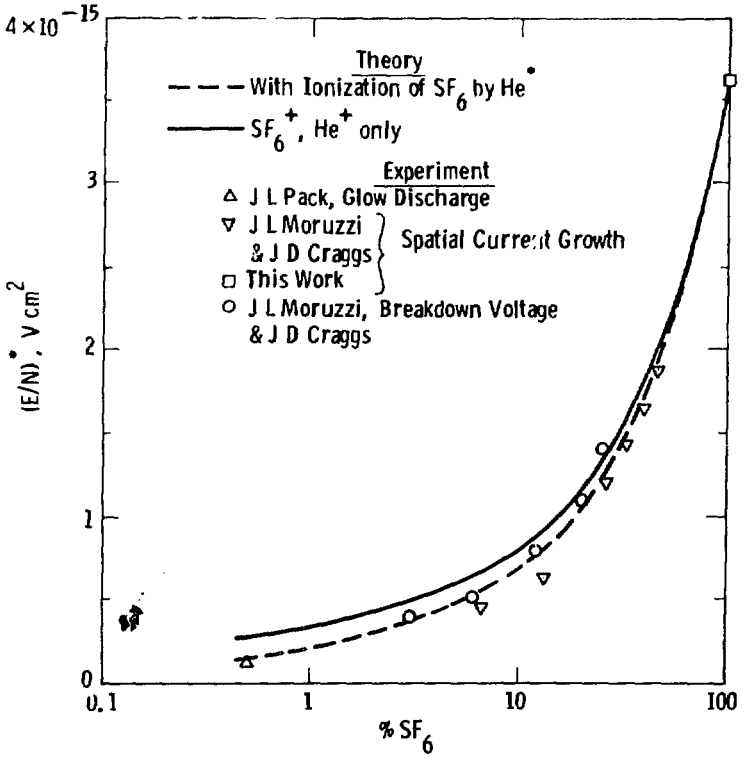

Figure 11 Comparison of measured and calculated values of the limiting breakdown voltage for SF_6-He mixtures vs. SF_6 concentration.

in a Penning ionization process. The lower curve for α/N neglects Penning ionization. The measured α/N values fall between these two curves in all cases. Resolution of the differences between the measured and calculated attachment coefficients requires further study.

The calculated values of $(E/N)^*$ are plotted as a function of SF_6 concentration in Fig. 11, along with the experimental data of Moruzzi and Craggs[27] who have measured $(E/N)^*$ in two ways. The calculated values of $(E/N)^*$ agree with the average of the measured values to within about 5% over the entire range of the experiments.

CONCLUSIONS

1. A set of cross sections which is consistent with measured swarm parameters has been determined for SF_6. The results are satisfactory in view of the limited cross section data available. Additional cross section measurements, particularly of inelastic loss processes, would permit better predictions of parameters.
2. The theoretical results for SF_6 show that the measured attachment cross sections are consistent with the measured attachment coefficients to within the estimated experimental errors. High energy (>2eV) attachment processes account for 39% of the predicted value of η at $(E/N)^*$.
3. Measured and calculated values of α and $(E/N)^*$ for SF_6-He mixtures agree well. The differences between the measured and calculated η values require further study.
4. The SF_6 cross sections can be used to predict the dielectric properties of mixtures of SF_6 and other gases, such as air, N_2, and CO_2, for which cross sections are available.

REFERENCES

1. R. G. Baumgartner, Proceedings Third International Conference on Gas Discharges, 1974, (I.E.E., London, 1974), p. 366.
2. L. S. Frost and A. V. Phelps, Phys. Rev. 136, A1538 (1964).
3. L.G.H. Huxley and R. W. Crompton, The Diffusion and Drift of Electrons in Gases, (Wiley, New York, 1974), Ch. 13.

4. J. J. Lowke, A. V. Phelps, and B. W. Irwin, J. Appl. Phys. 44, 4464 (1973).

5. P. J. Chantry, J. Chem. Phys. 51, 3369 (1969).

6. R. E. Fox, W. M. Hickam, D. J. Grove, and T. Kjeldaas, Rev. Sci. Instrum. 26, 1101 (1955).

7. P. J. Chantry, Rev. Sci. Instrum. 40, 884 (1969).

8. D. Rapp and P. Englander-Golden, J. Chem. Phys. 43, 1464 (1965).

9. B. Lehmann, Z. Naturf. 25a, 1755 (1970).

10. P. J. Chantry and C. L. Chen, Bull. Am. Phys. Soc. 21, 170 (1976).

11. D. K. Davies, J. Appl. Phys. 47, 1920 (1976).

12. D. K. Davies, J. APpl. Phys. 47, 1916 (1976).

13. R. Geballe and M. A. Harrison, in L. B. Loeb, Basic Processes of Gaseous Electronics, (University of California Press, 1955), p.415.

14. M. S. Bhalla and J. D. Craggs, Proc. Phys. Soc. Lond. 80, 151 (1962).

15. J. Dutton, F. M. Harris, and G. J. Jones, Nature 227, 702 (1970).

16. H. A. Boyd and G. C. Crichton, Proc. I.E.E. 118, 1872 (1971).

17. T. H. Teich and B. Sangi, Proc. Int. Symp. Hochspannungstechnik, Munich 1972, p. 391.

18. T. H. Teich and D. W. Branston, in Ref. 1, p. 109.

19. V. N. Maller and M. S. Naidu, Proc. I.E.E. 123, 107 (1976).

20. S. K. Srivastava, S. Trajmar, A. Chutjian, and W. Williams, J. Chem. Phys. 64, 2767 (1976).

21. K. Rohr, J. Phys. B 10, 1175 (1977).

22. J. A. Simpson, C. E. Kuyatt, and S. R. Mielczarek, J. Chem. Phys. 44, 4403 (1966).

23. S. Trajmar and A. Chutjian, J. Phys. B 10, 2943 (1977).

24. L. E. Kline and J. J. Lowke, Proc. 12th Inter. Conf. on Phenomena in Ionized Gases (North-Holland, Amsterdam, 1975) p. 9.

25. J. Dutton, F. M. Harris, and G. J. Jones, Proc. 10th Inter. Conf. on Phenomena in Ionized Gases (Donald Parsons, Oxford, 1971), p. 60.

26. M. S. Naidu and A. N. Prasad, J. Phys. D 5, 1090 (1972).

27. J. L. Moruzzi and J. D. Craggs, in Ref. 24, p. 225.

ACKNOWLEDGMENT

This work was supported in part by USERDA Division of Laser Fusion under Contract EY-76-C-02-4030, "Laser Discharges in Attaching Gases," and EPRI under Contract RP 847-1,"Gases Superior to SF_6 for Insulation and Interruption."

DISCUSSION

DUTTON: Relative to the question of the stabilization of the $(SF_6^-)^*$, do you obtain any pressure dependence of the reduced apparent ionization coefficient in your calculations? We observed such a dependence in some earlier experiments and speculated whether it might depend on this stabilization.

KLINE: No pressure dependence was seen in the measurements of λ_1. The attachment cross sections of Fig. 1 are assumed in the calculations, and the $(SF_6^-)^*$ stabilization is assumed to be instantaneous.

CHRISTOPHOROU: 1. I wonder if you have an explanation for the peak in the momentum transfer cross section at ~60 eV? 2. I would like, if I may, also to ask how your deduced cross sections for vibrational excitation of SF_6 compare with recent experimental data.

KLINE: 1. The measured momentum transfer cross section of Srivastava, et al., Ref. 20, was used. We do not have a physical explanation of the peak at 60 eV. 2. The peak vibrational cross section shown in Fig. 7 is about an order of magnitude smaller than the peak cross section measured by Rohr, Ref. 21. However, use of the larger cross section of Rohr has a negligible effect on the predicted values of α/N and η/N near $(E/N)^*$, as noted in the paper.

PAI: In a negative ion attachment experiment, negative ion decay can mask attachment since no collisional stabilization occurs due to collisions in your experiment. How would such a decay affect the cross sections that you measure?

CHANTRY: The question refers specifically to the measured cross section for SF_6^- production, and does not apply to the dissociative cross sections which require no stabilization. Discussion of this question was omitted from the oral presentation but is given in the written text, towards the end of the section on cross section measurements, to which the reader is referred.

DUTTON: I was interested in the agreement of your calculated values of w in SF_6 with the values we obtained from some very indirect measurements of the current as a function of d in a parallel plate gap. Could I ask a question on nomenclature-- what do you mean by an electronic cross section?

KLINE: The electronic cross section shown in Fig. 7 represents the sum of the cross sections for all electronic excitation processes.

FARISH: We have made some calculations of the breakdown voltage in protrusion-perturbed fields in SF_6/He mixtures, using values for $\bar{\alpha}$ interpolated on a partial pressure basis. For this mixture the calculations did not agree with experimental results, in that the mixtures were even less sensitive to the field enhancement than the calculation predicted. This might suggest that for a given mixture the true $\bar{\alpha}$ increases more slowly with E/P than our interpolated value. Is this true of your computed $\bar{\alpha}$ values and have you made any calculations of V_s in protrusion-perturbed or other nonuniform fields? Also, which is the highest value of E/P for which you can calculate $\bar{\alpha}$ for SF_6?

KLINE: 1. The measured values of λ_1 (or $\bar{\alpha}$) shown in Fig. 5 show that λ_1 increases approximately linearly with E/N up to 2100 Td $\approx$ 6 x (E/N)*. We have not calculated $\bar{\alpha}$ for larger values of E/N. 2. We have

not calculated V_s for nonuniform field systems. 3. The calculations can, in principle, be extended over a much wider range of E/N. Calculated values of α/N may be in error at very high values of E/N (see Ref. 24).

THE USE OF SF_6 OR C_2F_6 IN OIL FILLED TRANSFORMERS

E. J. Walsh
Westinghouse Electric Corporation, USA

ABSTRACT

Under a contract with the Electrical Power Research Institute (E.P.R.I.), studies are being conducted to evaluate the potential benefits of utilizing SF_6 or C_2F_6 saturated oils as an insulating medium in transformers.

The results to date have shown that the 60 Hz electric strengths, the corona inception voltages, the impulse strengths, and the material compatibilities for the SF_6 and C_2F_6 saturated oils are all similar to nitrogen saturated oils.

The effects of temperature and pressure on the solubility of these electro-negative gases in transformer mineral oil have also been investigated. It was found that both SF_6 and C_2F_6 were much more soluble than nitrogen in oil over the temperature and pressure range studied. Also studied was gas evolution under electric stress and a significant variation from nitrogen behavior was found in the Pirelli test results and in rates of gas evolution during arcing.

Thermally accelerated life testing using distribution transformers containing these new gas-oil mixtures are ongoing and to date, no transformer failures have been detected. However, it was found that it was necessary to vent some of the gases from the head space over the oil to avoid excess pressure buildup in the transformer tanks. The increased pressure was due to SF_6 or C_2F_6 in the oil being released at the elevated temperatures used in these tests.

INTRODUCTION

Traditionally, nitrogen gas has been used to fill the head space in many oil filled power transformers. The favorable experience in the use of SF_6 in gas insulated substations and the excellent performance of C_2F_6 in gas insulated "dry" type transformers indicated that the use

of these electronegative gases in oil filled transformers might provide a superior insulating system. In addition to the potential performance improvements, it was anticipated that a study of SF_6 oil systems and C_2F_6 oil systems would provide data for evaluating the necessity for continuing to provide special bushings to fully exclude SF_6 from nitrogen-oil insulated transformers.

Therefore, this study had two primary objectives. The first objective was to determine the potential for improved transformer performance with SF_6 or C_2F_6 oil insulation. The second objective was to evaluate the effects of SF_6 oil insulating medium on transformer performance to determine what detrimental effects, if any, could be expected if SF_6 gas entered an oil filled transformer.

To attain these goals, a series of chemical, physical, and electrical tests on SF_6 oil and C_2F_6 oil models was initiated.

EXPERIMENTAL

Solubility Studies

A survey of the literature indicated that some data was available on SF_6 oil solubilities but no information was available on C_2F_6 oil systems. The solubilities of these materials in a typical transformer oil were determined over a range of temperatures and pressures and also the effect of increasing temperature of the gas-oil mixtures in a model tank was examined to determine the pressure rise which could be expected during transformer operation. Table 1 summarizes the data from the solubility studies and Figure 1 is a plot of pressure vs. temperature for these gas-oil systems in a model transformer tank with 10% head space over the liquid.

Table 1. The Variation of Solubility, X, ml Gas @STP/ml Oil With Temperature and Pressure

	Temp. (°C)[a]	P (atm)[a]	Solubility; X ml gas at STP / ml oil	k[b] atm / Solubility
N_2 Gas	27	1	.073	13.8
	60	1	.076	13.2
	100	1	.078	12.8
	130	1	.080	12.5
	27	2	.143	13.9
	27	3	.226	13.3
SF_6 Gas	27	1	.418	2.41
	60	1	.328	3.05
	100	1	.262	3.87
	130	1	.218	4.58
	27	2	.816	2.45
	27	3	1.25	2.41
C_2F_6 Gas	27	1	.649	1.54
	60	1	.585	1.71
	100	1	.528	1.89
	130	1	.495	2.02
	27	2	1.07	1.88
	27	3	1.35	2.22

a - SI units; $^oC = {}^oK - 273$ 1 atm = 1.01325×10^5 Newtons/meters^2

b - k is Henry's low constant from the equation: $P = k \cdot X$

Chemical Studies

In an effort to determine what chemical effects SF_6 or C_2F_6 would have on transformer materials, a series of long term compatibility tests were conducted. Representative samples of tank steel, core steel, copper, aluminum, and insulating materials were immersed in the different saturated gas-oil mixtures for up to 180 days at temperatures up to

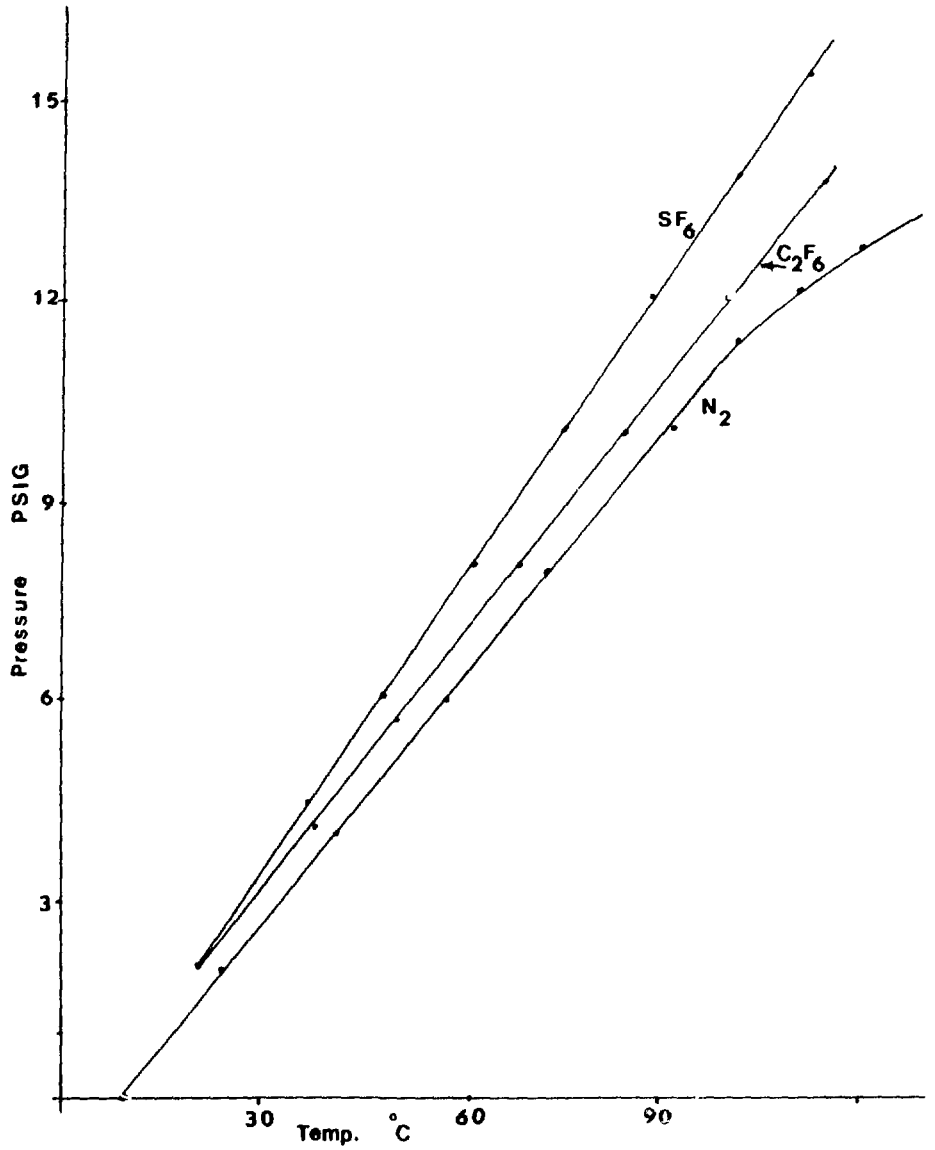

Fig. 1. Pressure rise as a function of temperature in sealed tanks with 10% head space.

150°C. The results of these tests were compared to nitrogen saturated oil results and evaluations made of the conditions of the materials and the quality of the liquid medium. No accelerated deterioration due to the presence of SF_6 or C_2F_6 or any of the materials, including the oil, could be detected by chemical and physical tests. The SF_6 and C_2F_6 performed as well as the nitrogen in these tests even though they were present in much higher concentrations.

In addition to the compatibility experiments, a series of experiments was carried out to determine the effects of prolonged arcing through these new mediums. The gases generated by arcing through the head space above the liquid were examined to determine what decomposition products resulted from the arc induced reactions.

Table 2 lists some of the gaseous products formed during these experiments. Table 3 compares the different arc energies used and the gas pressures generated from these arcs. In addition to the gas analysis,

Table 2. Gases Generated During 30 Minutes Arcing

Gas Evolved	Saturation Gas					
(Vol. %)	N_2	SF_6	C_2F_6	N_2	SF_6	C_2F_6
	Arcing Through Oil			Arcing Through Head Space		
N_2	91.62	.16	---	99.73	.18	.04
SF_6	-----	86.81	---	-----	99.65	----
C_2F_6	-----	-----	82.70	-----	-----	78.69
O_2	.65	.19	.03	.05	.02	----
CO_2	.02	.08	---	.02	.09	.57
H_2	6.54	12.28	16.71	.12	-----	-----
CO	-----	-----	---	.01	-----	-----
$CH_4 + CF_4$	.24	.48	.56	-----	.06	20.52
C_2H_2	.07	-----	---	-----	-----	-----
C_2H_4	.85	-----	---	-----	-----	-----
C_2H_6	.01	-----	---	-----	-----	-----
C_3's	.02	-----	---	.07	-----	-----

Table 3. Gas Generation From Arcing of Saturated Oils For 30 Minutes

Saturation Gas	Arcing Medium	Total Arc Energy K_w -Sec.	Change in Gas Pressure PSI	Change in Volume (CC)	Average CC/K_w -Sec.
N_2	Head Space	.95	.04	1.1	
N_2	Sat. Oil	30.7	3.51	125.2	4.08
SF_6	Head Space	6.25	.12	3.3	
SF_6	Sat. Oil	28.9	10.15	363.3	12.57
S_2F_6	Head Space	11.54	1.34	36.2	
S_2F_6	Sat. Oil	30.7	7.77	278.2	9.06

the liquid solution after arcing was examined for fluorinated hydrocarbon content by infrared spectroscopy and no significant quantities of such materials were detectable.

Electrical Studies

These new gas-oil mixtures were examined using standard or modified ASTM or IEEE test methods to determine electric strengths, dielectric constants, dissipation factors, impulse strengths in uniform and non-uniform fields, corona inception voltages, and gasing tendencies in a corona field. Table 4 gives the data on electric strengths for these solutions over a representative range of temperatures. Table 4 also contains the data from a series of electric strength tests in which a stream of bubbles of the gas under study was maintained between the electrodes during the tests.

Table 4. 60 Hz, Dielectric Breakdown Strength of Gas-Oil Mixture with Bubbling Between Electrodes

Gas-Oil Mixture	Temperature (°K)	Average Breakdown Values (KV) With Bubbles	Without Bubbles
N_2	296	29.8	35-46
N_2	353	36.4	38-46
SF_6	296	38.2	30-42
SF_6	353	39.0	33-44
C_2F_6	296	35.0	37-47
C_2F_6	353	40.2	47

A pressure of Gas 1 Lb. PSIG solution saturated 1 Hour Before Testing.

Table 5 summarizes the impulse test data for uniform and non-uniform fields. Table 6 contains the summarized data ..om the corona inception studies and Figure 2 is a graphical presentation of the gasing tendency runs using a Pirelli cell.

Work in Progress

At present, there is a continuing program of life testing using distribution type transformers, in accordance with IEEE 345, filled with different insulating mixtures. Also under examination is the potential solvation of the metallic materials in the oil due to the presence of the SF_6 or C_2F_6. To date, after 1000 hours of operation at 180°C hot spot, none of the SF_6 oil or C_2F_6 oil units have failed. However, occasional venting of the gases was needed to keep the pressure in the test tanks below 15 PSIG.

Table 5. Summary of Results
Electric Breakdown Tests on Oil Saturated with Gas

(a)
Average Breakdown Voltages

	Non-Uniform Field (b) Point to Plane				Uniform Field 1 Inch Spheres	
	60 Hz		Impulse (c)		60 Hz	Impulse
Gas	.1" Gap KV	.5" Gap KV	.1" Gap KV	.5" Gap KV	.1" Gap KV	.1" Gap KV
SF_6	20.6	41.3	54.3	110.3	43.8	114.0
C_2F_6	21.5	32.8	59.7	113.0	38.9	118.9
Nitrogen	24.9	36.9	56.5	104.9	30.9	129.8
Degassed Oil	30.4	45.5	61.9	106.1	41.1	135.8

(a) - The average of five runs
(b) - Needle negative
(c) - 7-50 μ sec. full wave impulse

Table 6. Corona Inception Voltages for Gas-Oil Mixtures

Gas-Oil Mixture	Corona Detected (KV)	Breakdown Voltage (KV)
N_2	23.0	24.0
SF_6	23.5	24.0
C_2F_6	23.5	24.0

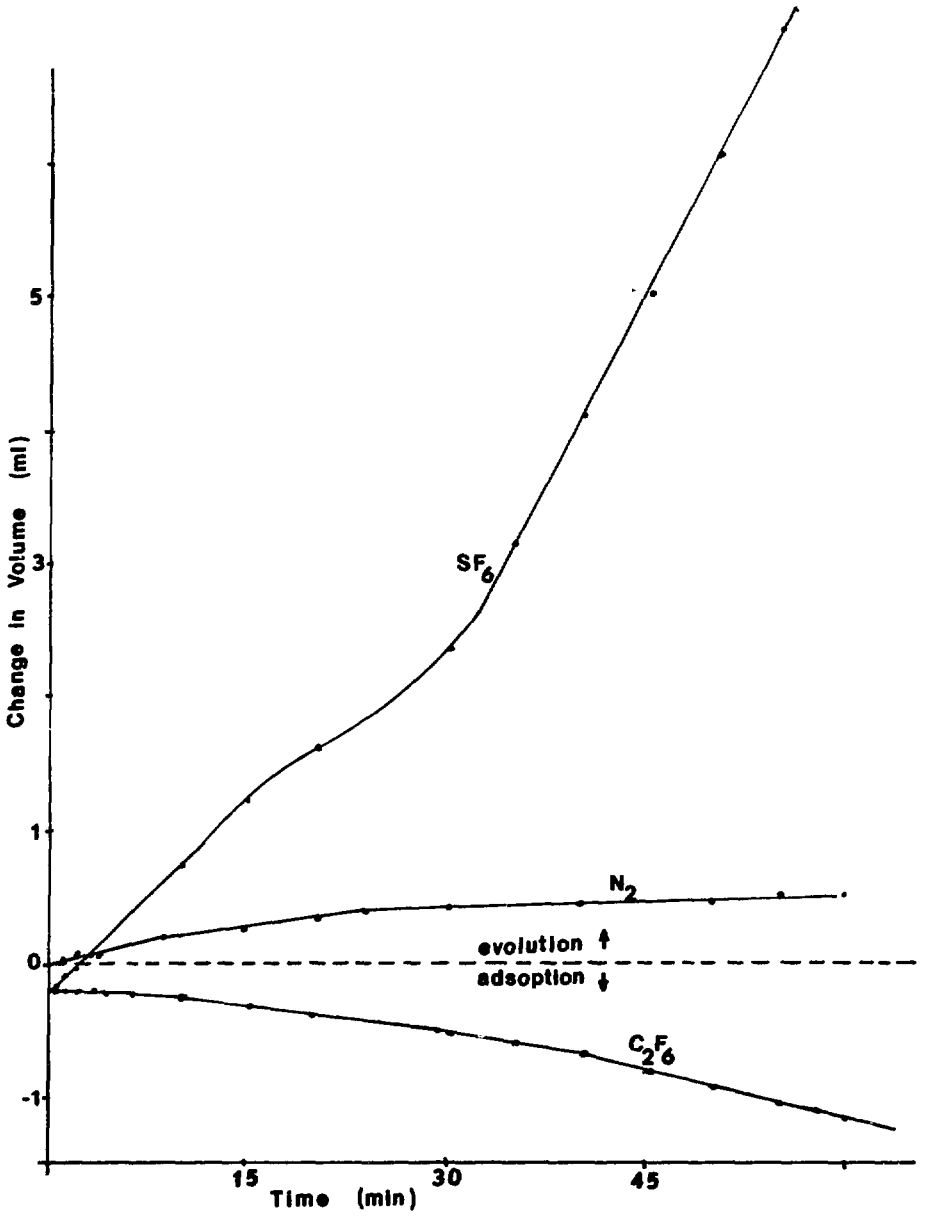

Fig. 2. Pirelli test results for gasing tendency at 80°C, 16 KV stress.

RESULTS AND DISCUSSION

It can be seen from the tests conducted to date that SF_6 and C_2F_6 oil solutions appear to be equivalent to nitrogen as an insulating medium. There are, however, certain observations which should be noted which indicate that some design changes would be necessary to utilize these materials in transformers.

Both SF_6 and C_2F_6 are significantly more soluble in oil than is nitrogen. Therefore, if a saturated solution of either of these gases is used in a sealed system, one obtains significantly higher pressures in the tank than with nitrogen. Also, in the presence of corona, there is rapid and significant evolution of SF_6 gas which may release bubbles into the transformer.

Counter balancing these observations is the data presented in Table 4 which indicates that SF_6 bubbles do not significantly reduce the dielectric strength of the insulating medium.

In summary, the data obtained to date indicates that either SF_6 or C_2F_6 could be introduced into a transformer without adversely affecting the insulating capability of the liquid insulation but that the introduction of significant quantities of SF_6 may require either a pressure relief device or a stronger transformer tank. Also, there is the possibility of increased decomposition of either SF_6 or C_2F_6 during arcing which generates more hydrogen than found for nitrogen saturated oils.

64442

COMPRESSED GAS INSULATED TRANSMISSION SYSTEMS: THE PRESENT AND THE FUTURE

286-313

A. H. Cookson
Westinghouse Electric Corporation
CGIT Laboratory
Westborough, Massachusetts

ABSTRACT

The present design of compressed gas insulated transmission lines (CGIT) consists basically of an isolated phase system with an aluminum conductor supported on cast epoxy insulators inside an aluminum sheath filled with sulfur hexafluoride (SF_6) gas typically at a pressure of 0.44 MPa (4.4 atm). These systems were first installed in 1971/72, and are now in service as high power (eg. 3000 A) transmission links or substation getaways at voltage levels of 145 kV through 550 kV. In addition, 800 kV designs have been developed and tested.

The basic CGIT design parameters are discussed with reference to the high voltage performance and operating conditions of the gaseous dielectric and the support insulators. A typical CGIT cost analysis indicates the critical parameters and the increasing importance of the SF_6 gas cost at the higher voltage levels. The significance of an improved gaseous dielectric is considered as to possible reduction of the CGIT size and the effect this would have on the design, current rating, and economics.

Future CGIT system developments are discussed, including: three phase designs, where the three conductors are mounted within the same aluminum sheath; flexible systems where the sheath is made from corrugated aluminum with a flexible conductor; high temperature design, where the conductor operates at a temperature of 150°C; 1200 kV systems, where the current rating of 5000 A will enable 10,000 MVA to be transmitted; and DC transmission systems.

INTRODUCTION

The basic design of a Compressed Gas Insulated Transmission Line consists of a conductor supported on discretely spaced insulators inside a metallic sheath, the high voltage insulation being provided by a compressed gas, typically sulphur hexafluoride (SF_6) at a pressure of 0.44 MPa (4.4 atmospheres). The first designs were proposed in the early 1940's[1], but the first lines were only installed on transmission systems in 1971-1972[2,3], although SF_6 insulated equipment such as circuit breakers, and current and power transformers had been developed in the 1950's. Already there are twenty seven systems in service or scheduled for service as high power transmission links or substation getaways at voltage levels of 145 kV through 550 kV[4]. In addition, 800 kV designs have been developed and tested, and 1200 kV systems are under development.[5]

This paper reviews the general construction and design criteria of CGIT systems. As one of the purposes of this Symposium is to review the progress in gaseous dielectrics and the potential applications, special attention is given to the design criteria for the gas insulation in CGIT systems. If a new gas or gas mixture with superior dielectric properties to the presently used SF_6 were developed, this could have significant effect. This is discussed as related to the general design, including the design value of the electric fields, and the effect on the current rating. The requirements and specifications for any new gaseous dielectric for application in CGIT systems are then discussed. The last section discusses future developments of advanced CGIT systems.

DESIGN OF CGIT SYSTEMS

General Design

Present CGIT lines are isolated phase systems, with an extruded aluminum conductor of high conductivity alloy (6101-T64) and typically 12.7 mm wall thickness, supported on cast epoxy insulators concentrically in an aluminum sheath that is either extruded or of spiral welded construction, typically with a wall of 6.4 mm thickness. The lines are made and shipped

in 18 m lengths, with the insulators every 6 m (Figure 1). A special conductor plug-in connector is used which acts as the field joint and also accommodates the differential thermal expansion between the conductor and the sheath. The sheath joint can be either welded or flanged, but the welded joint is preferred as this is a lower cost system and allows greater flexibility for installation in the field.

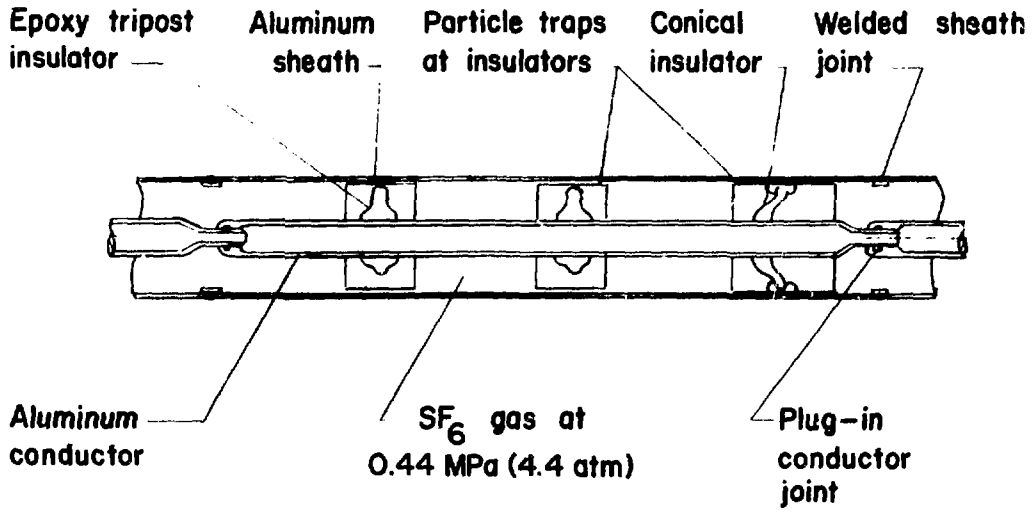

Fig. 1 Typical design of compressed gas insulated transmission line. Section length is 18 m with insulators every 6 m. Other designs may use only disc or conical insulators.

The dimensions and ratings of standard CGIT systems for buried conditions are shown in Table 1. These current and MVA ratings are conservative, based on close interphase separation, unity load factor, and a maximum sheath temperature of 60°C to prevent excessive drying of the soil. The aboveground ratings are typically 75% higher. The design and test voltages for the different ratings, and the values of the conductor field under operating and test conditions are given in Tables 2 and 3.

The cast epoxy insulator is the most critical component for the high voltage integrity of CGIT systems. Figure 2 shows two types of insulators that are frequently used, a tripost and conical design. Disc insulators are also used. There are several alternative methods whereby the insulators can be mounted on the conductor and inside the sheath. Basically the insulator is cast either directly onto the conductor, or onto a conductor

Table 1. Dimensions and Ratings of Buried CGIT Lines

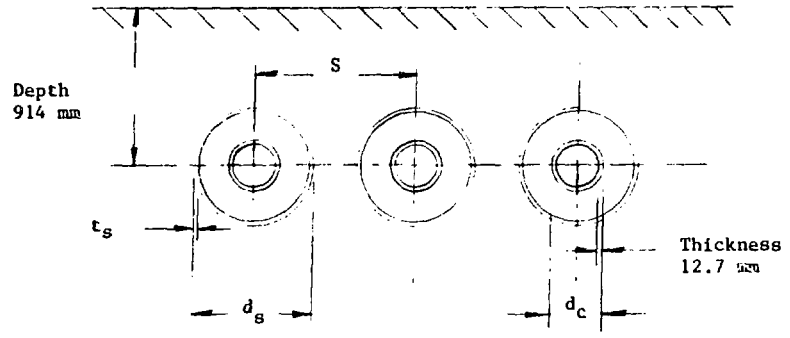

Voltage Rating AC Max/BIL kV	d_s mm	t_s [a] mm	d_c mm	S mm	Current Rating [a] A	MVA [b]
145/650	241	6.4	89	394	1400	335
242/900	307	6.6	102	457	1700	680
362/1050	381	7.6	127	559	2000	1200
550/1550	508	6.4	178	711	2350	2050
800/1800	635	6.4	203	813	2750	3650

a. Extruded sheath 145 kV through 362 kV, spiral welded sheath at 550 kV and 800 kV.

b. For 35°C sheath temperature rise in soil of thermal conductivity 90°C cm/W, with 25°C ambient and unity load factor.

Table 2. High Voltage Test Levels for CGIT Systems [a]

Maximum Rated System Voltage kV rms	Design Test BIL kV Peak	Design Test Sw. Surge kV Peak	Design and Factory Test 60 Hz, 1 Min kV rms	Field Test 60 Hz, 1 Min kV rms
145	650	-	310	230
242	900	-	425	320
362	900	-	425	320
	1050	825	500	375
550	1300	1050	615	460
	1550	1175	740	550
800	1800	1425	860	645

[a] Recommended Test Levels of IEEE Working Group 70.1, Document P468-1/D3 "Voltage Ratings of Gas Insulated Substations".

Table 3. Design Fields for Present and "Future" CGIT Lines

Maximum System Voltage kV	CGIT Dimensions		Field at Conductor MV/m			
	Sheath/Conductor Dia.		Present System		"Future" System	
	Present System mm	"Future" System mm	Continuous AC rms	BIL Peak	Continuous AC rms	BIL Peak
145	241/ 89	216/ 76	2.0	15.5	2.2	17.3
242	307/102	241/ 89	2.6	16.8	3.3	21.5
362	381/127	307/102	3.1	15.4	3.9	19.6
550	508/178	381/127	3.5	17.0	4.7	22.8
800	635/203	508/178	4.1	15.8	5.1	19.8

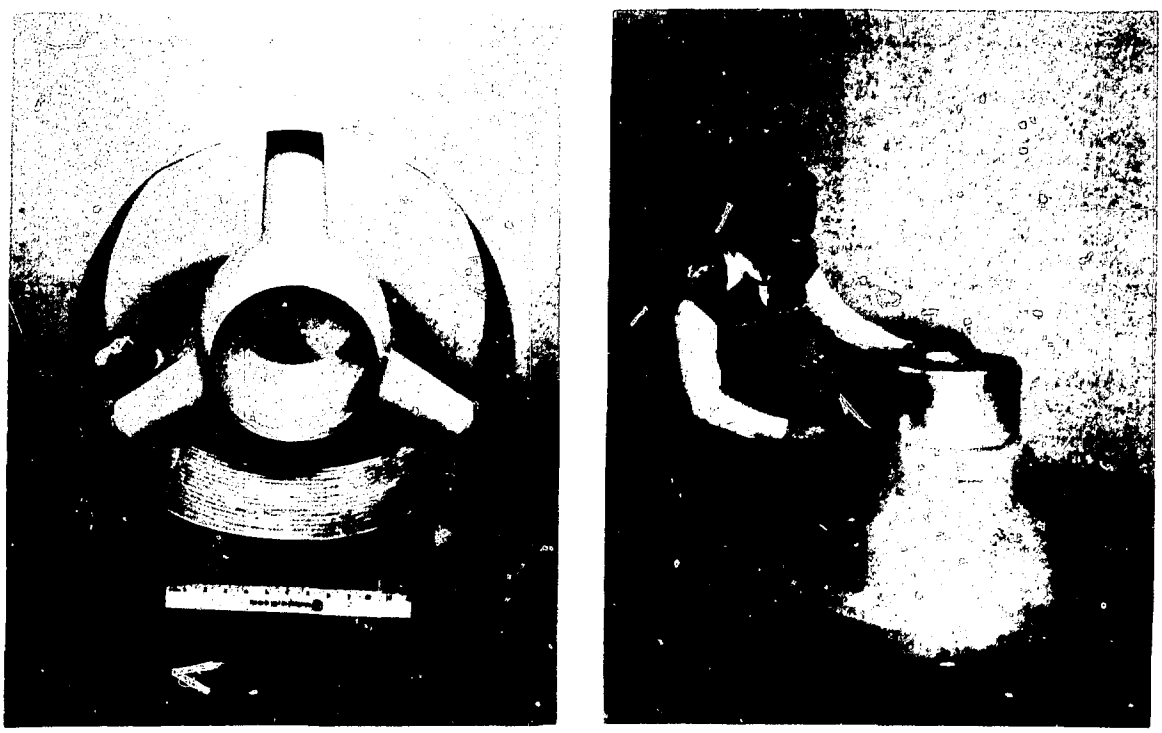

Fig. 2 Cast epoxy insulators for CGIT systems.
Left - 800 kV Tripost insulator with encircling particle trap system
Right -1200 kV conical insulator

sleeve which then fits over the conductor. The casting operation is performed under vacuum with highly controlled conditions during casting and curing in order to have a "void-free" insulator. Every insulator is then given an AC high voltage test to insure that it is discharge free to at least 1.5 times line-to-ground voltage. The design of the insulators is critical in order to limit the electric field along the insulator surface, and to have an acceptable field inside the epoxy. The epoxy material is also very important. Apart from the requirement of being able to operate under the continuous AC stress for the life of the CGIT line (typically 40 years), and having the required dielectric and mechanical properties, another specification is that the epoxy formulation be non-tracking. The reason is that during the high voltage field acceptance testing, "conditioning" sparks may sometimes occur for example due to contamination. It is essential that if an insulator flashes over under these conditions a conducting track is not formed so that the insulator is not degraded and the line can then be put in service after withstanding the specified test voltage.

Compressed SF_6 Insulation in CGIT Lines

The compressed gas serves two purposes: (i) To provide the basic high voltage insulation, (ii) To transfer the heat efficiently from the conductor to the sheath. The excellent thermal characteristics of compressed gases and particularly SF_6, are the reason for the high current carrying capability of CGIT lines compared with other cable systems employing solid dielectric material for high voltage insulation.

Present CGIT lines operate with the SF_6 gas typically at a pressure of 0.44 MPa (4.4 atm). Some earlier designs operated at lower pressures (0.2 MPa (2 atm)), but the higher pressure reduces the system size by enabling higher design fields.

For SF_6 insulated systems, the critical condition for the design is the lightning impulse level (BIL). This arises because high voltage breakdown investigations have shown that the impulse ratio (impulse to crest AC) for SF_6 is typically 1.3 to 1.4. From the high voltage test levels in Table 2 it can be seen that the ratio of BIL to crest AC design test is 1.48,

so that the lightning impulse value is the most critical case. Generally an accepted SF_6 maximum design level for lightning impulse is 17 MV/m which has been shown by extensive testing with the large diameter and long length of CGIT sections to be adequate. It should be noted that this level is substantially below the breakdown field that can be obtained with small, highly polished electrode configurations under controlled conditions of cleanliness in the laboratory. This demonstrates the difference in the design field that is necessary as a result of the finish and cleanliness typical of large practical systems fabricated in the factory and subsequently shipped and joined together in the field. This practical factor must be considered when new alternative gases are being evaluated.

These design field levels are for the simple, concentric conductor. In practice there will always be local areas where the field may be 15%-20% higher due to stress concentration, eg. at conductor joints and elbows. Special attention must be given here to the conductor finish and cleanliness. When the CGIT line is designed based on the BIL, the continuous AC conductor field during normal operation is usually less than 4.1 MV rms/m (Table 3). This continuous AC stress is more critical for the cast epoxy insulators than for the insulating gas. Extensive research is in progress to determine the maximum operating field for different formulations of cast epoxy as a function of the continuous operating field, operating temperature, and integrity of the epoxy insulator.[6]

All compressed gas insulated systems are susceptible to conducting contaminating particles.[7] These may be produced during manufacture, field installation or service. It has been shown that under the influence of the electric field, the particles become charged, then elevated and move between the conductors. The particles can then initiate breakdown either in the gas or along insulator surfaces. The resultant breakdown voltage can be as low as one-tenth the value for the particle-free system. This contamination problem is more severe with CGIT lines than, for example, SF_6 circuit breakers, as the fields in the line are typically double those in the breakers in order to reduce the CGIT size and cost. Techniques have therefore been developed to ensure a clean assembly in the factory and to prevent contamination being introduced during assembly or operation in the

field. In addition, a special device has been developed to dramatically reduce the potential problems due to contamination. This is the "particle trap"[8]. The basic philosophy is to design intentional areas at the sheath where the field is virtually zero. For the designs shown in Figure 2 there is a metallic ring encircling the insulators, with slots in the bottom portion of the ring. There is an electrical contact between this ring and the grounded aluminum sheath. Under the influence of the electric field any conducting particles are elevated and eventually move through these slots into the zero field region between the ring and the sheath. Once in this region there is no electric field to elevate the particles into the active insulating region, so that the particles are effectively mechanically and electrically trapped. This design of using the particle trap at every insulator is very effective as the insulator is particularly sensitive to surface contamination. During the high voltage AC acceptance test in the field, the particles are moved by the field into the traps.

Advantages of CGIT Systems

- CGIT systems have sufficiently high current ratings that one line can directly match that of an overhead transmission line. As a result the system has been used quite extensively, where, for example, it is required to join two substations together or as a dip beneath an overhead line [4] (Figure 3).
- The lines are a sealed and static system, requiring no maintenance or pumping stations.
- The capacitance of CGIT lines is relatively low (typically 49 pF/m) and this, together with the high current rating, results in a long critical length of hundreds of miles before reactive compensation is required.
- The gas-filled bushings required for the high voltage entrance are of a simple design (Figure 4) and relatively low cost compared with other solid dielectric bushings.
- The losses are low because the large aluminum conductor and sheath cross section area result in low resistive losses. In addition, the dielectric losses are negligible.

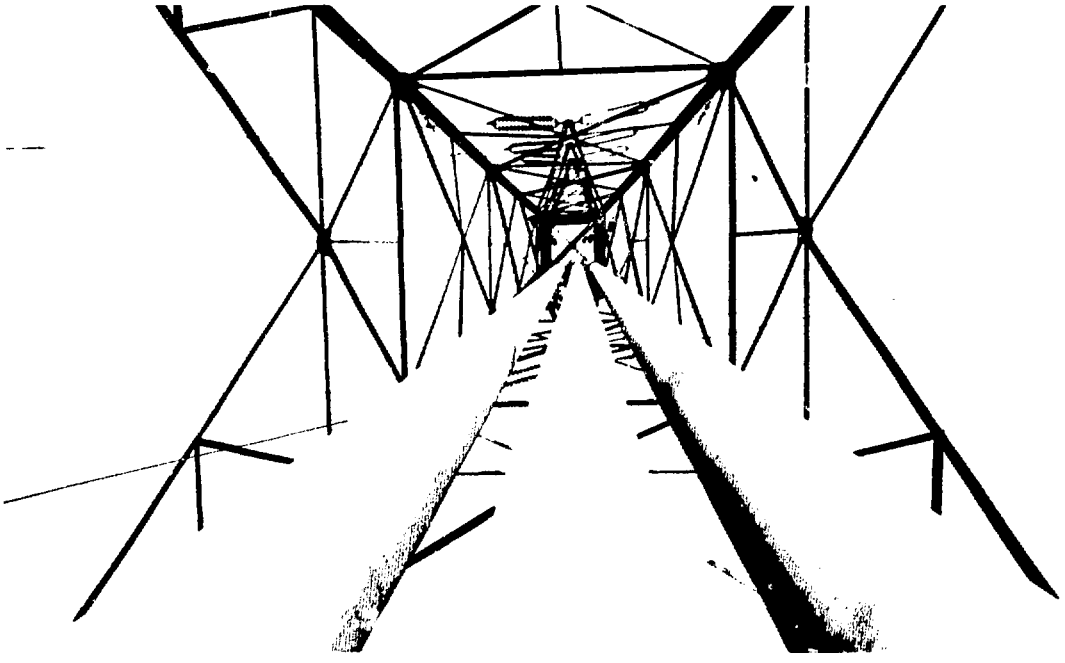

Fig. 3 Vertical 242 kV CGIT line inside transmission tower connecting overhead line to gas insulated substation.

The thick aluminum sheath is solidly grounded and of low resistance, so that voltage rises are acceptably low even under fault conditions.

These advantages have contributed to the rapid growth in the application of CGIT lines. To date the maximum length of a single line is of the order 600 m, but as confidence and experience is gained with these new systems it is expected that longer length transmission systems will be installed. Cost analysis has shown that for the higher voltages and high current rating (362 kV, 2000 amp) CGIT lines can then become competitive with other underground transmission systems for lengths of kilometers.[3]

Research and development are in progress to reduce the manufactured and installed costs of CGIT lines, by developing new, lower cost designs (Section 4), and by developing lower cost, better insulating gases.

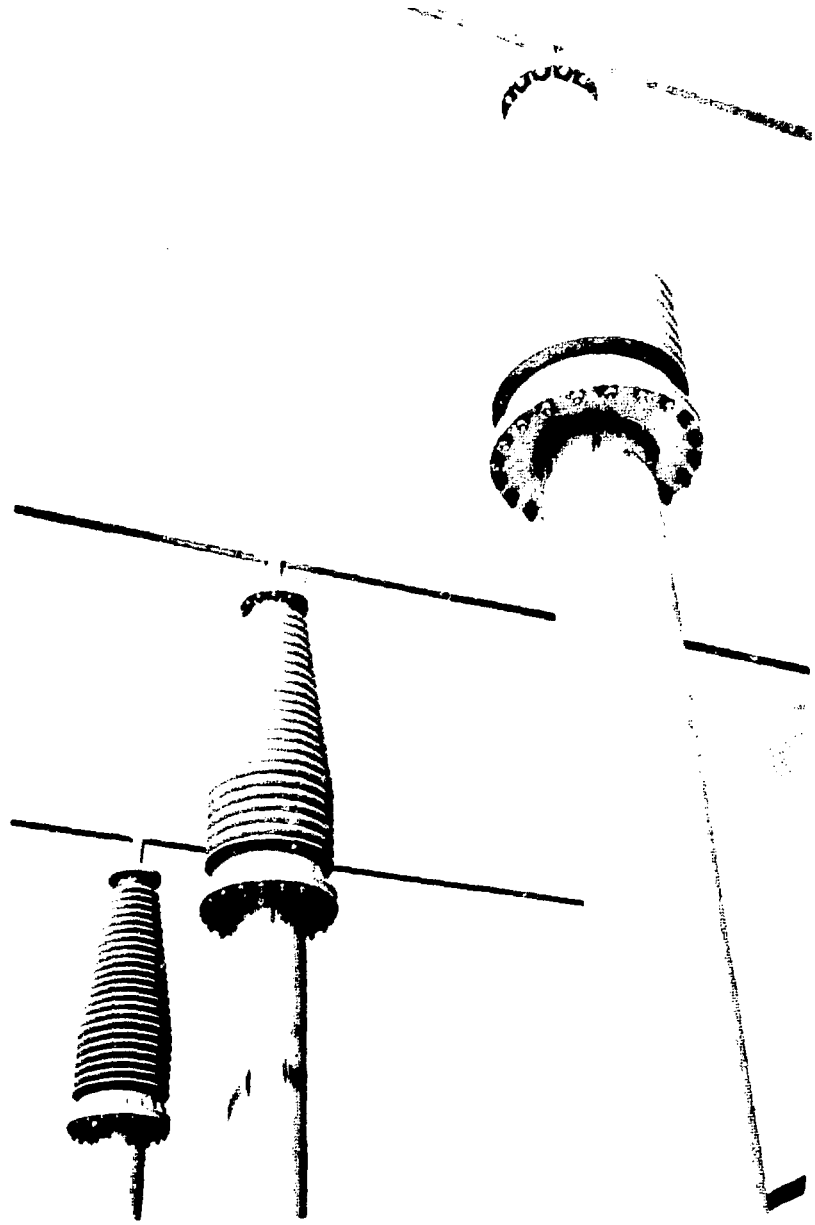

Fig. 4 Air-SF_6 bushings for 242 kV CGIT system.

EFFECT OF IMPROVED GASEOUS DIELECTRIC

Alternative Gases

There are several alternative approaches to developing a new gaseous dielectric as a replacement for the SF_6 presently used in CGIT systems. The new gas insulation system can be either: (i) Lower cost than SF_6 with

similar dielectric strength, and can be used as a direct replacement; (ii) Not necessarily cheaper than SF_6, but with a higher strength to enable a system to operate at a higher field and therefore effect a reduction in diameter and cost; (iii) Not necessarily lower in cost or able to use at a higher design field, but would, for example, be less susceptible to particle contamination or conductor surface roughness so that the system reliability could be improved. These alternatives are now discussed in more detail.

Effect of Reduced Gas Cost

The material cost breakdown of CGIT systems (excluding assembly) in Table 4 shows that the most costly single item is the aluminum sheath, which typically amounts to 40%. The percentage cost of the gas increases with the increase in the voltage rating and therefore size, such that at 800 kV it amounts to 21%. The conductor and insulators typically each account for 20% and 13%, respectively, of the material cost. Several of the new developments outlined in Section 4 are specifically being investigated with the intention of reducing the cost of the metallic sheath and so reduce the cost of manufacture. Table 4 demonstrates that the savings due to simply replacing the SF_6 gas with a lower cost gas (eg. 50% of the cost) and operating at the same fields, would probably be economically attractive for long length installations at the higher voltage ratings (362 kV and above). For the 800 kV system the cost of the SF_6 gas alone is now more than $142,000/km, giving an indication of the savings possible with lower cost alternatives.

Effect of Higher Design Field

A more significant effect is if a new gas permits higher design and operating fields. It is of interest to make a simple analysis of the present CGIT systems assuming it is possible to operate a CGIT line at the next voltage class; for example, operate a present 145 kV system at 242 kV. Table 5 shows the effect this would have on the MVA rating; the current rating is that for the same physical size system in Table 1, but the MVA rating is increased due to the higher voltage. The ratio of MVA rating for the "future" and "present" designs (MVA_f/MVA_p) is calculated. To give

Table 4. CGIT Material Cost Breakdown

Percentage Cost Analysis
No Assembly or Labor Included

Component	Max. System Voltage, kV				
	145	242	362	550	800
Sheath	39	45	44	44	44
Conductor	21	18	20	21	18
Insulators	16	13	13	10	8
Gas	9	10	13	16	21
Other Components	15	14	10	9	9

Table 5. Comparison of Ratings and Cost of Present and "Future" CGIT Systems Operating at Higher Field Level

Maximum System Voltage kV	Present System		"Future" System		MVA Ratio	Selling Price Ratio
	Sheath/ Conductor Diameter mm	MVA_p	Sheath/ Conductor Diameter mm	MVA_f	$\frac{MVA_f}{MVA_p}$	$\frac{\text{"Future" } \$_f}{\text{Present } \$_p}$
145	241/ 89	335	216/ 76	285	0.85	0.93
242	307/102	680	241/ 89	560	0.82	0.79
362	381/127	1200	307/102	1015	0.85	0.87
550	508/178	2050	381/127	1730	0.85	0.62
800	635/203	3650	508/178	3115	0.85	0.84

an indication of the effect this would have on the cost, the standard price list has been used to calculate the ratio of the "future" selling price (ie. with the smaller size system) to the present selling price, assuming no change in the designs.

It can be seen that the MVA rating of the "future" design is typically 15% less than the present, larger designs. The potential reduction in selling price is an average of 19%, with a maximum of 38%, depending on the voltage rating. This means that although the cost of the lower rated line is substantially lower, the cost of the CGIT line in $ per MVA rating is not greatly affected. However, for most applications the high current rating of present CGIT systems is not needed on a continuous basis, and therefore, for many applications the lower MVA rating will be quite adequate. For these installations the effect of an insulating gas with higher dielectric strength can have a significant effect on the cost of CGIT systems by enabling a reduction in the sheath diameter. This is economic even if the cost of the new gas system is double that of the SF_6 gas system.

The effect of reducing the sheath size is to increase the operating and test fields as shown in Table 3. The impulse field at the conductor for the "future" system would now be increased by 35% to typically 23 MV peak/m from 17 MV peak/m. More critical however, particularly for the insulators, will be the increase in the continuous AC field from typically a maximum of 4.1 MV rms/m to 5.1 MV rms/m. Recent research has shown that these field levels are probably acceptable with present epoxy insulators if suitable casting techniques are used.[6] The increase in the operating and test fields will probably also result in a greater degree of cleanliness being required than for present CGIT systems, and improved manufacturing, assembly and trapping techniques may need to be developed.

This simplified analysis has shown that if alternative gases are developed with better high voltage insulation characteristics than SF_6, then substantial reductions in the cost of CGIT systems may be possible by operating at a higher field and that the penalty of a lower current rating will usually be acceptable. The smaller diameter system gives a more compact installation which will also reduce the trenching and installation costs.

Improved Reliability

Flashover occurs in compressed gas insulated transmission systems either because of contamination, or because of surface imperfections on the conductor.

There has been extensive research on the effec of conducting contaminants initiating breakdown in SF_6 systems. This has shown that typically the maximum breakdown voltage with large contamination occurs at a pressure of 0.44 MPa and that the breakdown voltage can then fall drastically with increasing pressure.[7] Alternative gases may be developed which can substantially reduce the effect of the conducting particles. For example, previous work on mixtures of SF_6 and air has indicated that a 50-50 mixture (by volume) has a 30% higher breakdown voltage in the presence of wire-type aluminum contaminants at a pressure of 0.44 MPa than for SF_6 alone.[9] It is also relevant that a theoretical analysis of SF_6-nitrogen mixtures has indicated that the conductor surface finish may be less critical than for the SF_6 alone.[10]

By developing suitable gases with these characteristics it may be possible to reduce the susceptibility of the CGIT lines to minor conductor imperfections and contamination and thereby improve the system reliability.

Specifications for Improved Gaseous Dielectric

It is of interest to discuss some of the gaseous dielectric specifications and requirements that are required for an effective alternative gas to SF_6 in CGIT lines or other gas insulated equipment where no arc interruption is required.

Breakdown Strength

The gaseous dielectric should be able to operate at least under the conditions for which SF_6 insulated equipment is presently designed: ie, lightning impulse 17 MV peak/m, ac design test level 8 MV rms/m. To enable a CGIT line to be uprated to the next voltage level, the required design levels would be; lightning impulse 23 MV peak/m, AC test level 11.0 MV rms/m. These design levels apply to the full size, long length installations. The breakdown data obtained from small scale experiments should be investigated to

determine the effect of electrode area, "erratic" low breakdowns, scatter, practical finish on the conductor, and practical cleanliness conditions.[11] Investigations of the breakdown voltage-versus-time to breakdown characteristics are required to ensure that the required insulation coordination is obtained. The breakdown characteristics should be studied under deliberately contaminated conditions with AC, DC, lightning and switching impulse voltages to confirm that the new gas system is superior under these conditions.

Operating Conditions

Present CGIT lines have to operate under ambient temperature conditions of -30°C to +40°C. At the lower temperature it is important that the gaseous dielectric does not liquify. Under continuous operating conditions of maximum current loading the conductor temperature is typically not above 95°C, although some points may reach 105°C. Another factor is that under some conditions it may be necessary to do some minor welding repairs on the aluminum sheath when the line is filled with the gas. The temperature may then reach 180°C at localized areas for a period of a few minutes. No degradation or decomposition should occur under these conditions.

Although CGIT lines are designed to be corona free under operating conditions, corona may sometimes occur for brief periods, for example at conducting particles during the conditioning process. Degradation should not occur under these conditions.

Present CGIT systems typically operate at a pressure of 0.44 MPa. For most design systems this operating pressure could be doubled with only relatively minor design changes required in the system, primarily at the gas tight insulators, the air-SF_6 bushings, or connections to other SF_6-insulated equipment. The sheath has adequate mechanical strength for the higher operating pressure if it should be required. However, it should be pointed out that operating at a higher pressure must be evaluated to determine that the particle contamination problem does not become excessively severe, and that no liquifying occurs at the lower temperatures.

Physical and Chemical Properties

The gas should be non-flammable and should preferably be non-toxic or have only a very low level of toxicity. Tests should be made to insure that no highly toxic compounds are produced if a fault should occur.

The compatibility of the gas with the materials used in the CGIT line such as epoxy, aluminum, silver plating and gasketing should be verified for the conditions of operating temperatures and pressures, including the effect of the arced gas.

SF_6 is a very convenient gas to use as standard recovery carts are available for storing the gas in a liquid form. The utilization and recovery of alternative gases in the field must be considered.

Carbonization

An important factor in the evaluation of any gaseous alternative to SF_6 is the degree of carbonization in the gas that occurs with sparking or arcing. SF_6 is unique in that there is extensive recombination after an arc and no carbonization. There are two practical conditions to be considered where a flashover or a fault may occur in a CGIT line and this affects the carbonization specifications of the gas.

All CGIT lines have a high voltage field acceptance test to verify the integrity of the system. Presently the AC field test is the most commonly used and typical test levels are given in Table 2. Usually a transportable AC resonant transformer set is used. If a fault occurs with this system then only the energy stored in the line is dissipated and there is no power supplied by the test system. For example, with a 680 m length of a 362 kV system field tested to 375 kV with a resonant transformer set of 5 A capacity, the energy stored in the line will be of the order 2.5 kJ. It is essential that if a flashover occurs during the field acceptance test then no carbonization be produced in the gas or along the insulator.[12] This is so that the "spark conditioning" technique that is now used to condition a system up to the test voltage can continue to be utilized. If some carbonization were produced then although this might not necessarily cause flashover during the field acceptance test, at some later time in service

it might subsequently cause flashover and failure. Any testing of alternative gases should therefore include an evaluation of this carbonization.

The second and more severe fault condition can occur in service with a flashover and power arc, where a fault of 63 kA may exist for several cycles. It would be preferable if the alternative gas system were similar to SF_6 in that there may be severe arc damage but no carbonization. This arc damage to the CGIT components is usually rectified by cutting an access hole in the sheath and repairing and cleaning the system. If carbonization occurred with the alternative gas under this fault condition it would be a considerable disadvantage requiring a larger outage time, with more extensive cleaning and repair operations, and perhaps required replacement of the damaged section. However, if the new gas offered a substantial reduction in the size and cost of the system, then the CGIT line could be designed so that the carbonization would be confined to a short section (eg. 18m), and this section could be rapidly replaced with a spare section in the event of a fault.

FUTURE DEVELOPMENTS

There are several programs in progress for the development of new and lower cost CGIT systems. For all these systems an alternative superior gas to SF_6 could have the same significance as described above. However, operating conditions may be different and should be considered in the evaluation of the use of alternative gases.

Three Conductor CGIT System

In three conductor CGIT systems, the three conductors are mounted within the same aluminum sheath.[13] This results in a lower cost, more compact installation than for the three separate isolated phase lines. Figure 5 shows the prototype developed on an EPRI program of a 362 kV system with a buried current rating of 2000 amps. The three conductors are mounted on epoxy post insulators which are attached to the aluminum sheath. The sections are manufactured and shipped in 18 m lengths, and have the same plug-in conductor joint and sheath welded joint system as the isolated phase system. The insulating medium is SF_6 at 0.44 MPa and the design

fields are the same as the isolated phase system. This design allows a more compact installation than the isolated phase lines, has lower losses (10%-15%), and has an installed cost typically 15% lower.

Future developments are expected to further reduce the cost. A test installation on an Electric Utility system is planned to begin in 1978.

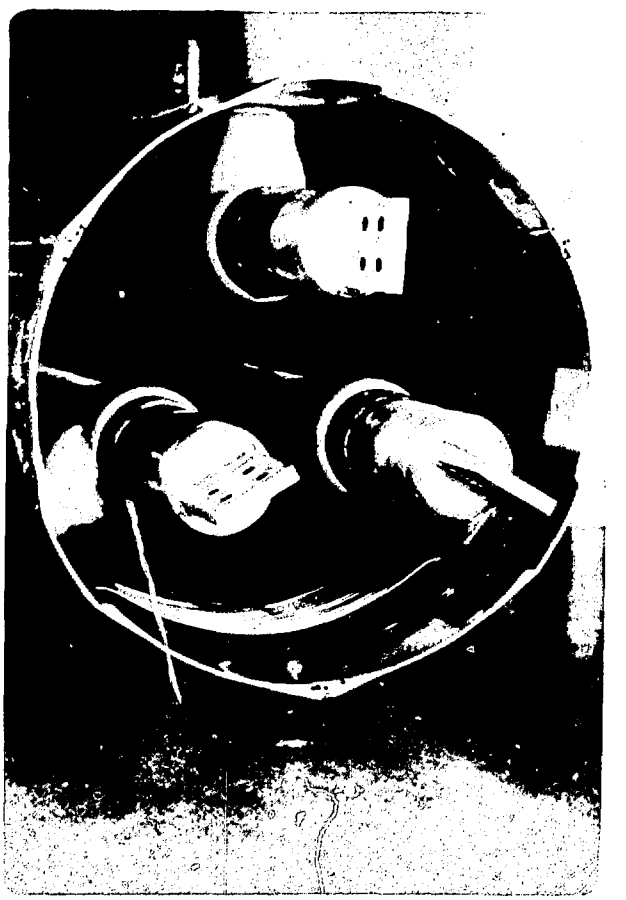

Fig. 5 Three conductor CGIT system. Above is short circuit prototype of 362 kV, 2000 A system. Bolted conductor connections were used for this test, but conductors usually have plug-in joints. Note particle trap between lower post insulators.

Flexible CGIT System

In order to reduce the cost of manufacture and installation, flexible CGIT lines are being developed. The design under development for EPRI[14] has a flexible corrugated conductor housing with a stranded, segmented con-

ductor inside (Figure 6). This is supported on low dielectric constant material insulators that are of a split design and snap around the conductor housing with an insulator separation of typically 0.6 m. The conductor system is manufactured and assembled inside a corrugated aluminum housing in a continuous operation on a special machine. The flexible CGIT line is planned to be wound on a drum of 4.3 m diameter. Long continuous lengths (eg. 92 m of 362 kV cable) can be shipped to the field, thereby reducing the field installation time and cost. The same design field as present systems is used.

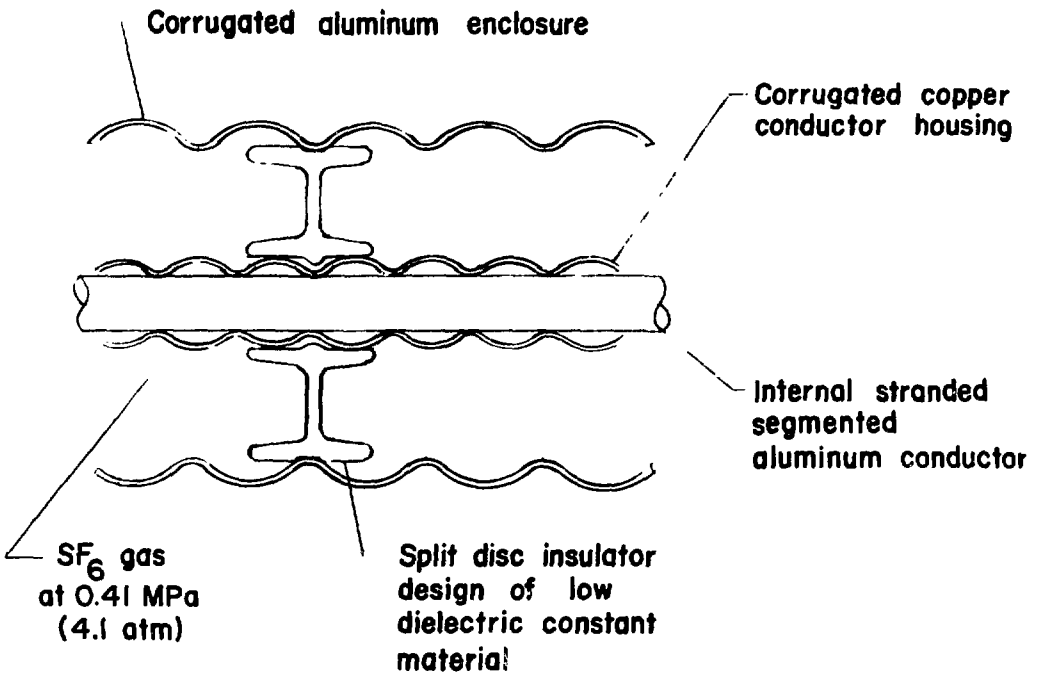

Fig. 6 Design of flexible gas cable under development for EPRI[14]. Typical insulator separation is 0.6 m.

The experimental flexible CGIT system under development in Europe[15] uses a dielectric-covered flexible conductor bundle which fits around the low dielectric constant material insulator (Figure 7). This unusual design very effectively shields the critical interface between the conductor and insulator. The conductor-insulator system is assembled in a flexible plastic pipe and is then either pulled into a corrugated housing or pulled into prelaid pipes. The sheath diameter for this design is half that of

present CGIT systems; i.e. the design fields are twice as high. An SF_6 gas mixture will probably be used at a pressure of the order 0.8 MPa (8 atm). The particle contamination problem may be severe at these high stresses.

An alternative "semi-flexible" CGIT system is about to be developed on a Department of Energy program specifically for the UHV levels where 18 m shipping lengths are rapidly joined in the field with a semi-automated joining and welding system.

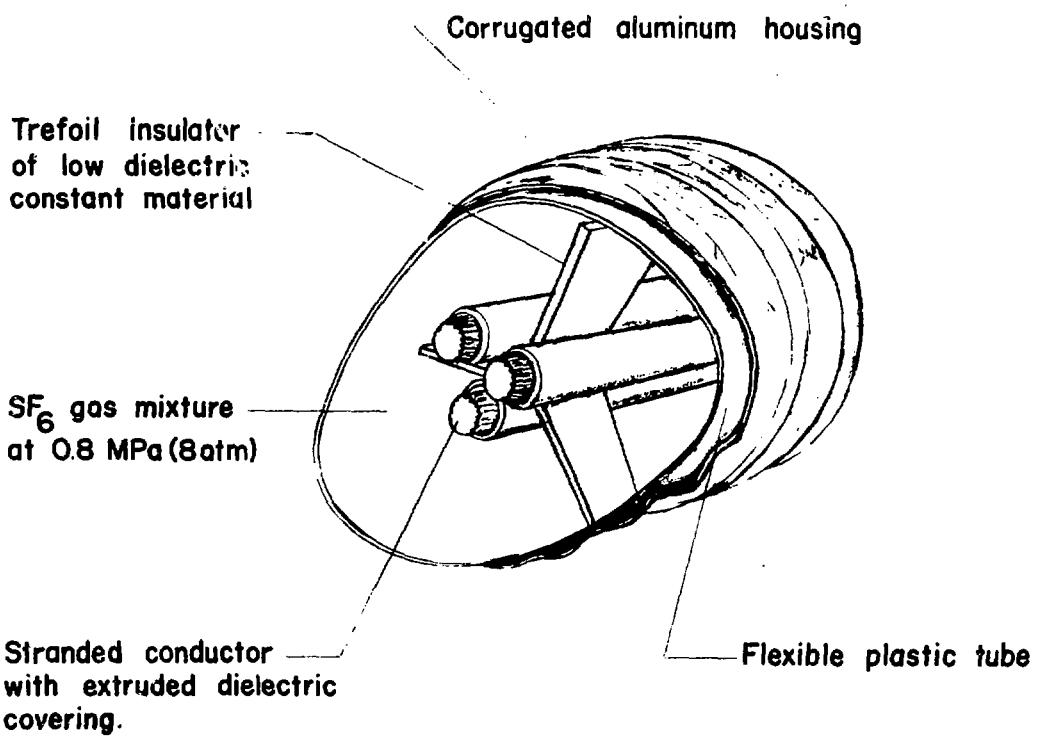

Fig. 7 Flexible design of gas cable where the conductor bundles (at same potential) fit around the insulator[15]. Typical insulator separation is 0.5 m.

High Temperature System

Another EPRI program is developing a CGIT line where the conductor operates at a temperature of 150°C. With this system the current rating is substantially increased compared with the normal case where the maximum conductor temperature hot spot temperature of 105°C is allowed. At these temperatures a special insulator material is necessary, and new developments are required for the conductor joints to operate at the higher temperature.

1200 kV System

The Department of Energy is funding a program for a 1200 kV CGIT system which is rated 5000 amps.[5] This system will be able to transmit 10,000 MVA. The design of this system is such that although the continuous lightning impulse field is the same as for lower voltage systems of 17 MV peak/m the continuous AC stress on the insulator is much higher at 4.8 MV rms/m. Special development work has therefore been necessary on the insulators. For this program an SF_6-air mixture will probably be used at 0.54 MPa (5.4 atm) instead of the SF_6 at 0.44 MPa. Figure 2 shows the conical insulator used in this program, giving an indication of the physical size system necessary for the lightning impulse design level of 2175 kV, AC one minute withstand test of 1200 kV rms, and the switching impulse level of 1800 kV crest.

DC Compressed Gas Insulated Transmission Lines

All present installed CGIT lines are AC systems. There are potential applications for DC CGIT systems on account of the very high rating that can be obtained with relatively small increase in cost. For example, if the 362 kV AC system (Table 1) were operated at $\pm$ 300 kV DC under the same burial conditions with the conductor solid instead of hollow, then two DC cables would have a power handling capability of the order 2520 MVA compared with 1200 MVA for the three AC cables.

There are several critical areas where development is required for a DC CGIT system. The voltage distribution across the insulators is controlled by the insulator resistance, compared with the capacitance controlled distribution for the AC case, and this will be more susceptible to surface impurities. A major problem is likely to be that the particle contamination problem is more severe as particles are more active under DC than AC[7]. Efficient, low cost particle trapping techniques taking into account the unique characteristics of DC systems might therefore need to be investigated. There is also the concern on a DC design level in the gas for long term operation. Alternative gases to SF_6 showing less susceptibility to contamination would be advantageous for DC gas cables.

CONCLUSIONS

Compressed gas insulated transmission lines are beginning to play an important part in transmission systems as high power, high voltage transmission links. Present CGIT lines have shown rapid development in the seven years since their introduction. It is expected that there will be similar progress in the next few years which will be brought about by extensive research and development programs for manufacturing new systems at a lower cost such as with the three conductor and flexible CGIT lines.

New and superior gases to SF_6 can have a big impact on CGIT lines, either by reducing the cost of the gas, or more importantly by allowing the CGIT lines to operate at higher fields, thereby enabling substantial reductions in size and cost of the equipment and installation.

REFERENCES

1. H. M. Hobart, J. Franklin Inst. 234, 251 and 331 (1942).

2. B. O. Pedersen, H. C. Doepken, Jr., and P. C. Bolin, IEEE Trans. Power Apparatus and Systems PAS 90, 2631 (1971).

3. EPRI Report 7825, ERDA Report E (49-18)-1615, Guide to the Use of Gas Cable Systems, and Optimized Design for Gas Cable Systems, Prepared by ITE-Imperial Corp. (1975).

4. R. F. Swoish, H. Gold, F. Jenkins, C. Demond and H. P. LeBlanc, Paper 23-08, CIGRE, Paris (1976).

5. A. H. Cookson, T. F. Garrity and R. W. Samm, Paper 21-09, CIGRE, Paris (1978).

6. T. W. Dakin and S. A. Studniarz, Voltage Endurance of Epoxy Resins with Microcavity Type Defects, Conf. Electrical Insul. and Dielect. Phenomena, Montreal, Canada (1976).

7. A. H. Cookson, P. C. Bolin, H. C. Doepken, Jr., R. E. Wootton, C. M. Cooke and J. G. Trump, Paper 15-09, CIGRE, Paris (1976).

8. J. G. Trump, Dust Precipitator, U.S. Patent 3,515,939 (1970).

9. A. H. Cookson and R. E. Wootton, Internat. Symposium High Voltage Tech., Zurich, 416 (1975).

10. O. Farish, O. E. Ibrahim and B. H. Crichton, Proc. IEE 123, 1047 (1976).

11. A. H. Cookson, Proc. IEE 117, 269 (1970).

12. R. E. Wootton, F. T. Emery and A. H. Cookson, Proc. of 13th Electrical/ Electronics Insulation Conference, 351 (1977).

13. EPRI Report 7816, ERDA Report E (49-18)-1560, Design and Test of Three Conductor Gas Insulated Cable, Prepared by High Voltage Power Corp. (1975).

14. R. W. Samm, EPRI Journal 1, 9, 14 (1976).

15. B. F. Hampton, D. N. Browning and R. M. Mayes, Proc. IEE 123, 159 (1976).

DISCUSSION

PACE: Over the forty-year lifetime, is there a possibility of saturating the particle traps? Do you see an area effect in testing enclosed lines? We should not automatically fear carbon-containing compounds concerning carbonization. Work at Du Pont (see Pace on page 256) and by Sauers at Oak Ridge National Laboratory indicates that solid breakdown products of fluorocarbons may not be pure carbon, and they may have high resistivity. However, this problem remains to be dealt with carefully in applications.

COOKSON: It is believed that the contamination likely to be most troublesome in gas-insulated systems is large particles left during manufacture or installation. These are deactivated by moving them into the traps during the high voltage field test and perhaps during the initial period the equipment is in service. Very few particles will be produced in service as, unlike a circuit breaker for example, there are very few moving parts. The only major movement is the plug-in conductor joint which also accommodates the conductor expansion. A special low wear contact has therefore been developed, and the design prevents any contamination that may be produced from entering the high stressed region in the line. The production of extensive insulating or even partially conducting particles with low energy sparks (e.g., during field test flashover conditions) should be treated with some caution. There is the possibility of very fine conducting particles or powder, usually not degrading, becoming deposited on the insulating particles and then effectively behaving like large conducting particles.

SIOMOS: You mentioned very often in your presentation that the basic research has to be of help to the problem under study. For example, better gases than SF_6 have to be found. Sometimes, however, these gases might not fulfill all your technological standards, but they might be superior in terms of dielectric strength and costs. Is the industry prepared to make some compromises in terms of its technological standards so that a cooperation between basic research and industry will be more successful?

COOKSON: If a superior gas is developed, then some modifications or compromises are possible, for example, if different insulator materials or shapes are required or if other materials need to be changed for compatibility purposes. Some low levels of toxicity may also be permissible if the technological or economic advantages are sufficient. Concerning the operating temperature, there is probably less room for compromise because of the environmental conditions. Lowering the maximum permissible hot-spot temperature on the conductor from the present 105°C could result in a substantial reduction in the current rating for some CGIT systems, particularly for above ground installations. This could have the effect of requiring a larger, more expensive system to meet the current rating. Possible relaxation of the lower temperature limit is discussed in response to another question. Although some compromises on the standards are possible from industry, they are very limited as these reflect possible conditions the equipment may actually experience in service, quite independent of the insulating system inside the equipment. These practical conditions should therefore always be

considered in developing gaseous insulating systems for application in transmission or distribution equipment.

de TOURREIL: Traps are effective to deal with particles on horizontal sections. Do particles present a problem on vertical sections of CGIT? If so, how are spacer surfaces protected from particle contaminants?

COOKSON: In vertical lines the open construction of the Tripost insulator is preferred, with a particle trap inserted at the bottom of the line to trap the particles that have fallen through. If gas-tight or semi-stop insulators are required, then conical insulators are used with the cone pointing upwards so that any particles will fall into the low field areas at the edge of the cone.

FARISH: I was very interested in your observation of a reduced switching impulse strength for SF_6/N_2 mixtures in relatively small coaxial-electrode systems. This is perhaps unexpected since one might expect that any impulse corona would have a greater inhibiting effect in the mixture than in pure SF_6. Do you have any explanation for this behavior?

COOKSON: At present, I cannot give a theoretical explanation of why the switching surge flashover is much lower in N_2/SF_6 mixtures than for SF_6/air or SF_6/CO_2 with the coaxial geometry we tested. It may be associated with the growth of the streamer across the gap and the development of the space charge being the optimum for this mixture, perhaps in a manner similar to that for long gap switching impulse breakdown in air.

VINCENT: What about efficiency of particle traps situated just below epoxy spacers? Is it possible that particles stick to the spacer instead of going into the trap when bouncing towards the low-field region?

COOKSON: The traps are situated at the spacer because the spacers are susceptible to contamination. By increasing the AC test voltage very slowly the particle motion can be controlled so that the particles move into the traps without being deposited on the dielectric surface.

NAKATA: Ms. Claire Vincent's concern regarding the location of particle traps directly under the support insulators of your gas bus is equally shared by me. In dealing with HVDC gas bus, we found, as will be shown in the film later, that particles which are trapped under shallow traps by the random scattering of particles are seemingly only conditionally trapped. By conditional trapping, I mean that the particle movement towards the inner recesses of the trap stops once the particle gets under the lip of such a trap since the field intensity suddenly drops off. Such trapped particles have been found to be relevitable out of the traps at moderate DC stresses. Since an AC gas bus can suddenly become a DC gas bus if a capacitive switching duty is performed, and any particle relevitated out of a trap under the insulator (to instantly cross the gas gap by DC stresses) could very likely electrostatically adhere to the insulator, might this not constitute a hazard as mentioned by Ms. Vincent? As a difference in philosophy, the HVDC gas bus which we designed for the EPRI HVDC installation is designed to <u>direct</u> the particles positively away from the proximity of insulators (rather than by random bouncing and

spreading) into deep particle traps from which we have never been able to relevitate out the particles.

COOKSON: As the insulators are susceptible to contamination, we design traps to protect the insulator in CGIT lines. The traps are designed to trap and deactivate the particles during AC testing and once trapped can withstand the DC voltages that may be experienced by AC systems. CGIT lines may be installed on systems where there is a pronounced slope depending on, for example, the contour of the land. Under these conditions it may not be possible to always install a system so that the particles always move away from the insulators. For these several and variable conditions the trap at the insulator will effectively remove the particles before they reach the dielectric.

SAMM: Why -30°C criteria? Is industry willing to compromise for underground installations below the frost line or for above ground installations in warmer climates?

COOKSON: Present U. S. standards are for -30°C but some utilities with less severe winters do specify -20°C. This low temperature limit is to ensure that no liquefying occurs with the equipment when it is disconnected from service. It may indeed be possible to relax this lower limit for a deeply buried line, but the system will need to be studied to ensure, for example, that the line is not being filled with gas before the soil covering is placed in position at low ambient temperatures. Also, the interface where the buried line comes above ground should be considered in evaluating the use of higher levels of the minimum ambient temperature.

INSULATION COORDINATION OF GAS-INSULATED SUBSTATIONS

Roland Eriksson
Swedish State Power Board, Stockholm
Sweden

Håkan Holmborn
ASEA AB, Ludvika, Sweden

ABSTRACT

Gas-insulated substations (GIS) are exposed to the same overvoltages as conventional stations. Since a flashover in a GIS may seriously affect the equipment the whole GIS must be protected against overvoltages. In this report the shapes of overvoltages which may occur are briefly discussed as well as factors influencing these overvoltages.

Critical characteristics of the surge wave, its propagation in the GIS and the influence of the size of the GIS are explained. The influence of the characteristics and location of different types of surge arresters on the maximum overvoltages is discussed, especially considering steep surges.

Recommendations on suitable insulation levels BIL are given under the assumption that reasonable measures are taken in order to limit the overvoltages. GIS with the recommended BIL turns out to be less expensive than conventional substations at higher voltages. Price relations are indicated.

1. INTRODUCTION

Gas-insulated substations (GIS) are exposed to the same overvoltages as conventional substations. However, the character of the GIS insulation and the consequenses of a failure lead to the necessity of a close analysis of the stresses imposed on the insulation under various conditions as well as an economic choice of means of protection against excessive stresses[1].

For a conventional substation it is normally deemed sufficient if the transformers, being the most valuable equipment and difficult to replace, are well protected against excessive overvoltage stresses. Even if a part of GIS normally can be exchanged comparatively quickly and on site, a failure would lead to a great disturbance in the operation of the system. Good overvoltage protection is thus needed for all gas-insulated parts of the substations. This leads to the need to pro-

tect also the distance from line entrances to an open circuit-breaker, which in turn demands an installation of lightning arresters at the line entrance when overhead lines are connected.

The real nature of the overvoltage phenomena in the GIS is probabilistic[2]. The main influencing parameters are

- Stroke location
- Stroke characteristics (e.g. current and steepness)
- Earthing conditions and line configuration at stroke location
- Operating conditions of GIS (number of connected lines, open switching devices)

By using the probability to obtain high stresses (stress function) and the probability of insulation withstand (strength function), the resulting probability of failure can be estimated.

2. TYPE OF OVERVOLTAGE STRESSES IMPOSED ON THE GIS

A suitable classification of the overvoltages into three groups is made by IEC 71[3].

1. Temporary overvoltages
2. Switching overvoltages
3. Lightning overvoltages

2.1 Temporary overvoltages

The temporary overvoltages have their main importance in that they determine the choice of reseal voltage for the arrester and thus, due to design reasons, the protective level.

The most important temporary overvoltages are those occurring due to earth faults and load rejection. Sometimes there can be a risk for

so-called resonance overvoltages caused by non-linearities, but such overvoltages should be avoided by suitable system design.

The temporary overvoltages during fault conditions are normally up to 1.6 p.u. on the line side of the circuit-breaker if the connected lines are comparatively long. On the bus side of the circuit-breaker the overvoltages are lower, 1.2-1.4 p.u. These figures are valid for earthed neutral EHV systems while in isolated neutral systems the overvoltages are about $\sqrt{3}$ p.u.

Figures 1 and 2 give a calculation example showing temporary overvoltages as a function of disconnected load and short-circuit power.

Due to the rather flat insulation withstand dependence of the GIS as a function of the fronttime of overvoltage, the withstand of the GIS against temporary overvoltages is satisfactory as the insulation must be designed for the much higher lightning impulse.

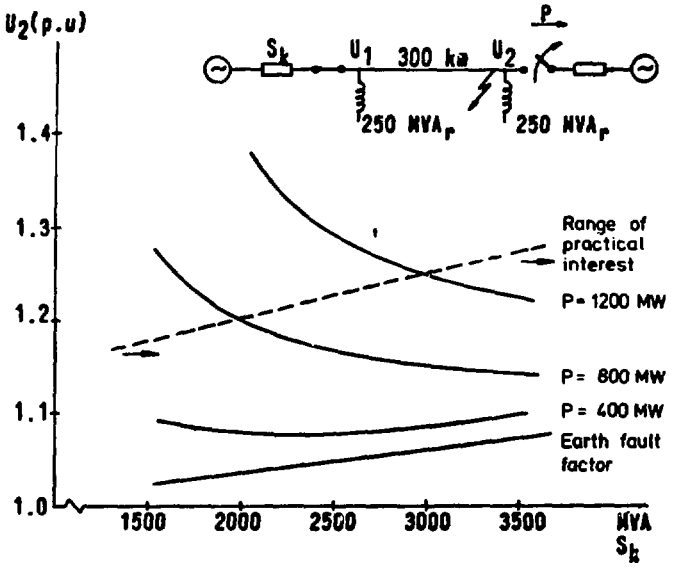

Fig. 1. Temporary overvoltages in receiving end for single phase faults combined with load rejection. 800 kV system. Early stage of system development.

Before fault: U_2 = 0.95 p.u.

S_k: Fault level in sending end (X_o/X_+ = 1.0)

P: Disconnected load (MW); cos φ = 1.0.

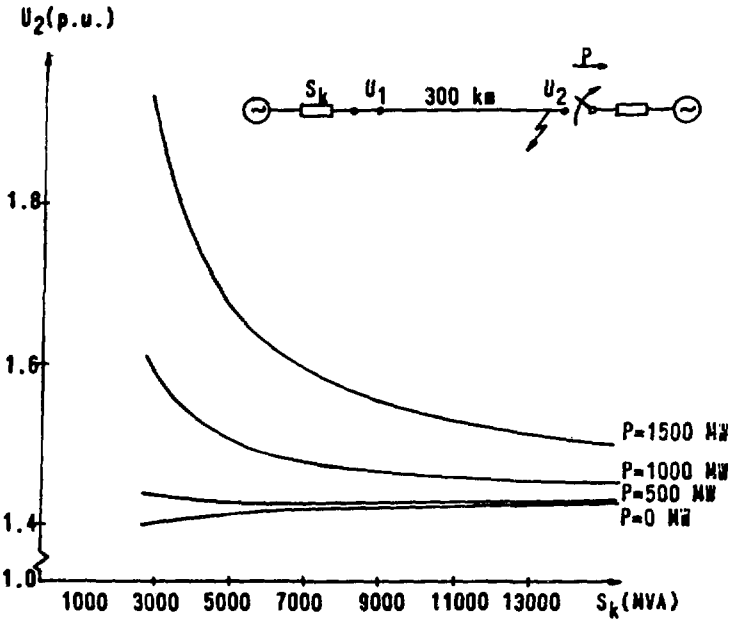

Fig. 2. Temporary overvoltages in receiving end for single phase faults combined with load rejection. 420 kV system.

Before fault: $U_1 = U_2 = 0.95$ p.u.

S_k: Fault level in sending end ($X_o/X_+ = 1.0$)

P: Disconnected load (MW).

2.2 Switching overvoltages

There are a lot of publications on switching overvoltages, their magnitudes, waveshapes and means of reduction and it is not possible here to go into details. Generally one can see three groups.

	"Maximum" overvoltage amplitudes p.u.
No special means of overvoltage reduction used	2.5 - 3.5
Some special steps for overvoltage control (closing resistors, shunt reactors)	2.0 - 2.5
Extreme reduction of overvoltage magnitude (multistep closing resistors, synchronous closing etc)	1.5 - 2.0

Many systems have a reliable operation without any special means for overvoltage reduction.

IEC 517[4] and IEEE [9] gives switching impulse withstand levels (SIWL) range 2.28 - 3.47 p.u. and it is necessary to protect the GIS against switching overvoltages excessive to those values. Normally this protection is obtained if the substation is well protected against lightning overvoltages. The maximum overvoltages within the GIS greatly depend on reflection phenomena. Since the steepness of the switching overvoltages are very low, there will be no overvoltages above the arrester sparkover voltage and thus a lower ratio between SIWL and protective level can be chosen. Further details about overvoltage propagation in the GIS is given in section 3.

2.3 Lightning overvoltages

Lightning overvoltages arise when a stroke hits the shielding wire or the phase wires. A stroke to the shielding wire or the tower will if the stroke current is sufficiently high cause flashover to a phase wire (backflashover) thereby generating an overvoltage on the phase wire. A stroke directly to the phase wire (shielding failure) will cause an overvoltage in any case, even if no flashover to the tower occurs. The magnitude and shape of the waves generated will depend greatly on the grounding conditions at the stroke location and the stroke characteristics.

Normally results reported in literature show mean values of stroke current amplitude and steepness of about 30 kA and 40 kA/µs respectively. Corresponding 10 % values could be about 70 kA and 70 kA/µs respectively. The structures comprising towers and overhead lines have, at least during the first µs after a stroke has hit the line, a waveimpedance of about 100 Ω. It is therefore understood that the steepness of generated surges can be up to 7000 kV/µs at the stroke origin. The amplitude of outgoing waves can be assumed to be about the insulation level of the line. If higher amplitudes are obtained at the stroke loca-

tion due to high stroke current or earth impedance, successive flashovers at adjacent towers will reduce the peak to a value close to the LIWL of the line.

When the wave travels along the line, the steepness will be reduced due to corona damping. A well known assumption is that the front-time will increase by 1 μs for each travelled km.

For insulation design of GIS substations it is also necessary to consider multiple strokes. After circuit-breaker opening due to the first stroke it will be stressed by a travelling wave generated by the second discharge. Since the wave will then meet an open line end the reflection conditions are changed and higher overvoltages may occur. This open breaker case is always considered at insulation coordination studies.

The reported[5,6] percentage of flashes consisting of more than one stroke varies in the range 20-50 %. As a mean the interval between the strokes is 30-60 ms.

It must also be noted in the GIS case that the insulation withstand is normally somewhat lower for negative than for positive polarity, while the air gaps normally have a higher withstand for the negative polarity. A "natural" coordination of line insulation and GIS insulation is therefore not obtained.

3. PROPAGATION OF LIGHTNING OVERVOLTAGES

3.1 Principal propagation

The wave impedance of an overhead line is considerably greater than that of a GIS and thus reflection phenomena will occur at the entrance of the GIS. At an open gap (disconnector, circuit-breaker) the surge will be totally reflected meaning a doubling of amplitude.

The way the voltage is built up is illustrated in Fig. 3.

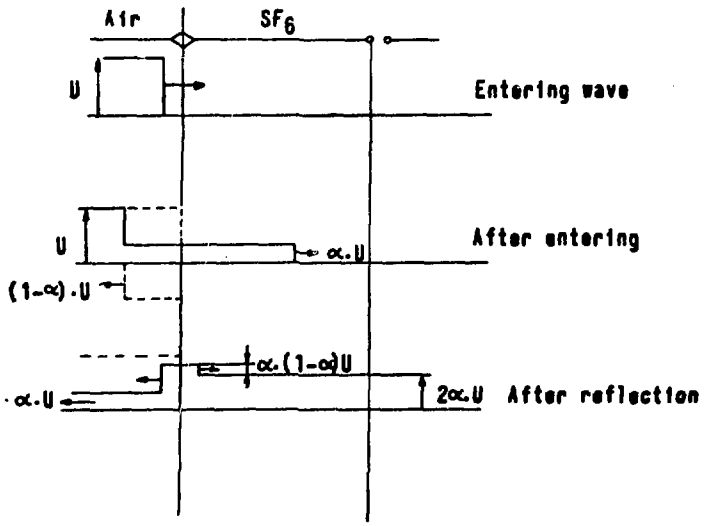

Fig. 3. Principal voltage build up.

After entering, one part, α, is transmitted into the substation and one part, (1-α), reflected back along the line. The entered wave is reflected at the open end and when reaching the GIS entrance reflected again. The growth of the overvoltage will follow the equation

$$\frac{U}{U_o} = 2 - (2-\alpha)(1-\alpha)^n \qquad (1)$$

where n is the number of reflections. For $n \to \infty$ $U/U_o = 2$.

3.2 The voltage build up for finite steepness of incoming wave

Compared to above where infinite steepness of incoming surges was studied, the voltage increase and reflection is not at all as severe for steepness where the front is longer than twice the wave travelling time in the substation, which is the usual case.

The theoretical voltage increase is shown in Fig. 4, where a constant rate of rise is assumed. Neglecting damping the voltage is expressed by the formulae (2), (3) and (4).

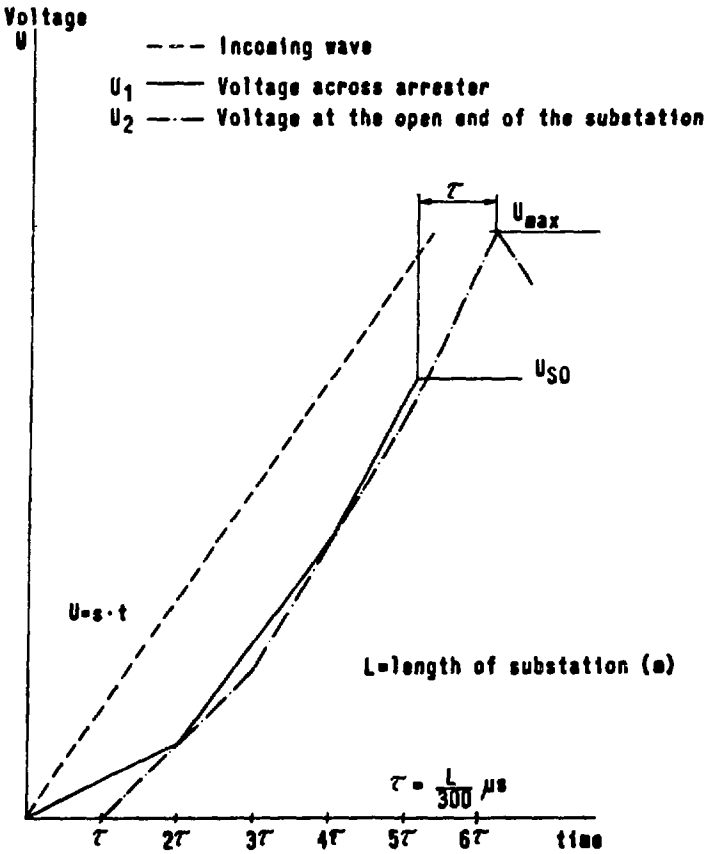

Fig. 4. Voltage build up for finite steepness.

s = steepness of wave on the overhead line

τ = wave travelling time in a GIS

L = length of GIS from entrance to open circuit in metres

$$\tau = \frac{L}{300} \ \mu s$$

n = number of reflections

Before the first reflection the voltage at the entrance is

$$U = s \cdot \alpha \cdot t \qquad (2)$$

Voltage at time t at the entrance after n reflections:

$$2(n-1) < \frac{t}{\tau} < 2n$$

$$U = s \cdot \alpha \left[t + \Sigma_{m=2}^{n} (1-\alpha)^{m-2}(2-\alpha)[t-(m-1)\tau] \right] \qquad (3)$$

Voltage at open end at time t:

$$2(n-1) < \frac{t}{\tau} < (2n+1)$$

$$U = s \cdot \Sigma_{m=1}^{n} 2(1-\alpha)^{m-1} \left[t-(2m-1)\ \tau\right] \qquad (4)$$

The voltage increase is dependent upon three parameters, steepness (s), ratio of wave impedances (α) and length of substation (L,τ).

As can be seen from Fig. 4 the voltage increase is constant between every reflection inside the GIS but is magnified for every reflection. After a number of reflections the steepness inside the GIS is therefore greater than that of the incoming surge.

The above expressions give an understanding of the wave propagation and voltage build up. Normally all calculations are made by computer[7].

4. OVERVOLTAGE LIMITATIONS BY ARRESTERS

The equations related above are valid before the instant of arrester sparkover only.

When the voltage has reached such a value that the arrester sparks over, it will take another travel time τ between arrester and the open bus end until the negative wave from the arrester arrives to the open end and the voltage is reduced. Therefore a higher steepness results in a higher overshot in voltage. Also for a longer SF_6 bus and thus a longer travel time the overshot is greater.

Figure 5 illustrates the overvoltage versus sparkover voltage of the GIS for different bus lengths when an enclosed arrester is located at the entrance.

The influence of surge steepness on arrester characteristics will affect the protection. Generally one can say that for short bus lengths

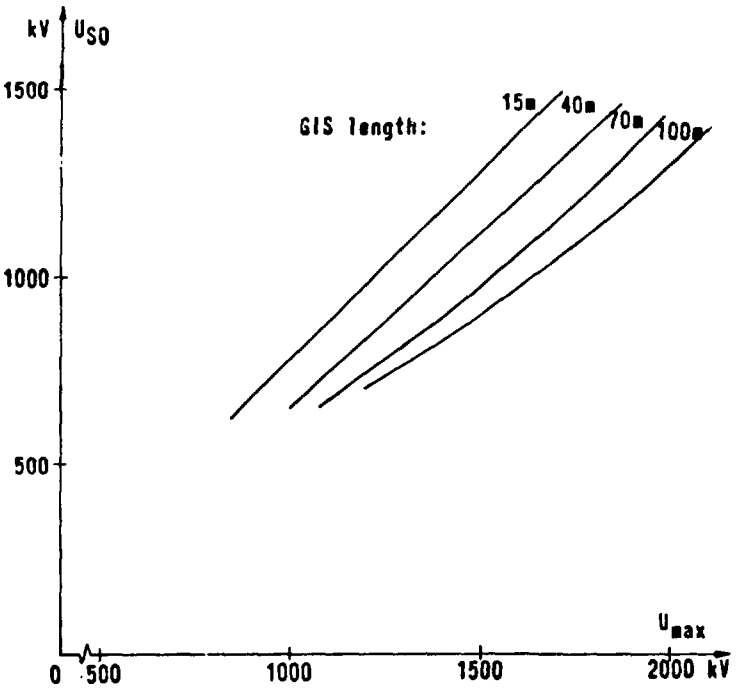

Fig. 5. Maximum overvoltage versus arrester sparkover voltage. Enclosed arrester at line entrance. 2000 kV/μs incoming wave.

the voltage increase is more rapid, resulting in higher sparkover voltage of the arrester, but on the other hand the voltage overshot is less. For longer buses the voltage increase is slower and the sparkover voltage is lower leading to a greater acceptable overshot. This will be discussed in detail in section 5.

5. INFLUENCE FROM STEEPNESS OF INCOMING SURGE TO VARIOUS GAS-INSULATED EQUIPMENT

5.1 Electric strength of SF_6 at short voltage duration

It is well-known that the electric strength of air of atmospheric pressure increases considerably when the voltage duration decreases. The increase starts for duration times shorter than about 100-1000 μs.

In SF_6-insulation a corresponding increase in electric strength occurs but the increase is less and starts at lower duration time, usually below 10 μs. The increase in breakdown voltage for steep waves - front time < 1 μs - is partly depending on the formative time lag which means that the breakdown initiation voltage at a steep front of wave can be exceeded before the breakdown will be observed. The formative time lag is very short, < 0.1 μs. The duration of the stress shall, however, be counted from the instant when the critical voltage is exceeded point C in Fig. 6 and the time lag will be sufficient to cause an increase of the observed breakdown voltage for fronts of waves shorter than about 1 μs. Another reason for the voltage withstand increase is statistical and is often referred to as statistical time lag. The physical back-ground for this time lag is the lack of primary electrons in critical locations. In an exactly uniform electrode gap with polished surfaces this time lag is very short, but in practical electrode systems the field is nonuniform with local field enhancements resulting in a long statistical time lag (1-100 μs).

Surface roughness, defects and particles will give field enhancements in a very small gas volume outside the defect. This is taken into account by designing the SF_6-equipment for a voltage gradient at LIWL of about half the theoretical breakdown value. The probability of existence of primary electrons in the small volumes with local field enhancement during the front time of a surge is rather low, resulting in a long statistical time lag which can cause an increase of the 100 % breakdown short duration voltage, up towards about twice the LIWL.

Also the macro field outside normally used electrode shapes is non-uniform and the overstressed volume outside the surface where primary electrons have to appear is depending on the voltage. The statistical time lag and consequently the statistical increase in breakdown voltage for steep fronts will thus depend on the size of the test object and of the field uniformity.

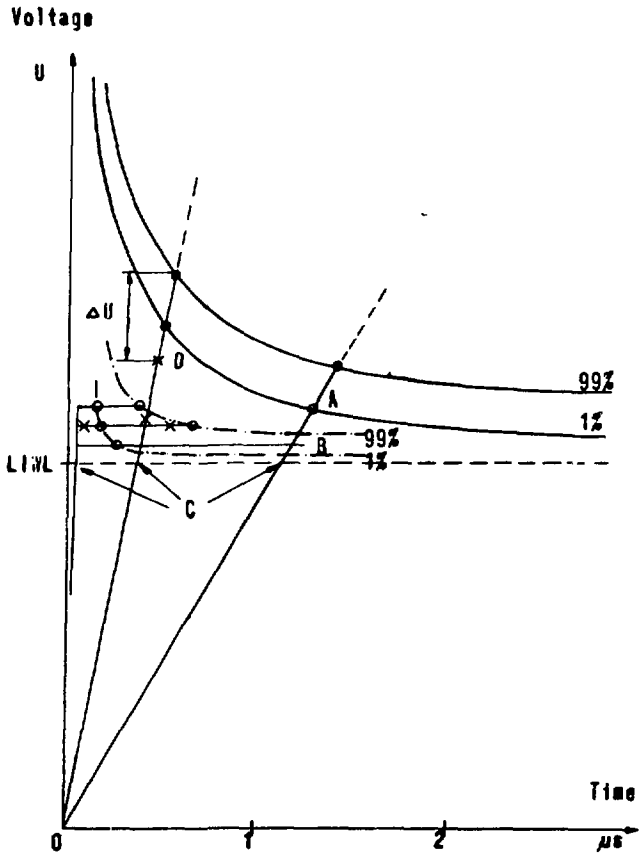

Fig. 6. Voltage time characteristics

A: v-t curve, front breakdown
B: v-t curve, step voltage impulse
C: Minimum breakdown initiation voltage
D: Example of breakdown initiation voltage
ΔU: Voltage increase due to formative time lag

Reported voltage-time (v-t) curves have been obtained with different test methods. Figure 6 shows some curves taken up with steep fronts giving all breakdowns on the front (A) and with a step voltage impulse (B).

The v-t curves with breakdowns on the front are most used for steep fronts and show a high voltage increase with decreased time due to the very short stress time at the highest voltage. This type of v-t curve can be used as a basis for insulation coordination with respect to steep fronts with high peak level and short duration. However, when coordinating the sparkover voltage of a surge arrester with the voltage

withstand of the GIS, the breakdown voltage according to the v-t curve must be reduced by a value, ΔU in Fig. 6, corresponding to the voltage rise during the formative time lag. The initiation of the breakdown has in fact started at a voltage below the v-t curve, e.g. at point D in Fig. 6.

The front breakdown type of v-t curve (A) is, however, not valid for coordination with respect to surges having a lower peak level causing a breakdown near the peak or on the back of the surge. In this case a lower breakdown voltage will be experienced and v-t curves (B) recorded during step voltage tests are more relevant.

5.2 Surge arrester characteristics for steep surges

The arrester sparkover voltage for steep surges is of great interest for the insulation coordination of GIS since the increase of the GIS voltage withstand level is limited for steep surges. Due to the flat SF_6 v-t characteristic it is necessary to have a low surge arrester sparkover voltage also for front times $\lesssim$ 1 μs.

Figure 7 shows a surge arrester specially designed for use in SF_6. The active gap stack is surrounded by grading rings interconnected with capacitors to establish a correct voltage distribution along the arrester. This arrester is housed in an SF_6 filled vessel.

With such enclosed arresters it is possible to choose a lower sparkover voltage due to the careful voltage grading and the steady ambient conditions of the arrester, especially the absence of pollution. Thus, the sparkover voltage of enclosed arresters can be reduced by approximately 10 % in relation to that of conventional arresters without changing the other characteristics.

Figure 8 shows the increase of the front of wave sparkover voltage for times to sparkover less than 1 μs. The curve is based on tests on both conventional and metal-enclosed arresters of different ratings,

Fig. 7. Surge arrester for enclosed application.

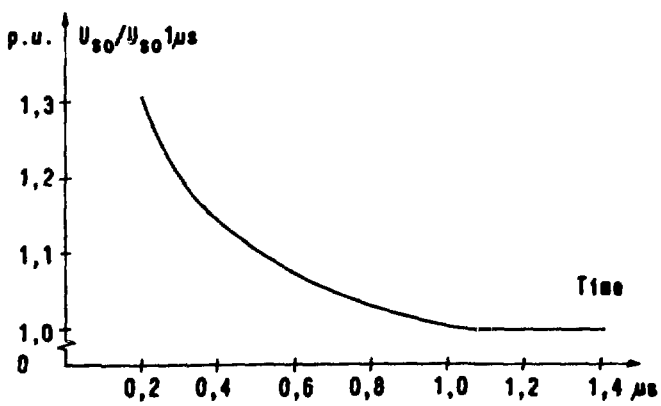

Fig. 8. Relative arrester sparkover voltage versus time to sparkover.

including one conventional and one metal-enclosed arrester rated 600 kV. Tests have been performed in accordance with IEC and ANSI Standards. The steepness has, however, been varied up to 2500 kV/μs, which is higher than prescribed in these standards.

The sparkover voltage in Fig. 8 has been assumed to be a function of the time to sparkover only. The shape of the applied voltage wave is judged to be of minor importance and thus the average steepness (determined by the 10 % - 90 % values) can be used to determine the sparkover increase at high steepnesses. The time to sparkover can be transformed into steepness of the applied voltage.

In Figure 9 the average rate-of-rise of the voltage across an arrester at the line entrance has been plotted versus the distance from entrance to an open gap in the GIS. With longer bus length the steepness across the arrester will decrease. Comparing with Fig. 8 it can be deduced that there is no significant increase in sparkover voltage of the arrester for bus lengths greater than 40 m even if the incoming wave has 2000 kV/μs steepness.

Taking into consideration the length of the GIS as well as the sparkover voltage increase for steep surges relations between maximum overvoltage and LIWL as seen in Figure 10 can be obtained.

6. SELECTION OF INSULATION LEVEL

6.1 Choice of arrester

The first important decision to make is the selection of surge arrester rated voltage (reseal voltage). Due to temporary overvoltages related in 2.1 a choice of reseal voltage equal to the temporary overvoltage results in reseal voltages 1.3 - 1.6 times normal phase to ground voltage. Being on the conservative side and covering most of the systems 145-420 kV, at least for Swedish conditions, a choice of rated

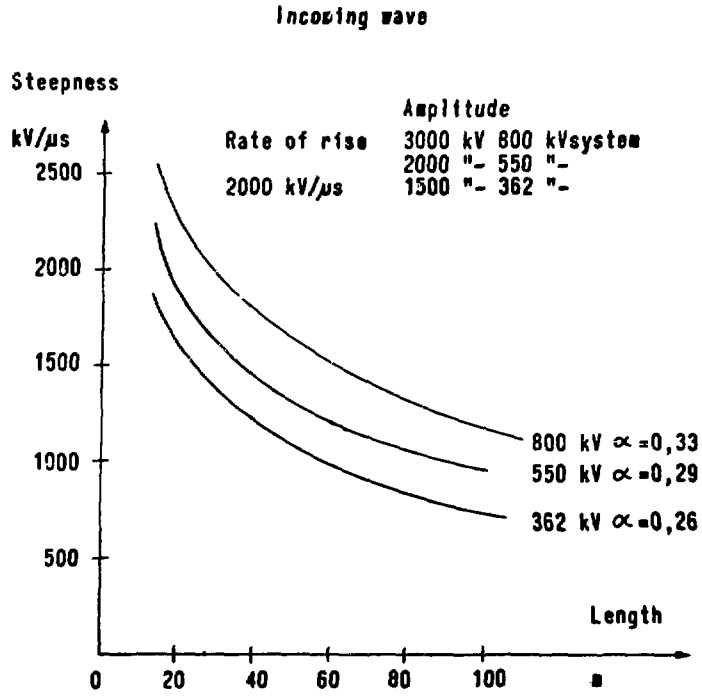

Fig. 9. Rate-of-rise of voltage at line entrance for 2000 kV/µs incoming wave.

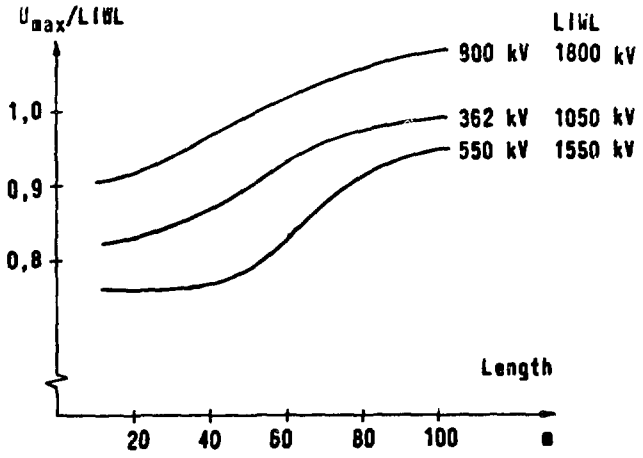

Fig. 10. Maximum overvoltage versus bus length with an enclosed arrester at line entrance. 2000 kV/µs incoming wave.

voltage 1.6 p.u. should be possible. For the 800 kV system value 1.3 could be chosen[8].

It is supposed that for higher system voltages the temporary overvoltages will be lower and thus a lower reseal voltage can be chosen.

Referred to the rated voltage (U_r) the following arrester characteristics can be easily obtained:

- Front of wave sparkover voltage $2.3 \times U_r$
- 1.2/50 μs sparkover voltage $2.1 \times U_r$
- Residual voltage at 10 kA $1.9 \times U_r$

6.2 Determination of overvoltage stresses. Choice of arrester locations

The overvoltage stresses on the GIS must be calculated for different rates-of-rise of incoming waves to determine the critical rate-of-rise (if any) above which the overvoltage exceeds the insulation level.

Arresters must be installed at the line entrance to ensure the protection during open breaker (or disconnector) conditions. Additional arresters may also be required close to the transformers or on the bus due to a long path to the line entrance. For these locations the calculation of overvoltages should be performed for different operating conditions. Normally a few operating conditions can be found more onerous compared to others. After considering the probability of these events, the calculations can be limited to analysing these critical cases (e.g. the open circuit-breaker case or one transformer and no additional lines connected to the bus).

When considering arrester locations there will also be a choice between enclosed and conventional arresters. The technical advantages of enclosed arresters are:

- the liberty to locate the arrester in the best place of the GIS from protection point of view

- there are no connection leads to ground and to conductors and thus no delay to the operation of the arrester occurs
- the enclosed arrester operates under steady ambient conditions compared to conventional arresters for which sparkover level could be disturbed by pollution.

6.3 Determination of probability of excessive overvoltage stresses, critical zones

Normally for each substation the calculations under 6.2 lead to the statement that protection is obtained for overvoltages with rate-of-rise up to a certain critical value.

A critical steepness of around 2000 kV/μs seems reasonable. Assuming this a critical zone between the GIS and a point on the connected overhead line can be determined assuming the front prolongation 1 μs/km. These zones have been estimated for Swedish conditions, see table below.

Table 1. Estimated critical zones

System voltage kV	Amplitude of incoming wave kV	Critical zones km	Probability of surges with origin within the critical zone % per year
800	3000	1.5	0.1
420	1500	0.75	0.2
245	1000	0.5	0.3

The figures refer to the cases where shielding wires are used. For 420 kV continuous shielding wires are used in the Swedish network, while for lower voltages a length leading up to the substation is shielded.

Assuming a substation having 5 incoming lines and the probability of the open breaker being 0.1 in case of a lightning stroke, the resulting failure probability of a substation for lightning will be of the

order 1/1000 per year, which is less than 1/100 of short-circuit failure rate of a conventional substation. A correct estimate of the failure probability requires a detailed knowledge of the overvoltage distribution stressing the SF_6 insulation and the insulation characteristics. Such a precise calculation could be very intricate to perform and it seems that the above procedure is quite sufficient.

Assuming this semi-probabilistic approach the ratio between insulation level and overvoltage peak should be assumed equal to 1.0. In this approach it is not recommended to take into account any significant increase of the withstand voltage for steep surges (curve B in section 5.1).

6.4 Insulation levels

Due to the great benefits of standardization the number of alternative insulation levels must be kept low. Recommended insulation levels by IEC[4] and IEEE[9] are given in the tables below.

Table 2. Insulation levels recommended by IEC

Rated voltage kV	Rated lightning impulse withstand voltage kV	Rated switching impulse withstand voltage kV
362	1175	950
420	1300	1050
525	1425	1175
765 (800)	1800	1425

Table 3. Insulation levels recommended by IEEE

Rated voltage kV	Rated lightning impulse withstand voltage kV	Rated switching impulse withstand voltage kV
362	900/1050	720/825
550	1300/1550	650/1240
800	1800	1425

Considering normal bus lengths the insulation levels in the tables can be well protected, compare figures 5 and 10.

7. ECONOMICAL ASPECTS ON INSULATION LEVEL

At an economical study the GIS can be divided into a number of parts which have their own cost influence due to the insulation level. The parts are

- GIS enclosure
- GIS apparatus
- surge arrester arrangements

The GIS enclosure which is a heavy part from economical point of view will increase its cost with LIWL. With given values of current, power frequency voltage etc. the GIS apparatus, apart from the enclosure, will vary its costs very little with LIWL. The surge arrester arrangements will be more costly at lower LIWL. The lower LIWL can lead to the introduction of enclosed arresters at different locations.

The total cost of the substation should be studied in order to select the best insulation level from both economical and technical point of view. Fig. 11 shows the cost variation versus LIWL for 245 kV, 550 kV and 800 kV. The cost variations would be still more pronounced if also the power transformer costs were considered. The cost relations are given under the assumption of free choice of enclosure dimensions. As seen in the figure standardized withstand levels for the 245 kV and

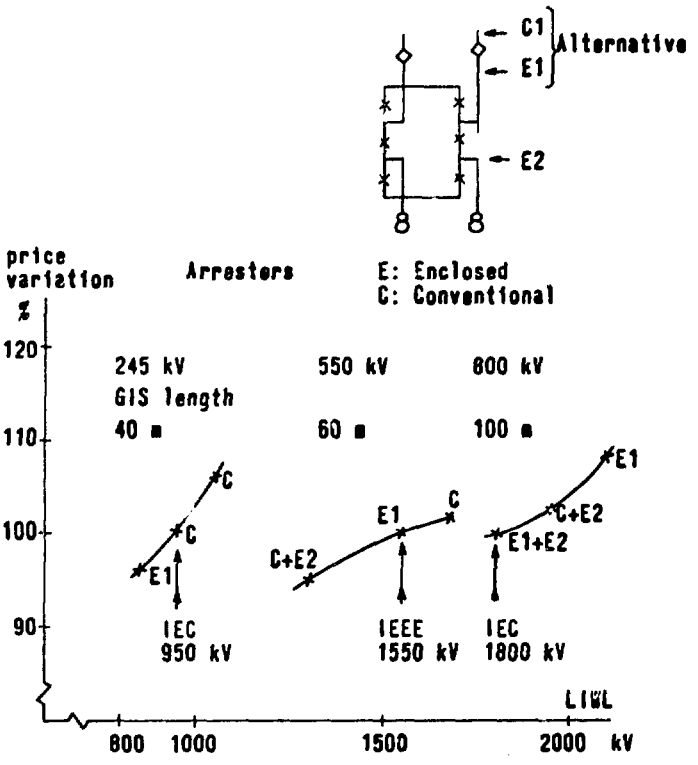

Fig. 11. Total GIS cost versus insulation level.

800 kV systems seems economically justified. For 550 kV a reduction of the higher level, 1550 kV, could be discussed.

8. CONCLUSIONS

Lightning overvoltages will have the greatest influence on insulation design of a GIS and they must be reduced by means of arresters. Arrester data and location as well as specific insulation costs must be analysed to get the most economical solution for each GIS layout.

A semi-probabilistic approach is suitable for insulation coordination of GIS. A critical steepness of 2000 kV/μs is considered to give an acceptable low probability of excessive overvoltage stresses.

The increased withstand of the GIS for impulses with short duration is not recommended to be taken into account when selecting insulation levels and protection schemes.

For very steep fronts the arrester sparkover voltage increases. At critical steepness of incoming wave this need only to be considered for short bus lengths. However, this fact will not in general influence the choice of insulation level for the complete substation.

REFERENCES

1. B Wahlström, H Holmborn, A Schei, Overvoltage protection of metal-enclosed SF_6-substations. Insulation coordination philosophy and surge arrester characteristics, Cigré 1976, Report 33-03.

2. J D Tranen, A probabilistic method for lightning protection of EHV SF_6 substations, IEEE paper A 77 729-7 presented at IEEE Summer Meeting 1977.

3. IEC Publication 71, Insulation co-ordination, (Part 1: Terms, definitions, principles and rules, Sixth edition, 1976. Part 2: Application guide, Second edition 1977).

4. IEC Publication 517, High-voltage metal-enclosed switchgear for rated voltage of 72.5 kV and above, first edition, 1975.

5. E Ruoss, H-J Vorwerk, Shutz offenstehender Leistungsschalter vor Blitzüberspannungen, BBM, pp 424-433, vol. 56, 1969.

6. K Berger, Novel Observations on lightning Discharges; Results of Research on Mont San Salvatore, Journal of the Franklin Institute, vol. 283, 6 (1967).

7. B Thorén, L Carlsson, A digital computer program for the calculation of switching and lightning surges on power systems, IEEE Transactions on Power Apparatus and Systems, pp 212-218, vol. 89, 2 (1970).

8. G Jancke, W Carlshem, R Engström, T Johansson, S Smedsfelt, The Swedish 800 kV system, Cigré 1974, Report 31-11.

9. IEEE P 468-1/D2, Gas Insulated Substations. Standards, recommended Practices and Guides, Prepared by working group 70.1 of the Substations Committee of IEEE, 1977.

DISCUSSION

TAKUMA: In your calculations 300 m/μsec (that is, the light velocity) is used as the surge velocity. According to measurements in Japan, the surge velocity is reported to be 10 to 20 % smaller than the light velocity. Would you comment on this point? Are there any measurements of the surge velocity on gas-insulated lines in your country?

ERIKSSON: We have set the traveling speed to that of light due to theoretical considerations. No detailed measurements of the surge velocity have been made. For overhead transmission lines a zero and positive sequence propagation can be noticed, the former with lower velocity than that of light leading to increased time to crest value. One could raise the question whether an influence of ground also exists for the gas-insulated bus.

SLETTEN: The GIS breakdown characteristics were discussed both for ramp and step voltages. Is the arrestor characteristic given in the paper obtained by ramp or step voltages?

ERIKSSON: The sparkover voltage has been assumed to be a function of time to sparkover only. The curve is a "mean curve" based upon tests on several different arrestors and with different rated voltages. The tests have been performed in accordance with IEC and ANSI standards.

MASHIKIAN: In your insulation coordination studies, you considered the effect of lightning surges. You mentioned that in the future gapless arrestors may help lower the level of surges seen by CGIT equipment. This,

in turn, may allow smaller size equipment to be designed. If this is done, however, the long-time effect of power frequency voltage, as well as the short-time power frequency voltage performance may become critical factors in the CGIT insulation coordination. The long-time effects include performance of the solid spacers. Have you considered any trade-off between designs based on lightning surge and those based on power frequency voltage performance?

ERIKSSON: A reduction of impulse strength must be taken with care. If the ratio between required impulse strength and normal power frequency voltage decreases, the normal operating conditions increase in importance as regards insulation consideration. The influence of particles and other contamination will them be more pronounced and necessary to further analyze. Today's tests required by standards can of course not give a complete guarantee at the substation behavior under normal operating conditions. Maybe then further test methods would be required.

04444

STATISTICAL APPROACH TO THE BREAKDOWN CHARACTERISTICS OF LARGE SCALE GAS INSULATED SYSTEMS

T. Nitta Y. Shibuya
Y. Arahata H. Kuwahara
Mitsubishi Electric Corp.,Amagasaki, Japan

338-354

ABSTRACT

Dielectric strength of compressed SF_6 gas insulation decreases with the scale of the system. The scale effect has been shown to be brought in by the statistical property of the weak points of breakdown such as protrusions on electrode and foreign particles in the system. Problems in evaluating the breakdown characteristics of a large scale system from the data of laboratory experiments are analyzed based on the Weibull statistics of those weak points of breakdown.

The Weibull Statistical analysis is applied on a long coaxial cylinder bus with spacers and some other gas insulated systems.

INTRODUCTION

The breakdown of a gas insulated system is subject to the irregularity factors such as the microscopic protrusions on electrode and foreign particles left in the system. Extensive efforts are being devoted to eliminate those irregularities. Particle trap to scavenge foreign particles, dust-free clean room for assembly shop and finer finishing of highly stressed metal surface are some of the efforts along this line. Still, it is not economical to produce large gas insulated systems to be free from the influence of some of those irregularities.

The irregularities have probabilistic property by nature and work as the "weak points" of electrical breakdown. The weakest point statistically existing in a system determines the breakdown of the system.

The disagreement between the breakdown data of laboratory experiments and the breakdown characteristics of a large scale system has been shown to be attributed to the statistical nature of the irregularities[1]. The appearance probability of a weak point having a certain influence on breakdown is higher in larger systems. When the breakdown is governed by the weakest point in the system, the statistical distribution of the breakdown can be shown mathematically to obey the extreme value distribution[2]. In the case of the electrical breakdown in compressed gas, it obeys Weibull distribution which is one special form of the extreme value distribution. If we know the probability distribution of the weak points from laboratory experiments, the insulation performance of large scale gas insulated systems can be evaluated theoretically,by the Weibull statistical analysis[3]. The problems and the limitations of the analysis are discussed in the first part of the present paper.

The Weibull statistical analysis is applied on a coaxial SF_6 gas insulated bus with spacers. In considering the breakdown characteristic of a gas system with complicated construction, the simplest approach will be to figure out the gap mostly stressed in the system and to check the breakdown characteristic of the gap. The approach is not correct for large scale system. The fact is clearly shown in the example chosen.

SCALE EFFECT IN THE BREAKDOWN CHARACTERISTIC OF GAS INSULATED SYSTEM

Breakdown voltage of a gap in compressed SF_6 is known to be strongly dependent on the maximum field strength of the gap. In most gas insulated systems in which sharp edges are eliminated, the breakdown of the system is determined by the maximum field strength E_{max} in the system[4]. We will discuss the breakdown characteristic of a given system by E_{max} at breakdown in the following discussions.

Uniformly Stressed Electrode System

Scale effect in the breakdown of gas insulation is most simply

understood when we apply the analysis on a system whose electrode surface is stressed uniformly at constant field strength throughout the system.

One simplest example is a long coaxial line without any spacers. The surface of the inner cylinder is stressed at E_{max} through its length. We neglect the effect of the outer cylinder, assuming that it is stressed fairly low in comparison with the inner cylinder.

Suppose we discuss the breakdown characteristic of a uniformly stressed system by the experimental data obtained on one n'th section of the whole system. The cumulative probability of E_{max} of the test section will be expressed by Weibull distribution as in Eq. (1)[3].

$$P_o(E) = 1 - \exp\left\{ - k \left(\frac{E - E_o}{E_d} \right)^m \right\} \qquad (1)$$

where, k, m and E_o are constants determined by the property of the irregularities in the system in question. E_d is the theoretical breakdown voltage of the system without the effect of the irregularities. The value of E_d is approximately given by Eq. (2)[4].

$$E_d \simeq 89\, p \ [\ kV/cm\ ] \qquad (2)$$

where, p is the gas pressure in atm (ab). The constants in Eq. (1) can be obtained by fitting experimental data on Weibull distribution paper as the thick solid line in Fig. 1.

The original system can be looked upon as the parallel connection of n test sections. The breakdown in one of the sections means the breakdown of the system. In this case, the breakdown probability is given as;

$$P(E) = 1 - \exp\left\{ - n\, k \left(\frac{E - E_o}{E_d} \right)^m \right\} \qquad (3)$$

The relation between $P_o(E)$ and $P(E)$ is shown in Fig. 1 for a few values of n.

We can clearly see that the breakdown voltage at a given probability decreases with the value of n. The analysis is mathematically correct but there are some difficulties in the practical application. We will discuss these later.

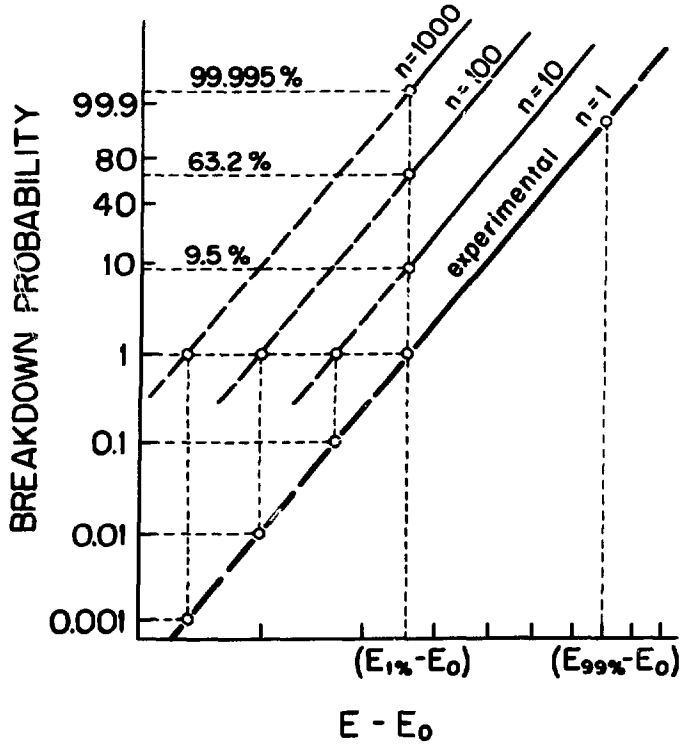

Fig. 1. Weibull Distributions of Breakdown Field Strength of Electrode Systems with Various Areas.

Nonuniformly Stressed Electrode System

In practical gas insulated systems, the surface of electrodes is stressed differently from part to part. This does not mean that the most highly stressed part determines the breakdown characteristic of the system. If the part is localized and besides that there exists a large electrode area stressed slightly lower than that, the breakdown of the system will be determined by the latter. It has been shown that the breakdown characteristic of the system of this kind can be discussed by the concept of "effective electrode area"[5].

In the effective electrode area analysis, the area stressed at E is converted to the "effective area" stressed at E_{max}. This can be done mathematically, provided the statistical property of the irregularities which governs the breakdown is same. The details of the conversion was given in the reference (5).

The effective electrode area S_{eff} is given by Eq. (4).

$$S_{eff} = -\int_{E_o}^{E_{max}} \left(\frac{E - E_o}{E_{max} - E_o} \right)^m \cdot \frac{dS(E)}{dE} \cdot dE \qquad (4)$$

E_o and m are the Weibull parameters in Eq. (1). S(E) represents the area of electrode where the field strength exceeds E. $S(E_{max})$ is null. The negative sign in Eq. (4) is attached, since S(E) is the decreasing function of E by nature.

By this calculation, we can convert a nonuniformly stressed electrode to the electrode area of S_{eff} stressed uniformly at E_{max}. Then, we can apply the Weibull statistical analysis just in the same way as in the previous section using the Weibull parameters obtained on uniformly stressed test electrode. Examples of the effective electrode area analysis will be given later on typical 500 kV gas insulated systems.

PROBLEMS IN THE WEIBULL STATISTICAL ANALYSIS

Determination of Weibull Parameters

The Weibull statistical analysis of the breakdown characteristic has a few problems to be kept in mind on its application. The first problem is the validity of the Weibull distribution itself. When we evaluate the characteristic of a coaxial line by the experimental data on one n'th section, we postulate the linear relation of the distribution in Fig. 1 throughout the range of $E - E_o$ on abscissa. Suppose we take the case of n = 100 and consider the breakdown probability down to 1%. This imposes the linear relation on the test section to be valid down to 0.01%. It is unrealistic to verify the relation experimentally to this low probability.

We remind that the Weibull distribution is an approximate expression proved experimentally. The true but unknown distribution is looked upon as Weibull type as far as $E - E_o$ on abscissa is within a certain range. By this reason, the scale of the test section should not be too small in comparison with the actual system.

The second problem is in the determination of the value of E_o. As

in Fig. 1, we plot the cumulative breakdown probability as a function of $E - E_0$. The value of E_0 is chosen so that the curve is straight on Weibull distribution paper. If all the experimental values of E are larger than E_0 by far —— this happens when the area of the test electrode is too small, the linearity of the distribution is not sensitive to the value of E_0. In this case, we have difficulty to choose one particular value of E_0. If we increase the area of the test section, the linearity of the Weibull distribution becomes more and more sensitive to the value of E_0. The area of the test section has to be large enough to specify the value of E_0 in acceptable accuracy.

Identity of the Distribution of Weak Points

Another type of difficulty exists in the Weibull statistical approach. The statistical property of the weak points in the test section and in the whole system has to be identical. That means the electrode finish, contamination and other irregularities in the system have to be in the same grade. This requirement seems to be fulfilled if the test section is large enough for the reliable determination of E_0 and is fabricated in the same procedure to the whole system. One way to assure the identity is to prepare a few test sections with different area and to confirm that the parameters obtained on these test sections converge to specific values with the increase in electrode area.

The identity of the weak point distributions is also disturbed by the repetitive breakdown of one test electrode. If the area of the test electrode is small, the number of the weak points on the electrode is limited. They can be cleared by breakdowns and breakdown voltage increases from shot to shot. The effect is known as "conditioning effect". On the contrary, if we do not limit the energy dissipation in the breakdown, electrode surface may be roughened by the breakdown. In this case, the test electrode is "deconditioned" by repetitive breakdowns. It is very important to limit the breakdown energy as low as possible.

The number of the breakdown experiments on a given test electrode has to be limited to the level for which the conditioning effect is negligible. If we want to get the distribution of the breakdown

voltages on a single test electrode, the area of the electrode has to be sufficiently large for the purpose[1].

NUMERICAL EXAMPLES OF WEIBULL PARAMETERS AND EFFECTIVE ELECTRODE AREA

Weibull parameters for the breakdown in compressed SF_6 had been studied on a few coaxial cylinder electrodes having various electrode areas. A part of the results has been reported before[1]. According to the study, the parameters in Eq. (1) are given as functions of material and finish of electrode and gas pressure. Typical example of the parameters for carefully machined factory grade aluminum are as in Eqs. (5).

$$\begin{aligned} E_o &= Ed \;/\; \{\, 1 + 0.355\; p^{0.7} \,\} \\ m &= 7.4 \\ \lambda &= k/S = 100 \exp (1.15\; p) \end{aligned} \tag{5}$$

In the expression, the parameter k is normalized by the area of the test electrode S in cm^2. The unit of gas pressure p is in atm (ab.).

The breakdown characteristic of a system having a given effective electrode area, S_{eff} is given by Eq. (3), substituting S_{eff}/S for n. Using the parameters in Eq. (5), the most probable breakdown field strengths of the system are calculated as a function of S_{eff}. The results are shown in Fig. 2. We can clearly see the decrease in the breakdown field strength with the scale of the system.

The largest electrode area used to obtain the Weibull parameters was about 3000 cm^2. One may think the area is too small for the parameters to be applied to large scale systems. However, we proved that the parameters are applicable to large full scale systems in excellent accuracy. The reasons are simple. Firstly, the effective electrode area of any practical system is not quite large, for highly stressed parts are rather localized in the system. We will show a few examples in the following. Secondly, if the area is sufficiently large, the breakdown characteristic is not very much dependent on the electrode area, by the nature of Weibull distribution.

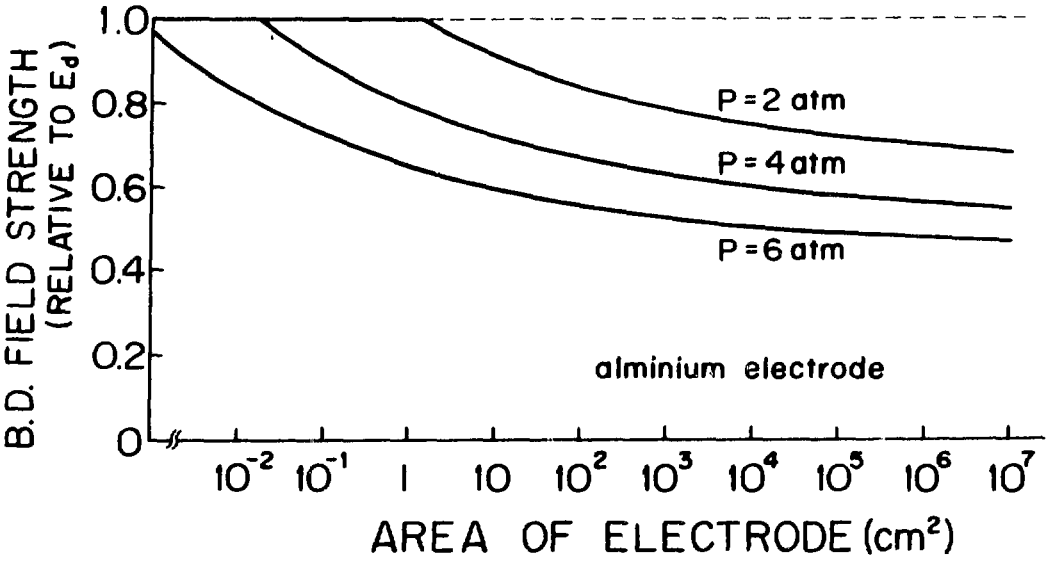

Fig. 2. Calculated Breakdown Field (Modal Value) for Aluminium Electrode.

The effective electrode area of gas systems can be evaluated substituting the parameters in Eq. (4), provided S(E) is known. S(E) can be obtained by a routine field analysis. As the applied voltage is not fixed, it is expressed as a function of E/E_{max}.

Examples of S(E)'s are shown on two different parts of 500 kV system in Fig. 3. Example (a) is a 10m long straight bus with a spacer. The maximum field locates at a point close to the spacer. The field strength on the surface of inner conductor is about 70% of the maximum field in this particular example. Example (b) is a disconnector section of the system. Using these S(E)'s, we can calculate the values of S_{eff}'s in Eq. (4) for these sections by the aid of a computer[3]. Effective areas of these sections of 500 kV system so obtained are:

(a) 10m Bus Section with a Spacer $S_{eff} \simeq 405\ cm^2$

(b) Disconnector Section $S_{eff} \simeq 628\ cm^2$

These values are not quite large and within the reach of our laboratory experiment approach.

Once we get the effective area of a system, we can easily analyze

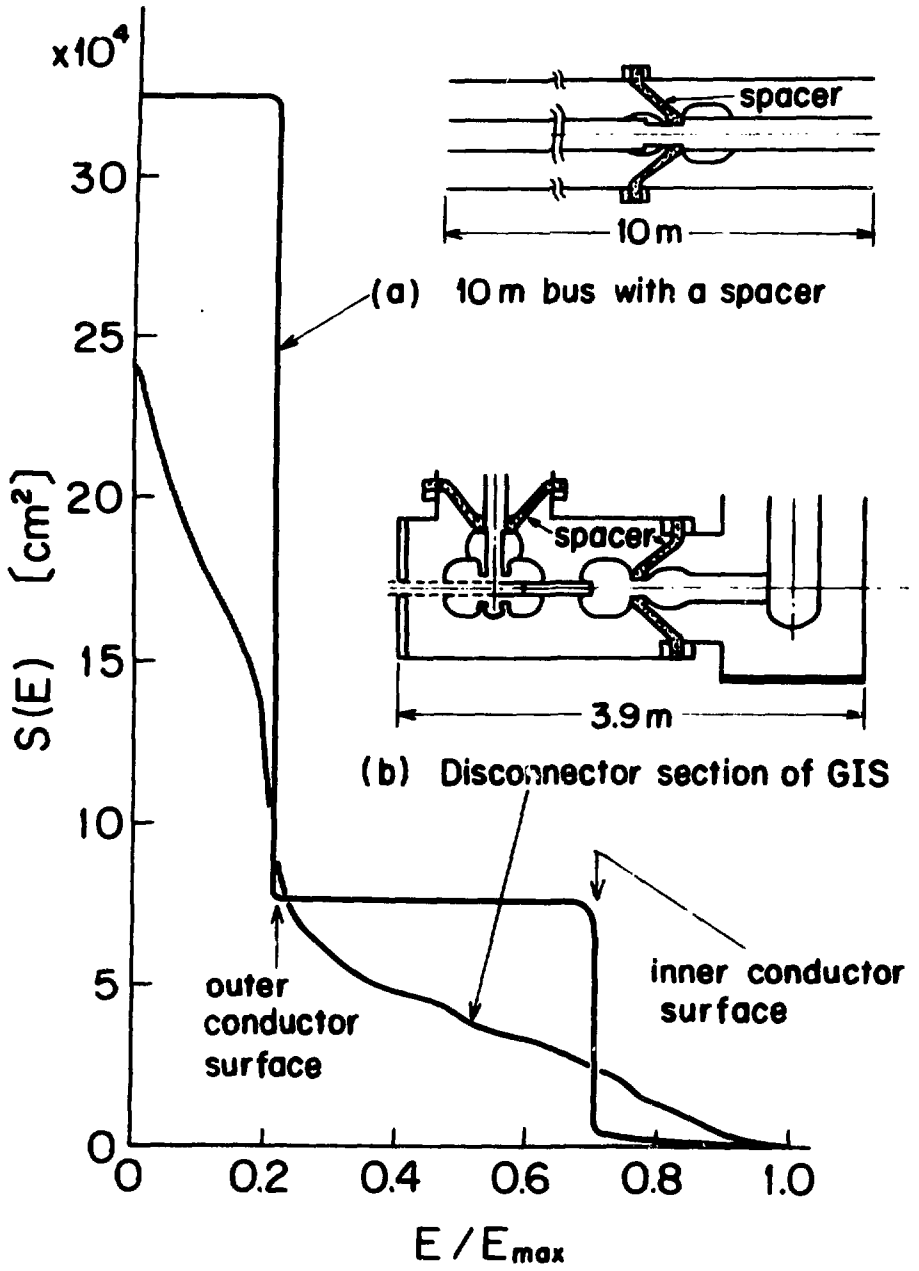

Fig. 3. S(E) Curves for 500 kV Gas Insulated Substation.

the breakdown field strength of the system using Eqs. (3) and (5). To convert the characteristic of E_{max} to that of the breakdown voltage, we need more information on the geometry and electric field distribution of the system.

VOLTAGE-TIME CHARACTERISTIC AND POLARITY EFFECT

In the previous sections, we have ignored the time factor of the influence of weak points on the breakdown characteristic. It has been shown that the influence diminishes gradually when the period of time of voltage application is decreased down to less than several microseconds.

An empirical relation on the time effect of applied voltage has been reported before[5]. For switching impulse and ac applied voltages, the breakdown voltages are as evaluated by the analysis in the previous sections. While the influence of the weak points is not appreciable for steep front impulse voltages, if the time to breakdown is less than submicroseconds. Because of the property, voltage-time characteristic of an electrode system is significantly influenced by the property of weak points.

In the previous sections, we assumed to sum up the electrode area distribution S(E) on both high voltage and grounded electrodes, considering ac breakdown. Actually the irregularities are effective only on the electrode at negative polarity. If we are interested in the breakdown for impulse voltages of both polarities, we have to sum up S(E)'s on both electrodes separately to evaluate the polarity effect of breakdown. The details of the technique are also given in the previous paper[3].

BREAKDOWN VOLTAGE CHARACTERISTIC OF A MODEL BUS WITH SPACERS

Model Bus Line

When we apply the Weibull statistical analysis to the breakdown voltage rather than to the electric field, we need the detailed infor-

mation on the geometry and the electric field distribution of the systems. To simplify our discussion, we will show the examples of the breakdown voltage analysis on a simple coaxial cylinder bus with spacers. The analysis will be of value to show the important aspects of the scale effect of gas insulation. The geometry of the model bus is given in the inset of Fig. 4. We will analyze the coaxial cylinder parts and the spacers separately. The weak points in the system are assumed to be given by the Weibull parameters in Eq. (5). Numerical examples at p = 4 atm are given in the present paper.

The design of the spacer is characterized by two factors. One is the ratio of the maximum field strength at around the spacer E_S and the field strength on the inner cylinder of coaxial line E_C. The ratio E_S/E_C is set at 1.25. This value may be a little lower than the values usually observed in practical design, but the value was chosen so as to show the breakdown characteristic of the system more clearly. The other factor is the effective area of the spacer. We set the area as 10 cm^2.

AC Breakdown Characteristic

The statistical distribution of ac breakdown voltage (kV peak) for the coaxial bus of unit length (1 meter) is obtained as follows. Electrode area S or the surface of the inner cylinder is 2.85×10^3 cm^2 per meter. Then, Weibull parameter at p = 4 atm is given by Eq. (5) as,

$$E_0 = 184 \text{ kV/cm}, \qquad m = 7.4, \qquad k = 10^4$$

Substituting these values in Eq. (1), the probability distribution of the field strength E_C at breakdown is obtained. The relation between E_C and the applied voltage V for the coaxial cylinder is;

$$E_C = \frac{2V}{D_1 \, \ell n \, D_2/D_1} = 0.223 \, V \tag{6}$$

where D_1 and D_2 are the diameters of inner and outer cylinders. Using the relation, the probability density distribution (dP/dV) for L = 1 m is calculated and shown by solid curve in Fig. 4.

The probability density distributions of the line of length n(m) are calculated in the similar manner using Eq. (3). The breakdown

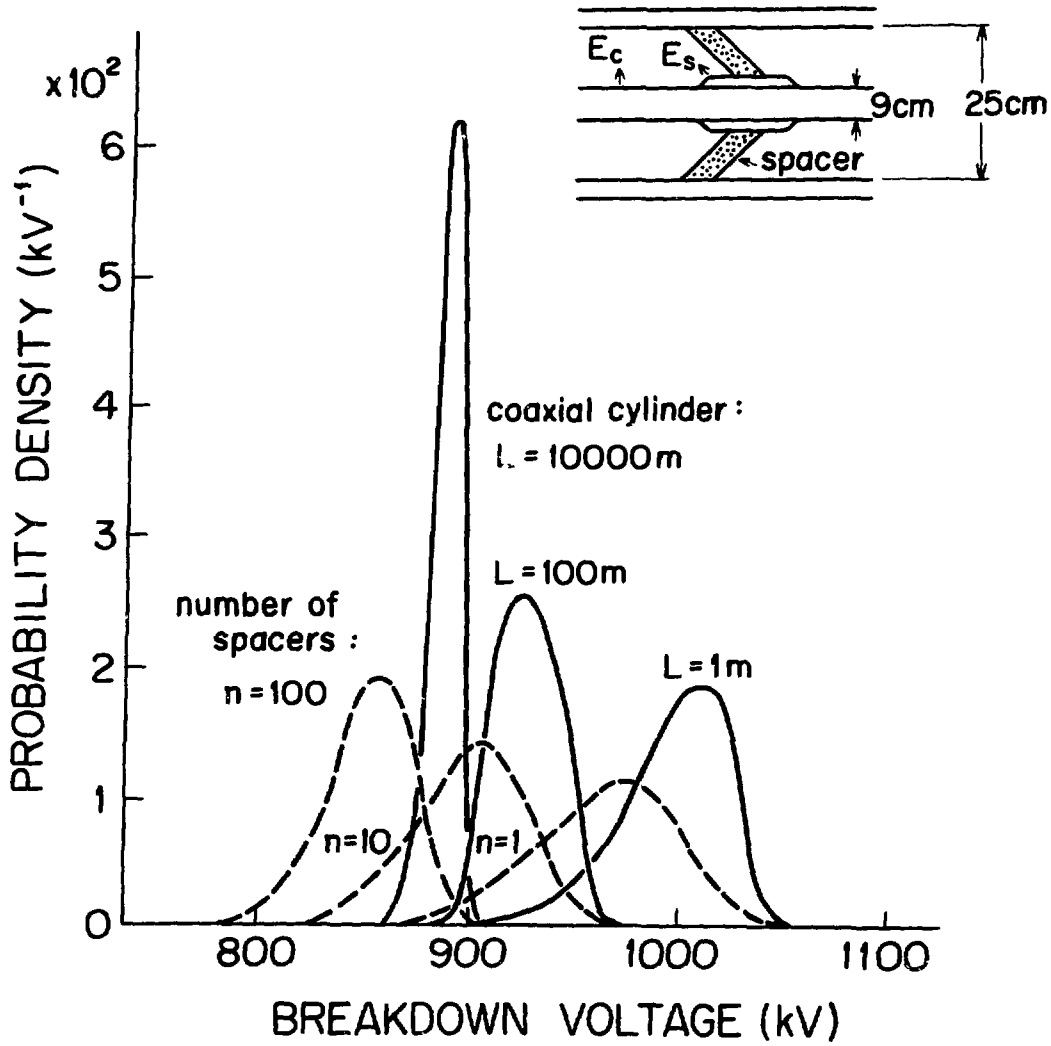

Fig. 4. Model Bus Line and Breakdown Probability Distribution Calculated for Coaxial Cylinder and Spacers.

voltage of 1 m bus ranges roughly from 930 kV to 1040 kV, whereas that of 10 km bus is in between 870 and 900 kV. We notice that the scattering of the breakdown voltage is much smaller for longer line.

The probability distribution of the maximum field strength E_S at the breakdown of one spacer is evaluated using the effective area of 10 cm^2 as specified. Since the maximum field strength E_S is specified as 1.25 times that of E_C, the relation between E_S and the applied voltage V is given as:

$$E_S = 1.25 \times 0.223\ V = 0.279\ V$$

Probability density distribution of V of the spacer is given by the dashed lines in Fig. 4. The same distributions for n parallel connections are also shown in the figure.

In comparing the distributions in Fig. 4, we can notice that the breakdown voltage of one spacer is similar to that of the coaxial cylinder of several meters length. But the scattering width of the former is a little wider. This is due to the difference in the electrode area of the two systems. We can see that most of the breakdowns will occur in the coaxial cylinder part, if a 100 m bus has only one spacer. Breakdown will occur at the spacer in the case that the bus has a hundred spacers. Both modes coexist in the case of the 100 m bus with 10 spacers. This relation of the breakdown voltage, of course, changes by the design factors S_{eff} and E_S/E_C of the spacer.

Voltage-Time Characteristic

The V-t characteristics of the model coaxial cylinder and the spacer are shown in Fig. 5, using the formula given in reference (5). The V-t curves are dependent on the scale of the system particularly in the time range longer than 10 μs. Further, the V-t curves for the cylinder part are steeper than that for the spacer. If the bus line of 100 m has only one spacer, the breakdown will occur mostly in the cylinder part for slowly rising switching impulse, but it will occur in the spacer region for steep front impulse.

The above relation is very much dependent on the design of the spacer. For quantitative discussions on a given gas insulated system,

we have to analyze the characteristics based on the detailed design of the system.

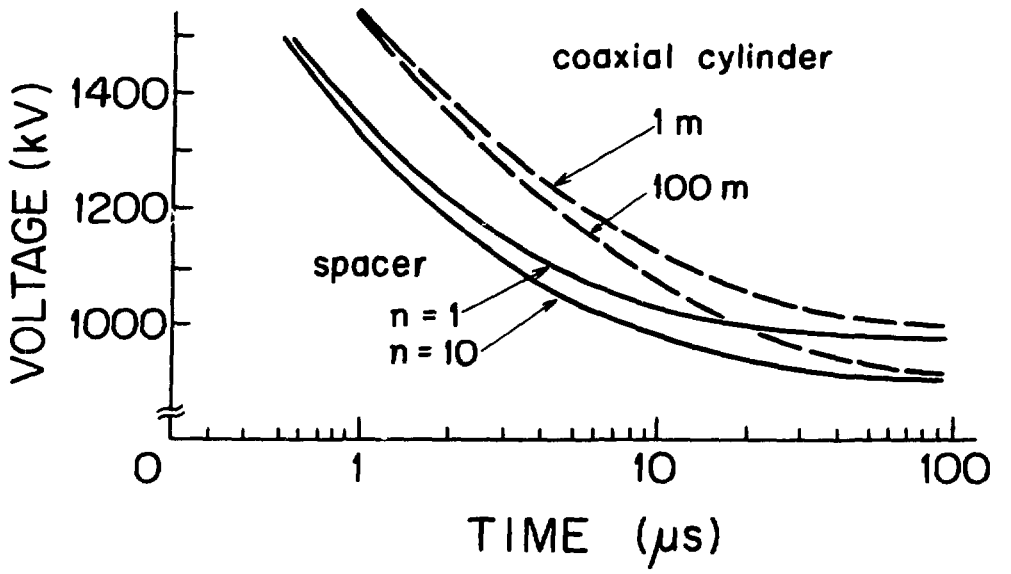

Fig. 5. V-t Characteristics Calculated for Coaxial Cylinder and Spacers.

REFERENCES

1. T. Nitta, N. Yamada, Y. Fujiwara, IEEE Tran. Power Apparatus and Systems, PAS-93, 623 (1974).

2. E.J. Gumbel, Statistical Theory of Extreme Values and Some Practical Applications, No.33, U.S. Gov't Printing Office (1954).

3. T. Nitta, Y. Fujiwara, F. Endo, J. Ozawa, CIGRE Paper 15-04 (1976).

4. T. Nitta, Y. Shibuya, IEEE Trans. Power Apparatus and Systems, PAS-90, 1065 (1971).

5. T. Nitta, Y. Shibuya, Y. Fujiwara, IEEE Trans. Power Apparatus and Systems, PAS-94, 108 (1975).

DISCUSSION

JOHANSEN: In the type of analysis performed it is not necessary to know the physical nature of the weak points in the system. The author considers, however, that microscopic protrusions on the electrode surface and particle in the gas volume are the physical reasons for these weak points. Do you have any indications as to which of these factors is the dominating one in representing weak points in the system?

NITTA: We cannot say which of these factors is dominating, since we do not control the factors quantitatively. But we found the following evidences as reported in Refs. 1 and 3: 1. Dark current of the order of $\mu A/cm^2$ is observed when the maximum field strength in the system E is in between E_o and E_d. This will indicate field emission from the cathode surface. 2. If we roughen the surface of the electrode, the breakdown voltage decreases in a similar way as we increase the area of the electrode. 3. The statistical properties of the weak points are very much dependent on the material of the electrode.

SLETTEN: Were the Weibull parameters obtained from AC or impulse measurements? Is the V-t characteristic shown for a ramp or step function?

NITTA: They were obtained from AC measurements. We also studied other types of applied voltage and found that they are the same within the accuracy of our measurement for negative DC and negative slow switching surges. The V-t characteristic is discussed on the basis of the experimental data obtained using standard lightning wave and some other

switching surge wave shapes. Since most of the breakdowns occur at the front or around the peak of the applied voltages, the characteristic is principally for ramp voltages.

COOKE: In the extrapolation of breakdown values to larger size systems you assume that the breakdown voltages can be described by Weibull statistics. Do you have evidence that Weibull statistics accurately describe breakdown voltages in compressed SF_6 at low probabilities?

NITTA: Yes, I think I have. But to obtain any meaningful values for the parameters you have to be very careful to choose the electrode on which you perform the test. As I discussed in the text, the area of the electrode has to be sufficiently large--sufficient to determine the value of E_o in acceptable accuracy and to assure the identity of the statistical distribution of the weak points through the breakdown measurement. According to our experience, the "effective" area of the electrode has to be at least a few thousand square centimeters. We can prove the validity of Weibull distribution at low and also at high probabilities by comparing the probability distributions on various electrodes having different areas. I think we have enough evidence to prove the validity of applying this analysis on a number of systems having a variety of effective areas.

DALE: Your flashover probability characteristics indicated that flashover for long bus lengths are more likely from the conductor and for short bus lengths across the spacer. Do you have any feeling for how the relative flashover probabilities will alter if the surface roughness of the conductor is changed? For example, could the probability of spacer flashover be reduced if the surface roughness of the conductor was much larger or vice versa?

NITTA: Yes, the roughening of the surface of the electrode shows very similar effect to the increase of the area. I reported on the effect in detail in Refs. 1 and 3 of the text.

THE DIELECTRIC STRENGTH OF SOME FREONS AND THEIR MIXTURES WITH NITROGEN AND SULPHUR HEXAFLUORIDE

E. Gockenbach
Technical University Darmstadt, West Germany

HVDC-converter stations have high requirements with respect to liquid coolant. Freons with a suitable boiling point are very well available for this application[1]. Therefore it is significant to investigate the dielectric strength of gaseous Freons, which can be used as insulation in combination with a liquid Freon-cooling. The dc breakdown voltage of Nitrogen (N_2) Sulphur Hexafluoride (SF_6), Trifluortrichloräthan ($C_2Cl_3F_3$), and some other Freons was investigated in a uniform electrical field configuration. The following table shows for example the measured field strength.

Table 1: Electrical field strength of the gases

Gas	N_2	SF_6	$C_2Cl_3F_3$	
Field strength	3o	88	185	kV/cm

Not only the pure gas but also the gas mixtures are interesting for technical application with regard to the economy. Moreover it is possible,that a gas mixture results from leakage. Therefore it is important to know the dielectric strength of the gas mixtures. At the ideal gas the Dalton's law holds exactly for the relationship between the partial pressure and the portion of volume. It is

$$V_1/V = p_1/p \qquad (1)$$

where V_1 = portion of volume of the gas 1
V = total volume of the gas mixture
p_1 = partial pressure of the gas 1
p = total pressure of the gas mixture

The legality of Eq.(1) was tested for all gas mixtures and by the following investigations the ratio of mixture is determined by Eq.(1). The measured field strength of the gas mixture N_2 - $C_2Cl_3F_3$ is shown in table 2.

Table 2: Field strength of the gas mixture N_2-$C_2Cl_3F_3$

Volume N_2	100	90	50	10	0 (%)
Volume $C_2Cl_3F_3$	0	10	50	90	100 (%)
Field strength	30	64	128	177	185 kV/cm

The increasing of the dielectric strength is especially important of small portion of a Freon. The breakdown voltage of the pure gas and the gas mixtures increases linearly with the gas pressure and the gap length. Knowing the ionization coeffizient α and the attachment coefficient η of the components of a gas mixture, the breakdown voltage can be calculated[2] by the known breakdown theories (generation and streamer mechanism)[3]. The reduced breakdown condition is

$$\bar{\alpha} = \alpha - \eta = 0 \qquad (2)$$

where $\bar{\alpha}$ = effective ionization coefficient, 1/cm
α = ionization coefficient, 1/cm
η = attachment coefficient, 1/cm

The effective coefficient $\bar{\alpha}$ of a gas is only a function of the field strength E and the gas pressure p. Therefore the measured ionization coefficient is given by the relation $\bar{\alpha}/p = f(E/p)$. This relation is for SF_6 [4]

$$\bar{\alpha}/p = k\ (E/p - (E/p)_{crit}) \qquad (3)$$

where p = gas pressure, bar
k = constant, 27/kV
E/p = refered electrical field strength, kV/cmbar
$(E/p)_{crit}$ = refered critical field strength, 88 kV/cmbar

and for N_2 [2]

$$\bar{\alpha}/p = A \exp(-B\ p/E) \qquad (4)$$

where A, B = constants

On the basis of Eq.(2) it is possible to calculate the breakdown voltage of a gas mixture, if Eq.(2) is transformed to

$$\frac{\bar{\alpha}_1\ p_1}{p_1} + \frac{\bar{\alpha}_2\ p_2}{p_2} = 0 \qquad (5)$$

where p_1, p_2 = partial pressure of gas 1 resp. gas 2.

The term $\bar{\alpha}_1/p_1$ or $\bar{\alpha}_2/p_2$ at a given field strength can be determined from Eq.(3) or Eq.(4), if on the left side of the two

relation the gas pressure p is replaced by the partial pressure p_1 or p_2, and on the right side the gas pressure p by the total pressure of the gas mixture.The breakdown of a N_2-Freon gas mixture is measured as a function of the volume portion of the Freon (table 2). Knowing the breakdown voltage of the various mixtures,the electrical field strength is calculated. Then the effective ionization coefficient of N_2 is determined from Eq.(4) and the unknown coefficient of Freon is determined from Eq.(5). The calculated effective ionization coefficient of the Freon is given in a modified form of Eq.(4) to

$$\bar{\alpha}/p = A \exp(-B\ p/E) + C \qquad (6)$$

where A, B, C = constants, listed in table 3

Table 3: Constants of the ionization coefficient $\bar{\alpha}/p$

Constants	A (1/cmbar)	B (kV/cmbar)	C (1/cmbar)
N_2	532o	2o8	------
$C_2Cl_3F_3$	1o2oo	315	- 185o

The breakdown voltage of SF_6-Freon mixtures is now measured to verify the legality of the calculation method.Comparison to the measurements the breakdown voltage is calculated from Eq.(5) with the ionization coefficient of Freon, which is determined from the N_2-Freon mixtures. The comparison between measured and calculated breakdown voltage gives satisfactory results for technical application, because the difference is by no means greater than 6%.

REFERENCES

1. H. Jaster; N. Singh; R. Nakata, IEEE Summer Power Meeting Paper F 77 678-6

2. A. Wieland, ETZ-A 94, p.37o (1973)

3. B. Gänger, Der elektrische Durchschlag in Gasen, Springer Verlag Berlin, (1953)

4. T. Nitta; Y. Shibuya, IEEE 9o, p. 1o65 (1971)

DISCUSSION

CHRISTODOULIDES: I do not know if you are aware of the implications these kind of freons - containing chlorine atoms - have in depleting the ozone (O_3) layer in the stratosphere. Some of these molecules are photochemically reactive. It is known that the fragments Cl or ClO attack O_3. It is estimated that 1,1,3-$C_2H_3Cl_3$ can survive for ∿15 years in the stratosphere, which means that it might be a potential reducer of O_3 for a long period of time. If one considers the large amounts used in the last ten years, as aerosol propellants for example, the amount of chlorine-containing freons accumulated in the stratosphere could indeed be very large and the expected effects on ozone depletion in the near future could be large as well.

GOCKENBACH: I know, that the fragments of Freon 113 can decompose O_3 to O_2. But up to now, it is not certain if this decomposition of O_3 takes place, and if the conversion from O_2 to O_3 as a result of the uv-light is really impossible. On the other hand, the Freon 113 is used in a closed and watched system, like a HVDC converted station for example, so that no gas or liquid reaches the air or the stratosphere.

ORFEO: On the basis of present scientific evidence, one can neuter, validate, or disprove the CFM/ozone issue. Furthermore, it is highly unlikely that this problem will be resolved within the next five years. Regulatory activity to date has focused on the evaluation of practical emission control standards and appropriate recovery and reclamation procedures. There is not intent to ban the use of chlorofluorocarbons in non-aerosol uses but rather to control release.

SIOMOS: There is enough evidence that indeed freons present a hazard for the atmospheric ozone layer. Detailed information on this important environmental problem one can obtain either from Professor D. Ehholt, Institute for Atmospheric Chemistry, KFA- Jülich, W. Germany, or from NOAA, Boulder, Colorado, USA.

NAKATA: The use of Freon 113 discussed by Dr. Gockenbach is in a specialized high voltage apparatus in a carefully controlled and maintained closed system. To compare the threat that such limited use might pose as compared to indiscriminate uncontrolled ejection of Freon (used as an aerosol propellant) prior to the banning, is unwarranted I feel. To ban the use of Freon 113 as a dielectric (in its limited application for the specialized HV application) can set an implied guilt precedent by which most stable dielectric fluids or gases might be questioned with dire consequences.

AVALANCHE STATISTICS AND THE STREAMER CRITERION

D.T.A. Blair B.H. Crichton I.C. Somerville
Department of Electrical Engineering, University of Strathclyde, United Kingdom

ABSTRACT

We have examined the streamer criterion for electronegative gases in uniform fields, allowing for avalanche statistics, and have performed numerical calculations for SF_6. A well-defined static breakdown voltage is to be expected, and the probability of streamer breakdown is vanishingly small for E/p (field strength/pressure) below the limiting value, even when an avalanche is initiated by a large number of electrons.

APPLICATION OF LEGLER'S ANALYSIS

Streamer theory is often interpreted as predicting breakdown when the average number of electrons per avalanche exceeds a critical value. We assume instead that breakdown occurs if a single avalanche contains a number of electrons greater than a critical value, and we must therefore take account of statistical variations in the number of electrons contained in an avalanche. We consider an electronegative gas in which detachment does not occur, we assume that the applied electric field is uniform, and we neglect the effect of the space charge of the avalanche. Legler[1] has discussed the statistics of such a case: if an avalanche is initiated by a single electron at the cathode ($z = 0$) then (with some simplifying assumptions) the probability that it will contain n electrons when it reaches the anode at $z = d$ is

$$p_n = ax^n \qquad (n \neq 0,\ \eta \neq \alpha) \qquad (1)$$

where $a = \bar{n}(1-\eta/\alpha)^2/[(\bar{n}-1)(\bar{n}-\eta/\alpha)]$, $x = (\bar{n}-1)/(\bar{n}-\eta/\alpha)$, η is the attachment coefficient, α the ionisation coefficient, and $\bar{n} = \exp(\alpha-\eta)d$. We apply this result to the case where $(\alpha-\eta)$ is positive and not too small, so we may take the breakdown probability p_b as the probability that n will equal or exceed the critical value N, and we obtain

$$p_b = \Sigma_N^\infty p_n = \Sigma_N^\infty ax^n = ax^N/(1-x) \qquad (2)$$

For large N this may be written

$$p_b \simeq (1 - \eta/\alpha)\exp[-(1 - \eta/\alpha)N/\bar{n}]. \qquad (N \gg 1) \qquad (3)$$

A MARKOV-CHAIN ANALYSIS

Here we consider the avalanche to experience transitions in each of which it either gains one electron (with probability p) or loses one electron (with probability $q = 1 - p$). In a uniform electric field p and q are constants. We assume that the avalanche continues until it either dies out ($n = 0$) or causes a breakdown ($n = N$). This analysis therefore applies to the case of an infinitely long gap.

To determine the value of p, we consider an avalanche containing n(z) electrons progressing in a uniform field from position z_1 to position z_2. The electrons in the avalanche will make, on average, n_i ionising collisions and n_a attaching collisions, with

$$n_i = \int_{z_1}^{z_2} \alpha n(z)\, dz \quad \text{and} \quad n_a = \int_{z_1}^{z_2} \eta n(z)\, dz$$

The total number of transitions will be $n_i + n_a$, and $p = n_i/(n_i + n_a)$. Consequently $p = \alpha/(\alpha+\eta)$, $q = 1 - p = \eta/(\alpha+\eta)$ and $q/p = \eta/\alpha$.

When stated in this form, the problem of avalanche growth is analogous to the "gambler's ruin" problem[2]. For the probability of streamer breakdown we obtain

$$p_b = [1-(q/p)^i]/[1-(q/p)^N] = [1-(\eta/\alpha)^i]/[1-(\eta/\alpha)^N] \qquad (\eta \neq \alpha) \qquad (4)$$

$$p_b = i/N \qquad (\eta = \alpha) \qquad (5)$$

where i is the number of electrons in the avalanche at the start of the process (for example at the cathode).

NUMERICAL VALUES

We have used Eq.(3) to calculate breakdown probabilities in SF_6 for $(\alpha - \eta)$ positive and not too small[3]. The results show that for a gap with moderate irradiation a well defined static breakdown voltage is to be expected, and that the breakdown probability rapidly becomes vanishingly small as E/p is reduced towards the limiting value at which $\alpha = \eta$.

Eq.(4) and (5) can be used to calculate breakdown probabilities at

and below the limiting value of E/p. For i =1 and N = 10^8, the breakdown probability at the limiting value is, from Eq.(5), 10^{-8}. This result applies to any electronegative gas (or gas mixture) that exhibits a limiting E/p. For SF_6 with E/p only 1 part in 10^6 below the limiting value, and with i = 1, p_b works out at the very low value of 6×10^{-134}. Increasing i to 10^7 increases this only to about 10^{-115}. These results apply to an infinitely long uniform-field gap at the given value of E/p: for a finite gap of any geometry in which the maximum E/p does not exceed that value, the breakdown probability will be even smaller. We conclude that avalanche statistics cannot explain breakdown in any gap where E/p is always below the limiting value.

Hauschild and Bürger[4] appear to have incorrectly predicted breakdown below the limiting E/p by failing to recognise that in a transition the ratio of the attachment probability to the ionisation probability is equal to the ratio of the attachment and ionisation coefficients ($q/p = \eta/\alpha$). Rein, Arnesen and Johansen[5] also predict breakdown below the limiting value on the basis of avalanche statistics, but their analysis requires that the average avalanche achieves the critical amplification in a finite distance, and it therefore cannot be valid for E/p below the limiting value.

ACKNOWLEDGEMENTS

The work reported here is supported by the Central Electricity Generating Board (UK) and the Science Research Council (UK).

REFERENCES

1. W. Legler, Z. Naturforsch. A, 16, 253 (1961).

2. J.G. Kemeny, J.L. Snell and G.L. Thompson, Introduction to Finite Mathematics, p. 144, Prentice-Hall, Englewood Cliffs, New Jersey, 1974

3. D.J. Tedford, B.H. Crichton and I.C. Somerville, to be published in 1977 Annu. Rep. Conf. Elec. Insul.

4. W. Hauschild and W. Bürger, Z. elektr. Inform.-u. Energietechnik, 5, 283 (1975).

5. A. Rein, A. Arnesen and I. Johansen, IEEE Trans. Power App. Syst., PAS-96, 945 (1977).

DISCUSSION

DUTTON: It is interesting to see that the statistical probability of breakdown at fields below the critical value is very low in a strongly electro-negative gas. We came to the same conclusion about hydrogen in earlier work on non-attaching gases. Can I ask why the larger initial number of electrons i gives a greater probability of breakdown (albeit still infinitesimally small) even though the statistical fluctuation will be greater the smaller is i?

BLAIR: When i initiating electrons leave the cathode simultaneously at the same point, the breakdown probability is the probability that the total number of electrons, produced by gas amplification of all the i electrons together, will reach the critical value N. This will always be greater than the probability that a single initiating electron will gas-amplify to that critical value on its own.

JOHANSEN: The conclusion of this paper is that no breakdown can take place below an E/P value of 8.9 kV/mm atm in SF_6 under ideal conditions. Although I have no reason to doubt the calculations perfomed, I disagree with the conclusion that there is no insight to be gained on the breakdown phenomena by studying the influence of the statistical distribution of avalanche sizes.

In his invited paper on Monday, Professor Dutton made the general remark about the understanding of the basic physics of gaseous dielectrics that in the region of low pressures and small distances one could, from basic physics, design a dielectric with known properties. On the other

hand, in the high pressure region, much was not known and one had to be careful with theoretical predictions. I agree entirely with this statement.

In the present situation, I think one has to follow several paths to a deeper understanding of the breakdown phenomena and to get information that is useful for design purposes. In the paper that the authors refer to (Ref. 1 of their paper) a distance very close to the cathode is chosen where the statistical distribution of avalanche sizes is studied and chosen as characteristic. I agree entirely with the author that this choice is not theoretically well justified. It gives however the advantage that the results coincide with measurements over a wide range of electrode areas, field inhomogeneities (although it is assumed that there is no corona before breakdown) and pressures. It also predicts the statistical spread of the experimental results rather well. These measurements are made with polished electrodes and with the gas cleaned as well as can be done under laboratory conditions. Any further refining of that technique did not improve the breakdown values. I think this path, where theoretical studies are guided by experiments and where all important parameters are varied, should be further studied. I would then recommend variations in the electrode area, also under fundamental research conditions.

At the present moment I think no ideas should be ruled out as explaining breakdown at higher pressures. If I should use my intuition, though, I doubt that particle contaminations will explain breakdown under refined laboratory conditions for impulse voltages. I believe that further insight might be obtained by studying the properties of the

surface, especially the problems of microprotrusions, although I don't think the now classical Pedersen's criterion will give the whole answer, and I believe that further insight into electron emission properties of the electrode and avalanche size statistics will be of importance. This is as far as impulse breakdown is concerned. When it comes to AC and DC breakdown, the situation is more complicated and also other factors have to be taken into account.

BLAIR: Strictly, the conclusion of this paper is that breakdown at E/P below the limiting value cannot be explained by statistical variations in avalanche growth. The experimental results reported by Professor Johansen and his co-workers are very valuable, and their model for predicting such results is most interesting. This model, however, is not physically realistic if it depends on an avalanche reaching the critical value for streamer formation in a finite distance over which E/P always lies below the limiting value.

BASIC DATA ON POSITIVE CORONA DISCHARGES

Joint paper from Laboratoire de physique des décharges
E.S.E. -C.N.R.S. équipe n°114
Plateau du Moulon 91190 Gif sur Yvette France

presented by F. Bastien

ABSTRACT

The discharges which cause dielectric losses are often transient discharges,more precisely of corona type.Besides the knowledge of I(t), q(t) and V(t) the electrical methods brought us accurate knowledge on conduction and influence currents.As for the optical methods,more particulary spectroscopic ones elaborated at the Lab.,they allowed us to obtain basic data on the vibrational and rotational temperature of the gas,the electron temperature,the current densities,the electron densities and the field.With the fundamental data thus obtained,it has been possible to build quantitative models describing the discharge evolution.

The present paper reports investigations carried out in the "Laboratoire de physique des décharges" of the physical mechanism active in the corona discharge.
Various techniques were employed to gain the information required for the basis of a quantitative analysis. Only the characteristic value of the results which have been obtained using these techniques will be given here.Futhermore results obtained in the Lab. concerning the important problem of D.C. current will not be presented.
Typically the discharges are performed in air or oxygen at atmospheric pressure between a sharp point and a plane with 1 cm gap.A steady positive potential is applied to the point across a resistance.The discharge is periodic with a filamentary aspect.The period is associated with ionic charges collection or with power supply circuit if a transitory arc occurred.
The initial development of the pulsative discharge is associated with a luminous spot related to a high rate of ionization termed the primary streamer which crosses the gap from point to plane in approximately 20 ns. Whereupon a luminous filament develops from the anode;this bright region is called secondary streamer or "channel".When the applied potential is large enough an arc follows the secondary streamer.The final step before arc formation, referred to as the "activated channel",is connected with some active processes.

PRIMARY STREAMER

G. Hartmann has employed spectroscopic methods to study the primary streamer at voltages below the breakdown potential.He has measured the rotational temperature (Tr) of nitrogen molecules.From band (0,2) of 2^d positive system ($C^3\Pi_u \rightarrow B^3\Pi_g$ transition) Tr=330 K has been obtained for voltages clearly below the breakdown potential.He has also determined the vibrational temperature from the vibrational levels relative populations of $C^3\Pi_u$ and $B^2\Sigma_u^+$ states.This method has already been described in full[1] . The obtained value Tv ≃1200 K for electronic ground state molecules shows that about 10% of molecules are vibrationally excited in a metastable state.This result has allowed the introduction of this important parameter in a primary streamer propagation model [2].Finally,Hartmann has measured the intensity ratio of the nitrogen molecular bands (0,0) from the first negative system (1S-) and the second positive system (1S+) which gives the electron energy within the primary streamer tip.Assuming a Maxwell distribution for the electrons, an energy of 12eV is obtained;this average energy is almost constant as the streamer conditions change [3].

SECONDARY STREAMER (see Marode [4])

When the primary streamer arrives at the plane the discharge,after a short phase (compensation phase) connected with redistribution of the electric field,gets a resistive behaviour.Then the discharge can be considered as a transient glow discharge where the filament track built up by the primary streamer is a positive column,that is to say a low ionizing region.This fact has been supported (Marode and Hartmann [5]) by a time resolved analysis of radiation emitted from neutral and ionized nitrogen.The intensity ratio of first negstive ($\rightarrow N_2^+$) and second positive system ($\rightarrow N_2$) gives an average electron energy of ε=1.4 eV the correspon--ding E/p value about 20 V/cm torr is lower than the value which is required for ionization.The existence of a cathode region of a glow discharge has been confirmed by temporal studies of light emission from metallic atoms ejected from the cathode (P.C.Johnson,G.Berger,M.Goldman[6])

"ACTIVATED CHANNEL" (see [8] [9] [10])

If the applied potential increased to a sufficient value the secondary streamer is followed by an arc.By introducing hydrogen traces in oxygen, Bastien and Marode have been able to perform Stark broadening measurements of hydrogen atom emission lines from the activated channel.The interpre--tation of the Stark profiles could not be made by means of the normal line broadening theory under the present conditions.It was necessary to add vectorially the local macroscopic field (Fc) to the ionic microfield. As a consequence the resulting field is no longer isotropically dis--tributed.The broadening theory has been developed according to these conditions[7] .The results show that the line shape is not only dependent upon the electron density Ne but also on the field Fc.However,in large

range of experimental conditions,it has been shown that broadening is related with the current density.Consequently the current density j has been measured as a function of time ;a characteristic value being $j \simeq 3.10^3 A/cm^2$.The knowledge of both the current density j and current i leads to a characteristic value of the filament radius:typically 20µm. Finally,the field Fc is evaluated from a discharge numerical simulation according to a method developed by Marode from which it has also been possible to obtain Ne ,thus $Fc \simeq 10$ KV/cm and $Ne \simeq 10^{15}$ cm^{-3}.
The electron density is too low to allow the assumption of a large energy transfer from electrons to ions by means of coulombic collisions.On the contrary,these values suggest that neutral species play an important role in the streamer-arc transition.
This last result has been presented elsewhere during the conference.
As a conclusion we can say that the foregoing results lead to the determination of the main mechanisms of different discharge events.

REFERENCES

1. G.HARTMANN,Thesis no1783,Université de Paris sud (1977)
2. G.HARTMANN and I.GALLIMBERTI,J.Phys.D,8,pp 670-680 (1975)
3. G.HARTMANN,Proc.3rd Int. Conf.on gas discharges London.I.E.E. Conf.Publ. no118 (1974)
4. E.MARODE,J.of Applied Physics,46,no5,pp2005-2015 and pp2016-2020 (1975)
5. E.MARODE and G.HARTMANN,C.R.Acad.Sci. B,269 ,748 (1969)
6. P.C.JOHNSON,G.BERGER andM.GOLDMAN,J.Phys. D, 10,pp2245-2256 (1977)
7. F.BASTIEN and E.MARODE J.Q.S.R.T.,17,no4,pp453-469 (1977)
8. F.BASTIEN,B.FERTIL and E.MARODE,J.Phys.D.9,L 155-158 (1976)
9. F.BASTIEN and E.MARODE Journal de Physique appliquée,12,pp1121-1125 (1977)
10. F.BASTIEN,Thesis no1871,Université de Paris sud (1977)

DISCUSSION

SIOMOS: Have you considered any other kind of line broadening than Stark broadening in your line profile measurements?

BASTIEN: All kinds of line broadening have been analyzed. Besides the Stark broadening, important factors are the Doppler broadening and the instrumental broadening. These factors are taken into account in order to obtain the theoretical profile.

PHELPS: Have you been able to measure the radial electric field in the discharge channel?

BASTIEN: No, we have not. Nevertheless, I think that the field is almost axial into the filament and it becomes almost radial on the boundary. The light emitted by the discharge essentially comes from the core of the filament. As a consequence, it is possible to assume an axial field in the Stark broadening studies.

NANOSECOND TIME AND SPATIAL RESOLVED INVESTIGATION OF BREAKDOWN DEVELOPMENT IN SF_6

Wolfgang Pfeiffer Wolfgang Schmitz

Institut für Hochspannungs-und Meßtechnik der Technischen Hochschule Darmstadt, West Germany

The whole range of breakdown development in SF_6 beginning from predischarge up to the voltage collapse has been investigated with electrical and optical methods. As already at normal pressure voltage collapse occurs within 10 ns, a special apparatus has to be used in order to measure and to store these transients. Simultaneously the light emission must be recorded and coordinated to the voltage signal. The test set-up including feeding capacitor is built up coaxially (fig.1). It includes the test gap with nearly homogeneous field distribution and it is suited for dc-voltages up to 150 kV. Investigations can be made with gas pressures up to p = 3 bar and gap widths up to s = 10 mm. Measuring of voltage collapse is possible with two non reactive capacitive voltage dividers [1] ($T_A = 0,1$ ns). The voltage signal is stored by a transient digitizer ($T_A = 0,7$ ns). Simultaneously the development of light emission is recorded with an image intensifier camera (IIC) of very short exposure time (2 ns) and stored on video tape by a low-light-level-camera. Both events measured may be coordinated with a time uncertainty of less than 0,5 ns . Triggering of the optical apparatus occurs by the voltage collapse. In order to investigate the earlier states of discharge development the image of the spark must be delayed. This has been achieved by a combination of several mirrors placed at different distances from the test gap , which reproduce an equivalent number of pictures of the spark at different well known moments. In fig. 2 this arrangement is shown with 3 concave mirrors of different focal lengths.By variation of the trigger-moment of the IIC with delay lines the moment of exposure can be changed continuously.The earliest moment of exposure is about 20 ns before voltage collapse occurs.

During measurements for each combination of test parameters the moment of exposure was varied from the earliest possible up to

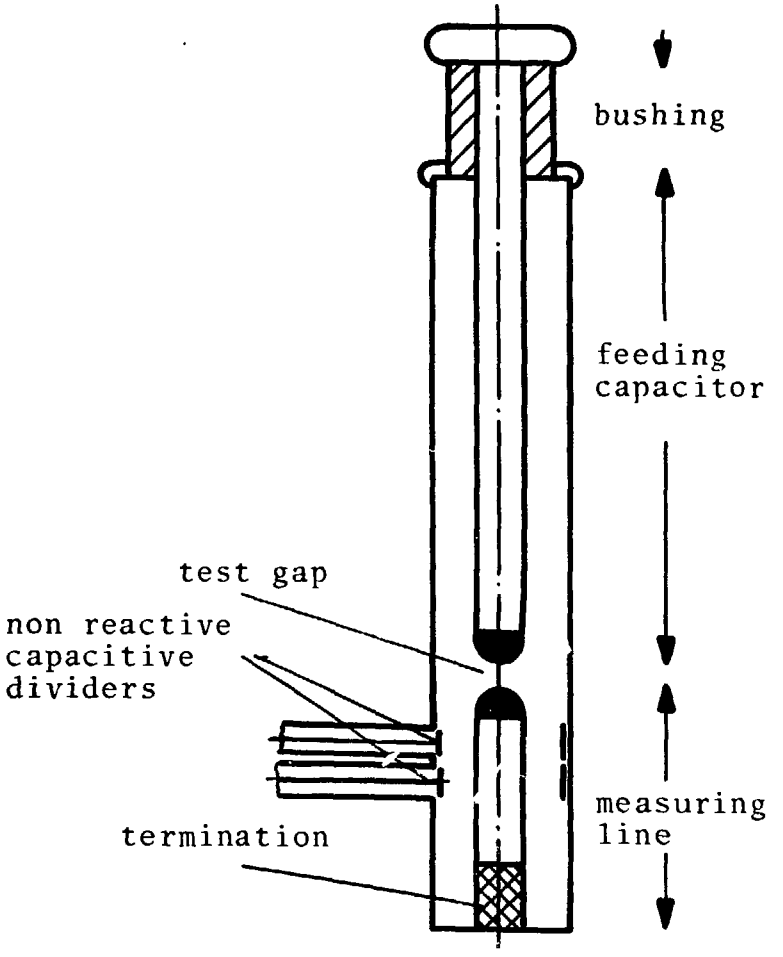

Figure 1: test set-up

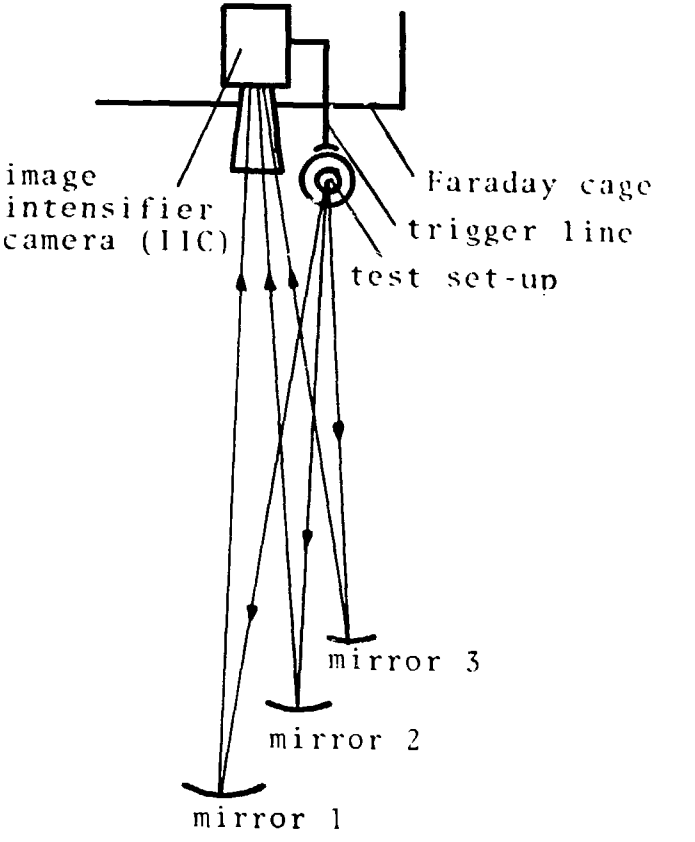

Figure 2: schematical arrangement of the optical delay paths

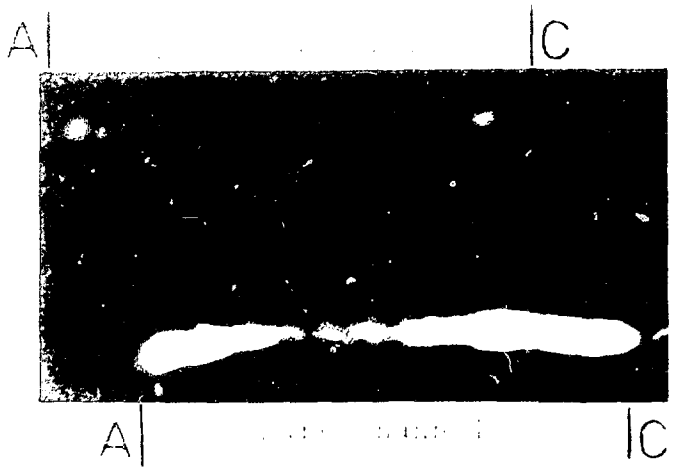

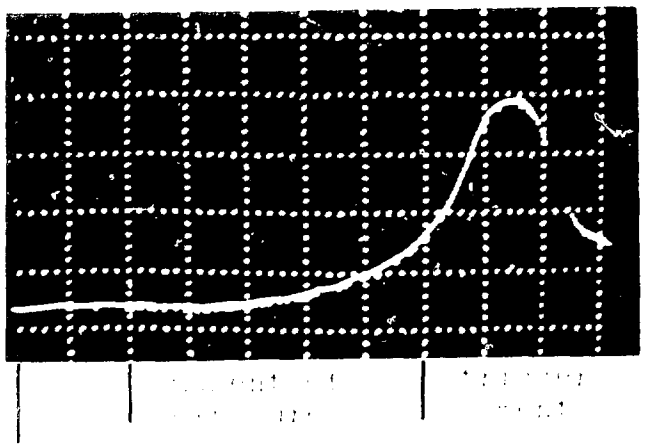

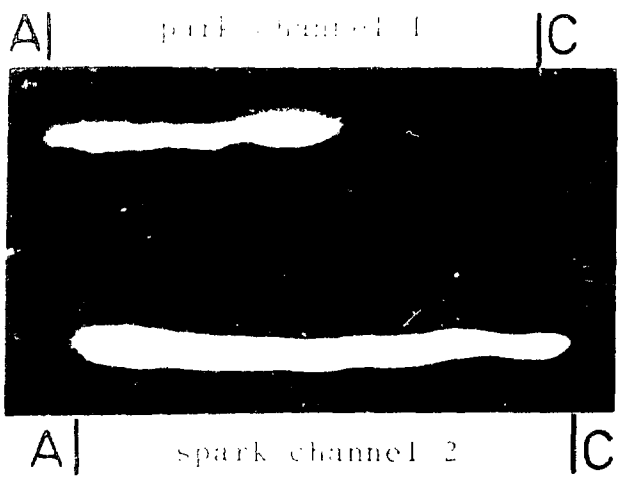

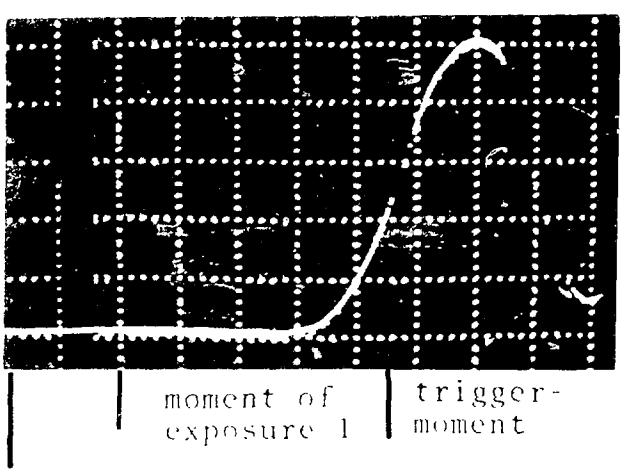

Figure 3c: spark development before voltage collapse of fig. 3d
A anode
C cathode

Figure 3d: voltage collapse and moments of exposure of the spark channels in fig. 3c

[illegible] Paschen's spark-law [4] [illegible] the [illegible] very well. The [illegible] predischarge in order to explore the mechanism [illegible] different [illegible] of discharge development.

1. W. Pfeiffer, etz-a 94 (1973), p. 91
2. W. Schmitz, etz-a 97 (1976), p. 24
3. W. Pfeiffer, IEE Conf. Publ. No. 143 (1976), p. 34
4. W. Pfeiffer, ISH Zürich (1975), Conf. Publ. p. 4C1

DISCUSSION

DUTTON: I think you have developed a significant new technique from which some very useful information can be obtained. Clearly from your photographs something significant is happening at the anode. Can you please tell us the nature and state of the electrodes and comment on the source of the pre-breakdown currents you mentioned.?

GOCKENBACH (for PFEIFFER): The electrode configuration is a sphere-sphere configuration and the roughness of the electrodes is about 5-10 μm. Because I don't work on this problem, I cannot explain the pre-discharge current occurring after 10 ns. But I think that the authors also need more results to explain these facts.

THE INFLUENCE OF ELECTRODE SURFACE ROUGHNESS AND PREDISCHARGE CURRENTS ON THE BREAKDOWN VOLTAGE IN COMPRESSED AIR

S. Berger
High Voltage Lab, Federal Institute of Technology,
Zurich, Switzerland

ABSTRACT

This paper deals with some of the reasons responsible for the deviations from Paschen's law in compressed air. Previous investigations of the influence of conductible electrode surface roughness on the breakdown voltage of uniform fields as well as on the predischarge or prebreakdown currents were continued in order to possibly improve the dielectric strength of electrode configurations with compressed air as an insulation medium. A typical result of these investigations is that at higher air pressures the breakdown voltage of uniform fields is not only governed by air pressure, gap spacing and intensified field and ionization due to the electrode surface roughness but also by thermic processes in the vicinity of precurrent leading protrusion tips.

INTRODUCTION

The deviations from Paschen's law in compressed gases are a traditional problem of high voltage technology. Earlier investigations showed that these deviations depend mainly on air pressure and electrode roughness[1], as well as on the area of the stressed electrodes[2] and on the electrode material[3,4]. Accompanying effects of the failure of Paschen's law are the conditioning effect[5], the occurence of precurrents in the nA- and µA-range[1,6] and bright spots in the vicinity of cathode irregularities[1,6,7]. In his literature review Cookson[8] displayed a broad spectrum of possible reasons for the failure of Paschen's law in compressed gases. During the last 5 years most of the investigators focussed their interest upon the problem of the onset or breakdown voltage reduction due to intensified field and ionization caused by some tens of µm high electrode surface protrusions[9,10,11,12]. As mentioned in a previous paper[13], the deviations from Paschen's law in compressed air cannot be satisfactorily explained only by the intensified ionization due to microroscopic protrusions. The reason is the insufficient agreement between measured[4] and computed breakdown voltage[14] of electrodes with some ten µm high surface protrusions. It is the aim of this paper to investigate other processes in the vicinity of electrode surface protrusions besides ionization.

EXPERIMENTAL RESULTS

The results of breakdown voltage measurements as well as scanning electron microscope investigations of electrode surfaces are displayed in two previous papers[4,13]. Due to the limited space of this publication it is however not possible to present the results of the predischarge current measurements in full detail. The summarized results of these measurements are the following:

1. Above a field gradient of about 50 $kVcm^{-1}$ polished or sand-blasted brass or aluminium cathodes show very slowly decreasing predischarge currents with current densities in the $nAcm^{-2}$-range. The reasons of these currents are not clear but it may be supposed that field emission on certain parts of the electrodes like protrusion tips and thin surface layers plays a role in the generation of these currents.

2. Besides the slowly decreasing nA-currents transient predischarge current pulses occured on sparked or sand-blasted cathodes with surface protrusions higher than approximate 50 µm, at pressures greater than about 5 bar and field gradients above approximate 100 $kVcm^{-1}$. The duration of these current pulses varies from about 0.5 msec to some sec, the current amplitude lies between approximate 0.5 and 50 µA. The air pressure related onset field gradient E_o/p of these pulses decreases with pressure increasing, e.g. at 5.4 bar E_o/p is 19 $kVcm^{-1}bar^{-1}$ and at 17.5 bar E_o/p is 12 $kVcm^{-1}bar^{-1}$. This pressure dependence is an evidence that the predischarge current pulses in the microampere range are started by ionization processes.

THERMIC PROCESSES IN THE VICINITY OF PREDISCHARGE CURRENT LEADING CATHODE PROTRUSIONS

The power density in a current leading medium is expressed by the following equation

$$P_m = E \cdot j \qquad (1)$$

where

P_m = power density $kWcm^{-3}$
E = field gradient $kVcm^{-1}$
j = current density Acm^{-2}

As seen from ref.[13], fig. 5b, the current leading area of the protrusion tip is in the order of some μm^2, the predischarge current lies in the range of some µA. This gives current densities in the order of $\mu A \mu m^{-2}$ or

100 Acm^{-2}. In the considered cases the macroscopic field gradient lies in the order of hundreds of $kVcm^{-1}$. The microscopic field gradients at the protrusion tips are without doubt greater than the macroscopic ones. If a microscopic field gradient of 500 $kVcm^{-1}$ is choosen the power density in the vicinity of the tips of predischarge current leading cathode protrusions is in the order of 500 $kVcm^{-1} \cdot 100\ Acm^{-2} = 50{,}000\ kWcm^{-3}$. If heat losses by diffusion and convection are neglected, the temporal temperature increasing rate $\partial T / \partial t$ is given by

$$\frac{\partial T}{\partial t} = \frac{P_m}{c_p} \qquad (2)$$

where

c_p = specific heat capacity of air

With P_m is 50,000 $kWcm^{-3}$ and c_p(20bar) is $2.6 \cdot 10^{-2}\ Wsec^{o}K^{-1}cm^{-3}$ $\partial T / \partial t$ has the value of approximate 2000 $^{o}K\,sec^{-1}$. This very simple model shows the possibilty of thermic processes in the vicinity of cathode surface protrusions.

THE INFLUENCE OF THERMIC PROCESSES ON THE BREAKDOWN VOLTAGE

The local heating of the insulation medium air causes a density reduction of the gas leading to greater ionization coefficients in this region as well as to a heating and destruction of the protrusion tips, see ref.[13], fig.5. Thermoemission by the "hot" protrusion tips must be assumed. An attempt to compute approximate the influence of the air density lowering in the vicinity of a cathode protrusion on the breakdown voltage is displayed in the discussion of ref.[13]. This computation showed that the breakdown voltage reduction by the gas density lowering due to the predischarge currents is some times greater than the breakdown voltage lowering caused by the intensified ionization due to the field enhancing protrusion.

CONCLUSION

This paper shows that thermic processes in the vicinity of electrode surface protrusions may considerably reduce the dielectric strength of compressed air. This knowledge leads to theoretical considerations, of ways in which the dielectric strength of electrode configurations with compressed air insulation may be improved; for instance by coating of the electrodes or by adding electronegative gases to the air.

ACKNOWLEDGEMENT

The author thanks Prof. Dr. W. Zaengl and Miss C. Zinsli for their support of this work.

REFERENCES

1. A. H. Howell, Trans. A.I.E.E. 58, 193 (1939)
2. M. J. Sysoev and V. V. Jakovlev, 1st Int. Conf. on Gas discharges, 485 (1970)
3. J. G. Trump, R. W. Mann, J. G. Cloud and E. P. Hanson, Elec. Eng. 69, 961 (1950)
4. S. Berger, 4th Int. Conf. on Gas discharges, 98 (1976)
5. H. M. Ryan and G. Spence, 2nd Int. Symposium High Volt. Techology, 17 (1975)
6. A. Boulloud, Ann. de Phy. 8(12), 909 (1953)
7. M. N. Félici and Y. Marchal, Rev. Gen. de L' Elec. 57, 155 (1947)
8. A. H. Cookson, Proc. IEE 117, 269 (1970)
9. A. Pedersen, IEEE Trans. PAS 94, 1749 (1975)
10. C. M. Cooke, IEEE Trans. PAS 94, 1518 (1975)
11. V. A. Avrustskii, Sov. Phy. - Tech. Phy. 18, 389 (1973)
12. W. Zaengl und R. Baumgartner, ETZ-A 96, 510 (1975)
13. S. Berger, IEEE Trans. PAS 96, 1179 (1977)
14. S. Berger, IEEE Trans. PAS 95, 1073 (1976)

DISCUSSION

MALIK: You mentioned that in the case of positive polarity, no pre-breakdown current was observed. Did you observe higher breakdown gradients in that case as compared to the case when protrusion was located on the cathode?

BERGER: At positive polarity of the electrode with the protrusion the pre-current pulses occurred at much higher voltages. The breakdown voltage of the positive rough electrode was some 10% higher than in the case of the negative rough electrode.

TAKUMA: I strictly agree with you that such a calculation is permitted only for the field without space charge. You showed very sharp pre-current on your slide. The first question is: Isn't this current caused by the ionization multiplication (corona onset)? The second question is: Shouldn't you apply the calculation to this pre-current onset voltage?

BERGER: The pre-current pulses are caused by ionization processes. On the other hand, an electron emitting process which supplies electrons to start the pre-current pulses is necessary. The answer to the second question is: A calculation of the onset-voltage of the pre-current pulses is possible if it is possible to calculate the field pattern in the vicinity of the surface protrusions.

DEVELOPMENT OF RADIOGRAPHIC PARAMETERS FOR EVALUATION OF ENERGIZED COMPRESSED GAS-INSULATED SYSTEMS

R.C. Lawrence
S.R. Doctor
E.C. Martin

Battelle-Northwest, U.S.A.

This paper discusses a feasibility study for the development of radiographic parameters for evaluation of energized compressed gas-insulated systems. It is vitally important for any utility to maintain mechanical and electrical integrity. To assist the utilities in meeting this challenge, we at BNW were requested by the Bonneville Power Administration to conduct a feasibility program for which we have slides and photos of work completed January 31, 1978. The research program was directed at measuring and evaluating potential degradation or decomposition of SF_6 and mixture of 50% SF_6 and N_2 in a radiation field such as would be used in radiography. The intent of the program was to assess the feasibility of radiography for use as a tool to evaluate the status of compressed gas-insulated components without dismantling.

A 25,000 curie ^{60}Co source and a Norelco-Phillips 300 kV x-ray generator and iridum-192 100 curie source was used to irradiate a test cell containing a point-plane high voltage electrode configuration. The temperature and pressure of the gases were monitored as well as corona with a standard differential amplifier technique. Gas samples for non-energized, energized pre-irradiation, post irradiation and control were analyzed using a gas chromatograph and mass spectrometer.

The experimental design set the high voltage within 3 to 4% of sparking with the point in corona. The irradiation was then performed at dose rates far greater than those typically used for making radiographs. In addition, total doses exceeded by a factor of 1 to 1000 those anticipated for using radiography as a maintenance tool in which 10 shots per year for 30 years was the reference.

In all the experiments the gas breakdown voltage was not lowered as a result of exposure to x-rays or gamma rays. Gas analysis determined no significant changes in the SF_6. For the control sample receiving over 1.2×10^7 rads of x-ray and gamma radiation, the largest chemical change measured was a doubling increase in SF_4 concentrations. This evidence clearly supports the conclusion that radiography can be employed to evaluate the status of energized gas-insulated equipment.

NOTE: Our conclusions are further justified by analytical work reported by H.H. Hubbell in L.G. Christophorou et al, High Voltage Research, (Semi-Annual Report, April 1 - September 30, 1977) ORNL - TM - 6133 (November 1977).

DISCUSSION

COOKSON: Does the radiation required for the x-ray inspection techniques cause any degradation of the material for the support insulators, either for the surface flashover or the volume internal strength? Is the corona onset voltage affected by the radiation? Can the technique detect a single flashover?

LAWRENCE: There is no evidence to date for all components of CGIS but a study was done at Battelle for components of high pressure oil filled cable such as (tape carbon) sheath, various plastics, and including oil. Using mechanical testing methods such as used in metallurgy, we detected no gross amounts of degradation. Yes, the corona from a point electrode was reduced as the irradiation was started. We have not attempted to radiograph a single flashover. However, it does appear possible with a radiation source of a size selected to provide a fast exposure such that the flashover duration is a significant portion of the film exposure time duration. It is our feeling that R&D is required to expand the capabilities for all CGIS components made by various manufacturers.

ELECTRIC FIELD PROBE AND BREAKDOWN VOLTAGE MEASUREMENTS USING IMPULSE VOLTAGES IN SF_6 AND SF_6/N_2 MIXTURES AT PRESSURES UP TO 8 BAR

E. A. Hamouda, F. Gabris and P. A. Chatterton
Department of Electrical Engineering and Electronics,
University of Liverpool, P.O. Box 147, Liverpool L69 3BX, U.K.

Higher values of A.C. and impulse breakdown strengths for certain SF_6/N_2 mixtures as opposed to pure SF_6 have been reported[1][2] for non-uniform field systems at high gas pressures, though no detailed explanation has yet been advanced for this effect. Enhanced values of the breakdown strengths are also observed in the present work using impulse voltages and a protrusion distorted uniform field system. The initially uniform field electrode geometry used had a 6.35 mm long hemispherically capped cylindrical protrusion attached centrally to one electrode. Two protrusion radii were used (0.5 mm and 0.1 mm). The breakdown results show four main features. For the smaller radii point it is shown that

(1) A peak occurs in the breakdown voltage composition curve for a mixture of 80-70% SF_6 20-30% N_2 at high gas pressures (≈ 8 Bar)

(2) A decrease in the breakdown voltage occurs when small concentrations of SF_6 are added to N_2 at high pressure

(3) An increase in the breakdown voltage occurs when small concentrations of SF_6 are added to N_2 at low pressures (2 - 3 Bar). When the radius of the protrusion is increased it is found that

(4) The main effects listed under (1),(2) and (3) still occur but the magnitudes of the effects are diminished. The breakdown voltages are shown not to be predicted on the basis of the streamer onset theory. This might be expected since for sufficiently distorted field systems the theory should only predict the corona onset.[3][4] Electric field probes[5] were used to measure charge injection into the electrode system being investigated at times prior to breakdown using the 1/50μs test waveform. The results taken show that for the positive point no detectable charge injection was observed about 5 Bar in pure SF_6, whereas for the negative point charge injection was apparent up to 8 Bar. In the case of

a 20% N_2/80% SF_6 mixture however charge injection for positive and negative points was measured up to 8 Bar. The charge injection onset voltages can be associated with impulse corona onset voltages and are shown to agree well with the streamer onset theory in SF_6 but not in the SF_6/N_2 mixture. These results suggest that the enhanced breakdown performance is probably due to a form of corona stabilisation and that simple techniques[4][6] for calculating streamer onset voltages in gas mixtures may be unreliable. The extent of the corona cloud is shown to be small so that only very small protrusions would be expected to exhibit the large improvements in insulation level.

References

1) T. Watanabe and T. Takuma, J. Appl. Phys. 48, 3281-3287 (1977).

2) O. Farish, S. J. Dale and A. M. Sletten, IEEE PAS 95, 1639-1647 (1976).

3) T. Nitta and Y. Shibuya, IEEE PAS 90, 1065-.070 (1971).

4) O. Farish, O. E. Ibrahim and B. M. Crichton, Proc. IEE 123, 1047-1056 (1976).

5) E. D. Hamouda, Proc. IEE 117, 653-659 (1970).

6) M. Ermel, Elektrotech. ZA96, 231-235 (1975).

DISCUSSION

MILCAHY: If you get an increase in breakdown voltage-sharp peak - by addition of ~10% N_2 to SF_6 - why do you not get a further increase when you add more N_2?

CHATTERTON: We have no proven understanding of this problem. However it is not difficult to see that the addition of N_2 to SF_6 may have two effects: (1) to improve charge injection and corona stabilization and (2) to reduce the intrinsic uniform field strength of the SF_6. The peak therefore may be considered as a reflection of these two competing processes.

FARISH: Did you record time lags to breakdown and if so, can you say whether breakdown occurred on the wavefront or wavetail for pure SF_6 and for the SF_6/N_2 mixtures which showed the highest impulse strength?

CHATTERTON: No detailed studies of time lags to breakdown were performed. However, the determination of V_B consisted of measuring the actual value of the voltage at breakdown for every waveform. All the breakdowns in this instance occurred at the peak of the impulse wave for the 0.2 m diameter protrusion.

IMPULSE AND AC BREAKDOWN CHARACTERISTICS OF SF_6 WITH BARE AND COVERED ELECTRODES

Antonios E. Vlastós and Sune Rusck
The Royal Institute of Technology, S-100 44 Stockholm, Sweden

The impulse and AC (one minute) breakdown voltage and the breakdown probabilities of SF_6 and air were examined in a coaxial cylinder electrode configuration (electrode diameters 70/30 mm, length 250 mm) with bare or coated inner electrode in the pressure range of 1-9 bar_a (0.1-0.9 MP_a). The main purpose of the work was to study the influence of thin epoxy or aluminum oxide coatings on the breakdown voltage of SF_6 and air and the influence of previous voltage applications and breakdowns on the breakdown probabilities of these gases.

The AC breakdown voltage was determined by the one minute test procedure in which the voltage was first raised to a value corresponding to about 80 % of the expected breakdown voltage at a rate of 2-3 kV/s and later raised in small steps corresponding to 2-3 % of the applied voltage at intervals of 1 minute. The results obtained show that, when the first breakdown on a new pair of steel electrodes is considered the one minute AC breakdown voltage for SF_6 and air is improved appreciably by coating the inner electrode with a thin epoxy coating adhering to the electrode. It was found that the improvement of the 1 minute AC breakdown voltage by coating the inner electrode is higher for rough electrodes than for smooth (polished) electrodes and can be of the order of magnitude 30 % or higher. However, if one considers the mean value of the breakdown voltage obtained from a series of measurements on the same electrode pair and then compares the results obtained with a bare and with a coated inner electrode, one may find the influence of the electrode coating on the breakdown voltage confusing. The reason for this confusion seems to be the successive improvement of the breakdown voltage in the case of the bare electrodes which is due to the spark conditioning and on the other hand the successive reduction of the breakdown voltage for the covered electrodes which is due to the perforations of the coatings caused by previous breakdowns. This may be the reason for the contradictory results reported by different researches on the influence of the electrode coating on the breakdown of SF_6.

The impulse breakdown voltage in the present work was determined by applying a set of impulses at a particular voltage level followed by similar sets at increasing voltage levels until breakdown occurred. Sequential tests in which the voltage level for a particular trial is determined by the outcome of the previous trial (up-and-down method) or tests with linearly increasing voltages leading each time to breakdown were found unrealistic since they do not allow a direct comparison of the breakdown voltages obtained with bare and covered electrodes because the breakdown voltage of covered electrodes is modified by the perforations due to breakdown.

The results reported in this paper refer mainly to measurements performed with negative standard lightning impulses (1.2/50 µs) on steel or aluminium electrodes in the pressure range of 1-7 bar_a. Comprehensive measurements were also performed with other impulse voltage forms [0.5/50 µs, 0.5/(50)6 µs (a 0.5/50 µs impulse chopped after 6 µs), 0.5/(50)1.5 µs, 1.2/(50)6 µs and 1.2/(50)2 µs impulses] and with positive impulse voltages at a pressure of 5 bar_a. Since the perforation of the coatings may, as already mentioned, be crucial for the outcome of the results the impulse breakdown strength for both bare and covered electrodes was determined starting with a set of 100 impulses at a voltage level leading to breakdown probabilites lower than 1 % and followed by similar tests at increasing voltage levels with steps of 1-2 % of the previous voltage level until breakdown occurs. At voltages leading to higher breakdown probabilities the number of impulses was reduced to twenty. When a breakdown probability higher than 95 % was reached the voltage was reduced successively until the breakdown probability was reduced to values below 5 %. However, this procedure has a drawback: the low probability impulse breakdown voltage improves due to a voltage conditioning caused by the successive application of the impulse voltage. This improvement was verified for both bare and coated electrodes. Additionally it was found that after the first breakdowns the breakdown probability increases rapidly to high values. A decrease of the voltage level after reaching a high breakdown probability does not lead immediately to a decrease of breakdown probability. As a consequence the plots of the breakdown probability versus the crest value of the applied impulse voltage show a hysteresis effect. The form of the hysteresis loop may change shape in subsequent series of measurements on the same electrode pair and in measurements on identically prepared electrodes depending on the number of applied pulses not leading to breakdown and the appearance of the first breakdown.

The results obtained with polished bare steel electrodes with negative voltage impulses 0.5/50 µs and 1.2/50 µs show that the breakdown happens at the tail of the voltage impulse and that the breakdown voltage for these two impulse shapes is not appreciably different.

The results obtained by chopping the 0.5/50 µs impulse after 6 respectively 1.5 µs and the 0.5/50 µs impulse after 6 respectively 2 µs show an increase of the breakdown in the order of 10 %. The results obtained with steel electrodes covered by thin epoxy coatings show that the breakdown voltage improves appreciably and that the breakdown occurs near the crest of the applied impulse. Therefore chopping the impulses after 1.5-6 µs does not lead to a further improvement of the breakdown voltage. The experiments were repeated with an inner electrode of relatively pure commercial aluminium and of an aluminium-copper alloy (5 % Cu). The results obtained with bare polished commercial pure aluminium inner electrode and with identical electrode which was oxidized show a significant improvement higher than 20 % of the breakdown voltage due to the oxide layer on the electrode. The breakdown voltage of the bare aluminium-copper alloy electrode was found to be higher than for the pure aluminium approaching that of the oxidized electrode. However, an oxidizing of this electrode gives only a limited improvement of the breakdown voltage. This may be due to the ineffectiveness of the applied method of oxidizing the aluminium in the presence of copper and in getting homogeneous oxide

layer on the electrode. For oxidized electrodes the deterioration of the oxide layer by previous breakdown was limited and the pronounced hysteresis loop observed with epoxy covered electrodes was limited.

Repeated sets of measurements on the same electrode pair with an oxidized inner electrode led to almost the same results as those obtained when the electrode was new.

Measurements with positive polarity lead to higher breakdown voltages both for bare and covered electrodes.

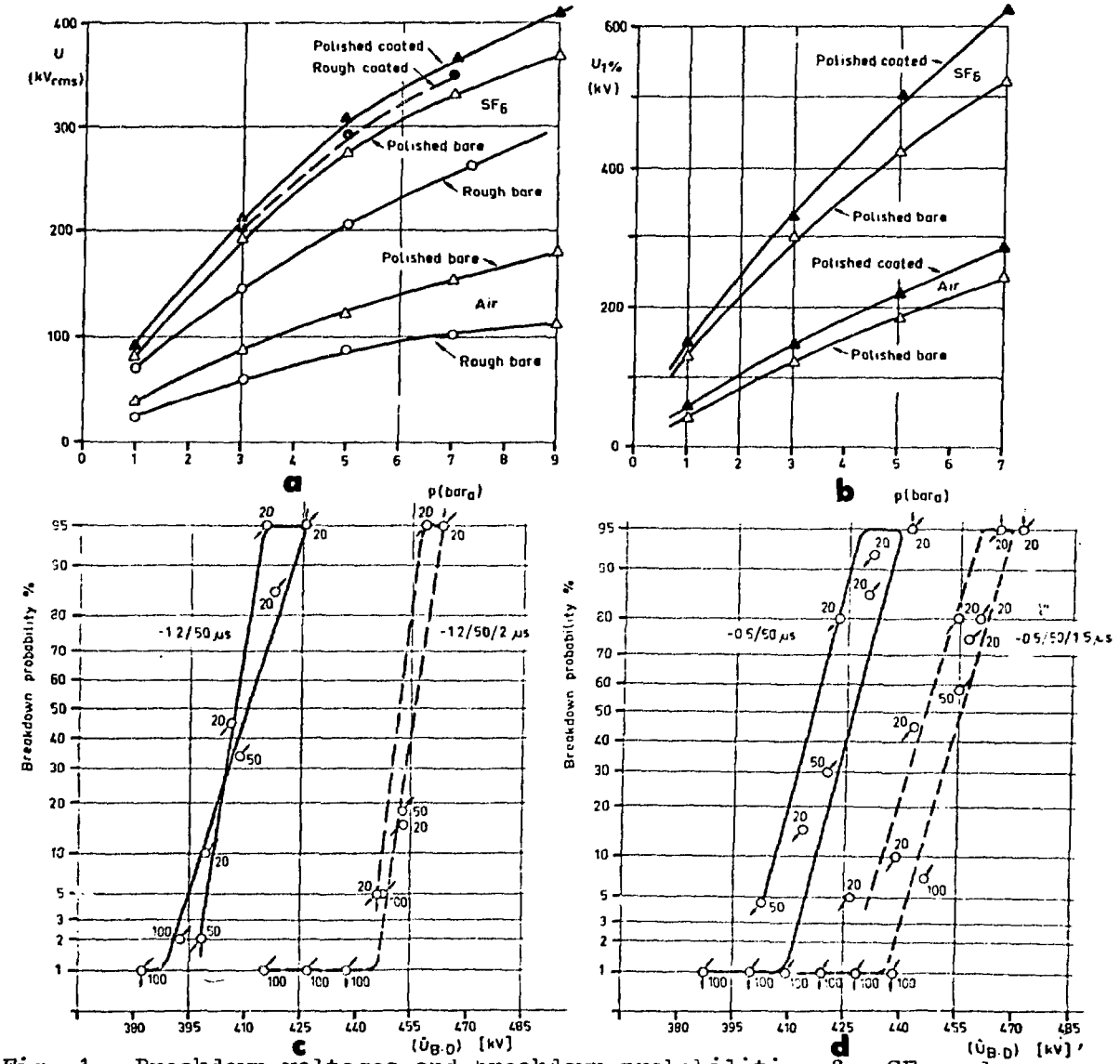

Fig. 1. Breakdown voltages and breakdown probabilities for SF_6 and air for 70/30 mm coaxial cylinder steel electrodes with bare and epoxy resin coated inner electrode. a. AC breakdown voltages. b. 1 % negative lightning impulse (1.2/50 µs) breakdown voltages. c. Breakdown probabilities at 5 bar_a (bare electrodes) for negative 1.2/50 µs (chopped) impulse voltages. d. Breakdown probabilities at 5 bar_a (bare electrodes) for negative 0.5/50 µs and 0.5/(50)1.5 µs (chopped impulse voltages).

DISCUSSION

DALE: Have you tried pre-stressing of the electrodes without breakdown by DC or AC and then determined the probability distribution? Such pre-stressing may give a distribution closer to that first shown in your results.

VLASTÓS: We have done some pre-stressing of the electrodes without breakdown by AC and then we tried to determine the probability distribution. The pre-stressing gave a distribution which was close to that obtained when we obtained the distribution by applying many impulses at different voltage levels starting from low voltage levels not leading to breakdown. However, one has to remember that our purpose was to study the influence of coatings on new electrodes which were not deteriorated (conditioned) either by spark or long term voltage conditioning. In this respect our measurements are different from those presented previously by other authors.

DAKIN: How was the oxide coating achieved--by anodization or high temperature air oxidation?

VLASTÓS: The coating was achieved by anodization using the same method to oxidize domestic aluminum.

COOKSON: We found (Macalpine and Cookson, Proc. IEE,1970) in studies of the effect of electrode coatings on the first impulse breakdown value in N_2 and SF_6 at 15 atm that there was a dependence on the coating material, which we placed on the center conductor of a coaxial geometry. Also there was an increase in the positive and negative impulse breakdown

field in SF_6, but only for the negative value in N_2. Have the authors noted similar effects?

VLASTÓS: We found that for pressures 1 to 9 bar (absolute) the impulse breakdown voltage by coating the center electrode was improved for both positive and negative polarities; the improvement has been much greater for the negative polarity than for the positive. This was observed both for air and SF_6

ON THE BREAKDOWN MECHANISM OF AIR IN UNIFORM AND NONUNIFORM FIELDS

M. Abdel-Salam
High Voltage Institute, Technical University, Munich, W. Germany

ABSTRACT

For uniform fields: A method is described for computing the spark-breakdown voltages in air. The method is based on the formulation of the physical processes that govern the growth of the streamer towards the anode (positive-streamer) or to the cathode (negative-streamer). Therefore, two criteria are considered for evaluating both the positive- and negative-breakdown voltages. For nonuniform fields: A method is also described for computing the positive inception voltages of both the burst-pulse and the onset-streamer, being observed experimentally in air at inception. Different from the positive case, Trichel pulse is the only mode of negative corona at inception. Therefore, a method based on the condition necessary for the Trichel pulse to be self-recurred is suggested for computing the inception voltages of negative corona.

CRITERIA OF BREAKDOWN

In Uniform Fields

Breakdown is Materialized by Positive-Streamer

Assuming that an electron starts to propagate from at the cathode,(Fig. 1a) it creates a primary avalanche with N_e electrons at its head. The head is assumed[1] spherical with equivalent radius R. The ion density within the head of the primary avalanche equals $N_e(x)/(4\pi R^3(x)/3)$. Simultaneously with the creation of the avalanche, photons have been produced in proportion to $N_e(x)$. The rate of production of photons increases fast as the avalanche progresses towards the anode. Within the ionization zone, the cathode is only irradiated by a negligible fraction of these photons. Most of the photons get absor-

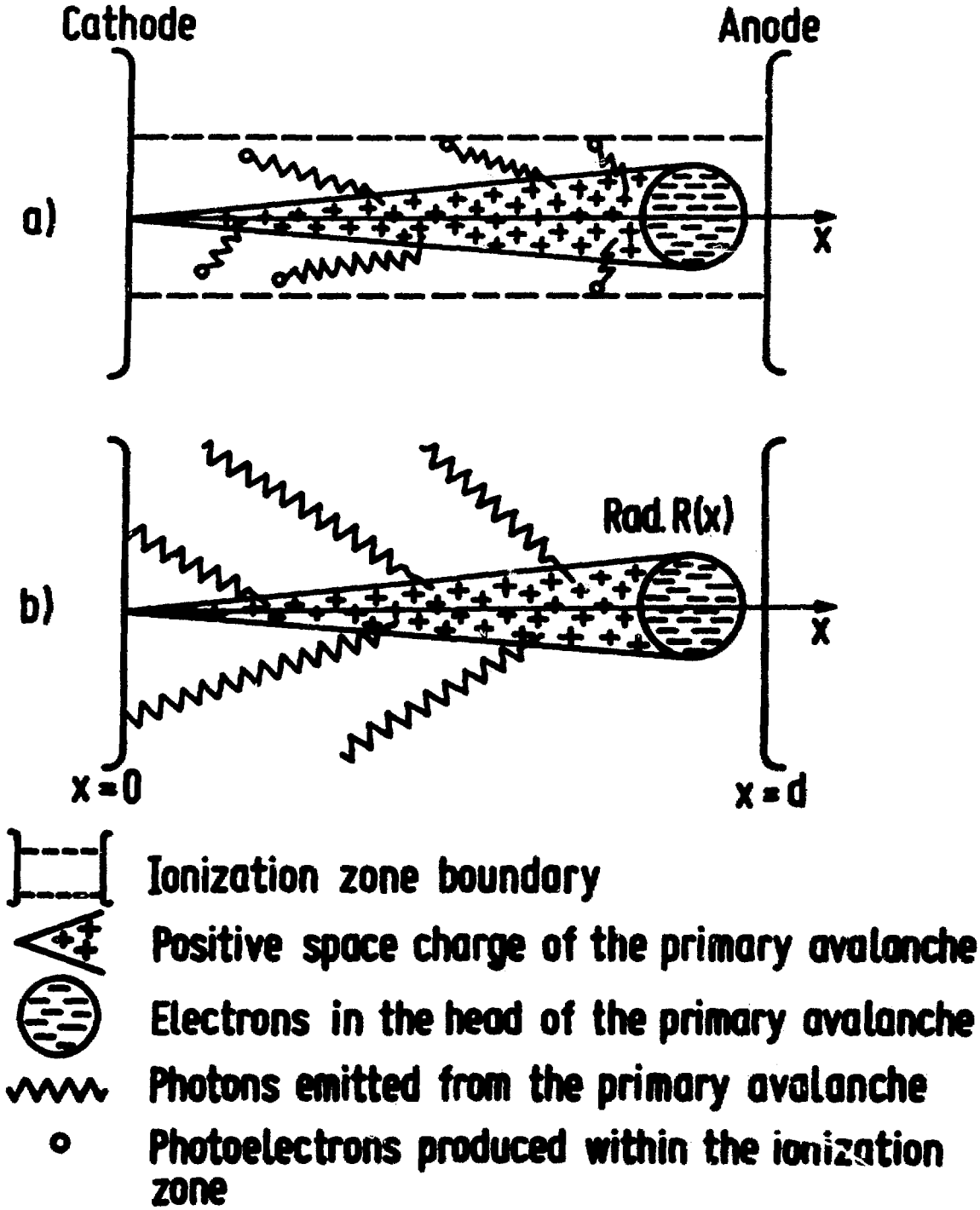

Fig. 1. A schematic diagram illustrating the development of an avalanche to (a) a positive-streamer or to (b) a negative-streamer in uniform field.

bed by air molecules and some of them lead to photoionization. Each photoelectron produced within the ionization zone will be accelerated by the prevailing field strength from its point of origin and starts one avalanche of the succeeding generation. When the ion density of the second generation equals that for the primary avalanche, the applied voltage is the breakdown value[2].

Breakdown is Materialized by Negative-Streamer

In this case, the primary avalanche propagating towards the anode,(Fig. 1b) emits photons, meanwhile with increased distance from the cathode the latter receives a smaller percentage of these photons. This results in photoemission of electrons from the cathode to start successor avalanches that form the second generation. For negative streamer to propagate the growth of the primary avalanche as a whole succeeds[2] to produce one photoemitted-electron from the cathode. Then, the applied voltage is the breakdown value.

Breakdown at High Pressures

The breakdown voltage is known to increase with the pressure linearly up to a critical value[3]. Above the critical value the ratio of the prevailing field strength to pressure becomes so low[4] that $\eta > \alpha$; η and α are the attachment and ionization coefficients. Therefore the breakdown cannot take place except through a consideration of electrons emitted from the cathode. If one of the emitted electrons succeeds[4,5] to reach the anode the gap is short-circuited by dense electrons and negative ions that form a conducting channel between the electrodes, the applied voltage is then the breakdown value. In Fig. 2, the negative breakdown voltages agree with experiment[6] in comparison with those positive-computed. It is satisfying to observe that the computed positive and negative values put the limits that bound the measured values. Such values depend on the electrode material, surface condition and air pressure.

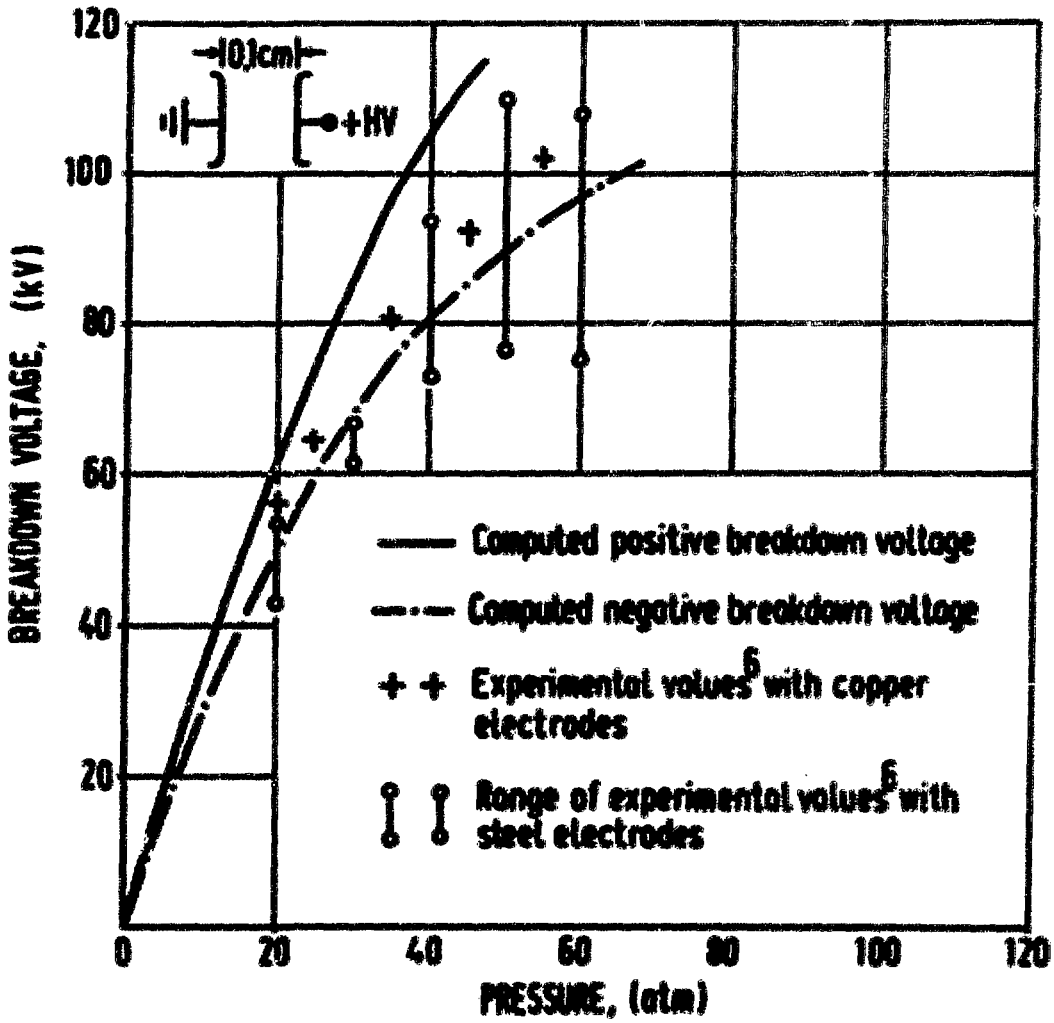

Fig. 2. Computed positive and negative breakdown voltages of a uniform field gap against the experimental values[6].

In Nonuniform Fields

Inception Voltage of Burst-Pulse

The electron triggering the primary avalanche is assumed to grow along the gap axis from the ionization-zone boundary (α$\hat{\gamma}$). The criterion for burst-pulse inception is suggested as: During the growth of the primary avalanche, the ionization zone boundary must receive photoelectrons of the same number as that starting the primary avalanche. The number of photoelectrons is corrected to account for the fact that the greater the angle θ, the smaller the size of the avalanche (Fig. 3a). The validity of this criterion is checked by comparing the computed values with those measured[8], Fig. 3b.

Inception Voltage of Onset-Streamer

For the onset-streamer to propagate, the number of positive ions developed by the primary avalanche must be sufficient to produce[7] a radial field of the same order as the applied field. The photoelectrons produced in the immediate vicinity of the primary avalanche will be drawn into it, Fig. 3c, and will not be directed to the anode. This yields for the streamer to grow along the gap axis. A comparison between the computed and measured[9,10] inception voltages is made in Table 1.

Inception Voltage of Trichel-Pulse

The condition of self-sustenance of Trichel pulses is identical to that of the uniform field, each electron must -by photoemission from cathode surface- provide[11] for a successor. In Fig. 4, the inception voltages measured[12] are lower than those computed because the hv conductor was assumed to be perfectly smooth cylinders in the computation.

CONCLUSIONS

1. The computed positive- and negative-breakdown voltages in uniform fields bound the experimental values that depend on the electrode material, surface condition and air pressure.

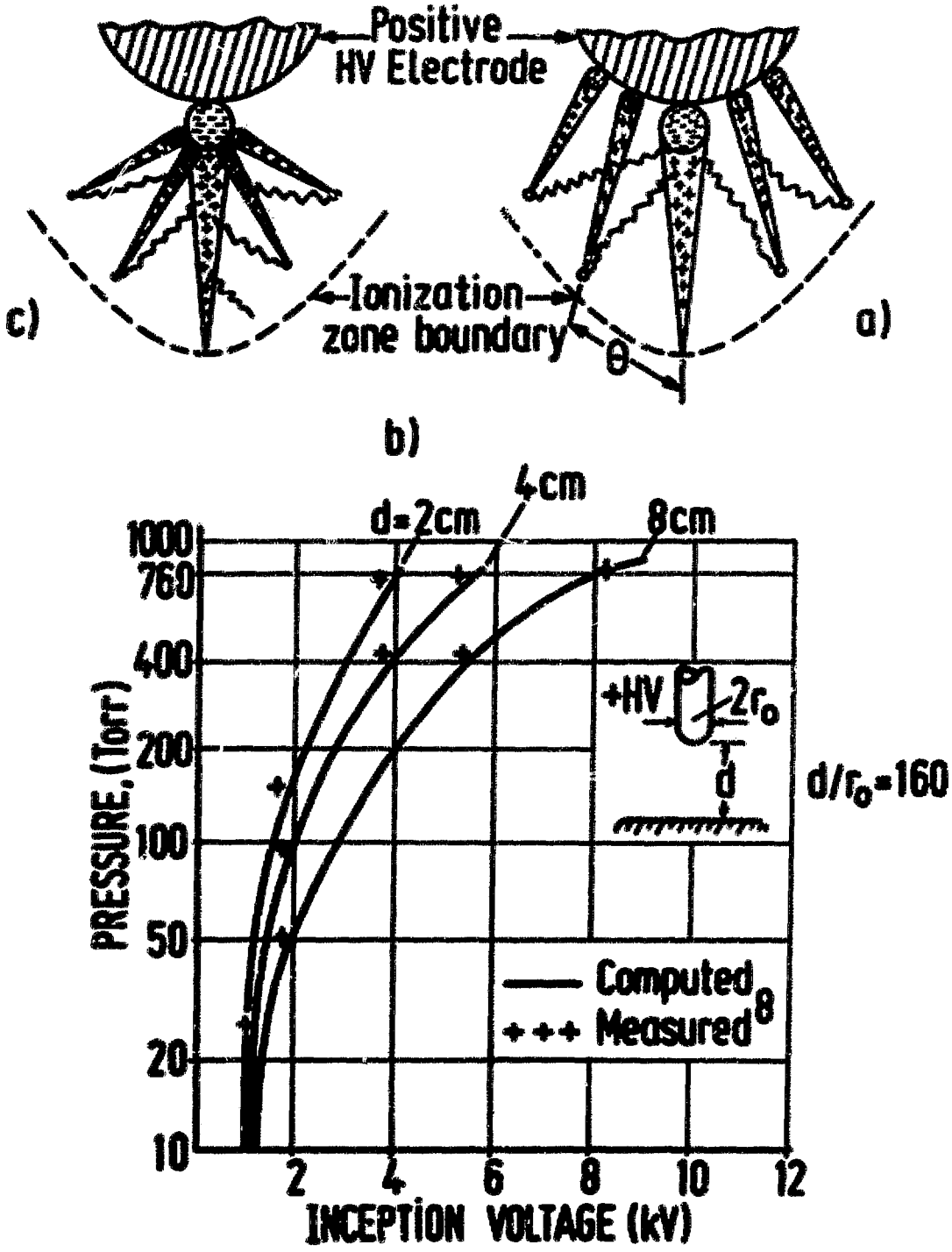

Fig. 3. Illustrating the growth of both the primary avalanche and its successors to sustain (a) a burst-pulse or (b) an onset-streamer. Part (c) is to report a comparison between the computed and measured[8] values of burst-pulse inception voltages.

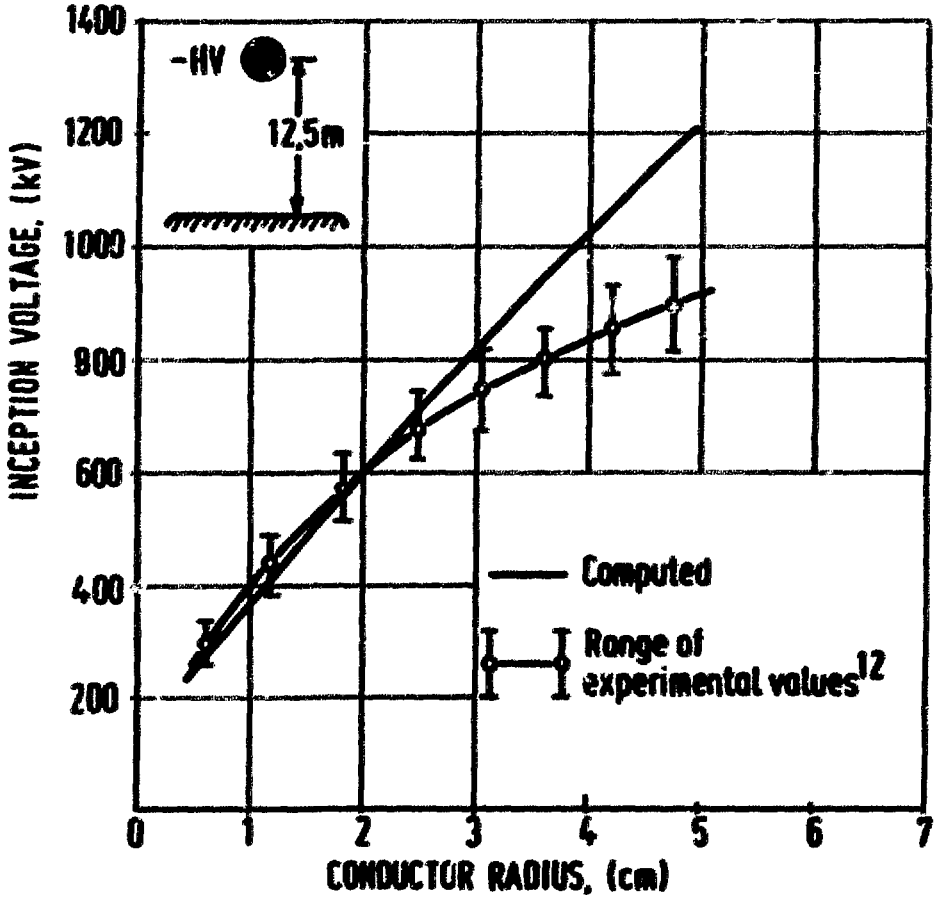

Fig. 4. Negative corona inception voltage for a full-scale test line; computations versus experiment[12].

2. The computation of the inception voltages of breakdown in uniform and nonuniform fields of both positive and negative polarities is based purely on the theory of gas discharges.

Table 1. Inception Voltages of Onset-Streamer for Rod-Plane Gaps(r_o=rod radius and d=gap length)

r_o	Inception Voltage		d/r_o	Reference
	Measured	Computed		
0.100	11.7	12.2	40	9
0.125	13.6	14.1	40	9
0.300	22.5	23.5	10	10

ACKNOWLEDGMENT

Dr. Abdel-Salam is with the High Voltage Institute, TU Munich, W. Germany. He is now on leave from Assiut University, Assiut, Egypt. He wishes to acknowledge Prof. Dr. Boeck, the Head of the Institute, for his interest. Also, the author is grateful for the financial support he received from Alexander-von-Humboldt Foundation.

REFERENCES

1. L. B. Loeb, Electrical Coronas, p. 65, Berkeley, Univ. of California Press, 1965.
2. M. Abdel-Salam and M. Abdellah, Acta Physica, 40,155(1976)
3. J. D. Cobine, Gaseous Conductors, p. 168, Dover, New York, 1958.
4. M. Abdel-Salam and M. Abdellah, IEEE Trans., IA-13(1977).
5. M. Khalifa, M. Abdel-Salam, R. Radwan and Kh. Ali, IEEE Trans., PAS-96,886(1977).
6. E. H. Cohen, Proc. IEE, 103A,57(1956).
7. M. Abdel-Salam, A. Zeitoun and M. El-Ragheb, IEEE Trans., PAS-95,1019(1976).
8. H. W. Bandel, see Ref. 1, p. 109-110.
9. M. R. Amin, J. Appl. Phys., 25,358(1954).
10. Y. Miyoshi and T. Hosokawy, J. Phys. D., 6,730(1973).
11. M. Khalifa, M. Abdel-Salam and M. Abou-Seada, IEEE paper C 73-160-9,1973.
12. W. Mosca, P. Ostana and G. Rumi, IEEE Trans. PAS-90,138 (1971).

DISCUSSION

DUTTON: I would like to suggest that we should stop making qualitative speculations about the effect of space charges linked with photoionization in cases where quantitative calculations are now possible. Such speculations can be misleading. For example, it is now well known that (i) static breakdown in uniform electric fields involves cathode processes even at high values of Pd and (ii) that under impulse over-voltage conditions where space charge becomes significant, detailed calculations show that the space charge field is not well represented by that due to a sphere of charge.

ABDEL-SALAM (response obtained by correspondence): The discusser stated that the static breakdown in uniform electric fields involves cathode processes even at high values of Pd. This agrees with what is outlined in the paper. At high pressures that exceed the critical value, the ratio of the prevailing field strength to pressure becomes so low that the attachment coefficient exceeds that for ionization. Therefore, the breakdown cannot take place except through a consideration of electrons emitted from the cathode. Such emission is a cathodic process, being accounted for within two views (see Ref. 4 in the paper). The first is a macroscopic view, in which the field emission takes place from the cathode surface as a whole with the cathode field being equal to the applied value. The second view is a microscopic one, in which the emission takes place from localized sites on the cathode surface. The field values at such sites are orders of the applied value.

Regarding the simulation of the space-charge field, the author assumed a spherical shape for the positive-ion cloud at the primary-

avalanche head. This assumption is generally valid and commonly adopted in the literature (see Ref. 1 in the paper). Recently these positive ions were represented (M. Khaled, ETZ-A, Vol. 95, pp. 369-373, 1974) by a number of ring charges. A comparison of the two approaches is given in Fig. 5, which gives the field values due to the positive ions left by the primary-avalanche in a rod-to-plane gap. The comparison is conducted along

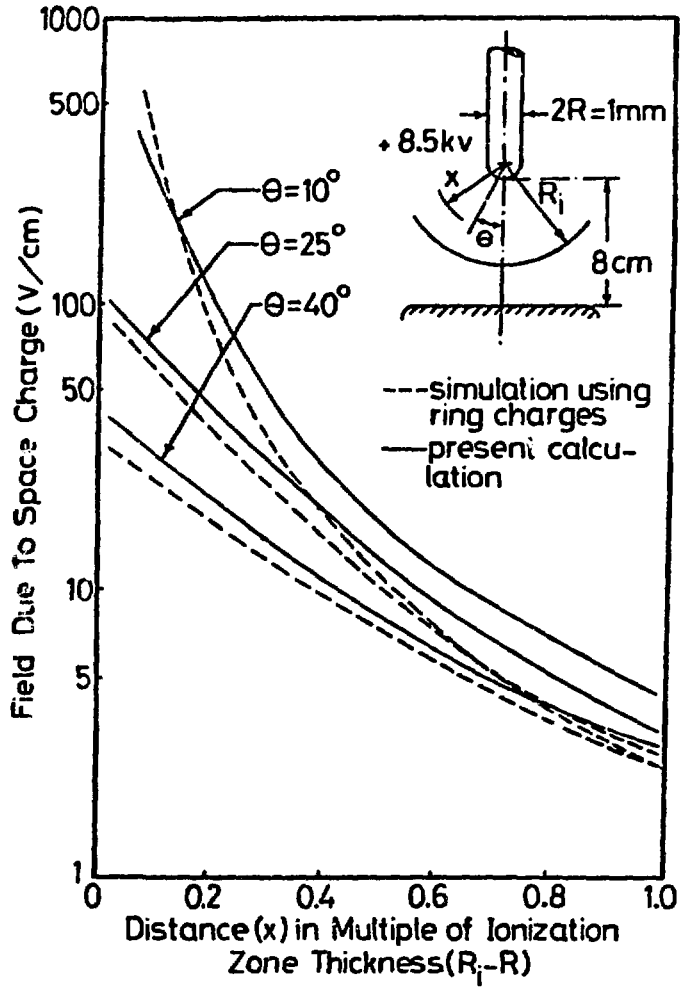

Fig. 5. Field due to space charge left by the primary avalanche.

different directions, Θ, within the ionization zone. For the values in Fig. 5, five ring charges are considered to represent the positive ions that left in wake of the primary avalanche, the rings are with charges given in Table 2. The data in Table 2 show that the last ring mainly

Table 2: Charge distribution over the rings that simulate the positive ion cloud left by the primary avalanche

Ring No.	1	2	3	4	5
Charge x 10^{-19} (Coul.)	0.16	0.72	4.96	46.4	4.96×10^{4}

represents the ion cloud. It is rather difficult to make a definite decision about the feasible approach. Certainly, the assumption of spherical cloud representation is simpler and in comparison with the ring representation, it needs shorter computing time. On the other hand, the ring representation (M. Khaled, ETZ-A, Vol. 95, pp. 369-373, 1974) is so simple that it cannot simulate the ion cloud correctly. Actually, the field-induced motion of ions makes the calculations to be time dependent. In this case, the magnitudes of the ring charges are determined by solving a set of equations formulated using suitably boundary conditions. Such a procedure was recently developed (M. Abdel-Salam et al., IEEE-IAS paper, Proc. of the Industrial Society Annual Meeting, Chicago, USA, Oct. 1976, pp. 654-659) to extend the charge-simulation technique for calculating the field due to ionic space charges.

DISCHARGE EXTENSION OF LONG GAPS IN COMPRESSED SF_6 GAS AND GAS MIXTURES

T. Takuma T. Watanabe
Y. Aoshima
Electric Engineering Laboratory, Central Research Institute of Electric Industry, Japan

Discharge characteristics of nonuniform gaps were studied at large electrode separations to 50 cm in SF_6 gas up to about 7 atm and in gas mixtures containing SF_6 at atmospheric pressure. The tested electrode arrangement was a rod-to-plane gap or a small shere-to-plane; i.e. the upper electrode was a square-cross section rod of 1.25 × 1.25 cm, a 2 cm diameter sphere or others. The gap was enclosed in a cylindrical vessel 3.8 m in height and 2 m in diameter.

The breakdown voltage was measured in compressed SF_6 gas with three impulse waves : 1.7 (2.8) × 42 μsec, 35 (50) × 370 μsec and 280 (400) × 2300 μsec expressed as nominal wave front from the 30% ~ 90% method (real wavefront) × wavetail. For extremely nonuniform gaps of the square rod-to-plane, the breakdown voltage of SF_6 gas shows a marked saturation tendency against the electrode separation compared with that of atmospheric air. The SF_6 gas breakdown voltage is about 1.5 to 2 times higher at a 10 cm gap for both voltage polarities than the air breakdown voltage, but it intersects with the latter at about 40 ~ 50 cm for positive polarity and at about 20 ~ 40 cm for negative polarity in all of three tested impulse waveforms. In this electrode arrangement, the negative breakdown voltage is roughly twice as high as the positive. Furthermore, it was found that even if SF_6 gas pressure is raised to about 7 atm, the low breakdown voltage scarcely increases, except for a 280 × 2300 μsec impulse with negative polarity.

For somewhat uniform gaps of the 2 cm diameter sphere-to-plane, the breakdown voltage is much the same with that of the square rod-to-plane for both voltage polarities at atmospheric pressure. However, the positive breakdown voltage increases almost linearly with SF_6 gas pressure. This causes the breakdown voltage with positive polarity to rise higher at pressures above 3 to 5 atm than with negative polarity.

Current oscillograms showed that for the two slower impulse waves, discharge took place briefly only a short period of the impulse duration. Therefore, the time-resolved analysis was performed for a standard impulse voltage with an image converter camera. Voltages near the 50% flashover voltage were always applied. Some characteristic results are summarized as follows:

(a) The discharge channel generally extends with intermittent reillumination (steps) along spatially identical paths in long nonuniform gaps of compressed SF_6 gas.

(b) In these conditions, negatively charged channels are generally brighter than positive ones. Furthermore, they advance more slowly with longer pause times, despite the applied voltage being about twice higher than for positive channels.

(c) With negative polarity, the extension velocity of a channel is typically $3 \sim 4$ cm/μsec in average for 50 cm gaps when it leads to breakdown. This value remains almost constant over a wide range of SF_6 gas pressure up to 7 atm, corresponding to the fact that the breakdown voltage is near 735kV for 50 cm gaps regardless of pressure. Pause times between steps are typically $1.1 \sim 1.6$ μsec at 1 atm, $0.3 \sim 0.5$ μsec at 3 atm and below 0.2 μsec at above 5 atm. This dependence of the pause time on pressure means that the intermittent extension in SF_6 is not caused by the voltage application circuit but by the nature of discharge.

(d) With positive polarity, for 50 cm gaps at atmospheric pressure, the channel extension velocity is in the order of $10 \sim 20$ cm/μsec and the pause time typically $0.1 \sim 0.2$ μsec or shorter. At above 3 atm of a 2 cm diameter sphere-to-plane gap where breakdown occurs at a high voltage without preceding corona discharge, the breakdown is completed almost instantaneously with the discharge occurrence by a luminous, thick channel.

(e) The discharge channel in SF_6 has no broad corona streamer regions as can be seen in discharge figures in atmospheric air or gas mixtures containing a relatively small percentage of SF_6. However, the channel is always the most luminous at its tip. With negative polarity, frequently two luminous points were recorded at one step tip.

(f) Microdischarges appearing apart in front of a channel tip were photographed by still cameras for negative polarity. They are especially distinct for SF_6 gas at below atmospheric pressure and for gas mixtures containing SF_6 and nitrogen.

(g) Current oscillograms showed that with negative polarity, the positive pulsive current flowed on the wavetail of impulse voltages. This is the "back discharge" caused by the reversed field between the upper electrode and space charge in the midgap, when an applied voltage decreases relatively rapidly. The occurrence of the back discharge means that the discharge channel in long nonuniform gaps of SF_6 remains somewhat conductive during several tens of microseconds.

(h) These discharge characteristics in SF_6 have a strong resemblance to those of stepped leaders in lightning discharge. The intermittent channel extension was also observed in gas mixtures of nitrogen-SF_6 and air-SF_6 as well as even in compressed air. However, the time-resolved extension pattern with negative polarity in SF_6 is especially distinct and regular with relatively constant pause times.

DISCUSSION

FARISH: I was very interested to see that the authors have been able to apply time-resolved schlieren techniques to the streamer discharge and to detect the propagation of a relatively small density perturbation. We have used a similar technique for long gaps in air (10-30 cm) although we have used a high-speed camera to record the schlieren image directly, rather than a photomultiplier technique. For such gaps, we have been able to observe the radial development of the leader channel once it has reached ∿0.2 mm diameter, and have found that, while the channel thermal boundary saturates at ∿0.6 mm, a shock wave continues to propagate at 350 m/s, as found by the authors for short-gap streamer. Figure 1 shows the channel with the surrounding shock wave for positive-impulse breakdown of a 10-cm gap. (In this case, the time to breakdown was such that

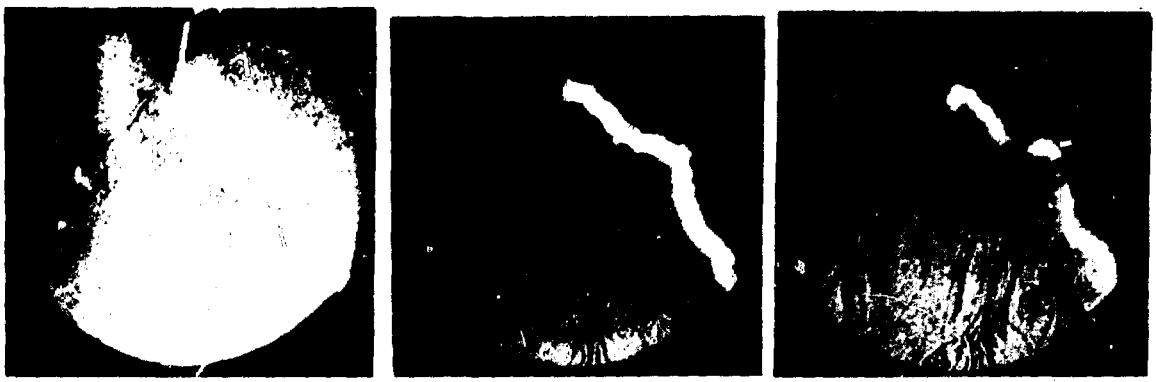

(i) t = 2.8 μs (ii) t = 4.2 μs (iii) t = 12.6 μs

Fig. 1. Leader and spark channel development in a 10 cm gap. Applied voltage: 85 kV (= V_{50}), 2 μs/16 μs impulse.

the main spark channel occurred before the leader channel became detectable by schlieren system so that the spark also appears on the records.) We have used the measured maximum channel diameters to calculate the

times required for the hot channel to cool and have found that after internal rapid cooling to ~2000°, the subsequent cooling to ambient conditions may take ~200 μs: this means that, in the case of long-gap breakdown, where stepped propagation at 10-100 μs intervals is observed, enhanced ionization in the reduced-density columns will have to be considered in any mechanism proposed to explain the intermittent restriking of the leader channel.

DAKIN: In recent photographic studies in our laboratory of streamer propagation in transformer oil, we have observed bright spots at the negative streamer tips--as the authors of this paper see in long gas gaps. There seems to be great similarity between streamer propagation in liquid and in gases.

TAKUMA: In my opinion, the stepwise extension occurs in media where there is much loss during the discharge extension through the gap and especially when the main channel is not guided by the corona streamers, such as in liquids, electronegative gases, or extra-long air gaps (lightning discharge). There is certainly a great similarity between them. Thank you very much for your comment.

DESIGN OF COMPRESSED-SF_6-INSULATED SYSTEMS FOR EHV TRANSMISSION

F.A.M. Rizk C. Vincent
N.G. Trinh C. de Tourreil
Hydro Quebec Institute of Research, Quebec, Canada

ABSTRACT

This paper summarizes the research activities at IREQ, sponsored by the Canadian Electrical Association, in the design and dimensioning of compressed-SF_6-insulated cables for underground transmission at EHV levels. Different aspects were investigated including the selection of epoxy-resin formulations, the design of epoxy spacers and actual testing of real-size coaxial conductors for energy transmission at 550 and 800 kV levels.

SELECTION OF EPOXY FORMULATIONS

Several epoxy-resin formulations, composed of epoxy resin, hardener and alumina filler in different proportions were tested and evaluated for their dielectric and mechanical properties. All formulations are degased and molded under vacuum. Gelling and curing took place at atmospheric pressure. Five different epoxy-resin formulations, supplied by CIBA-GEIGY Corp., were evaluated. The most promising formulation, using 1 pbw of a combined bisphenolic and heterocyclic resin, 1 pbw of hardener and 4 pbw of tabular alumina filler, was selected for the spacer design study. Typical characteristics of this epoxy resin formulation are:

- dry arc resistance (ASTM Test D-495): 192 s at 15 kV
- tracking resistance (ASTM Test D-2303): 3.25 kV (68 min)
- point to plane breakdown voltage (unfilled epoxy): 33 kV, 2.2 mm gap, 50 μm tip radius
- dielectric constant: 5.3 measured at 60 Hz
- dielectric losses (tan δ): $8.6\ 10^{-3}$ measured at 60 Hz
- impact resistance (Charpy test, ASTM Test D-256): 0.18 kg-m (1.3 lb-ft)
- thermal deflection temperature (ASTM Test D-648): 122°C

SPACER DESIGN

Two spacer configurations, namely the cone and disc, were investi-

gated. Calculation of the field distribution along a conical gas-dielectric interface, showed that uniform field distribution along the interface can be obtained for an optimal angle θ between the interface and the conductor (as measured in the dielectric side). For epoxy dielectric, with a relative dielectric constant of $\varepsilon = 6$, the optimal angle is $\theta = 75^{\circ}$. For smaller values of θ, a high field region is formed near the outer envelope; while for larger values of θ, the high field region is located near the central conductor. Disc-shaped spacers are therefore, particularly effective in controlling the uniformity of the field distribution along the spacer interface. Longer creepage distances are readily obtained with cone-shaped spacers, this advantage is however partly attenuated by the poor field distribution along the lower surface of the spacer.

Practical design problems were investigated with small spacers in a 2.54/7.9 cm, 50 cm long coaxial conductor system. Breakdowns were observed to occur along the epoxy interface, initiating from the metal-epoxy-SF_6 junctions. Improvement of the spacer insulation and partial discharge performances were found possible by:

- providing a good bonding between the metal-epoxy surfaces. Vacuum casting is most suitable to eliminate small voids at the metal-epoxy junctions, which are responsible for initiating corona discharges and breakdown of the gap;
- introducing metallic inserts which effectively reduce the local field intensity at the metal-epoxy-SF_6 junctions, and hence prevent the development of corona discharges as illustrated by the results of Fig. 1.

TEST ON REAL-SIZE COAXIAL CONDUCTORS

Insulation tests were performed on coaxial cables of 17.8/53 and 20.3/61 cm, 6 m long, with associated epoxy spacers. Test voltages include standard lightning and switching impulses and 60 Hz ac voltage. The withstand voltage of the test cable was determined using a modified α-β test procedure to minimize the number of flashovers. The expected breakdown voltage U_{exp} of the coaxial cable was estimated from a series of measurements with increasing test voltage. The α withstand voltage U_{α} was determined by the first breakdown in a second series of measurements. The test voltage is raised in step of $\Delta U \simeq 0.02\ U_{exp}$, starting from a level of

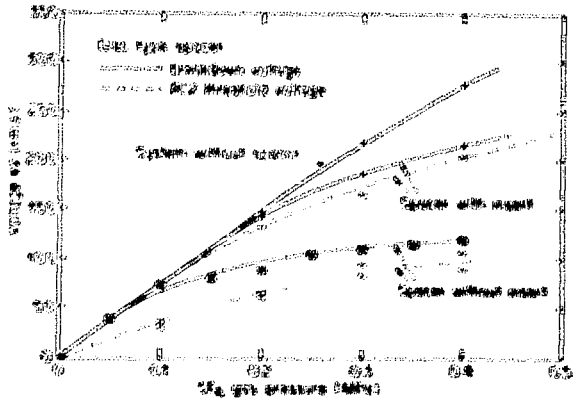

FIG. 1 Improvement of the insulation and partial discharge performances of disc-shaped spacers by the use of metallic inserts

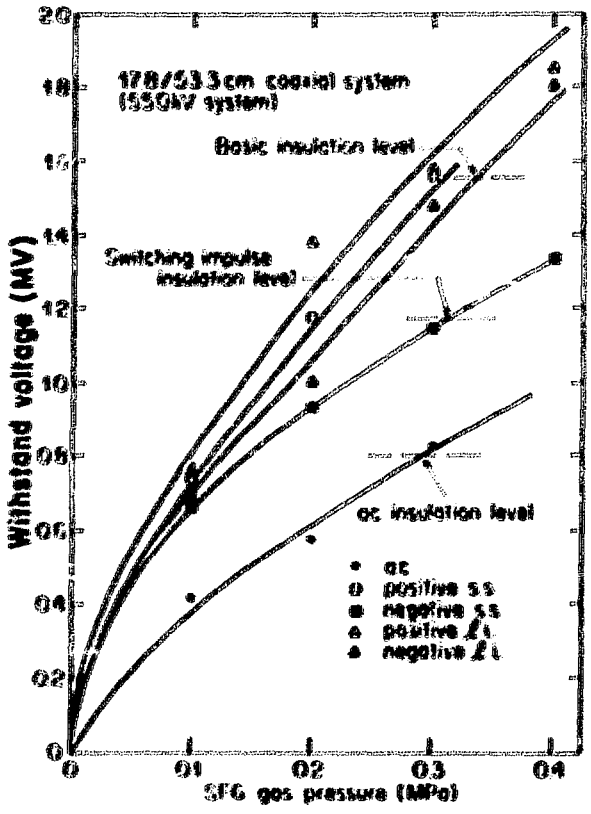

FIG. 2 Insulation performance of 17.8/53.3 cm coaxial cable.

low breakdown probability with three voltage applications at each test voltage level. The 5 withstand voltage U_{5} is determined by a third series of measurements with decreasing test voltages, starting from U_{α}-4% and having 10 voltage applications at each test voltage level. U_{5} is determined as the highest voltage level at which 10 consecutive withstands are obtained. Test results obtained indicate a high degree of consistency in the determination of U_{α}. The relatively greater dispersions in the measurement of U_{exp} and U_{5} are believed to be related to the relatively large statistical time lag in SF_6 as well as to conditioning effects. Typical test results are presented in Fig. 2 for the 17.8/53 cm conductor, using Y-shaped spacers. The results obtained indicate that with actual insulation requirements for gas-insulated equipment, the tested cables could be operated at 550 and 800 kV (marginally) with gas pressures of 0.35 and 0.45 MPa respectively, limited by the negative lightning impulse withstand voltage.

DISCUSSION

SPENCER: 1. Why limit the study to epoxies?

2. How does IREQ propose to demonstrate that the material selected has an adequate life?

de TOURREIL: 1. Filled epoxy resin was chosen as the initial material to be studied for the following reasons:

(i) the main aim of the work was concerned with the study of the CGIT system as a whole, for possible use in the Hydro Quebec and

(ii) filled epoxy resin has the advantage to allow coating of large insulators with embedded metallic inserts. Mechanical properties remain good at elevated temperatures.

Other materials will be considered as possible candidates.

2. Long term aging studies have not been included in this program.

RELIABILITY ASSURANCE OF 550 kV GAS INSULATED SWITCHGEAR

T. Ushio S. Tominaga
H. Kuwahara S. Matsuda
Mitsubishi Electric Corporation, Itami Works, Japan

INTRODUCTION

The first 550 kV full gas insulated switchgear (GIS) has been put into commercial service on December 1976, in Japan. This GIS with 1800 BIL rating is entirely insulated with SF_6 gas in metal enclosed weather casing, and equipped with metal enclosed SF_6 gas gap surge arresters.

We MELCO, started manufacturing of gas circuit breaker in 1965, and has shipped out more than 3500 sets rated from 24 kV to 550 kV by the end of 1977.

As the development of SF_6 GIS progressed at the same period as that of GCB, the basic research and the application technology of SF_6 gas were effectively used to complete GIS. In 1968, the first 84 kV GIS was installed in the power system and by the end of 1977 the total units of GIS amounts to more than 500 units rated from 72 kV up to 550 kV. The first application of GIS for 550 kV system in Japan started in 1973 using the hybrid GIS, which is a gas insulated switching equipment combined with aerial buses. Now 50 units of 550 kV hybrid GIS are in commercial operation. Therefore, we can say that this first commercial operation of 550 kV GIS has been achieved based on the accumulated field experiences of these gas circuit breakers and GIS.

The reliability of GIS should be assured as the integrated system, because GIS is composed of many components having the different characteristics. There are many technologies on design, manufacturing and testing, supporting the quality of 550 kV full GIS.

RATINGS OF 550 kV FULL GIS

Rated Voltage:	550 kV
Rated Current:	4,000A/2,000A
Rated Short Circuit Current:	50 kA, 2 sec.
Dielectric Strength, Power Frequency:	750 kV
Switching Impulse Voltage:	1,175 kV
Lightning Impulse Voltage:	1,800 kV

FUNDAMENTAL STUDY ON DIELECTRIC CHARACTERISTICS OF SF_6 GAS

There are many factors affecting the dielectric strength of gas insulated equipment. To make clear those factors, the basic research was conducted and many papers were published by our colleagues.

Area effect, surface finishing roughness, v - t characteristics, effect of solid impurities and humidity in gas space etc. are investigated. Depending on those studies the practical design technique was established.

CAST EPOXY INSULATOR

All cast epoxy insulators are designed and manufactured in our factory.

To manufacture insulators of stable and excellent quality, the strict control is made all over the manufacturing processes. Each completed insulator is subjected to dielectric test and measured partial discharge using the specially constructed testing installation. Mechanical destruction test, heat shock test, creep test etc., are also made. Since 1970, a long term voltage endurance test for epoxy insulators has been carried out at 550 kV and above.

MANUFACTURING, ASSEMBLING AND TESTING IN THE FACTORY

Parts and components, which amount to an enormous cost, should be manufactured under strict control and should be balanced between each other as much as possible. Pressure vessels for enclosures are manufactured by the skilled, high level welding technique, which eliminates leakage of gas through welding portions. Machining of materials is made by precision

numerical controlled machines to get the stable quality of parts.

The gas leakage depends on the finishing condition of sealing surfaces and O-ring. Many experiments were made to select the good condition of their combination. O-ring with a sealing material is the best solution for gas sealing.

Assembling work is performed under particular attention to avoid solid impurities to enter into SF_6 gas space. The several sections of assembly units are totally assembled in the factory and tested to assure the integrated ability of GIS. This work reduces the installation work at site in abominable conditions. For this purpose a large building under clean condition was built. Dielectric withstand test, partial discharge test, gas leak test and operation tests of switchgears are made at the factory as the routine test.

INSTALLATION ON SITE

Usually the site installation work is made outdoor. To protect against dust during the setting up, dustproof sheet is provided around the area, making connections between flanges of the vessels. Open portions of buses are covered also with vinyl sheet and clean air is fed into vessel. Individual component is transported filled with the low SF_6 gas pressure.

FUTURE APPLICATION

The present GIS is designed to withstand A.C. 840 kV according to the old standards. Therefore this GIS may be able to be employed as a switchgear rated at 765 kV without modification according to IEC standard. The further reduction in the size of GIS is required due to the economical and environmental reasons. This reduction is achieved by the proved reliability and reasonable design of insulation coordination combined with the newly developed metal oxide surge arrester, which has the excellent v - i characteristics and is small in size.

The efforts to develop and manufacture GIS with high reliability and lower price are continued based on the technologies acquired from the field experiences.

DISCUSSION

MASHIKIAN: 1. Dr. Kuwahara, during the 10 years of operation of GIS systems, and with the 500 units now in service, you have presumably experienced some failures. Could you comment on the types and frequencies of occurrence of major faults experienced?

2. I noticed that conventional cables rather than gas-insulated lines were used in your nuclear power plants. Was there a special reason for this choice?

KUWAHARA: 1. We have never experienced in the field major insulation faults. Our practice is to manufacture GIS totally assembled in our factory and then voltage withstand tests are conducted to assure the integral reliability of the system. By this practice erection work on site is minimized and reliability is guaranteed.

2. In Japan, oil-filled cable for 500 kV is an excellent one. Then in a small current region, such as 1,000 A or 2,000 A continuous current ratings, oil filled cable is more economical than Gas Insulated Lines. But in a higher current region, such as more than 4,000 A, the cable needs many parallel circuits and, then, Gas Insulated Lines become economical. In this current region, Gas Insulated Lines will be used in Japan.

BASIC DISCUSSION PANEL SUMMARY*

R.Y. Pai, Oak Ridge National Laboratory, U.S.A., and T.F. Garrity, U.S. Department of Energy

PAI: Important Physical Parameters in Gas Breakdown Studies. Breakdown in a gas is basically a change of state. The system changes from electrons moving in a gas into a plasma where the electrons experience collective effects. All changes of state are extremely complex, little-understood phenomena. Their study is difficult. It is proposed that the study of pre-breakdown processes is easier than the study of breakdown phenomena and that the former can lead to insights into the inhibition and control of breakdown.

The important parameters in studying these pre-breakdown phenomena are cross sections: attachment cross sections, ionization cross sections, and electron scattering cross sections. These, together with the electron energy distribution, will determine the behavior of the electrons in the gas. In particular the electron density at a given E/P value in the gas will be known and thus the electrical stress necessary to allow the change of state to occur will be determined.

The basic parameters of interest are:

a. the electron-molecule cross sections for elastic and inelastic scattering σ_{el}, σ_{inel},

b. the electron attachment cross section, σ_a,

c. the electron-impact ionization cross section, σ_i, and

d. the electron energy distribution function, $f(\varepsilon,E/P)$.

Recent advances in measurement techniques allow all of these processes to

*Based on the recordings of the proceedings.

be measured. We can now, for the first time, begin to examine the true microscopic properties of the gas and determine how they ultimately affect gaseous breakdown.

MASTROIANNI: Some measurements of better dielectric gases indicate that, at higher pressures, the breakdown strength of these gases relative to SF_6, is not as good as at lower pressures. Could you study pressure effects?

PAI: Care must be taken in making these measurements that one measures the intrinsic dielectric strength of the gas and not changes in the dielectric strength due to the effects of surfaces and other extraneous properties of the apparatus. We have found that when care is taken to control the energy that is dumped into a gas at discharge, these gases exhibit uniform behavior at all pressures with respect to SF_6.

ZAENGL: If care is taken in making measurements, sulfur hexafluoride at pressures up to 20 bar, shows no deviation from Paschen's law. Many of the Paschen's law deviations that are observed by various investigators appear to be due to the effects of surface roughness, the area effect and inhomogeneities in the field.

FARISH: It is perhaps time for all investigators to agree on a definition of what is desirable in new gases. The dielectric strength under uniform field conditions does not appear to be the only desirable characteristic in practical apparatuses. Thus, atmospheric air may well be better as a dielectric for 50 cm gaps than 6 bar SF_6 under impulse conditions. Perhaps it is time to discuss standards and desirable character-

ies of gases such as insensitivity to locally high electrical stresses and one of the major accomplishments of this symposium might well be a start in setting of some standards for improved gaseous dielectrics.

CHANTRY: Given that one knows the distribution function for one particular gas, it is not clear how one would use this knowledge in applying it to another gas or to a gas mixture. The cross sections for all of these electron-gas processes can be used and applied to a Boltzmann transport equation to solve for the final α's and η's and thus characterize the gas much more easily than just using the distribution functions which are not transferable between gases.

PAI: Merely knowing the cross sections for the processes is not enough. Solutions of the Boltzmann transport equation are not well enough developed and are so tedious that in the end, perhaps, one would tend to perform the experiment rather than perform the calculation in the interest of time.

CHANTRY: Measurement of Physical Properties for Gaseous Dielectrics. The determination of the physical properties of gaseous dielectrics is crucially determined by the parameter $\bar{\alpha}$, i.e., $\alpha - \eta$, the ionization rate minus the attachment rate. When this quantity becomes greater than zero, net increase in electron density will occur and this increase will lead to breakdown. At E/P values below the critical value for $\bar{\alpha}$ there will be no net ionization, and thus no electron multiplication and no breakdown. The quantities α and η are derived from the convolution of the ionization cross section with the electron energy distribution and the attachment cross section with the electron energy distribution. The question then becomes at what value of E/P will these convolutions yield a net quantity of $\alpha - \eta$

above zero. If we know the transport coefficients and the coefficients for inelastic processes, then we can compute what the electron distribution function will be. This is done by applying the known values for these cross sections and coefficients in a Boltzmann transport program.

There are many such programs available in various parts of the world and the agreement among these programs is good. Given that we know the electron energy distribution for a gas such as nitrogen, for low mixtures, say less than 1% of SF_6, knowing the attachment cross section and ionization cross section for SF_6, we can compute the value of $\bar{\alpha}$ and thus find the breakdown strength of this mixture. However, knowing the distribution function for dilute mixtures of an attaching gas is of no use if one wishes to know the breakdown strength for mixtures containing, say 50 to 100% of attaching gases. Then the distribution function is not known and one must go to the cross sections and use these in a transport equation solution.

From the papers presented earlier it is seen that attachment cross sections have been heavily emphasized in this field. The reason for this is that one finds the ionization coefficients for many of these attaching gases to be similar. Thus, the only variable that we have is the attachment cross section since the ionization cross section does not appear to be a strong function of the gas.

ZAENGL: It appears that the sensitivity of these gases to inhomogeneities in the electric field could be reduced by changing the slope of the net ionization coefficient $\bar{\alpha}$ so that it is not quite so steep a function of E/P. Is changing the slope possible from a physical point of view?

CHRISTOPHOROU: Ionization near the threshold does vary considerably and is perhaps the most important energy regime to consider. It may be possible to employ molecules which dissociate rather than ionize in this region and thus control the ionization coefficient and therefore affect the breakdown processes.

LUCAS: With regard to the first topic it is very important to know the electron energy distributions. We have made many attempts to measure this, but have been stymied by the fact that sampling does not appear to give the measurement that we want. The cross sections are relatively easy to measure. If we could find the distribution functions then these quantities, α and η, could be calculated very easily. Use of Monte Carlo and Boltzmann transport equation methods to compute the electron energy distribution are unsatisfactory but the only possible way to go at this time. It would be extremely useful to have the energy distribution functions.

CHANTRY: Changing the mixture will change the distribution function and you would have to remeasure.

LUCAS: But you could do that directly.

PHELPS: The electron energy distribution would be a very useful parameter to know. There is some dissatisfaction with present methods of determining these electron energy distributions and some effort is being made to try to improve this situation. The electron energy distribution, at times, need not be known that accurately. Possibly at the thresholds it would be important, but calculations have been made which show that in certain discharges assuming a Maxwellian function does not

seriously affect the result even though a Maxwellian function is clearly wrong.

Going to a gas with a high attachment coefficient implies that one will be able to go to high electric fields. This in turn implies that the ionization coefficient will rise sharply. Thus, one is in a situation where improving the dielectric strength of a gas may well make it more susceptible to nonuniform fields.

CHANTRY: It would be helpful to modify the slope of the net ionization coefficient as a function of the E/P value.

PAI: If one can change the electron energy distribution, one should in principle be able to change the slope of the net ionization coefficient.

LUCAS: Uniform Electric Field Considerations. There are three operating regimes of interest in our work. The first regime is the low pressure discharge region, the second regime is the high pressure discharge region, in which secondary electrons are important, and the third regime is for the high pressure region in which only primary electrons are considered, that is the measurement of swarm coefficients. In the low pressure regime we find that breakdowns will occur over longer paths since greater multiplication can be achieved. Thus, electrode designs are made with the consideration that the actual position of breakdown should be the longest path between electrodes. In the high pressure regime in which secondary electrons are important, we have basically three different uniform-field geometries, the standard Bruce profile, the Rogowsky profile, and a profile calculated by Harrison by a computer simulation in which the effect of the wall geometry is taken into consideration.

In the regime for measurement of swarm coefficients an effective uniform field geometry is to have guard rings which determine the field at regularly spaced intervals around the periphery of the interaction region. Here, as long as the electrons do not approach the periphery of the interaction region, one can effectively have a uniform field geometry. One final method for maintaining uniform fields is to set up a positive column, in which case, the net charge density would maintain a uniform field over very long distances up to one meter. Use of the positive column allows one to pass very large currents up to 100 milliamperes without worrying about space charge.

BERGER: Electrode Coating Effects. At low pressure and for small apparatus, breakdown strength of a gas depends on the gas composition, the electric field and the geometry of the electrodes. However, when we go to high pressures and larger electrodes, the condition of the gap, the roughness, any coatings, etc., become important. Differences between the breakdown measurements of different investigators in supposedly the same gas at the same pressure may well be due to differences in the condition of the electrodes that they have used. Coatings on electrodes can reduce the pre-breakdown current from 10^{-5} to 10^{-6} amps down to 10^{-9} amps. These coatings also improve the breakdown voltage. There are questions as to the exact mechanisms by which coatings improve the dielectric strengths of the electrode gas combinations. Possible mechanisms are, (i) the reduction of the precurrent may delay the onset of breakdown, (ii) the coating may reduce the field gradient in the critical region between the electrode and the gas, and (iii) the coating may restrict particle motion which is known to cause breakdown at much lower voltages than would

otherwise be anticipated.

MASHIKIAN: Have you measured the effects of the permeativity of the coating?

BERGER: No.

MASHIKIAN: What are the effects of pinholes in the coating for the electrodes?

BERGER: The most important technical problem involved with coatings for improving dielectric strength of electrode-gas combination are the pinholes. Pinholes must be avoided at all costs.

SHARBAUGH: In addition to the other improvements made by putting a coating on an electrode, you must take into account the fact that you have replaced a medium of low dielectric strength, namely the gas, by a medium of high dielectric strength, namely the solid coating, in the region of the asperities where the fields are nonuniform.

VLASTOS: In my work on coatings, a 20 mm gap was able to withstand 500 kV before breakdown. Positive and negative breakdown voltages were comparable. The coatings that seem to work best were aluminum oxide and these coatings did not change their breakdown strength with sparking. This aluminum oxide coating seems to be much better than epoxy in controlling breakdown.

PARKER: Aluminum oxide coatings always exist on aluminum surface, thus, adding aluminum oxide is merely adding to the oxide coating. The effect of additional oxidation is not clear. Perhaps the coating process is more

complicated than we realize.

COOKE: We have found that coatings need not be perfect. The effect of punctures of epoxy coating sometimes reduced breakdown strengths, but other times did not. Close examination of these punctures indicates that the probable cause of the reduction is due to metal deposits on the coating caused by vaporization. Thus, it is not necessary that coatings be perfect.

MASTROIANNI: Nonelectrical Aspects of Gaseous Dielectrics. Industrial testing of the electrical properties of a new gaseous dielectric would require large amounts of the compound. A chemical company, before it could sell such large quantities, would have to make tests of the toxicity of such compounds. These tests would include an LC_{50} test, a mutagenic test, and a teratogenic test. The total amount of material necessary for such tests would probably be of the order of one ton. The cost of such materials may affect the willingness of a chemical company to supply a gas for electrical testing.

Certain general statements can be made about the toxicity of chemical compounds. Total fluorination of a simple compound makes it very nontoxic. Replacement of the fluorine by hydrogen increases the toxicity. Inclusion of chlorine also increases the toxicity. These considerations may be important in the initial search for new gases.

Another consideration for a new gas is arc stability. Arc stability of fluorinated hydrocarbons seems to depend on the complexity of the carbon/carbon bond. Thus, single bonded carbon structures are more stable than double bonded ones. These in turn are more stable than triple bonded

systems. Consideration of these chemical properties of compounds should be taken into account in looking for new dielectric gases. We have found that in arcing a set of related fluorocarbons, more deposits were left by a triple-bonded system than by a double-bonded system and even less deposits were left by a compound with only single bonds.

VIGREUX: Basic Considerations of Gaseous Dielectric Performance in Electrical Apparatus. Electrical switchgear has its own mechanical properties which characterize the gear. Dielectric gases on the other hand have properties and characteristics of their own. For practical equipment we must match the properties of the gas to the properties of the switchgear.

Many dielectric gases have been known for many years. Thus, compressed air has been considered as one possible candidate for switchgear applications. But metal clad switchgear has only been in production with the introduction of SF_6 as the dielectric gas. The cost of the mechanical equipment is one of paramount consideration, and the pressure of the gas has a very serious effect on the cost. SF_6 can be used at much lower pressures than air, this lower pressure reduces the mechanical strength needed and therefore the cost of the equipment.

Consideration should also be taken of the production capability of gas manufacturers. A 500 kV line of 100 km length would require more SF_6 than the total production capability of the entire world for one year.

Differences between laboratory apparatus used in the measurement of the properties of dielectric gases and switchgear very much influence the behavior of the gas. Laboratory apparatus is small, the roughness is known, and the conditions are very well controlled. Switchgear on the other

hand is manufactured in a factory and it must be large; it is impossible to control the conditions under which it operates as well as can be done on equipment in a laboratory.

From a switchgear point of view the most important advance in dielectric gases would be a gas which is less sensitive to nonuniform fields. Such gas would both moderate the effect of scratches and machining in switchgear as well as allow the elimination of devices such as particle traps in the gear.

Use of SF_6-N_2 mixtures may well be the next important advance in gaseous dielectrics. We have measured a 50% SF_6-50% N_2 mixture in which the impulse breakdown is better than SF_6. The standard deviation is also small. We are continuing investigations of these mixtures. One final consideration to be taken into account is that users would like to have the same gas in all switchgear. Using different gases in the same substation is not practical. Also no carbon deposits can be tolerated in any of the equipment under any circumstance.

FARISH: Baumgartner seems to have also found a SF_6-N_2 mixture which was better than pure SF_6. These mixtures may also be good as arc interruption media.

SPENCER: If a mixture of gases is to be used, users must be able to measure what is in the equipment. Pressure measurements are not enough.

GARRITY: The arc interruption test referred to earlier was only for synchronous interruption. Non-synchronous interruption may be different.

COOKSON: In a long CGI transmission line one may be able to use a gas

mixture that is different from that used in a substation, but the gas used inside a substation should be common to all equipment.

DAKIN: Consideration should be given to the durability, thermal stability and compatibility with other materials of a dielectric gas.

MULCAHY: Research Needs on Gaseous Dielectrics Related to User Needs. Equipment users have stringent requirements for gas switchgear. Reliability, in both long and short terms, must exceed 99%. Compact systems are desirable, both in terms of costs and in terms of space available to the user in installing systems. The systems used are very large both in terms of the energy stored in them and in terms of the energy transmitted. Another requirement is ease of assembly of the equipment. Finally, we would like the gaseous component to be nontoxic and nonhazardous in any form. Also, demonstration programs should be taken on life-sized systems, and not laboratory-size systems to show that gaseous dielectrics being proposed are indeed good.

CHRISTOPHOROU: Before we can introduce better dielectric materials we must know not only what is needed from the material point of view but also what makes one material better than another. Basic research is necessary before we can provide the users with what they want.

MULCAHY: I agree.

SPENCER: In field installation the gas must be put into an evacuated system. The vacuum that is drawn will not be good. Thus, the gas must be compatible with what material is left in the system. These materials include water, air, and cleaning fluid that was used to clean the system.

Also it must be realized that these systems will leak. A large substation in which only 2% of the SF_6 leaks out per year will lose 1000 lbs of SF_6 per year. Toxicity limits must take this large leakage into account.

VIGREUX: We have found that in actual installations, the leakage rate is small. Over a ten-year period some of our equipment has lost only one per cent of their gas, and with diffusion, the residual concentration of the gas will be small. What is perhaps of greater concern is a break in the line, not only under operation conditions, but also in refilling operations. Then, a large quantity of gas may be spilt into the atmosphere and the danger may be great.

CHRISTODOULIDES: In your toxicity tests what is the reliability of the numbers that you produce?

MASTROIANNI: We, of course, use outside laboratories to perform these tests, and thus remove any bias.

SAUERS: Have you analyzed the residues that you found in your experiments?

MASTROIANNI: No.

SHARBAUGH: The toxicity of any new compounds should be tested. We are presently testing a nitro compound which looks very promising and hopefully will not be too toxic.

CHRISTOPHOROU: Many possible fluorocarbons can be found which will have high dielectric strengths but since they contain carbon one would

have to expect some carbon formation in the case of a breakdown. The question that is posed to the manufacturer is: "Can solid insulators be designed so as to tolerate the formation of small amounts of carbon?"

COOKSON: In field tests of installed CGI equipment, no carbon formation can be tolerated. Any carbon formed in a field test may lead to long-term degradation of the system, thus, no possibility of carbon can be tolerated by the manufacturer or user. In regard to this question of degradation of insulators, one should consider the interaction of the solid insulator with the gas; it may be possible to find a combination of insulator and gas which will out-perform the present combination and it is the insulator-gas interface which is the weak point at this time. A final practical problem with using mixtures as gaseous insulators is that at some point the equipment may have a failure and we will wish to pump out the gas. Some system must be designed which will pump out the gas and allow a refill with the proper mixtures at the time of refill.

APPLIED DISCUSSION PANEL SUMMARY*

M.O. Pace, University of Tennessee, U.S.A., and V.H. Tahiliani, Electric Power Research Institute, U.S.A.

TAHILIANI: Introduction. This is the last session of this Symposium. We have spent the bulk of the three days reporting what has been done. In this session I would like to entertain discussion on current problems and the work that remains to be done. This applications panel consists of Roy Wootton of Westinghouse, Roy Nakata of General Electric Company, Marshall Pace of the Electrical Engineering Department at University of Tennessee, Inge Johansen of the Electrical Engineering Department at Norwegian Institute of Technology, Martin Hudis of R.T.E. Corporation, and Ed Spencer of Gould, Inc.

I would like to begin with a brief overview of the state of the art of gaseous dielectrics in the electric power industry. EHV and UHV substations are experiencing increased acceptance of dead tank, gas insulated equipment. Compactness, improved aesthetics, and freedom from electrostatic fields, coupled with lower installed costs, especially at higher voltages, are expected to increase the usage of gas insulated equipment. In spite of the readily available equipment up to 500 kV, the usage is somewhat limited by some reliability questions. These result from uncertainties of protection, from steep surges, and contamination from particles and moisture. Also the lack of suitable fault location methods and excessive repair time deter the usage.

Transmission voltages of 1200 to 1500 kV are likely by the late 1980's; according to many experts, substations for these voltages are

---

*Based on the recordings of the proceedings.

certain to be dead tank, gas insulated design. While the actual needs are far into the future we must develop the basic technology for improving today's application, as well as developing the technology for the future.

Although gas insulated cables are now in use for short runs, the economics makes them less competitive for transmission over long distances. Here again, we must develop the base technology and improve the economics. I hope the discussions during this panel will focus on current problems, enabling us to develop the base technology for future equipment. One of the problems we all recognize is effect of particle contamination in gas and its effect on its dielectric strength. When we think of particles, we think of them in motion under the influence of electric fields, and further, we are tempted to move these into zero-field regions to immobilize them. Understanding this phenomenon is very important, not only to the design of gas-insulated equipment, but also to the user since he must employ a particle scavenging technique to condition the system prior to energization. To start off this discussion, I would like to invite the comments of Mr. Roy Wootton of Westinghouse Electric Corporation.

WOOTTON: Particle Contamination, Primarily in AC Fields. Mr. Wootton showed three films of particle motion and breakdown, first at real-time speed, and then slowed-down by about a factor of 100. The first of three films showed plane electrodes with inclined boundary regions to prevent particles from escaping from the system. The AC voltage was ramped linearly. Particle-initiated breakdown was extremely fast and in this real-time film, often occurred between frames. Particle motion has been simulated on a computer, and this agrees well with observations.

Film 2 was a high-speed (2000-3000 frames per second) film taken at Westinghouse with a laser by Owen Farish. This technique provided a "shadowgram" which showed density differences in the moving gas after each breakdown. Particles could be seen hovering and oscillating, with electric wind streaming from them. The electrodes were quasi-plane, as in film No. 1. The gas in the first two films was SF_6 at 200 psi. Film 3 showed a co-axial electrode system with curved axis to prevent escape of the particles. The gas was SF_6 at 150 psi. The aluminum particles were 1/4 in. long. Hovering motion and particle acceleration at the electrode could be seen. The particle hit the center electrode many times without causing breakdown.

I would like to discuss where we are concerning particle-initiated breakdown. Initially the examination of breakdown was difficult due to particles hitting a surface because you didn't know where they would hit or on which impact a breakdown would occur. More recently, we have been able to get the same results with fixed particles isolated from the electrodes as with moving particles. This will allow us to bring more instrumentation to bear on the problem. There has been an increased confidence in particle traps. One result of finding the "two-gap" process of breakdown with the particles is that the 60 Hz breakdown behavior is related to the impulse response of the gas.

TAHILIANI: Instead of inviting questions on particles, I propose to have the next panel speaker now and we will entertain the questions later. While gas-insulated AC equipment is widely used, application of gaseous dielectrics is catching on in the DC converter stations as well. We also recognize that it is only a matter of time before we install longer

lengths of gas-insulated transmission cable. This means that the preferred AC testing method will no longer be practical, and we must resort to testing the equipment with DC or other suitable test methods. Let us examine how the particles behave when the equipment is energized with DC. I would like to introduce Roy Nakata of G.E. to discuss his experiences on how the particles behave under DC excitation.

NAKATA: Particle Contamination, Primarily in DC Fields. As DC becomes more widely used in transmission and in testing, we do indeed need to know more about particle behavior in DC. Also an AC system can experience DC due to trapped charge. In practical apparatus one must consider not only the cylindrical field, but also the axial field--for example, at elbow bends and disconnect switches.

In a practical test vehicle, we have shown that small particles will move downhill, and large particles will move uphill. Now let us show films of particles in DC fields. The first film shows an 8" enclosure filled with 30 psig SF_6 with a 3" diameter conductor. Some particles are free; others are cemented. The negative polarity due to its severity was selected. A major problem with DC is that particles will levitate and stick to the insulator tenaciously. In the film we see the particles bouncing, and falling into the trap. Particle motion in AC is also shown in the film. In this case, we are using directed trapping.

From the film we conclude that we can indeed trap particles, but the traps must be properly designed. A practical system must be capable of trapping all types of particles. We have never been able to re-levitate particles that have been trapped. Practical design thus developed is one where the particle trap is located downhill so that gravitational as well

as electric-field forces help push the particles into the trap. In practical apparatus, we begin scavenging particles at 75 kV, and go up to 400 kV in about one hour. We have built a 400 kV gas-bus system for E.P.R.I, which is 95% complete, and ready for final testing. Thank you.

TAHILIANI: Are there any questions?

GARRITY: What is practical for a substation bus may not be practical for long underground transmission. AC scavenging is all right for substations, but may not be suitable for long transmission lines, especially underground. In underground transmission, slopes and contours may negate the effects of particle traps; therefore, we must accept particles and find ways to control the undesirable effects of particle contamination. AC scavenging is not acceptable for long underground lines, due to large charging current requirements. Also, AC systems may be subjected to DC stresses after de-energization. Therefore, particle traps must hold particles under all field conditions. A question I have is this: After you scavenged the particles, did you subject the system to a reverse polarity switching surge?

NAKATA: Yes, we did. We would stabilize the system for hours at 500 kV first. Then instantaneously, that is in microseconds, we would reverse the polarity.

TAHILIANI: Let us ask ourselves 'what are we looking for in new gases?' We now call on Marshall Pace from the University of Tennessee.

PACE: Developing and Applying New Gases. Let us discuss what we should be doing to prepare gaseous dielectrics for the present and the future.

As an electrical engineer, I will stand in the applied arena and direct comments to the basic workers, emphasizing the need for close cooperation between the basic and applied workers. One group of workers occupies itself with fundamental electron-molecule interactions, while another works with larger-scale phenomena, described generally by $\bar{\alpha}$ and other coefficients. And then, of course, there is the third group of workers in the applications area, where the pay-off exists for all. Here the problems are particles, rough surfaces, flash-over, etc.--all those problems we have discussed so far.

The synthesis of new gas dielectrics must be done on the basis of knowledge on fundamental electron-molecule interactions. In using $\bar{\alpha}$, we analyze given gas mixtures and, just as important, develop engineering design rules for their use in applications. And, of course, in the third group, the applications, we have all the problems which we are all trying to solve. The workers in this last group must direct their problems to the other two groups. We might label the first two groups as the basic workers; those in the applications would then be the applied workers. There must be a constant interplay among these three distinct and important groups.

The three parts to my question are: How should these groups interact? Where should improvements be made, and where can improvements be made? What do the applications people need from the basic workers?

I will now give my own answers to these questions. The three groups I have named seem to have certain common observations. The applied workers observe that the dielectric strength of SF_6 is ultimately quite good, but many problems such as particles and rough surfaces keep us from

realizing that strength. The workers using $\bar{\alpha}$ observe, meanwhile, that the $\bar{\alpha}$ for SF_6 as a function of electric field has an intercept at quite high electric field, which makes its ultimate dielectric strength high. However, the very steep slope of this relation of $\bar{\alpha}$ as a function of E is not satisfactory, because the steepness leads to problems in applications. Any field enhancements, even over volumes as small as one cubic millimeter, may cause $\bar{\alpha}$ to be positive and to launch a streamer, which leads to breakdown, even though the field may be well controlled everywhere else. Meanwhile, in the world of basic studies, we find that SF_6 provides very good control of electrons of low energy, that is, below $\sim$0.4 eV, but above this energy range control decreases abruptly. Unfortunately, electrons in a gas under electric stress do have a wide range of energies.

I think each of these three groups sees practically the same phenomenon, each in its own way. I think we can reasonably hope to obtain improvements in many areas by dealing with this common observation.

What improvements do the applications people need? Gaseous dielectrics must be able to tolerate particle contamination, rough surfaces, and flash-over at the insulators; the dielectric strength should be easily increased by raising the pressure; we need compatibility with all materials; we need a better impulse ratio, which is disappointing in SF_6 compared to impulse characteristics of other gases relative to their DC strengths. We need good simple field test methods; we need good methods of fault detection and perhaps incipient fault detection. There are other characteristics which are absolutely necessary, though not so electrical in nature, such as the temperature characteristics, the methods of handling

and storing gases, the mixing characteristics of any mixtures, and of course, the toxicity.

A major way that basic researchers can improve the gaseous dielectric is to make it much less sensitive to field enhancements. A complication concerning the particle problem is that particles are field enhancements which move. For new gases it is difficult to speculate on this point. For example, how would particles move in different gases? How do we want particles to move in gases? As a particle approaches a surface, perhaps of opposite charge, we have a discharge gap which varies continuously from a large value all the way down to zero. I think we might see a diminished area effect in improved gaseous dielectrics because of an improvement in sensitivity to rough surfaces and particles, which underlie this area effect. We can hope to obtain better impulse characteristics by making the dielectric form streamers less easily than SF_6 does. This would cause the volume of streamer formation to increase, which would possibly increase the formative time lag, but decrease the statistical time lag.

Now, concerning the third question, what do applied workers need from basic workers? The answer is: an improved dielectric in the ways we have outlined, but also a set of engineering design rules for using this dielectric. These design rules could be divided into two parts: (i) for existing equipment we need design rules on how to optimize the gaseous dielectric for given conditions of surface roughness, particle contamnation, etc. and (ii) for the future we need engineering design rules to guide the designer of new equipment to reach the very best condidions for a given gas. I think it is the job of the basic worker to deliver a

finished product to the applied worker. The basic worker is able to run smaller experiments, which are faster. The applied worker has many current problems of his own. The applications workers are the customers in this relationship. The finished product needed is not only improved gaseous dielectrics, but also engineering rules on how to use them.

And so, in conclusion, I have tried to outline the problems and approaches for the future, with an optimistic view of what can be accomplished by controlling the sensitivity to field enhancements by means of control of free electrons.

TAHILIANI: Are there any questions?

COOKSON: Roy Wootton and I looked at particles in nitrogen, and found them to be more active there than in SF_6. This was because of increased corona at the tips of the particles. You are right; particle motion can be different in different gases.

DUTTON: This cogent analysis of the situation is the sort of thing I hoped might come out of this meeting from the very beginning. No matter which group you fall into, those of cross section, those of coefficients, or those of applications, we all need data. There is a vast amount of data available, but it is widely scattered and disorganized. Should we set up some panel to decide what data is needed, how to gather that data and most importantly, to critically analyze the data. I would like to put this to this body as a suggestion.

JOHANSEN: The relation between basic and applied sides is better in this field than most others. For example, concerning solid insulation,

you would rarely find basic and applied people meeting as we are doing here. I feel it is harder for the basic person to understand the applied side than vice-versa. The cooperation can be made even better, in one way, by industry and utilities placing more research in the universities.

FARISH: I think we all agree we need a better gas than SF_6, especially concerning non-uniform fields. In seeking this improved gas, we must evaluate the candidates as cheaply and quickly as possible. We need more discussion on ways to do this. With various gases and mixtures, the measured strength depends on geometry; one can study the strength in many geometries, but that is a long process. Therefore, better methods of testing candidate gases is quite important in developing improved dielectrics. If anyone can suggest standardized test methods, that would be a very useful result of this conference.

ERIKSSON: Our company now uses gas insulated substations in Sweden. We must deal with temperatures down to -50° C, which is a problem with pure SF_6. A solution may be a mixture of SF_6 and nitrogen. In fact, we have ordered circuit breakers with that mixture.

NAKATA: I would like to make a comment on studies that might be done in the future. We have developed, for example, a resistive coating for insulators which would help grade the field and carry charge to neutralize the particles. It worked quite well, but was too expensive. Basic studies could lead to toleration of particles, at least on the insulators in this case.

CHRISTOPHOROU: Is -40 to 150° C the temperature range

in which new gases should be used? (Several members of the audience indicated agreement.) Another question is: do you not worry about the water content of gas? Let us seek gases tailored to the many particular needs, rather than just one universal gas. Also, I would like for Professor Dutton to form a committee to follow up on his suggestion of a few minutes ago.

TAHILIANI: I would now like to call on Inge Johansen from the Electrical Engineering Department of the Norwegian Institute of Technology.

JOHANSEN: Gas Insulation in Europe. In Europe, gas insulation is well established. There is a large number of installations with good operating record. In my country of Norway, GIS has made installation of hydroelectric stations economical. We have seven such stations in operation with perfect operating record. Fifteen more are being planned or are on order. Concerning safety, gas insulation has already saved many lives, being safer than conventional systems, where contact with high voltage is a danger.

We have made full-scale tests on faults in power apparatus. We looked at the pressure rise, the gases resulting from arcs, and the effects on the equipment. Spring-loaded domes released when pressure reached a certain value. Tests were made at 20 kA and 40 kA. We found that about half the arc energy goes to increase pressure, and the rest goes to heat the system. Arcs on aluminum electrodes gave an exo-thermal reaction. Many reaction products involve the aluminum and the epoxy insulators. Some of the gaseous by-products were toxic, but the risk to people some distance away is small. These systems should be safe with

good design and ventilation.

TAHILIANI: Thank you. Are there any questions? Are there any questions on reliability?

GARRITY: How do we get confidence for a 30 to 40-year operating lifetime? What tests can be made? Also, I believe safety measures based on rupture discs are safety hazards in themselves.

JOHANSEN: The gas must not degrade under stress with time; the reliability problem is then mainly with the solid insulators. One of my main concerns is when pressures are raised in the future and the voltages are raised to the 500 to 800 kV range.

CHANTRY: I would like to go back to earlier comments on corona. We basic workers should admit that we are not able to tell you with cross sections why your systems will not operate at the ultimate dielectric strength of SF_6. The toleration of rough surfaces and particles depends on the degree of corona stabilization. Therefore, more needs to be known about the photon processes in gases.

TAHILIANI: While we speak of gas dielectric applications, we instinctively think of EHV equipment; however, this insulating medium is widely used on distribution class voltage apparatus such as load break switches, low fault interruptors and vapor-cooled transformers. This specific application demands some understanding of the requirements. I would like to invite Dr. Hudis of RTE Corporation to discuss his thoughts on what we can look for in this area.

HUDIS: Gas Insulation in Distribution Equipment. I wish to discuss the trends in distribution and the impact of gas insulation in distribution. I will deal with the sealed switching area, and with medium voltages. There is a huge world of distribution which is slowly moving from open equipment to sealed equipment--which opens the possibility of new gas insulation.

There are five types of switching apparatus moving from an open to a sealed form which are: (i) fuses, (ii) disconnect switches, (iii) load-break switches, (iv) high-voltage contactors, and (v) distribution breakers. The voltages involved in these five are 2,400 volts to 38,000 volts. The currents range from a few hundred amperes up to 80,000 amperes.

These devices can be subdivided into three categories according to operation. There are plain-break devices, ablation interruptors, and gas-flow interruptors. With plain-break devices, we can put in a new gas in place of air to interrupt currents of a few hundred amperes. Ablation interruptors come in a wide variety of forms, in which an arc impinges on some kind of ablation material. In choosing a gas, interactions with the ablation material must be studied. For example, SF_6 cannot be used in a current-limiting fuse because of interactions with silver. The gas flow devices can be subdivided into four variations: two-pressure flow devices, single pressure puffer devices,magnetically driven arc devices, and those combining magnetic arc driving with a puffer. Most studies of enclosed equipment with gases so far have been performed with SF_6. Other gases and gas mixtures should be considered for use in these devices.

PACE: Do you expect to deal with the same problems in distribution equipment that we have been discussing earlier on this panel for higher

voltages?

HUDIS: The number of operations is of prime consideration in this equipment. This leads to concerns over materials, arc products, and their interactions, and aging. Problems that we have discussed concerning higher voltages, such as particles, would be less severe with distribution voltages.

TAHILIANI: A big challenge to the designer of gas-insulated equipment is supporting the high voltage conductors with appropriate distance from the grounded conductors. This means incorporating insulating supports that are equal or superior to the gas dielectric medium. This aspect is quite complex. Here to discuss this problem is Mr. Ed Spencer, of Gould Inc., who will speak on his concerns on how to life-test these insulators.

SPENCER: Solid Insulation in Gas Systems. There is often doubt about the long term stability of insulators in use now. These have been made of epoxies of various types, with different fillers. Epoxies have some serious drawbacks. The high dielectric constant disturbs the field considerably. This restricts the shapes which can be used. Epoxy insulators are difficult to make, which makes them expensive and require great quality control. They are opaque, which restricts inspection. This necessitates costly and drastic electrical testing. Epoxy insulators generally use conducting inserts, which limit design and add thermal constraints. There is some tracking with epoxy insulators. High temperatures are a problem, because epoxy is limited to a maximum of 105 to 120° C. Epoxies have one very great advantage: They have an operating performance history which provides a basis for reliability understanding.

At Gould, we have obtained a new material which we would call "X" which will not track at all. It has a low dielectric constant, approximately three, which disturbs the field much less and gives the designer more freedom. It is injection moldable which makes manufacture fast. The material is transparent. It does not need inserts due to its low dielectric constant. It permits operation at a much higher temperature than does epoxy. The major drawback of this new material is that it has no history.

We are considering this material for a new flexible cable being developed under E.P.R.I. sponsorship. This gas-filled flexible cable has corrugated conductor and corrugated outer cylinder, which allows us to put it on a reel. Flexing of this cable causes it to require many more insulators than a nonflexible cable, up to about ten times as many. The insulator which is made in two segments can be snapped on to the center conductor from the side. This insulator material has performed extremely well in short-term tests. Our job now is to determine that this material will have a long life in SF_6 or any other gas. We must know what kind of tests should be done. A production laboratory generally does not have time for these tests.

TAHILIANI: Thank you. Are there any questions?

SCHWEINLER: What is this material?

SPENCER: I do not know exactly. This is a developmental material and we have a secrecy agreement with our supplier. It is not on the market.

SLETTEN: What, again, was its dielectric constant?

SPENCER: The dielectric constant is about 3. It has an almost flat characteristic as its temperature goes up to almost 140 or 150° C.

SOMMERMAN: In arc interruptor nozzles and barriers, we have used teflon with considerable success.

SPENCER: We tried teflon, but discarded it partly because of poor arc resistance when an arc actually contacts it; and, of course, it is expensive.

DAKIN: In testing, we should determine the deteriorating factors first. For example, if temperature is a problem, we can accelerate life tests by using higher temperatures. One should run creep tests at higher temperatures also, because this is apparently a thermoplastic, since it is moldable. Also, life under voltage should be determined either by accelerating tests with higher voltage or with higher frequency.

SPENCER: We have considered tests at higher frequencies, but for these you need a known corona level. We have been unable to detect partial discharges at all so far. We have run it for many hours at four times the normal voltage.

TAHILIANI: We have three more minutes, and I would like to invite comments on any subject related to applications in general.

SLETTEN: In this conference I have missed, from the basic people, discussion of time as a parameter in breakdown, although some experimental work has been reported.

GARRITY: The one major question that has emerged as a result of this symposium, as I see it, is what do we mean by "better"? We must make a good definition. To some people "better" is lower cost; to others it means better dielectric performance; to others, it means stability and non-toxicity. We should leave with some definition of what we mean by "better".

WOOTTON: Figure 1 shows a vertical plot of voltages with the ultimate dielectric strength of SF_6 at the top. Lower strengths are shown for realistic conditions, such as rough surfaces, particles. These figures have been compiled from many laboratory tests. Also shown in Fig. 1 are the stresses we experience in practical equipment. The fields used are generally 10 to 15% of that which the gas ought to be able to stand in ideal conditions. The design limit is generally the BIL limit. However, Alan Cookson mentioned that in some mixtures the switching surge may be the limit. We can see that the problems with SF_6 are rough surfaces, dust, and large areas. We have heard the area effect discussed, but we have no indication of what it is caused by or what relation it may have with time.

Tests of new gases and gas mixtures should be performed in fields which have both microscopic nonuniformities and macroscopic nonuniformities. In practical coaxial systems, the macroscopic field factor is about 1.8 bu. with bends and other geometries considered it is at least 2. The microscopic field factor is due to surface roughness and microparticles. Electrical tests should, therefore, include both microscopic and macroscopic nonuniformities.

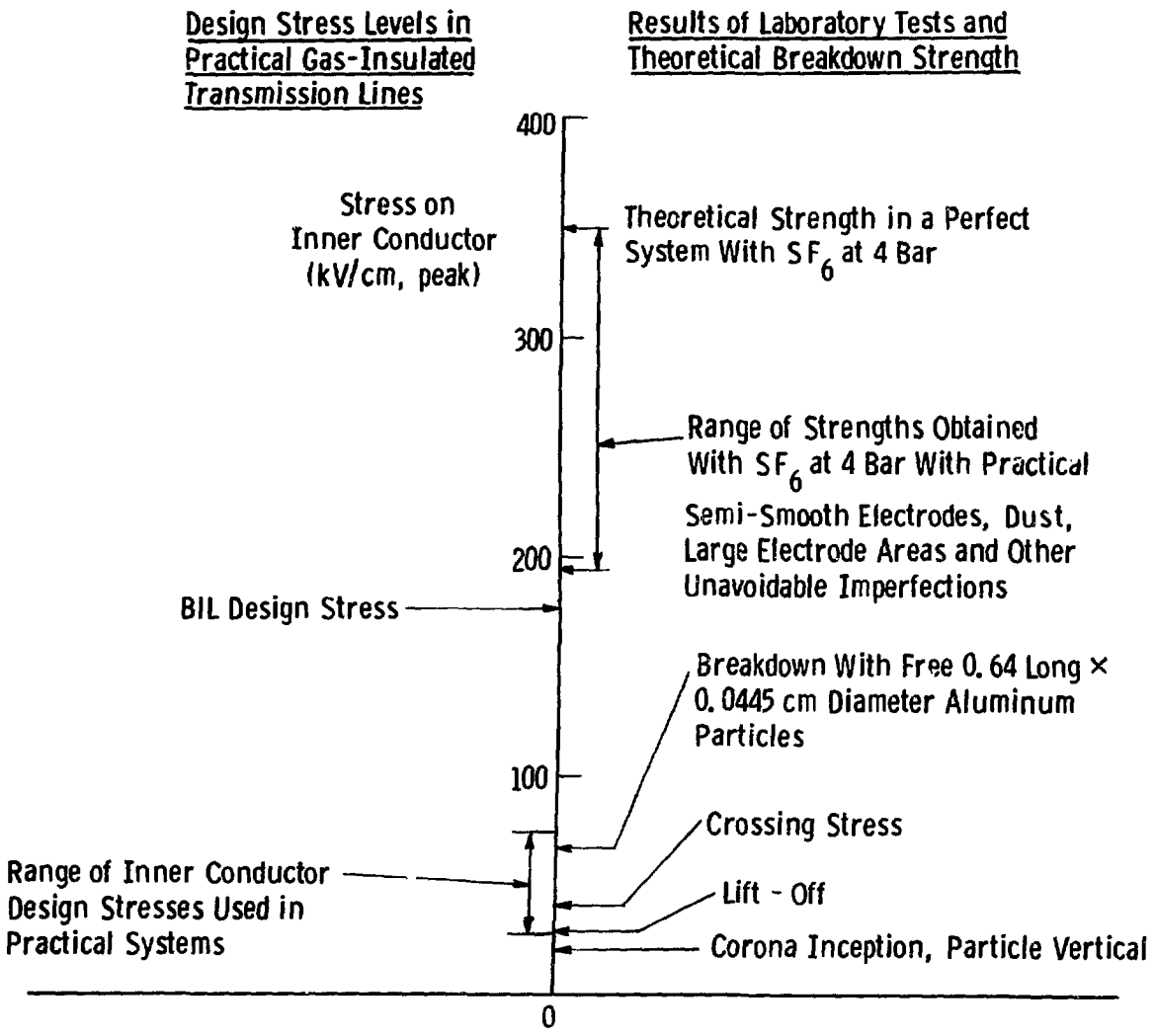

Fig. 1 — Relationship between the design stress in practical gas insulated systems and stresses at which various particle phenomena occur in a laboratory 7.5 cm/25 cm coaxial system with SF_6 at 4 bar

One possible interpretation of the situation is that we might choose to give up some ultimate uniform field dielectric strength in order to gain tolerance to these complicating factors. Gas mixtures might achieve this aim. However, there are other factors such as toxicity, carbonization, and cost. In using mixtures, compromises must be made in improving the different problems. We have found that mixtures of SF_6 with helium, or SF_6 with air, can be found which tolerate particles better than SF_6 or the other gas used alone. The behavior of mixtures in nonuniform fields can be quite different from that in uniform fields. Therefore, there is a limit to the merit of testing in purely uniform fields.

HUDIS: Concerning the question of "what is good?', I don't think we can produce an uniform answer for all applications. It is going to depend on the manufacturers' capabilities and on the users' needs.

I think it is quite important to converge on a uniform way of making measurements and reporting data. We now have considerable difficulty in comparing data from different sources. I think this is our first obstacle, and after we overcome that it is up to the manufacturer and the user to determine what they want.

TAHILIANI: I wish to thank this panel for their discussions. This being the last session of the symposium, I wish to extend thanks to all of you participants for your participation and to Dr. Christophorou and his people at Oak Ridge National Laboratory.

This is the end of the applied panel sesssion.

AUTHOR INDEX